



**Experimental Studies of Transpiration Cooling
With Shock Interaction in Hypersonic Flow**

MAY 1994

This experimental program was conducted under NASA Grant Number NAG 1-790. The analysis and publication of measurements was funded internally and with the contract with UDRI

Prepared By:

**Michael S. Holden
Calspan-UB Research Center
P.O. Box 400
Buffalo, New York 14225**

Prepared For:

**NATIONAL AERONAUTICS AND SPACE ADMINISTRATION
LANGELY RESEARCH CENTER
Hampton, Virginia 23665-5225**

ABSTRACT

This report describes the result of experimental studies conducted to examine the effects of the impingement of an oblique shock on the flowfield and surface characteristics of a transpiration-cooled wall in turbulent hypersonic flow. The principal objective of this work was to determine whether the interaction between the oblique shock and the low-momentum region of the transpiration-cooled boundary layer created a highly distorted flowfield and resulted in a significant reduction in the cooling effectiveness of the transpiration-cooled surface. As a part of this program, we also sought to determine the effectiveness of transpiration cooling with nitrogen and helium injectants for a wide range of blowing rates under constant-pressure conditions in the absence of shock interaction. This experimental program was conducted in the Calspan 48-Inch Shock Tunnel at nominal Mach numbers of 6 and 8, for a Reynolds number of 7.5×10^6 . For these test conditions, we obtained fully turbulent boundary layers upstream of the interaction regions over the transpiration-cooled segment of the flat plate.

The experimental program was conducted in two phases. In the first phase, we examined the effects of mass-addition level and coolant properties on the cooling effectiveness of transpiration-cooled surfaces in the absence of shock interaction. In the second phase of the program, we examined the effects of oblique shock impingement on the flowfield and surface characteristics of a transpiration-cooled surface. The studies were conducted for a range of shock strengths with nitrogen and helium coolants to examine how the distribution of heat transfer and pressure and the characteristics of the flowfield in the interaction region varied with shock strength and the level of mass addition from the transpiration-cooled section of the model. The effects of the distribution of the blowing rate along the interaction regions were also examined for a range of blowing rates through the transpiration-cooled panels. The regions of shock-wave/boundary layer interaction examined in these studies were induced by oblique shocks generated with a sharp, flat plate, inclined to the freestream at angles of 5° , 7.5° , and 10° . It was found that, in the absence of an incident shock, transpiration cooling was a very effective method for reducing both the heat transfer and the skin friction loads on the surface. The helium coolant was found to be significantly more effective than nitrogen, because of its low molecular weight and high specific heat. The studies of shock-wave/transpiration-cooled surface interaction demonstrated that the interaction region between the incident shock and the low-momentum transpiration-cooled boundary layer did not result in a significant increase in the size of attached or separated interaction regions, and did not result in significant flowfield distortions above the interaction region. The increase in heating downstream of the shock-impingement point could easily be reduced to the values without shock impingement by a relatively small increase in the transpiration cooling in this region. Surprisingly, this increase in cooling rate did not result in a significant increase in size of the region ahead of the incident shock or create a significantly enlarged interaction region with a resultant increase in the distortion level in the inviscid flow. Thus, transpiration cooling appears to be a very effective technique to cool the internal surfaces of scramjet engines, where shocks in the engine would induce large local increases in wall heating and create viscous/inviscid interactions that could significantly disturb the smooth flow through the combustor. However, if hydrogen is used as the coolant, burning upstream of shock impingement might result in localized hot spots. Clearly, further research is needed in this area.

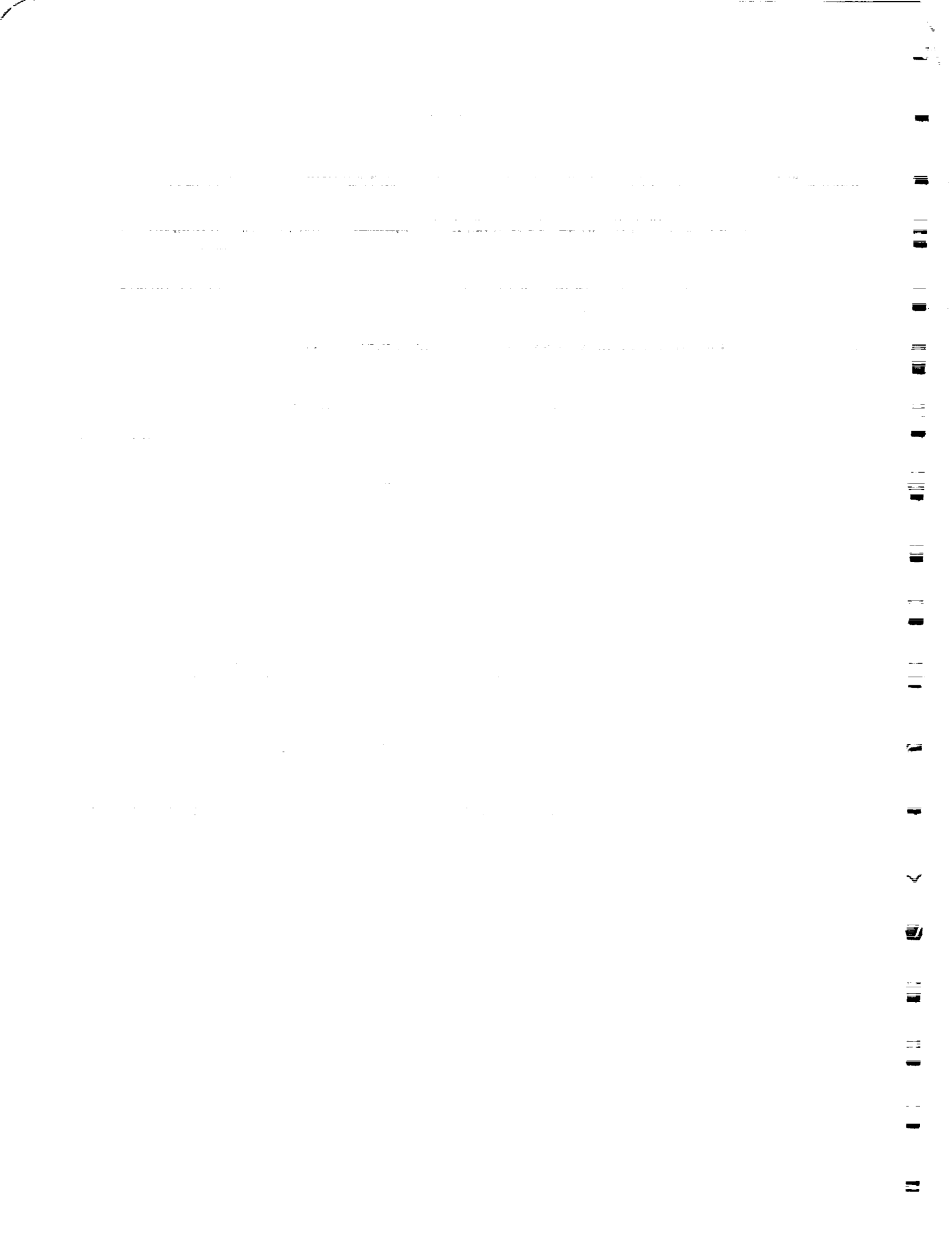


TABLE OF CONTENTS

<u>Section</u>	<u>Page</u>
ABSTRACT.....	ii
NOMENCLATURE.....	ix
1 INTRODUCTION.....	1
2 EXPERIMENTAL PROGRAM.....	3
2.1 PROGRAM OBJECTIVES AND DESIGN.....	3
2.2 EXPERIMENTAL FACILITIES AND TEST CONDITIONS.....	4
2.2.1 Experimental Facilities.....	4
2.2.2 Evaluation Of Test Conditions.....	6
2.2.3 Accuracy of Test Conditions.....	7
2.2.4 Airflow Calibrations of the "A" Nozzle.....	10
2.3 MODEL AND INSTRUMENTATION.....	10
2.3.1 Description of Transpiration-Cooled Flat-Plate/Shock-Generator Model.....	10
2.3.2 Calibration of Transpiration-Cooled Segments.....	13
2.3.3 Heat Transfer Instrumentation.....	20
2.3.4 Pressure Instrumentation.....	20
2.3.5 Measurement Recording System.....	21
2.3.6 Flow Visualization.....	21
3 RESULTS AND DISCUSSION.....	25
3.1 INTRODUCTION.....	25
3.2 BOUNDARY LAYER PROFILE MEASUREMENTS UPSTREAM OF TRANSPIRATION-COOLING SECTIONS.....	25
3.3 CORRELATION OF FLAT-PLATE TRANSPIRATION-COOLING DATA.....	27
3.4 STUDIES OF THE TRANSPIRATION COOLING OF SHOCK/BOUNDARY LAYER INTERACTION REGIONS.....	37
3.4.1 Introduction.....	37
3.4.2 Studies of Shock-Wave/Coolant-Layer Interaction at Mach 6.....	40
3.4.3 Studies of Shock-Wave/Transpiration-Cooled Layer Interaction at Mach 8.....	48
3.5 CORRELATION OF HEATING MEASUREMENTS ON SMOOTH AND TRANSPIRATION-COOLED SURFACE.....	57
3.5.1 Shock-Induced Heating on Non-Blowing Configuration.....	57
3.5.2 Shock-Induced Heating on Transpiration-Cooled Surfaces.....	57

TABLE OF CONTENTS (Cont.)

<u>Section</u>	<u>Page</u>
4 CONCLUSIONS	65
REFERENCES.....	66
APPENDIX A	A-1
APPENDIX B	B-1
APPENDIX C	C-1

LIST OF FIGURES

<i>Figure</i>	<i>Page</i>
1 Performance Characteristics of Calspan's Shock Tunnel	5
2 Mach Number Distributions for Test Conditions 1 and 3 in the "A" Nozzle	11
3 Transpiration-Cooled Flat-Plate Model in Test Section of the Calspan-48-Inch Shock Tunnel.....	12
4 Shock Generator Supported Above the Transpiration-Cooled Flat Plate.....	12
5 Schematic Diagram of Surface Geometry of Transpiration-Cooled Surface.....	14
6a Subchamber of the Model Showing Passages to Evenly Distribute the Coolant to the Transpiration-Cooled Surface	15
6b Back of Model Showing Instrumentation Harness and Ports for "Valcor" Fast-Acting Valves.....	15
7a Shock Generator Supported Above the Transpiration-Cooled Surface.....	16
7b Heat Transfer and Pressure Instrumentation Installed in the "Lands" Between the Injection Orifices.....	16
8 Schematic Diagram Showing Gage Positions Along the Flat-Plate Transpiration-Cooled Model	22
9 Pitot and Total Temperature Flowfield and Boundary Layer Rakes.....	26
10 Heat Transfer Distributions Along Flat Plate-Transpiration Surface Without Cooling at Mach 6 and 8	28
11 Heat Transfer and Pressure Distributions Along Flat Plate-Transpiration Surface and Nitrogen Coolant at Mach 6	29
12 Heat Transfer and Pressure Distributions Along Flat Plate-Transpiration Surface for Helium Coolant at Mach 6.....	30
13 Heat Transfer and Pressure Distributions Along Flat Plate-Transpiration-Cooled Surface for Nitrogen Coolant at Mach 8	31
14 Heat Transfer and Pressure Distributions Along Flat Plate-Transpiration-Cooled Model for Helium Coolant at Mach 8.....	32
15 Correlation of Heat Transfer Measurement with Transpiration Cooling in Terms of Simple Blowing parameter for Nitrogen Coolant at Mach 6.....	33
16 Correlation of Heat Transfer Measurement with Transpiration Cooling in Terms of Simple Blowing Parameter for Nitrogen Coolant at Mach 8.....	33
17 Correlation of Heat Transfer Measurement with Transpiration Cooling in Terms of Simple Blowing Parameter for Helium Coolant at Mach 6	34

LIST OF FIGURES (Cont.)

<i>Figure</i>		<i>Page</i>
18	Correlation of Heat Transfer Measurement with Transpiration Cooling in Terms of Simple Blowing Parameter for Helium Coolant at Mach 8	34
19	Correlation of Heat Transfer Measurements with Transpiration Cooling at Both Mach 6 and 8 for Nitrogen Coolant.....	35
20	Correlation of Heat Transfer Measurements with Transpiration Cooling at Both Mach 6 and 8 for Helium Coolant	35
21	Correlation of Heat Transfer Measurements for Nitrogen and Helium Coolants with Simple Blowing Parameter	36
22	Correlation of All Transpiration-Cooling Heat Transfer Measurements with Modified Blowing Parameter	36
23	Correlation of Heat Transfer Measurements for Nitrogen and Helium Coolants with Simple Blowing Parameter	38
24	Correlation of All Transpiration-Cooling Heat Transfer Measurements with Modified Blowing Parameter	38
25	Correlation of Pressure Measurements Over Transpiration-Cooled Surface with Modified Blowing Parameter	39
26	Correlation of Heat Transfer Measurements Over Transpiration-Cooled Surface with Modified Blowing Parameter.....	39
27	Heat Transfer and Pressure Measurements at Mach 6 on Nitrogen-Cooled Transpiration Surface with Shock Interaction From 5.3° Shock Generator	41
28	Heat Transfer and Pressure Measurements at Mach 6 on Helium-Cooled Transpiration Surface with Shock Interaction From 5.3° Shock Generator	42
29	Heat Transfer and Pressure Measurements at Mach 6 on Nitrogen-Cooled Transpiration Surface with Shock Interaction From 7.35° Shock Generator.....	43
30	Heat Transfer and Pressure Measurements at mach 6 on Helium-Cooled Transpiration Surface with Shock Interaction From 7.35° Shock Generator.....	44
31	Heat Transfer and Pressure Measurements at Mach 6 on Nitrogen-Cooled Transpiration Surface with Shock Interaction From 10.1° Shock Generator.....	45
32	Heat Transfer and Pressure Measurements at Mach 6 on Helium-Cooled Transpiration Surface with Shock Interaction From 10.1° Shock Generator.....	46
33	Heat Transfer and Pressure Measurements at Mach 8 on Nitrogen-Cooled Transpiration Surface with Shock Interaction From 5.2° Shock Generator.....	49
34	Heat Transfer and Pressure Measurements at Mach 8 on Nitrogen-Cooled Transpiration Surface with Shock Interaction From 5.0° Shock Generator	50

LIST OF FIGURES (Cont.)

<u>Figure</u>	<u>Page</u>
35 Heat Transfer and Pressure Measurements at Mach 8 on Helium-Cooled Transpiration Surface with Shock Interaction From 5.0° Shock Generator	51
36 Heat Transfer and Pressure Measurements at Mach 8 on Nitrogen-Cooled Transpiration Surface with Shock Interaction From 7.7° Shock Generator	52
37 Heat Transfer and Pressure Measurements at Mach 8 on Helium-Cooled Transpiration Surface with Shock Interaction From 7.7° Shock Generator	53
38 Heat Transfer and Pressure Measurements at Mach 8 on Nitrogen-Cooled Transpiration Surface with Shock Interaction From 10.1° Shock Generator.....	55
39 Heat Transfer and Pressure Measurements at Mach 8 on Helium-Cooled Transpiration Surface with Shock Interaction from 10.1° Shock Generator	56
40 Correlation of Maximum Heating in Wedge- and Externally Generated Shock-Induced Turbulent Separated Flows	58
41 Comparison of Peak Heating Measurements Downstream of Shock Impingement for Tests Without Coolant Flow (P_{max}/P_0 vs. q_{max}/q_0)	59
42 Correlation of Heating Reduction Ratio with Blowing Parameter Based on Local Conditions Downstream of the Re-Compression Shock for 5° Shock Generator.....	60
43 Correlation of Heating Reduction Ratio with Blowing Parameter Based on Local Conditions Downstream of the Re-Compression Shock for 7.5° and 10° Shock Generators.....	61
44 Correlation of All Heating Reduction Ratio with Blowing Parameter Based on Local Conditions Downstream of the Re-Compression Shock for 5°, 7.5° and 10° Shock Generators.....	62
45 Correlation of All Heating Reduction Ratio with Blowing Parameter Based on Local Conditions Downstream of the Re-Compression Shock for 5°, 7.5° and 10° Shock Generators.....	62
46 Correlation of Heating Reduction Ratio with Modified Blowing Parameter $\dot{m} / (\rho_s U_s C_{H_s}) (\tilde{M}_{fs} / \tilde{M}_{inj})$ for Shock-Generator Angles of 5°, 7.5° and 10° and Both Nitrogen and Helium Coolants.....	64
47 Correlation of Heating Reduction Ratio with Modified Blowing Parameter $\dot{m} / (\rho_s U_s C_{H_s}) (C_{pinf}/C_{pfs})^{0.7} (\tilde{M}_{fs} / \tilde{M}_{inj})^{0.5}$ for Shock-Generator Angles of 5°, 7.5°, and 10° and Both Nitrogen and Helium Coolants.....	64

LIST OF TABLES

<i>Table</i>		<i>Page</i>
1	Summary of Test Conditions.....	8
2	Summary of Transpiration-Cooled Flat-Plate Study.....	18
3a	Gage Locations in the 28-Inch Smooth Leading Edge Flat Plate.....	23
3b	Gage Locations in the Transpiration-Cooled Sections of the Flat-Plate Model.....	24

NOMENCLATURE

A*	Area of Orifice
a	Speed of Sound
C _D	Discharge Coefficient
C _H , C _h	$q/(\rho_{\infty} U_{\infty}(H_0 - H_w))$, Stanton Number
C _p	Pressure Coefficient, Equation 12
c _p	Specific Heat at Constant Pressure
D	Nozzle Diameter (inches)
H	Total Enthalpy
K(λ)	$= \sqrt{\frac{\gamma}{R} \left(\frac{2}{\gamma+1}\right)^{\frac{\gamma+1}{\gamma-1}}}$
l	Characteristic Dimension
M	Mach Number
M _i	Incident Mach Number
\tilde{M}	Molecular Weight
m	Mass
\dot{m}	Mass Flow Rate
p	Static Pressure
p _{o'}	Pitot Pressure
Q, q	Heat Transfer
\dot{q}	Heat Transfer Rate
q _∞	Dynamic Pressure
R	Gas Constant
\bar{R}	Gas Constant (=1717.91 ft-lb/slug-°R)
Re	= Ul/ν , Reynolds Number
S.G.	Shock Generator
T	Temperature
T _w	Initial Model Surface Temperature, Table 3
TC	Test Condition
t	Time
U	Velocity
V	Volume
v _c	Coolant Velocity

GREEK SYMBOLS

α	Reattachment Angle
β	Time Constant
γ	Specific Heat Ratio (~1.4)
ΔP	Change in Pressure
λ	$(\rho_w U_w)/(\rho_\infty U_\infty)$, Blowing Parameter
μ, Mu	Viscosity
ν	Kinematic Viscosity
ρ, Rho	Density
τ	Dimensionless Time

SUBSCRIPTS

0	Undisturbed Stagnation Value
1, initial	Initial Value
2	Value at Second Transpiration-Cooling Section
6	Driver Value
aw	Adiabatic Wall Value
b	In Boundary Layer
c	Coolant
D	Diameter
e	Edge of Boundary Layer, Local Condition (with λ)
f, final	Final Value
fs	Freestream Value
i	Incident
IDEAL	Ideal Value
inj	Injectant
p	Perfect
peak	Peak Value
REAL	Real Value
rake	Boundary Layer Rake Value
room	Ambient Conditions
A	Local Conditions Downstream of Incident Shock
theor.	Theoretical Value
w	Wall Value
∞	Freestream Value

Section 1 INTRODUCTION

Transpiration cooling and film cooling are two techniques that have been proposed to reduce the large heating loads on the walls of a scramjet combustor. Film-cooling techniques have also been used to reduce the aerothermal loads on the optical windows of hypersonic seeker heads, and to alleviate the heating levels in the combusting flows downstream of the injectors in scramjet engines. Employing film cooling is attractive, because of the positive aspects of the direct momentum addition to the freestream in the engine. However, recent studies (References 1 through 3) have demonstrated that relatively large levels of mass addition are required to maintain a cooling film over the length of the combustor. Also, if shocks generated in the inlet section and the combustion region of an engine impinge on the film-cooled surface, they can easily return the heating levels to uncooled values. Transpiration-cooling techniques have been used successfully to reduce the heating and skin friction levels on the nosetips and frusta of conical hypersonic reentry vehicles (References 4 through 6). Transpiration cooling is also advantageous in that they can significantly reduce the wall skin friction (which is a major component of the engine drag). However, the resulting low-momentum region adjacent to the wall can potentially be easily separated by a shock system impinging on the wall. The sensitivity to flow separation on a transpiration-cooled surface was demonstrated in studies (Reference 7) of transpiration-cooled maneuvering reentry vehicles (MRVs), where flap effectiveness was significantly reduced by the introduction of a low-momentum layer adjacent to the surface upstream of the flaps. Based on this latter observation, we believed that a transpiration-cooled surface might be very sensitive to shock interactions, which would significantly reduce cooling effectiveness and create significant flowfield distortions. We are not aware that any studies have been conducted to evaluate the effects of shock impingement on the effectiveness of transpiration-cooled surfaces. Thus, this experimental program was devised to obtain definitive information on this phenomenon.

In this experimental program, we designed and constructed a transpiration-cooled model and the associated instrumentation to explore the effects of shock impingement on the effectiveness of transpiration cooling and the distortions that could be developed in the inviscid flow in, and downstream of, the interaction region. The flat-plate/porous-wall configuration used was designed to be run at high Reynolds number freestream conditions such that a fully turbulent boundary layer would be developed on the non-porous surface well upstream of the transpiration-cooled sections. To most efficiently introduce the transpiration cooling, the porous surface of the model was divided into a number of distinct blowing regions so that the coolant could be introduced differentially into regions of high heating rates developed by shock/cooling-layer interaction. Here, we wished to avoid boundary layer blowoff in the regions ahead of the impinging shock that could result if high levels of transpiration cooling were introduced into this region of the flow. To evaluate the effects of coolant properties on transpiration-cooling effectiveness, and

the susceptibility to flow separation, measurements were made with both nitrogen and helium coolants. The studies were made at local nominal Mach numbers of 6 and 8 for high Reynolds number conditions to ensure that the flows ahead of the transpiration-cooled region were fully turbulent. The strength of the incident shock was varied to generate both attached and separated interaction regions over a non-porous wall configuration. In the following section of this report, we first discuss the objectives and design of the experimental program. We then describe the experimental facilities and test conditions used in this program, together with the analysis associated with developing freestream properties. We provide detailed descriptions of the model and instrumentation used in this program. We also describe the calibration and data recording and reduction procedures. The flow-visualization techniques used in these studies are briefly discussed. The results of the experimental program and their comparison with earlier studies and analysis are next described. Measurements are presented for each of the two Mach numbers, first for the flow in the absence of shock impingement and then for transpiration-cooled surfaces with shock impingement. Correlations of the heat transfer measurements in the transpiration-cooled regions in the absence of shock interaction are presented for comparison with measurements made in earlier studies. The measurements made in the studies of shock-wave transpiration-cooled surface interaction are discussed in detail. Correlations are presented to enable the designer to calculate the cooling requirements downstream of shock impingement for a given injectant. The results of the program are summarized, and the conclusions developed are presented.

Section 2 EXPERIMENTAL PROGRAM

2.1 PROGRAM OBJECTIVES AND DESIGN

The principal objective of these experimental studies was to determine whether shock impingement on transpiration-cooled surfaces resulted in significant localized flow distortion and loss of cooling effectiveness. A secondary objective was to examine the influence of coolant properties on the cooling effectiveness, both in the presence and in the absence of shock interaction. Local Mach numbers of close to 6 and 8 were selected for the studies to be representative of the largest Mach numbers that would be developed inside a supersonic-combustion ramjet (scramjet) combustor. The high Reynolds number conditions at which the studies were conducted were selected to ensure that the boundary layers upstream of the interaction were fully turbulent to minimize problems associated with boundary layer separation, transition, and strong flow distortions that could be generated by the rapid change in the boundary condition at the discontinuities between the non-porous and porous surfaces. The flat plate ahead of the porous section was highly instrumented with heat transfer and pressure gages to define the position and structure of the transition regions and the turbulent boundary layer just ahead of the porous surface. Pitot pressure and total temperature surveys were also made across the boundary layer just upstream of the porous surface to provide flowfield velocity and temperature data for code validation. Using information based on correlations of measurements from our earlier transpiration-cooling and shock-interaction studies (References 7 and 8), we positioned the high-density region of instrumentation in the porous surface to examine the structure of the shock-interaction regions at approximately 30 boundary layer thicknesses from the beginning of transpiration cooling to ensure that the boundary layer had adjusted to the blowing before the shock interaction was induced. We also designed the transpiration-cooled surface so that it could be differentially fed from three separate streamwise chambers to enable greater cooling to be applied to the region of high heating downstream of the incident shock.

A two-dimensional shock generator was designed to generate shocks whose strengths would generate both attached and separated regions on the model in the absence of transpiration cooling. The transpiration-cooling system was designed to operate with hydrogen, helium, or nitrogen coolants. The feed-system passages were designed such that the flow through the system was established in less than 12 milliseconds from valve opening, which enabled us to accurately actuate the system with triggers from passage of the incident shock in the driven tube of the shock tunnel. The porous surface was designed to obtain sonic injection from 0.032-inch-diameter passages, fed by orifices embedded 0.050 inch below the surface. Employing sonic orifices prevented changes in pressure over the model surface from influencing the coolant flow rate. Positioning the sonic orifices relatively close to the surface minimized the transient in the coolant passages during flow establishment through the tunnel to a fraction of a millisecond. Both

the heat transfer and the pressure gages were installed into the "lands" between the holes in the transpiration-cooled surface so that there were no distortions in the local surface geometry or cooling flow pattern.

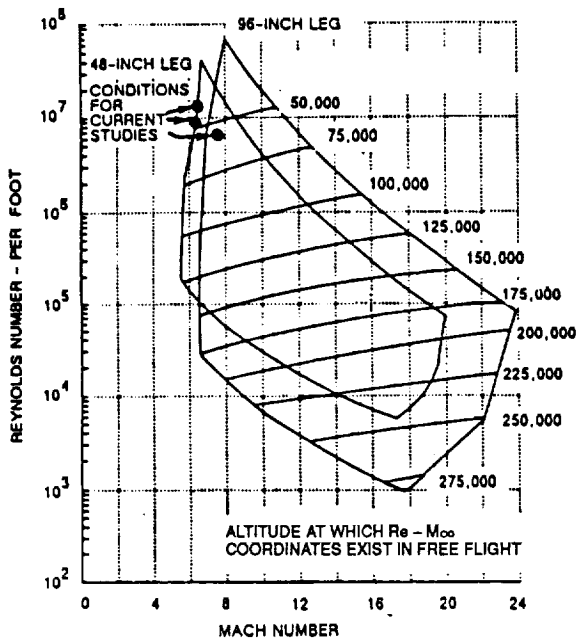
2.2 EXPERIMENTAL FACILITIES AND TEST CONDITIONS

2.2.1 Experimental Facilities

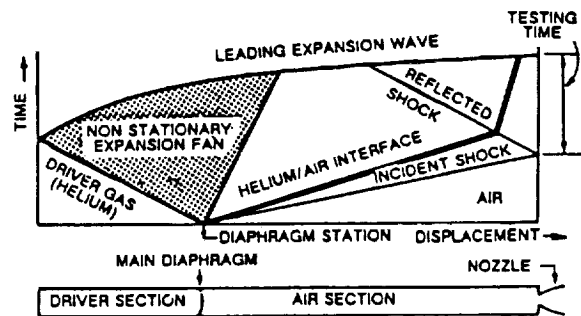
The experimental studies were conducted in Calspan's 48-Inch Shock Tunnel at Mach numbers of 6.4 and 7.9. The facility and its performance characteristics are described in Reference 9. The freestream conditions at which the current experimental program was conducted are plotted on the map of Mach number versus unit Reynolds number shown in Figure 1a.

The shock tunnel is basically a "blowdown tunnel" with a shock-compression heater. The operation of the shock tunnel in the reflected-shock mode is shown with the aid of the wave diagram in Figure 1b. The tunnel is started by rupturing a double diaphragm, permitting high-pressure helium in the driver section to expand into the driven section. This generates a normal shock, which propagates through the low-pressure air. A region of high-temperature, high-pressure air is produced between this normal-shock front and the gas interface (often referred to as the contact surface) between the driver and driven gases. When the incident shock strikes the end of the driven section, it is reflected, leaving a region of almost stationary, high-pressure, heated air. This air is then expanded through a nozzle to the desired freestream conditions in the test section.

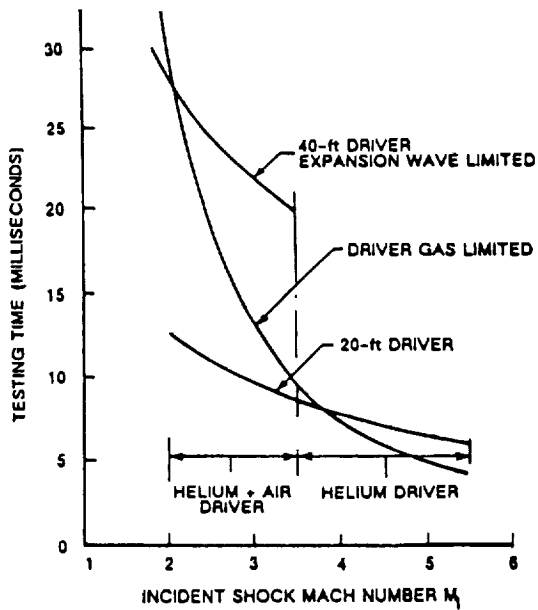
The duration of the flow in the test section is controlled by the interactions between the reflected shock, the driver/driven gas interface, and the leading expansion wave generated by the non-stationary expansion process occurring in the driver section. We normally control the initial conditions of the gases in the driver and driven sections so that the gas interface becomes transparent to the reflected shock. This is known as operating under "tailored-interface" conditions. Under these conditions, the test time is controlled by the time taken for the driver/driven interface to reach the throat, or for the leading expansion wave to deplete the reservoir of pressure behind the reflected shock. The flow duration is, therefore, either driver-gas-limited or expansion-limited. Figure 1c shows the flow duration in the test section as a function of the Mach number of the incident shock. In the current program, we obtained flow durations of 6 to 10 milliseconds.



(a) Performance map



(b) Wave diagram for tailored-interface shock tube



(c) Test time available for tailored-interface operation of the shock tunnel

Figure 1 PERFORMANCE CHARACTERISTICS OF CALSPAN'S SHOCK TUNNEL

2.2.2 Evaluation Of Test Conditions

The stagnation and freestream test conditions were determined from measurements of the incident-shock-wave speed, U_i ; the initial temperature of the test gas (in the driven tube), T_1 ; the initial pressure of the test gas, p_1 ; and the pressure behind the reflected shock wave, p_0 . We calculated the incident-shock-wave Mach number, $M_i = U_i/a_1$, where the speed of sound, a_1 , is a function of p_1 and T_1 . The freestream Mach number, M_∞ , was determined from correlations of M_∞ with M_i and p_0 . These correlations were based on airflow calibrations of the "A" nozzle and are discussed in Section 2.2.4.

Freestream test conditions of pressure, temperature, Reynolds number, etc., were computed based on isentropic expansion of the test gas from the conditions behind the reflected shock wave to the freestream Mach number. Real gas effects were taken into account for this expansion under the justified assumption that the gas was in thermochemical equilibrium. In the freestream, the static temperature, T_∞ , was sufficiently low that the ideal gas equation of state, $p_\infty = \rho \bar{R} T_\infty$, was applicable, where \bar{R} is the gas constant for the test gas.

The stagnation enthalpy, H_0 , and temperature, T_0 , of the gas behind the reflected shock wave were calculated from:

$$H_0 = (H_4/H_1)H_1 \text{ and } T_0 = (T_4/T_1)T_1 \quad (1)$$

where (H_4/H_1) and (T_4/T_1) are functions of U_i (or M_i) and p_1 and are given in Reference 10 for air. H_1 was obtained from Reference 11 for air, knowing p_1 and T_1 .

The freestream static temperature was found from the energy equation, knowing H_0 and M_∞ ,

$$T_\infty = \frac{H_0}{c_p} \left(\frac{1}{1 + \frac{(\gamma-1)}{2} M_\infty^2} \right) \quad (2)$$

where $c_p = 6006 \text{ ft-lb/slug-}^\circ\text{R}$ and $\gamma = 1.40$.

The freestream static pressure was calculated from

$$p_\infty = \frac{p}{p_p} p_0 \left(1 + \frac{(\gamma-1)}{2} M_\infty^2 \right)^{\frac{-\gamma}{\gamma-1}} \quad (3)$$

where

$$\frac{p}{p_p} = \frac{(p_\infty/p_0)_{\text{REAL}}}{(p_\infty/p_0)_{\text{IDEAL}}} \quad (4)$$

is the real gas correction to the ideal gas static-to-total pressure ratio as described in Reference 12. The sources for the real gas data used in this technique are References 13 and 14.

The freestream velocity was determined from

$$U_\infty = M_\infty a_\infty \quad (5)$$

where

$$a_\infty = \sqrt{\gamma \bar{R} T_\infty} \quad (6)$$

the speed of sound.

The freestream dynamic pressure was found from

$$q_\infty = \frac{1}{2} \gamma p_\infty M_\infty^2 \quad (7)$$

and the freestream density then was calculated from the ideal gas equation of state

$$p_\infty = \rho_\infty (\bar{R} T_\infty) \quad (8)$$

where $\bar{R} = 1717.91$ ft-lb/slug-°R for air. Values of the absolute viscosity, μ , used to compute the freestream Reynolds number per foot were obtained using the technique described in Reference 15.

The test-section pitot pressure, p_0' , was determined from q_∞ and the ratio (p_0'/q_∞) . This ratio has been correlated as a function of M_∞ and H_0 for normal-shock waves in air in thermodynamic equilibrium.

2.2.3 Accuracy of Test Conditions

The test conditions at which these studies were conducted are listed in Table 1. At these conditions, where real gas effects are negligible, the uncertainty in the pitot pressure measurement from errors in calibration and recording is $\pm 2.5\%$. The reservoir pressure can be measured with an uncertainty of $\pm 2\%$, and the total enthalpy (H_0) can be determined from the driven-tube pressure and the incident-

Table 1
SUMMARY OF TEST CONDITIONS

RUN	MI	Po	Ho	To	M	U	Q	Re/ft	Po'	T	P	Rho	Mu
7	2.800	2108.	1.340E+07	2104.	6.42	4892.	2.504E+01	7.438E+06	46.66	241.20	8.662E-01	3.013E-04	1.982E-07
8	2.888	3705.	1.429E+07	2221.	7.87	5145.	1.843E+01	6.947E+06	34.03	177.90	4.248E-01	2.000E-04	1.485E-07
12	2.816	2082.	1.357E+07	2128.	6.42	4922.	2.471E+01	7.204E+06	46.07	244.60	8.564E-01	2.938E-04	2.007E-07
13	2.806	2125.	1.341E+07	2104.	6.42	4893.	2.525E+01	7.497E+06	47.06	241.30	8.737E-01	3.038E-04	1.983E-07
14	2.804	2118.	1.349E+07	2117.	6.42	4909.	2.512E+01	7.389E+06	46.82	242.90	8.691E-01	3.003E-04	1.994E-07
15	2.810	2119.	1.360E+07	2132.	6.42	4927.	2.510E+01	7.303E+06	46.79	244.80	8.688E-01	2.978E-04	2.009E-07
16	2.786	2093.	1.329E+07	2089.	6.43	4872.	2.487E+01	7.478E+06	46.34	239.10	8.597E-01	3.017E-04	1.966E-07
17	2.814	2144.	1.355E+07	2126.	6.42	4920.	2.542E+01	7.430E+06	47.39	244.00	8.797E-01	3.025E-04	2.003E-07
18	2.786	2111.	1.338E+07	2102.	6.43	4889.	2.503E+01	7.454E+06	46.64	240.70	8.650E-01	3.016E-04	1.978E-07
19	2.805	2134.	1.344E+07	2109.	6.42	4899.	2.534E+01	7.498E+06	47.22	241.90	8.765E-01	3.041E-04	1.987E-07
20	2.809	2134.	1.351E+07	2119.	6.42	4911.	2.531E+01	7.436E+06	47.18	243.10	8.759E-01	3.023E-04	1.996E-07
21	2.818	2190.	1.364E+07	2138.	6.42	4936.	2.592E+01	7.509E+06	48.22	249.30	8.957E-01	3.064E-04	2.014E-07
22	2.838	2187.	1.383E+07	2165.	6.42	4970.	2.586E+01	7.337E+06	48.32	245.50	8.963E-01	3.064E-04	2.014E-07
23	2.794	3660.	1.353E+07	2117.	7.89	5008.	1.825E+01	7.492E+06	33.68	167.50	4.184E-01	2.096E-04	2.043E-07
24	2.842	3500.	1.389E+07	2167.	7.87	5074.	1.746E+01	6.868E+06	32.24	172.80	4.023E-01	1.954E-04	1.443E-07
26	2.865	3453.	1.364E+07	2127.	7.86	5026.	1.739E+01	7.018E+06	32.09	169.90	4.013E-01	1.983E-04	1.420E-07
27	2.805	3721.	1.348E+07	2109.	7.89	4999.	1.859E+01	7.673E+06	34.31	166.90	4.263E-01	2.143E-04	1.396E-07
28	2.878	3660.	1.425E+07	2216.	7.87	5139.	1.820E+01	6.899E+06	33.60	177.30	4.194E-01	1.985E-04	1.480E-07
29	2.857	3507.	1.378E+07	2149.	7.87	5053.	1.758E+01	6.999E+06	32.44	171.50	4.052E-01	1.982E-04	1.433E-07
30	2.856	3536.	1.389E+07	2165.	7.87	5073.	1.767E+01	6.950E+06	32.63	172.80	4.073E-01	1.978E-04	1.444E-07
31	2.860	3598.	1.409E+07	2193.	7.87	5109.	1.791E+01	6.902E+06	33.08	175.20	4.127E-01	1.977E-04	1.463E-07
32	2.882	3683.	1.432E+07	2225.	7.87	5150.	1.829E+01	6.881E+06	33.79	178.10	4.127E-01	1.987E-04	1.487E-07
33	2.862	3590.	1.400E+07	2181.	7.87	5093.	1.791E+01	6.963E+06	33.07	174.20	4.127E-01	1.989E-04	1.455E-07
34	2.920	3772.	1.468E+07	2274.	7.86	5214.	1.869E+01	6.768E+06	34.52	182.90	4.314E-01	1.980E-04	1.525E-07
35	2.884	3666.	1.433E+07	2227.	7.87	5153.	1.821E+01	6.837E+06	33.63	178.40	4.199E-01	1.975E-04	1.489E-07
36	2.867	3675.	1.402E+07	2183.	7.87	5097.	1.833E+01	7.113E+06	33.84	174.30	4.221E-01	2.032E-04	1.456E-07
37	2.901	3646.	1.444E+07	2242.	7.86	5172.	1.812E+01	6.718E+06	33.47	180.00	4.183E-01	1.950E-04	1.502E-07
38	2.901	3633.	1.447E+07	2246.	7.86	5178.	1.805E+01	6.670E+06	33.33	180.40	4.167E-01	1.939E-04	1.505E-07

Table 1
SUMMARY OF TEST CONDITIONS (Cont.)

RUN	Mi	Po	Ho	To	M	U	Q	Re/ft	Po'	T	P	Rho	Mu
41	2.846	4086.	1.389E+07	2165.	7.89	5073.	2.030E+01	8.027E+06	37.47	171.80	4.649E-01	2.271E-04	1.435E-07
42	2.955	3936.	1.487E+07	2300.	7.86	5249.	1.949E+01	6.919E+06	36.01	185.40	4.503E-01	2.038E-04	1.546E-07
43	2.940	4000.	1.473E+07	2280.	7.87	5223.	1.981E+01	7.145E+06	36.60	183.40	4.569E-01	2.091E-04	1.529E-07
44	2.995	4087.	1.522E+07	2347.	7.86	5310.	2.018E+01	6.919E+06	37.31	190.00	4.668E-01	2.062E-04	1.582E-07
45	3.005	4179.	1.535E+07	2364.	7.86	5234.	2.060E+01	6.979E+06	38.08	191.50	4.763E-01	2.087E-04	1.594E-07
46	2.949	4228.	1.479E+07	2288.	7.87	5234.	2.089E+01	7.503E+06	38.60	183.80	4.810E-01	2.197E-04	1.532E-07
47	2.955	4109.	1.488E+07	2300.	7.87	5250.	2.031E+01	7.219E+06	37.53	185.20	4.684E-01	2.123E-04	1.543E-07
48	2.993	4213.	1.528E+07	2356.	7.86	5320.	2.075E+01	7.081E+06	38.35	190.50	4.792E-01	2.111E-04	1.586E-07
49	2.980	4442.	1.496E+07	2310.	7.87	5264.	2.192E+01	7.741E+06	40.51	185.90	5.047E-01	2.278E-04	1.549E-07
50	3.041	4528.	1.562E+07	2400.	7.86	5378.	2.222E+01	7.348E+06	41.08	194.60	5.131E-01	2.212E-04	1.619E-07
51	3.055	4399.	1.591E+07	2441.	7.85	5429.	2.153E+01	6.915E+06	39.83	198.80	4.985E-01	2.105E-04	1.652E-07
52	3.036	4652.	1.550E+07	2384.	7.87	5359.	2.282E+01	7.641E+06	42.20	192.90	5.262E-01	2.289E-04	1.605E-07
54	2.878	3934.	1.418E+07	2205.	7.88	5126.	1.954E+01	7.473E+06	36.09	176.00	4.492E-01	2.142E-04	1.469E-07
55	2.914	3891.	1.452E+07	2252.	7.87	5186.	1.930E+01	7.113E+06	35.66	180.60	4.443E-01	2.067E-04	1.507E-07
56	2.913	3882.	1.446E+07	2244.	7.87	5176.	1.928E+01	7.143E+06	35.61	180.00	4.443E-01	2.072E-04	1.502E-07
57	2.922	3883.	1.462E+07	2265.	7.87	5203.	1.925E+01	7.020E+06	35.56	182.00	4.440E-01	2.047E-04	1.518E-07
59	2.911	3879.	1.430E+07	2221.	7.87	5147.	1.932E+01	7.279E+06	35.69	177.90	4.454E-01	2.100E-04	1.485E-07
60	2.900	3892.	1.431E+07	2222.	7.87	5148.	1.935E+01	7.293E+06	35.73	177.80	4.457E-01	2.103E-04	1.485E-07
62	2.895	3959.	1.432E+07	2225.	7.88	5151.	1.965E+01	7.399E+06	36.29	177.90	4.521E-01	2.133E-04	1.485E-07
63	2.906	3967.	1.439E+07	2233.	7.87	5162.	1.922E+01	7.179E+06	35.49	179.00	4.428E-01	2.077E-04	1.493E-07
64	2.920	3911.	1.460E+07	2264.	7.87	5201.	1.938E+01	7.080E+06	35.80	181.70	4.468E-01	2.063E-04	1.516E-07
65	2.908	3770.	1.455E+07	2257.	7.86	5191.	1.869E+01	6.863E+06	34.53	181.20	4.312E-01	1.998E-04	1.511E-07
66	2.924	3907.	1.464E+07	2268.	7.87	5207.	1.936E+01	7.045E+06	35.76	182.20	4.464E-01	2.056E-04	1.520E-07
67	2.926	3930.	1.469E+07	2276.	7.87	5217.	1.945E+01	7.041E+06	35.93	182.90	4.485E-01	2.058E-04	1.525E-07
68	2.908	3841.	1.441E+07	2236.	7.87	5166.	1.909E+01	7.113E+06	35.26	179.30	4.400E-01	2.060E-04	1.496E-07
69	2.921	3903.	1.463E+07	2268.	7.87	5206.	1.933E+01	7.010E+06	35.71	182.10	4.458E-01	2.054E-04	1.519E-07
70	2.915	3882.	1.462E+07	2266.	7.87	5204.	1.922E+01	7.010E+06	35.51	181.90	4.431E-01	2.044E-04	1.517E-07
71	2.922	3858.	1.448E+07	2246.	7.86	5179.	1.918E+01	7.089E+06	35.43	180.30	4.424E-01	2.059E-04	1.504E-07
72	2.921	3935.	1.456E+07	2258.	7.87	5194.	1.951E+01	7.157E+06	36.04	181.20	4.497E-01	2.083E-04	1.512E-07
73	2.920	3906.	1.464E+07	2259.	7.87	5208.	1.934E+01	7.038E+06	35.73	182.20	4.459E-01	2.054E-04	1.520E-07
76	2.899	3898.	1.439E+07	2234.	7.87	5163.	1.934E+01	7.228E+06	35.73	178.90	4.454E-01	2.090E-04	1.493E-07
77	2.831	2248.	1.370E+07	2148.	6.43	4948.	2.659E+01	7.650E+06	49.58	246.70	9.195E-01	3.128E-04	2.023E-07
78	2.828	2252.	1.370E+07	2146.	6.43	4946.	2.664E+01	7.674E+06	49.66	246.40	9.208E-01	3.136E-04	2.021E-07
79	2.811	2207.	1.358E+07	2129.	6.43	4924.	2.612E+01	7.624E+06	48.69	244.20	9.027E-01	3.103E-04	2.004E-07
80	2.824	2232.	1.375E+07	2153.	6.43	4955.	2.637E+01	7.559E+06	49.16	247.30	9.115E-01	3.093E-04	2.028E-07
81	2.826	2233.	1.375E+07	2154.	6.43	4956.	2.638E+01	7.558E+06	49.19	247.40	9.122E-01	3.094E-04	2.029E-07
82	2.883	2393.	1.416E+07	2211.	6.42	5029.	2.822E+01	7.745E+06	52.63	255.10	9.766E-01	3.213E-04	2.086E-07
83	2.865	2340.	1.427E+07	2228.	6.42	5048.	2.748E+01	7.464E+06	51.26	256.90	9.508E-01	3.105E-04	2.100E-07
87	2.878	2363.	1.421E+07	2218.	6.42	5038.	2.783E+01	7.601E+06	51.90	256.00	9.633E-01	3.158E-04	2.093E-07
88	2.871	2366.	1.411E+07	2204.	6.42	5020.	2.789E+01	7.696E+06	52.10	254.10	9.648E-01	3.187E-04	2.079E-07
89	2.891	2395.	1.429E+07	2229.	6.42	5051.	2.820E+01	7.642E+06	52.61	257.50	9.766E-01	3.183E-04	2.104E-07
90	2.886	2385.	1.435E+07	2238.	6.42	5062.	2.803E+01	7.553E+06	52.30	258.50	9.707E-01	3.151E-04	2.112E-07
91	2.883	2383.	1.434E+07	2237.	6.42	5060.	2.800E+01	7.551E+06	52.24	258.30	9.694E-01	3.149E-04	2.110E-07

shock Mach number with an uncertainty of $\pm 2\%$. These measurements combine to yield an uncertainty in the Mach number and dynamic pressure measurements of $\pm 0.8\%$ and $\pm 3.5\%$, respectively.

2.2.4 Airflow Calibrations of the "A" Nozzle

Detailed flowfield surveys were made across the exit plane of the "A" nozzle to determine flow uniformity and core sizes at the Mach 6 and 8 conditions at which the first experimental studies were conducted. Additional data were provided from measurements of the axial static-pressure distribution along the flat plate. From the flowfield measurements of pitot pressure and total temperature, and the static pressure, we can determine the flow properties across the test section. Figures 2a and 2b show the Mach number distributions across the exit plane of the nozzle for the Mach 6 and 8 conditions. It can be seen that the core size for this condition was 20 inches, and that the variation in Mach number across the test core was less than 2%.

2.3 MODEL AND INSTRUMENTATION

2.3.1 Description of Transpiration-Cooled Flat-Plate/Shock-Generator Model

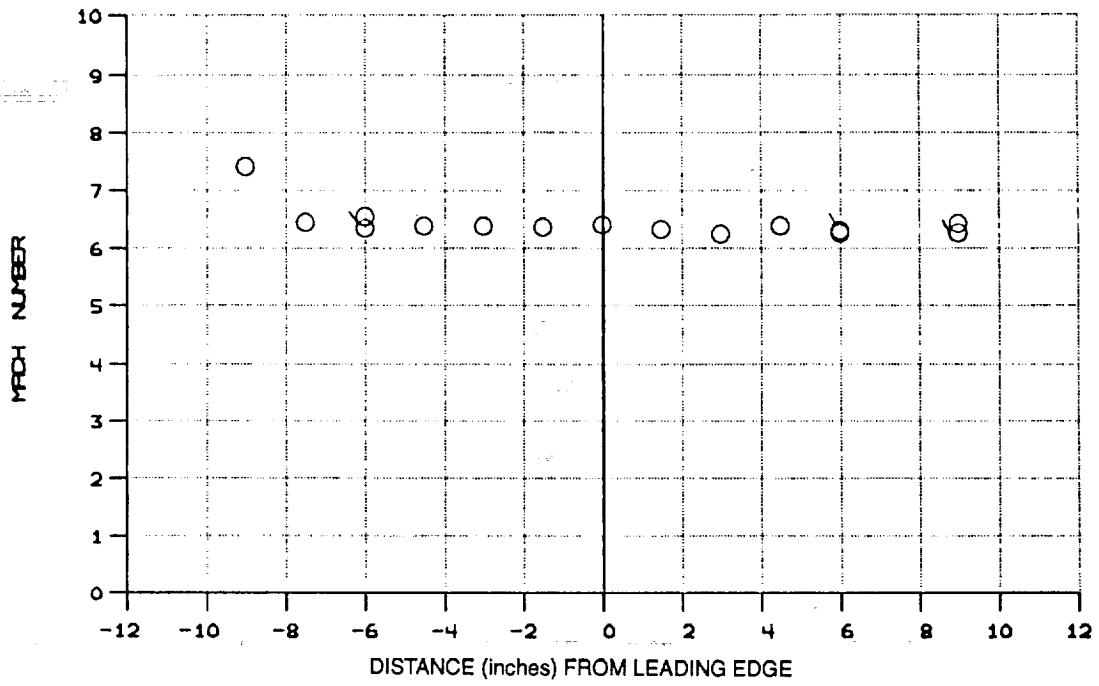
General Configuration

The flat-plate/transpiration-cooled model was constructed in two segments--a smooth flat plate, 28 inches in length, followed by a transpiration-cooled porous surface composed of three independently fed transpiration-cooled segments, each 5 inches in length. Both the porous and the non-porous surfaces were fully instrumented with heat transfer and pressure instrumentation. The transpiration-cooled flat plate model is shown in Figure 3. A two-dimensional shock generator was supported above the flat-plate surface by arms attached to the model support at the rear of the model as shown in Figure 4. This shock generator could be translated in the streamwise direction to position the point of shock impingement for each shock strength in the center of the region of maximum instrumentation.

Construction of the Porous Surface

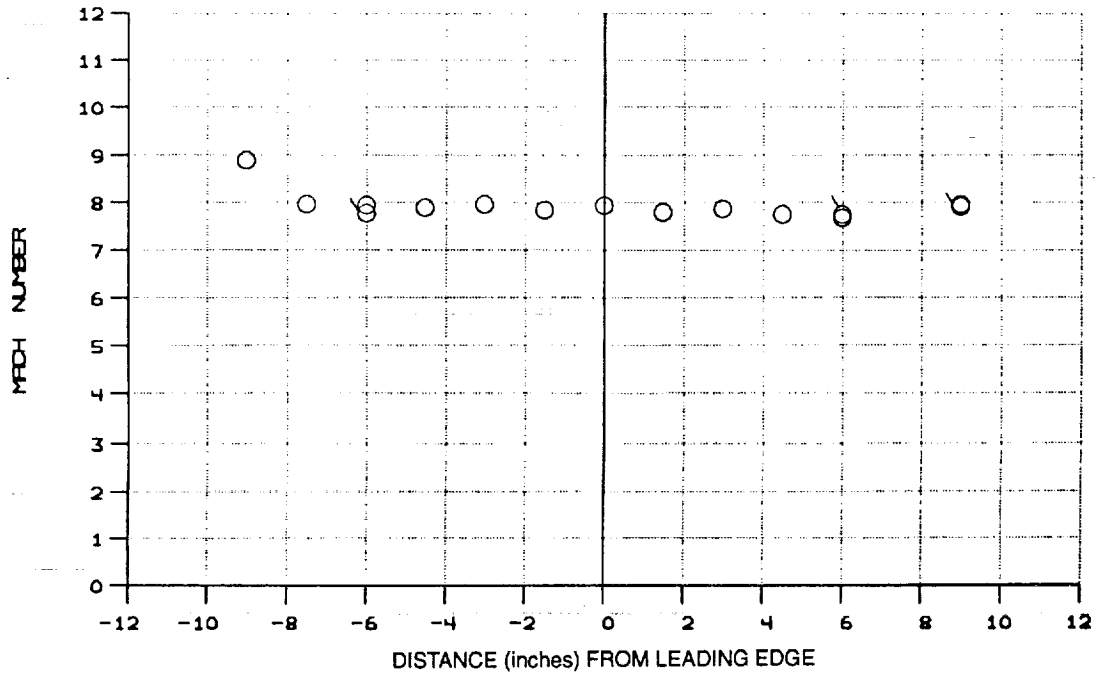
The porous surface was constructed from a composite sandwich of two porous plates, a surface plate and an orifice plate, glued tightly together. The porous surface was constructed from 0.2-inch-thick stainless steel plate, perforated with 0.039-inch holes that were spaced 0.070 inch apart in an hexagonal array. At the base of each of these holes was a plate in which there were three 0.0039-inch-diameter

AIRFLOW MACH NUMBER PROFILE
 RUN 1161 D 2.570 P6 4000. P1 55.10 $\frac{1}{4}$ 68.0 M1 2.78



(a) $M_{\infty} = 6.4$

AIRFLOW MACH NUMBER PROFILE
 RUN 1164 D 1.600 P6 5200. P1 72.00 $\frac{1}{4}$ 68.0 M1 2.90



(b) $M_{\infty} = 7.9$

Figure 2 MACH NUMBER DISTRIBUTIONS FOR TEST CONDITIONS 1 AND 3 IN THE "A" NOZZLE

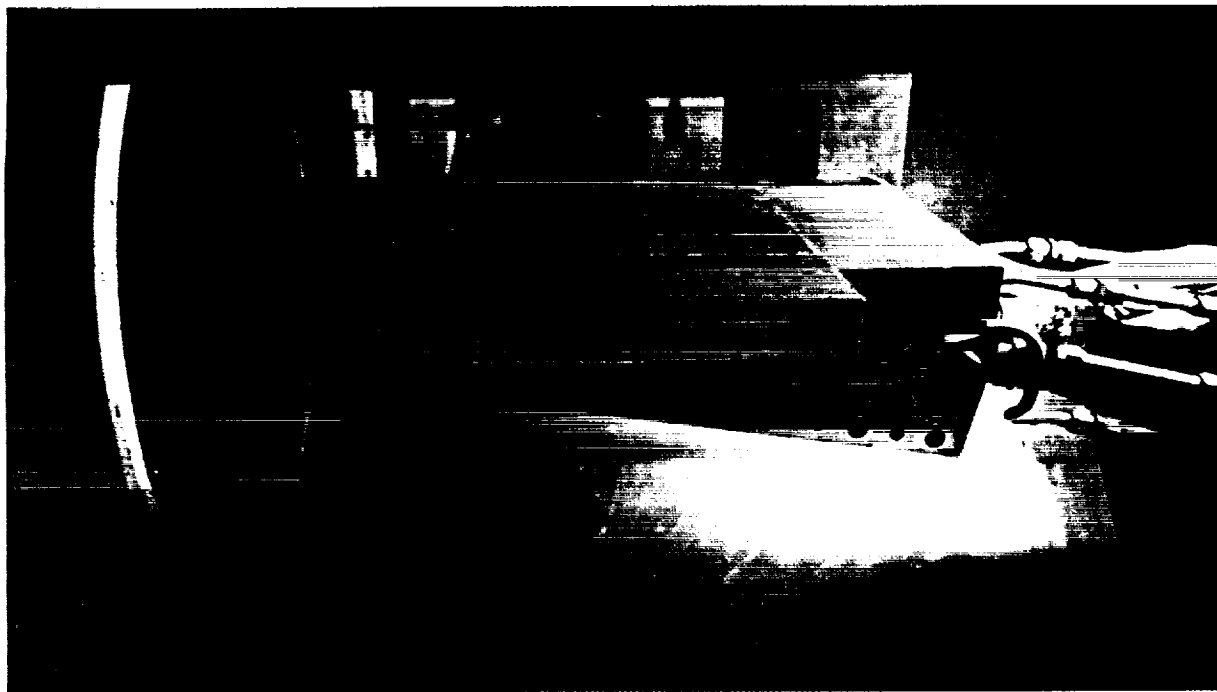


Figure 3 **TRANSPIRATION-COOLED FLAT-PLATE MODEL IN TEST SECTION OF THE CALSPAN 48-INCH SHOCK TUNNEL**

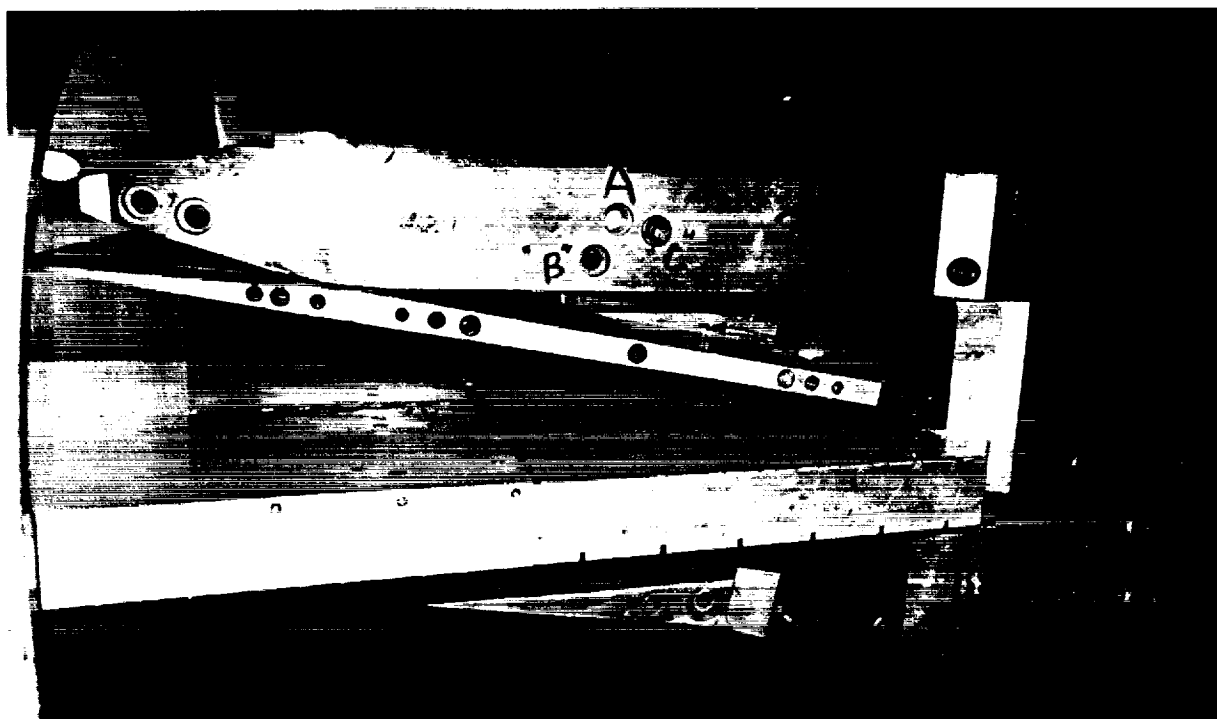


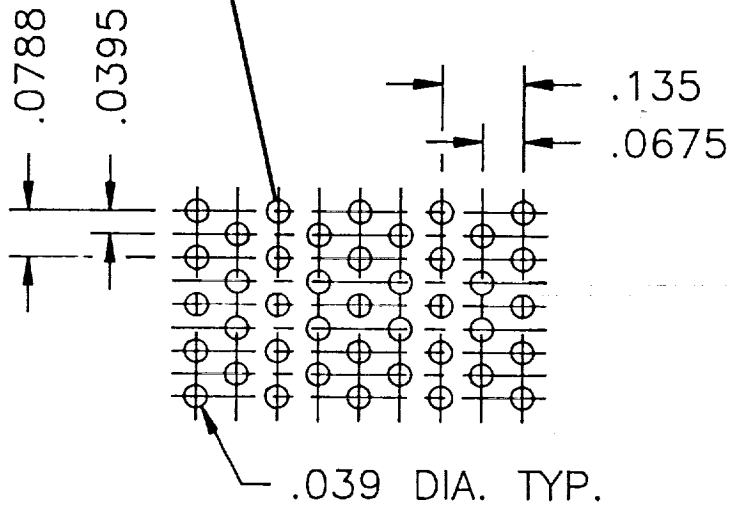
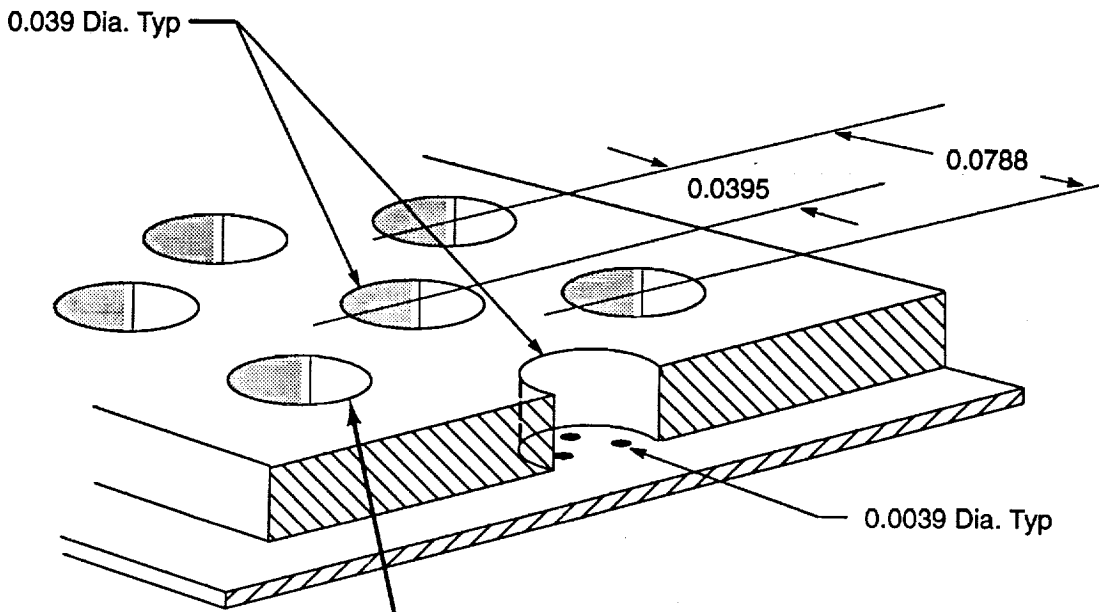
Figure 4 **SHOCK GENERATOR SUPPORTED ABOVE THE TRANSPIRATION-COOLED FLAT PLATE**

orifices, positioned uniformly across the area. (A schematic diagram of the surface geometry is shown in Figure 5.) These were the sonic orifices, which controlled the flow rate through the surface. Because the combined area of the orifices was a small fraction of that of each surface hole, and because the depth of these holes was sufficient for the sonic jets to mix to form a uniform subsonic flow, we obtained a uniform flow between the lands over the surface (≈ 100 ft/sec). The schlieren photographs of the flow demonstrate that there were no significant disturbances generated close to the surface as a result of the interaction between the injectant and the base of the boundary layer. This method of construction gave precise knowledge of the surface geometry and blowing characteristics, and the use of sonic orifices ensured precise control of the mass-flow rates, which remained independent of starting transients or the distribution of pressure over the model. This was not the case for models constructed with sintered porous surfaces. The porous segment of the model was fed from three separate plenum chambers (shown in Figure 6), positioned sequentially in the streamwise direction; each chamber was 5 inches in length and spanned the full width of the model. This enabled us to differentially cool the regions ahead of and behind the incident shock. Each chamber was fed from an extensive network of passages to ensure uniform flow through the surface. We installed miniature (0.033- and 0.062-inch-diameter) heat transfer gages and pressure transducers, respectively, in the lands between the holes in the porous surface (see Figure 7) so that this instrumentation would not locally disturb the flow in any way.

2.3.2 Calibration of Transpiration-Cooled Segments

Each of the transpiration-cooled sections of the model was calibrated by evacuating the model passages and the large test chamber to a low pressure (10 microns) and then releasing injectant gas from a large high-pressure reservoir through the model's choked surface orifices. This was done for a range of initial reservoir pressures. Both helium and nitrogen injectant gases were employed in this calibration.

The mass-flow rates of the coolant were calculated under the assumption of isentropic flow issuing from the coolant reservoirs through the choked surface orifices. Calibrations at various reservoir pressures were conducted, and an orifice calibration coefficient was experimentally determined from a comparison of experimental and theoretical reservoir changes in mass, which occurred during a short-duration blowdown of the coolant reservoirs. The experimental change in mass measured the difference between the initial state of the reservoir pressure at room temperature and the final state, reached once the valves closed after blowdown and heat transfer from the surroundings returned the reservoir gas to room temperature. The theoretical change in mass of the reservoir was calculated as the difference between the initial reservoir mass at the initial pressure and at room temperature and the final mass, achieved by an isentropic blowdown through a known choked throat area. Since the isentropic relation is a function of time, the mass of the reservoir was calculated at the end of the calibration blowdown and was compared to



HOLE PATTERN
FOR PLATE
SCALE 4/1

Figure 5 SCHEMATIC DIAGRAM OF SURFACE GEOMETRY OF TRANSPIRATION-COOLED SURFACE

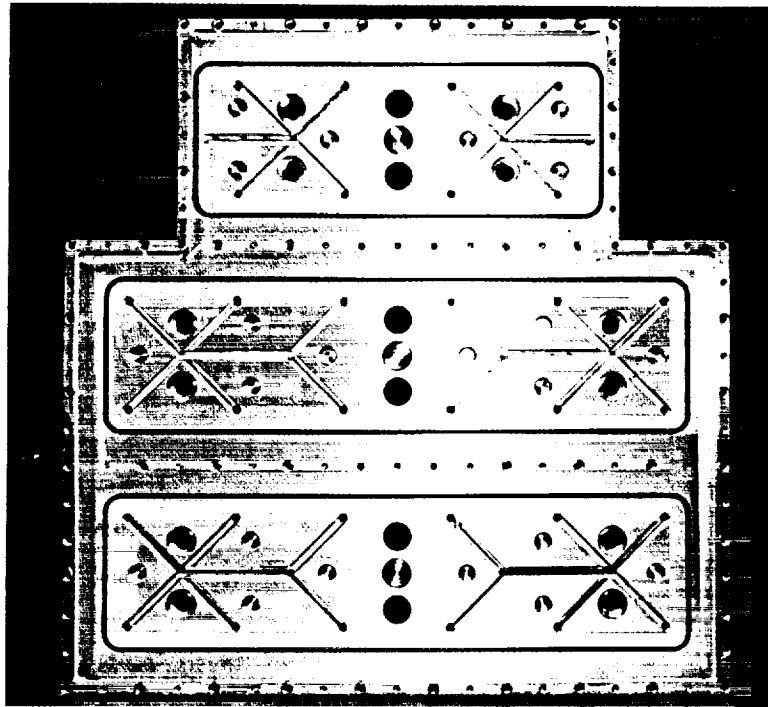


Figure 6a SUBCHAMBER OF THE MODEL SHOWING PASSAGES TO EVENLY DISTRIBUTE THE COOLANT TO THE TRANSPIRATION-COOLED SURFACE

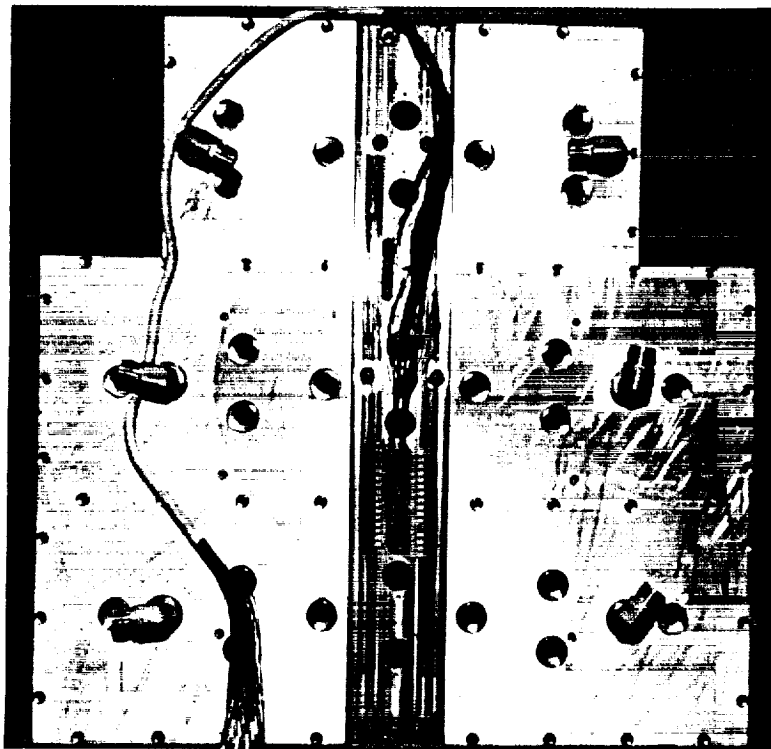


Figure 6b BACK OF MODEL SHOWING INSTRUMENTATION HARNESS AND PORTS FOR "VALCOR" FAST-ACTING VALVES

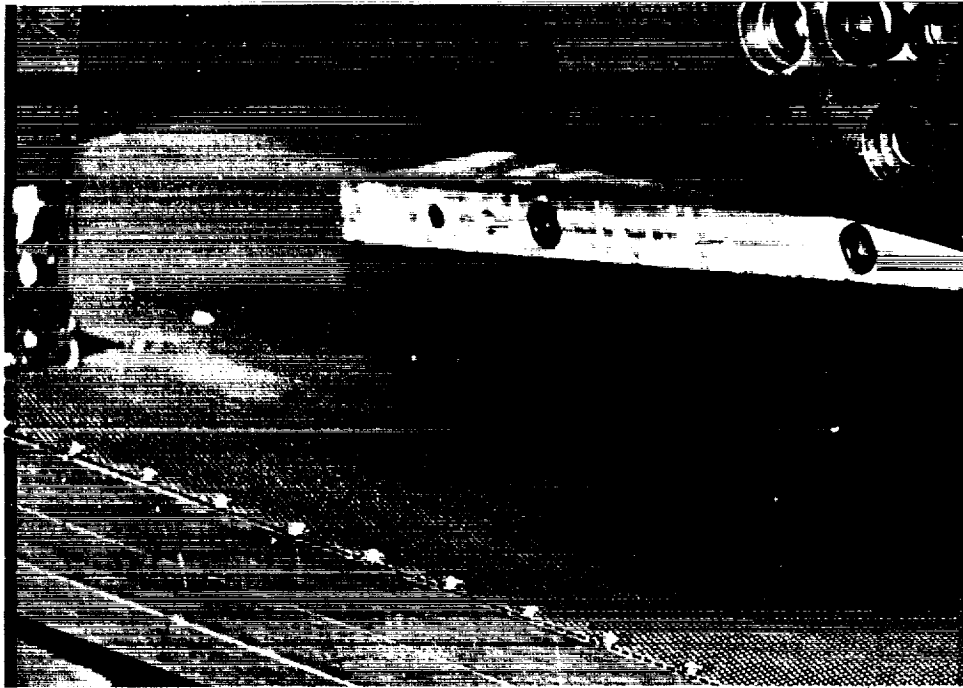


Figure 7a SHOCK GENERATOR SUPPORTED ABOVE THE TRANSPIRATION-COOLED SURFACE

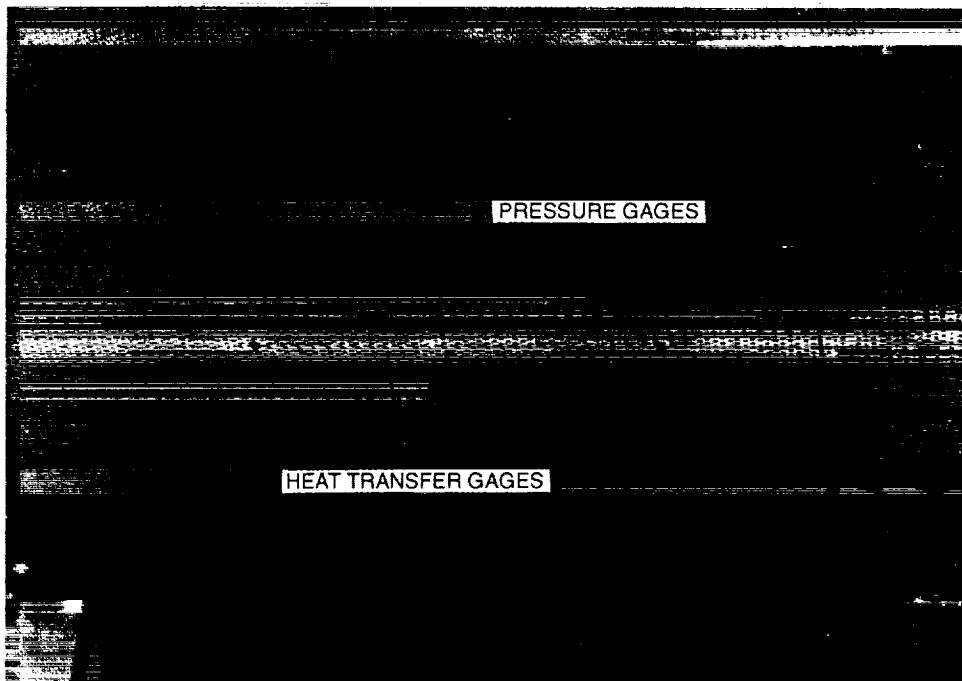


Figure 7b HEAT TRANSFER AND PRESSURE INSTRUMENTATION INSTALLED IN THE "LANDS" BETWEEN THE INJECTION ORIFICES

the experimental results to obtain the orifice discharge coefficient, as shown in Equation 9. Once the discharge coefficient had been calculated, the isentropic blowdown equations could be utilized to determine the mass-flow rate at any time t . In both methods, real gas effects were neglected, since the pressure drops were relatively small.

$$C_D \int_0^{\tau_f} \dot{m}_{\text{theor.}} d\tau = \dot{m}_{\text{final}} - \dot{m}_{\text{initial}} \quad (9)$$

Hence,

$$C_D = \frac{\Delta P \left(\frac{V}{RT_{\text{room}}} \right)}{\frac{\dot{m}(0)}{\gamma} \left[1 - \left(1 + \frac{\gamma-1}{2} \tau_{\text{final}} \right)^{\frac{2\gamma}{\gamma-1}} \right]}$$

Using the isentropic blowdown through a choked orifice of known discharge coefficient, the mass-flow rates experienced during the tunnel run time can be calculated from Equation 10. These results are recorded in Table 2. As a check, the theoretical change in mass of the reservoirs was compared to that of the actual change, and the difference was typically within 5%.

$$\frac{\dot{m}(\tau)}{\dot{m}(0)} = \left[1 + \frac{\gamma-1}{2} \tau \right]^{\frac{\gamma+1}{\gamma-1}} \quad (10)$$

where

$$\tau = \frac{t}{\beta}$$

$$\beta = \frac{V}{C_D A^* a(0)} \left(\frac{2}{\gamma+1} \right)^{\frac{\gamma+1}{2(1-\gamma)}}$$

$$\dot{m}(0) = \frac{p(0)}{\sqrt{T(0)}} A^* C_D K(\gamma)$$

V = Volume of Reservoir
 C_D = Discharge Coefficient
 A^* = Area of Orifice
 $a(0) = \sqrt{\gamma RT(0)}$ of Reservoir at $t=0$

Table 2
SUMMARY OF TRANSPIRATION-COOLED FLAT-PLATE STUDY
WITHOUT SHOCK GENERATOR

RUN	TC	Mach	ReL	GAS	Section		
					m1	m2 (lbm/sec)	m3
7	1	6.4	2.8E+07	-	-	-	-
9	3	7.9	2.6E+07	-	-	-	-
12	1	6.4	2.7E+07	N2	.0766	.0859	.0664
13	1	6.4	2.9E+07	N2	.0952	.0941	.0873
14	1	6.4	2.8E+07	N2	.1248	.1266	.1035
15	1	6.4	2.8E+07	N2	.1630	.1650	.1282
16	1	6.4	2.8E+07	N2	.2383	.2292	.2050
17	1	6.4	2.8E+07	He	.0137	.0143	.0128
18	1	6.4	2.8E+07	He	.0261	.0262	.0222
19	1	6.4	2.9E+07	He	.0488	.0376*	.0408
20	1	6.4	2.8E+07	He	.0745	.0697	.0520
21	1	6.4	2.9E+07	He	.0111	.0122	.0107
22	1	6.4	2.8E+07	N2	.0557	.0522	.0436
23	3	7.9	2.8E+07	N2	.0407	.0361	.0332
24	3	7.9	2.6E+07	N2	.0294	.0424	.0471
26	3	7.9	2.7E+07	N2	.0593	.0664	.0736
27	3	7.9	2.9E+07	N2	.0759	.0891	.0843
28	3	7.9	2.6E+07	N2	.0909*	.1086*	.0869*
29	3	7.9	2.7E+07	N2	.0283	.0270	.0290
30	3	7.9	2.6E+07	He	.00465	.00495	.00402
31	3	7.9	2.6E+07	He	.00636	.00686	.00654
32	3	7.9	2.6E+07	He	.00526	.00787	.00815
33	3	7.9	2.6E+07	He	.00809	.00923	.00958
34	3	7.9	2.6E+07	He	.0111	.0129	.0147
35	3	7.9	2.6E+07	He	.0114	.0151	.0161
36	3	7.9	2.7E+07	He	.0150	.0169	.0148
37	3	7.9	2.6E+07	He	.00704	.00806	.00670
38	3	7.9	2.5E+07	N2	.1303	.1320	.0882

* approximate value

Table 2
SUMMARY OF TRANSPIRATION-COOLED FLAT-PLATE STUDY (Cont.)

WITH SHOCK GENERATOR

RUN	TC	Mach	ReL	GAS	Section			S.G. Angle (deg.)
					m1	m2 (lbm/sec)	m3	
41	3	7.9	3.1E+07	-	-	-	-	5.217
42	3	7.9	2.6E+07	-	-	-	-	5.217
43	3	7.9	2.7E+07	N2	.0235	.0267	.0201	5.217
44	3	7.9	2.6E+07	N2	.0451	.0422	.0414	5.217
45	3	7.9	2.7E+07	N2	.0484	.0784	.0951	5.217
46	3	7.9	2.9E+07	N2	.0689	.1346	.1122	5.217
47	3	7.9	2.7E+07	N2	.0597	.2543	.0991	5.217
48	3	7.9	2.7E+07	N2	.0607	.1473	.1273	5.217
49	3	7.9	2.9E+07	N2	.0687	.2007	.1672	5.067
50	3	7.9	2.8E+07	N2	.0587	.2189	.1836	5.067
51	3	7.9	2.6E+07	N2	.0582	.2448	.2145	5.067
52	3	7.9	2.9E+07	N2	.0901	.2550	.2240	5.067
54	3	7.9	2.8E+07	-	-	-	-	-
55	3	7.9	2.7E+07	He	.0185	.0783	.0618	5.0167
56	3	7.9	2.7E+07	He	.00445	.0516	.0431	5.0167
57	3	7.9	2.7E+07	He	.0169	.0543	.0434	5.0167
59	3	7.9	2.8E+07	He	.0170	.0416	.0346	5.0167
60	3	7.9	2.8E+07	-	-	-	-	7.7
62	3	7.9	2.8E+07	He	.0171	.0522	.0428	7.7
63	3	7.9	2.7E+07	He	.0111	.1061	.0891	7.667
64	3	7.9	2.7E+07	He	.0168	.1531	.1283	7.667
65	3	7.9	2.6E+07	He	.0183	.2301	.1918	7.667
66	3	7.9	2.7E+07	N2	.0936	.3893	.3517	7.667
67	3	7.9	2.7E+07	N2	.1060	.7421	.5595	7.667
68	3	7.9	2.7E+07	N2	.1100*	1.167	.8860	7.667
69	3	7.9	2.7E+07	N2	.1488	1.144	1.027	7.667
70	3	7.9	2.7E+07	-	-	-	-	10.1
71	3	7.9	2.7E+07	N2	.0556	.4513	.3618	10.1
72	3	7.9	2.7E+07	N2	.4060*	1.109	1.034	10.1
73	3	7.9	2.7E+07	He	.00631	.1201	.1033	10.1
75	3	7.9	2.7E+07	He	.01003	.2020	.1656	10.1
76	3	7.9	2.7E+07	He	.0320	.2554	.2135	10.1
77	1	6.4	2.9E+07	-	-	-	-	7.35
78	1	6.4	2.9E+07	N2	.0244	.6671	.4579	7.35
79	1	6.4	2.9E+07	N2	.2900*	1.147	.8537	7.35
80	1	6.4	2.9E+07	He	.00955	.1603	.1302	7.35
81	1	6.4	2.9E+07	-	-	-	-	5.233
82	1	6.4	2.9E+07	N2	.0582	.4704	.3310	5.3167
83	1	6.4	2.8E+07	N2	.1129	.5533	.2443	5.3167
87	1	6.4	2.9E+07	He	.0166	.0974	.0770	5.3167
88	1	6.4	2.9E+07	-	-	-	-	10.117
89	1	6.4	2.9E+07	N2	.0171	.9713	.6843	10.117
90	1	6.4	2.9E+07	N2	.6560*	1.498	1.026	10.117
91	1	6.4	2.9E+07	He	.0307	.4099	.3463	10.117

* approximate value

2.3.3 Heat Transfer Instrumentation

The miniature heat transfer instrumentation used in the transpiration-cooled surface is based on the thin-film heat transfer technique, in which a thin-film platinum resistance thermometer is used to sense the surface temperature of a low-conductivity surface. Because of the large streamwise heat transfer gradients in these flows to prevent measurement errors, it is extremely important to employ instrumentation with low surface conductivity. The transient response of this instrumentation is such that it is ideally suited to the detection of turbulent bursts and the unsteady nature of both transition regions and regions of shock-wave/boundary layer interaction.

The thin-film heat transfer gage is a resistance thermometer that reacts to the local surface temperature of the model. The first step of the data reduction was to convert the measured voltage time history for each gage to a temperature time history, taking into account the gage resistance, the current through the gage, the gage calibration factor, and the amplifier gain. The theory of heat conduction was used to relate the surface temperature to the rate of heat transfer. The platinum resistance element has negligible heat capacity and, hence, negligible effect on the Pyrex-substrate surface temperature. The substrate can be characterized as being homogeneous and isotropic. Furthermore, because of the short duration of a shock tunnel test, the substrate can be treated as a semi-infinite body. The final data reduction was done using the Cook-Felderman (Reference 16) algorithm.

The Stanton number, C_h , based on the freestream conditions, was calculated from the following

$$C_h = \frac{\dot{q}}{\rho_\infty U_\infty (H_o - H_w)} \quad (11)$$

where H_o and H_w are the total enthalpy of the free stream and the air at the wall.

For the thin-film heat transfer instrumentation, the uncertainties associated with the gage calibration and the recording equipment are estimated to be $\pm 5\%$ for the levels of heating obtained in the current studies.

2.3.4 Pressure Instrumentation

We used flush-mounted high-frequency Kulite pressure transducers (0.062 inch in diameter) in the leading edge of the flat-plate model to obtain measurements of the mean and fluctuating pressure levels through the interaction regions. PCB pressure transducers were used in the flat plate and for internal

passages mounted beneath small orifices. Their positions and gage numbers are shown in Figure 8 and Table 3.

The pressures were converted to absolute pressures (psia) by adding the measured initial vacuum pressure in the test section. This was the reference pressure for the transducers. The pressures were then averaged over an interval of time in which steady flow was established over the model, to obtain an average value for each position. The values of the pressure coefficients, C_p , were calculated from

$$C_p = p / \left(\frac{1}{2} \rho_{\infty} U_{\infty}^2 \right) \quad (12)$$

The uncertainties in the pressure measurements associated with the calibration and recording apparatus are $\pm 3\%$. Again, the variations associated with the unsteady nature of the fluid dynamics can be as large as $\pm 15\%$.

2.3.5 Measurement Recording System

All data were recorded on the 128-channel Calspan Digital Data Acquisition System (DDAS II). The DDAS II system consists of 128 Marel Co. Model 117-22 amplifiers, an Analogic ANDS 5400 data acquisition and distribution system, and a Sun SparcStation 2 computer. The Analogic system functions as a transient-event recorder in that it acquires, digitizes, and stores the data in real time. Immediately after each test run, the data were transferred to the Sun computer for processing. The Marel amplifiers provide gains up to 1000 for low-level signals, can be AC or DC coupled to the transducers, and have selectable low-pass filters with cutoff frequencies of 300, 1000, or 3000 Hz. The Analogic system contains a sample-and-hold amplifier, a 12-bit analog-to-digital converter, and a 4096-sample memory for each channel.

2.3.6 Flow Visualization

Flow visualization in these studies was accomplished via a standard off-axis, Z-type schlieren system, which uses 16-inch-diameter, $f/7.5$ schlieren-grade spherical mirrors as schlieren heads. A horizontal source-slit/knife-edge combination provides sensitivity in the vertical plane of 5 arc seconds, with test-section resolution better than 0.005 inch. A 1.5-microsecond FWHM (full-width, half-maximum) light pulse was generated from a high-voltage spark in air, triggered close to the end of the steady run time. The image was recorded on Kodak Tri-X panchromatic film.

GAGE LABEL	DIST. FROM L.E. OF IND. PLATE (inches)	DIST. FROM L.E. (inches)
L28H1	1.05	1.05
L28H2	3.05	3.05
L28H3	4.05	4.05
L28H4	5.05	5.05
L28H5	6.05	6.05
L28H6	7.05	7.05
L28H7	9.05	9.05
L28H8	10.05	10.05
L28H9	11.05	11.05
L28H10	12.05	12.05
L28H11	13.05	13.05
L28H12	15.05	15.05
L28H13	16.05	16.05
L28H14	17.05	17.05
L28H15	18.05	18.05
L28H16	19.05	19.05
L28H17	21.05	21.05
L28H18	22.05	22.05
L28H19	24.05	24.05
L28H20	25.05	25.05
L28H21	26.05	26.05

GAGE LABEL	DIST. FROM L.E. OF IND. PLATE (inches)	DIST. FROM L.E. (inches)
L28P1	5.05	5.05
L28P2	9.05	9.05
L28P3	11.05	11.05
L28P4	17.05	17.05
L28P5	21.05	21.05
L28P6	25.05	25.05

GAGE LABEL	DIST. FROM L.E. OF IND. PLATE (inches)	DIST. FROM L.E. (inches)
L28+Gap	0.800	27.861
TH1	1.352	29.213
TH2	1.892	29.753
TH3	2.438	30.299
TH4	2.984	30.847
TH5	3.527	31.388
TH6	4.069	31.926
TH7	4.609	32.461
TH8	5.148	32.993
TH9	5.685	33.522
TH10	6.221	34.048
TH11	6.755	34.571
TH12	7.287	35.091
TH13	7.817	35.608
TH14	8.345	36.122
TH15	8.871	36.633
TH16	9.395	37.141
TH17	9.917	37.646
TH18	10.437	38.148
TH19	10.955	38.647
TH20	11.471	39.143
TH21	11.985	39.636
TH22	12.497	40.126
TH23	13.007	40.613
TH24	13.515	41.097
TH25	14.021	41.578
TH26	14.525	42.056
TH27	15.027	42.531
TH28	15.527	43.003
TH29	16.025	43.472
TH30	16.521	43.938
TH31	17.015	44.401
TH32	17.507	44.861
TH33	18.000	45.318
TH34	18.495	45.772
TH35	18.991	46.223
TH36	19.485	46.671
TH37	19.977	47.116
TH38	20.467	47.558
TH39	20.955	47.997
TH40	21.441	48.433
TH41	21.925	48.866
TH42	22.407	49.296
TH43	22.887	49.723
TH44	23.365	50.147
TH45	23.841	50.568
TH46	24.315	50.986
TH47	24.787	51.401
TH48	25.257	51.813
TH49	25.725	52.222
TH50	26.191	52.628

GAGE LABEL	DIST. FROM IND. PLATE (inches)	DIST. FROM L.E. (inches)
L28+Gap	0.801	27.861
TP1	1.439	28.752
TP2	2.528	29.309
TP3	3.078	30.939
TP4	3.750	31.211
TP5	3.620	31.481
TP6	3.892	31.754
TP7	4.164	32.027
TP8	4.440	32.301
TP9	4.712	32.573
TP10	4.984	32.845
TP11	5.253	33.114
TP12	5.531	33.392
TP13	5.804	33.665
TP14	6.352	34.212
TP15	6.624	34.485
TP16	7.164	35.025
TP17	8.256	36.117
TP18	9.349	37.210
TP19	10.445	38.304
TP20	12.620	40.481
TP21	14.802	42.644

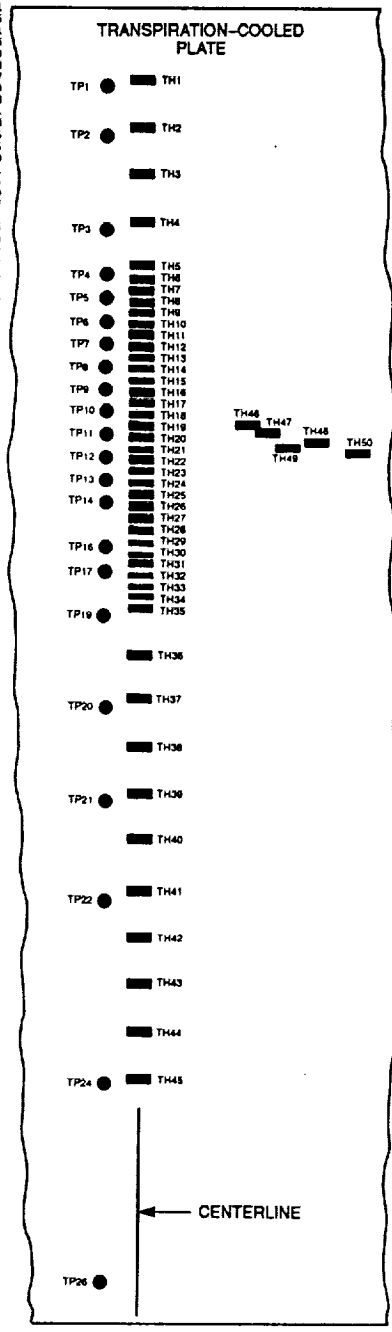
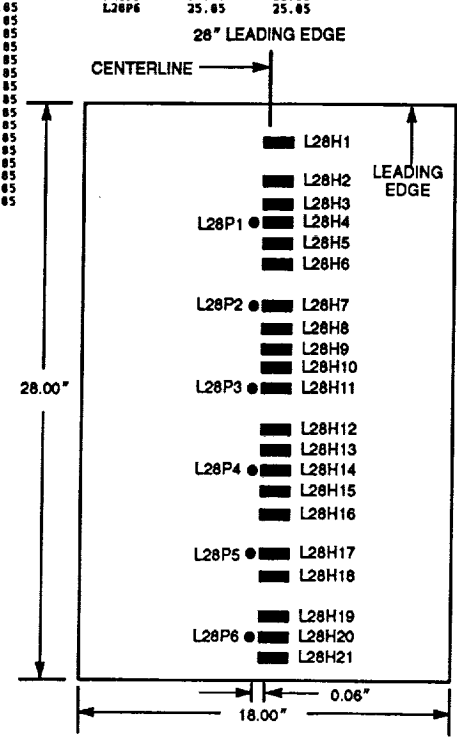


Figure 8 SCHEMATIC DIAGRAM SHOWING GAGE POSITIONS ALONG THE FLAT-PLATE TRANSPIRATION-COOLED MODEL

Table 3a
GAGE LOCATIONS IN THE 28-INCH SMOOTH LEADING EDGE FLAT PLATE

GAGE LABEL	DIST. FROM L.E. OF IND. PLATE (inches)	DIST. FROM L.E. (inches)	GAGE LABEL	DIST. FROM L.E. OF IND. PLATE (inches)	DIST. FROM L.E. (inches)
L28H1	1.85	1.85	L28P1	5.85	5.85
L28H2	3.85	3.85	L28P2	9.85	9.85
L28H3	4.85	4.85	L28P3	13.85	13.85
L28H4	5.85	5.85	L28P4	17.85	17.85
L28H5	6.85	6.85	L28P5	21.85	21.85
L28H6	7.85	7.85	L28P6	25.85	25.85
L28H7	9.85	9.85			
L28H8	10.85	10.85			
L28H9	11.85	11.85			
L28H10	12.85	12.85			
L28H11	13.85	13.85			
L28H12	15.85	15.85			
L28H13	16.85	16.85			
L28H14	17.85	17.85			
L28H15	18.85	18.85			
L28H16	19.85	19.85			
L28H17	21.85	21.85			
L28H18	22.85	22.85			
L28H19	24.85	24.85			
L28H20	25.85	25.85			
L28H21	26.85	26.85			

Table 3b
GAGE LOCATIONS IN THE TRANSPIRATION-COOLED SECTIONS OF THE FLAT-PLATE MODEL

GAGE LABEL	DIST. FROM L.E. OF IND. PLATE (inches)	DIST. FROM L.E. (inches)	GAGE LABEL	DIST. FROM L.E. OF IND. PLATE (inches)	DIST. FROM L.E. (inches)
L28+Gap		27.861	L28+Gap		27.861
TH1	0.800	28.661	TP1	0.891	28.752
TH2	1.352	29.213	TP2	1.439	29.300
TH3	1.892	29.753	TP3	2.528	30.389
TH4	2.438	30.299	TP4	3.078	30.939
TH5	2.986	30.847	TP5	3.350	31.211
TH6	3.127	30.988	TP6	3.620	31.481
TH7	3.255	31.116	TP7	3.893	31.754
TH8	3.400	31.261	TP8	4.166	32.027
TH9	3.533	31.394	TP9	4.440	32.301
TH10	3.669	31.530	TP10	4.712	32.573
TH11	3.808	31.669	TP11	4.984	33.845
TH12	3.941	31.802	TP12	5.253	33.114
TH13	4.078	31.939	TP13	5.531	33.392
TH14	4.209	32.070	TP14	5.804	33.665
TH15	4.348	32.209	TP16	6.352	34.213
TH16	4.486	32.347	TP17	6.624	34.485
TH17	4.620	32.481	TP19	7.164	35.025
TH18	4.755	32.616	TP20	8.256	36.117
TH19	4.896	32.757	TP21	9.349	37.210
TH20	5.025	32.886	TP22	10.445	38.306
TH21	5.169	33.030	TP24	12.620	40.481
TH22	5.302	33.163	TP26	14.803	42.664
TH23	5.444	33.305			
TH24	5.580	33.441			
TH25	5.715	33.576			
TH26	5.850	33.711			
TH27	5.984	33.845			
TH28	6.128	33.989			
TH29	6.262	34.123			
TH30	6.396	34.257			
TH31	6.532	34.393			
TH32	6.671	34.532			
TH33	6.800	34.661			
TH34	6.939	34.800			
TH35	7.075	34.936			
TH36	7.625	35.486			
TH37	8.169	36.030			
TH38	8.720	36.581			
TH39	9.263	37.124			
TH40	9.808	37.669			
TH41	10.356	38.217			
TH42	10.903	38.764			
TH43	11.445	39.306			
TH44	11.987	39.848			
TH45	12.546	40.407			
TH46	4.896	32.757			
TH47	4.967	32.828			
TH48	5.095	32.956			
TH49	5.169	33.030			
TH50	5.222	33.083			

Section 3 RESULTS AND DISCUSSION

3.1 INTRODUCTION

This experimental program was conducted in two phases. In the first phase of this program, the work was focused on obtaining measurements to examine the effects of coolant blowing rate and coolant properties on the performance of a transpiration-cooling system at Mach numbers of 6 and 8. Here, we employed nitrogen and helium gases at room temperature as coolants. The blowing rates in these experiments were varied from coolant flows where the boundary layer remained attached to larger flow rates, where the boundary layer was lifted from the surface. One of the secondary objectives of this phase of the program was to determine, from changes in the surface-pressure distribution, when the boundary layer occurred and how it could be correlated with the blowing rate and the properties of the injectant. In the major (second) phase of this program, the principal objective was to determine the levels of transpiration cooling required to reduce the peak heating rates in regions of shock/boundary layer interaction to the values comparable to those upstream of the interaction in the absence of cooling and, under such conditions, whether the inviscid flow was significantly distorted by the blowing.

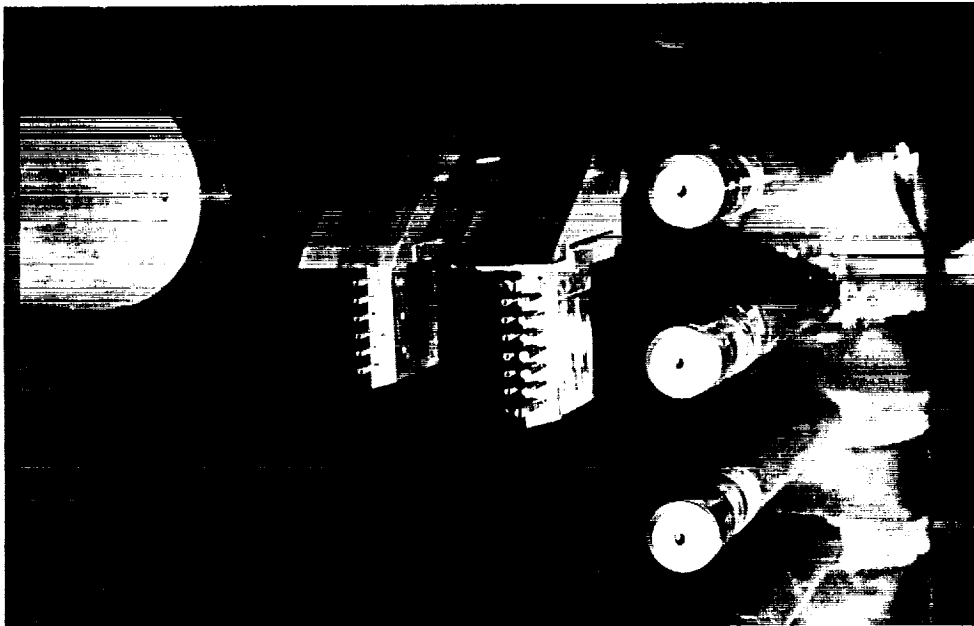
3.2 BOUNDARY LAYER PROFILE MEASUREMENTS UPSTREAM OF TRANSPIRATION-COOLING SECTIONS

Flowfield surveys across the boundary layer just upstream of the exit plane of the slot were made to provide information both for experimental correlations and for computational fluid dynamics (CFD) code validation. To make these measurements, we employed two specially constructed boundary layer rakes containing pitot pressure and total temperature instrumentation. The measurements made with this instrumentation, combined with the static-pressure measurements on the plate, provided a set of information to define the mean structure of the boundary layer just upstream of the nozzle lip. The pitot pressure and total temperature rakes used in this study are shown in Figure 9. We employed 0.062-inch-diameter Kulite strain gage transducers to obtain the pitot pressure measurements and shielded total temperature probes of the same diameter with thin-wire platinum-rhodium thermocouple sensing elements. Each rake contained eight probes, spaced 0.1 inch between centers. The Mach number distribution and velocity distribution across the flow can be determined by combining these two sets of measurements with the measurement of static pressure on the plate:

$$\frac{\rho_{\text{rake}}}{\rho_{\text{plate}}} = \left[\frac{(\gamma+1) M_b^2}{2} \right]^{\frac{\gamma}{\gamma-1}} * \left[\frac{\gamma+1}{2\gamma M_b^2 - (\gamma-1)} \right]^{\frac{1}{\gamma-1}} \quad (13)$$



a. AIRFLOW CALIBRATION RAKE



b. BOUNDARY LAYER SURVEY RAKES BEING CALIBRATED IN AIRFLOW RAKE

Figure 9 PITOT AND TOTAL TEMPERATURE FLOWFIELD AND BOUNDARY LAYER RAKES

$$\frac{U_b}{U_e} = \left(\frac{M_b}{M_e}\right) \left(\frac{T_{ob}}{T_{oe}}\right)^{1/2} \left(\frac{1+m_e}{1+m_b}\right)^{1/2} \quad (14)$$

where

$$m_b = \frac{\gamma-1}{2} M_b^2 \quad \text{and} \quad m_e = \frac{\gamma-1}{2} M_e^2$$

Tabulations of the measurements and the derived velocity distributions obtained in this set of studies are shown in Appendix B.

3.3 CORRELATION OF FLAT-PLATE TRANSPIRATION-COOLING DATA

The heat transfer and pressure measurements made on the flat-plate/transpiration-cooling configuration were conducted at Mach numbers of 6 and 8 with both nitrogen and helium coolants. At each of the two Mach numbers, we ran a series of coolant rates through the transpiration-cooled section of the model. First measurements were made along the model at each test condition for the no-blowing case, and the heat transfer distributions shown in Figure 10a and 10b present the results. For both of these cases, transition was well upstream of the transpiration-cooled segment of the model, with over 100 turbulent boundary layer thicknesses needed to reach turbulent equilibrium before blowing was initiated. While, at test condition 3, the intrinsic roughness of the porous surface did not enhance the heating level, at the higher Reynolds number 8 (test condition 1), the gages in the lands between the holes experienced heating rates larger than the smooth-flat-plate value. However, once blowing was initiated, surface roughness was not a factor for this surface configuration. The effects of the blowing rate and the properties of the coolant on the effectiveness of transpiration cooling are shown in Figures 11 through 15 for the Mach 6 and 8 conditions. At the Mach 6 condition, a mass-addition level of 1.5% caused a 50% reduction in the heating rate for nitrogen; using helium, this reduction was accomplished with one-third of the mass-flow rate. Once a 70% reduction in heating level was obtained with a nitrogen coolant, a further reduction in the heating rate required significantly more coolant. For helium, this "knee" occurred at approximately a 90% reduction. The effectiveness of transpiration cooling was not strongly influenced by Mach number at these high Mach number conditions. Correlations of the cooling ratios for nitrogen and helium coolants in terms of the blowing parameter $\lambda/\rho_e U_e C_{H_0}$ are shown in Figures 15 through 18. The heat transfer measurements for a range of blowing rates of each coolant correlate reasonably well at each test condition, and, as shown in Figures 19 and 20, coolant data from both test conditions correlate well, indicating relatively little Mach number effect. Plotting all the data together, as shown in Figure 21, graphically indicates the superior characteristics of helium as a coolant. To correlate the measurements from the two different coolants, we must account for the effects of both specific heat and molecular weight of the coolant. The greater specific heat of helium provided the capacity to absorb a greater quantity of

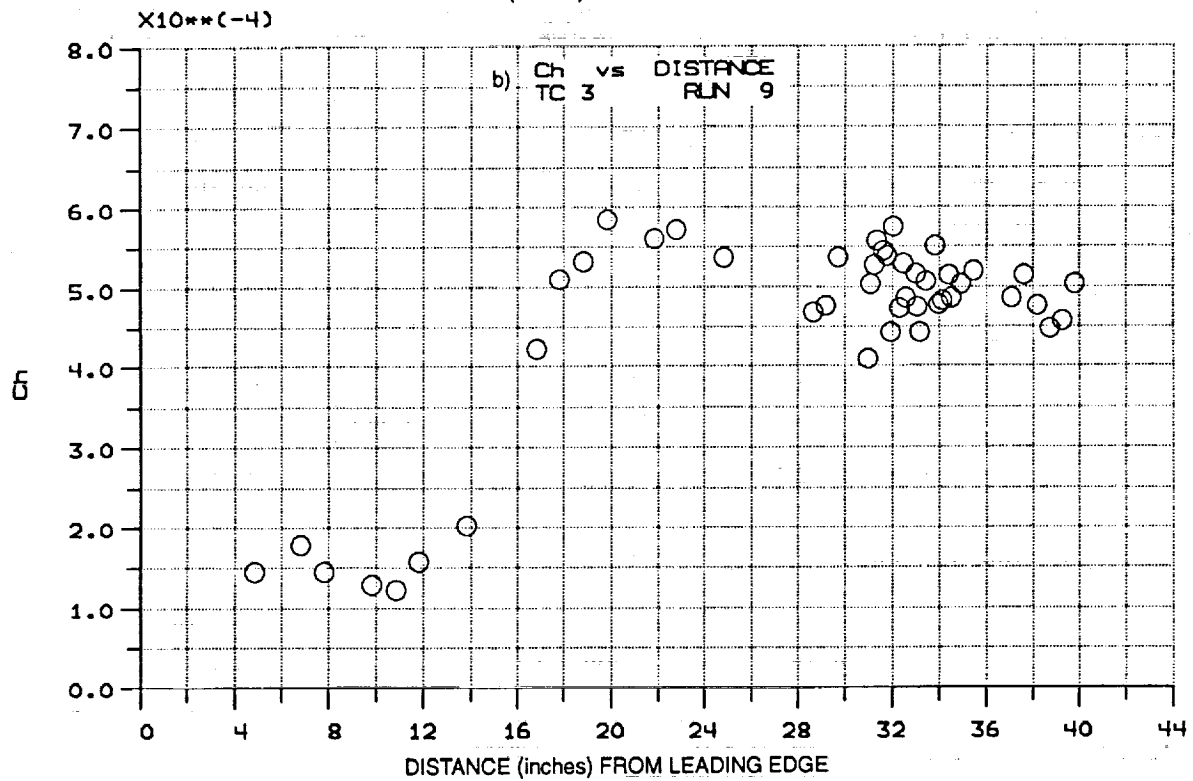
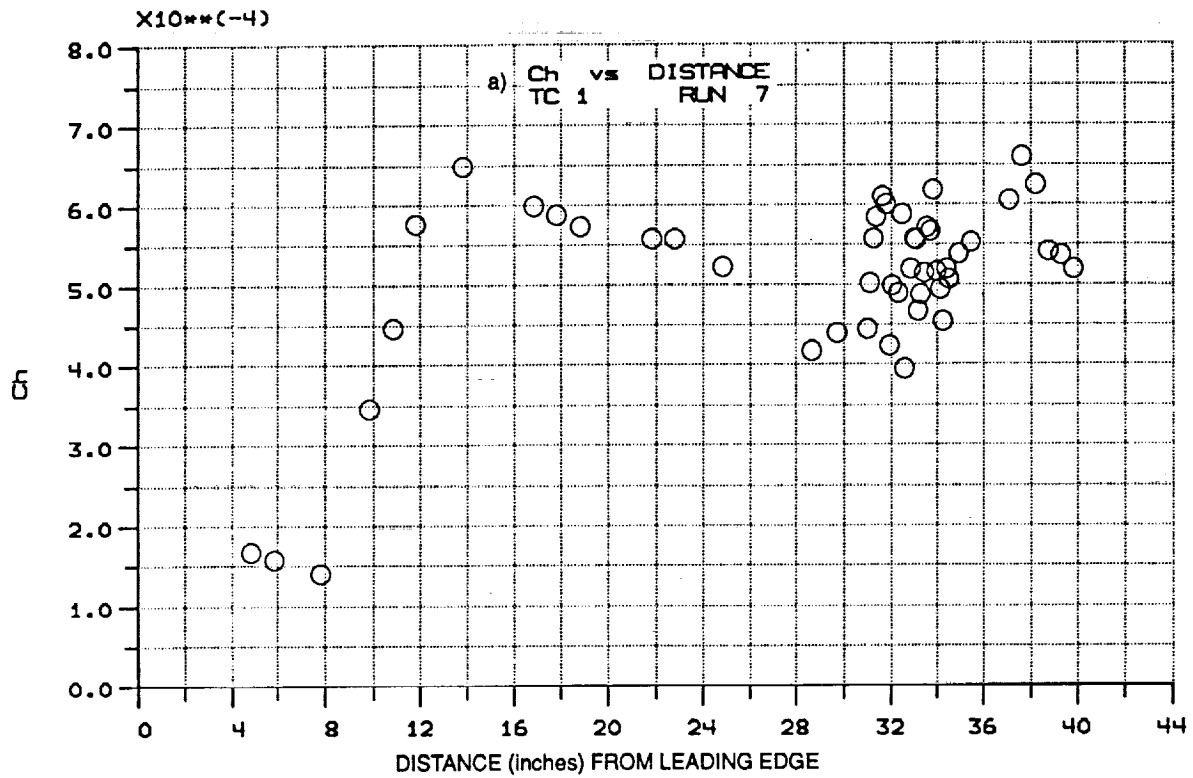


Figure 10 HEAT TRANSFER DISTRIBUTIONS ALONG FLAT PLATE - TRANSPARATION SURFACE WITHOUT COOLING AT MACH 6 AND 8

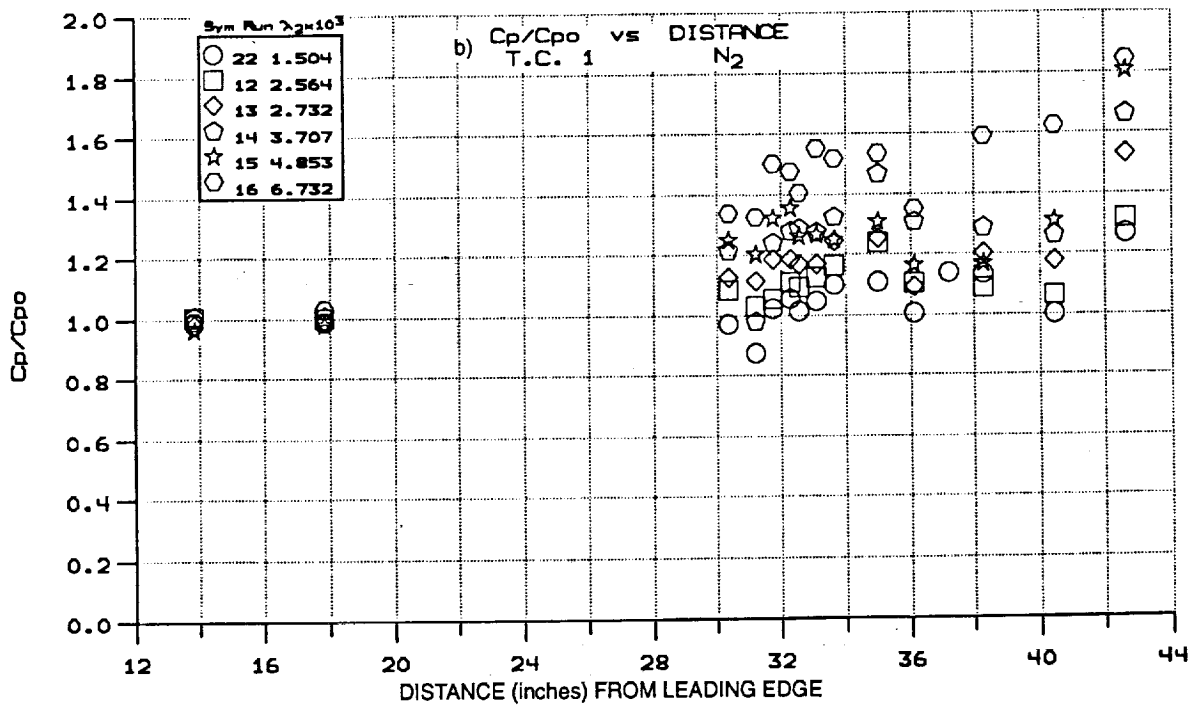
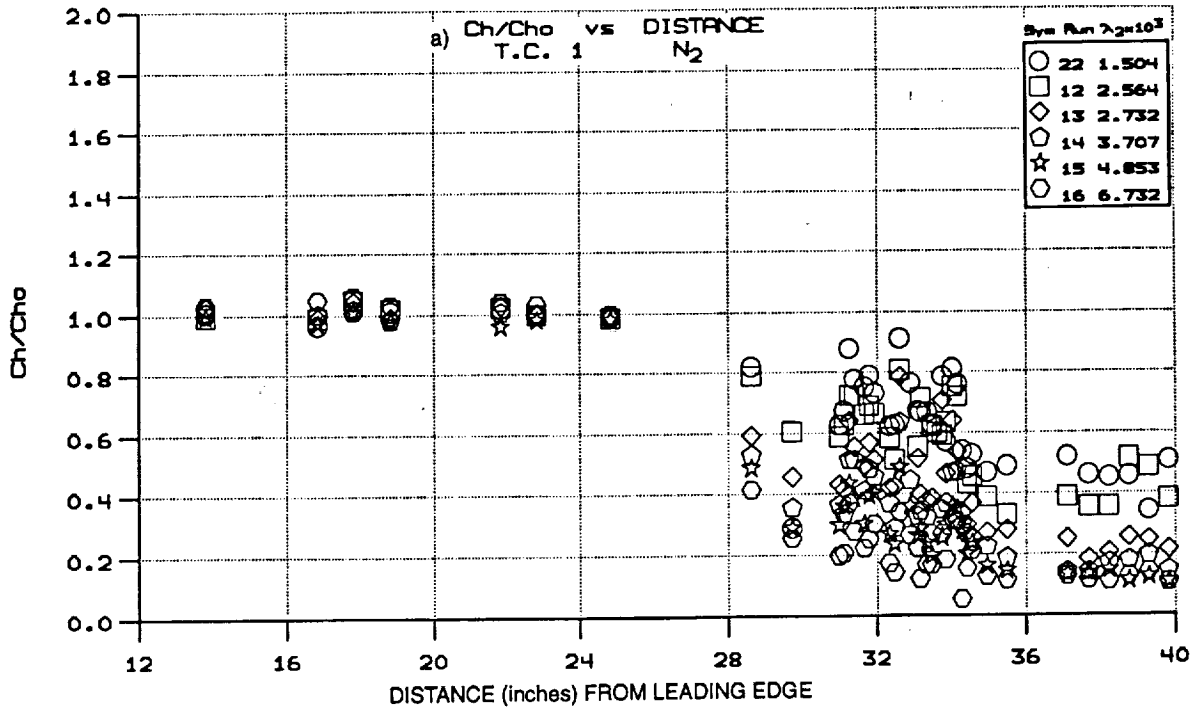


Figure 11 HEAT TRANSFER AND PRESSURE DISTRIBUTIONS ALONG FLAT PLATE –
TRANSPIRATION SURFACE FOR NITROGEN COOLANT AT MACH 6

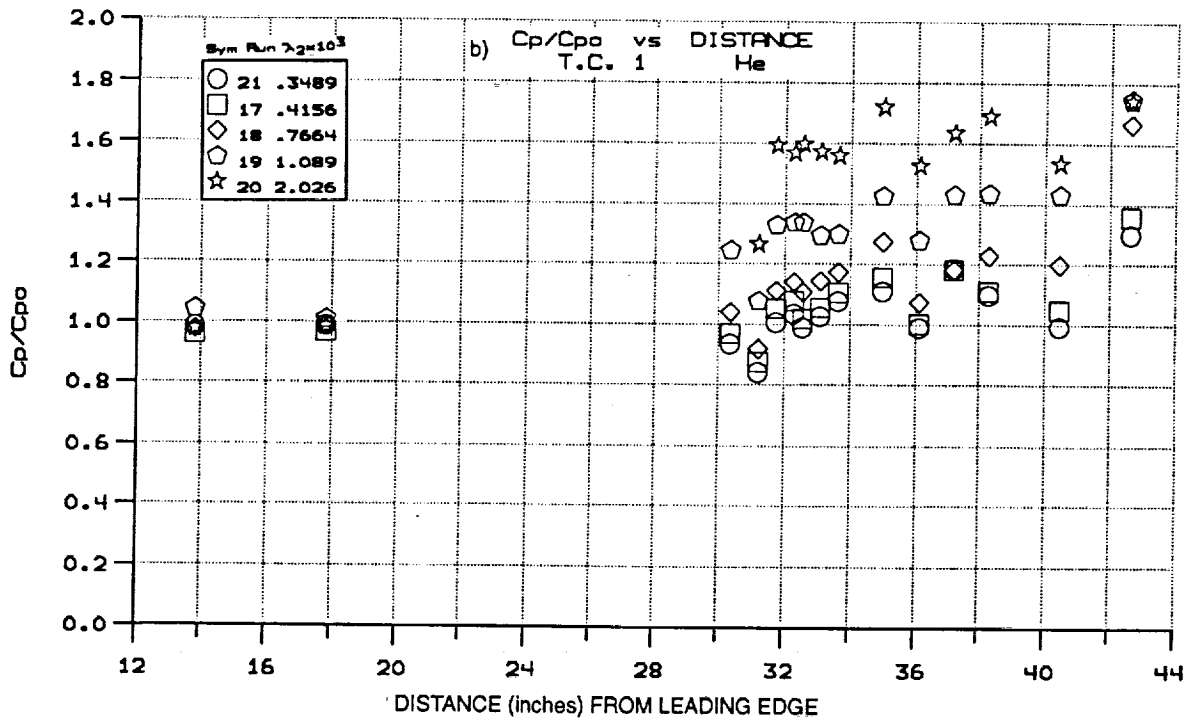
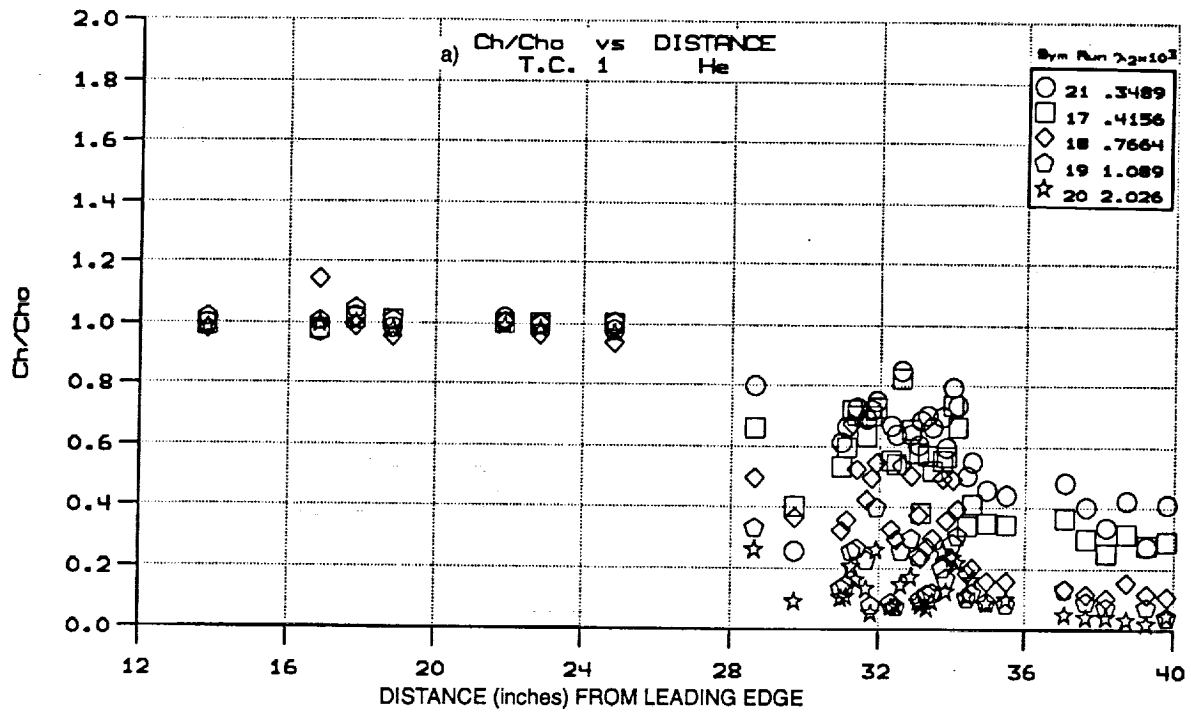


Figure 12 HEAT TRANSFER AND PRESSURE DISTRIBUTIONS ALONG FLAT PLATE -
TRANSPIRATION SURFACE FOR HELIUM COOLANT AT MACH 6

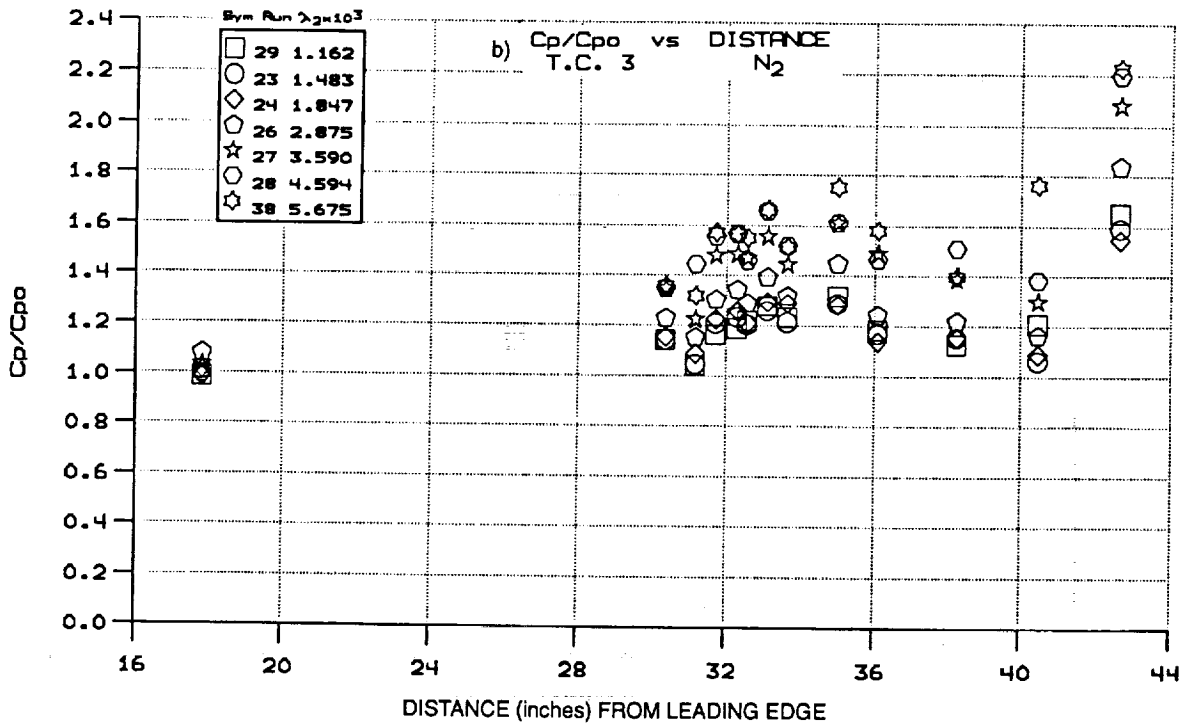
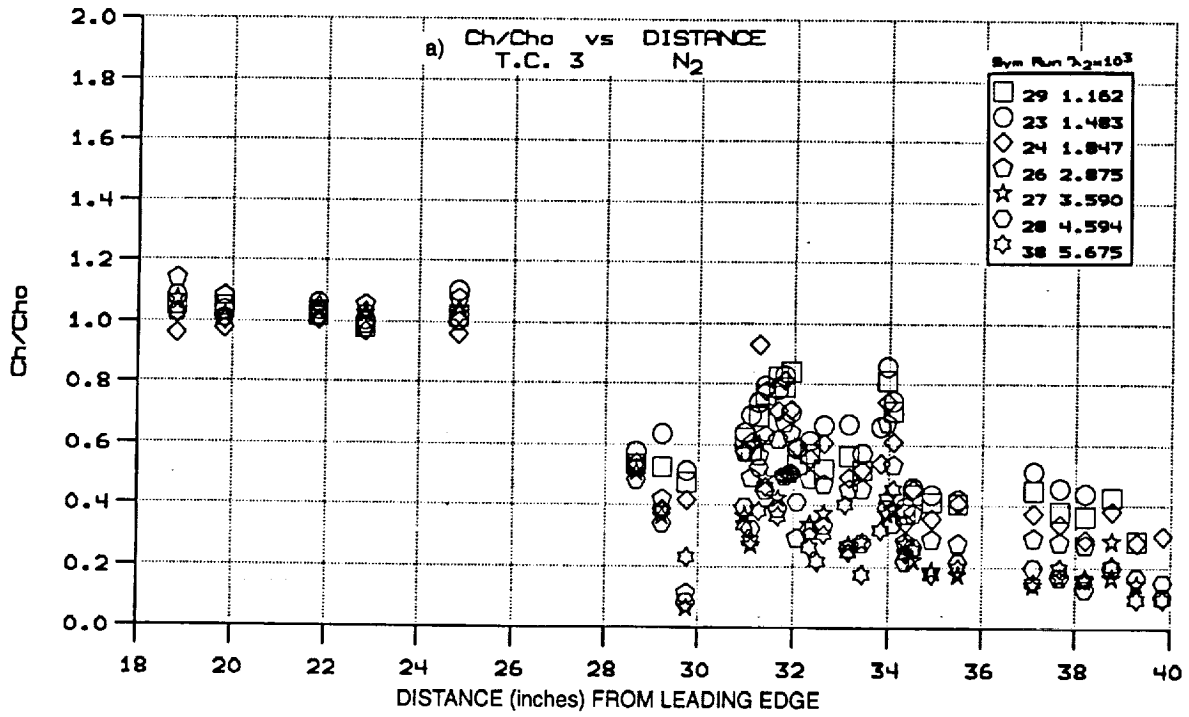


Figure 13 HEAT TRANSFER AND PRESSURE DISTRIBUTIONS ALONG FLAT PLATE –
TRANSPIRATION-COOLED SURFACE FOR NITROGEN COOLANT AT MACH 8

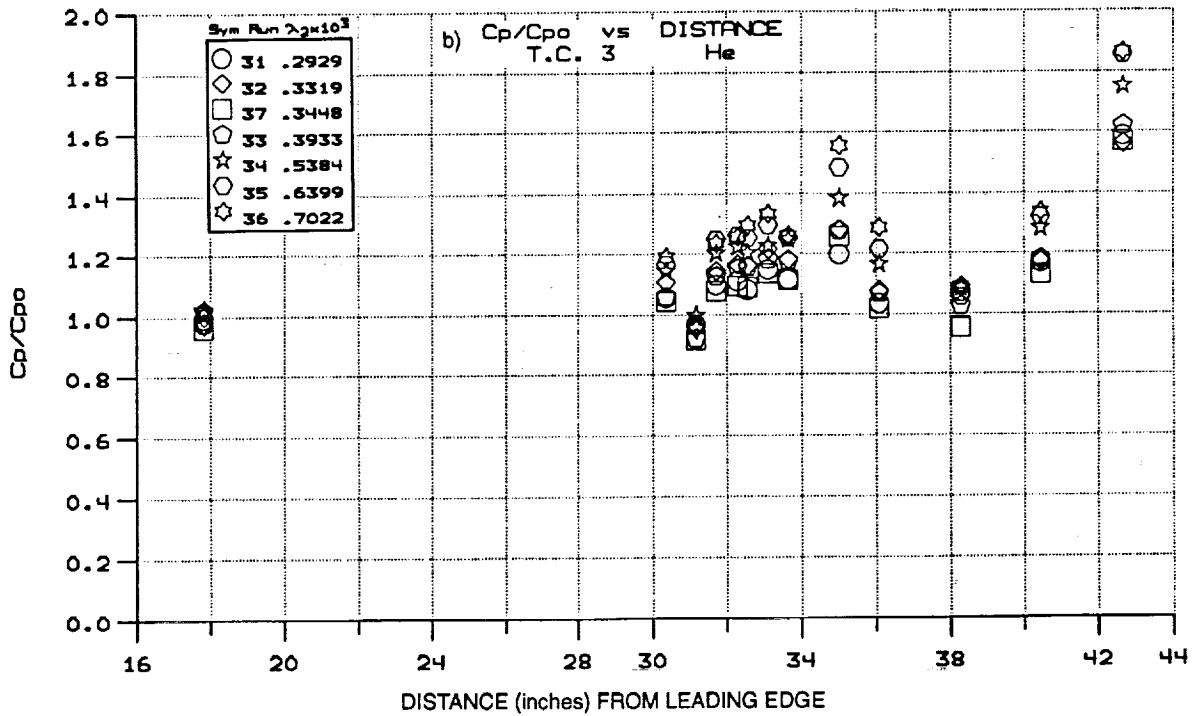
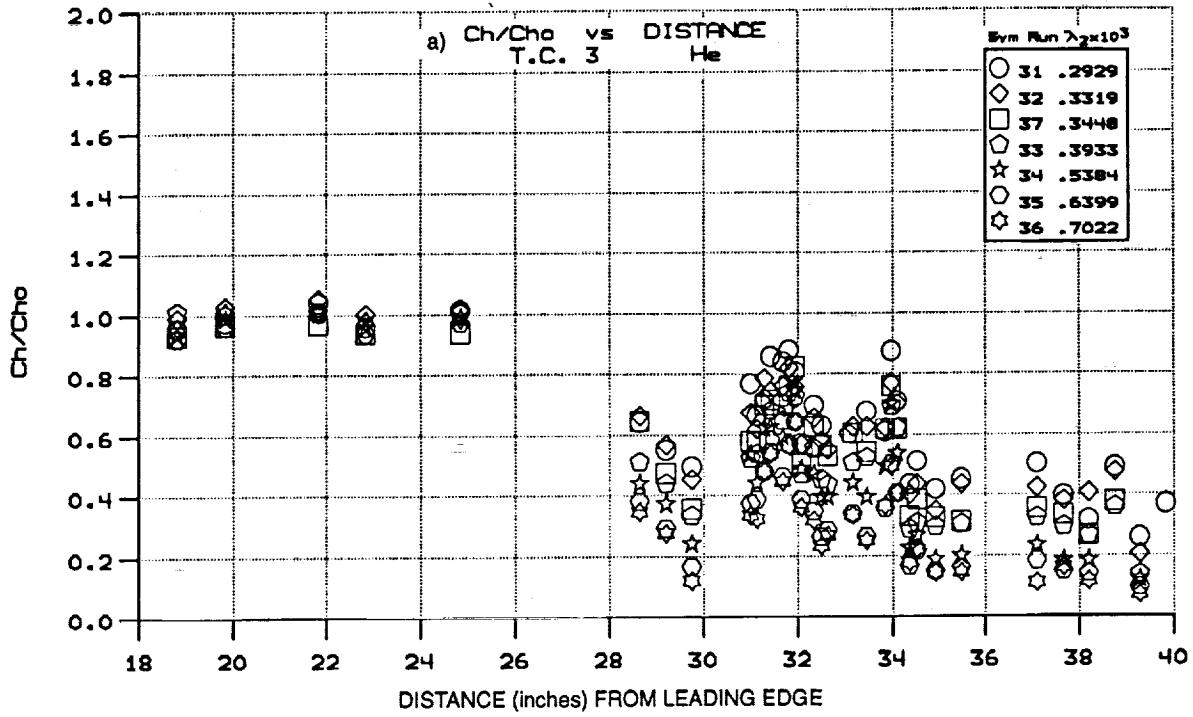


Figure 14 HEAT TRANSFER AND PRESSURE DISTRIBUTIONS ALONG FLAT PLATE -
TRANSPIRATION-COOLED MODEL FOR HELIUM COOLANT AT MACH 8

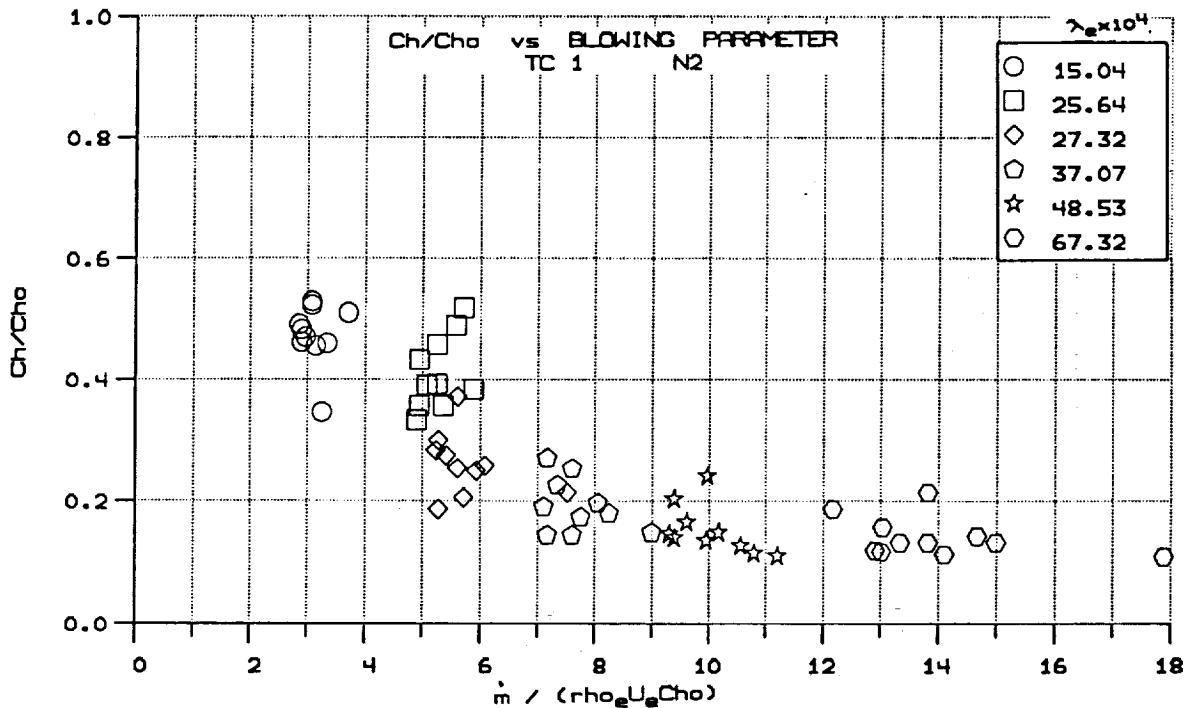


Figure 15 CORRELATION OF HEAT TRANSFER MEASUREMENT WITH TRANSPIRATION COOLING IN TERMS OF SIMPLE BLOWING PARAMETER FOR NITROGEN COOLANT AT MACH 6

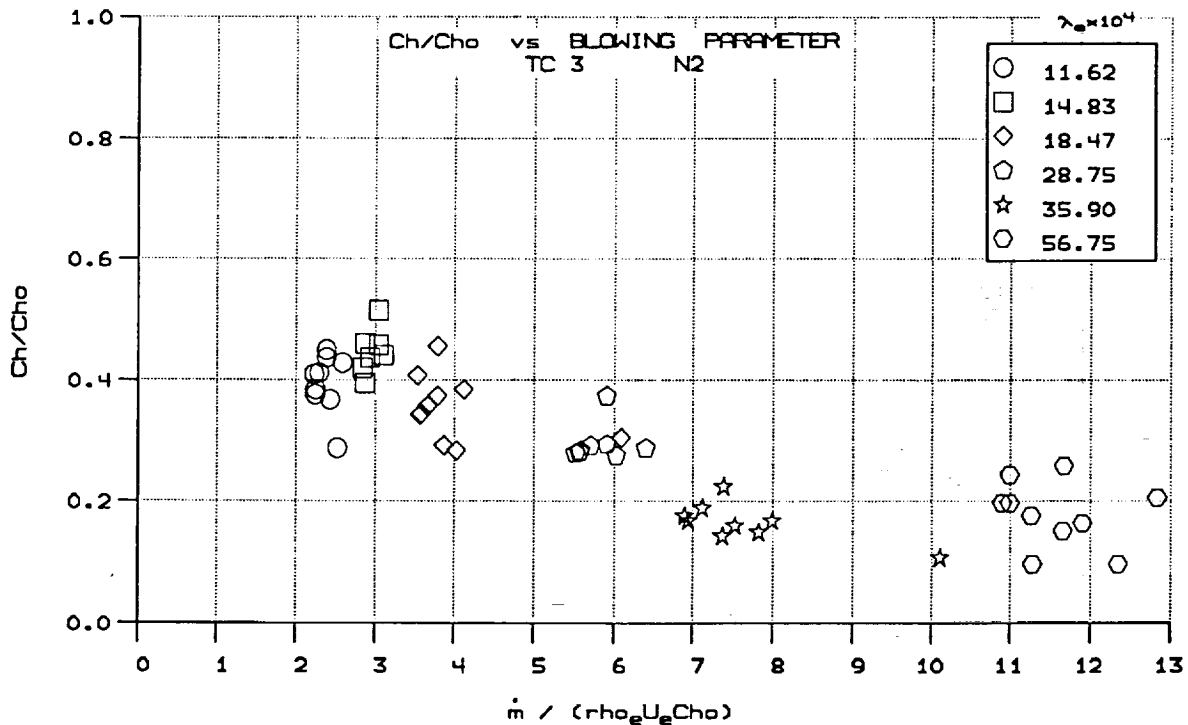


Figure 16 CORRELATION OF HEAT TRANSFER MEASUREMENT WITH TRANSPIRATION COOLING IN TERMS OF SIMPLE BLOWING PARAMETER FOR NITROGEN COOLANT AT MACH 8

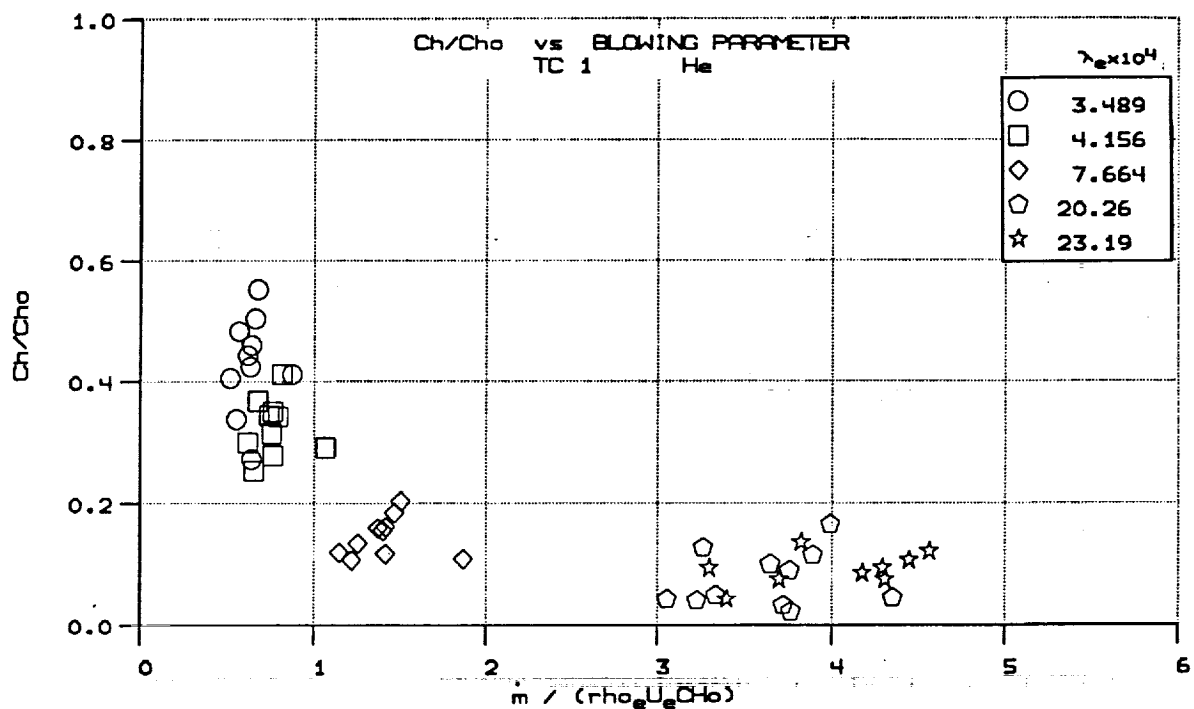


Figure 17 CORRELATION OF HEAT TRANSFER MEASUREMENTS WITH TRANSPIRATION COOLING IN TERMS OF SIMPLE BLOWING PARAMETER FOR HELIUM COOLANT AT MACH 6

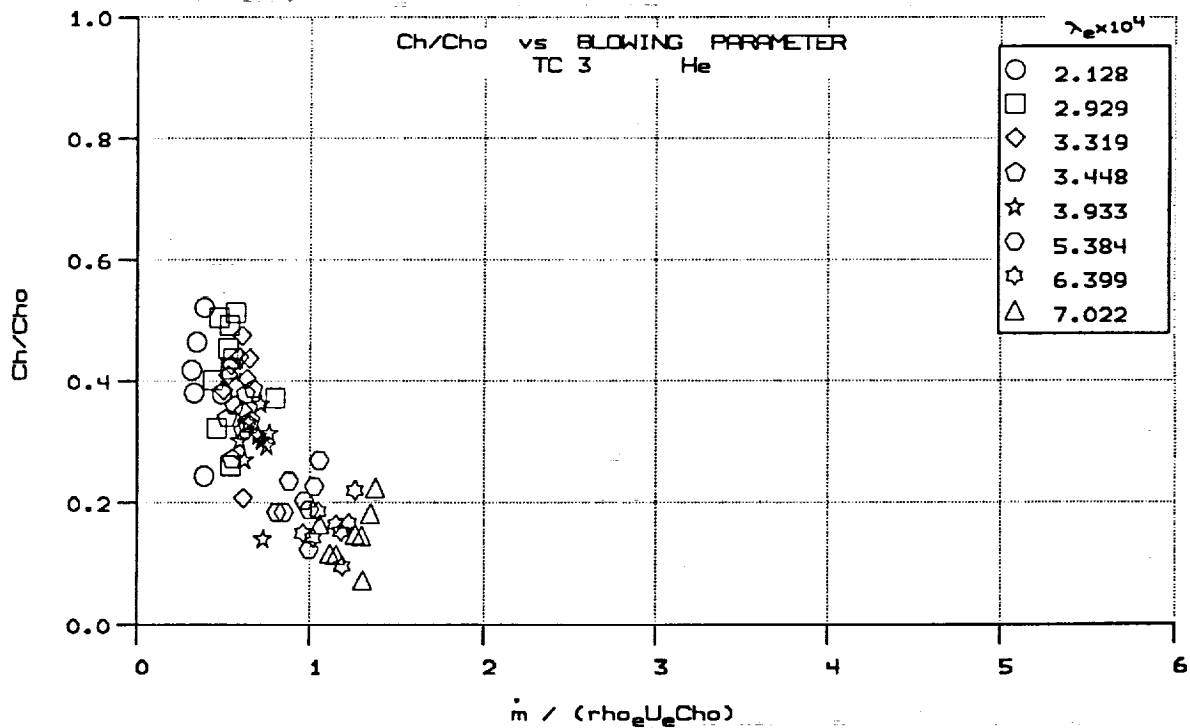


Figure 18 CORRELATION OF HEAT TRANSFER MEASUREMENTS WITH TRANSPIRATION COOLING IN TERMS OF SIMPLE BLOWING PARAMETER FOR HELIUM COOLANT AT MACH 8

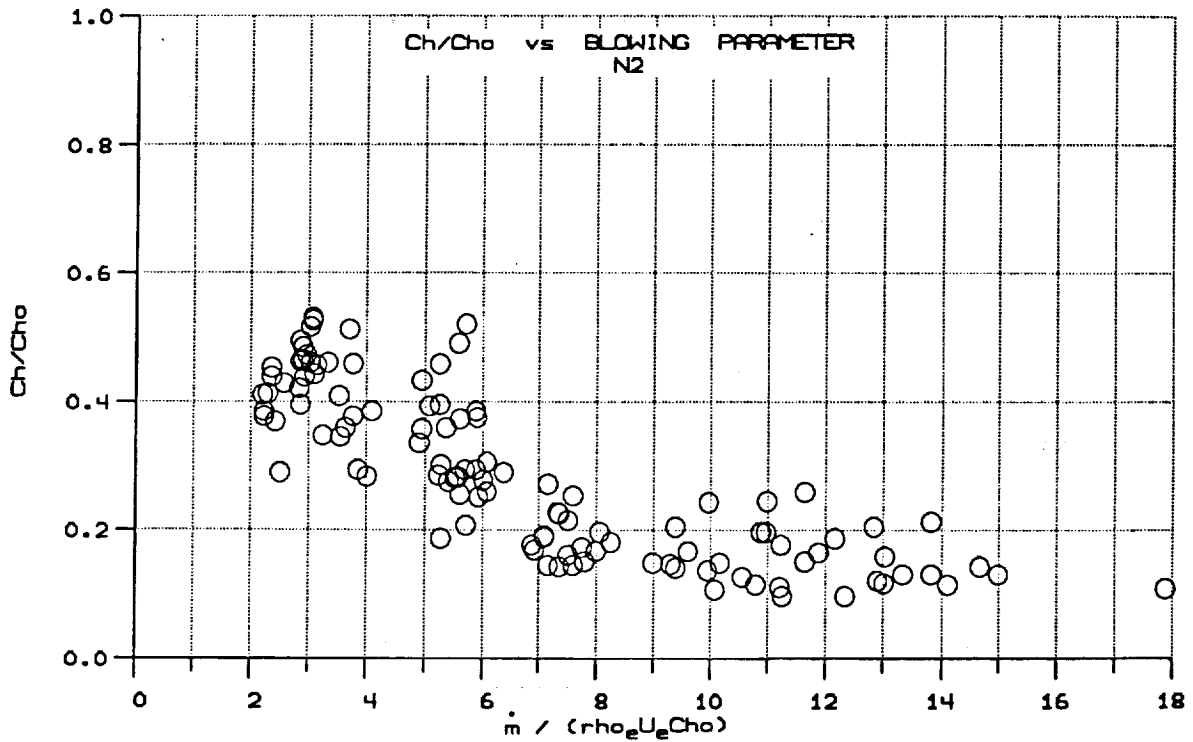


Figure 19 CORRELATION OF HEAT TRANSFER MEASUREMENTS WITH TRANSPIRATION COOLING AT BOTH MACH 6 AND 8 FOR NITROGEN COOLANT

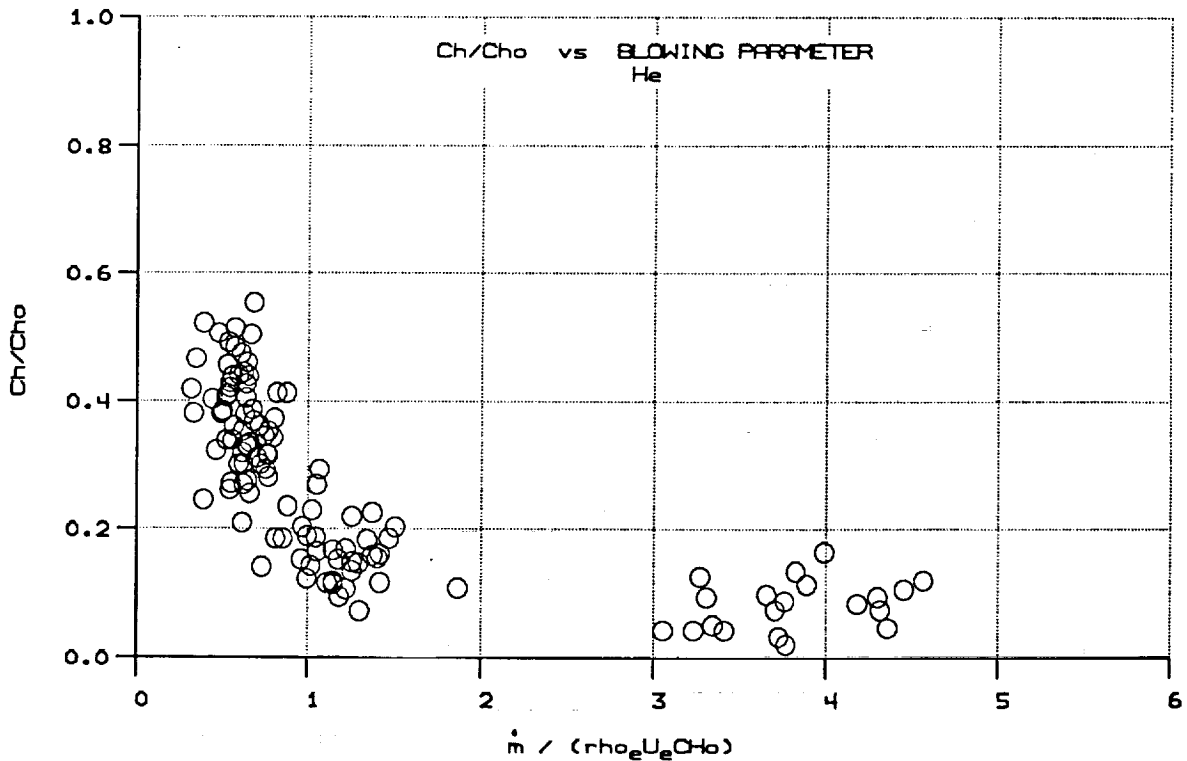


Figure 20 CORRELATION OF HEAT TRANSFER MEASUREMENT WITH TRANSPIRATION COOLING AT BOTH MACH 6 AND 8 FOR HELIUM COOLANT

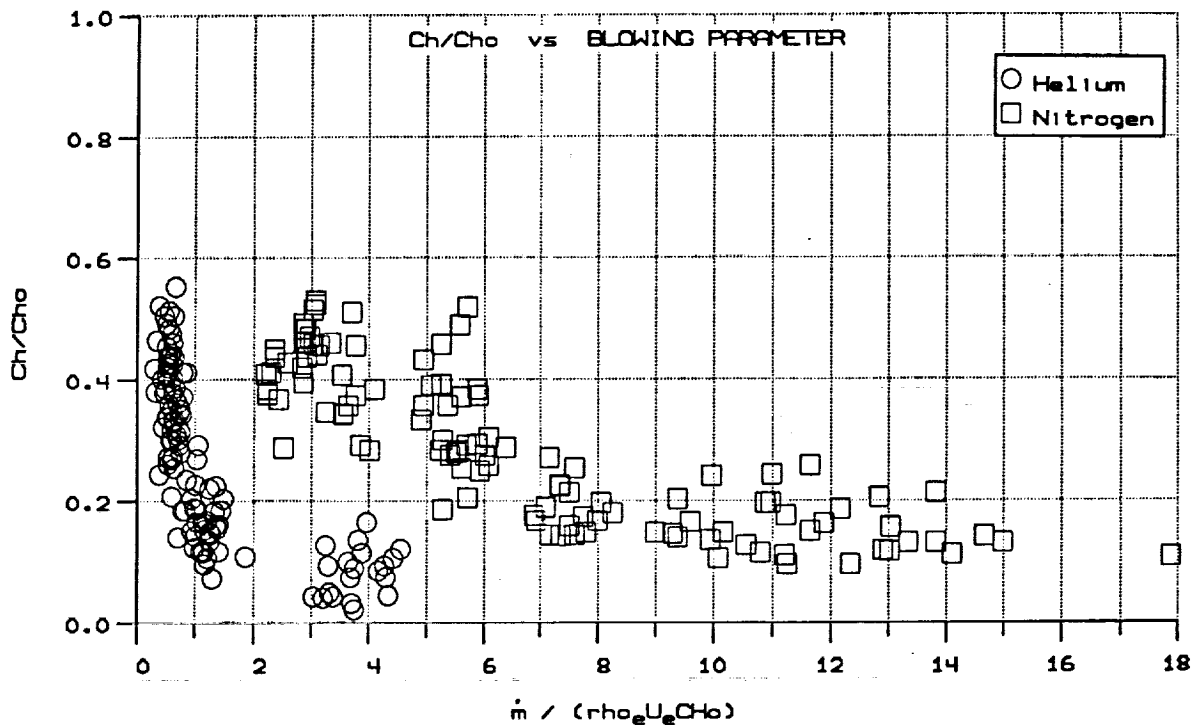


Figure 21 CORRELATION OF HEAT TRANSFER MEASUREMENTS FOR NITROGEN AND HELIUM COOLANTS WITH SIMPLE BLOWING PARAMETER

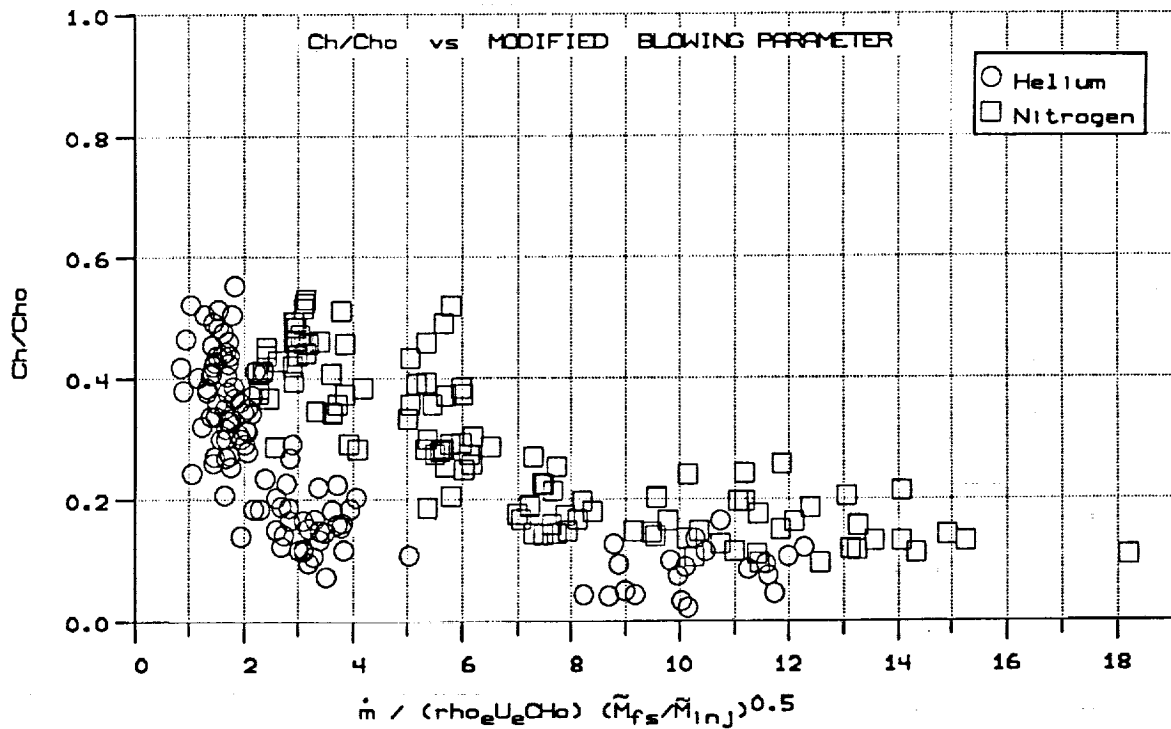


Figure 22 CORRELATION OF ALL TRANSPIRATION-COOLING HEAT TRANSFER MEASUREMENTS WITH MODIFIED BLOWING PARAMETER

heat than nitrogen for the same mass-flow rate; the lower molecular weight of helium resulted in a larger blockage effect, because there was a greater volume of helium in the boundary layer for the same mass flow rate. To account for these effects, we employed modified blowing parameters, as shown in Figures 22 through 24, to correlate the measurements from both injectant gases and the two test conditions. The measurements made in this program are brought into reasonable alignment using the correlation parameters shown in Figure 24. We have been able to correlate the changes in heat transfer with blowing rate and injectant properties in the form

$$\frac{C_{H_0} - C_{H_s}}{C_{H_0}} = 0.92 (1 - e^{-B'/4}) \quad (15)$$

where B' is defined as either

$$B' = \dot{m} / (\rho_s U_s C_{H_s}) (\tilde{M}_{fs} / \tilde{M}_{inj}) \quad (16)$$

or

$$B' = \dot{m} / (\rho_s U_s C_{H_s}) (C_{p_{inf}} / C_{p_{fs}})^{0.7} (\tilde{M}_{fs} / \tilde{M}_{inj})^{0.5} \quad (17)$$

The conditions under which boundary layer blowoff occurs and the effects of injectant properties on this phenomenon are of significant interest to designers. From correlation of the surface-pressure ratio with the mass-addition parameter, it is clear that pressure measurements can be used to define when blowoff occurs, and that the injectant properties can significantly influence this process. Modifying the blowing parameter by incorporating the molecular weight to allow for the different volumetric flow rates for the same mass-flow rate, as shown in Figure 25, also brings the sets of measurements into good alignment. It is also noted that, as shown in Figure 26, all the heat transfer measurements correlate well with this parameter, indicating the importance of blockage effects on heating reduction.

3.4 STUDIES OF THE TRANSPIRATION COOLING OF SHOCK/BOUNDARY LAYER INTERACTION REGIONS

3.4.1 Introduction

The major objective of this phase of the experimental program was to obtain heat transfer and pressure measurements with which we could determine the levels of mass addition required to cancel the increase in heating generated downstream of the incident shock in a region of shock-wave/transpiration-cooled turbulent boundary layer interaction. For these values of mass-addition levels, we also sought to

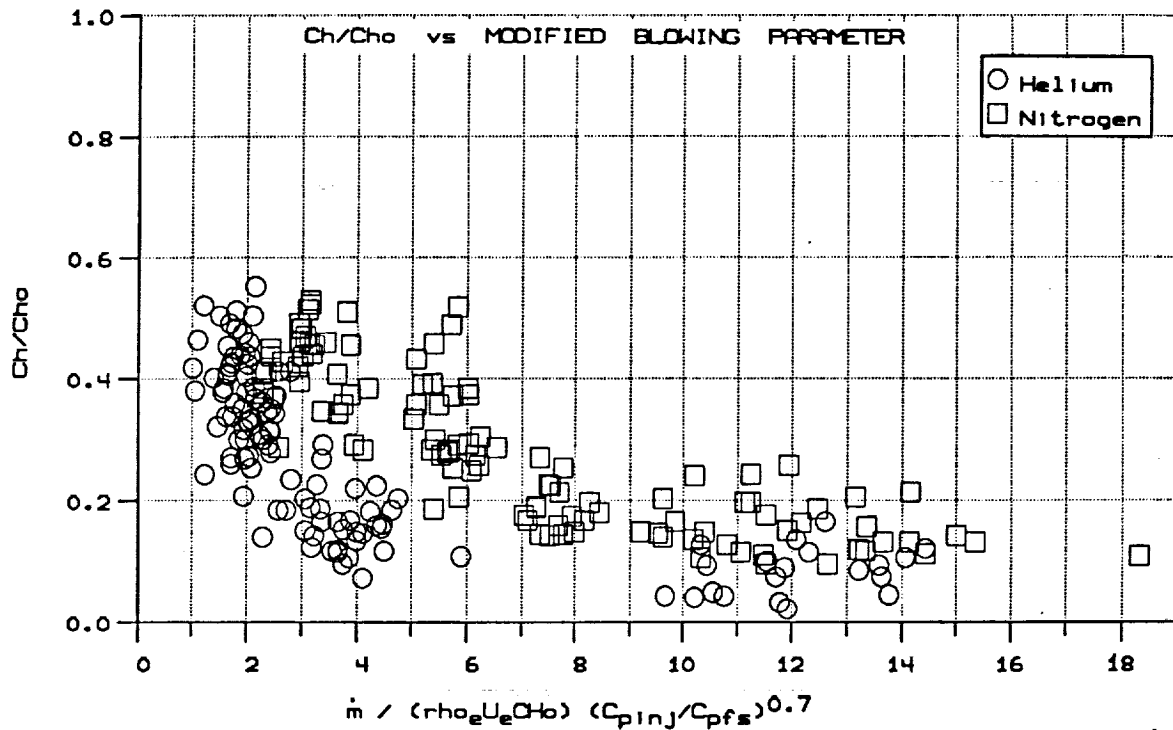


Figure 23 CORRELATION OF HEAT TRANSFER MEASUREMENTS FOR NITROGEN AND HELIUM COOLANTS WITH SIMPLE BLOWING PARAMETER

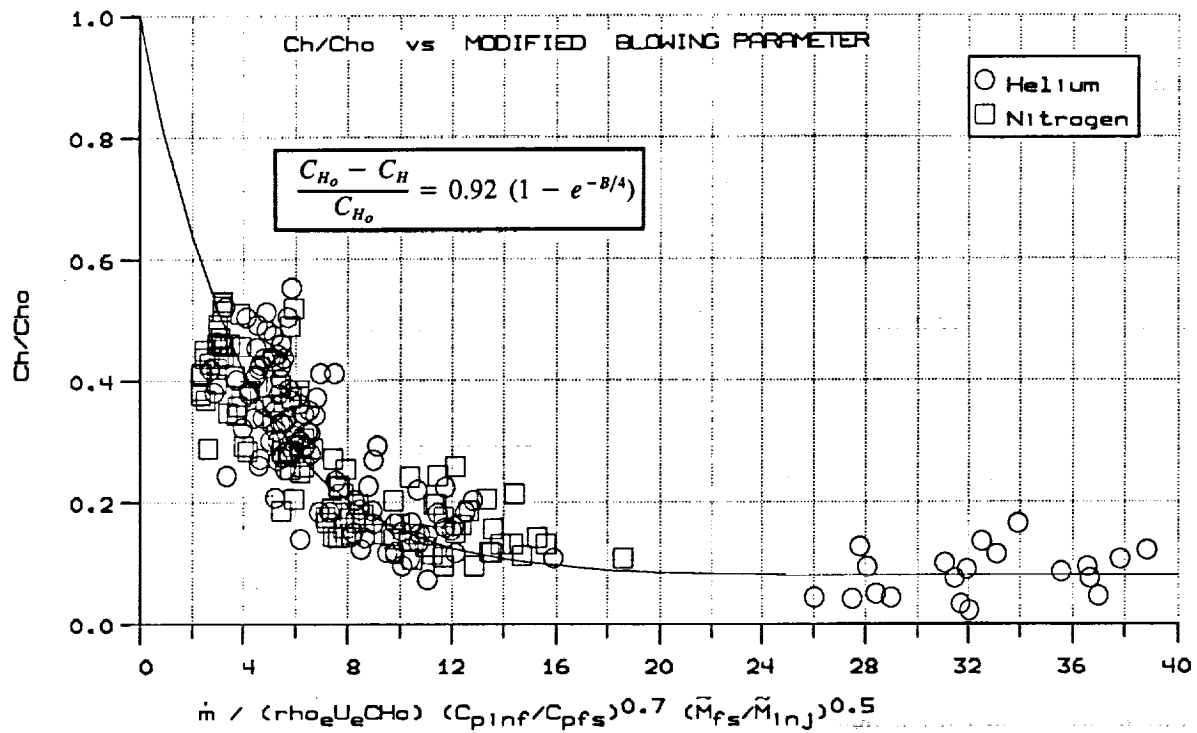


Figure 24 CORRELATION OF ALL TRANSPIRATION-COOLING HEAT TRANSFER MEASUREMENTS WITH MODIFIED BLOWING PARAMETER

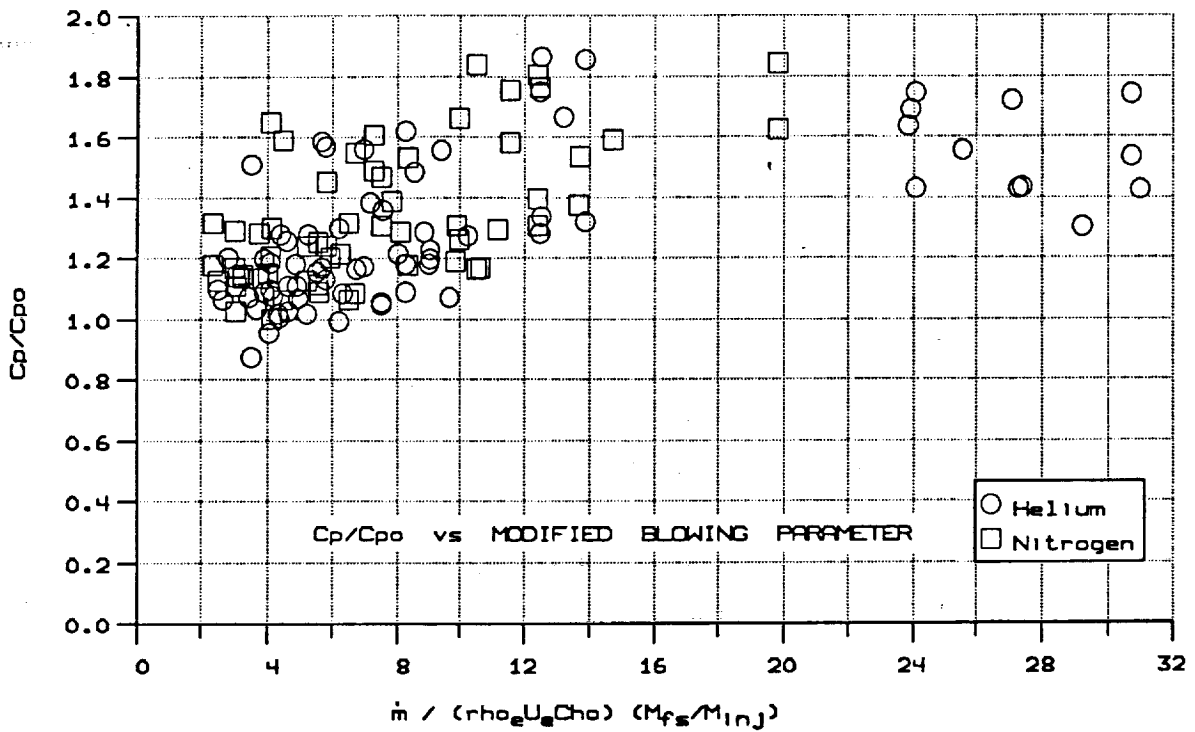


Figure 25 CORRELATION OF PRESSURE MEASUREMENTS OVER TRANSPIRATION-COOLED SURFACE WITH MODIFIED BLOWING PARAMETER

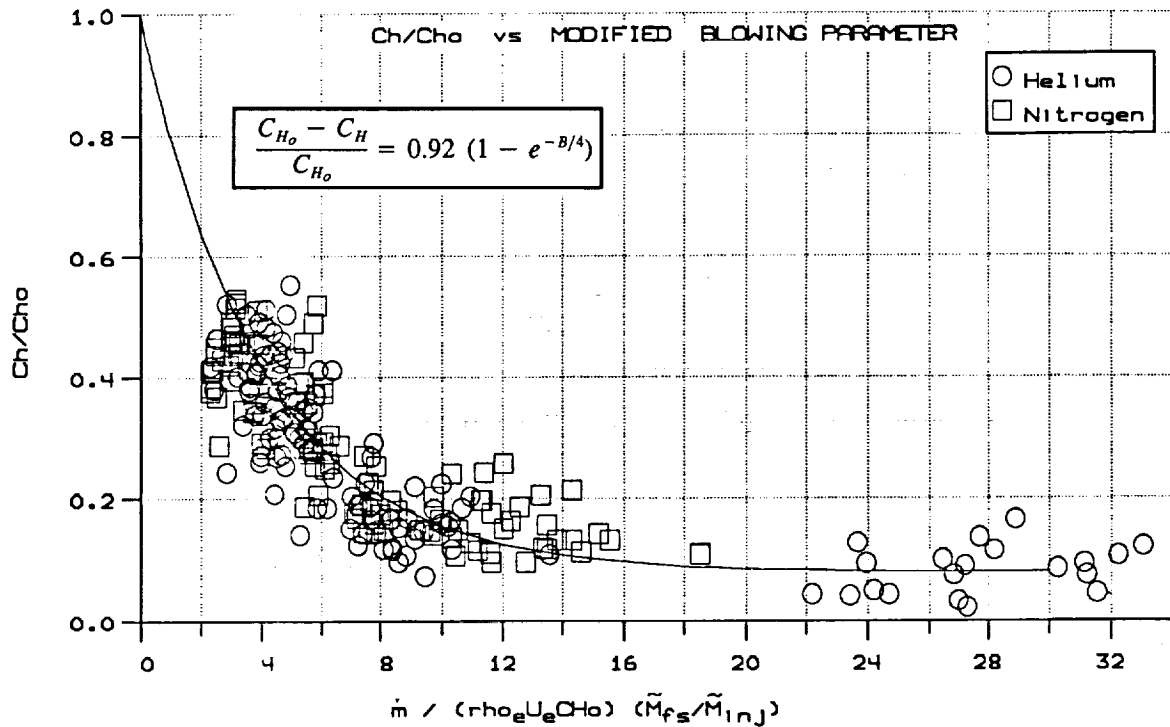


Figure 26 CORRELATION OF HEAT TRANSFER MEASUREMENTS OVER TRANSPIRATION-COOLED SURFACE WITH MODIFIED BLOWING PARAMETER

determine the degree to which the shock-wave/transpiration-cooled layer interaction resulted in significant distortions in the viscous and inviscid flowfields. This investigation was conducted at the same two freestream conditions (Mach 6 and Mach 8) at which the earlier studies without shock interaction were run. The test gas was air, and both helium and nitrogen coolants were injected through the porous surface of the model. Externally generated shocks were introduced by planar shock generators mounted above the transpiration-cooled plate. Shock generator angles of 5° , 7° , and 10° were selected so that, in the absence of transpiration cooling on a smooth surface, the strength of the interactions would be such that attached, incipient separated, and well-separated regions, respectively, would be generated close to the point of shock impingement. The position of the point of shock impingement on the transpiration-cooled surface was selected by adjusting the shock-generator plate such that the incident shock fell in the region of highest instrumentation density. As discussed earlier, the pressure and heat transfer instrumentation were positioned in the transpiration-cooled surface such that the maximum density of gages was in the middle of the second, transpiration-cooled section of the model. In these experimental studies, we typically varied the coolant level through the interaction regions such that the mass-addition levels introduced in and downstream of the point of shock impingement were significantly larger than those employed upstream of this point. In this way, we sought to bring the heating levels along each of the transpiration-cooled segments in alignment with those upstream of the interaction over the non-porous leading-edge flat plate. Here, our key objective was to determine how much coolant was required to achieve relatively uniform heating along the entire model and how the viscous and inviscid flow structure in the interaction region changed with strong cooling.

A summary of the model configurations and freestream conditions at which the measurements were obtained is presented in Table 2. The experimental studies conducted at the Mach 8 condition are listed for runs 41 through 76, while those at Mach 6 are listed for runs 77 to 91. As can be seen from this table, we systematically investigated cooling requirements for different incident-shock strengths at each of the two freestream conditions, employing a range of blowing rates to achieve the stated objectives for both nitrogen and helium coolants. In all of these studies, the test conditions were such that the boundary layer was fully turbulent over the smooth, flat plate upstream of the region of shock-wave/transpiration-cooled layer interaction.

3.4.2 Studies of Shock-Wave/Coolant-Layer Interaction at Mach 6

The heat transfer and pressure measurements made in the studies conducted at the Mach 6 test condition are presented in Figures 27 through 32. Shown first in Figures 27 and 28 are the sets of measurements taken with a 5.3° shock generator. Figures 27a and 27b show the heat transfer and pressure measurements obtained for a nitrogen coolant. For the no-blowing case, the shock interaction caused a

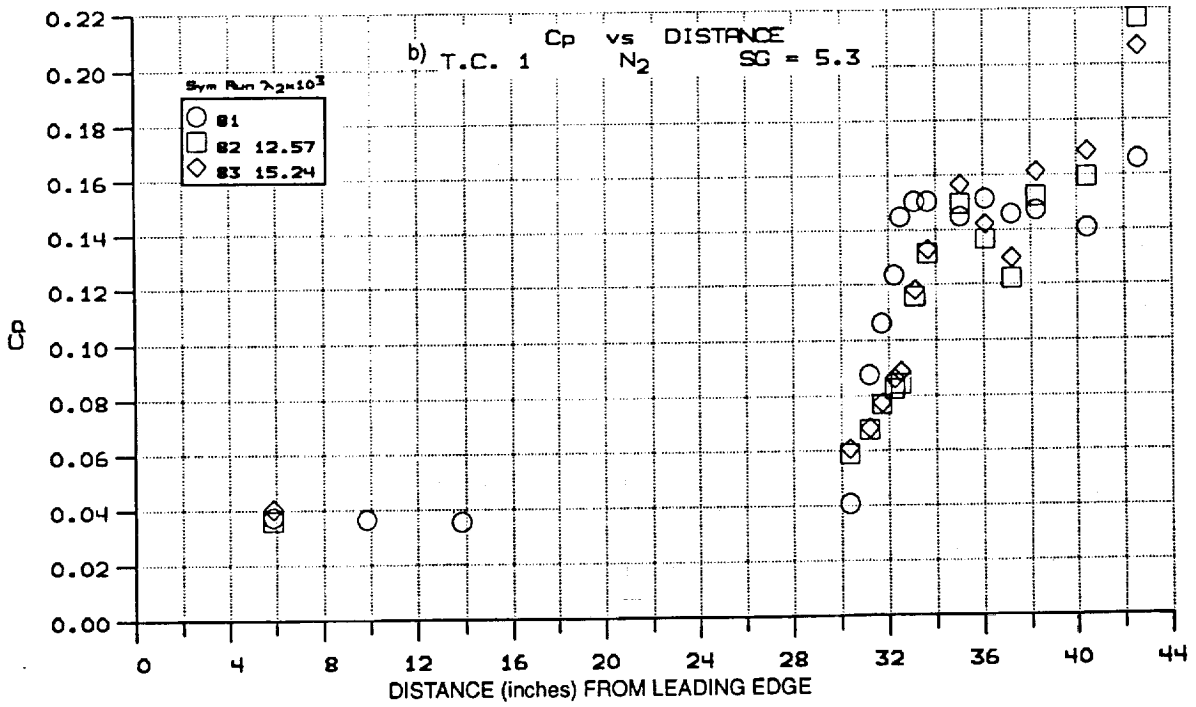
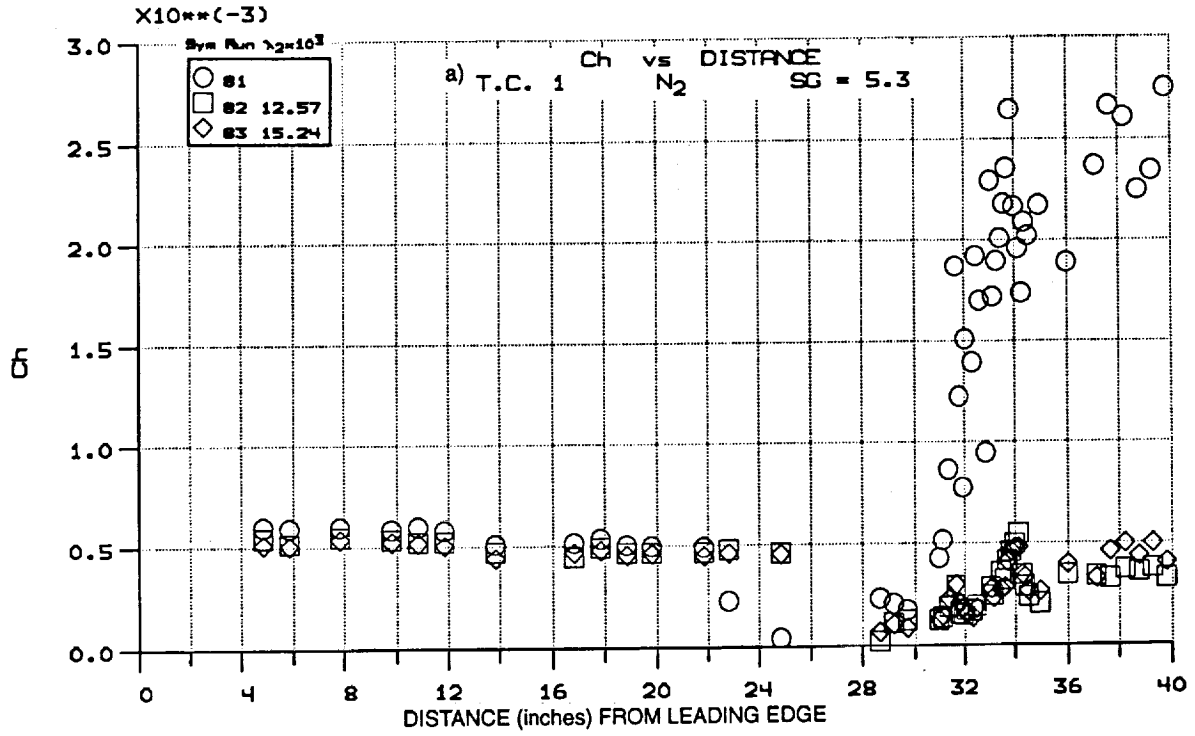


Figure 27 HEAT TRANSFER AND PRESSURE MEASUREMENTS AT MACH 6 ON NITROGEN-COOLED TRANSPIRATION SURFACE WITH SHOCK INTERACTION FROM 5.3° SHOCK GENERATOR

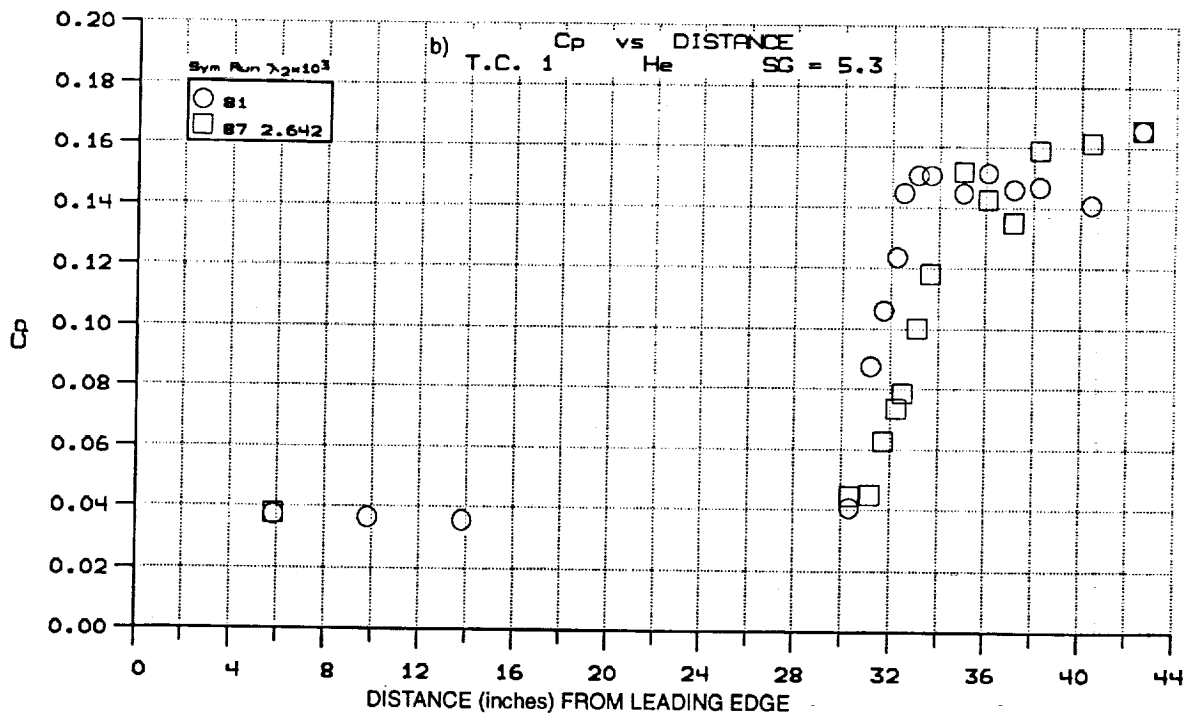
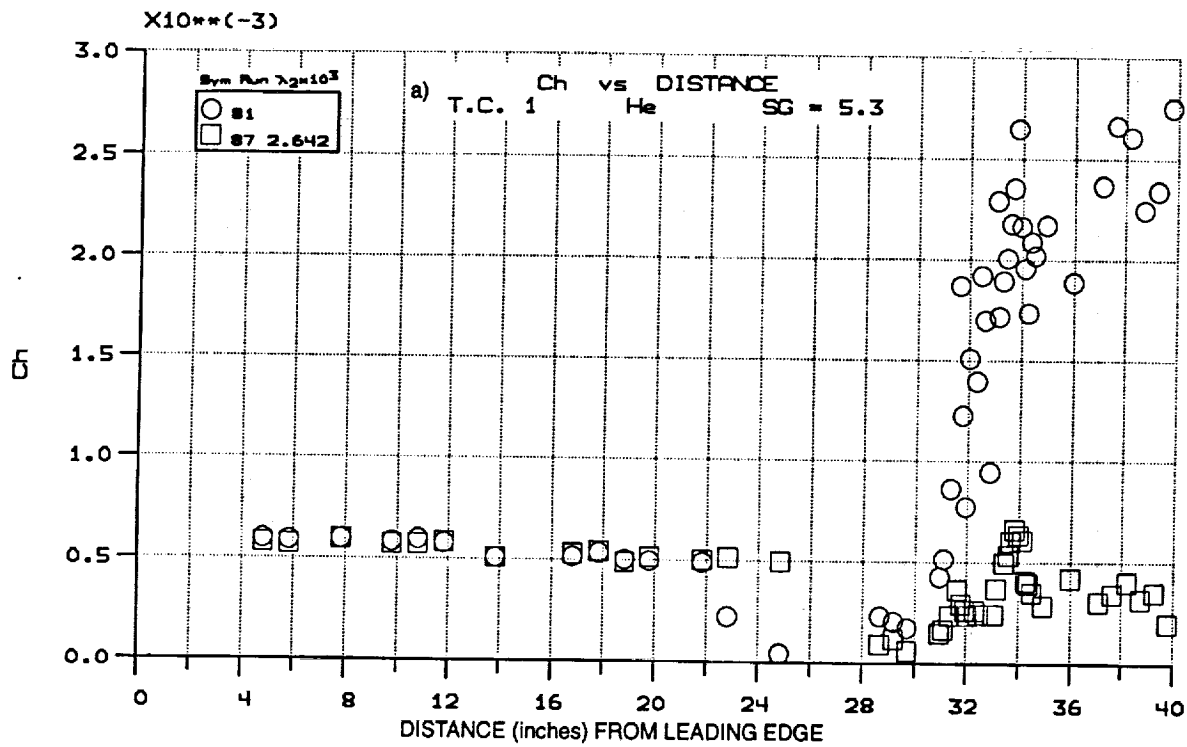


Figure 28 HEAT TRANSFER AND PRESSURE MEASUREMENTS AT MACH 6 ON HELIUM-COOLED TRANSPARATION SURFACE WITH SHOCK INTERACTION FROM 5.3° SHOCK GENERATOR

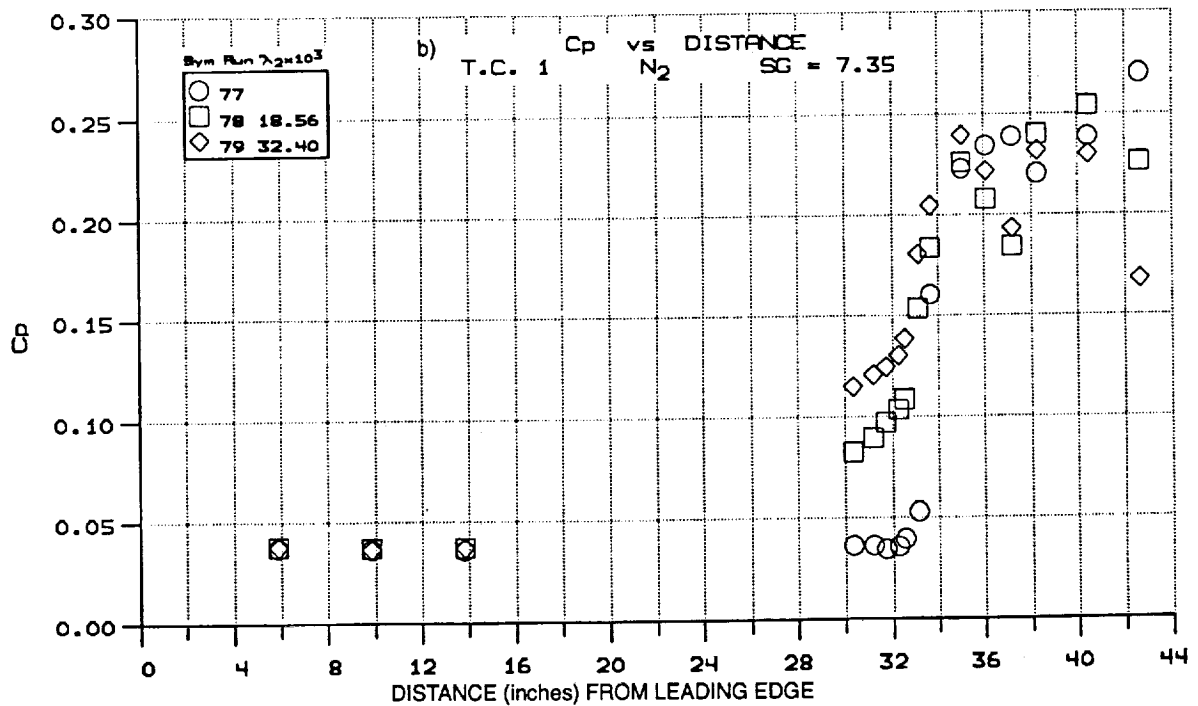
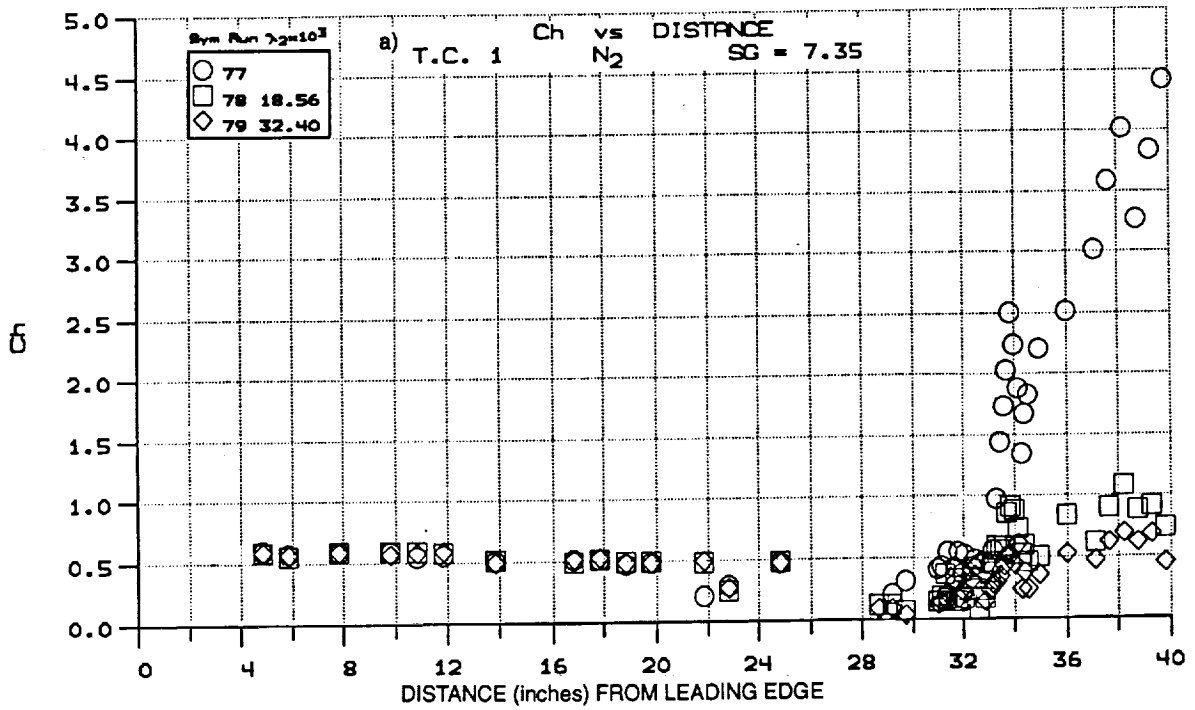


Figure 29 HEAT TRANSFER AND PRESSURE MEASUREMENTS AT MACH 6 ON NITROGEN-COOLED TRANSPARATION SURFACE WITH SHOCK INTERACTION FROM 7.35° SHOCK GENERATOR

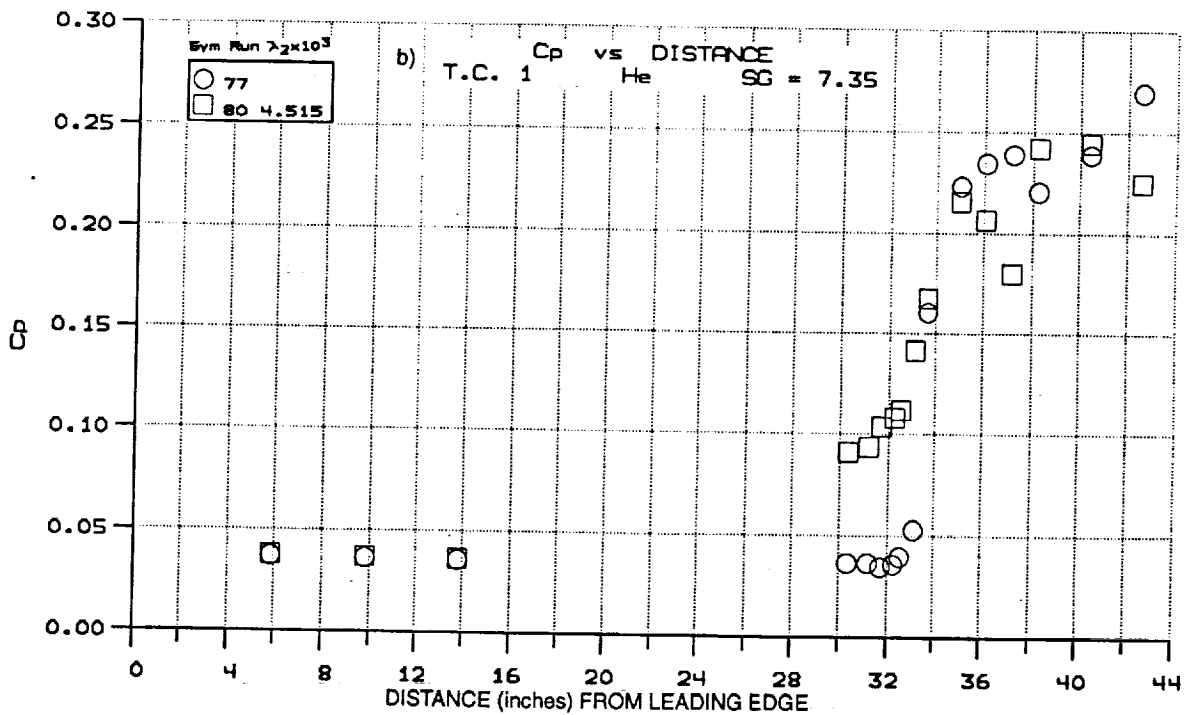
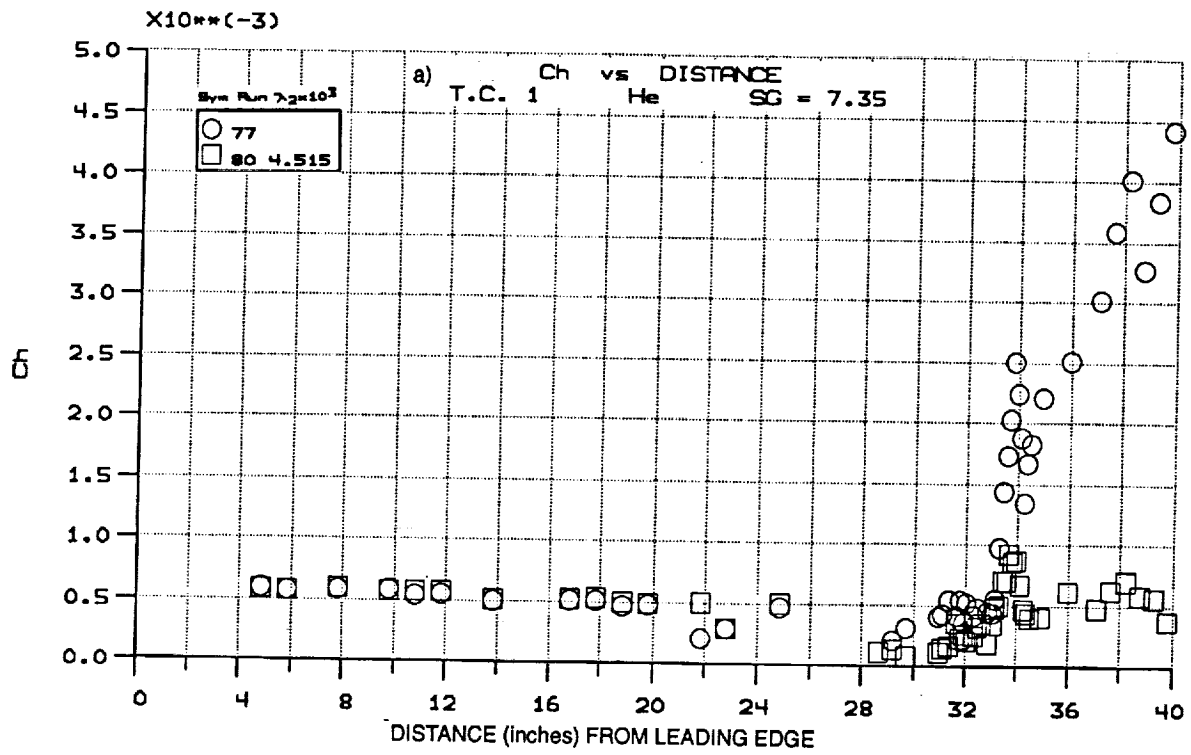


Figure 30 HEAT TRANSFER AND PRESSURE MEASUREMENTS AT MACH 6 ON HELIUM-COOLED
 TRANSPIRATION SURFACE WITH SHOCK INTERACTION FROM 7.35° SHOCK
 GENERATOR

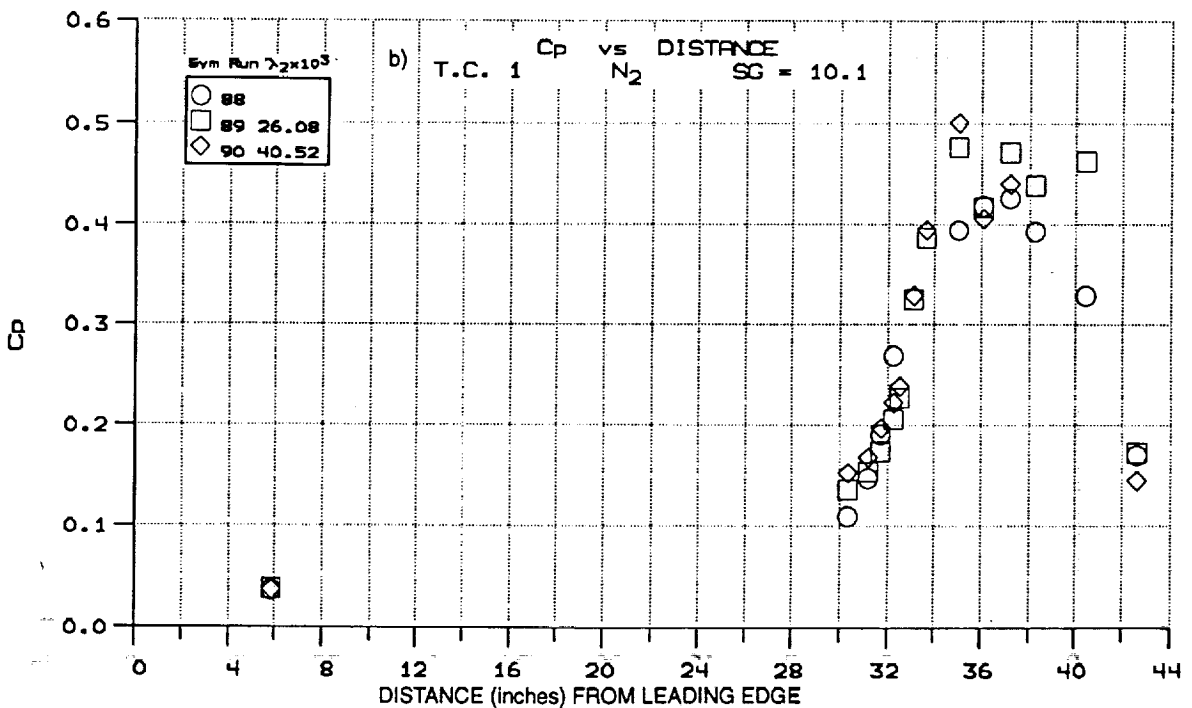
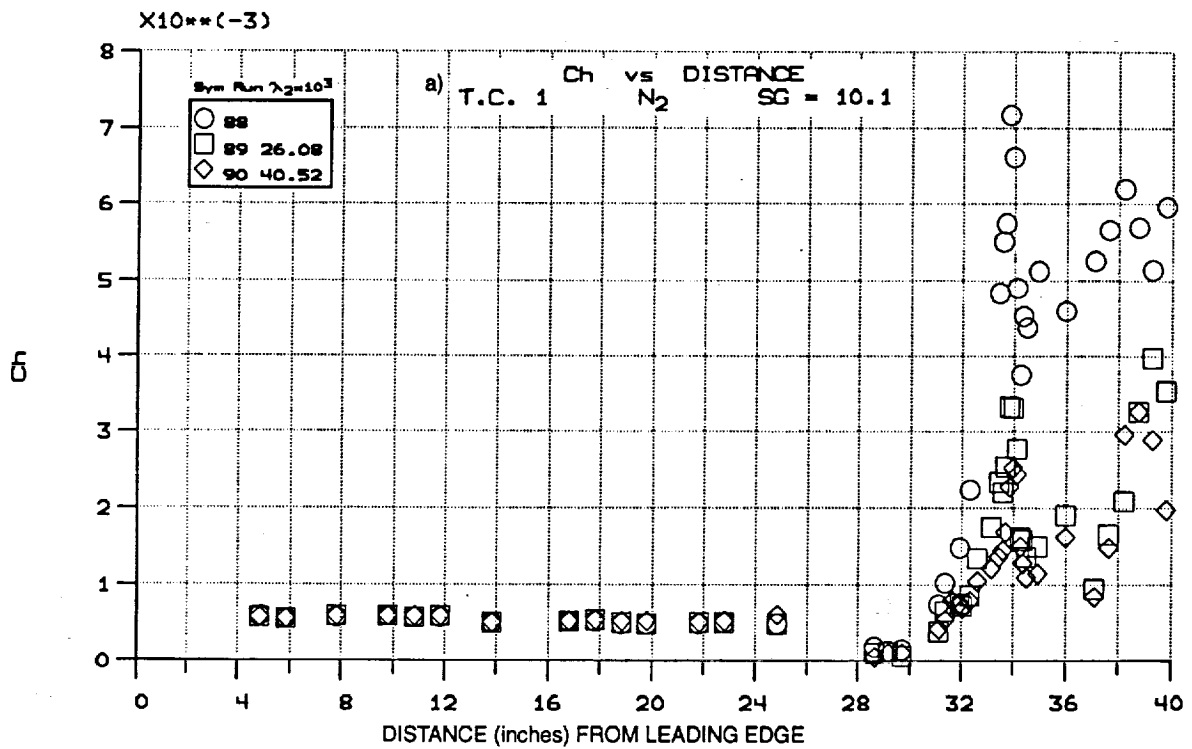


Figure 31 HEAT TRANSFER AND PRESSURE MEASUREMENTS AT MACH 6 ON NITROGEN-COOLED TRANSPIRATION SURFACE WITH SHOCK INTERACTION FROM 10.1° SHOCK GENERATOR

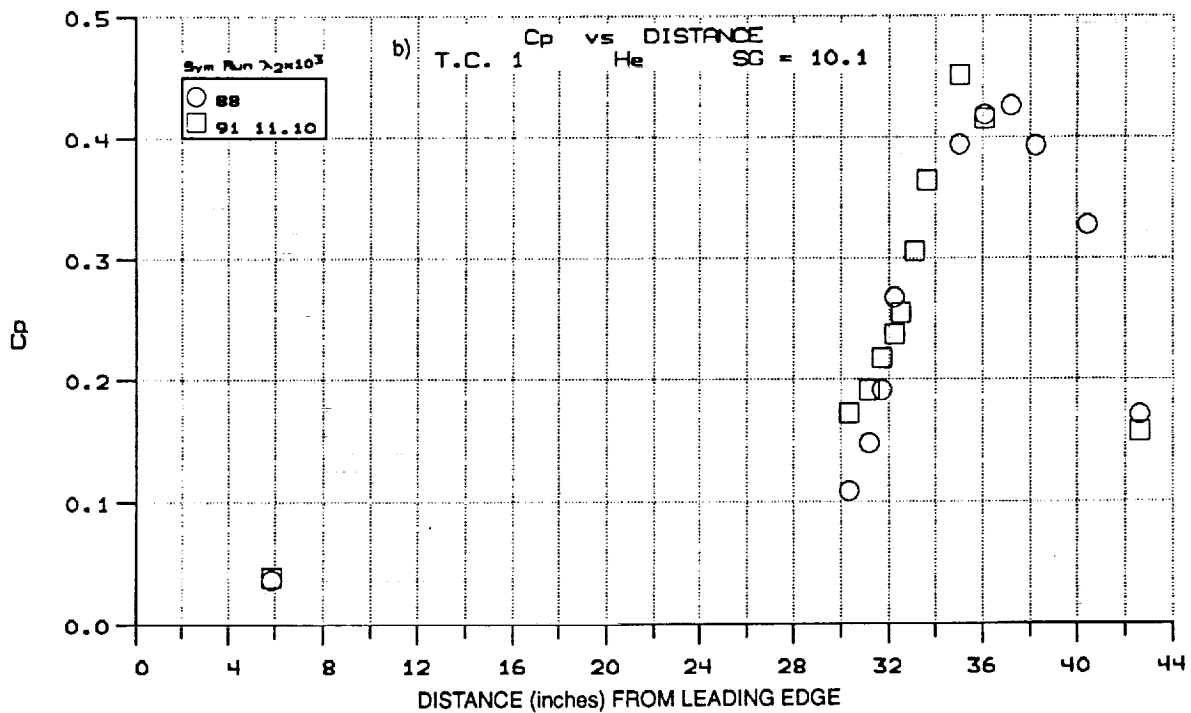
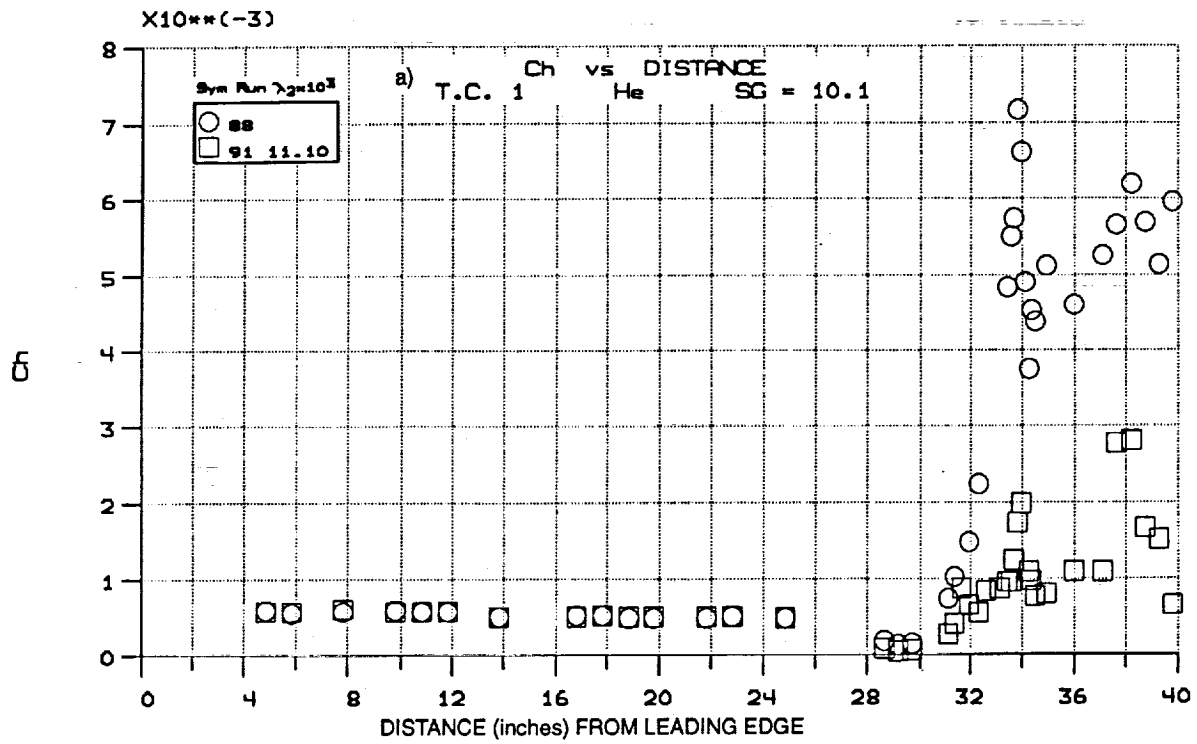


Figure 32 HEAT TRANSFER AND PRESSURE MEASUREMENTS AT MACH 6 ON HELIUM-COOLED TRANSPARATION SURFACE WITH SHOCK INTERACTION FROM 10.1° SHOCK GENERATOR

pressure increase that was fed from downstream of the shock through the transpiration-cooled surface, introducing air into the sublayer upstream of the shock interaction. In this region the heat transfer was reduced dramatically, even with coolant addition; however, it can be seen from the pressure distribution shown in Figure 27b, that the pressure upstream of the shock was not significantly modified by this influx of freestream gas into the base of the boundary layer. As can be seen from Figure 27a, it was only necessary to introduce nitrogen coolant at a rate of less than 5% to reduce the heating levels downstream of shock impingement to less than those upstream of the shock on the smooth flat plate. For these blowing rates, the pressure distributions shown in Figure 27b indicate that there was little disturbance induced in the inviscid flow by the introduction of the coolant. The measurements shown in Figures 28a and 28b demonstrate that employing helium as a coolant resulted in a reduction of heating behind the incident shock to the upstream flat-plate value for coolant mass-flow rates that were close to one-third of those for nitrogen. Again, as can be seen from the pressure distributions in Figure 28b, the pressures upstream of shock impingement were not significantly modified by the introduction of gas through the transpiration surface from behind the incident shocks, with or without significant cooling. Even when the strength of the interaction was increased by employing a shock generator angle of 7.35° , it can be seen from Figures 29 and 30 that there was very little upstream influence of the shock in the absence of transpiration cooling. In a manner similar to that discussed above, it can be seen from Figure 29 and Figure 30, that a decrease in heat transfer rate upstream of the incident shock (as seen for this case) resulted from flow under the porous surface from one side of the shock to the other. Once coolant was introduced, there was a small upstream influence as a result of flow separation, which is evident from the appearance of a plateau in the pressure distribution (see Figures 29b and 30b). However, from the schlieren photographs (See Appendix A), this is seen not to cause a strong distortion in the inviscid flow. The pressure levels and distribution downstream of shock impingement were basically uninfluenced by the introduction of coolant for these interaction strengths. As can be seen, the heat transfer downstream of the incident shock can be reduced to flat-plate levels by the introduction of 5% and 2.5% of the freestream mass-flow rate of nitrogen and helium coolant gases, respectively, into the base of the boundary layer; see Figures 29a and 30a. Again, the pressures downstream of the incident shock were relatively uninfluenced by coolant addition (see Figures 29b and 30b).

For the studies run with the 10.5° shock generator, the flow upstream of the point of shock impingement was fully separated in the absence of transpiration cooling, and the separated region increased in size as coolant was added. The heat transfer and pressure measurements obtained for this shock generator configuration are shown in Figures 31 and 32. Both sets of measurements indicate that the flow was separated in the interaction region; however, the size or properties of the interaction region did not appear to be strongly influenced by the rate of coolant addition. However again, as indicated in Figure 31b and 32b, the pressures downstream of the shock-impingement point were not significantly

influenced by even the largest coolant flow rates employed downstream of shock impingement. For these, the strongest of the interactions studied, only a 13% mass-addition level was required for the nitrogen coolant, and approximately one-half that value of helium coolant was required to return the level of heating downstream of the shock to the pre-shock flat-plate level.

3.4.3 Studies of Shock-Wave/Transpiration-Cooled Layer Interaction at Mach 8

The studies conducted at the Mach 8 freestream conditions were performed for the three shock-generator configurations employed in the Mach 6 studies. However, because of the increased Mach number, the strengths of the interactions were correspondingly stronger. Also, the leading edge of the shock generator was moved forward to place the impingement point of the incident shock in the region of high instrumentation density at the center of the second blowing section of the transpiration-cooling panels. As in the studies at Mach 6, in the absence of transpiration cooling, the interaction regions over a smooth surface were attached, incipient separated, and well separated for the shock generator angles of 5° , 7.5° , and 10.5° respectively. The distributions of heat transfer and pressure obtained in this segment of the experimental program are shown in Figures 33 through 39. In the first of this series of measurements with transpiration cooling, the incident shock was positioned just upstream of the introduction of high surface blowing rates; thus, in the heat transfer distributions shown in Figure 33a, we observe an initial increase in heating in the recompression regions before the transpiration-cooling effects reduced the heating to a relatively constant level. Shown in Figures 33 and 34 are the pressure and heat transfer distributions for the 5.25° shock generator for a range of flow rates with the nitrogen coolant. As can be seen from Figures 33b and 34b, the pressure distributions for this group of experiments demonstrate that the injection of coolant did not significantly influence the interaction between the viscous and inviscid flows.

Figure 35 shows the measurements made in the studies conducted with the 5° shock generator and the helium coolant. As we observed for the nitrogen coolant, injecting helium to bring the heat transfer downstream of the shock to the level on the flat plate did not significantly alter the pressure distribution in or downstream of the interaction region. Figures 36 and 37 shows heat transfer and pressure distributions obtained with the 7.5° shock generator. (For helium coolant fluxes approximately 1% of the freestream flux level, the heat transfer rate was readily reduced to the level before the interaction region.) As in Mach 6 studies, we observed that the pressure downstream of the interaction was fed forward below the transpiration-cooled surface, causing a decrease in the heat transfer rate upstream of the shock-impingement point. Again, we observed that helium is a far more effective coolant than nitrogen and has little or no effect on the outer inviscid flow.

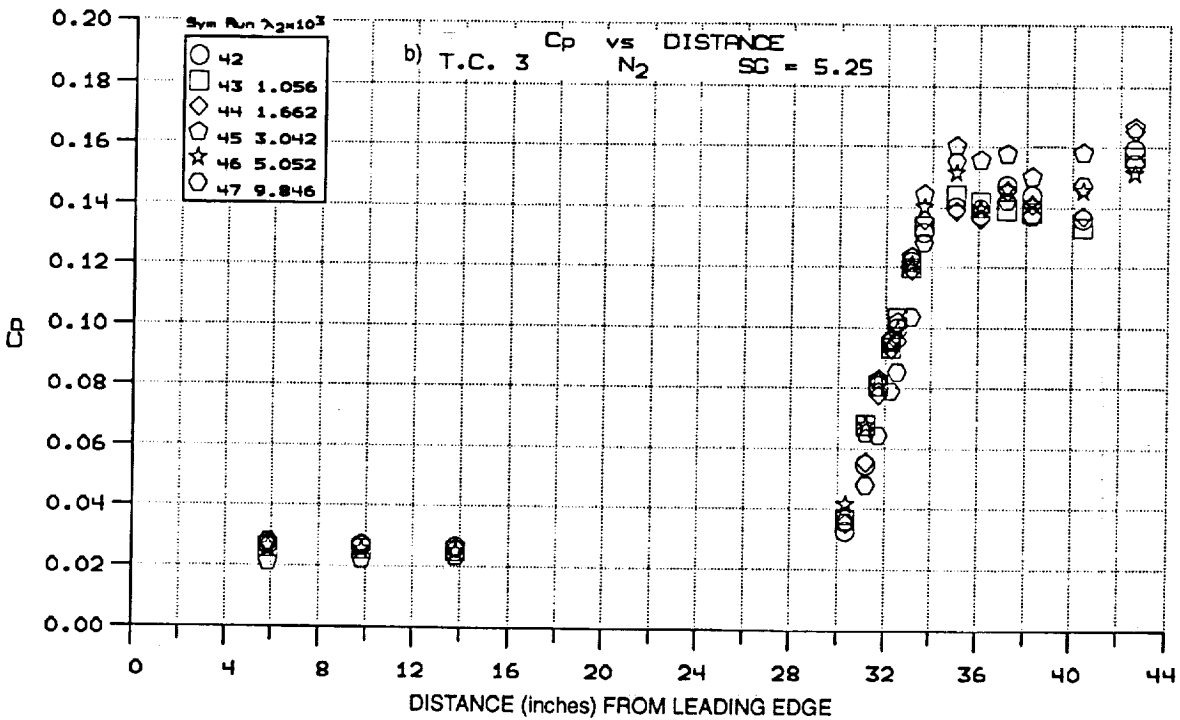
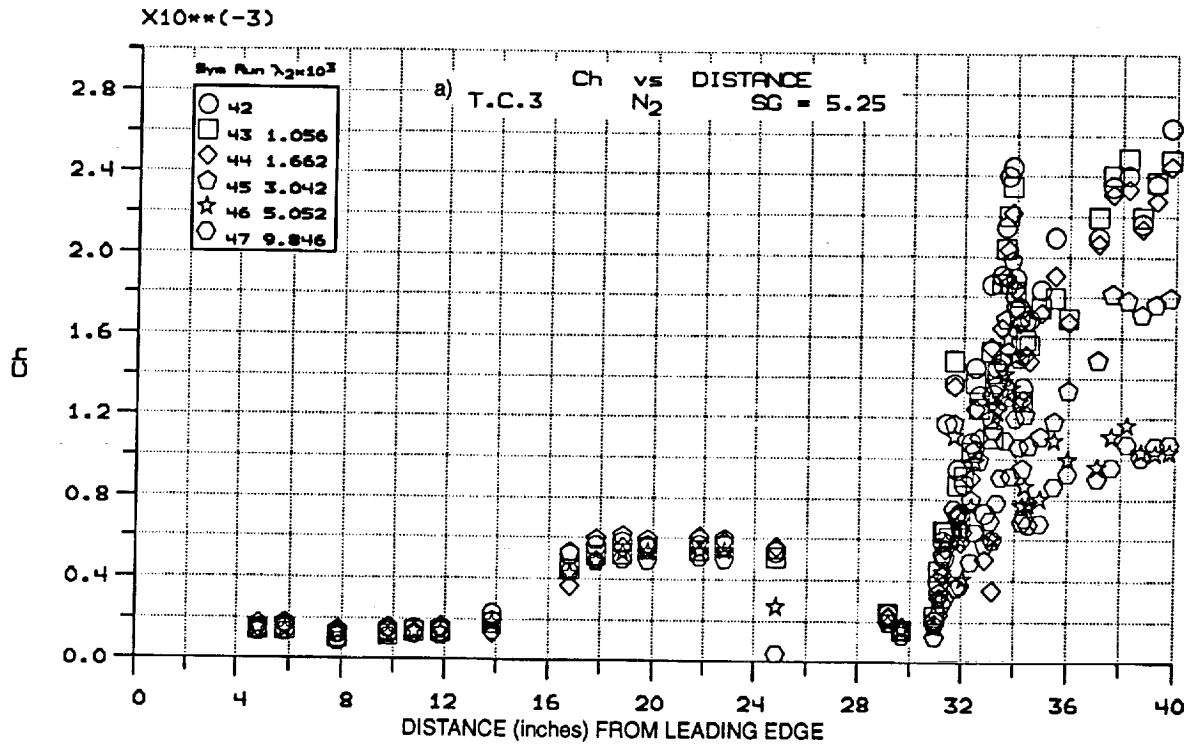


Figure 33 HEAT TRANSFER AND PRESSURE MEASUREMENTS AT MACH 8 ON NITROGEN-COOLED TRANSPARATION SURFACE WITH SHOCK INTERACTION FROM 5.2° SHOCK GENERATOR

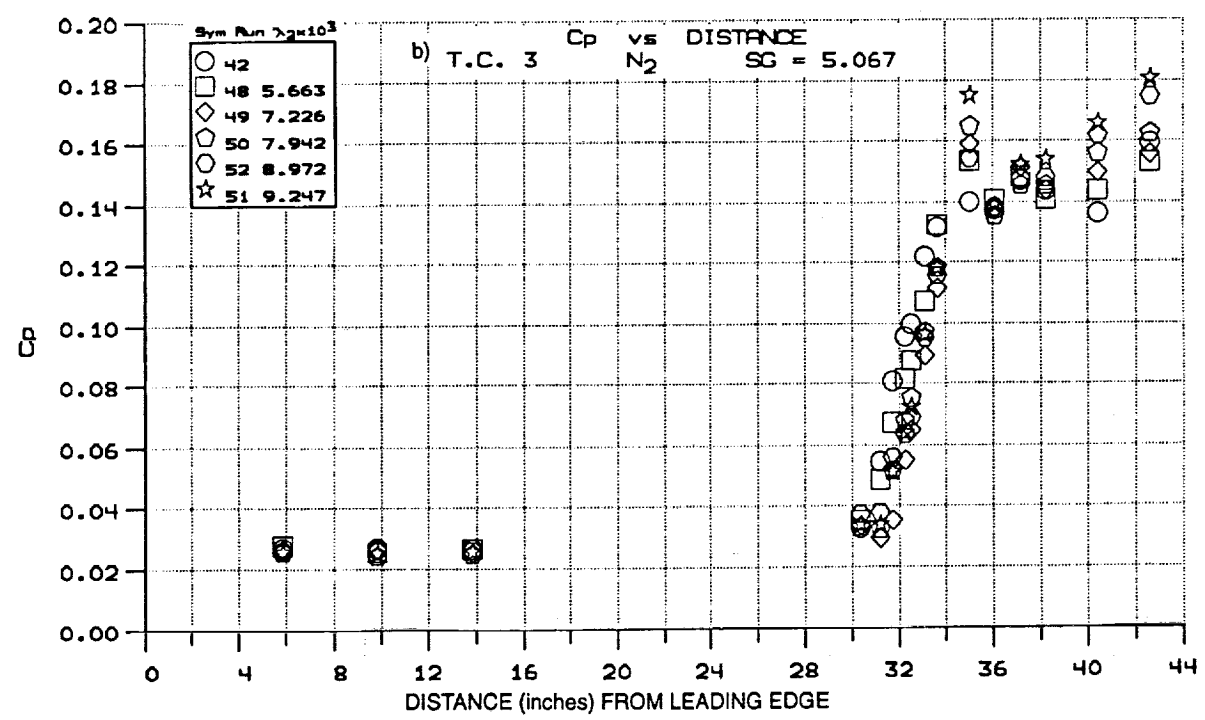
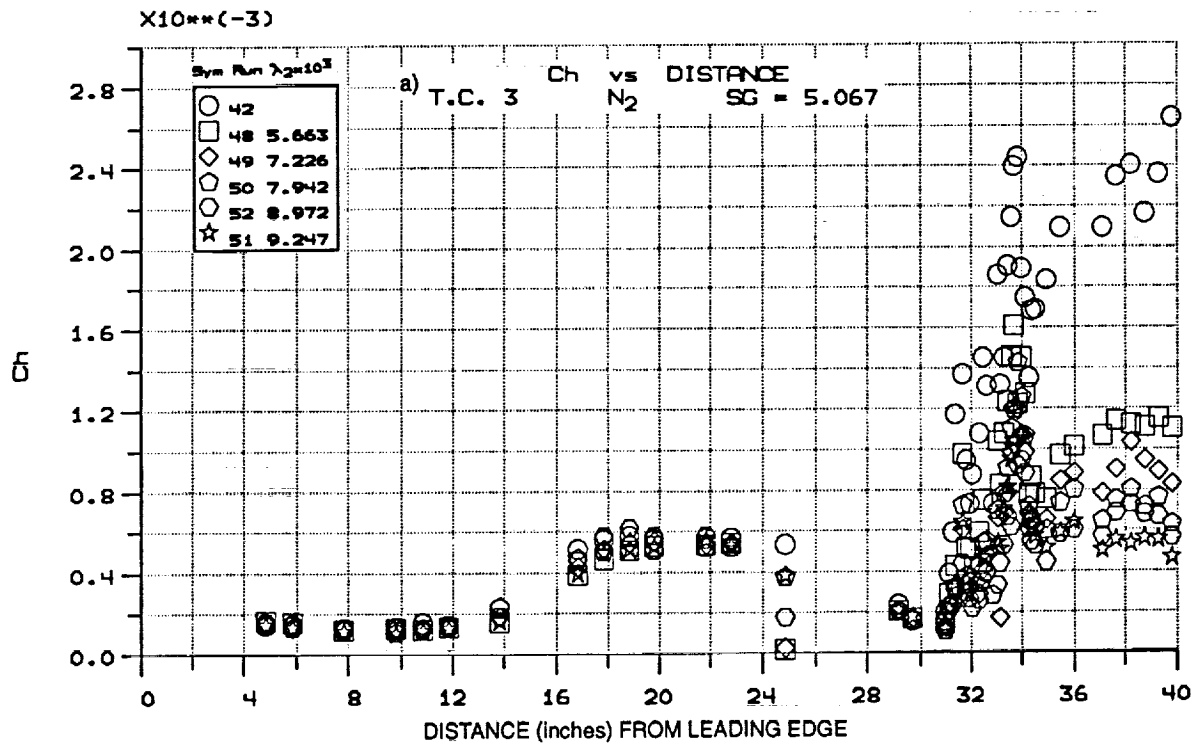


Figure 34 HEAT TRANSFER AND PRESSURE MEASUREMENTS AT MACH 8 ON NITROGEN-COOLED TRANSPIRATION SURFACE WITH SHOCK INTERACTION FROM 5.0° SHOCK GENERATOR

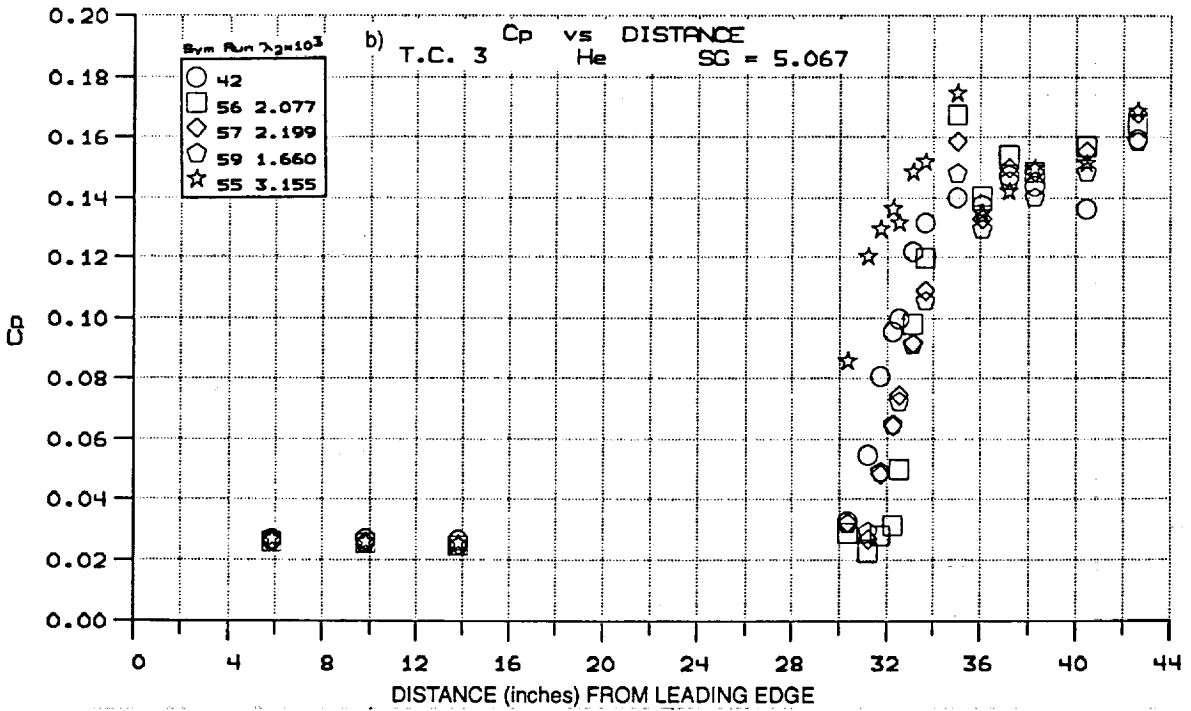
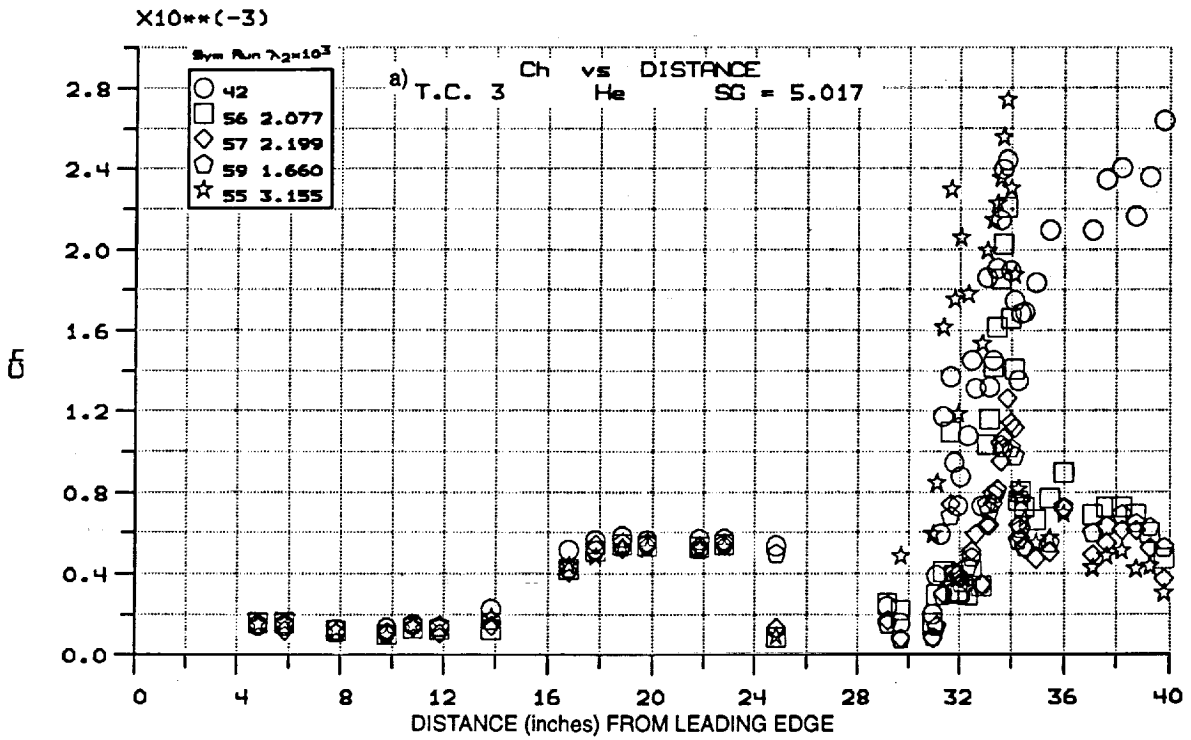


Figure 35 HEAT TRANSFER AND PRESSURE MEASUREMENTS AT MACH 8 ON HELIUM-COOLED TRANSPARATION SURFACE WITH SHOCK INTERACTION FROM 5.0° SHOCK GENERATOR

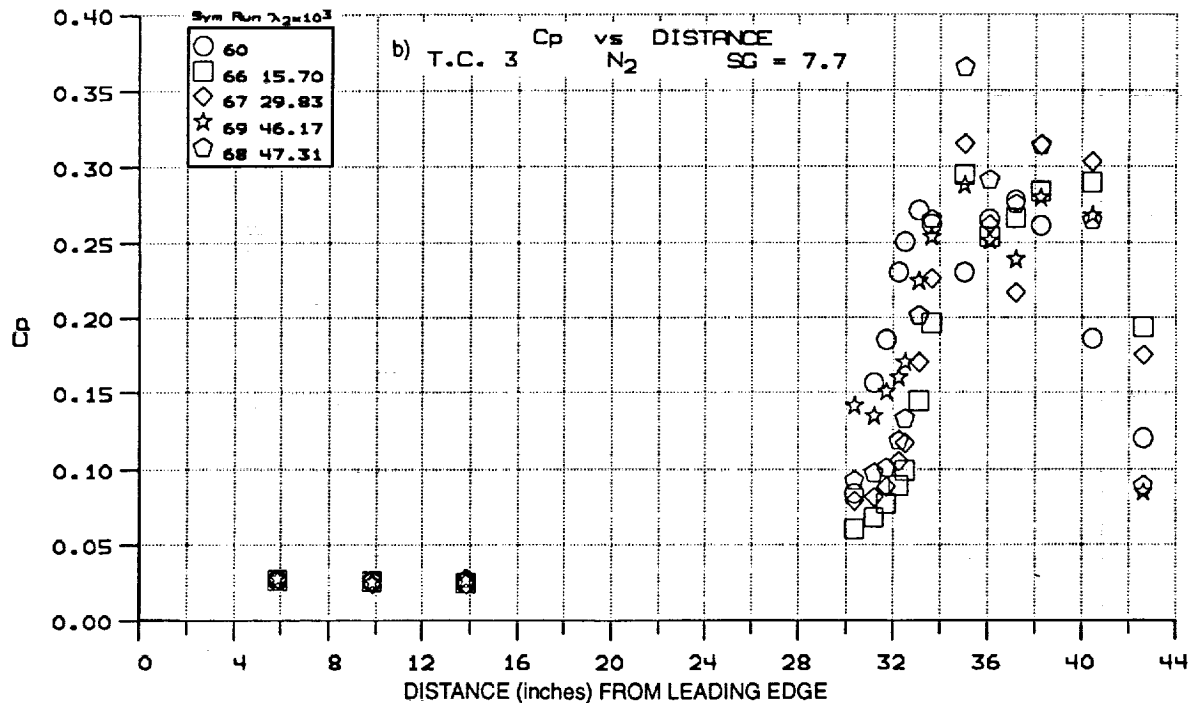
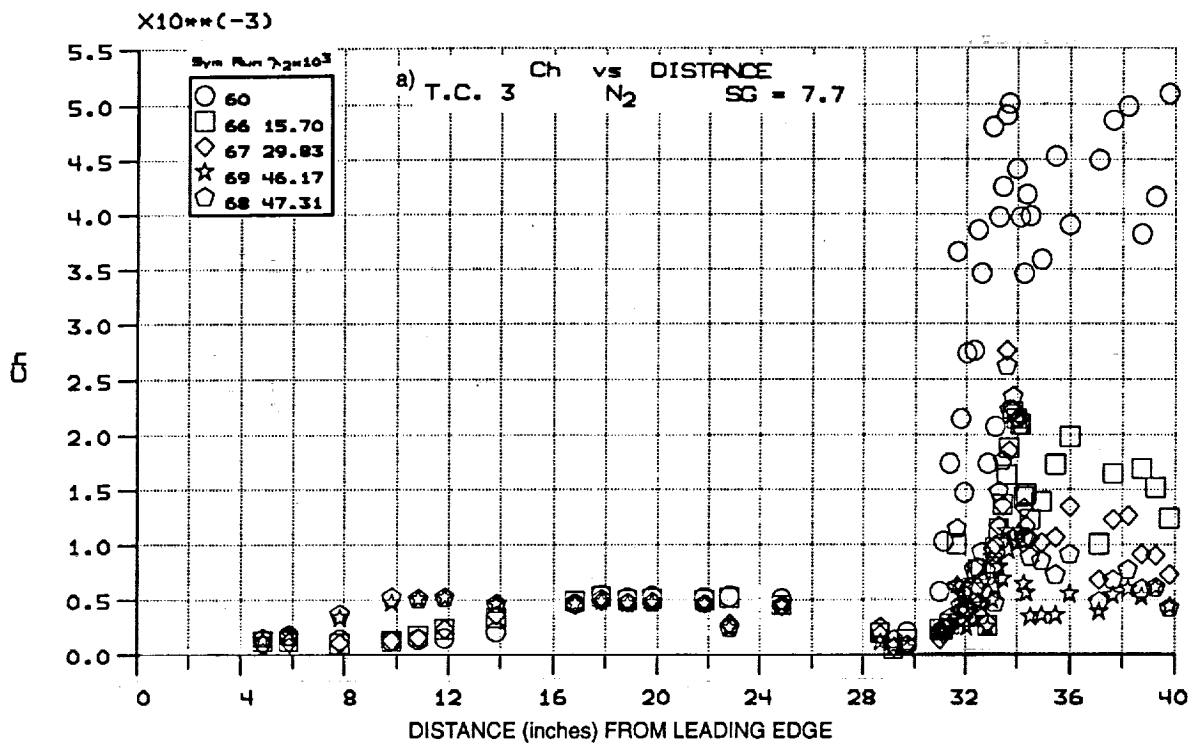


Figure 36 HEAT TRANSFER AND PRESSURE MEASUREMENTS AT MACH 8 ON NITROGEN-COOLED TRANSPIRATION SURFACE WITH SHOCK INTERACTION FROM 7.7° SHOCK GENERATOR

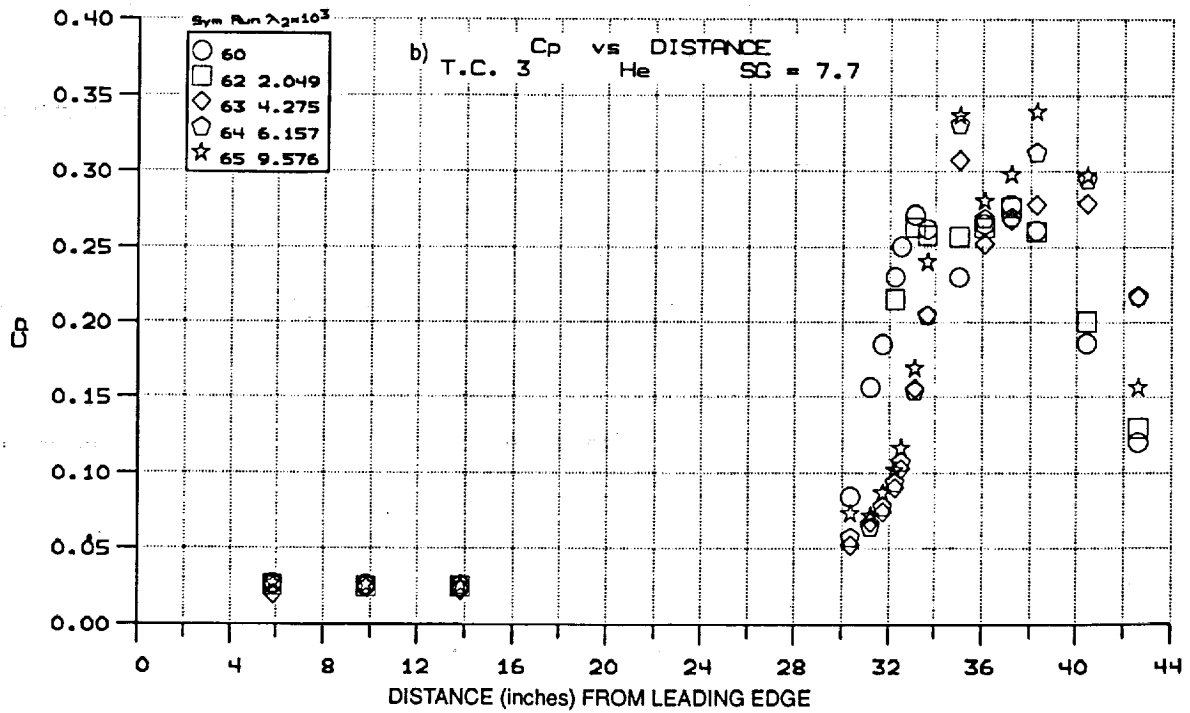
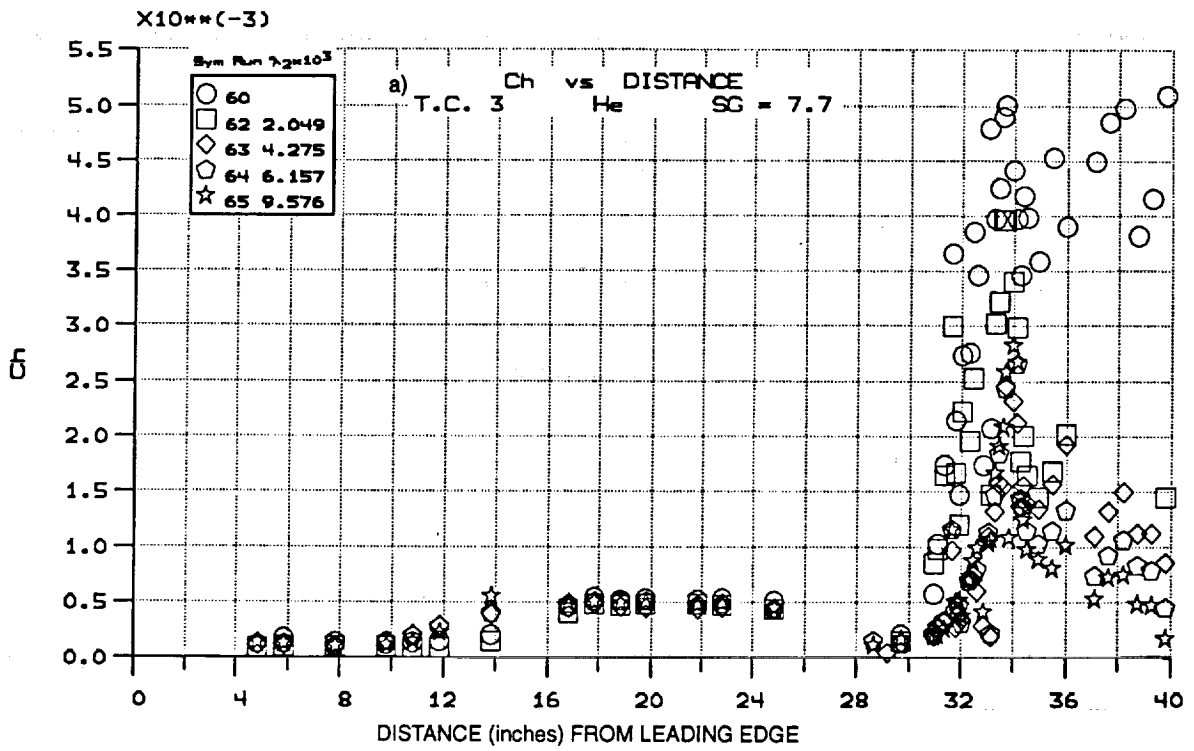


Figure 37 HEAT TRANSFER AND PRESSURE MEASUREMENTS AT MACH 8 ON HELIUM-COOLED TRANSPARATION SURFACE WITH SHOCK INTERACTION FROM 7.7° SHOCK GENERATOR

For a shock generator angle of 7.5° , there was a definite indication from the pressure distributions (see Figure 36b) that a small separated region was formed upstream of the shock. This region seems slightly enlarged for the highest blowing rates. Looking at the heat transfer rates for this case, shown in Figure 36a, it can be seen that for 5% nitrogen flux rates, we can bring the heat transfer rate down to its flat-plate values. Under these conditions, the heat transfer rates just prior to shock impingement were significantly below this level. As discussed earlier, we believe that this reduction in heat transfer rate stemmed from the forward propagation of coolant fluid through the transpiration-cooled surface, providing a cooling layer next to the surface without significantly altering the pressure distribution upstream of the shock-impingement point. Once again, we observed that employing helium as a coolant achieved the same heating reduction as did two to three times as much nitrogen. Again, we observed the region of extremely low heat transfer rates as the coolant was fed upstream into the separated region. The addition of mass into and downstream of the shock-impingement point did not appear to significantly change the pressure levels through the interaction, again indicating that the inviscid flowfield was not significantly modified by the transpiration cooling.

The heat transfer and pressure measurements showing the effects of cooling on the distribution of heating for the largest shock generator angle of 10.5° are shown in Figures 38a and 38b for nitrogen coolant and in Figures 39a and 39b for helium coolant. For this strong interaction, there was significant flow separation, both for the case with zero blowing and for the cases where we had significant transpiration cooling. As can be seen from the pressure distributions for the nitrogen coolant in Figure 38b, for the highest blowing rates we would anticipate significant levels of distortion in the freestream. It can be seen from Figure 38a that the levels of heat transfer upstream of the shock impingement were reduced to almost zero for the highest blowing rates. A mass flux ratio of 13% brought, brings the heating level down to the smooth-flat-plate value. The heat transfer downstream of shock impingement shows a more complex distribution, indicating a disturbing influence of the injection process on the structure of the interaction region. Again, employing helium rather than nitrogen for this interaction strength, as shown in Figure 39, reduced the mass flux requirements to reach a parity between the heating downstream of reattachment and that on the flat plate by a factor of three. And, although the volumetric addition rate for the helium coolant was significantly larger than for nitrogen, we did not observe significant distortions in the pressure distribution and, hence, in the flowfield downstream of the shock-impingement point. Both the pressure and the heat transfer distributions upstream of the point of shock impingement showed that the size of the separated interaction region was significantly enlarged.

In summary, for all the shock strengths at Mach 8, we found, as we did for Mach 6, that employing helium coolant not only is far more effective in terms of mass flux requirements but also creates significantly less distortion in the freestream, both upstream and downstream of shock impingement.

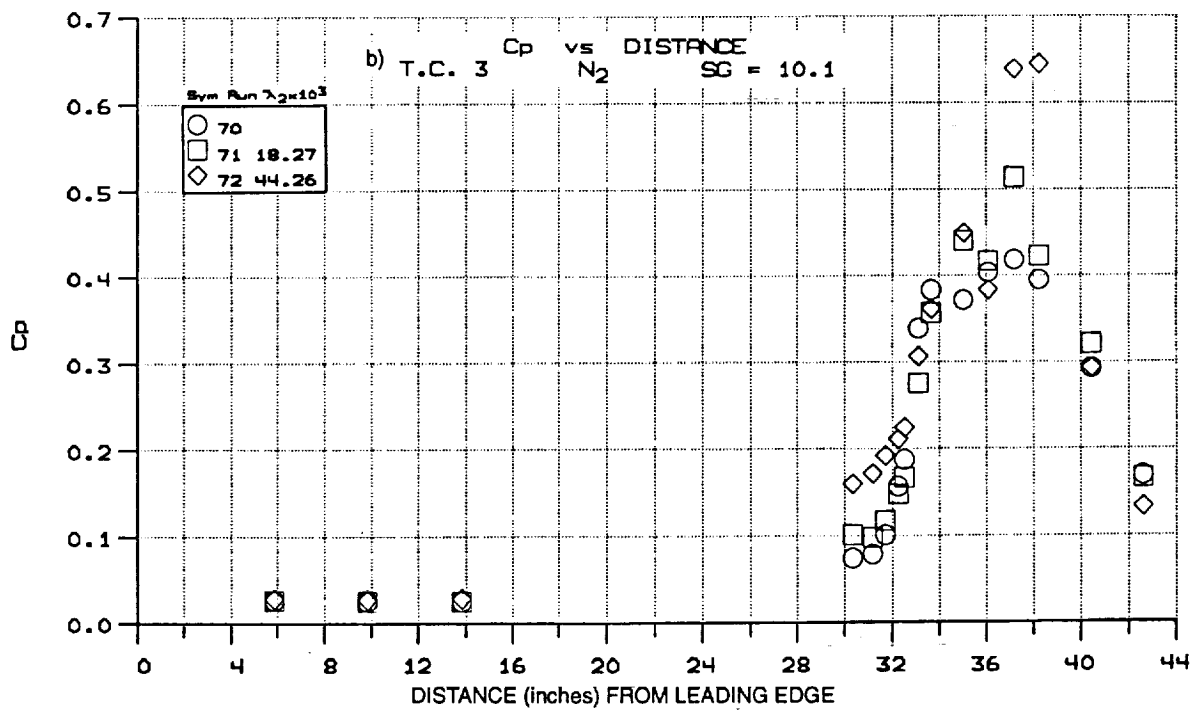
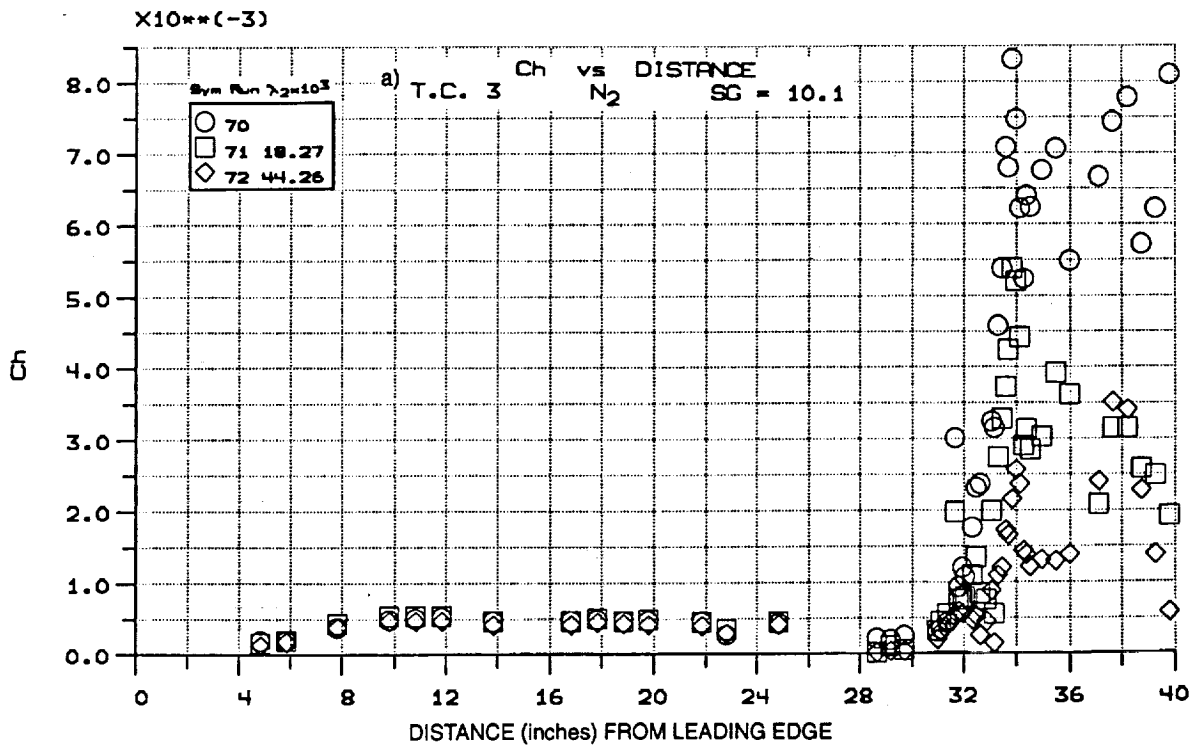


Figure 38 HEAT TRANSFER AND PRESSURE MEASUREMENTS AT MACH 8 ON NITROGEN-COOLED TRANSPIRATION SURFACE WITH SHOCK INTERACTION FROM 10.1° SHOCK GENERATOR

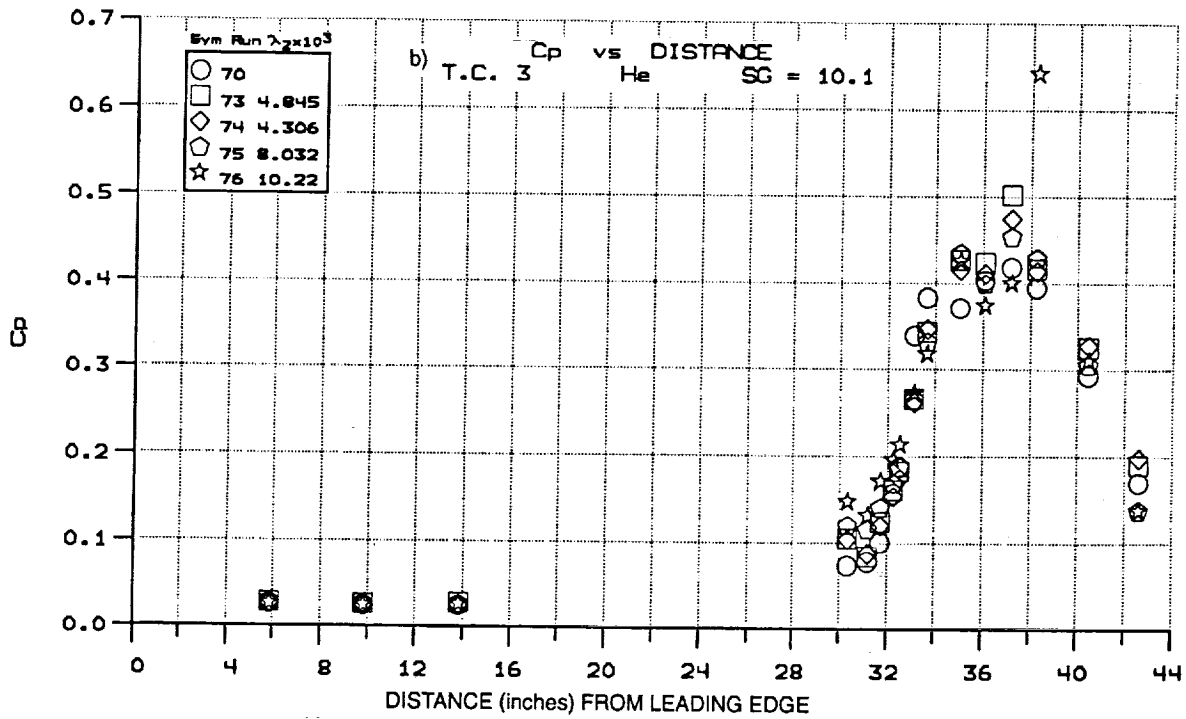
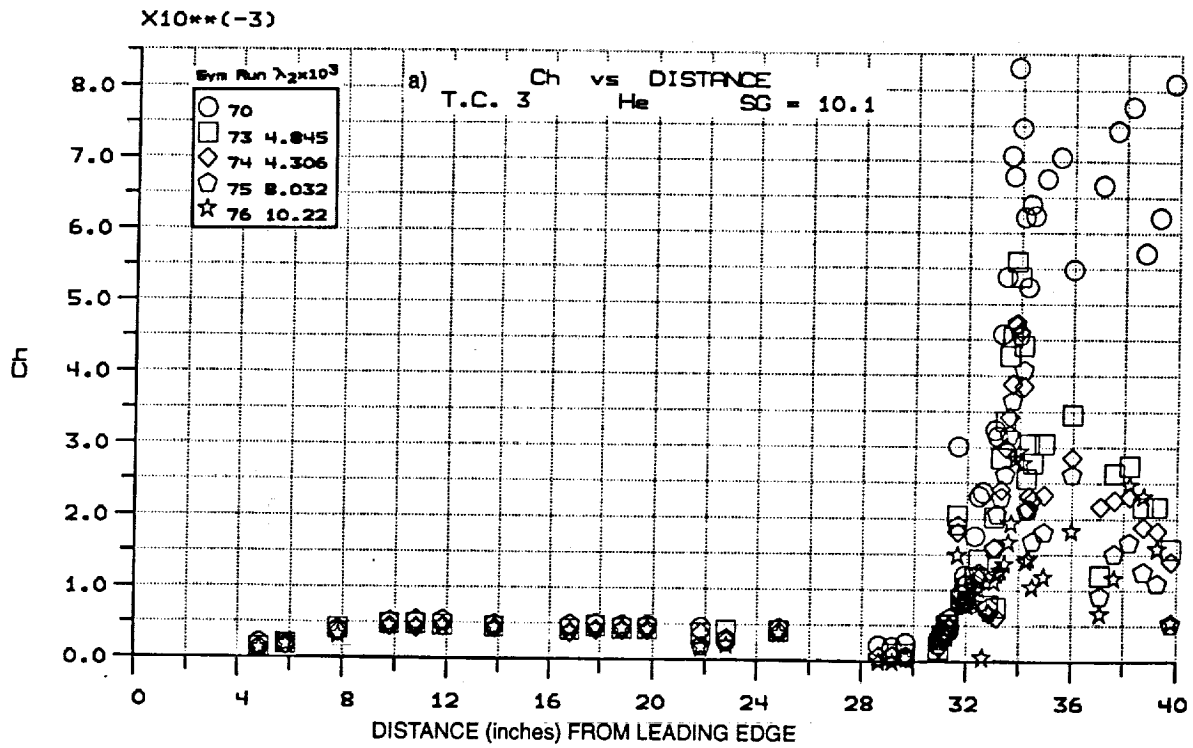


Figure 39 HEAT TRANSFER AND PRESSURE MEASUREMENTS AT MACH 8 ON HELIUM-COOLED TRANSPARATION SURFACE WITH SHOCK INTERACTION FROM 10.1° SHOCK GENERATOR

3.5 CORRELATION OF HEATING MEASUREMENTS ON SMOOTH AND TRANSPIRATION-COOLED SURFACE

3.5.1 Shock-Induced Heating on Non-Blowing Configuration

Heat transfer and pressure measurements were made on the flat-plate transpiration-cooled model without coolant addition at the Mach 6 and 8 conditions for shock-generator angles of 5° , 7.5° , and 10° . For this flow and model configuration, the interaction region occurred over the transpiration surface, which, as noted from the heat transfer measurements discussed in section 3.3, presented an effectively rough surface to the flow. Because the boundary layer thinned significantly through the shock-interaction region, the roughness-induced heating enhancement was even more pronounced at the end of the pressure rise downstream of the interaction. A large body of information is available on the heat transfer increase across a shock-interaction region on smooth surfaces, and a correlation of such measurements from Reference 8 is presented in Figure 40. The measurements made in the present study for the non-blowing cases are compared with the correlation in Figure 41, and it can be seen that the surface roughness does increase the maximum heating levels. However, here, as in earlier studies, we observed that, for this porous surface, even the smallest levels of blowing eliminated roughness-induced heating augmentation.

3.5.2 Shock-Induced Heating on Transpiration-Cooled Surfaces

An extensive set of heat transfer measurements, presented in section 3.4, provides the data necessary to determine the coolant requirements for transpiration-cooled surfaces with oblique shock interaction. The most important information in this data set is that which defines the cooling requirements necessary to reduce the peak heating to levels acceptable in the system design. To provide such information in the most concise form, we have correlated the heat transfer measurements made downstream of the incident shock, where the pressure and heat transfer rates reach a maximum, against a blowing parameter based on the local conditions in the inviscid flow in the region. Examples of such correlations for shock generator angles of 5° , 7.5° , and 10° are shown in Figures 42 and 43. It can be seen that the peak heating is reduced by local cooling in a uniform manner similar to that for the flows without shock interaction. In fact, by employing correlations basing the heat transfer coefficients and blowing parameters on the local inviscid flow conditions downstream of the reflected shock, we can collapse the data sets from the different interaction strengths and test conditions as shown in Figures 44 and 45. Here, it can be seen that the measurements from the strong interaction regions generated by the 10.5° shock generator are not as well correlated as those from the weaker shocks. Employing similar modified blowing parameters as employed in section 3.3 to incorporate the effects of the molecular weight and

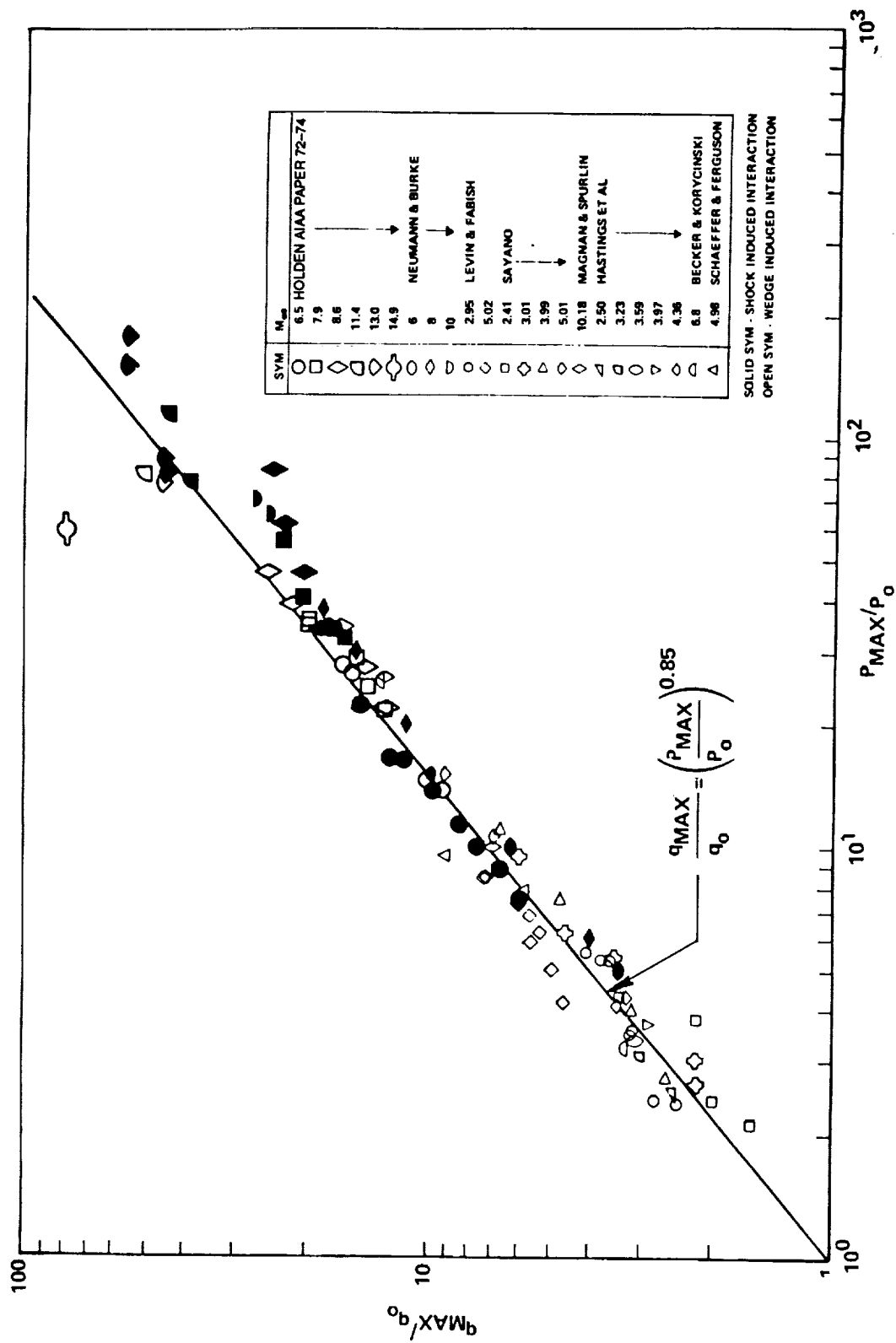


Figure 40 CORRELATION OF MAXIMUM HEATING IN WEDGE- AND EXTERNALLY GENERATED SHOCK-INDUCED TURBULENT SEPARATED FLOWS

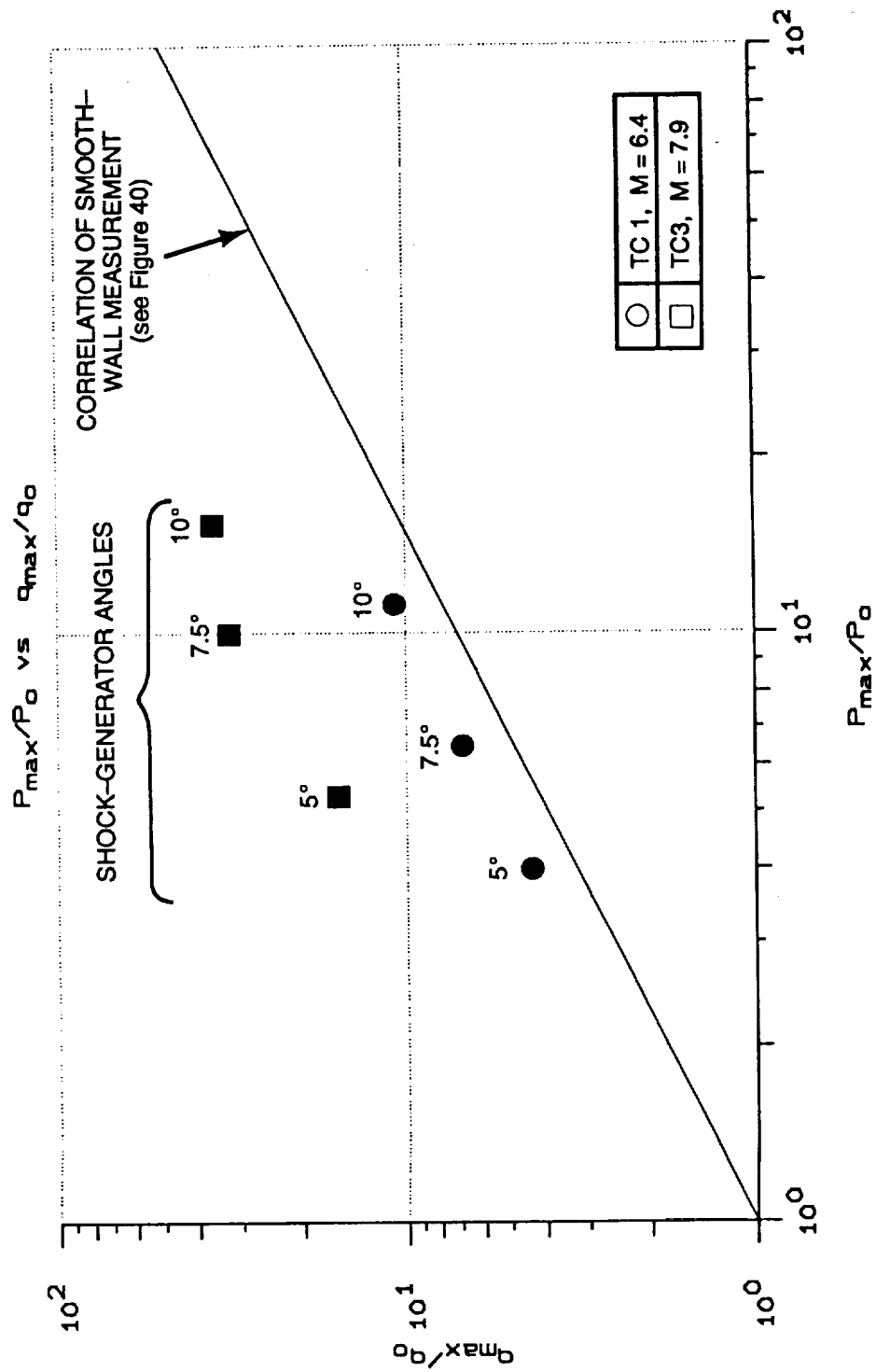


Figure 41 COMPARISON OF PEAK HEATING MEASUREMENTS DOWNSTREAM OF SHOCK IMPINGEMENT FOR TESTS WITHOUT COOLANT FLOW (P_{max}/P_0 vs. q_{max}/q_0)

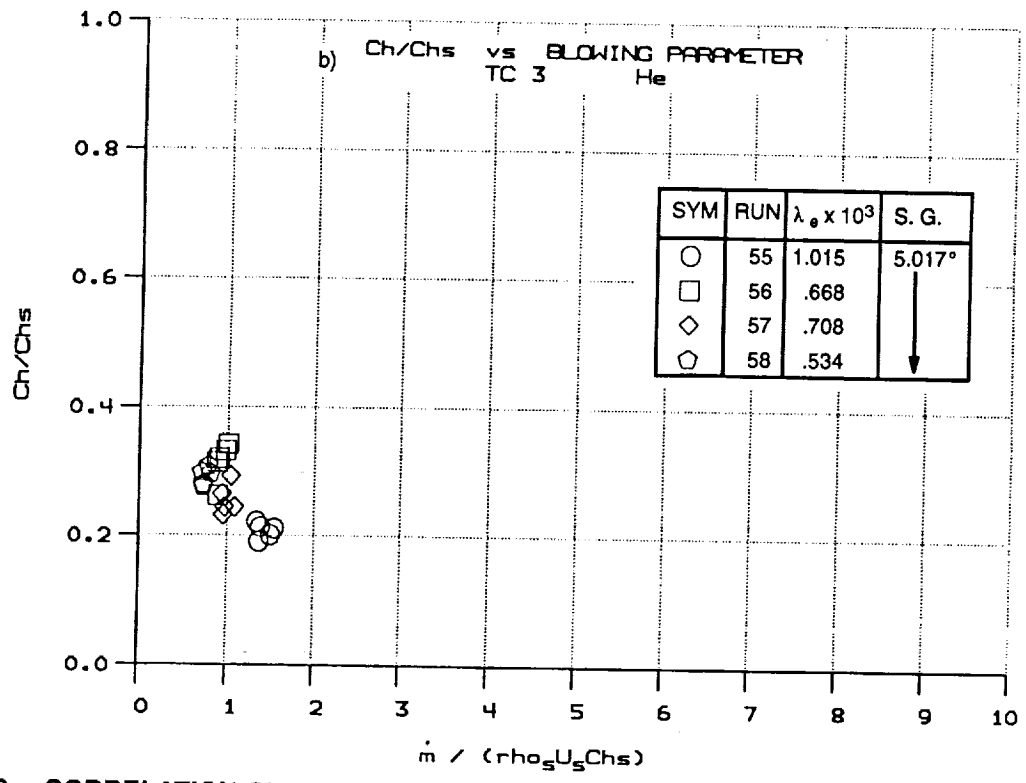
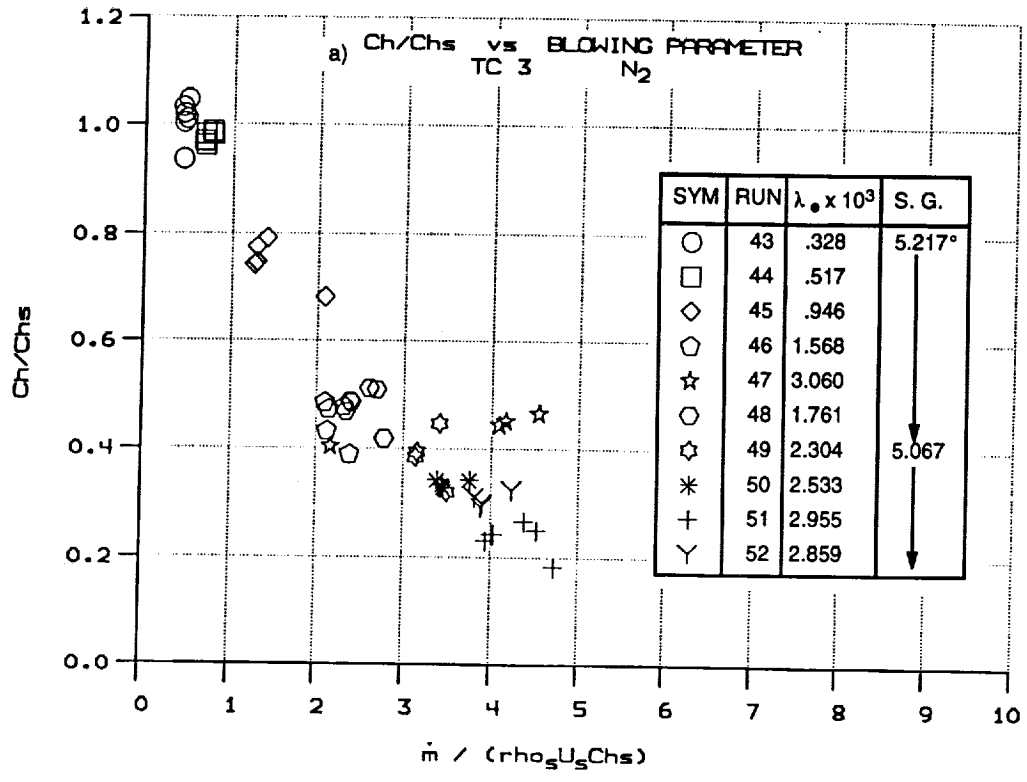


Figure 42 CORRELATION OF HEATING REDUCTION RATIO WITH BLOWING PARAMETER BASED ON LOCAL CONDITIONS DOWNSTREAM OF THE RE-COMPRESSION SHOCK FOR 5° SHOCK GENERATOR

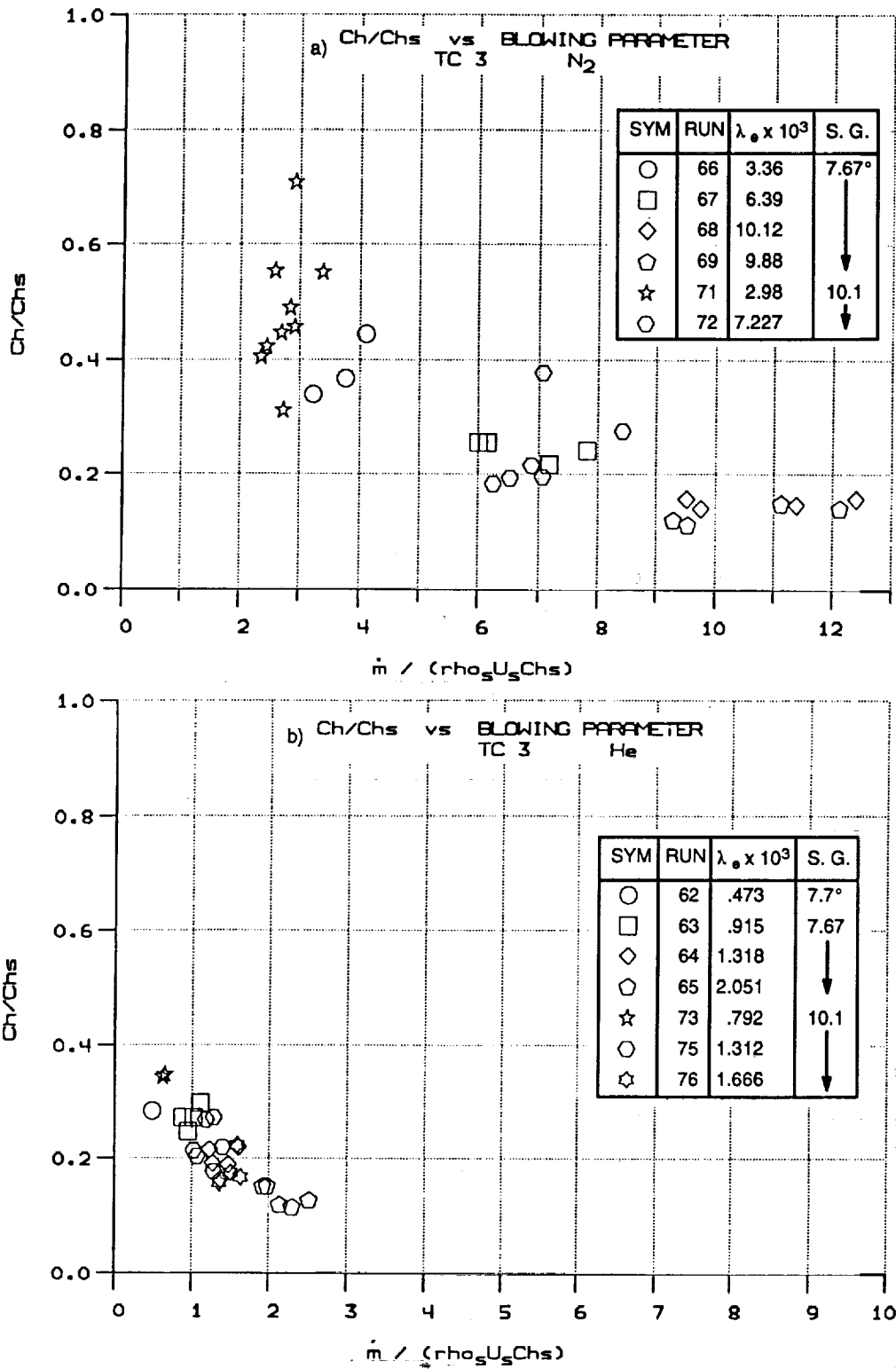


Figure 43 CORRELATION OF HEATING REDUCTION RATIO WITH BLOWING PARAMETER BASED ON LOCAL CONDITIONS DOWNSTREAM OF THE RE-COMPRESSION SHOCK FOR 7.5° AND 10° SHOCK GENERATORS

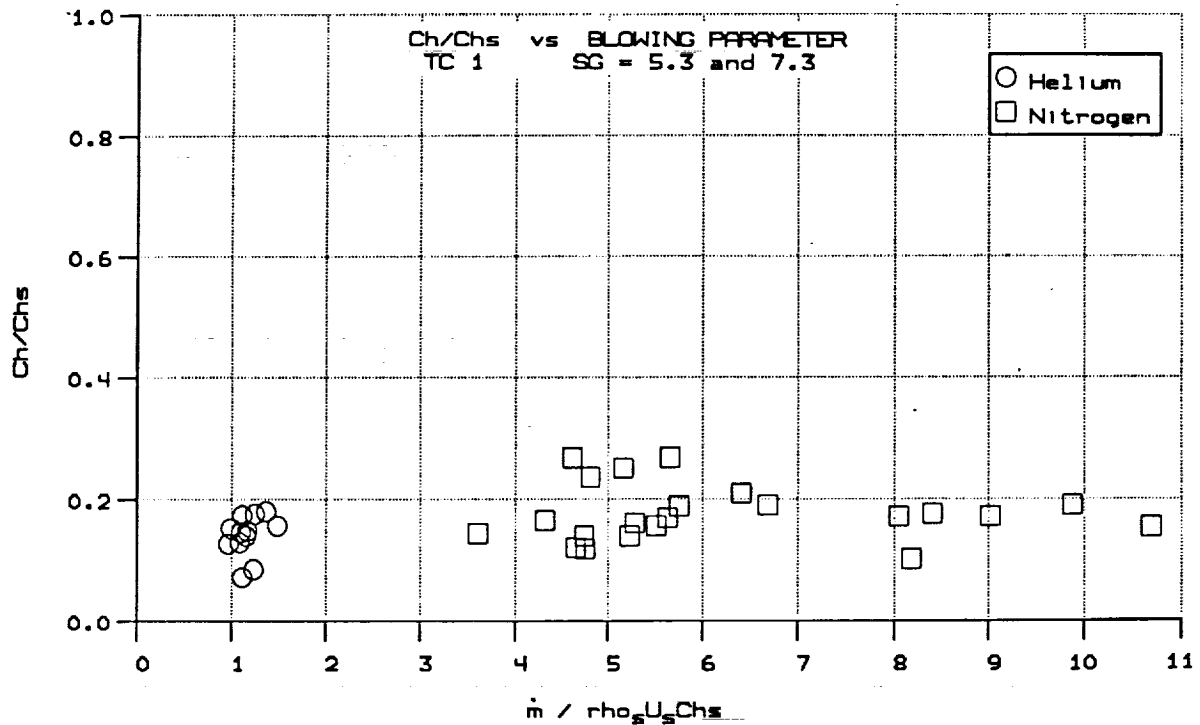


Figure 44 CORRELATION OF ALL HEATING REDUCTION RATIO WITH BLOWING PARAMETER BASED ON LOCAL CONDITIONS DOWNSTREAM OF THE RE-COMPRESSION SHOCK FOR 5°, 7.5° AND 10° SHOCK GENERATORS

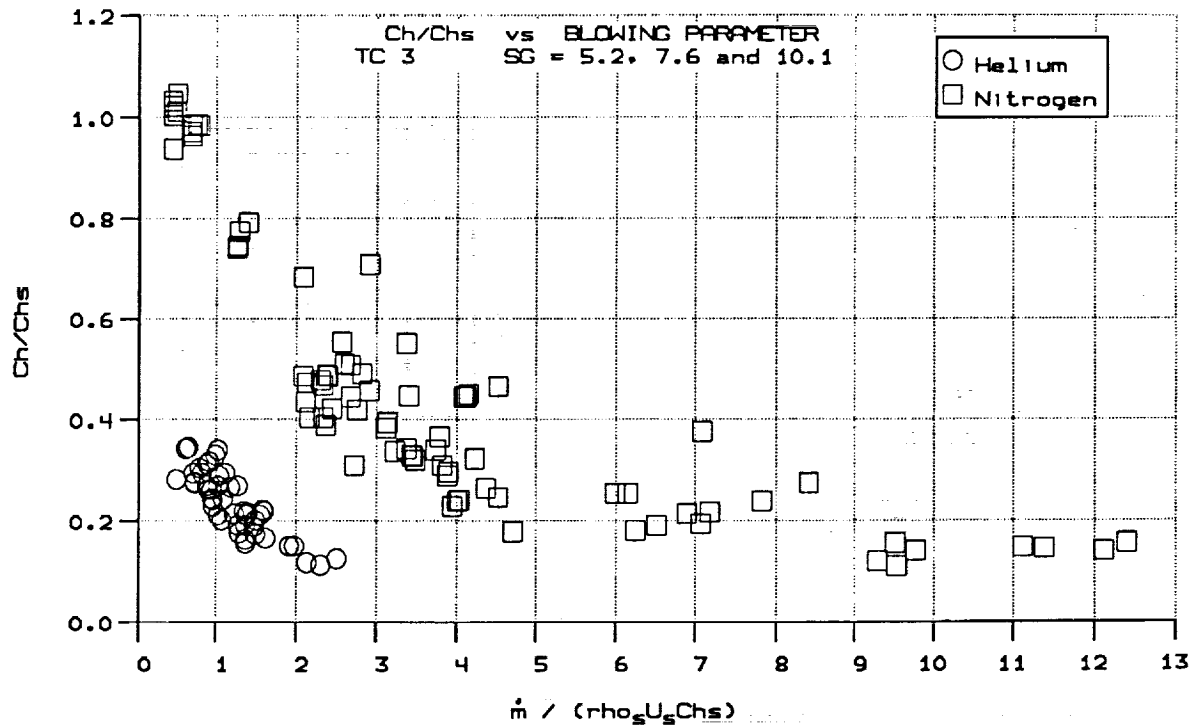


Figure 45 CORRELATION OF ALL HEATING REDUCTION RATIO WITH BLOWING PARAMETER BASED ON LOCAL CONDITIONS DOWNSTREAM OF THE RE-COMPRESSION SHOCK FOR 5°, 7.5° AND 10° SHOCK GENERATORS

specific heat of the injectant, we are able to correlate the measurements with the nitrogen and helium coolants as shown in Figures 46 and 47. Employing this correlation,

$$\frac{C_{H_0} - C_{H_s}}{C_{H_0}} = 0.92 (1 - e^{-B'/4}) \quad (18)$$

where B' is defined as either

$$B' = \dot{m} / (\rho_e U_e C_{H_s}) (\tilde{M}_{fs} / \tilde{M}_{inj}) \quad (19)$$

or

$$B' = \dot{m} / (\rho_e U_e C_{H_s}) (C_{pinf} / C_{pfs})^{0.7} (\tilde{M}_{fs} / \tilde{M}_{inj})^{0.5} \quad (20)$$

together with simple calculations of the local inviscid flow in the interaction region, it is possible to provide good design estimates for transpiration-cooling requirements in shock-interaction regions.

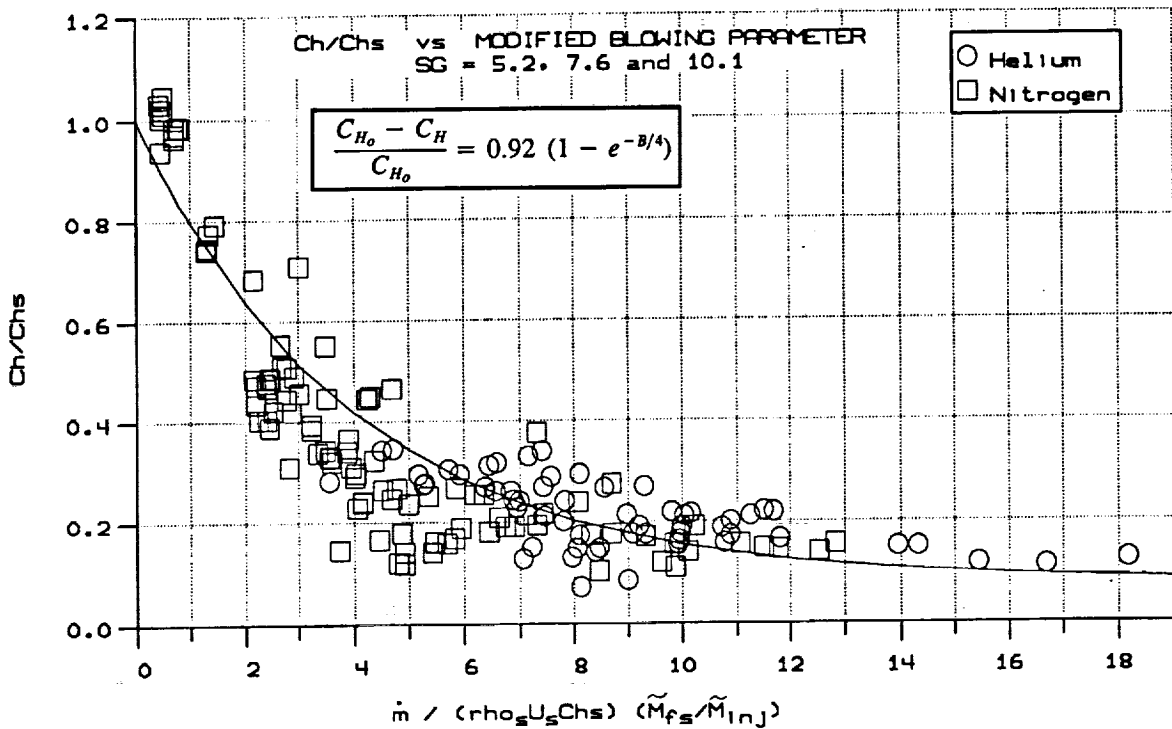


Figure 46 CORRELATION OF HEATING REDUCTION RATIO WITH MODIFIED BLOWING PARAMETER $\dot{m}/(\rho_s U_s Ch_s) (\tilde{M}_{fs}/\tilde{M}_{inj})$ FOR SHOCK-GENERATOR ANGLES OF 5°, 7.5°, AND 10° AND BOTH NITROGEN AND HELIUM COOLANTS

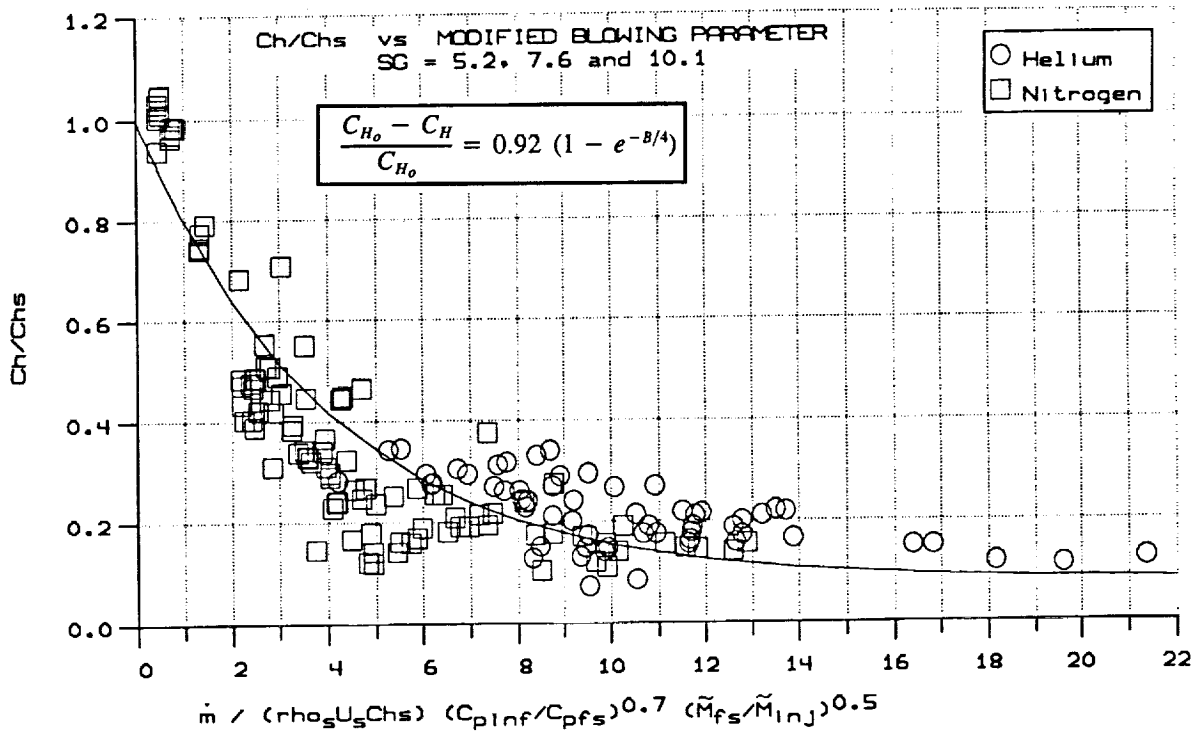


Figure 47 CORRELATION OF HEATING REDUCTION RATIO WITH MODIFIED BLOWING PARAMETER $\dot{m}/(\rho_s U_s Ch_s) (C_{p_{inf}}/C_{p_{fs}})^{0.7} (\tilde{M}_{fs}/\tilde{M}_{inj})^{0.5}$ FOR SHOCK-GENERATOR ANGLES OF 5°, 7.5°, AND 10° AND BOTH NITROGEN AND HELIUM COOLANTS

Section 4 CONCLUSIONS

Experimental studies have been conducted to investigate the use of transpiration cooling to reduce the peak-heating loads in regions of induced shock interaction. The experimental studies were conducted in the Calspan 48-inch shock tunnel at Mach numbers of 6.4 and 7.9 for unit Reynolds numbers of 7.5×10^6 and 7.1×10^6 , respectively. In these studies, the boundary layer was fully turbulent well upstream of the shock-wave/coolant-layer interaction. Detailed heat transfer and pressure measurements were obtained ahead and throughout the interaction region for the cooling-effectiveness studies, first without, then with, a shock incident on the coolant layer. The oblique shocks were generated with sharp, flat plates, inclined to the freestream at angles of 5° , 7.5° , and 10° . Both nitrogen and helium coolants were employed in this investigation.

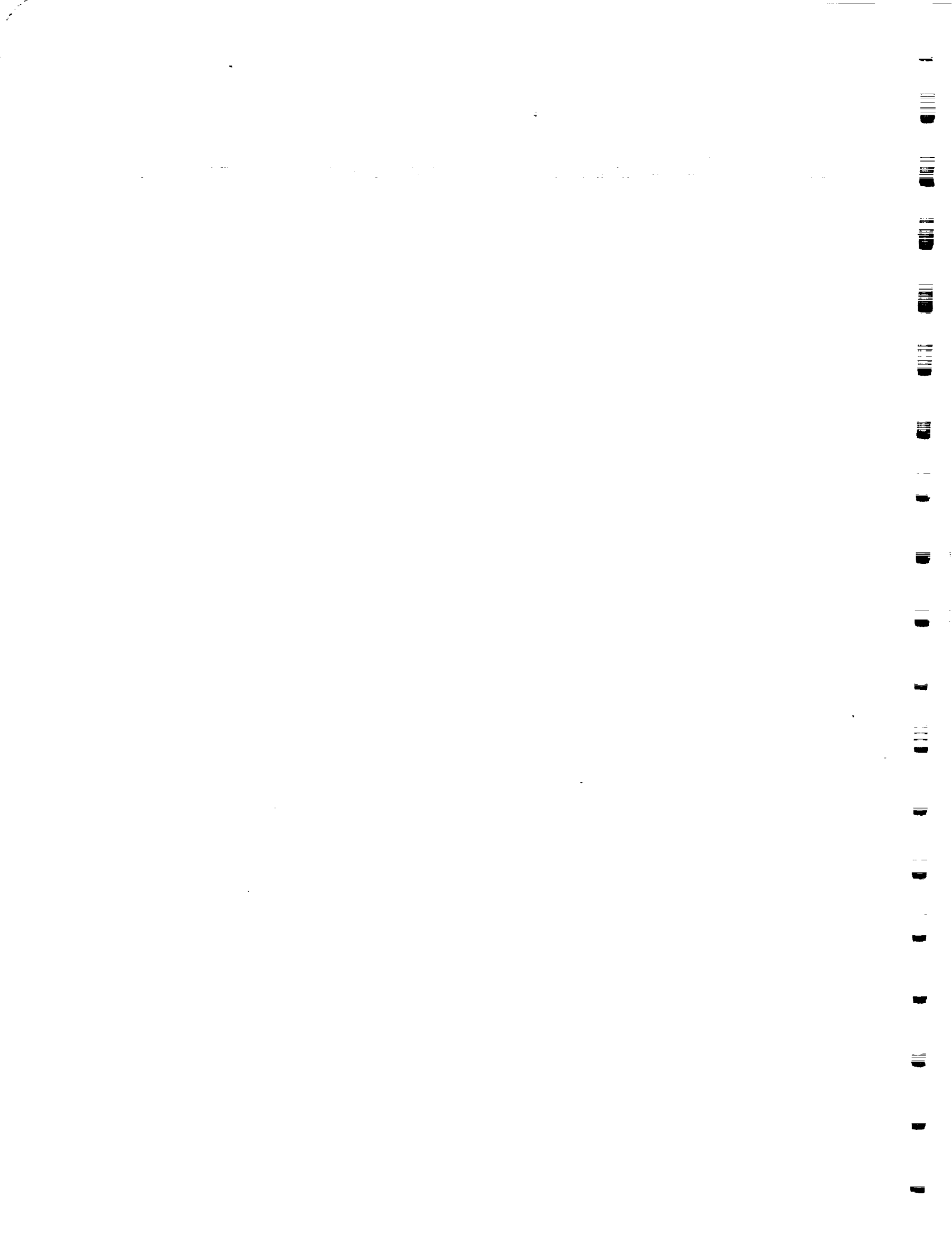
The measurements made in the first part of the program, where we studied transpiration-cooling effectiveness in the absence of incident shocks, demonstrated that transpiration cooling is an extremely effective method for surface cooling in hypersonic flows. Helium, because of its lower molecular weight and higher specific heat, was found to be a significantly more effective coolant than nitrogen. We were able to correlate the cooling effectiveness of the two gases for a large range of blowing rates up to boundary layer blowoff with parameters incorporating the non-blowing heating coefficient, the blowing rate, and the thermal properties of the coolant. The blowoff conditions were correlated in terms of a modified blowing parameter incorporating the molecular-weight ratio. The studies of shock-wave/transpiration-cooled-surface interaction demonstrated that the interaction region between the incident shock and the low-momentum transpiration-cooled boundary layer did not result in a significant increase in the size of attached or separated interaction regions, and did not result in significant flowfield distortions above the interaction regions. The increase in heating downstream of the shock-impingement point could easily be reduced to the values without shock impingement by a relatively small increase in the transpiration cooling in this region. Surprisingly, this increase in cooling rate did not result in a significant increase in the size of the region ahead of the incident shock or create a significantly enlarged interaction region with a resultant increase in the distortion level in the inviscid flow. Thus, transpiration cooling appears to be a very effective technique to cool the internal surfaces of scramjet engines, where shocks in the engine would induce large local increases in wall heating and create viscous/inviscid interactions that could significantly disturb the smooth flow through the combustor. Correlations in terms of local heating and flow parameter and the thermal property of the coolant are presented to enable the transpiration-cooling-rate requirements for shock interaction regions to be estimated. However, if hydrogen is used as the coolant, burning upstream of shock impingement might result in localized hot spots. Clearly, further research is needed in this area.

REFERENCES

1. Edney, B., "Anomalous Heat Transfer and Pressure Distributions on Blunt Bodies at Hypersonic Speeds in the Presence of an Impinging Shock," FFA Report 115, Aeronautical Research Institute of Sweden, 1968.
2. Baker, N.R., Kamath, Pradeep, S., McClinton, C.R. and Olsen, G.C., "A Film Cooling Parametric Study for NASP Engine Applications Using the 'SHIP' Code," Paper No. 40, Presented at the Fifth National AeroSpace Plane Technology Symposium, October 1988.
3. Majeski, J.A. and Weatherfor, R.H., "Development of an Empirical Correlation for Film-Cooling Effectiveness," AIAA 88-2624, June 1988.
4. Holden, M.S., "An Experimental Simulation of Massive Blowing from a Nosedip During Jovian Entry," in Thermophysics of Atmospheric Entry, Vol. 82, Progress in Astronautics and Aeronautics, Edited by T.E. Horton, Dept. Mech. Eng., The University of Mississippi, Published by AIAA 1982.
5. Holden, M.S., Rodriguez, K.M. and Nowak, R.J., "Studies of Shock/Shock Interaction on Smooth and Transpiration-Cooled Hemispherical Nosedips in Hypersonic Flow," AIAA-91-1765, Paper presented at the AIAA 22nd Fluid Dynamics, Plasma Dynamics and Lasers Conference, Honolulu, Hawaii, 24-26 June 1991.
6. Holden, M.S., "Studies of Surface Roughness and Blowing Effects on Hypersonic Turbulent Boundary Layers Over Slender Cones," AIAA-89-0458, Paper presented at the AIAA 27th Aerospace Sciences Meeting, Reno, Nevada, 9-12 January 1989.
7. Holden, M.S., Neumann, R.D., Burke, J. and Rodriguez, K.M., "An Experimental Study of the Effects of Injectant Properties on the Aerothermal Characteristics of Transpiration-Cooled Cones in Hypersonic Flow," AIAA-90-1487, Paper presented at the AIAA 21st Fluid Dynamics, Plasma Dynamics and Lasers Conference, Seattle, Washington, 18-20 June 1990.
8. Holden, M.S., "Shock Wave - Turbulent Boundary Layer Interaction in Hypersonic Flow," AIAA 15th Aerospace Sciences Meeting, 77-45, 1977.
9. "Calspan Hypersonic Shock Tunnel, Description and Capabilities Brochure," 1975.
10. Lewis, C.H. and Burgess, E.G., III, "Charts of Normal Shock Wave Properties in Imperfect Air (Supplement: $M=1$ to 10)," AEDC-TR-196, September 1965.
11. Hilsenrath, J., et al., "Tables of Thermal Properties of Gases," NBS Circular 565, 1955.
12. Reece, J.W., "Test Section Conditions Generated in the Supersonic Expansion of Real Air," Journal of Aeronautical Sciences, Vol. 29, No. 5, May 1962, pp. 617 and 618.
13. Hilsenrath, J., et al., "Tables of Thermodynamic Properties of Air Including Dissociation and Ionization from 1500°K to 15,000°K," AEDC-TR-59-20, December 1959.
14. Neil, C.A., and Lewis, C.H., "Interpolations of Imperfect Air Thermodynamic Data II at Constant Pressure," AEDC-TDR-64-184, September 1964.
15. Hirschfelder, J. O., Curtis, C.S., and Bird, R. B., "Molecular Theory of Gases and Liquid," J. Wiley and Sons, 1954.

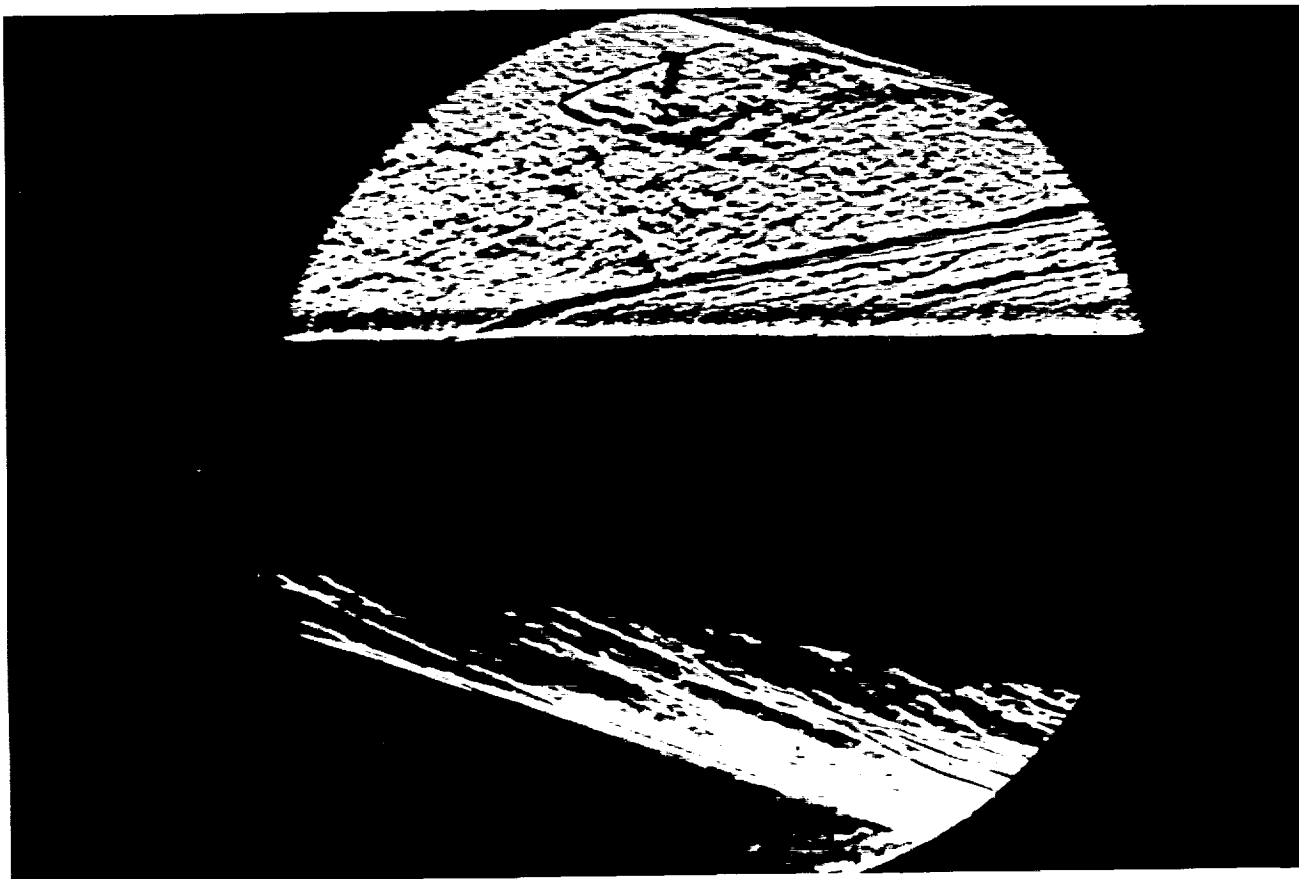
REFERENCES (Cont.)

16. Cook, W.J., "Determination of Heat Transfer Rates from Transient Surface Temperature Measurements," AIAA Journal, Vol. 8, No. 7, July 1970, pp. 1366-1368.



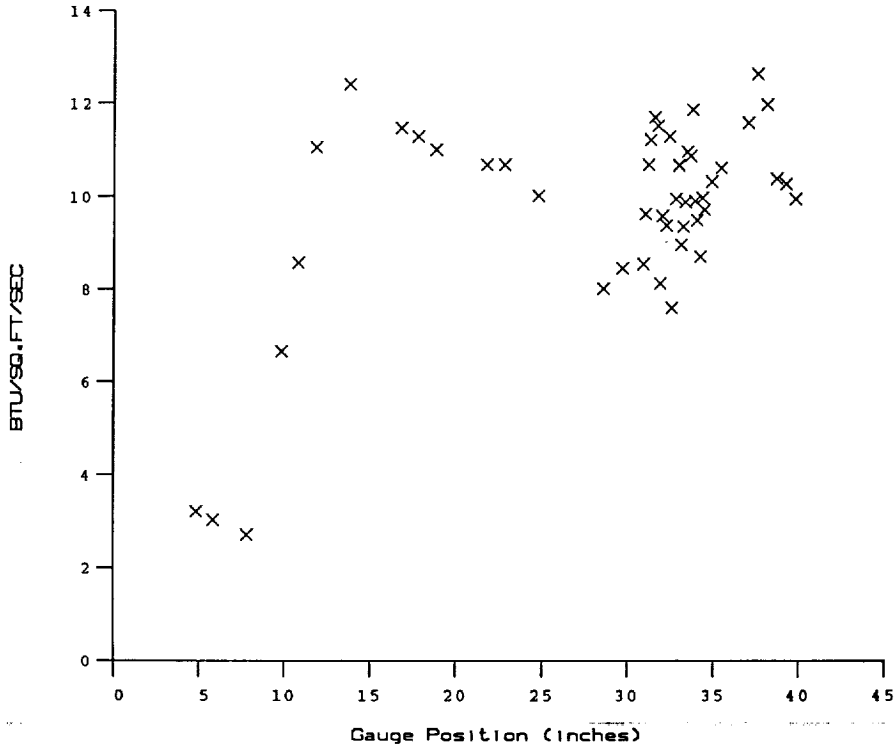
Appendix A

**TRANSPIRATION COOLING WITH SHOCK
INTERACTION STUDY DATA**

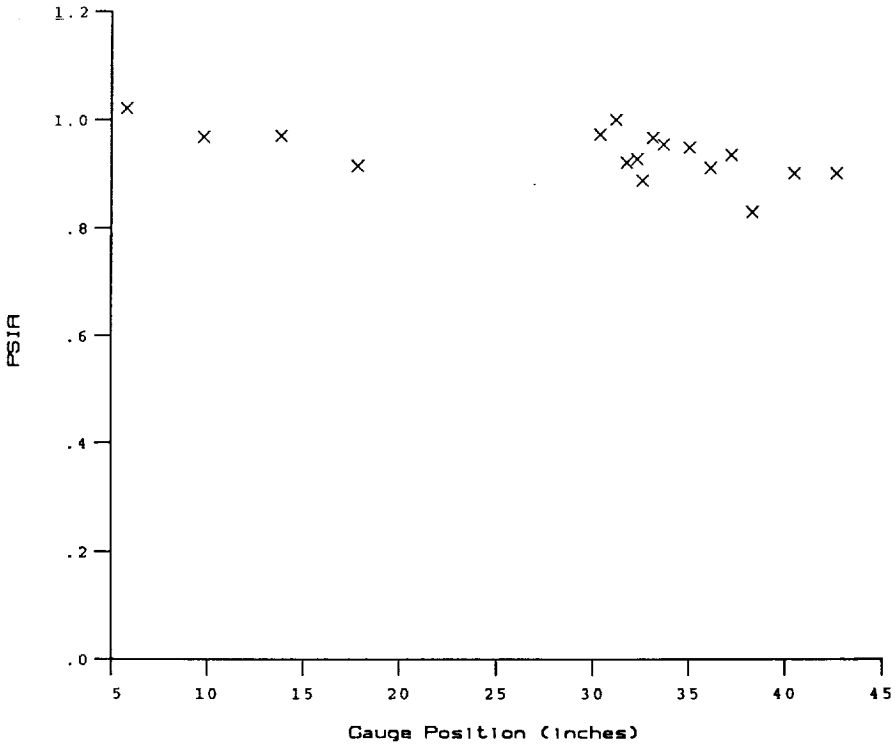


Test Conditions for Run 7 :

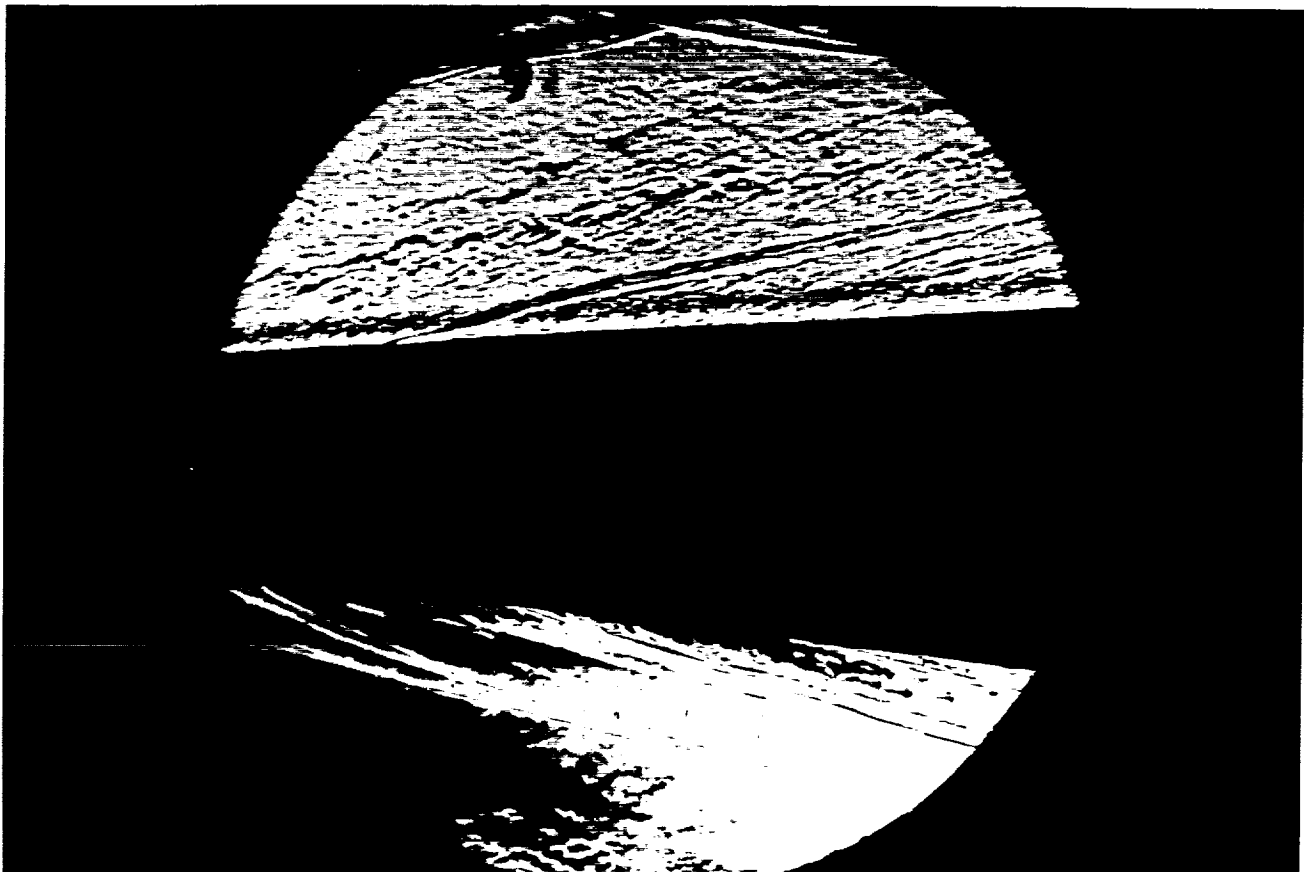
Po	= 2.108E+03 PSIA	Reservoir Total Pressure
Ho	= 1.340E+07 (Ft/sec) ²	Reservoir Total Enthalpy
To	= 2.104E+03 degR	Reservoir Total Temperature
M	= 6.423E+00	Freestream Mach Number
U	= 4.892E+03 Ft/sec	Freestream Velocity
T	= 2.412E+02 degR	Freestream Temperature
P	= 8.662E-01 PSIA	Freestream Static Pressure
Rho	= 3.013E-04 Slugs/Ft ³	Freestream Density
Mu	= 1.982E-07 Slugs/Ft-sec	Freestream Viscosity
Re	= 7.437E+06 1/Ft	Freestream Reynolds Number
Po'	= 4.666E+01 PSIA	Pitot Pressure
Q	= 2.504E+01 PSIA	Dynamic Pressure (Rho U ² /288)
Mi	= 2.800E+00	Shock Tube Incident Shock Mach Number
Tw	= 5.300E+02 degR	Wall Temperature (Test Gas = Air)
Hw	= 3.183E+06 (Ft/sec) ²	Wall Enthalpy (Cp Tw)
CPf	= 3.994E-02 1/PSIA	Pressure to CP factor (1/Q)
CHf	= 5.165E-05 Ft ² -s/BTU	Heat Rate to CH factor (778/(Rho U (Ho-Hw)))
QoFR	= 5.575E+01 BTU/Ft ² -s	Fay-Riddell Heat Transfer (.25' Diam Cylin.)



HEAT TRANSFER vs Gauge Position
Run 7

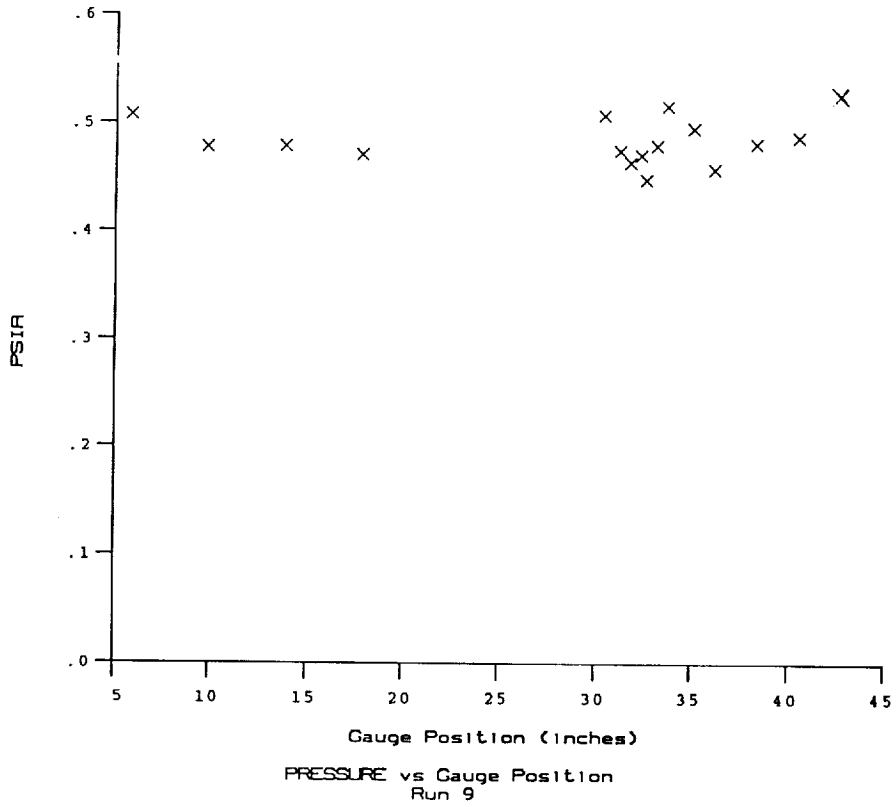
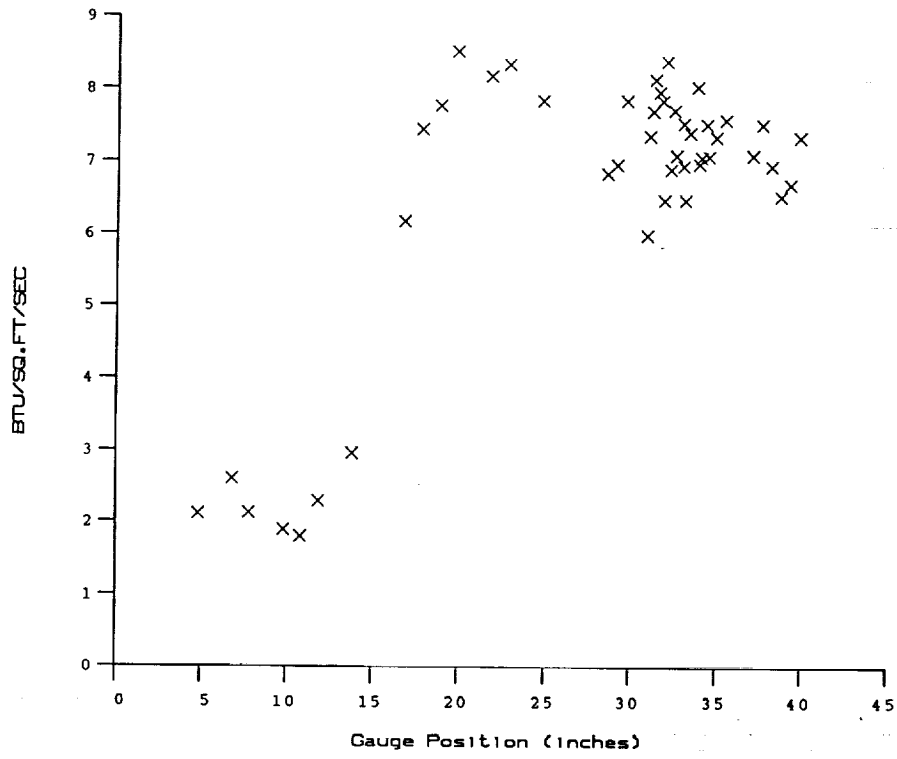


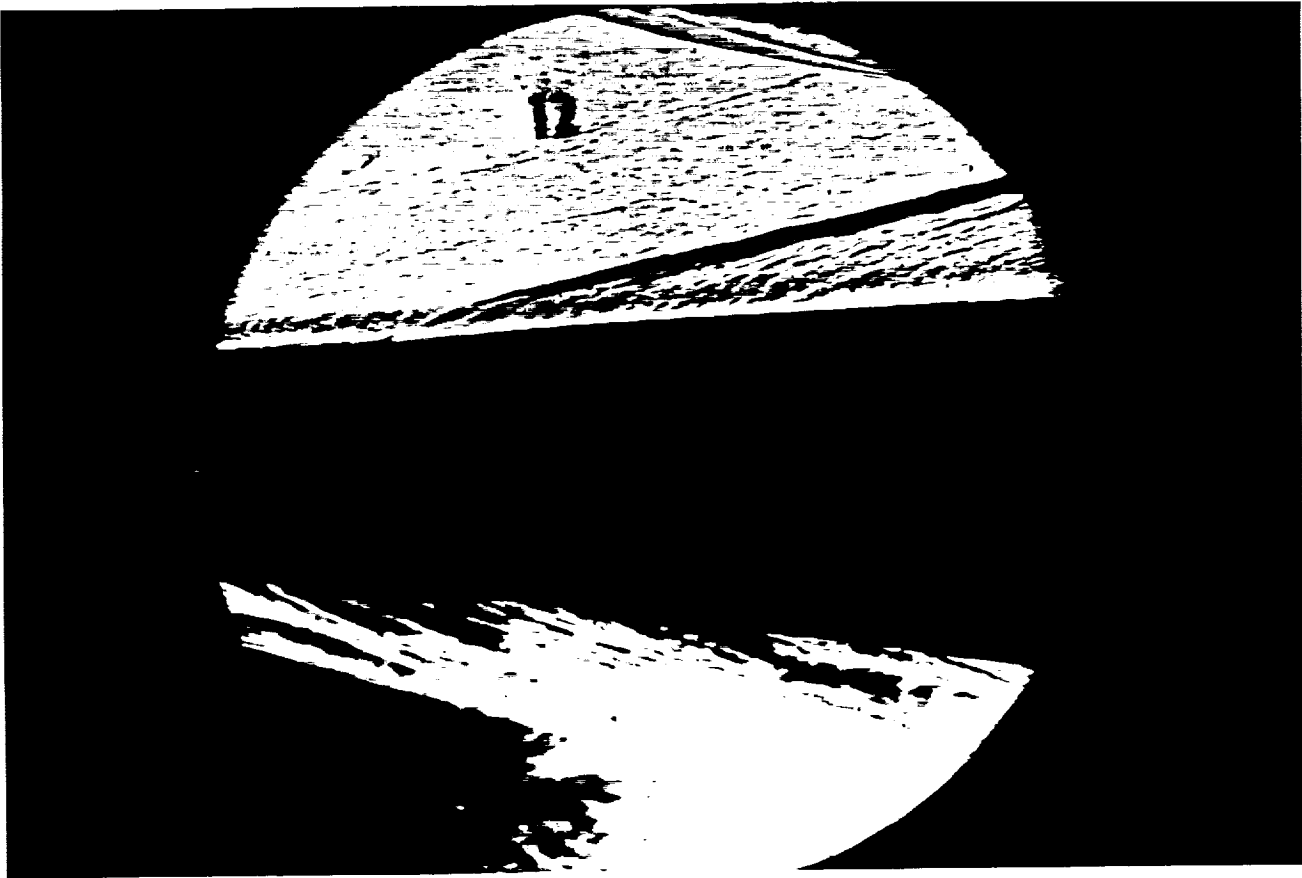
PRESSURE vs Gauge Position
Run 7



Test Conditions for Run 9 :

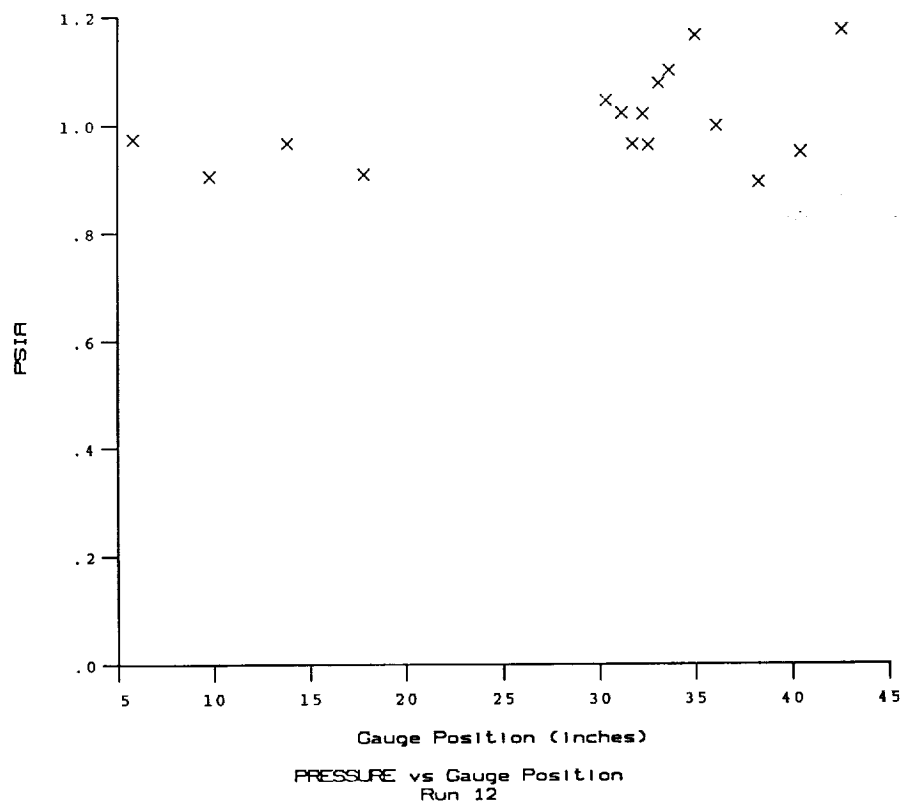
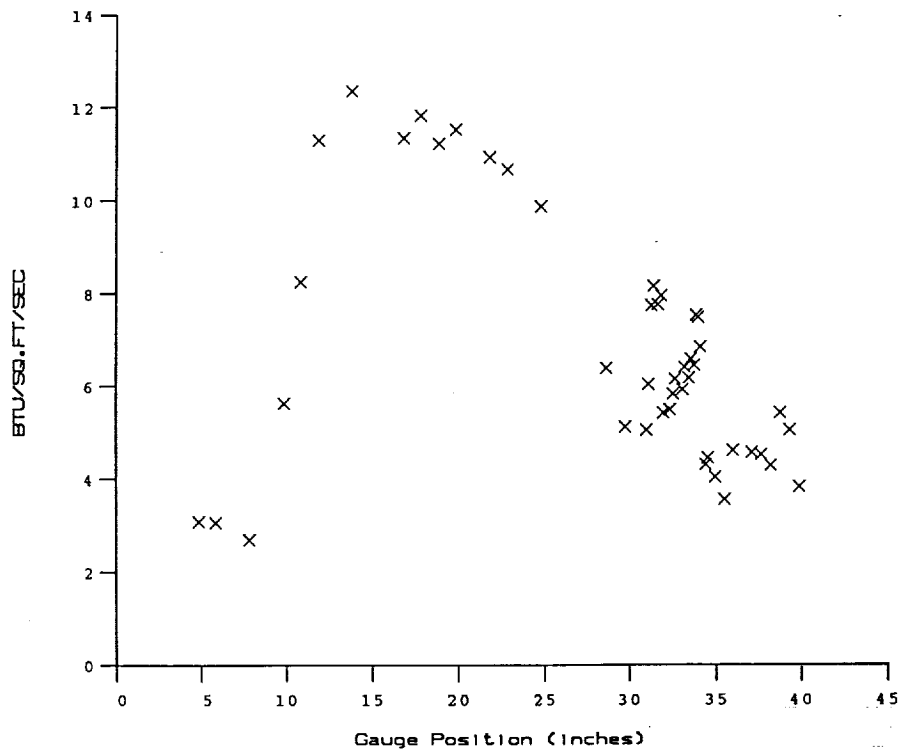
Po	= 3.705E+03 PSIA	Reservoir Total Pressure
Ho	= 1.429E+07 (Ft/sec) ²	Reservoir Total Enthalpy
To	= 2.221E+03 degR	Reservoir Total Temperature
M	= 7.868E+00	Freestream Mach Number
U	= 5.145E+03 Ft/sec	Freestream Velocity
T	= 1.779E+02 degR	Freestream Temperature
P	= 4.248E-01 PSIA	Freestream Static Pressure
Rho	= 2.004E-04 Slugs/Ft ³	Freestream Density
Mu	= 1.485E-07 Slugs/Ft-sec	Freestream Viscosity
Re	= 6.947E+06 1/Ft	Freestream Reynolds Number
Po'	= 3.403E+01 PSIA	Pitot Pressure
Q	= 1.842E+01 PSIA	Dynamic Pressure (Rho U ² /288)
Mi	= 2.888E+00	Shock Tube Incident Shock Mach Number
Tw	= 5.300E+02 degR	Wall Temperature (Test Gas = Air)
Hw	= 3.183E+06 (Ft/sec) ²	Wall Enthalpy (Cp Tw)
CPf	= 5.427E-02 1/PSIA	Pressure to CP factor (1/Q)
CHf	= 6.791E-05 Ft ² -s/BTU	Heat Rate to CH factor (778/(Rho U (Ho-Hw)))
QoFR	= 5.208E+01 BTU/Ft ² -s	Fay-Riddell Heat Transfer (.25' Diam Cylin.)

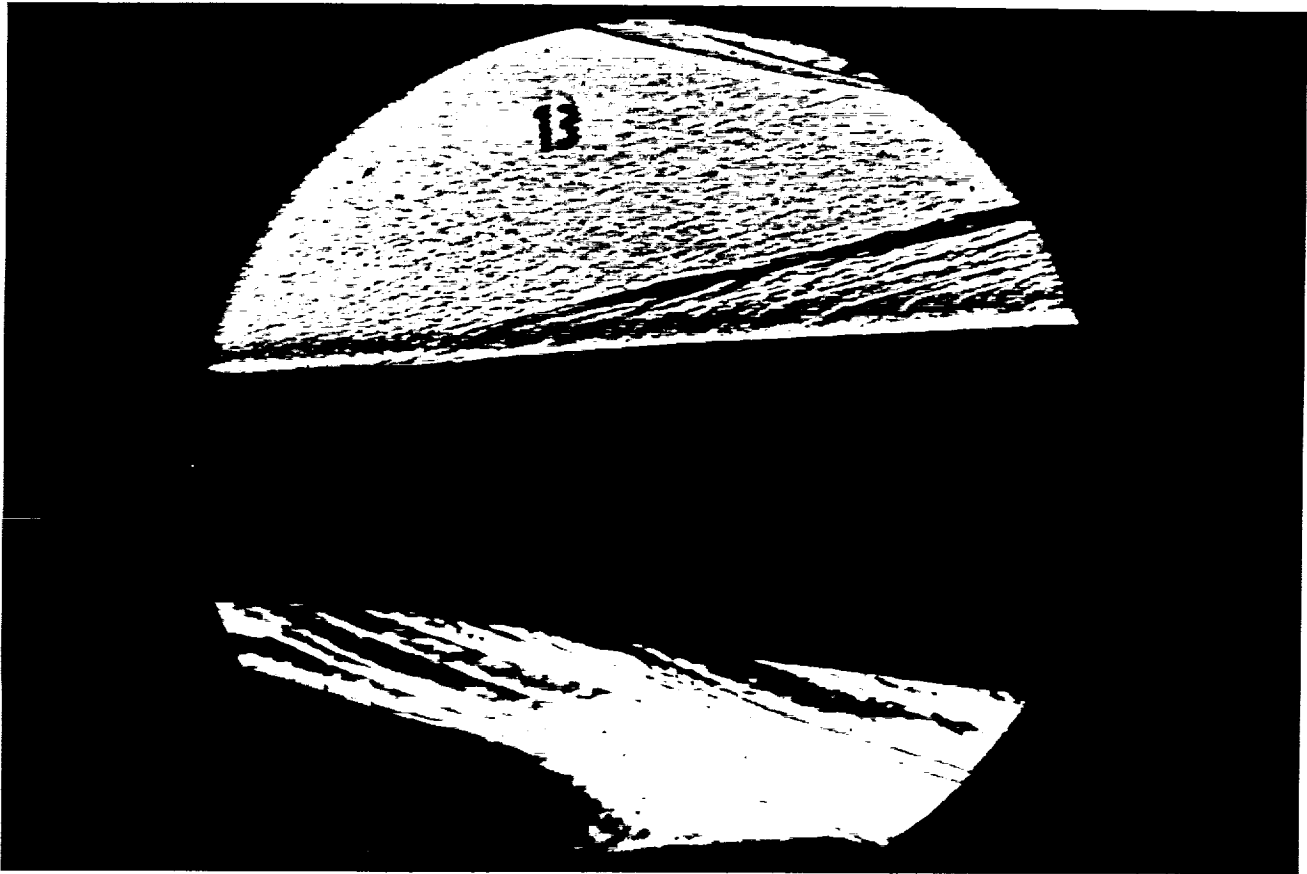




Test Conditions for Run 12 :

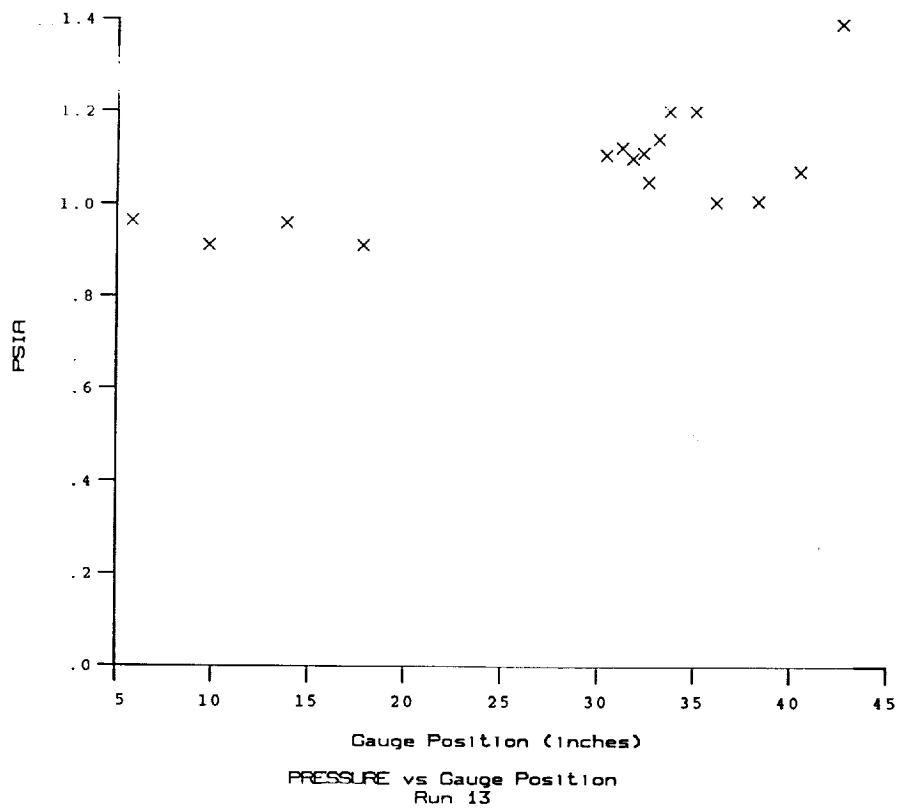
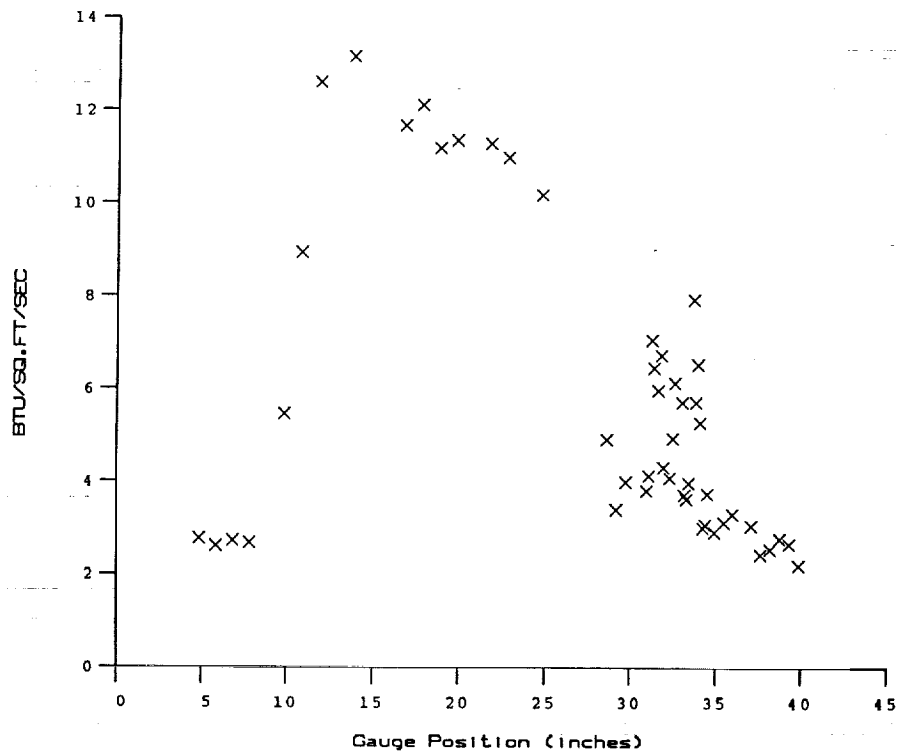
Po	= 2.082E+03 PSIA	Reservoir Total Pressure
Ho	= 1.357E+07 (Ft/sec) ²	Reservoir Total Enthalpy
To	= 2.128E+03 degR	Reservoir Total Temperature
M	= 6.417E+00	Freestream Mach Number
U	= 4.922E+03 Ft/sec	Freestream Velocity
T	= 2.446E+02 degR	Freestream Temperature
P	= 8.564E-01 PSIA	Freestream Static Pressure
Rho	= 2.938E-04 Slugs/Ft ³	Freestream Density
Mu	= 2.008E-07 Slugs/Ft-sec	Freestream Viscosity
Re	= 7.203E+06 1/Ft	Freestream Reynolds Number
Po'	= 4.607E+01 PSIA	Pitot Pressure
Q	= 2.471E+01 PSIA	Dynamic Pressure (Rho U ² /288)
Mi	= 2.816E+00	Shock Tube Incident Shock Mach Number
Tw	= 5.300E+02 degR	Wall Temperature (Test Gas = Air)
Hw	= 3.183E+06 (Ft/sec) ²	Wall Enthalpy (Cp Tw)
CPf	= 4.046E-02 1/PSIA	Pressure to CP factor (1/Q)
CHf	= 5.180E-05 Ft ² -s/BTU	Heat Rate to CH factor (778/(Rho U (Ho-Hw)))
QoFR	= 5.636E+01 BTU/Ft ² -s	Fay-Riddell Heat Transfer (.25' Diam Cylin.)

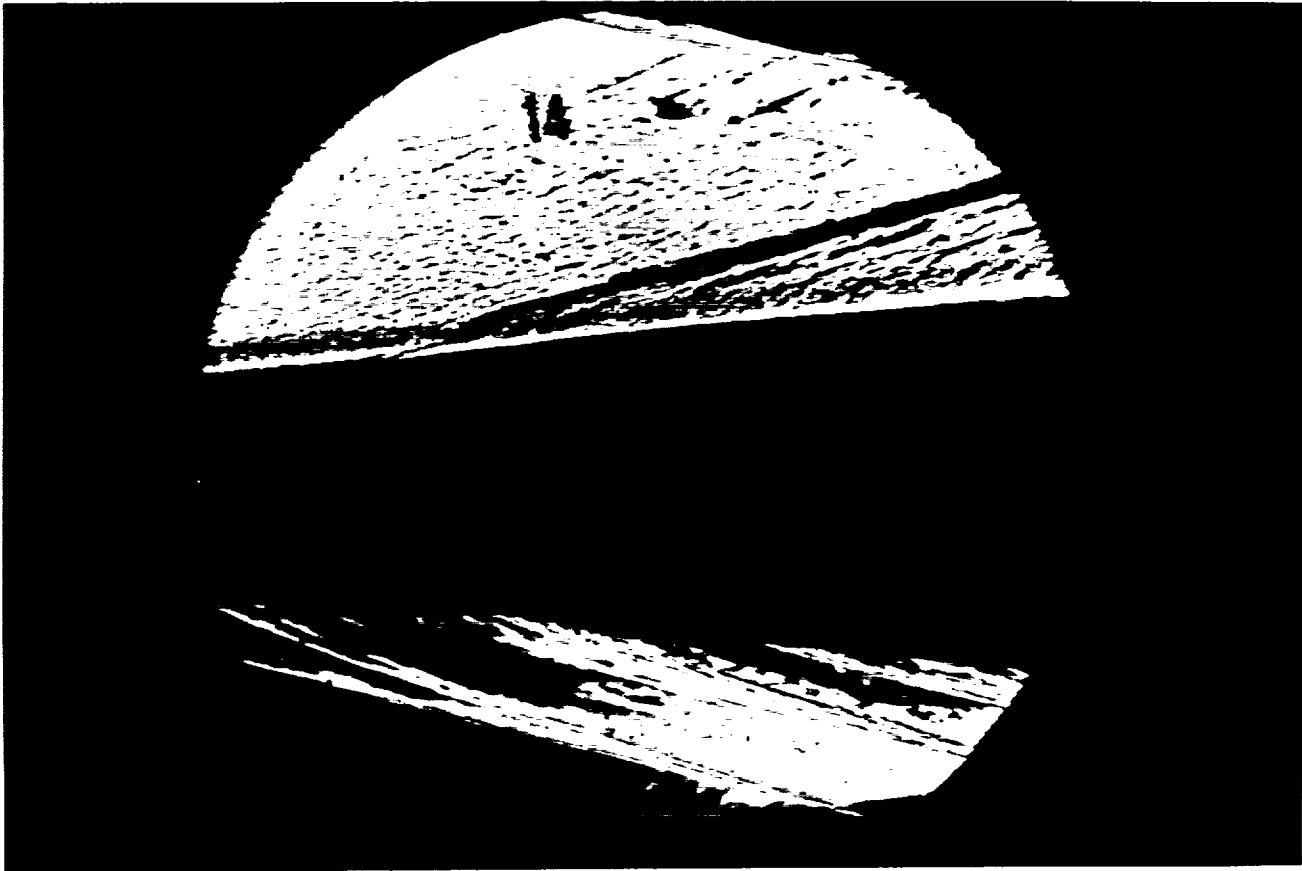




Test Conditions for Run 13 :

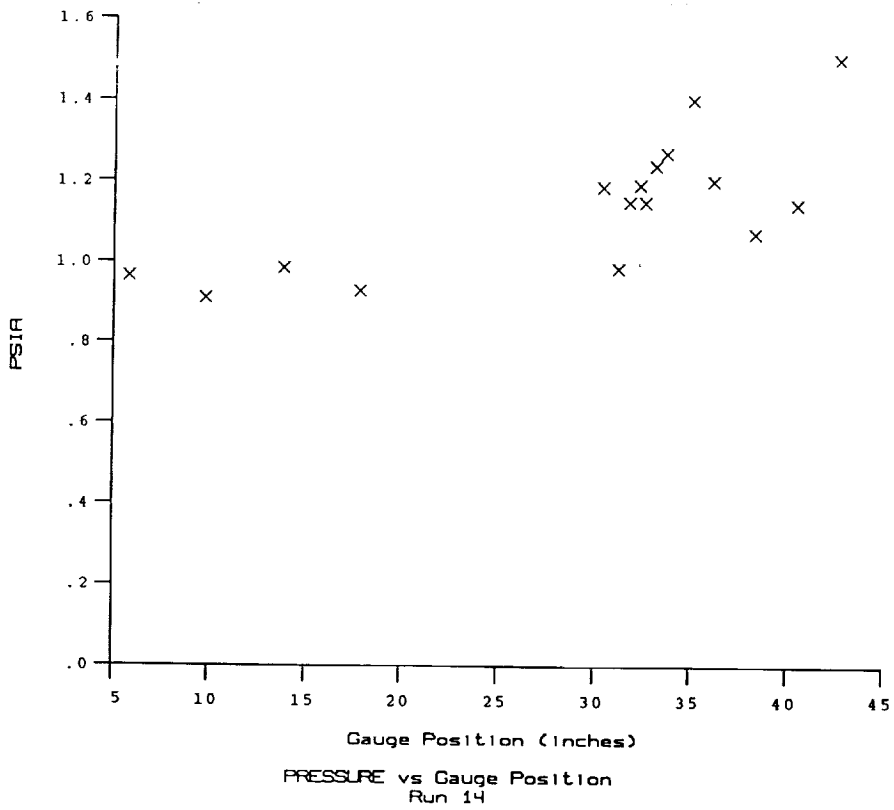
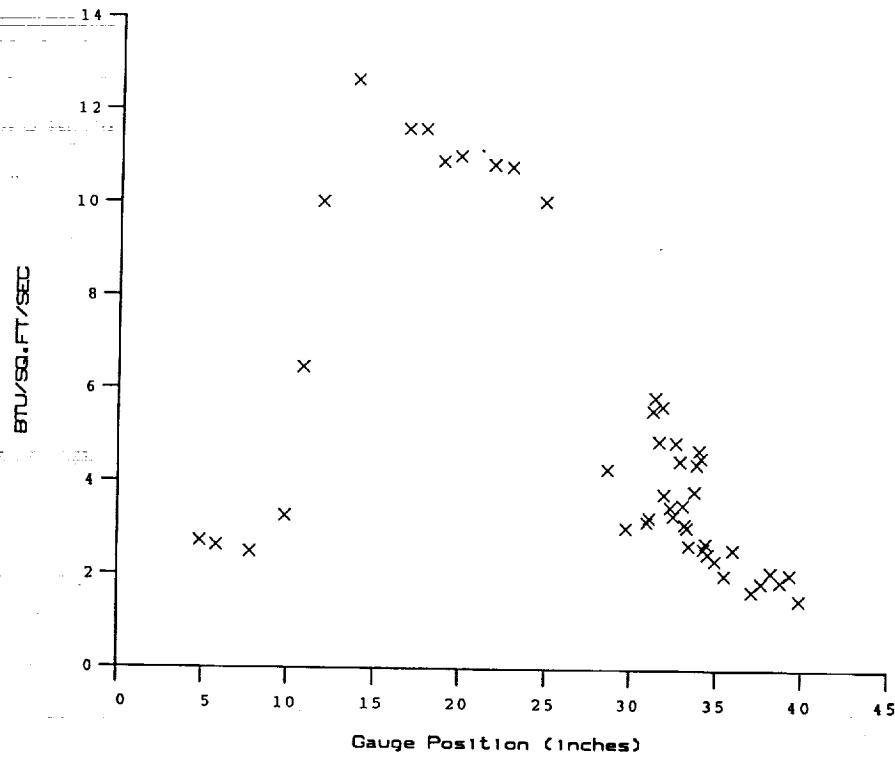
Po	= 2.125E+03 PSIA	Reservoir Total Pressure
Ho	= 1.341E+07 (Ft/sec) ²	Reservoir Total Enthalpy
To	= 2.104E+03 degR	Reservoir Total Temperature
M	= 6.422E+00	Freestream Mach Number
U	= 4.893E+03 Ft/sec	Freestream Velocity
T	= 2.413E+02 degR	Freestream Temperature
P	= 8.737E-01 PSIA	Freestream Static Pressure
Rho	= 3.038E-04 Slugs/Ft ³	Freestream Density
Mu	= 1.983E-07 Slugs/Ft-sec	Freestream Viscosity
Re	= 7.496E+06 1/Ft	Freestream Reynolds Number
Po'	= 4.706E+01 PSIA	Pitot Pressure
Q	= 2.525E+01 PSIA	Dynamic Pressure (Rho U ² /288)
Mi	= 2.806E+00	Shock Tube Incident Shock Mach Number
Tw	= 5.300E+02 degR	Wall Temperature (Test Gas = Air)
Hw	= 3.183E+06 (Ft/sec) ²	Wall Enthalpy (Cp Tw)
CPf	= 3.960E-02 1/PSIA	Pressure to CP factor (1/Q)
CHF	= 5.120E-05 Ft ² -s/BTU	Heat Rate to CH factor (778/(Rho U (Ho-Hw)))
QoFR	= 5.602E+01 BTU/Ft ² -s	Fay-Riddell Heat Transfer (.25' Diam Cylin.)

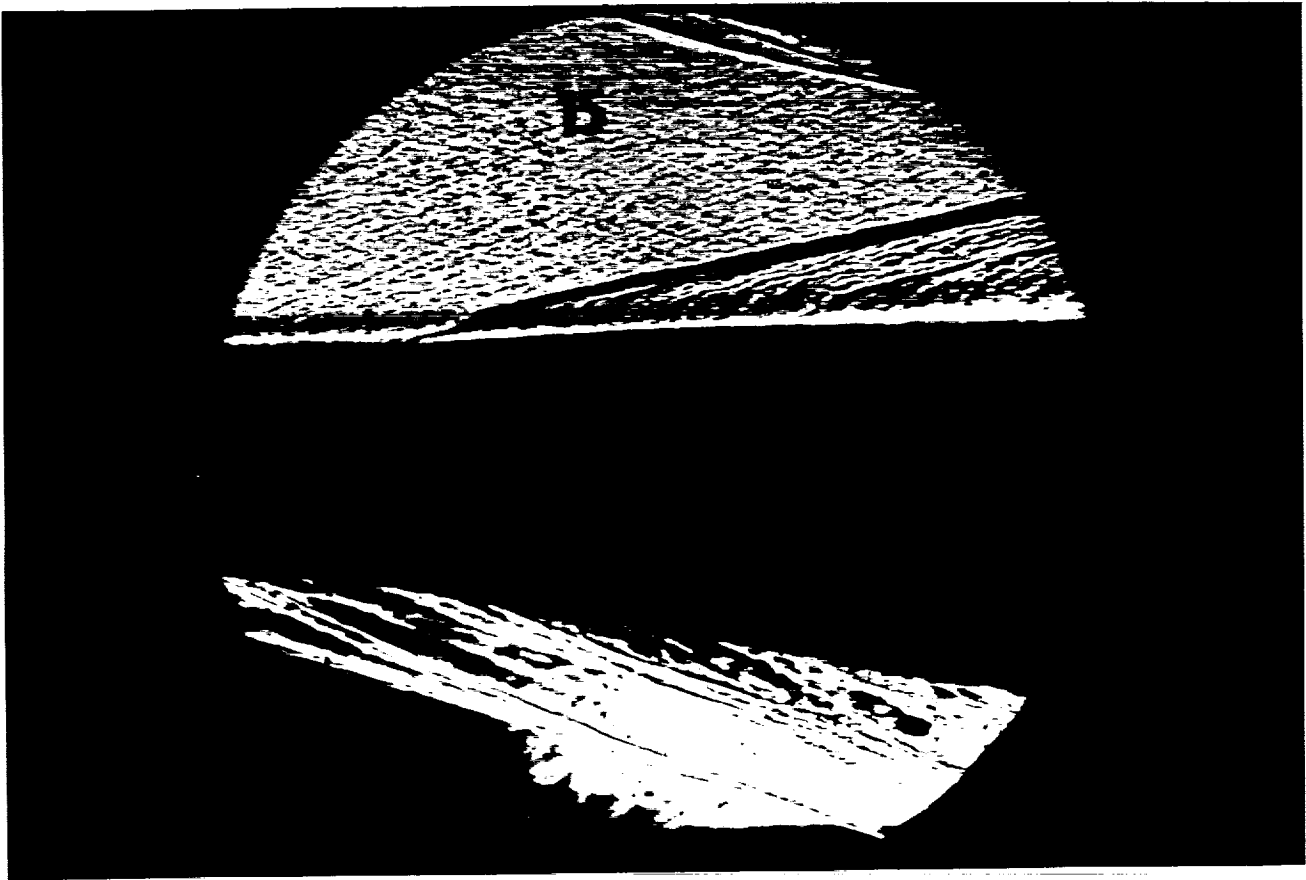




Test Conditions for Run 14 :

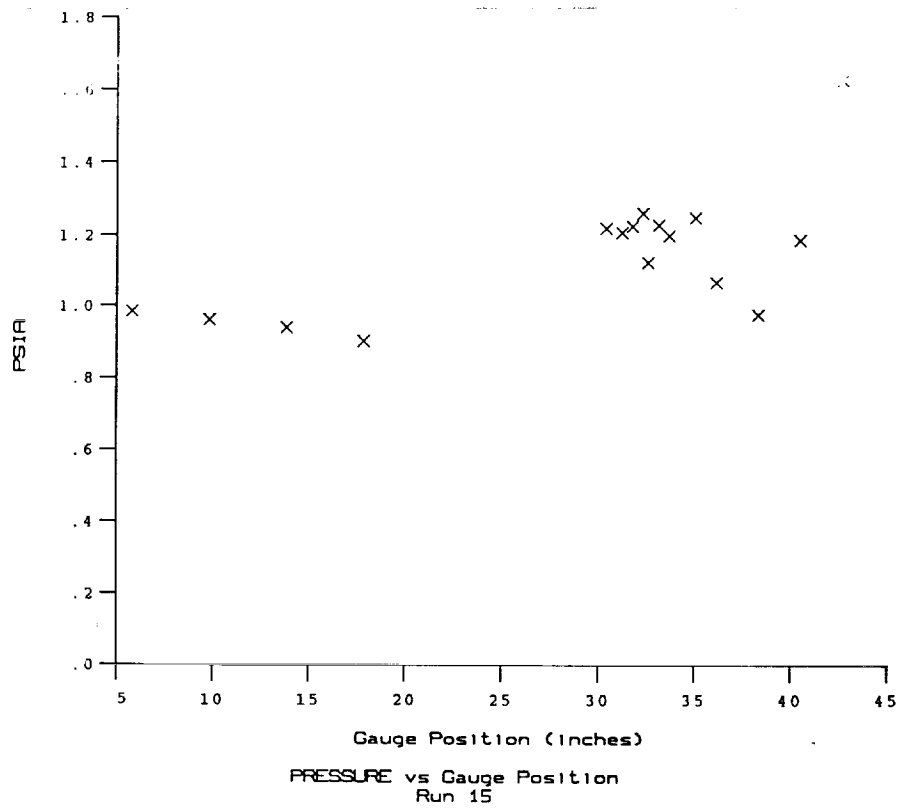
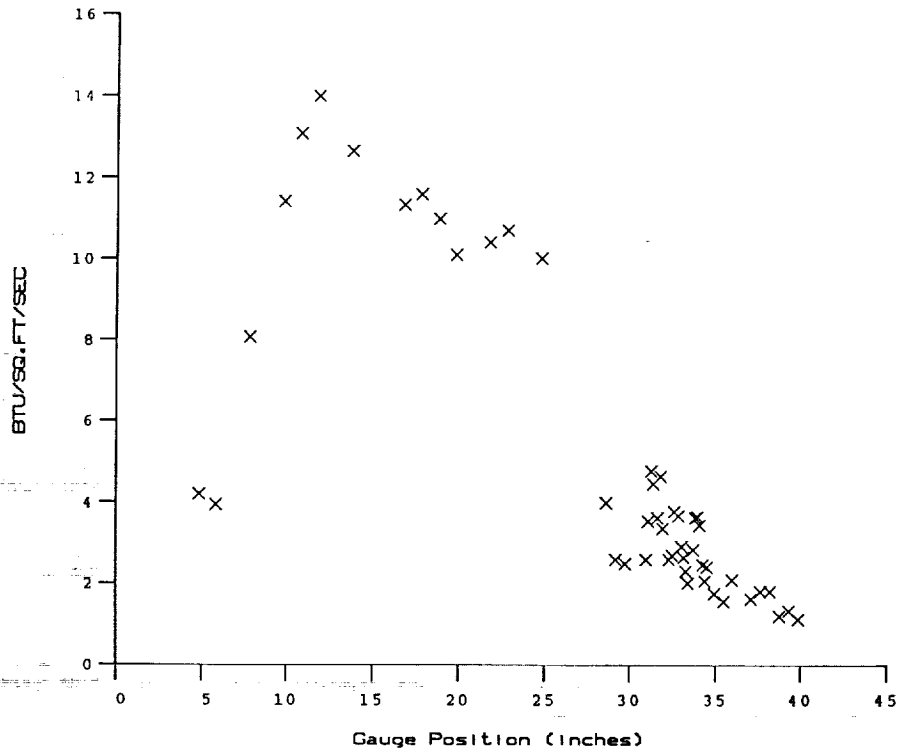
Po	= 2.118E+03 PSIA	Reservoir Total Pressure
Ho	= 1.349E+07 (Ft/sec) ²	Reservoir Total Enthalpy
To	= 2.117E+03 degR	Reservoir Total Temperature
M	= 6.422E+00	Freestream Mach Number
U	= 4.909E+03 Ft/sec	Freestream Velocity
T	= 2.429E+02 degR	Freestream Temperature
P	= 8.691E-01 PSIA	Freestream Static Pressure
Rho	= 3.002E-04 Slugs/Ft ³	Freestream Density
Mu	= 1.995E-07 Slugs/Ft-sec	Freestream Viscosity
Re	= 7.389E+06 1/Ft	Freestream Reynolds Number
Po'	= 4.682E+01 PSIA	Pitot Pressure
Q	= 2.512E+01 PSIA	Dynamic Pressure (Rho U ² /288)
Mi	= 2.804E+00	Shock Tube Incident Shock Mach Number
Tw	= 5.300E+02 degR	Wall Temperature (Test Gas = Air)
Hw	= 3.183E+06 (Ft/sec) ²	Wall Enthalpy (Cp Tw)
CPf	= 3.981E-02 1/PSIA	Pressure to CP factor (1/Q)
CHf	= 5.120E-05 Ft ² -s/BTU	Heat Rate to CH factor (778/(Rho U (Ho-Hw)))
QoFR	= 5.638E+01 BTU/Ft ² -s	Fay-Riddell Heat Transfer (.25' Diam Cylin.)

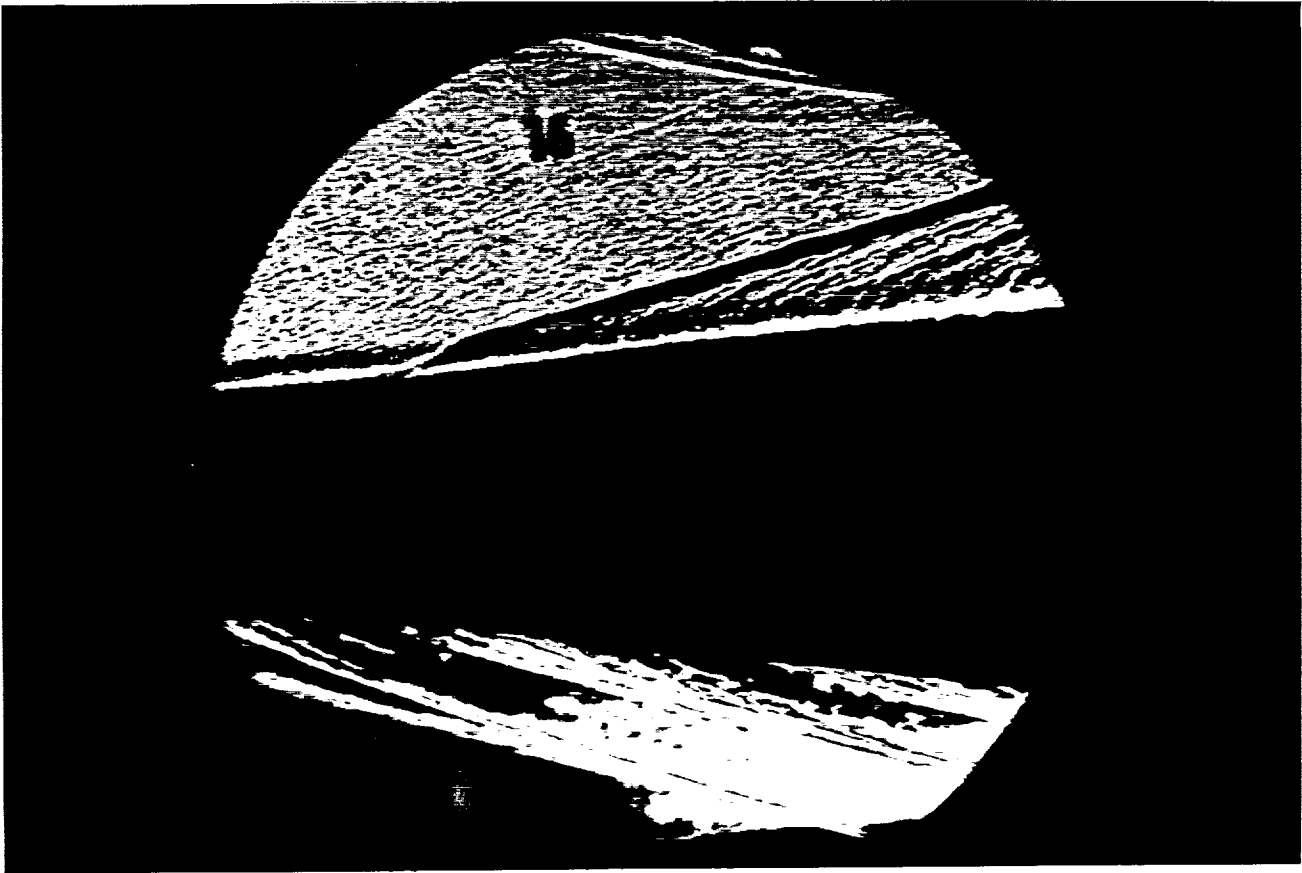




Test Conditions for Run 15 :

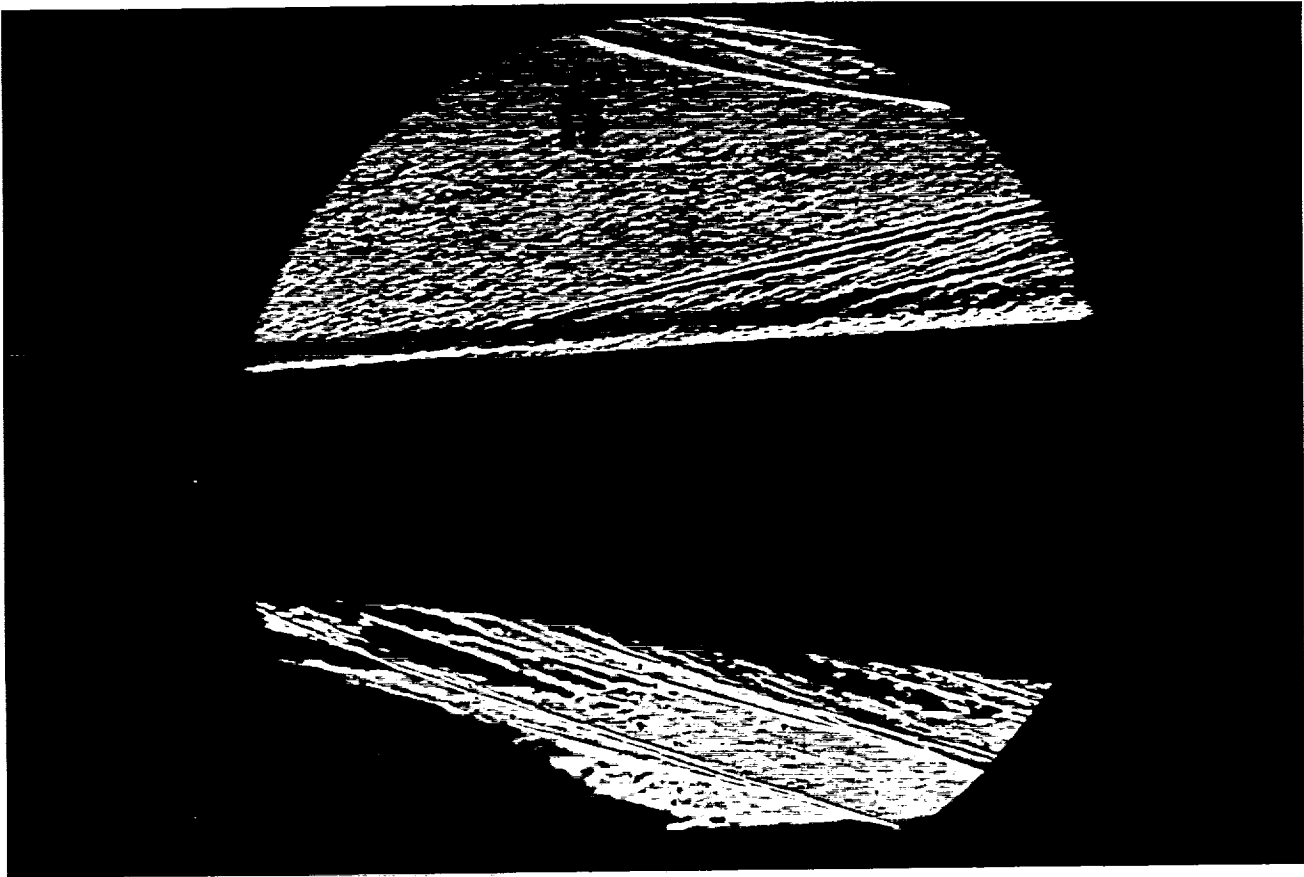
Po	= 2.119E+03 PSIA	Reservoir Total Pressure
Ho	= 1.360E+07 (Ft/sec) ²	Reservoir Total Enthalpy
To	= 2.132E+03 degR	Reservoir Total Temperature
M	= 6.421E+00	Freestream Mach Number
U	= 4.927E+03 Ft/sec	Freestream Velocity
T	= 2.448E+02 degR	Freestream Temperature
P	= 8.688E-01 PSIA	Freestream Static Pressure
Rho	= 2.978E-04 Slugs/Ft ³	Freestream Density
Mu	= 2.009E-07 Slugs/Ft-sec	Freestream Viscosity
Re	= 7.302E+06 1/Ft	Freestream Reynolds Number
Po'	= 4.679E+01 PSIA	Pitot Pressure
Q	= 2.510E+01 PSIA	Dynamic Pressure (Rho U ² /288)
Mi	= 2.810E+00	Shock Tube Incident Shock Mach Number
Tw	= 5.300E+02 degR	Wall Temperature (Test Gas = Air)
Hw	= 3.183E+06 (Ft/sec) ²	Wall Enthalpy (Cp Tw)
CPf	= 3.984E-02 1/PSIA	Pressure to CP factor (1/Q)
Chf	= 5.092E-05 Ft ² -s/BTU	Heat Rate to CH factor (778/(Rho U (Ho-Hw)))
QoFR	= 5.696E+01 BTU/Ft ² -s	Fay-Riddell Heat Transfer (.25' Diam Cylin.)





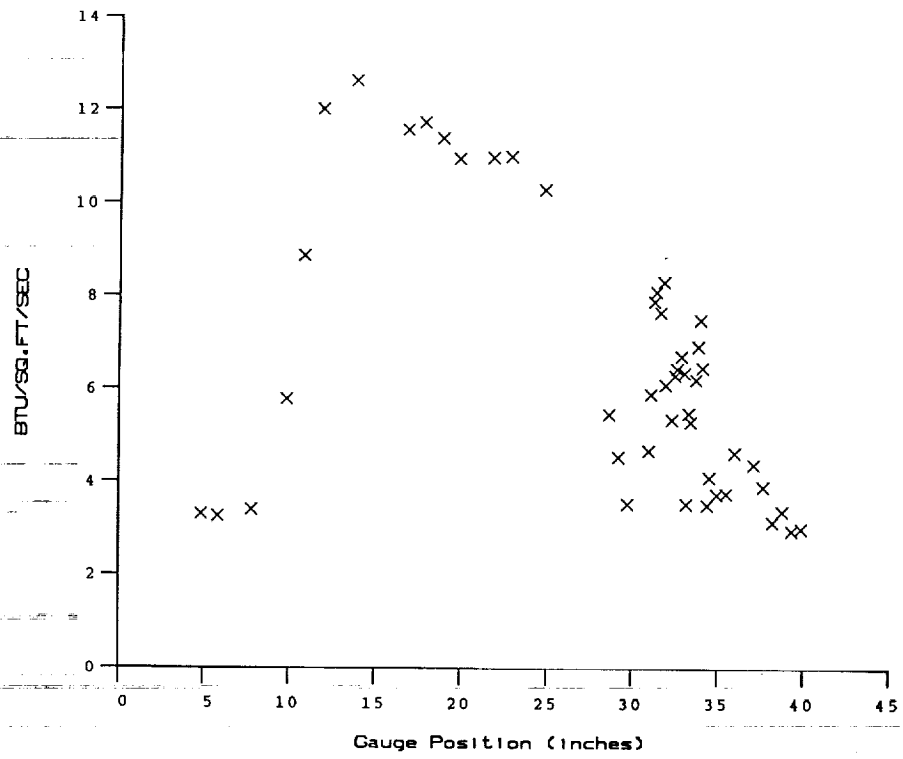
Test Conditions for Run 16 :

Po	= 2.093E+03 PSIA	Reservoir Total Pressure
Ho	= 1.329E+07 (Ft/sec) ²	Reservoir Total Enthalpy
To	= 2.089E+03 degR	Reservoir Total Temperature
M	= 6.425E+00	Freestream Mach Number
U	= 4.872E+03 Ft/sec	Freestream Velocity
T	= 2.391E+02 degR	Freestream Temperature
P	= 8.597E-01 PSIA	Freestream Static Pressure
Rho	= 3.017E-04 Slugs/Ft ³	Freestream Density
Mu	= 1.966E-07 Slugs/Ft-sec	Freestream Viscosity
Re	= 7.477E+06 1/Ft	Freestream Reynolds Number
Po'	= 4.634E+01 PSIA	Pitot Pressure
Q	= 2.487E+01 PSIA	Dynamic Pressure (Rho U ² /288)
Mi	= 2.786E+00	Shock Tube Incident Shock Mach Number
Tw	= 5.300E+02 degR	Wall Temperature (Test Gas = Air)
Hw	= 3.183E+06 (Ft/sec) ²	Wall Enthalpy (Cp Tw)
CPf	= 4.022E-02 1/PSIA	Pressure to CP factor (1/Q)
CHf	= 5.236E-05 Ft ² -s/BTU	Heat Rate to CH factor (778/(Rho U (Ho-Hw)))
QoFR	= 5.493E+01 BTU/Ft ² -s	Fay-Riddell Heat Transfer (.25' Diam Cylin.)

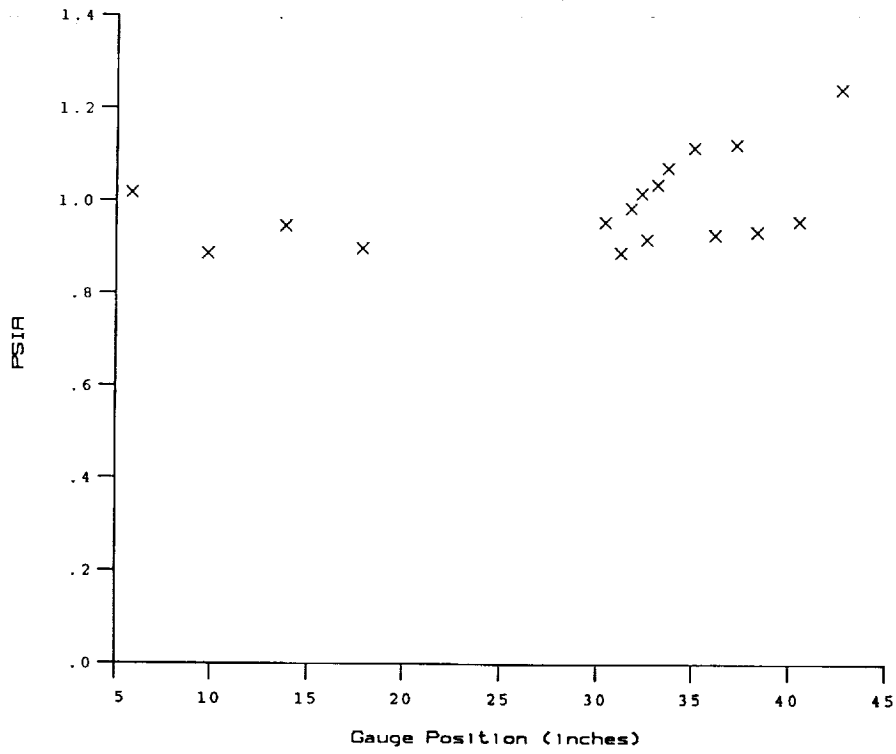


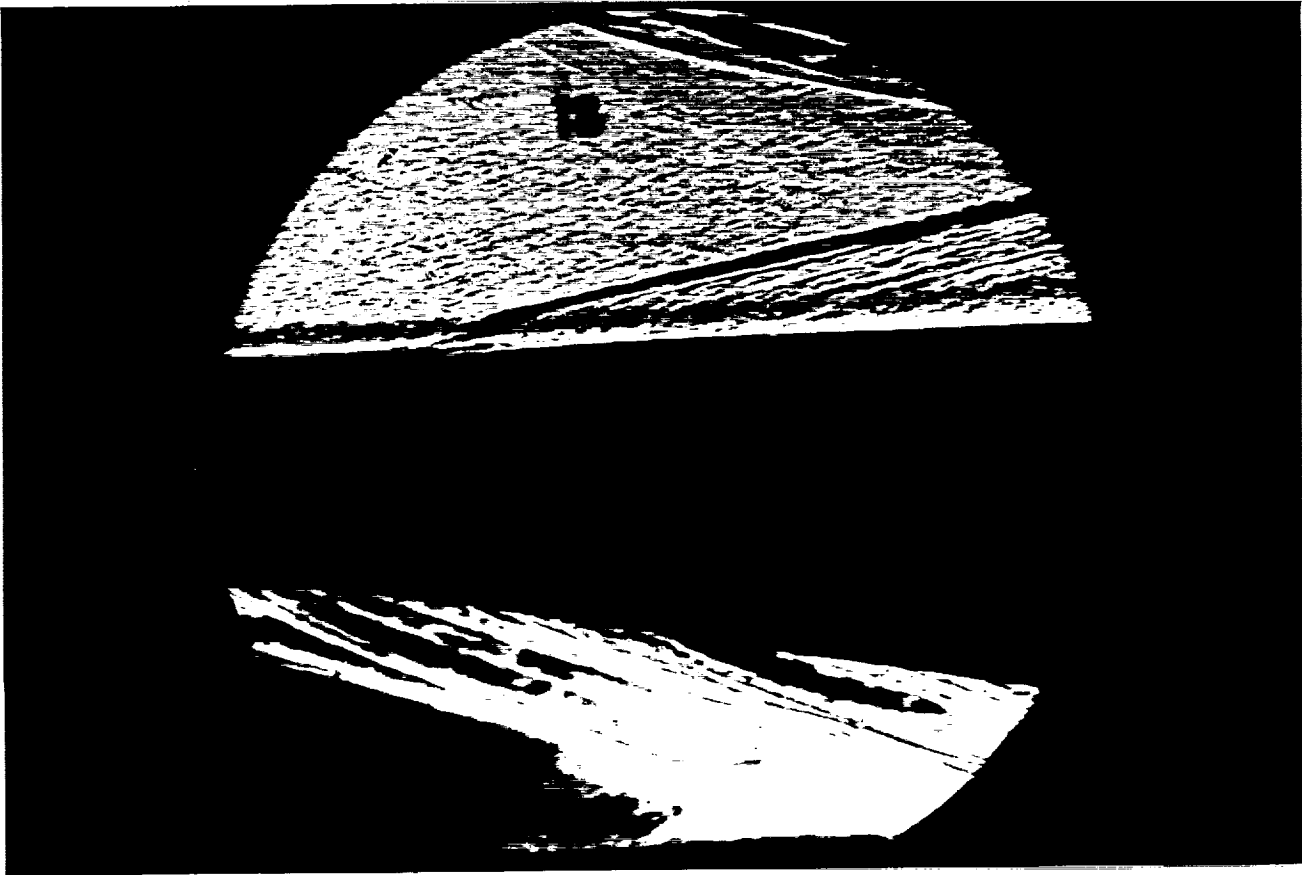
Test Conditions for Run 17 :

Po	= 2.144E+03 PSIA	Reservoir Total Pressure
Ho	= 1.356E+07 (Ft/sec) ²	Reservoir Total Enthalpy
To	= 2.126E+03 degR	Reservoir Total Temperature
M	= 6.422E+00	Freestream Mach Number
U	= 4.920E+03 Ft/sec	Freestream Velocity
T	= 2.440E+02 degR	Freestream Temperature
P	= 8.797E-01 PSIA	Freestream Static Pressure
Rho	= 3.025E-04 Slugs/Ft ³	Freestream Density
Mu	= 2.003E-07 Slugs/Ft-sec	Freestream Viscosity
Re	= 7.429E+06 1/Ft	Freestream Reynolds Number
Po'	= 4.739E+01 PSIA	Pitot Pressure
Q	= 2.542E+01 PSIA	Dynamic Pressure ($\rho U^2/288$)
Mi	= 2.814E+00	Shock Tube Incident Shock Mach Number
Tw	= 5.300E+02 degR	Wall Temperature (Test Gas = Air)
Hw	= 3.183E+06 (Ft/sec) ²	Wall Enthalpy ($C_p T_w$)
CPf	= 3.933E-02 1/PSIA	Pressure to CP factor (1/Q)
CHf	= 5.040E-05 Ft ² -s/BTU	Heat Rate to CH factor ($778/(\rho U (H_o - H_w))$)
QoFR	= 5.708E+01 BTU/Ft ² -s	Fay-Riddell Heat Transfer (.25' Diam Cylin.)



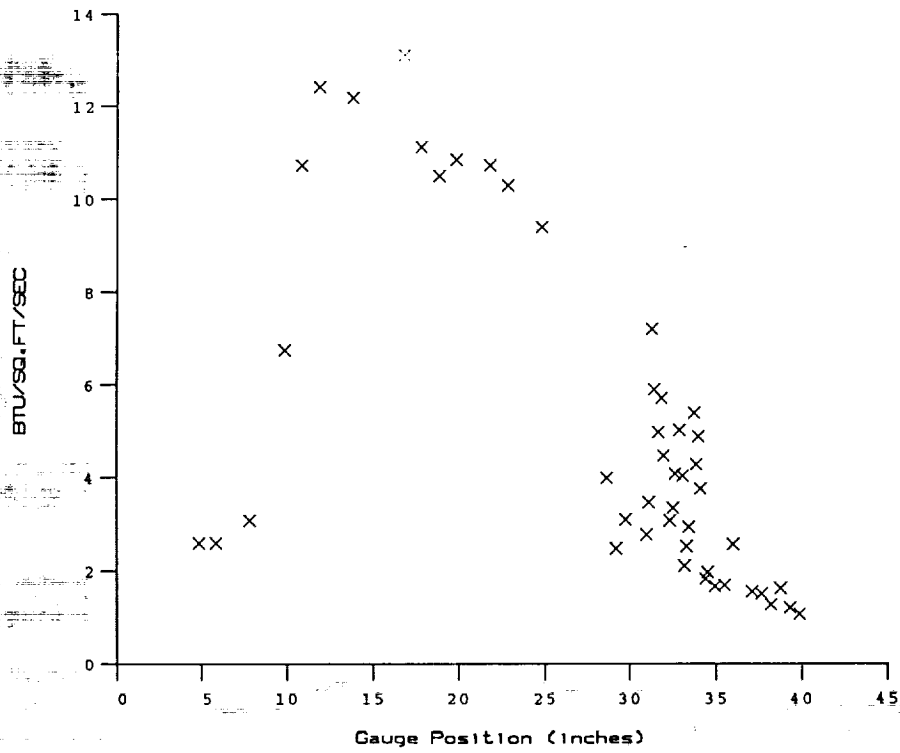
HEAT TRANSFER vs Gauge Position
Run 17



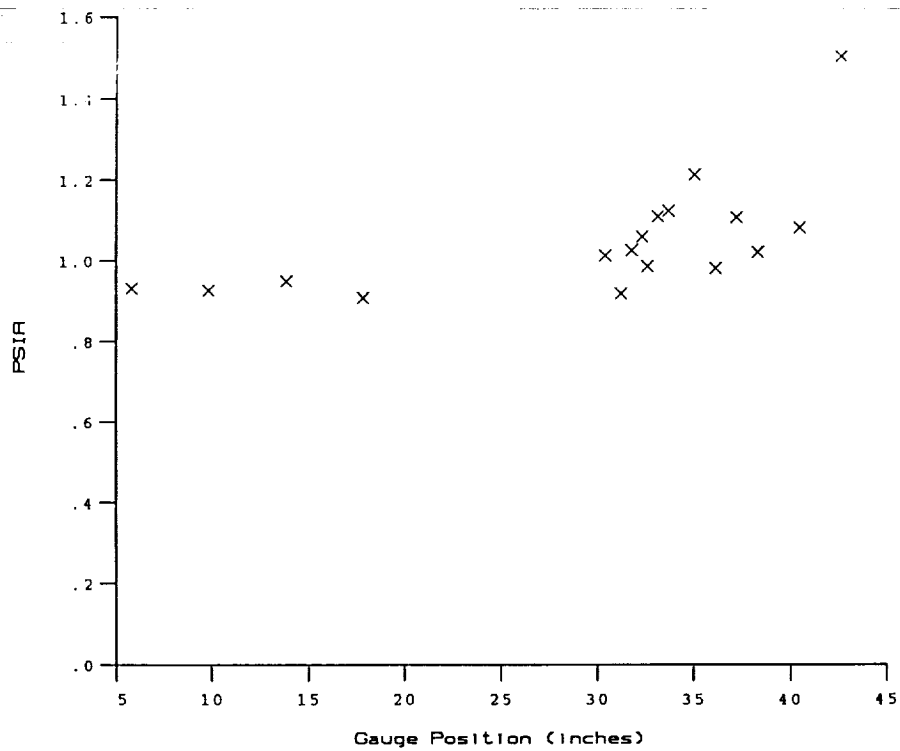


Test Conditions for Run 18 :

Po	= 2.111E+03 PSIA	Reservoir Total Pressure
Ho	= 1.338E+07 (Ft/sec) ²	Reservoir Total Enthalpy
To	= 2.102E+03 degR	Reservoir Total Temperature
M	= 6.426E+00	Freestream Mach Number
U	= 4.889E+03 Ft/sec	Freestream Velocity
T	= 2.407E+02 degR	Freestream Temperature
P	= 8.650E-01 PSIA	Freestream Static Pressure
Rho	= 3.016E-04 Slugs/Ft ³	Freestream Density
Mu	= 1.978E-07 Slugs/Ft-sec	Freestream Viscosity
Re	= 7.454E+06 1/Ft	Freestream Reynolds Number
Po'	= 4.664E+01 PSIA	Pitot Pressure
Q	= 2.503E+01 PSIA	Dynamic Pressure (Rho U ² /288)
Mi	= 2.786E+00	Shock Tube Incident Shock Mach Number
Tw	= 5.300E+02 degR	Wall Temperature (Test Gas - Air)
Hw	= 3.183E+06 (Ft/sec) ²	Wall Enthalpy (Cp Tw)
CPf	= 3.996E-02 1/PSIA	Pressure to CP factor (1/Q)
CHf	= 5.173E-05 Ft ² -s/BTU	Heat Rate to CH factor (778/(Rho U (Ho-Hw)))
QoFR	= 5.564E+01 BTU/Ft ² -s	Fay-Riddell Heat Transfer (.25' Diam Cylin.)

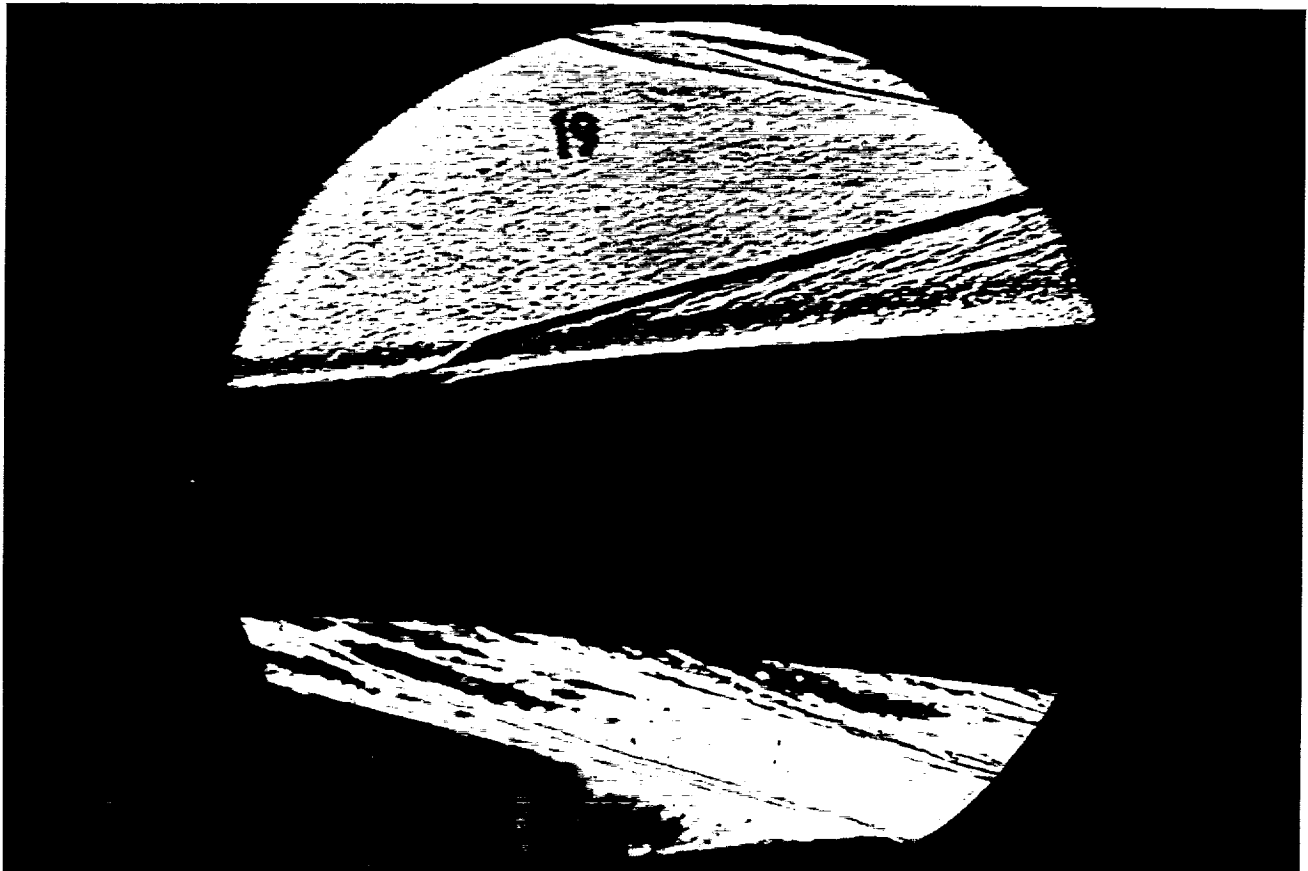


HEAT TRANSFER vs Gauge Position
Run 18



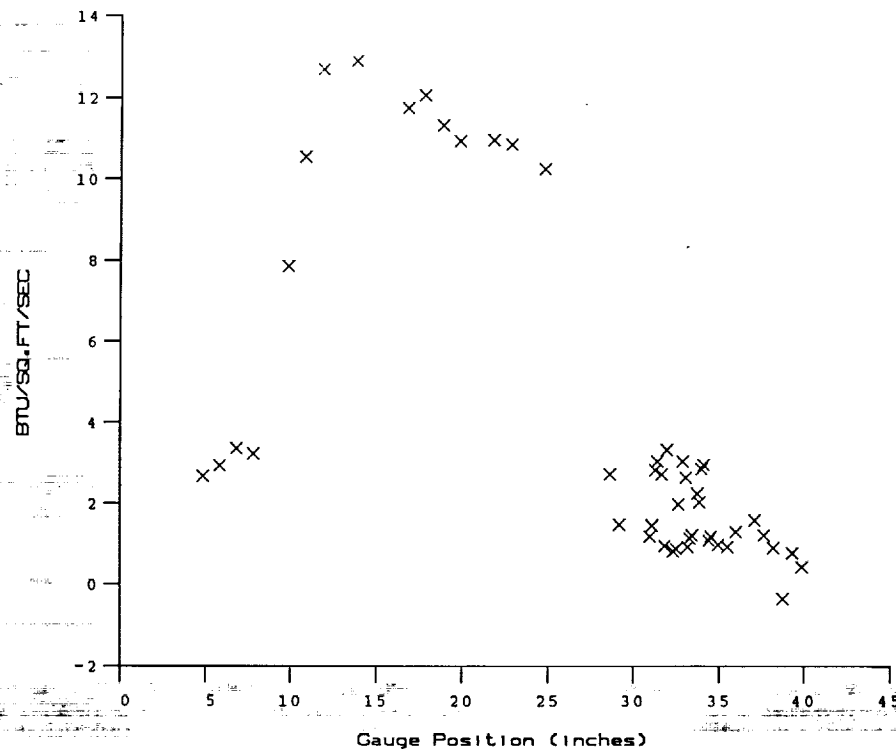
PRESSURE vs Gauge Position
Run 18

C-2

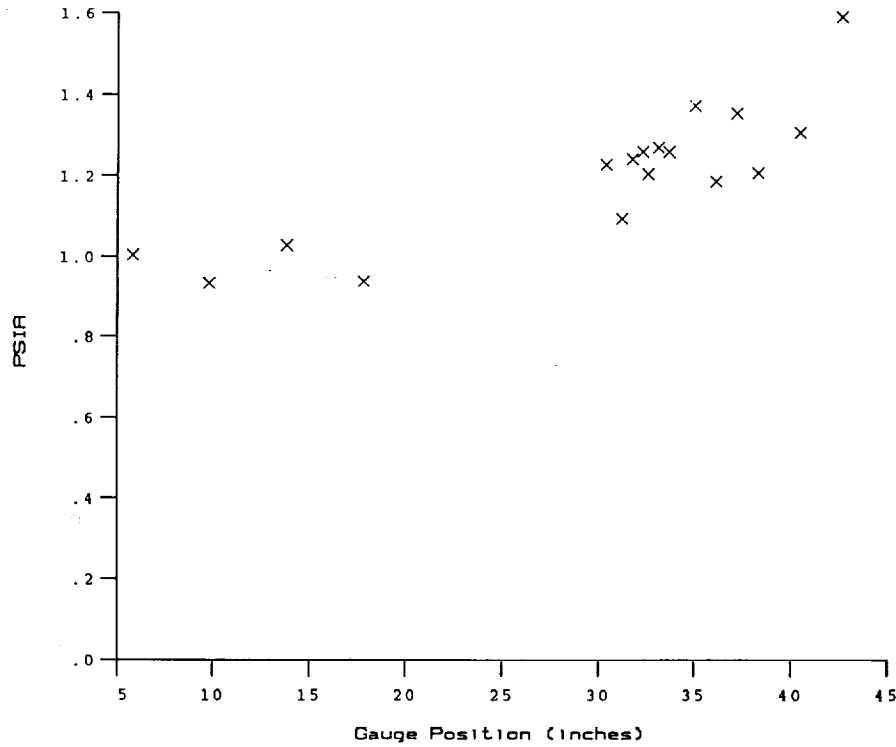


Test Conditions for Run 19 :

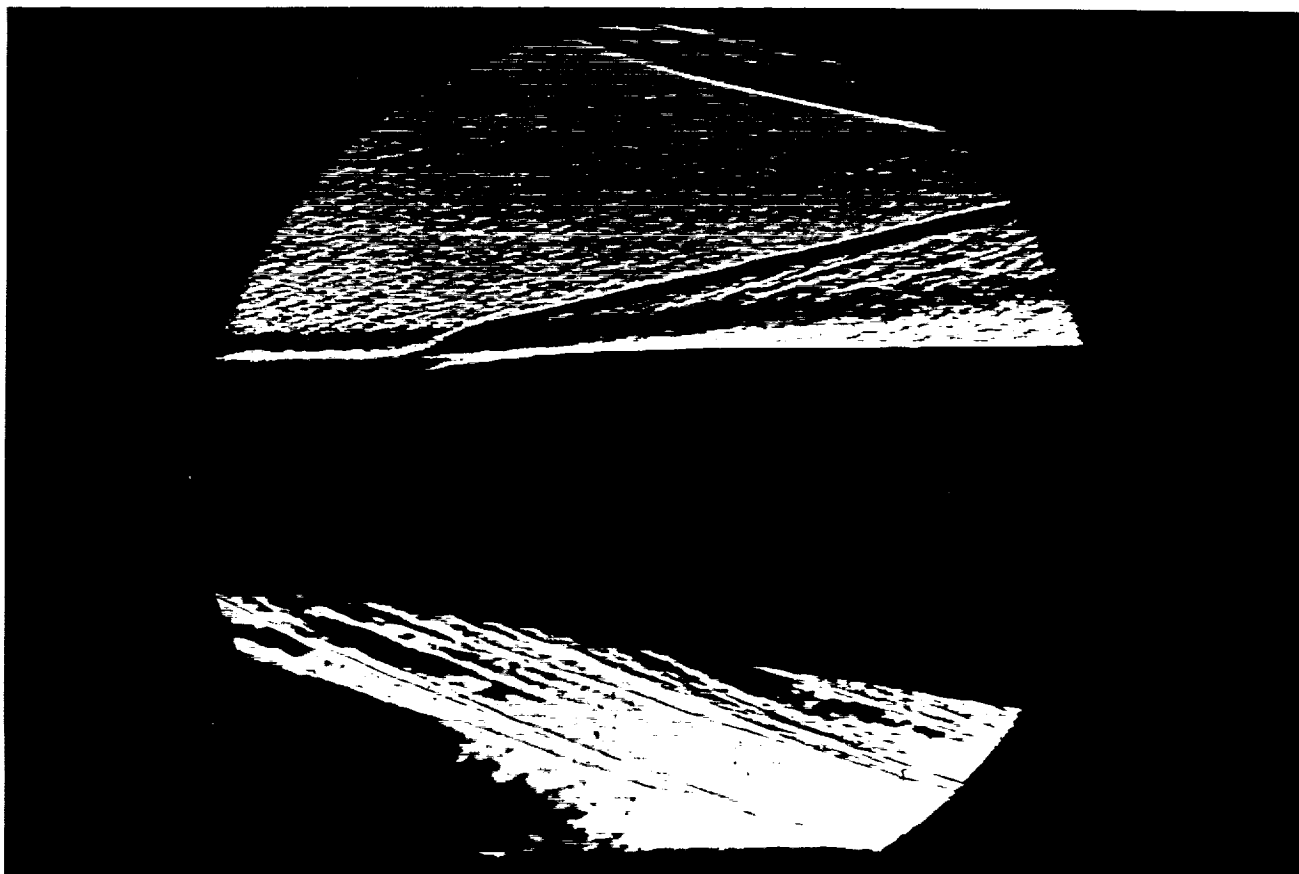
Po	= 2.134E+03 PSIA	Reservoir Total Pressure
Ho	= 1.344E+07 (Ft/sec) ²	Reservoir Total Enthalpy
To	= 2.109E+03 degR	Reservoir Total Temperature
M	= 6.423E+00	Freestream Mach Number
U	= 4.899E+03 Ft/sec	Freestream Velocity
T	= 2.419E+02 degR	Freestream Temperature
P	= 8.765E-01 PSIA	Freestream Static Pressure
Rho	= 3.041E-04 Slugs/Ft ³	Freestream Density
Mu	= 1.987E-07 Slugs/Ft-sec	Freestream Viscosity
Re	= 7.498E+06 1/Ft	Freestream Reynolds Number
Po'	= 4.722E+01 PSIA	Pitot Pressure
Q	= 2.534E+01 PSIA	Dynamic Pressure (Rho U ² /288)
Mi	= 2.806E+00	Shock Tube Incident Shock Mach Number
Tw	= 5.300E+02 degR	Wall Temperature (Test Gas = Air)
Hw	= 3.183E+06 (Ft/sec) ²	Wall Enthalpy (Cp Tw)
CPf	= 3.947E-02 1/PSIA	Pressure to CP factor (1/Q)
CHf	= 5.093E-05 Ft ² -s/BTU	Heat Rate to CH factor (778/(Rho U (Ho-Hw)))
QoFR	= 5.630E+01 BTU/Ft ² -s	Fay-Riddell Heat Transfer (.25' Diam Cylin.)



HEAT TRANSFER vs Gauge Position
Run 19

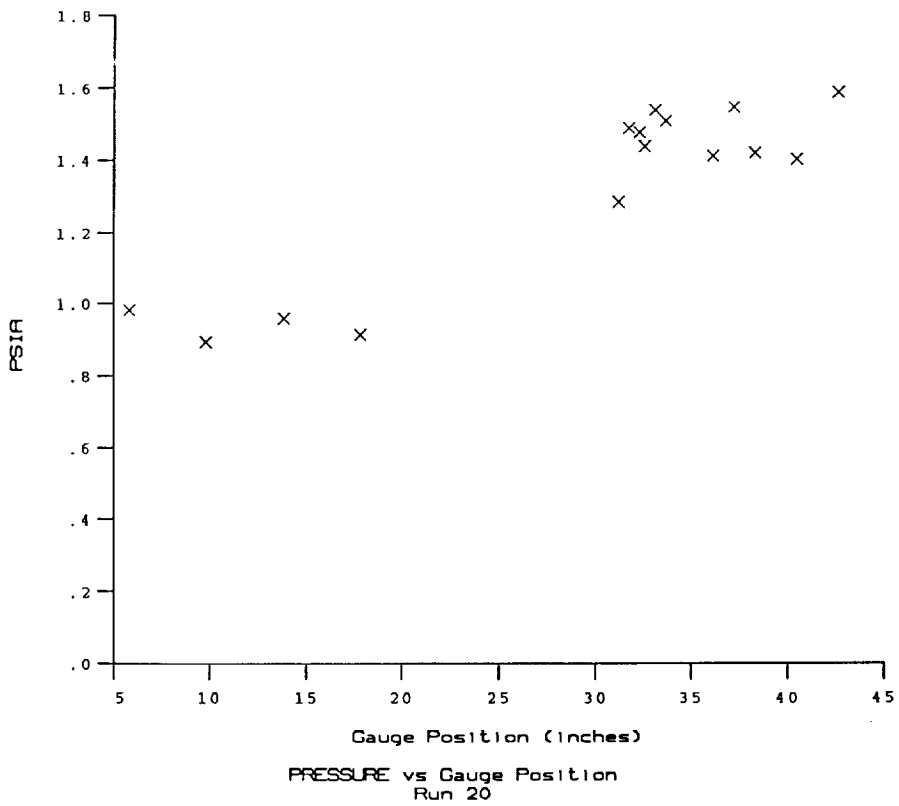
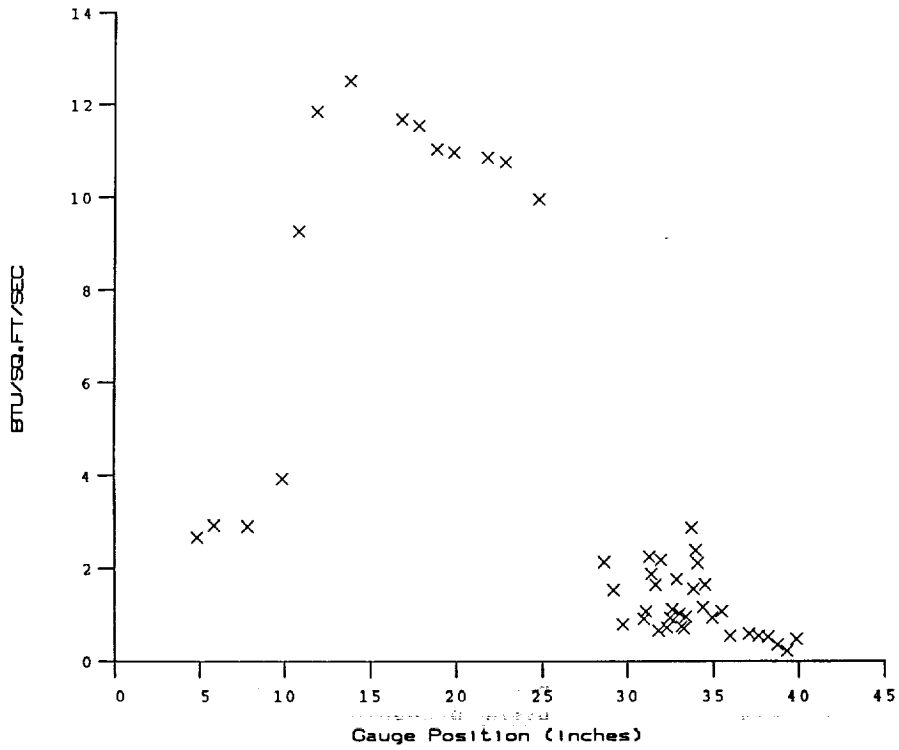


PRESSURE vs Gauge Position
Run 19



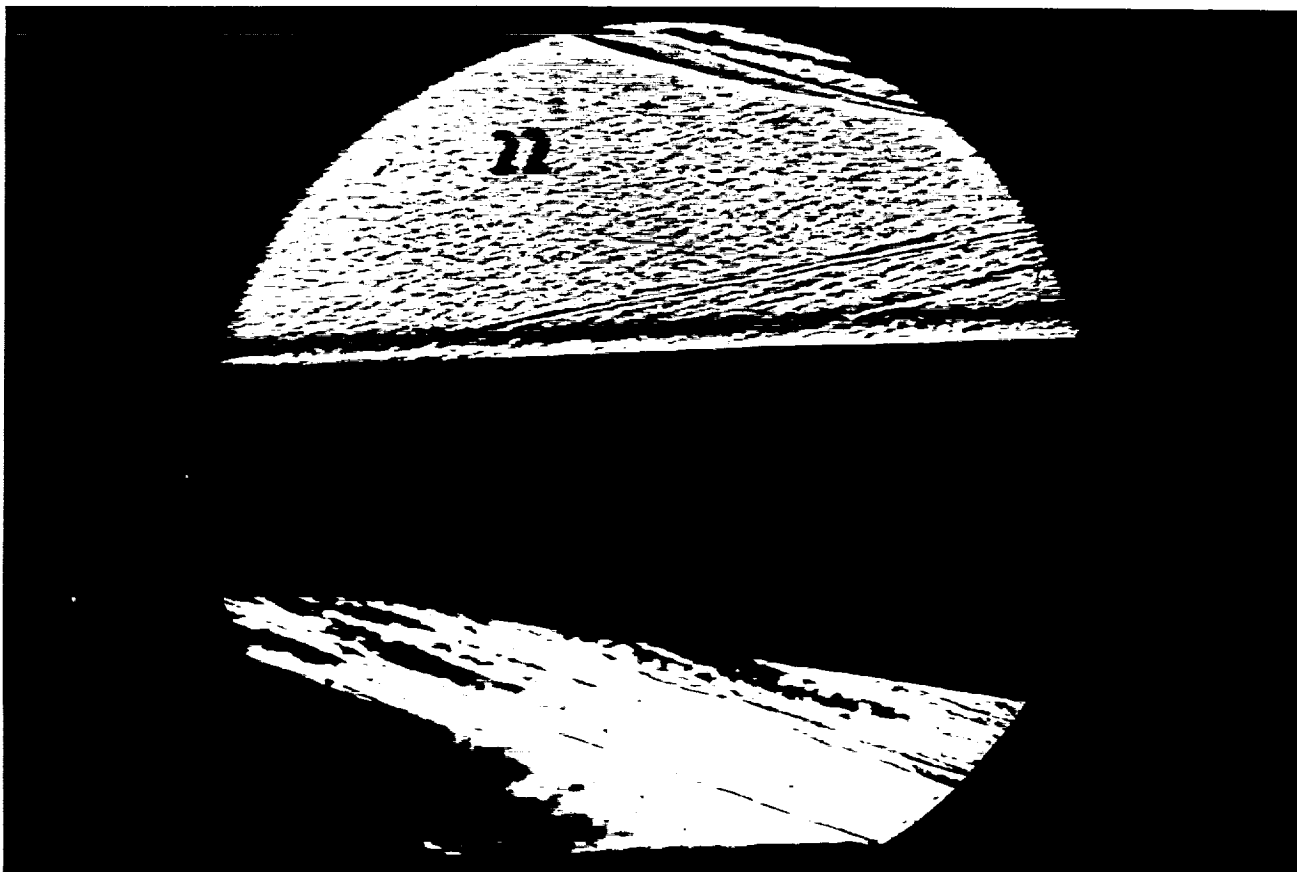
Test Conditions for Run 20 :

Po	= 2.134E+03 PSIA	Reservoir Total Pressure
Ho	= 1.351E+07 (Ft/sec) ²	Reservoir Total Enthalpy
To	= 2.119E+03 degR	Reservoir Total Temperature
M	= 6.422E+00	Freestream Mach Number
U	= 4.911E+03 Ft/sec	Freestream Velocity
T	= 2.431E+02 degR	Freestream Temperature
P	= 8.759E-01 PSIA	Freestream Static Pressure
Rho	= 3.023E-04 Slugs/Ft ³	Freestream Density
Mu	= 1.997E-07 Slugs/Ft-sec	Freestream Viscosity
Re	= 7.436E+06 1/Ft	Freestream Reynolds Number
Po'	= 4.718E+01 PSIA	Pitot Pressure
Q	= 2.531E+01 PSIA	Dynamic Pressure (Rho U ² /288)
Mi	= 2.809E+00	Shock Tube Incident Shock Mach Number
Tw	= 5.300E+02 degR	Wall Temperature (Test Gas = Air)
Hw	= 3.183E+06 (Ft/sec) ²	Wall Enthalpy (Cp Tw)
CPf	= 3.950E-02 1/PSIA	Pressure to CP factor (1/Q)
CHf	= 5.076E-05 Ft ² -s/BTU	Heat Rate to CH factor (778/(Rho U (Ho-Hw)))
QoFR	= 5.668E+01 BTU/Ft ² -s	Fay-Riddell Heat Transfer (.25' Diam Cylin.)



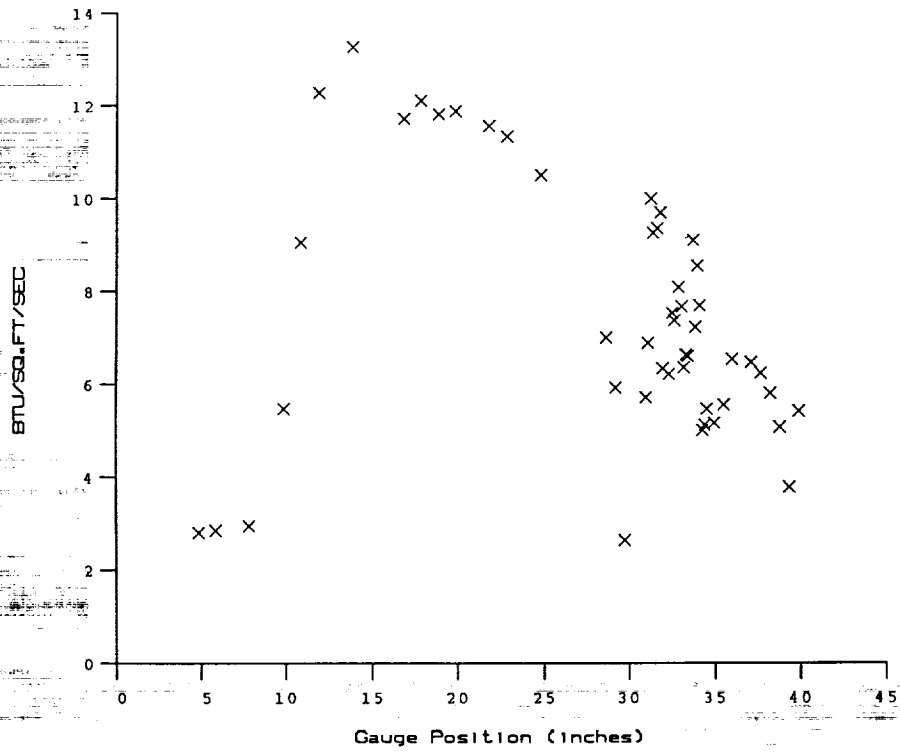
Test Conditions for Run 21 :

Po	- 2.190E+03 PSIA	Reservoir Total Pressure
Ho	- 1.364E+07 (Ft/sec) ²	Reservoir Total Enthalpy
To	- 2.138E+03 degR	Reservoir Total Temperature
M	- 6.424E+00	Freestream Mach Number
U	- 4.936E+03 Ft/sec	Freestream Velocity
T	- 2.455E+02 degR	Freestream Temperature
P	- 8.963E-01 PSIA	Freestream Static Pressure
Rho	- 3.064E-04 Slugs/Ft ³	Freestream Density
Mu	- 2.014E-07 Slugs/Ft-sec	Freestream Viscosity
Re	- 7.508E+06 1/Ft	Freestream Reynolds Number
Po'	- 4.832E+01 PSIA	Pitot Pressure
Q	- 2.592E+01 PSIA	Dynamic Pressure (Rho U ² /288)
Mi	- 2.818E+00	Shock Tube Incident Shock Mach Number
Tw	- 5.300E+02 degR	Wall Temperature (Test Gas = Air)
Hw	- 3.183E+06 (Ft/sec) ²	Wall Enthalpy (Cp Tw)
CPf	- 3.858E-02 1/PSIA	Pressure to CP factor (1/Q)
CHF	- 4.918E-05 Ft ² -s/BTU	Heat Rate to CH factor (778/(Rho U (Ho-Hw))
QoFR	- 5.816E+01 BTU/Ft ² -s	Fay-Riddell Heat Transfer (.25' Diam Cylin.)

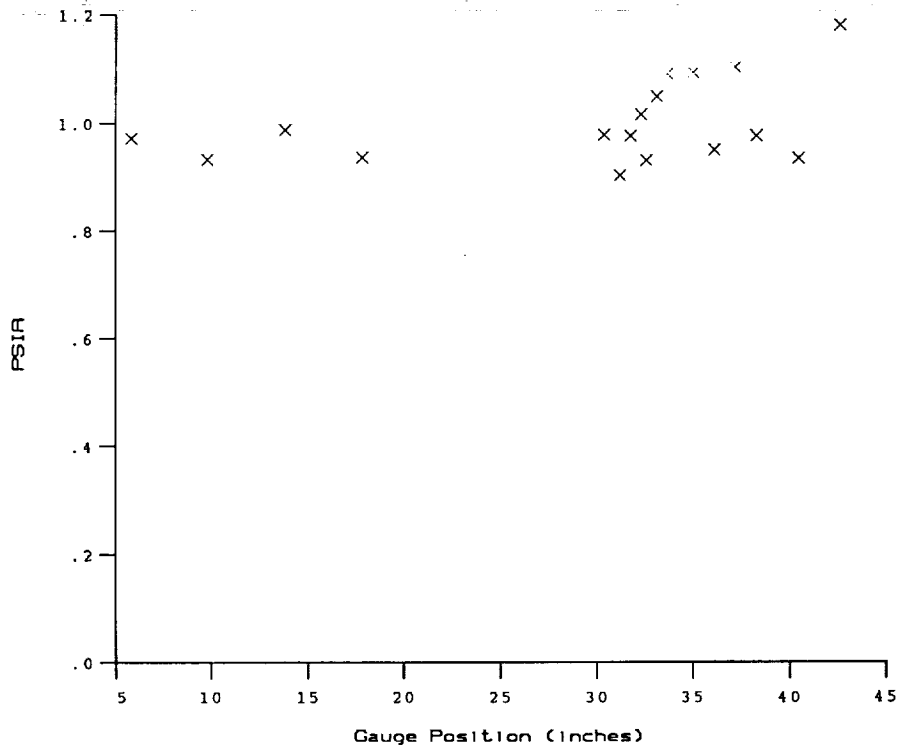


Test Conditions for Run 22 :

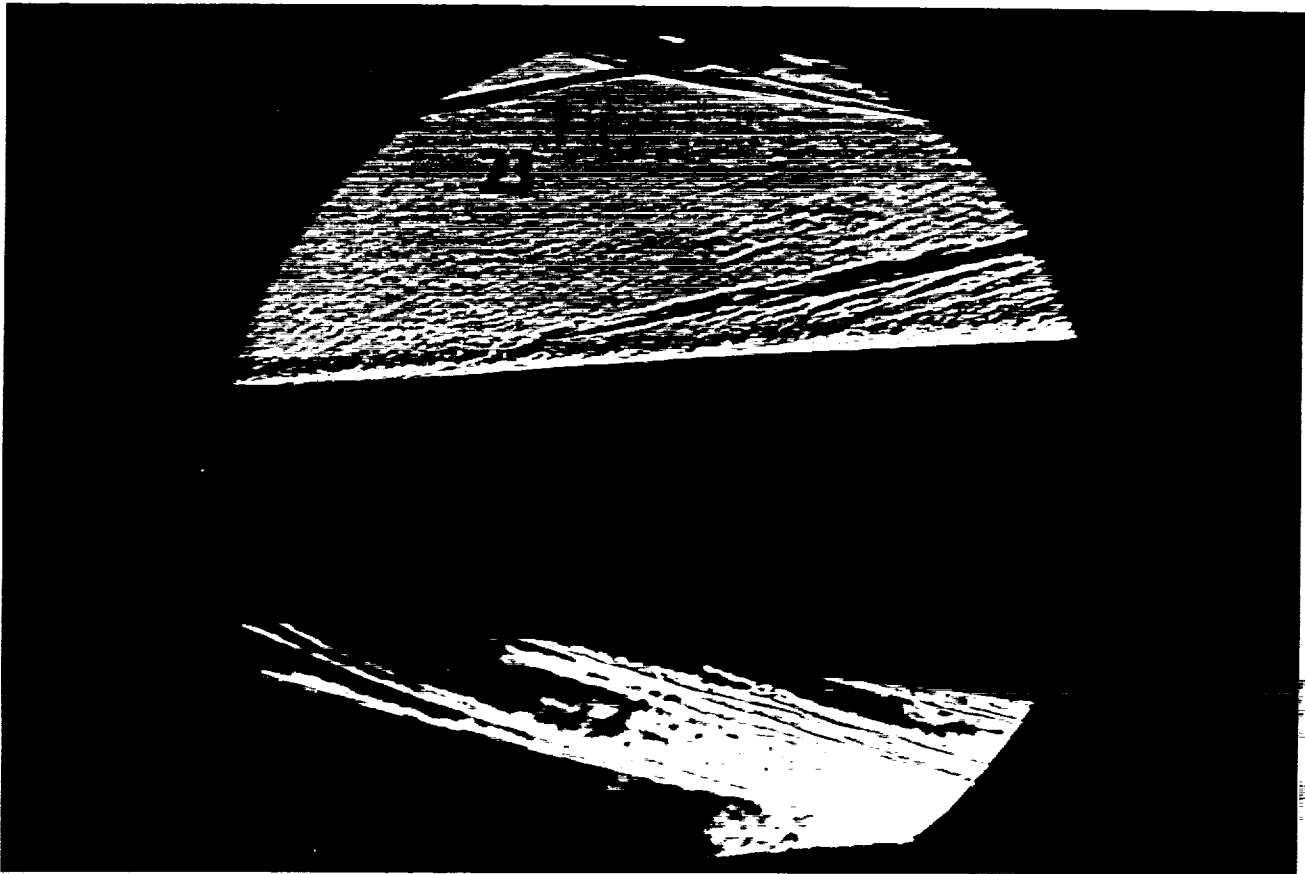
Po	= 2.187E+03 PSIA	Reservoir Total Pressure
Ho	= 1.384E+07 (Ft/sec) ²	Reservoir Total Enthalpy
To	= 2.165E+03 degR	Reservoir Total Temperature
M	= 6.419E+00	Freestream Mach Number
U	= 4.970E+03 Ft/sec	Freestream Velocity
T	= 2.493E+02 degR	Freestream Temperature
P	= 8.957E-01 PSIA	Freestream Static Pressure
Rho	= 3.016E-04 Slugs/Ft ³	Freestream Density
Mu	= 2.043E-07 Slugs/Ft-sec	Freestream Viscosity
Re	= 7.337E+06 1/Ft	Freestream Reynolds Number
Po'	= 4.822E+01 PSIA	Pitot Pressure
Q	= 2.586E+01 PSIA	Dynamic Pressure (Rho U ² /288)
Mi	= 2.838E+00	Shock Tube Incident Shock Mach Number
Tw	= 5.300E+02 degR	Wall Temperature (Test Gas = Air)
Hw	= 3.183E+06 (Ft/sec) ²	Wall Enthalpy (Cp Tw)
CPf	= 3.866E-02 1/PSIA	Pressure to CP factor (1/Q)
CHf	= 4.873E-05 Ft ² -s/BTU	Heat Rate to CH factor (778/(Rho U (Ho-Hw)))
QoFR	= 5.923E+01 BTU/Ft ² -s	Fay-Riddell Heat Transfer (.25' Diam Cylin.)



HEAT TRANSFER vs Gauge Position
Run 22



PRESSURE vs Gauge Position
Run 22

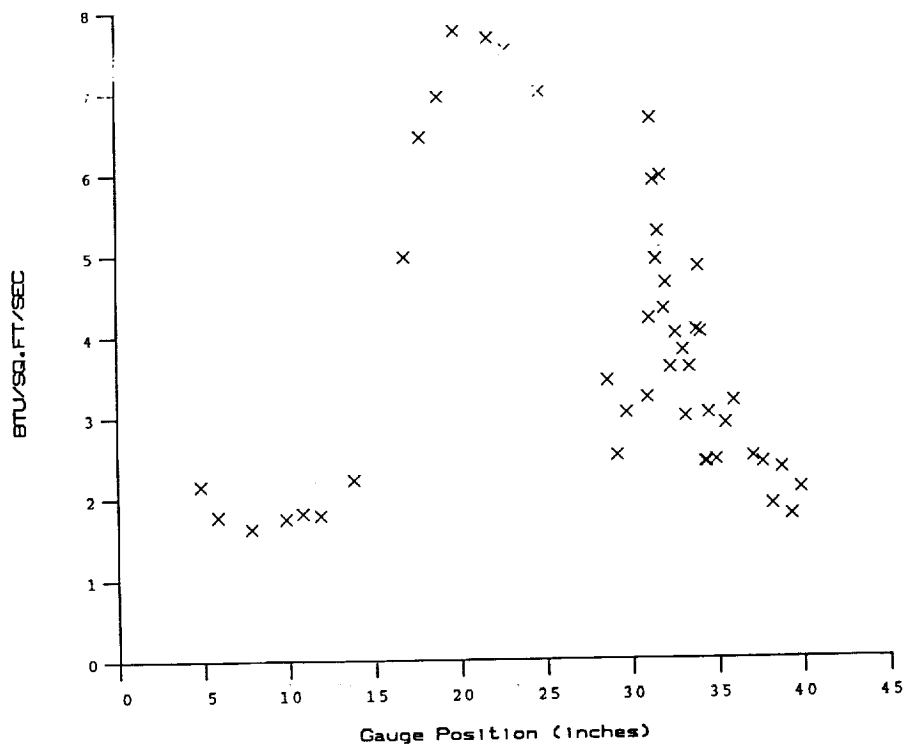


Test Conditions for Run 23 :

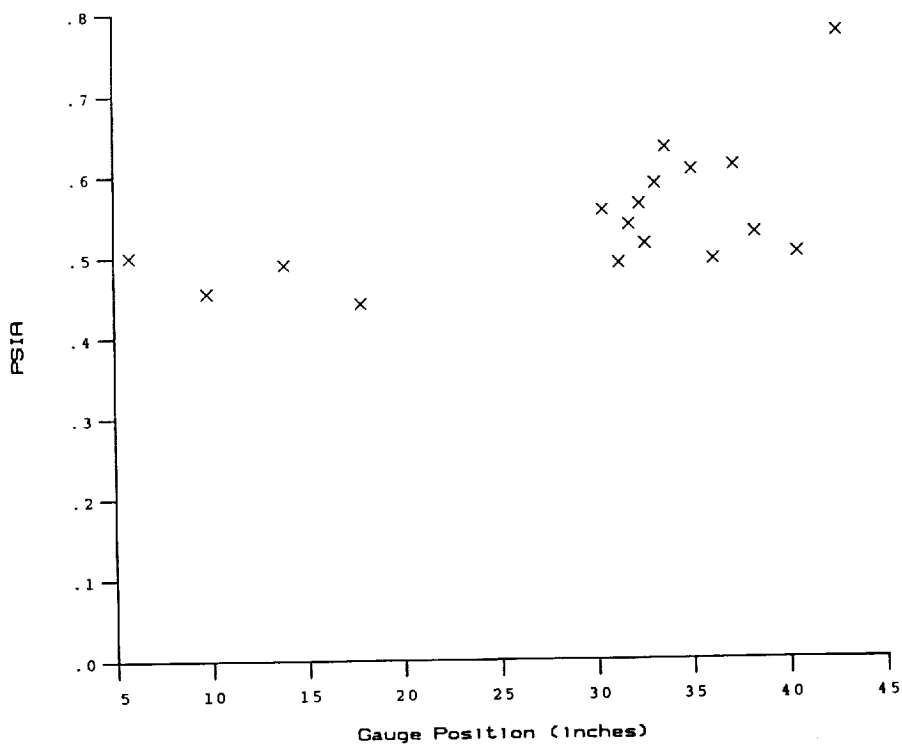
Po	= 3.660E+03 PSIA	Reservoir Total Pressure
Ho	= 1.353E+07 (Ft/sec) ²	Reservoir Total Enthalpy
To	= 2.117E+03 degR	Reservoir Total Temperature
M	= 7.890E+00	Freestream Mach Number
U	= 5.008E+03 Ft/sec	Freestream Velocity
T	= 1.675E+02 degR	Freestream Temperature
P	= 4.184E-01 PSIA	Freestream Static Pressure
Rho	= 2.096E-04 Slugs/Ft ³	Freestream Density
Mu	= 1.401E-07 Slugs/Ft-sec	Freestream Viscosity
Re	= 7.492E+06 1/Ft	Freestream Reynolds Number
Po'	= 3.368E+01 PSIA	Pitot Pressure
Q	= 1.825E+01 PSIA	Dynamic Pressure ($\rho U^2/288$)
Mi	= 2.793E+00	Shock Tube Incident Shock Mach Number
Tw	= 5.300E+02 degR	Wall Temperature (Test Gas = Air)
Hw	= 3.183E+06 (Ft/sec) ²	Wall Enthalpy ($C_p T_w$)
CPf	= 5.479E-02 1/PSIA	Pressure to CP factor ($1/Q$)
CHf	= 7.163E-05 Ft ² -s/BTU	Heat Rate to CH factor ($778/(\rho U (H_o - H_w))$)
QoFR	= 4.807E+01 BTU/Ft ² -s	Fay-Riddell Heat Transfer (.25' Diam Cylin.)

Test Conditions for Run 24 :

Po	= 3.500E+03 PSIA	Reservoir Total Pressure
Ho	= 1.390E+07 (Ft/sec) ²	Reservoir Total Enthalpy
To	= 2.167E+03 degR	Reservoir Total Temperature
M	= 7.871E+00	Freestream Mach Number
U	= 5.074E+03 Ft/sec	Freestream Velocity
T	= 1.728E+02 degR	Freestream Temperature
P	= 4.023E-01 PSIA	Freestream Static Pressure
Rho	= 1.954E-04 Slugs/Ft ³	Freestream Density
Mu	= 1.443E-07 Slugs/Ft-sec	Freestream Viscosity
Re	= 6.868E+06 1/Ft	Freestream Reynolds Number
Po'	= 3.224E+01 PSIA	Pitot Pressure
Q	= 1.746E+01 PSIA	Dynamic Pressure (Rho U ² /288)
Mi	= 2.842E+00	Shock Tube Incident Shock Mach Number
Tw	= 5.300E+02 degR	Wall Temperature (Test Gas - Air)
Hw	= 3.183E+06 (Ft/sec) ²	Wall Enthalpy (Cp Tw)
CPf	= 5.726E-02 1/PSIA	Pressure to CP factor (1/Q)
CHf	= 7.326E-05 Ft ² -s/BTU	Heat Rate to CH factor (778/(Rho U (Ho-Hw)))
QoFR	= 4.878E+01 BTU/Ft ² -s	Fay-Riddell Heat Transfer (.25' Diam Cylin.)



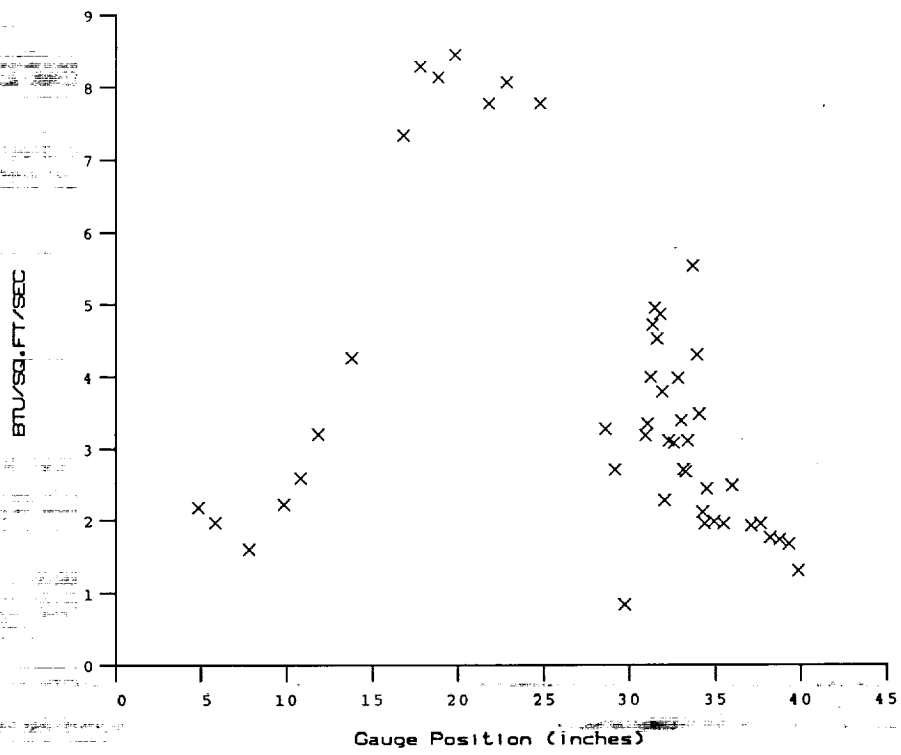
HEAT TRANSFER vs Gauge Position
Run 24



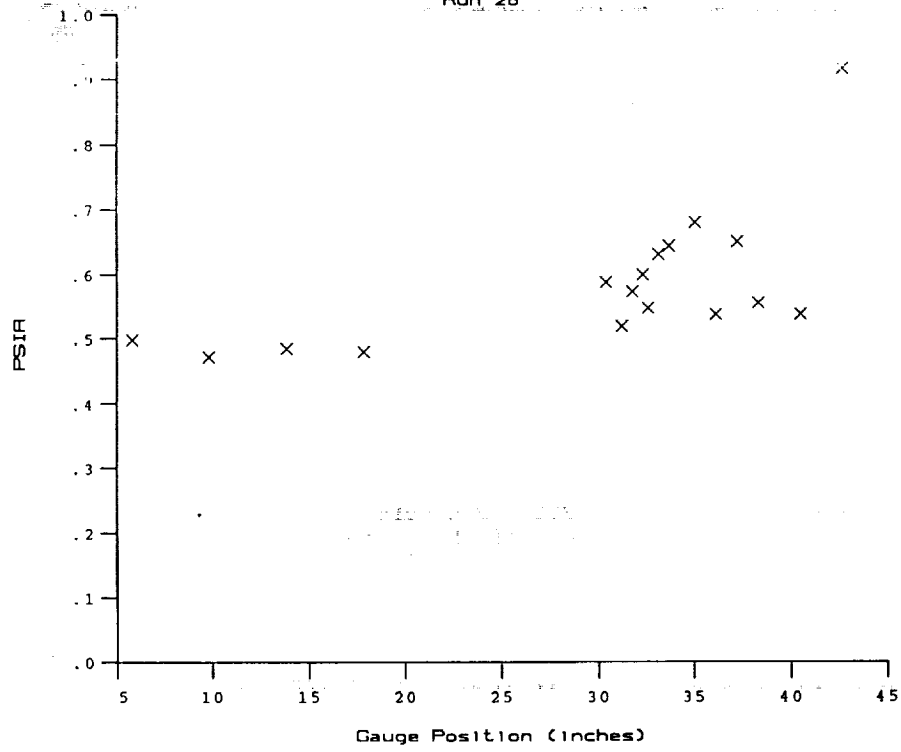
PRESSURE vs Gauge Position
Run 24

Test Conditions for Run 26 :

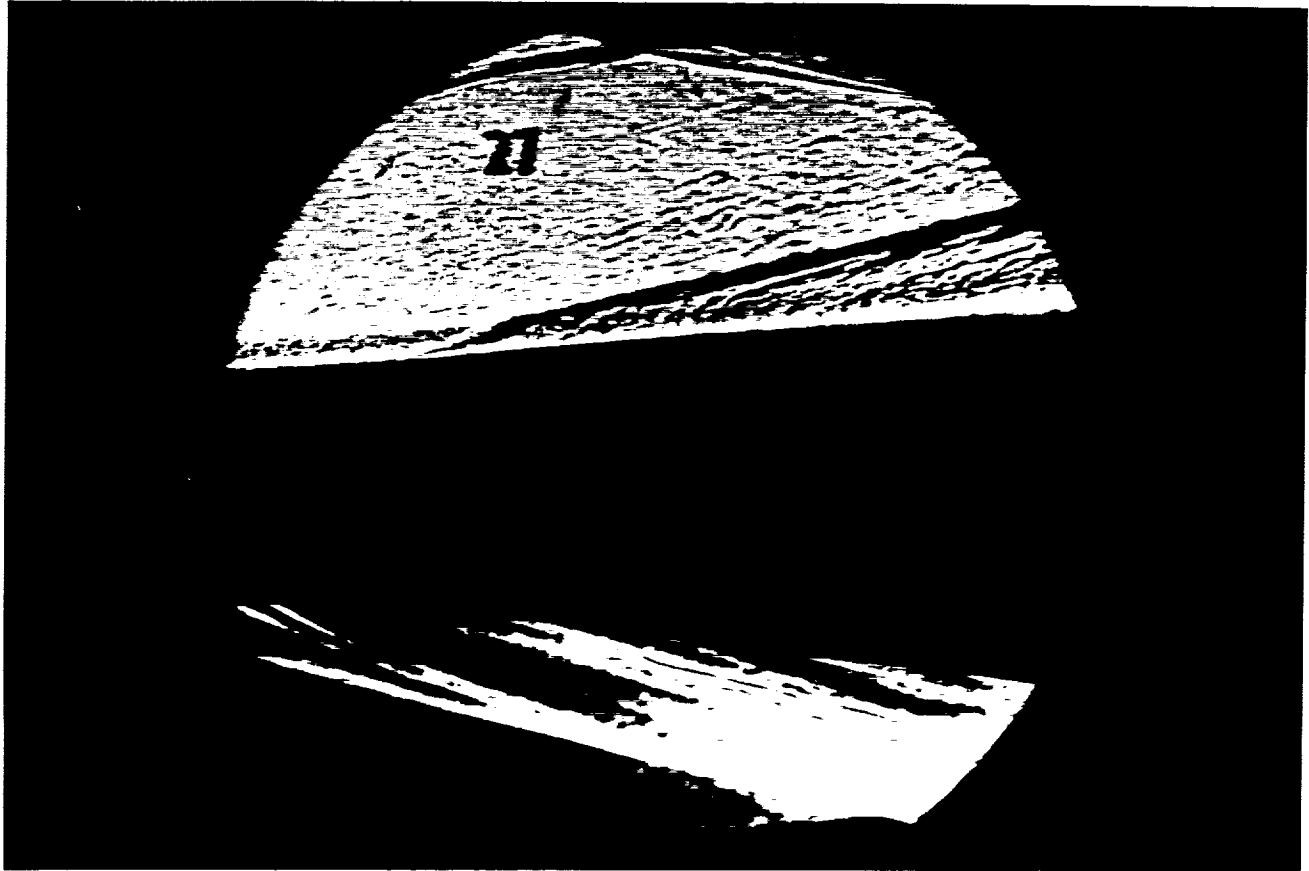
Po	= 3.455E+03 PSIA	Reservoir Total Pressure
Ho	= 1.364E+07 (Ft/sec) ²	Reservoir Total Enthalpy
To	= 2.128E+03 degR	Reservoir Total Temperature
M	= 7.864E+00	Freestream Mach Number
U	= 5.026E+03 Ft/sec	Freestream Velocity
T	= 1.699E+02 degR	Freestream Temperature
P	= 4.013E-01 PSIA	Freestream Static Pressure
Rho	= 1.983E-04 Slugs/Ft ³	Freestream Density
Mu	= 1.420E-07 Slugs/Ft-sec	Freestream Viscosity
Re	= 7.018E+06 1/Ft	Freestream Reynolds Number
Po'	= 3.209E+01 PSIA	Pitot Pressure
Q	= 1.739E+01 PSIA	Dynamic Pressure (Rho U ² /288)
Mi	= 2.865E+00	Shock Tube Incident Shock Mach Number
Tw	= 5.300E+02 degR	Wall Temperature (Test Gas = Air)
Hw	= 3.183E+06 (Ft/sec) ²	Wall Enthalpy (Cp Tw)
CPf	= 5.751E-02 1/PSIA	Pressure to CP factor (1/Q)
CHf	= 7.469E-05 Ft ² -s/BTU	Heat Rate to CH factor (778/(Rho U (Ho-Hw)))
QoFR	= 4.742E+01 BTU/Ft ² -s	Fay-Riddell Heat Transfer (.25' Diam Cylin.)



HEAT TRANSFER vs Gauge Position
Run 26

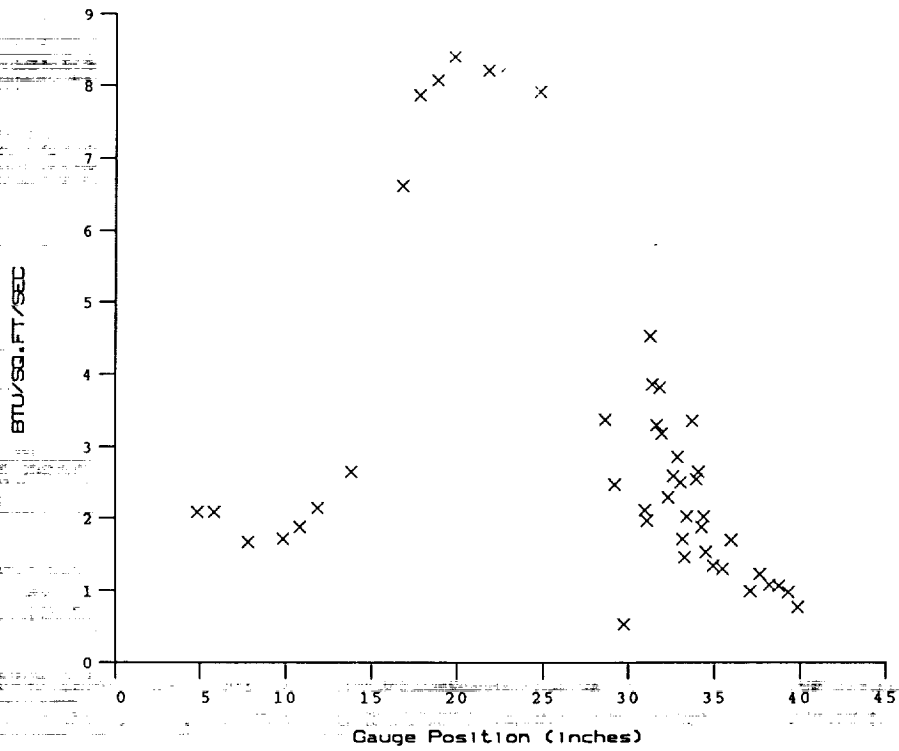


PRESSURE vs Gauge Position
Run 26

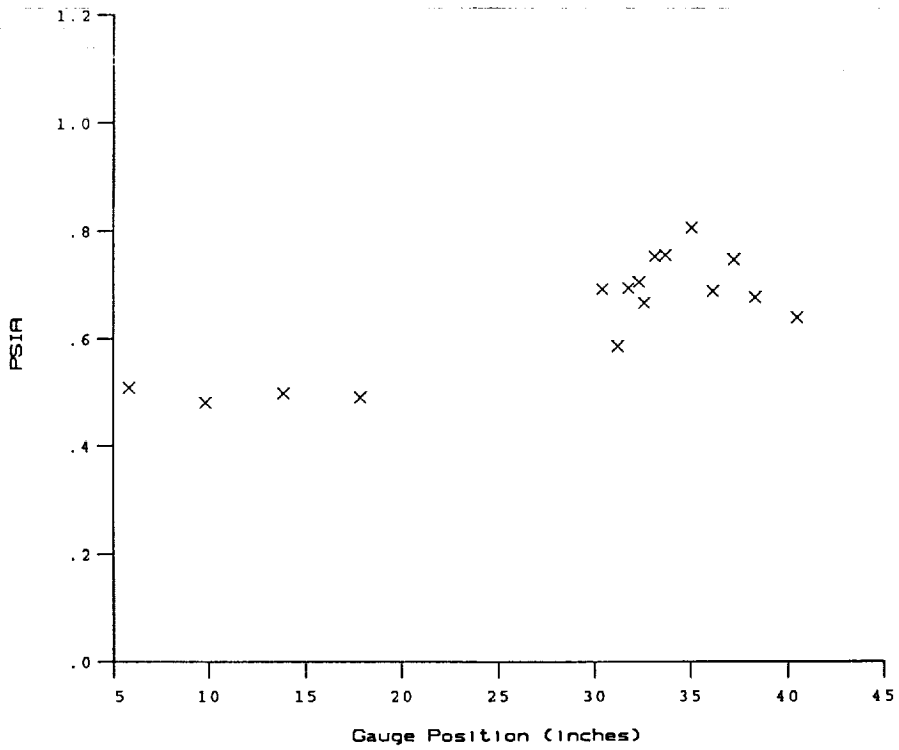


Test Conditions for Run 27 :

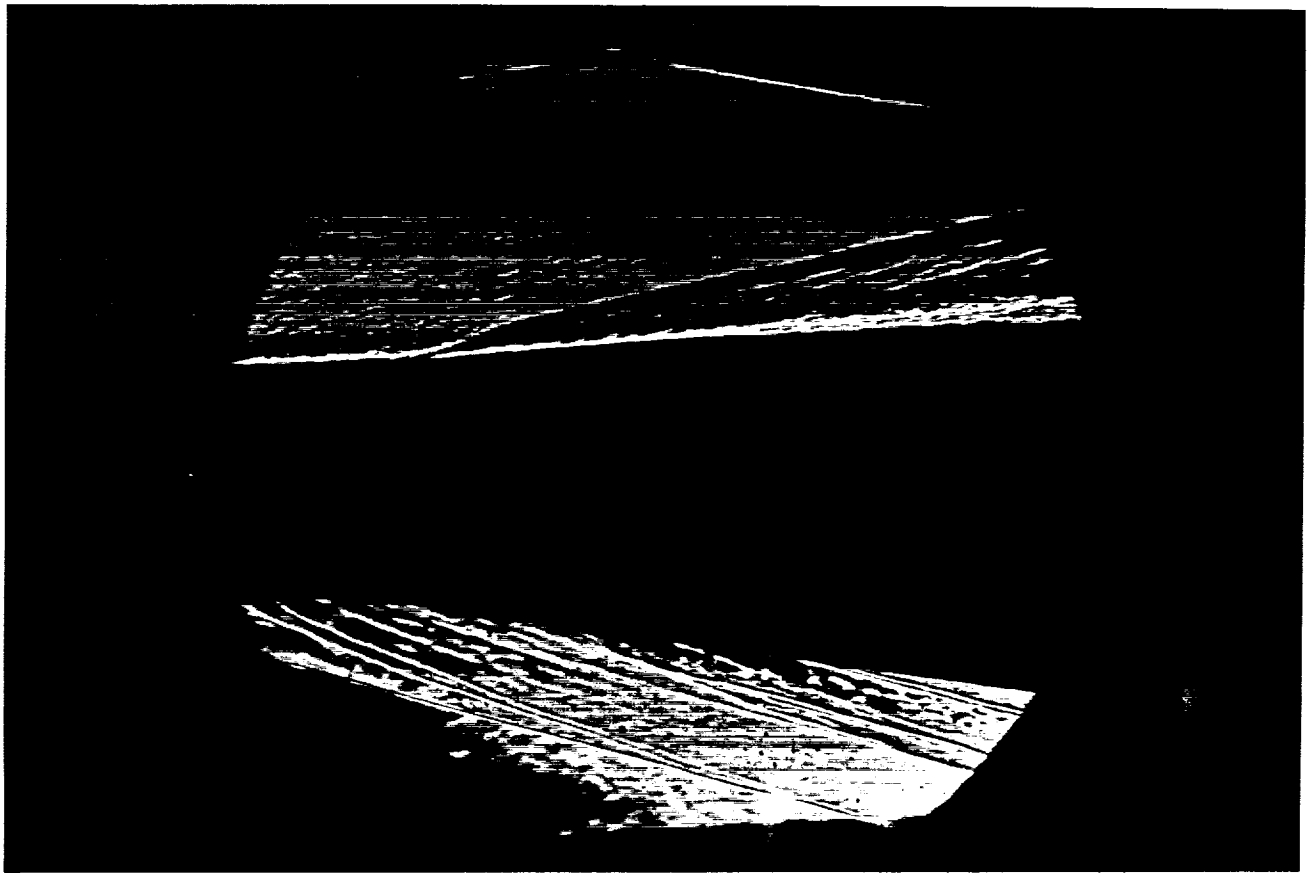
Po	= 3.721E+03 PSIA	Reservoir Total Pressure
Ho	= 1.348E+07 (Ft/sec) ²	Reservoir Total Enthalpy
To	= 2.109E+03 degR	Reservoir Total Temperature
M	= 7.889E+00	Freestream Mach Number
U	= 4.999E+03 Ft/sec	Freestream Velocity
T	= 1.669E+02 degR	Freestream Temperature
P	= 4.263E-01 PSIA	Freestream Static Pressure
Rho	= 2.143E-04 Slugs/Ft ³	Freestream Density
Mu	= 1.396E-07 Slugs/Ft-sec	Freestream Viscosity
Re	= 7.672E+06 1/Ft	Freestream Reynolds Number
Po'	= 3.431E+01 PSIA	Pitot Pressure
Q	= 1.859E+01 PSIA	Dynamic Pressure (Rho U ² /288)
Mi	= 2.805E+00	Shock Tube Incident Shock Mach Number
Tw	= 5.300E+02 degR	Wall Temperature (Test Gas = Air)
Hw	= 3.183E+06 (Ft/sec) ²	Wall Enthalpy (Cp Tw)
CPf	= 5.378E-02 1/PSIA	Pressure to CP factor (1/Q)
CHf	= 7.050E-05 Ft ² -s/BTU	Heat Rate to CH factor (778/(Rho U (Ho-Hw)))
QoFR	= 4.828E+01 BTU/Ft ² -s	Fay-Riddell Heat Transfer (.25' Diam Cylin.)



HEAT TRANSFER vs Gauge Position
Run 27

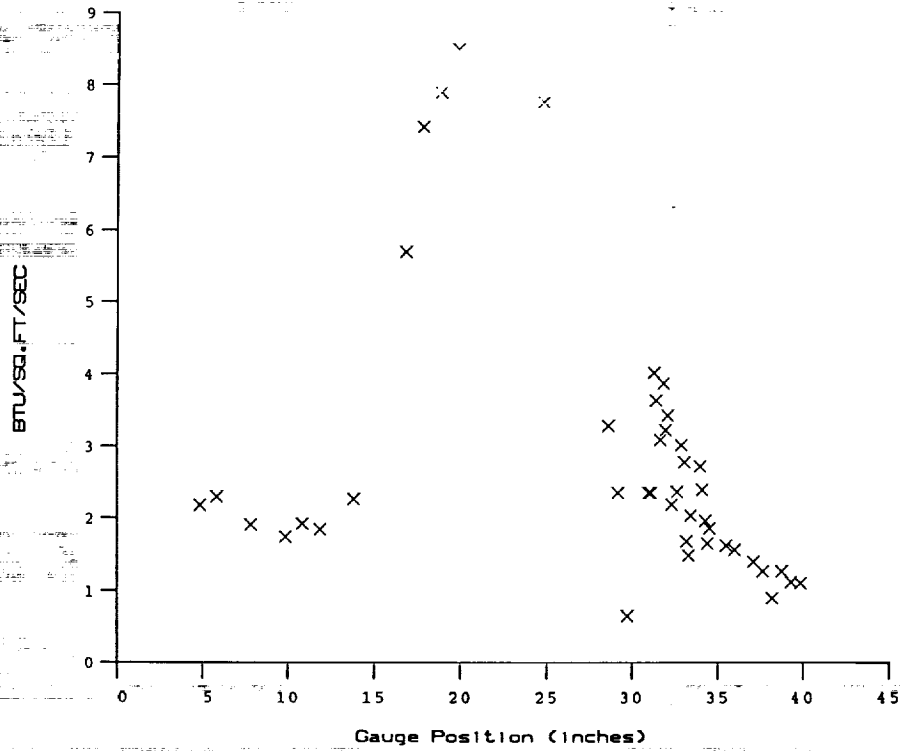


PRESSURE vs Gauge Position
Run 27

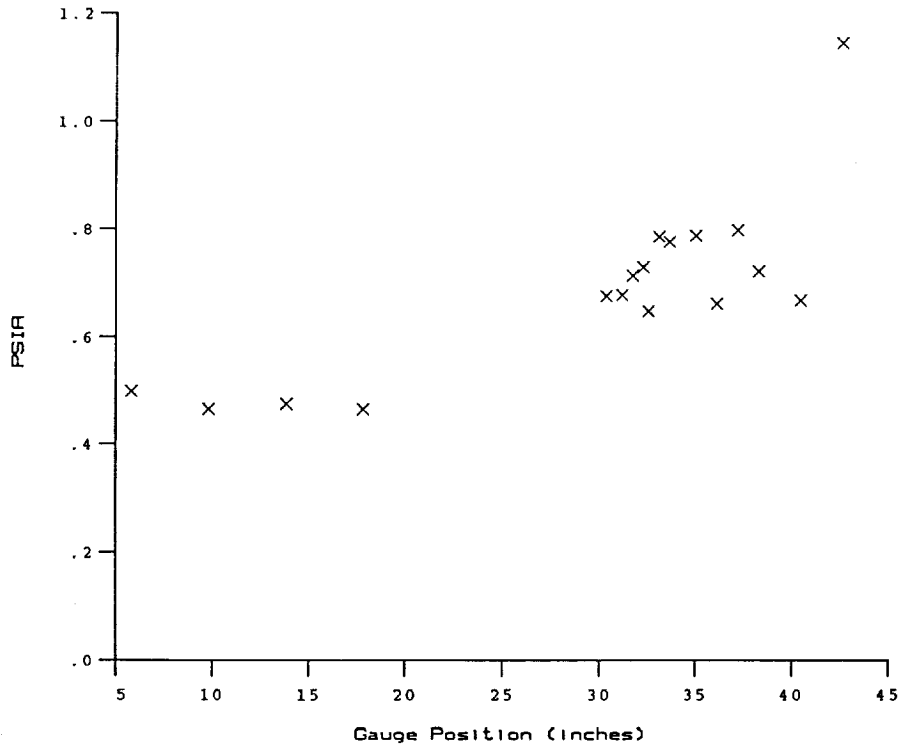


Test Conditions for Run 28 :

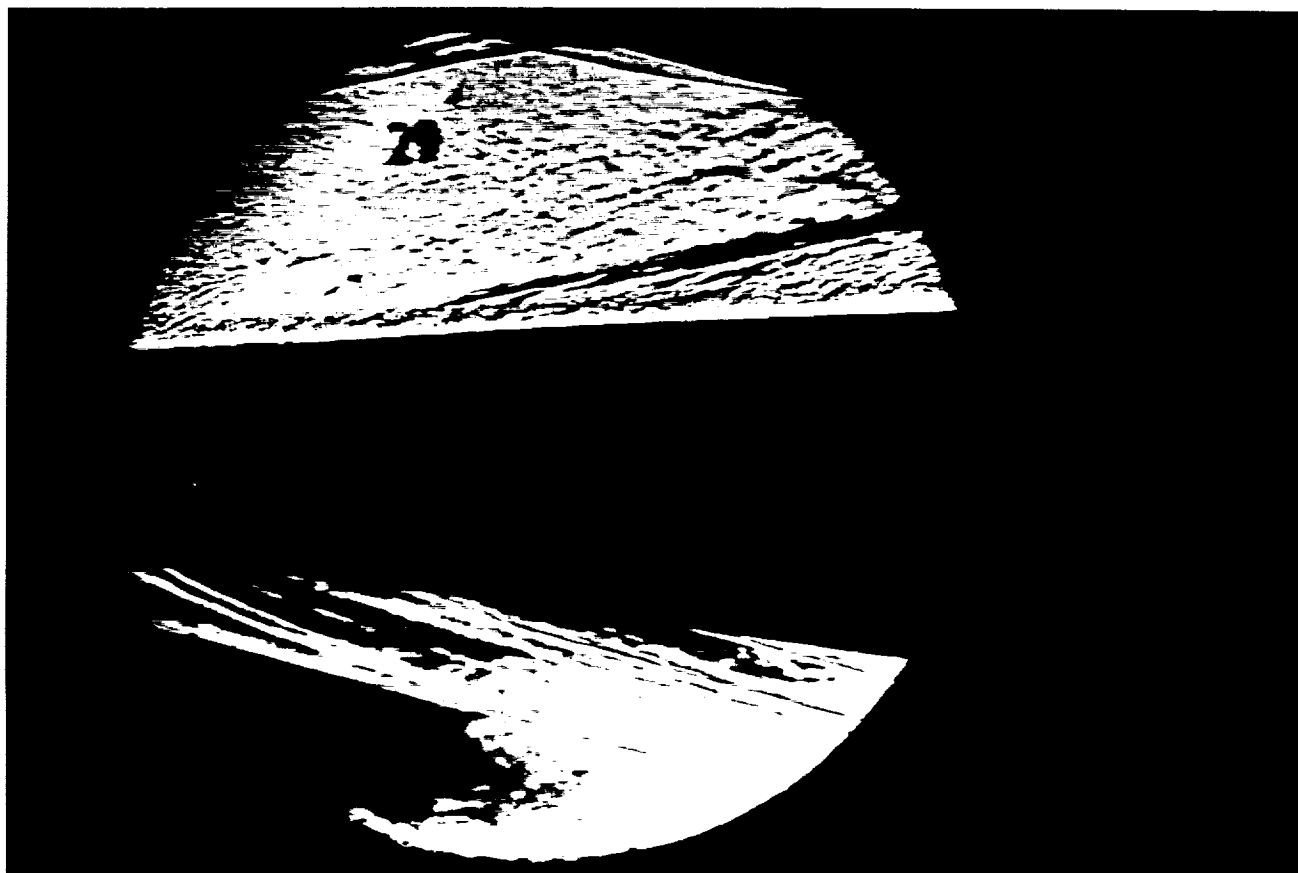
Po	- 3.660E+03 PSIA	Reservoir Total Pressure
Ho	- 1.425E+07 (Ft/sec) ²	Reservoir Total Enthalpy
To	- 2.216E+03 degR	Reservoir Total Temperature
M	- 7.869E+00	Freestream Mach Number
U	- 5.139E+03 Ft/sec	Freestream Velocity
T	- 1.773E+02 degR	Freestream Temperature
P	- 4.194E-01 PSIA	Freestream Static Pressure
Rho	- 1.985E-04 Slugs/Ft ³	Freestream Density
Mu	- 1.481E-07 Slugs/Ft-sec	Freestream Viscosity
Re	- 6.889E+06 1/Ft	Freestream Reynolds Number
Po'	- 3.360E+01 PSIA	Pitot Pressure
Q	- 1.820E+01 PSIA	Dynamic Pressure (Rho U ² /288)
Mi	- 2.878E+00	Shock Tube Incident Shock Mach Number
Tw	- 5.300E+02 degR	Wall Temperature (Test Gas = Air)
Hw	- 3.183E+06 (Ft/sec) ²	Wall Enthalpy (Cp Tw)
CPf	- 5.495E-02 1/PSIA	Pressure to CP factor (1/Q)
CHf	- 6.890E-05 Ft ² -s/BTU	Heat Rate to CH factor (778/(Rho U (Ho-Hw)))
QoFR	- 5.157E+01 BTU/Ft ² -s	Fay-Riddell Heat Transfer (.25' Diam Cylin.)



HEAT TRANSFER vs Gauge Position
Run 28

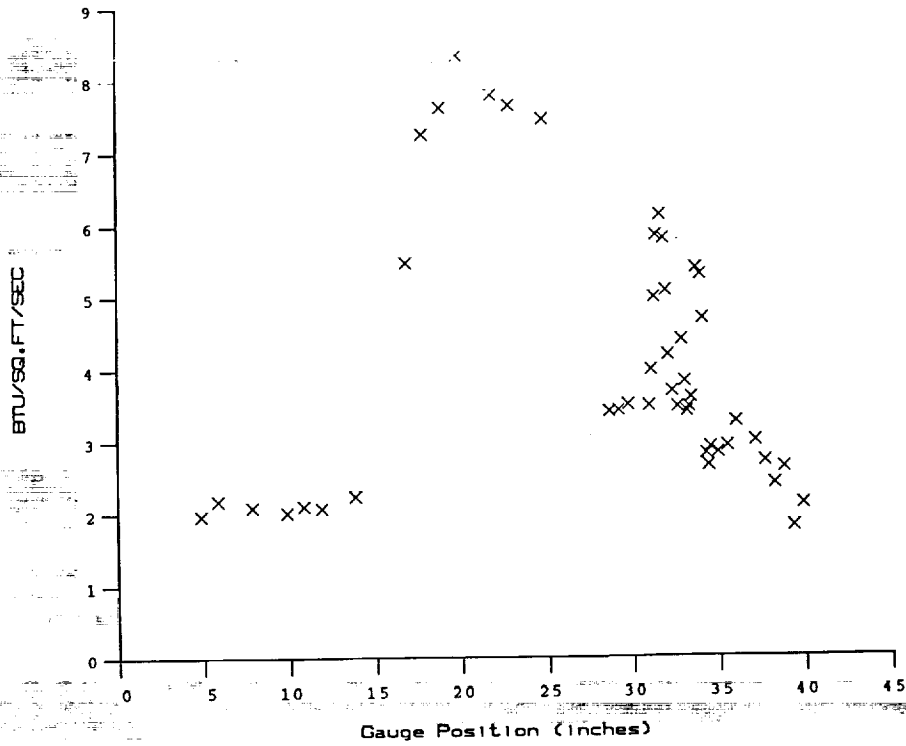


PRESSURE vs Gauge Position
Run 28

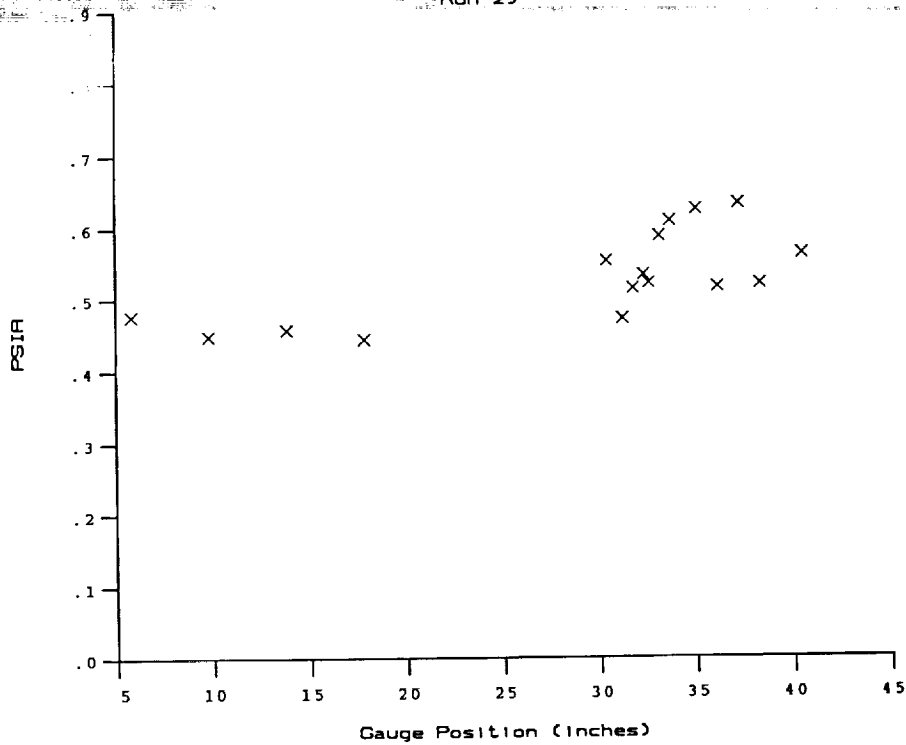


Test Conditions for Run 29 :

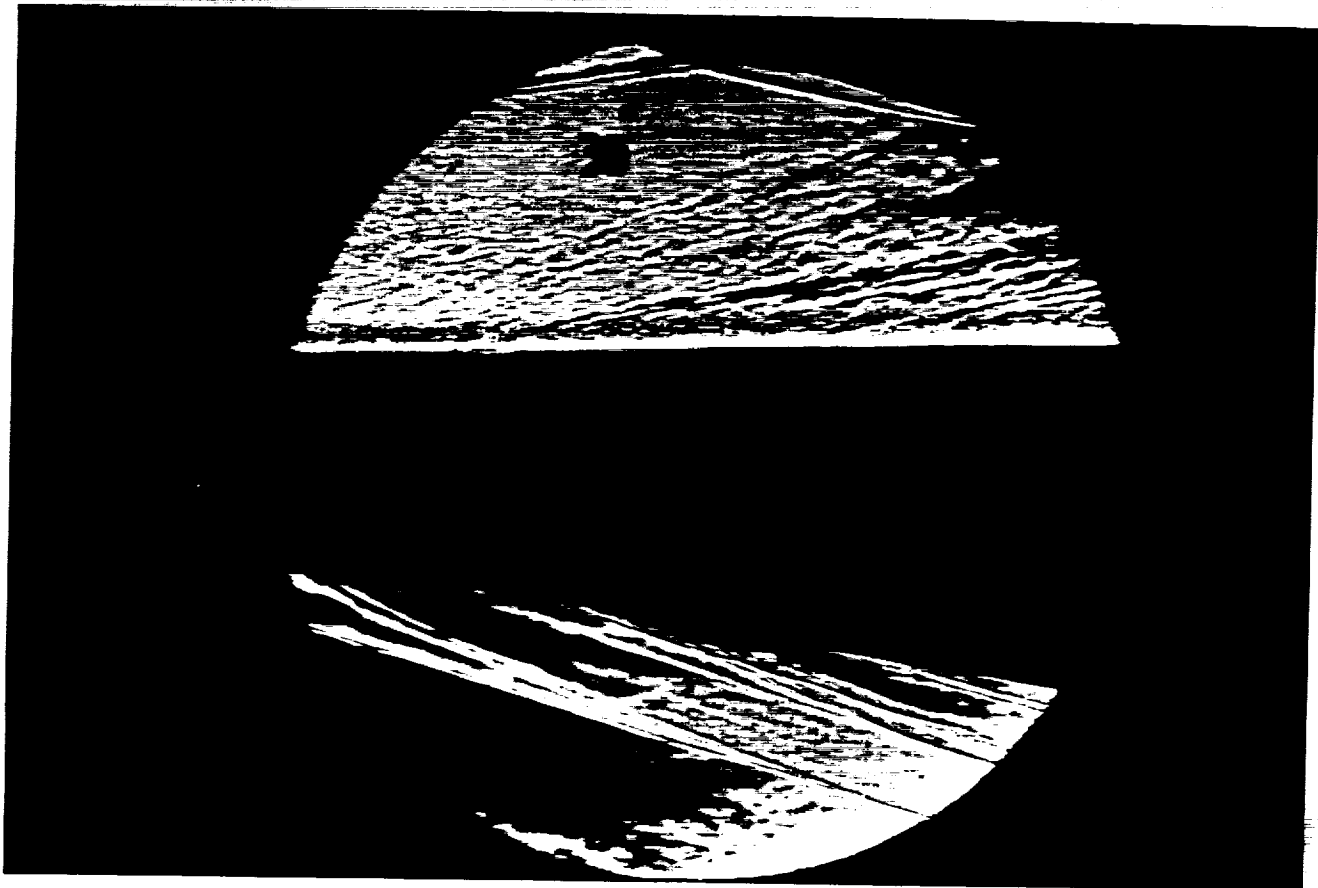
Po	= 3.507E+03 PSIA	Reservoir Total Pressure
Ho	= 1.378E+07 (Ft/sec) ²	Reservoir Total Enthalpy
To	= 2.149E+03 degR	Reservoir Total Temperature
M	= 7.868E+00	Freestream Mach Number
U	= 5.053E+03 Ft/sec	Freestream Velocity
T	= 1.715E+02 degR	Freestream Temperature
P	= 4.052E-01 PSIA	Freestream Static Pressure
Rho	= 1.982E-04 Slugs/Ft ³	Freestream Density
Mu	= 1.433E-07 Slugs/Ft-sec	Freestream Viscosity
Re	= 6.989E+06 1/Ft	Freestream Reynolds Number
Po'	= 3.244E+01 PSIA	Pitot Pressure
Q	= 1.758E+01 PSIA	Dynamic Pressure (Rho U ² /288)
Mi	= 2.857E+00	Shock Tube Incident Shock Mach Number
Tw	= 5.300E+02 degR	Wall Temperature (Test Gas = Air)
Hw	= 3.183E+06 (Ft/sec) ²	Wall Enthalpy (Cp Tw)
CPf	= 5.690E-02 1/PSIA	Pressure to CP factor (1/Q)
CHF	= 7.327E-05 Ft ² -s/BTU	Heat Rate to CH factor (778/(Rho U (Ho-Hw)))
QoFR	= 4.839E+01 BTU/Ft ² -s	Fay-Riddell Heat Transfer (.25' Diam Cylin.)



HEAT TRANSFER vs Gauge Position
Run 29



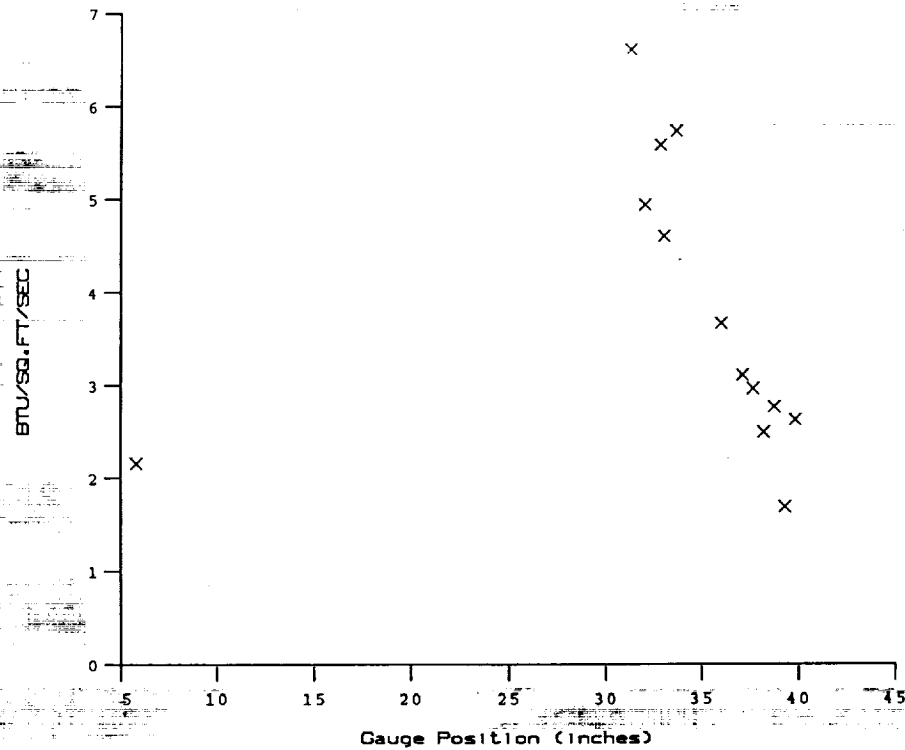
PRESSURE vs Gauge Position
Run 29



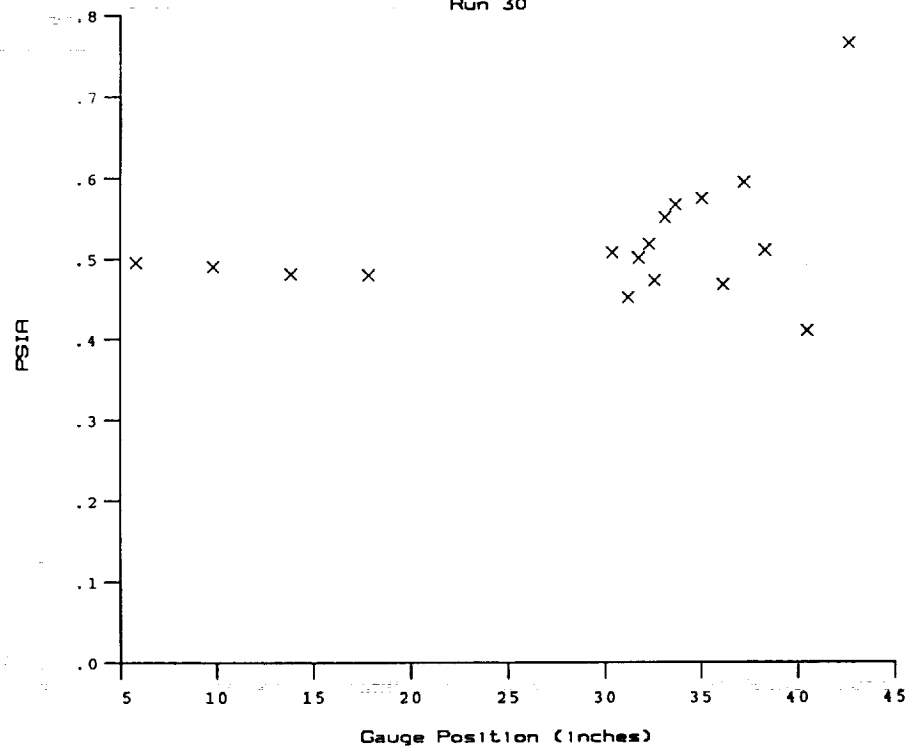
Test Conditions for Run 30 :

Po - 3.536E+03 PSIA
 Ho - 1.389E+07 (Ft/sec)²
 To - 2.165E+03 degR
 M - 7.869E+00
 U - 5.073E+03 Ft/sec
 T - 1.728E+02 degR
 P - 4.073E-01 PSIA
 Rho - 1.978E-04 Slugs/Ft³
 Mu - 1.444E-07 Slugs/Ft-sec
 Re - 6.950E+06 1/Ft
 Po' - 3.263E+01 PSIA
 Q - 1.767E+01 PSIA
 Mi - 2.856E+00
 Tw - 5.300E+02 degR
 Hw - 3.183E+06 (Ft/sec)²
 CPf - 5.658E-02 1/PSIA
 CHf - 7.241E-05 Ft²-s/BTU
 QoFR - 4.905E+01 BTU/Ft²-s

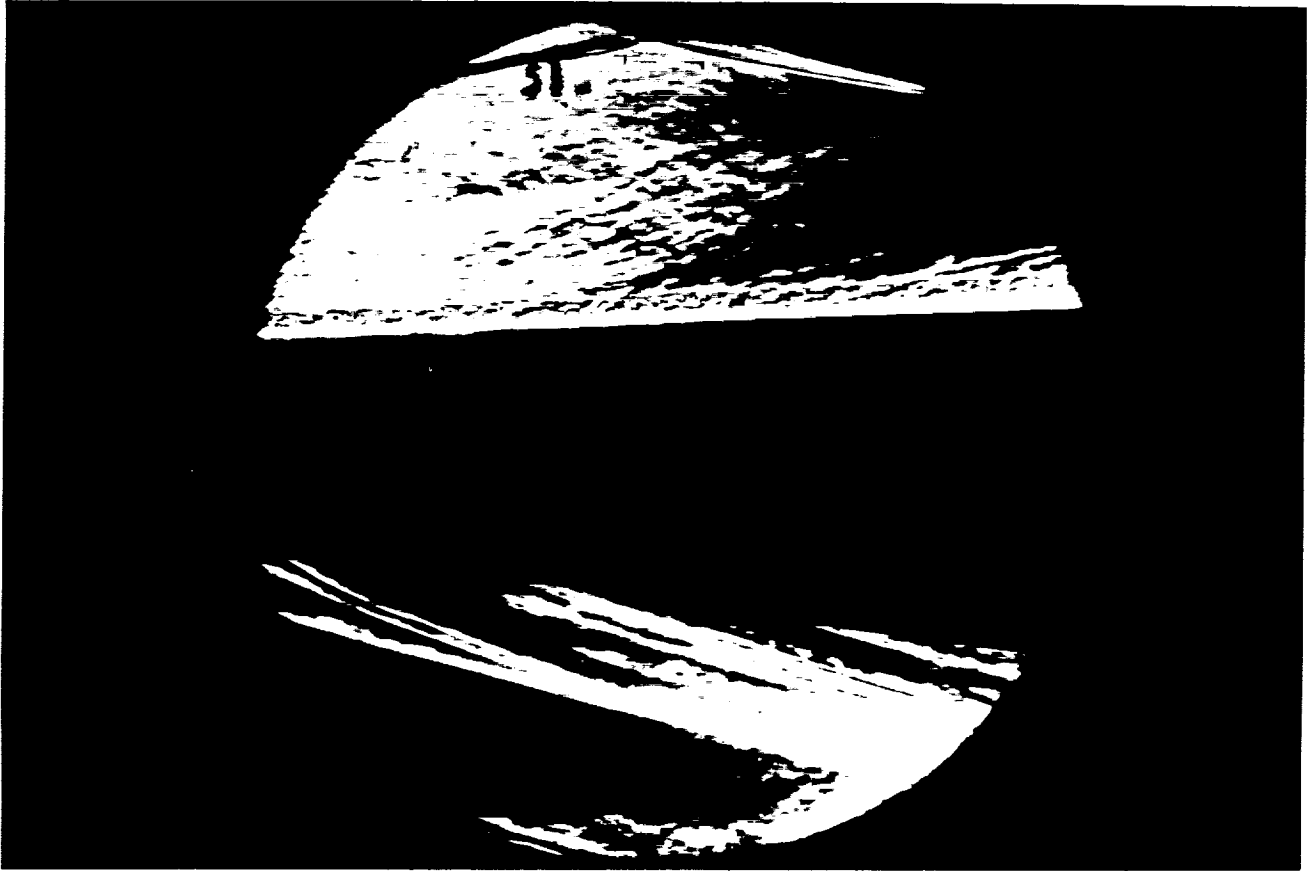
Reservoir Total Pressure
 Reservoir Total Enthalpy
 Reservoir Total Temperature
 Freestream Mach Number
 Freestream Velocity
 Freestream Temperature
 Freestream Static Pressure
 Freestream Density
 Freestream Viscosity
 Freestream Reynolds Number
 Pitot Pressure
 Dynamic Pressure (Rho U²/288)
 Shock Tube Incident Shock Mach Number
 Wall Temperature (Test Gas = Air)
 Wall Enthalpy (Cp Tw)
 Pressure to CP factor (1/Q)
 Heat Rate to CH factor (778/(Rho U (Ho-Hw)))
 Fay-Riddell Heat Transfer (.25' Diam Cylin.)



HEAT TRANSFER vs Gauge Position
Run 30

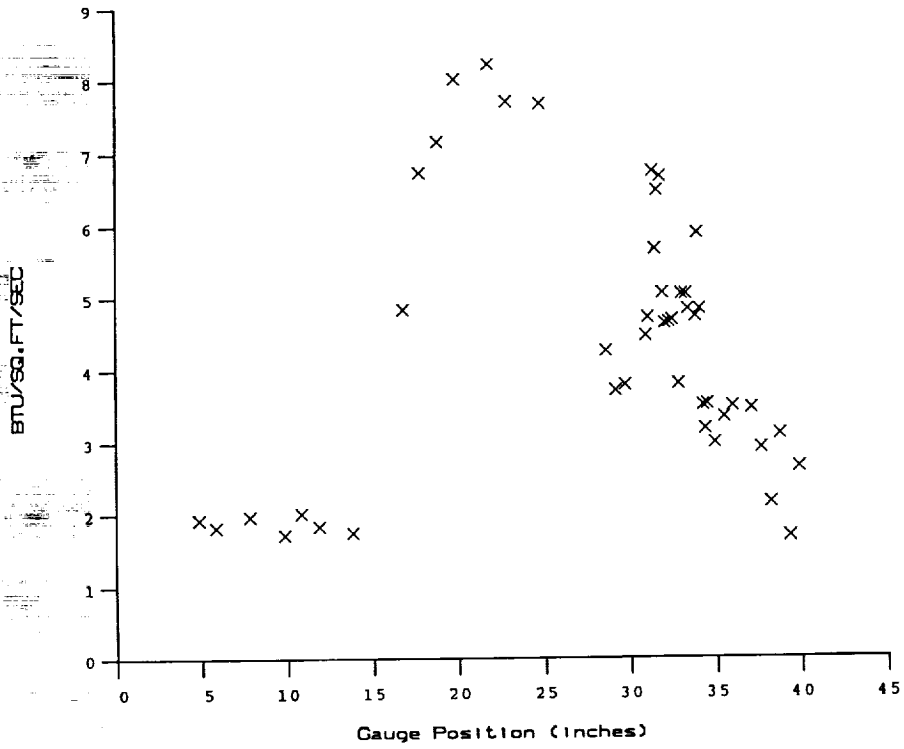


PRESSURE vs Gauge Position
Run 30

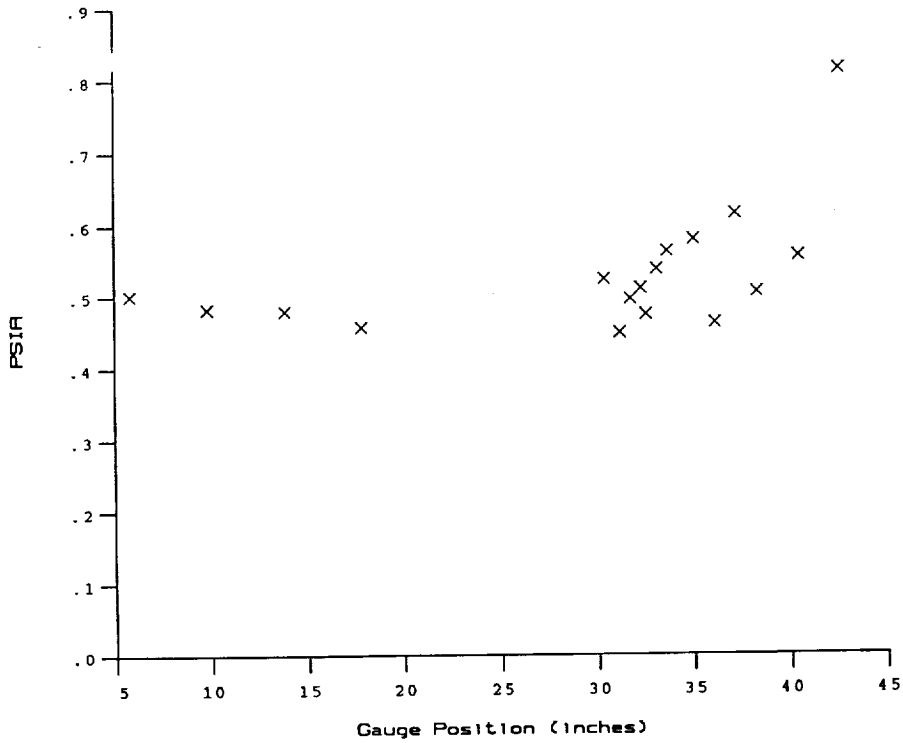


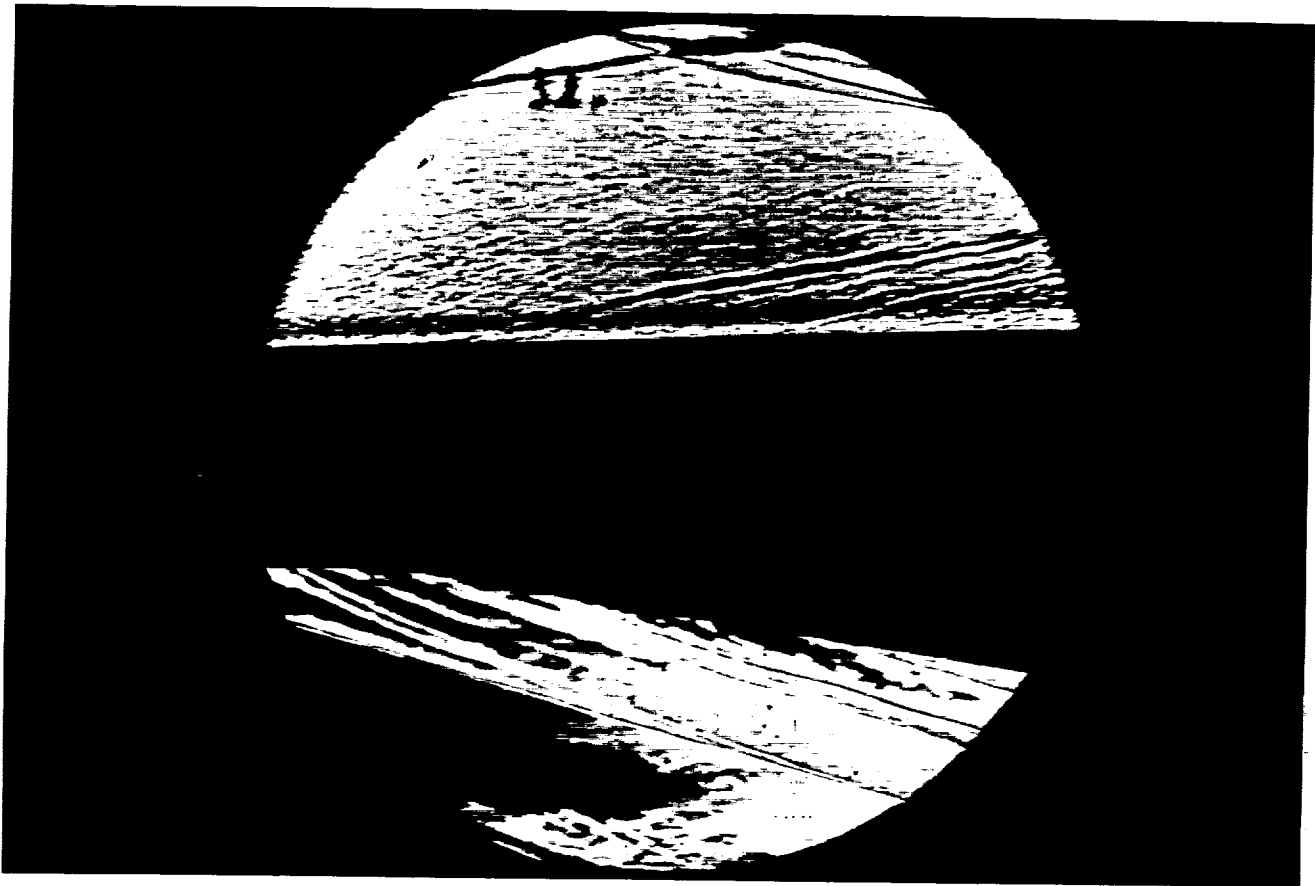
Test Conditions for Run 31 :

Po = 3.598E+03 PSIA	Reservoir Total Pressure
Ho = 1.409E+07 (Ft/sec) ²	Reservoir Total Enthalpy
To = 2.193E+03 degR	Reservoir Total Temperature
M = 7.871E+00	Freestream Mach Number
U = 5.109E+03 Ft/sec	Freestream Velocity
T = 1.752E+02 degR	Freestream Temperature
P = 4.127E-01 PSIA	Freestream Static Pressure
Rho = 1.977E-04 Slugs/Ft ³	Freestream Density
Mu = 1.463E-07 Slugs/Ft-sec	Freestream Viscosity
Re = 6.902E+06 1/Ft	Freestream Reynolds Number
Po' = 3.308E+01 PSIA	Pitot Pressure
Q = 1.791E+01 PSIA	Dynamic Pressure (Rho U ² /288)
Mi = 2.860E+00	Shock Tube Incident Shock Mach Number
Tw = 5.300E+02 degR	Wall Temperature (Test Gas = Air)
Hw = 3.183E+06 (Ft/sec) ²	Wall Enthalpy (Cp Tw)
CPf = 5.583E-02 1/PSIA	Pressure to CP factor (1/Q)
CHf = 7.065E-05 Ft ² -s/BTU	Heat Rate to CH factor (778/(Rho U (Ho-Hw)))
QoFR = 5.035E+01 BTU/Ft ² -s	Fay-Riddell Heat Transfer (.25' Diam Cylin.)



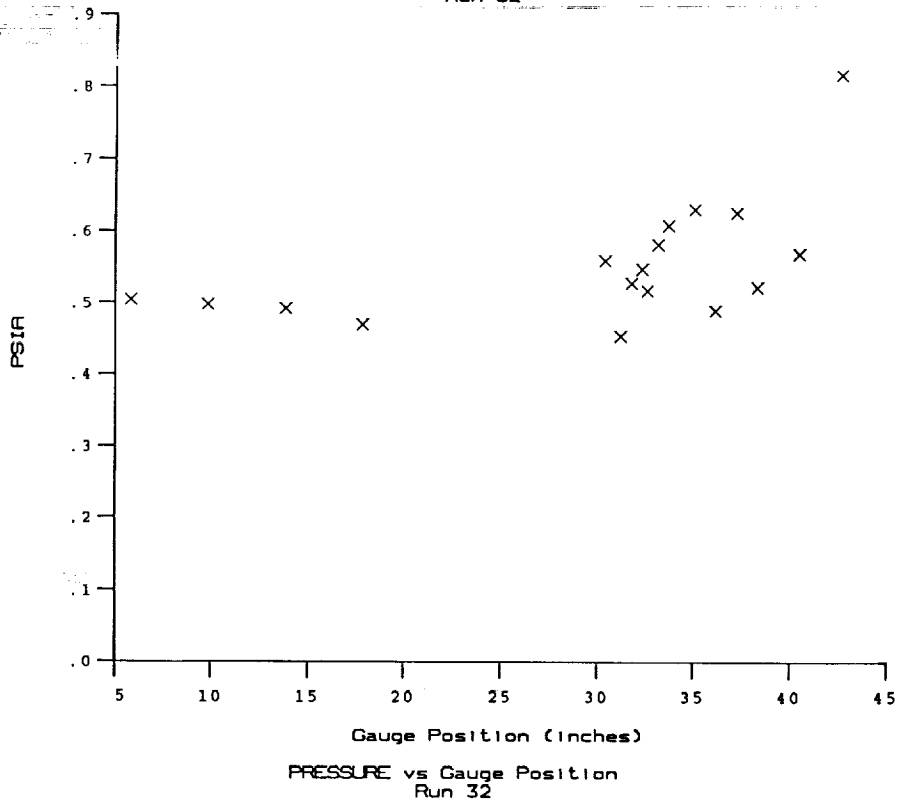
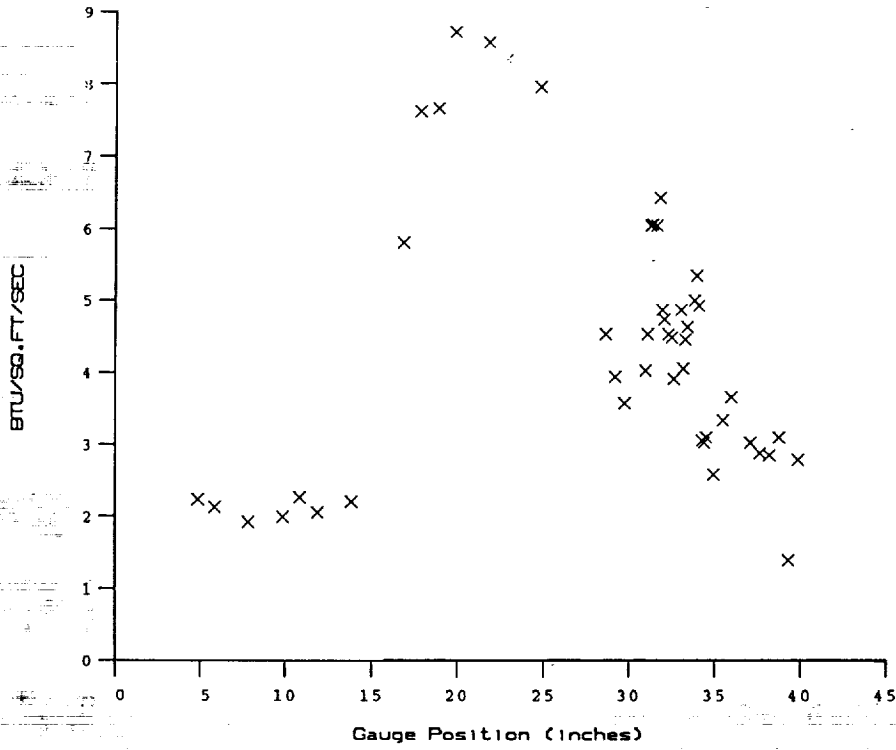
HEAT TRANSFER vs Gauge Position
Run 31

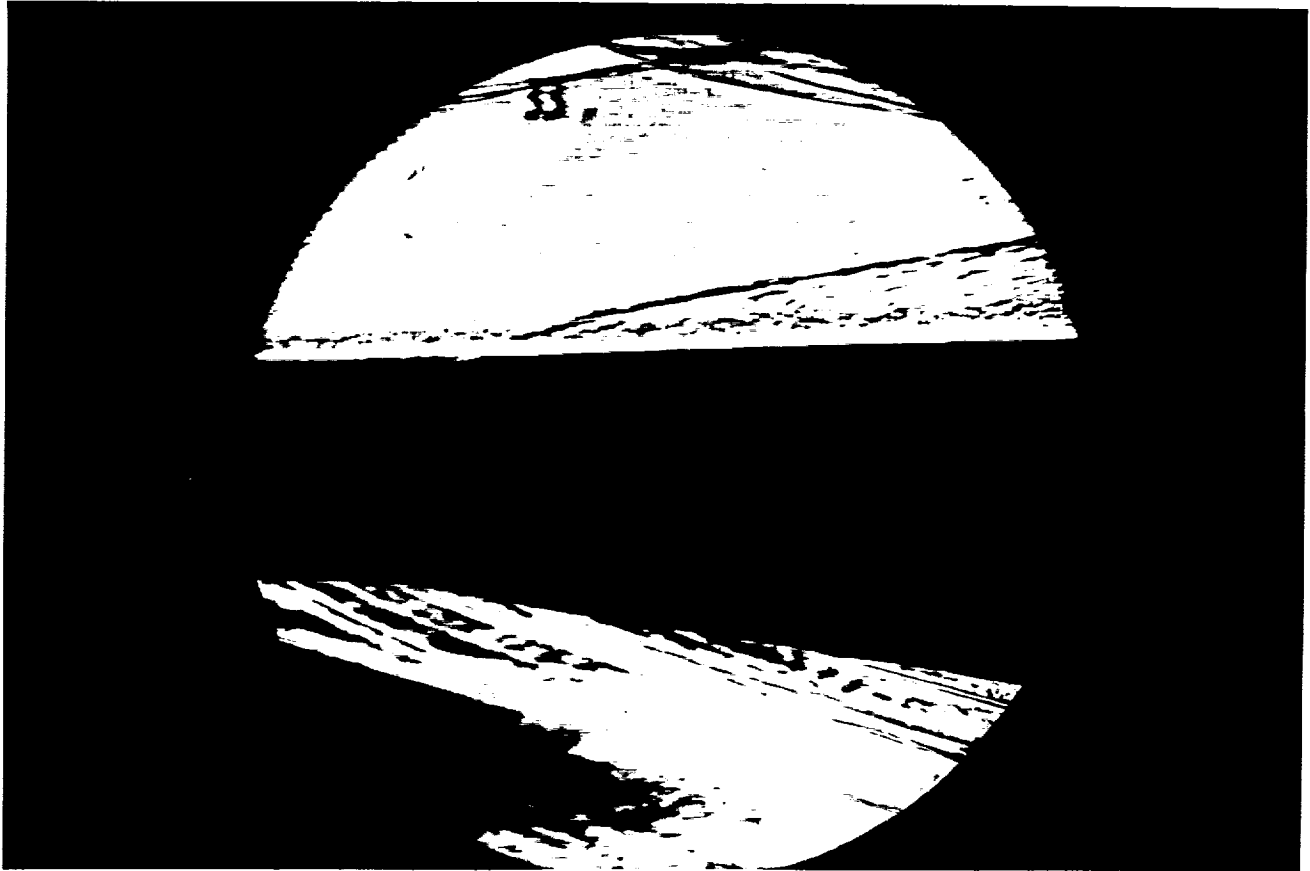




Test Conditions for Run 32 :

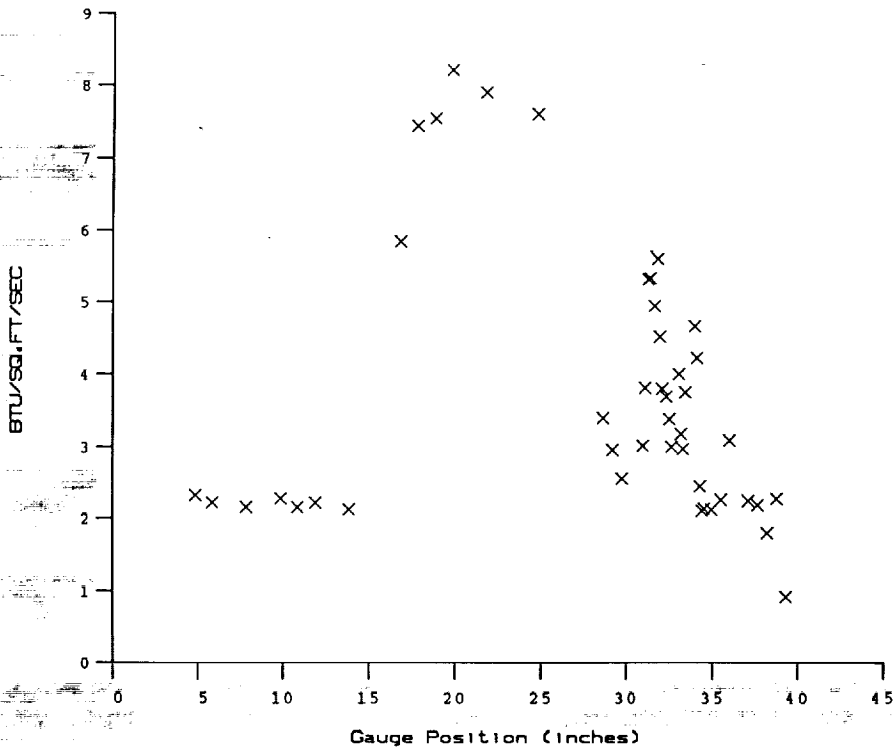
Po	= 3.683E+03 PSIA	Reservoir Total Pressure
Ho	= 1.432E+07 (Ft/sec) ²	Reservoir Total Enthalpy
To	= 2.225E+03 degR	Reservoir Total Temperature
M	= 7.868E+00	Freestream Mach Number
U	= 5.150E+03 Ft/sec	Freestream Velocity
T	= 1.781E+02 degR	Freestream Temperature
P	= 4.217E-01 PSIA	Freestream Static Pressure
Rho	= 1.987E-04 Slugs/Ft ³	Freestream Density
Mu	= 1.487E-07 Slugs/Ft-sec	Freestream Viscosity
Re	= 6.881E+06 1/Ft	Freestream Reynolds Number
Po'	= 3.379E+01 PSIA	Pitot Pressure
Q	= 1.829E+01 PSIA	Dynamic Pressure (Rho U ² /288)
Mi	= 2.882E+00	Shock Tube Incident Shock Mach Number
Tw	= 5.300E+02 degR	Wall Temperature (Test Gas = Air)
Hw	= 3.183E+06 (Ft/sec) ²	Wall Enthalpy (Cp Tw)
CPf	= 5.466E-02 1/PSIA	Pressure to CP factor (1/Q)
CHf	= 6.830E-05 Ft ² -s/BTU	Heat Rate to CH factor (778/(Rho U (Ho-Hw)))
QoFR	= 5.202E+01 BTU/Ft ² -s	Fay-Riddell Heat Transfer (.25' Diam Cylin.)



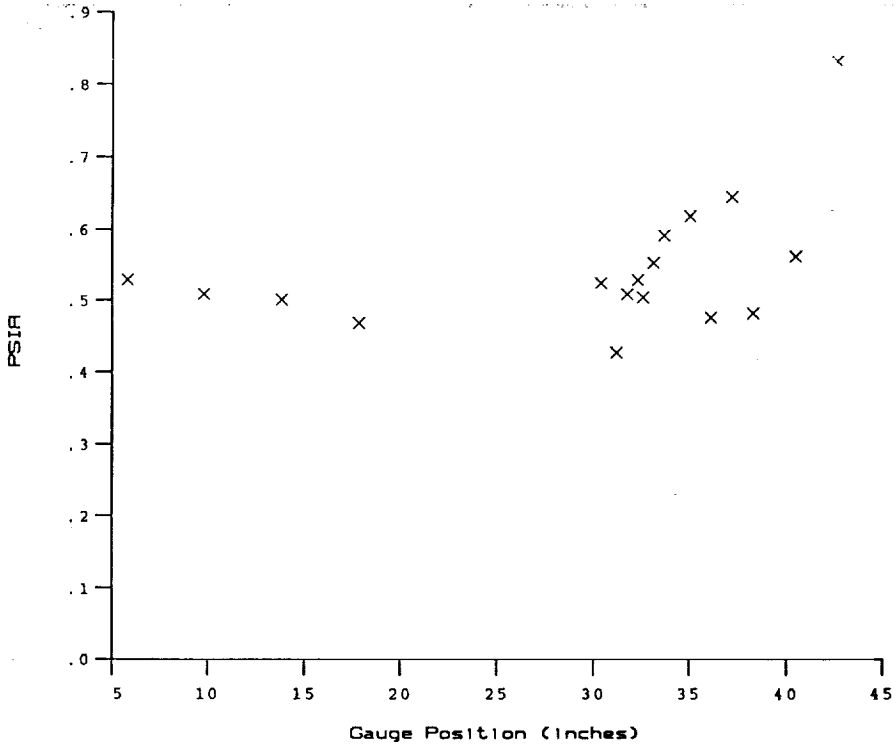


Test Conditions for Run 33 :

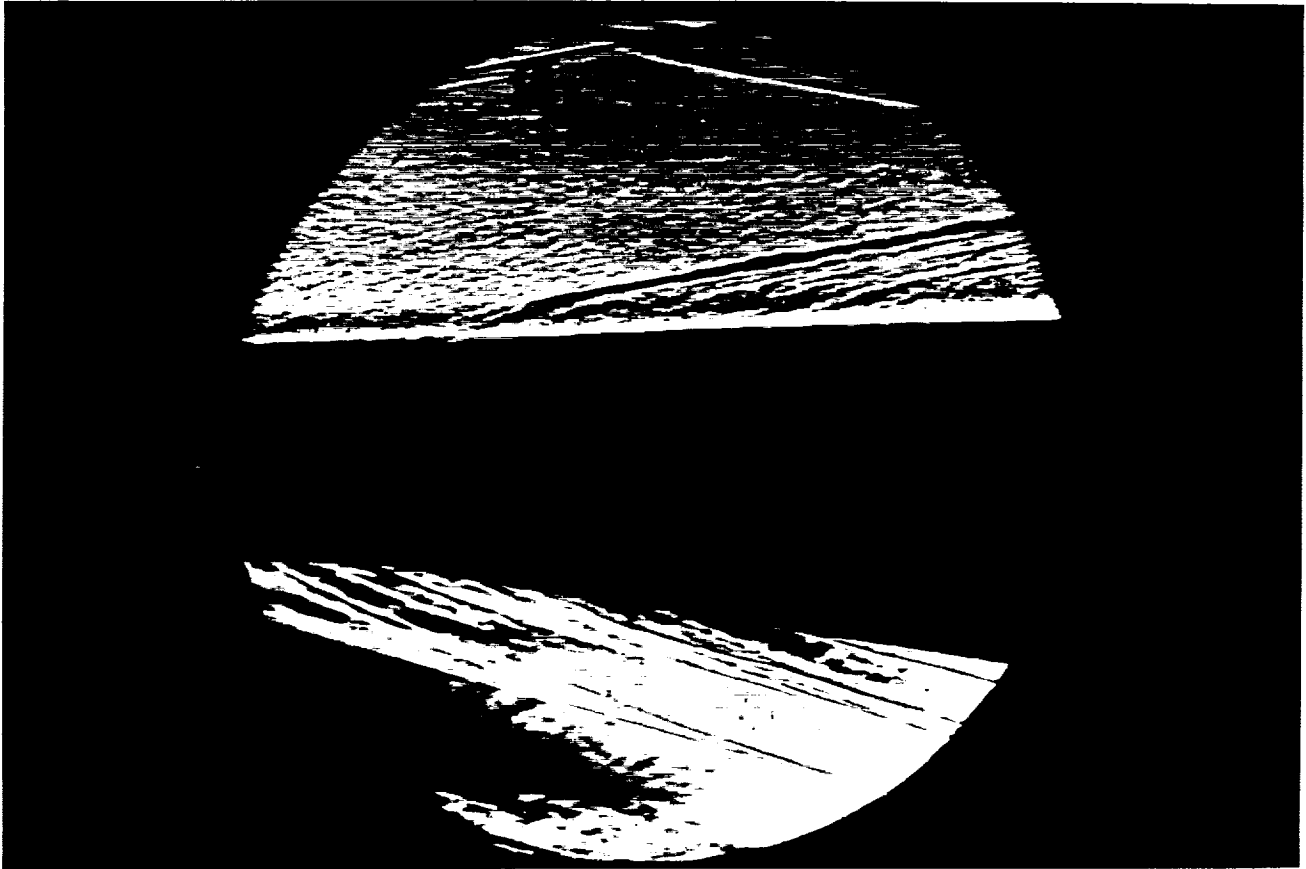
Po	= 3.590E+03 PSIA	Reservoir Total Pressure
Ho	= 1.400E+07 (Ft/sec) ²	Reservoir Total Enthalpy
To	= 2.181E+03 degR	Reservoir Total Temperature
M	= 7.870E+00	Freestream Mach Number
U	= 5.093E+03 Ft/sec	Freestream Velocity
T	= 1.741E+02 degR	Freestream Temperature
P	= 4.127E-01 PSIA	Freestream Static Pressure
Rho	= 1.989E-04 Slugs/Ft ³	Freestream Density
Mu	= 1.455E-07 Slugs/Ft-sec	Freestream Viscosity
Re	= 6.963E+06 1/Ft	Freestream Reynolds Number
Po'	= 3.307E+01 PSIA	Pitot Pressure
Q	= 1.791E+01 PSIA	Dynamic Pressure (Rho U ² /288)
Mi	= 2.862E+00	Shock Tube Incident Shock Mach Number
Tw	= 5.300E+02 degR	Wall Temperature (Test Gas = Air)
Hw	= 3.183E+06 (Ft/sec) ²	Wall Enthalpy (Cp Tw)
CPf	= 5.583E-02 1/PSIA	Pressure to CP factor (1/Q)
CHf	= 7.100E-05 Ft ² -s/BTU	Heat Rate to CH factor (778/(Rho U (Ho-Hw)))
QoFR	= 4.992E+01 BTU/Ft ² -s	Fay-Riddell Heat Transfer (.25' Diam Cylin.)



HEAT TRANSFER vs Gauge Position
Run 33

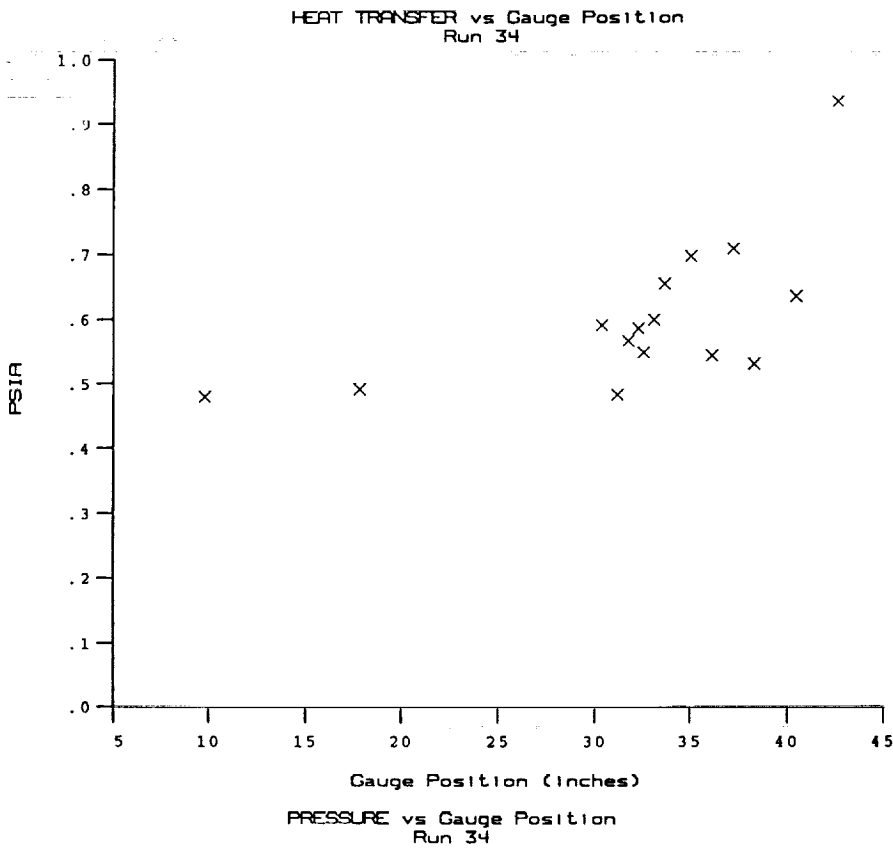
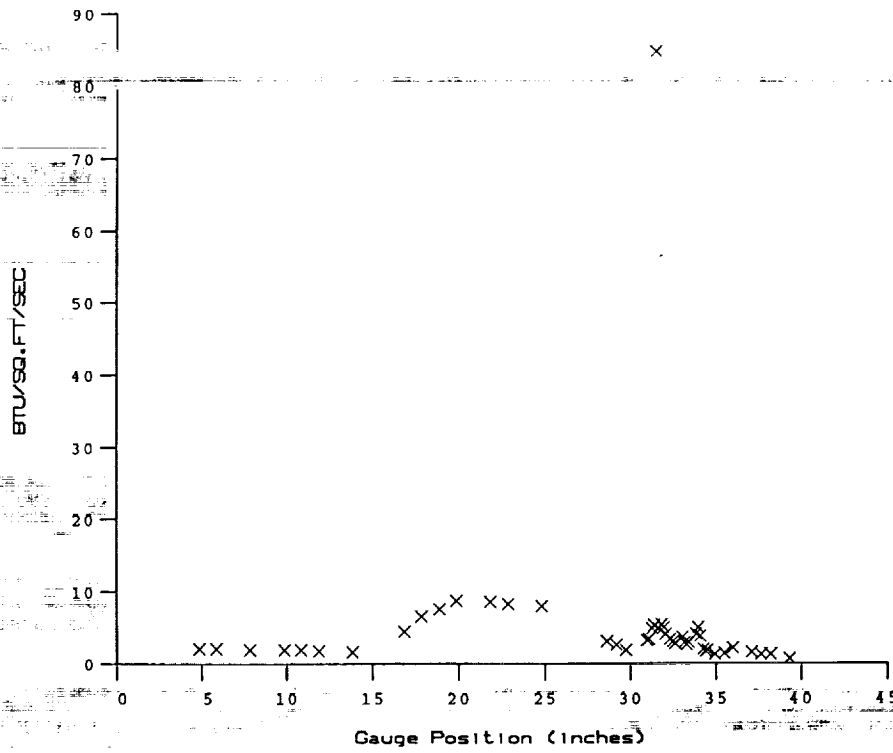


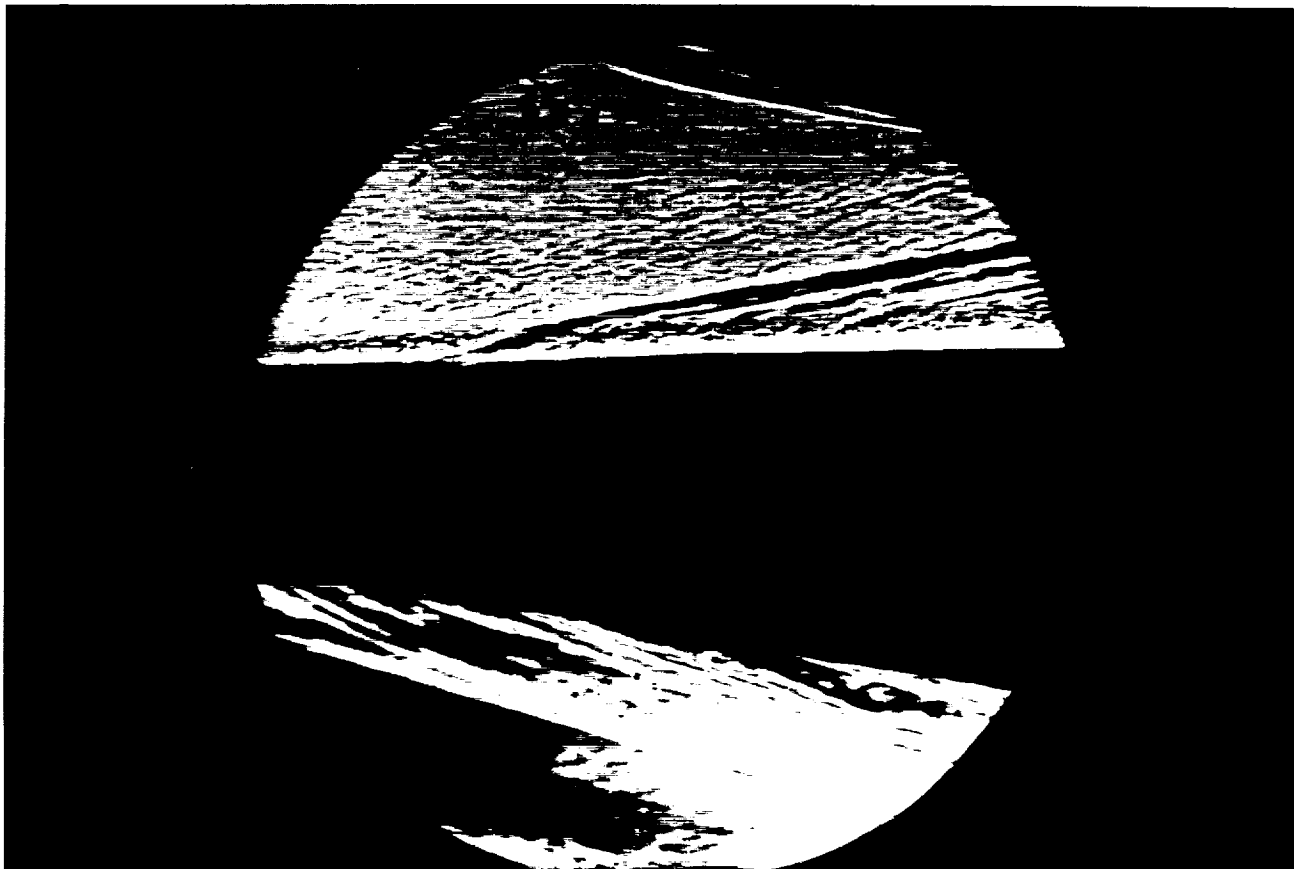
PRESSURE vs Gauge Position
Run 33



Test Conditions for Run 34 :

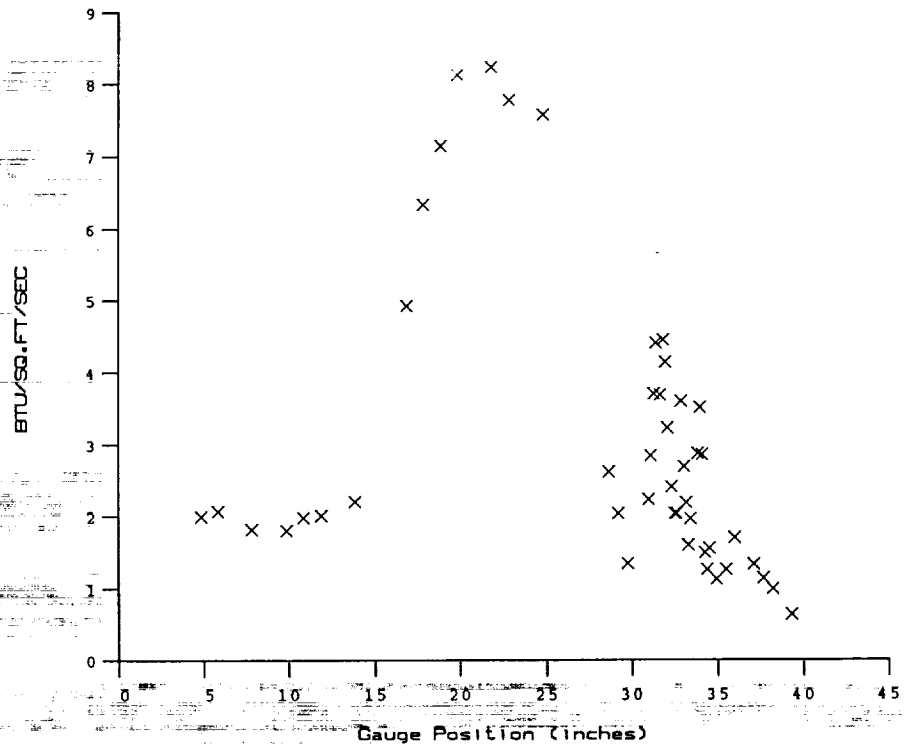
Po	= 3.772E+03 PSIA	Reservoir Total Pressure
Ho	= 1.468E+07 (Ft/sec) ²	Reservoir Total Enthalpy
To	= 2.274E+03 degR	Reservoir Total Temperature
M	= 7.862E+00	Freestream Mach Number
U	= 5.214E+03 Ft/sec	Freestream Velocity
T	= 1.829E+02 degR	Freestream Temperature
P	= 4.314E-01 PSIA	Freestream Static Pressure
Rho	= 1.980E-04 Slugs/Ft ³	Freestream Density
Mu	= 1.525E-07 Slugs/Ft-sec	Freestream Viscosity
Re	= 6.768E+06 1/Ft	Freestream Reynolds Number
Po'	= 3.452E+01 PSIA	Pitot Pressure
Q	= 1.869E+01 PSIA	Dynamic Pressure ($\rho U^2/288$)
Mi	= 2.920E+00	Shock Tube Incident Shock Mach Number
Tw	= 5.300E+02 degR	Wall Temperature (Test Gas = Air)
Hw	= 3.183E+06 (Ft/sec) ²	Wall Enthalpy ($C_p T_w$)
CPf	= 5.351E-02 1/PSIA	Pressure to CP factor (1/Q)
Chf	= 6.558E-05 Ft ² -s/BTU	Heat Rate to CH factor ($778/(\rho U (H_o - H_w))$)
QoFR	= 5.438E+01 BTU/Ft ² -s	Fay-Riddell Heat Transfer (.25' Diam Cylin.)



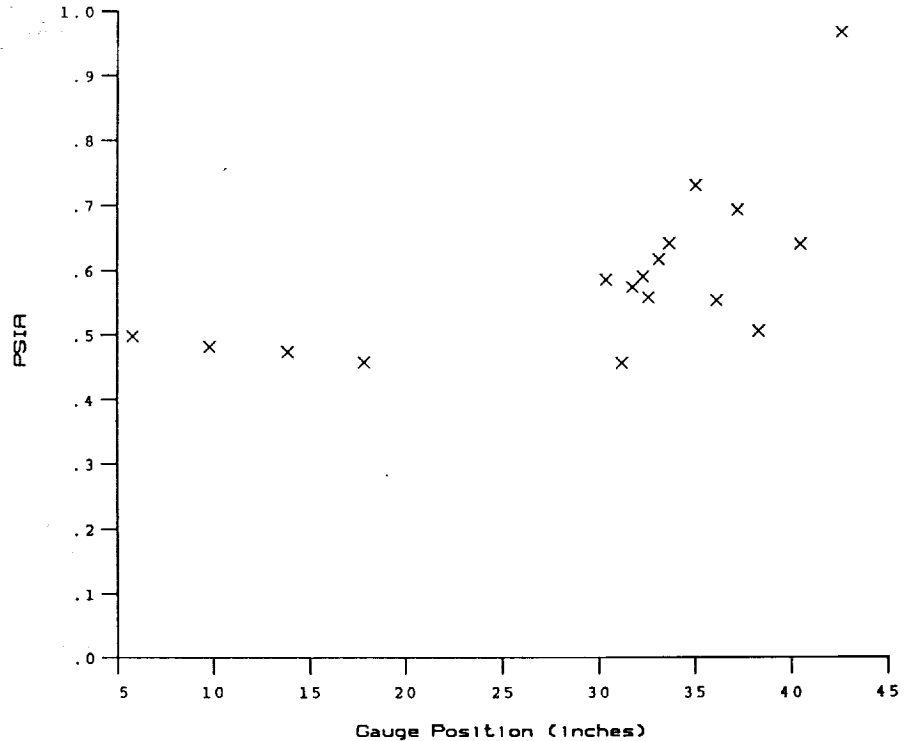


Test Conditions for Run 35 :

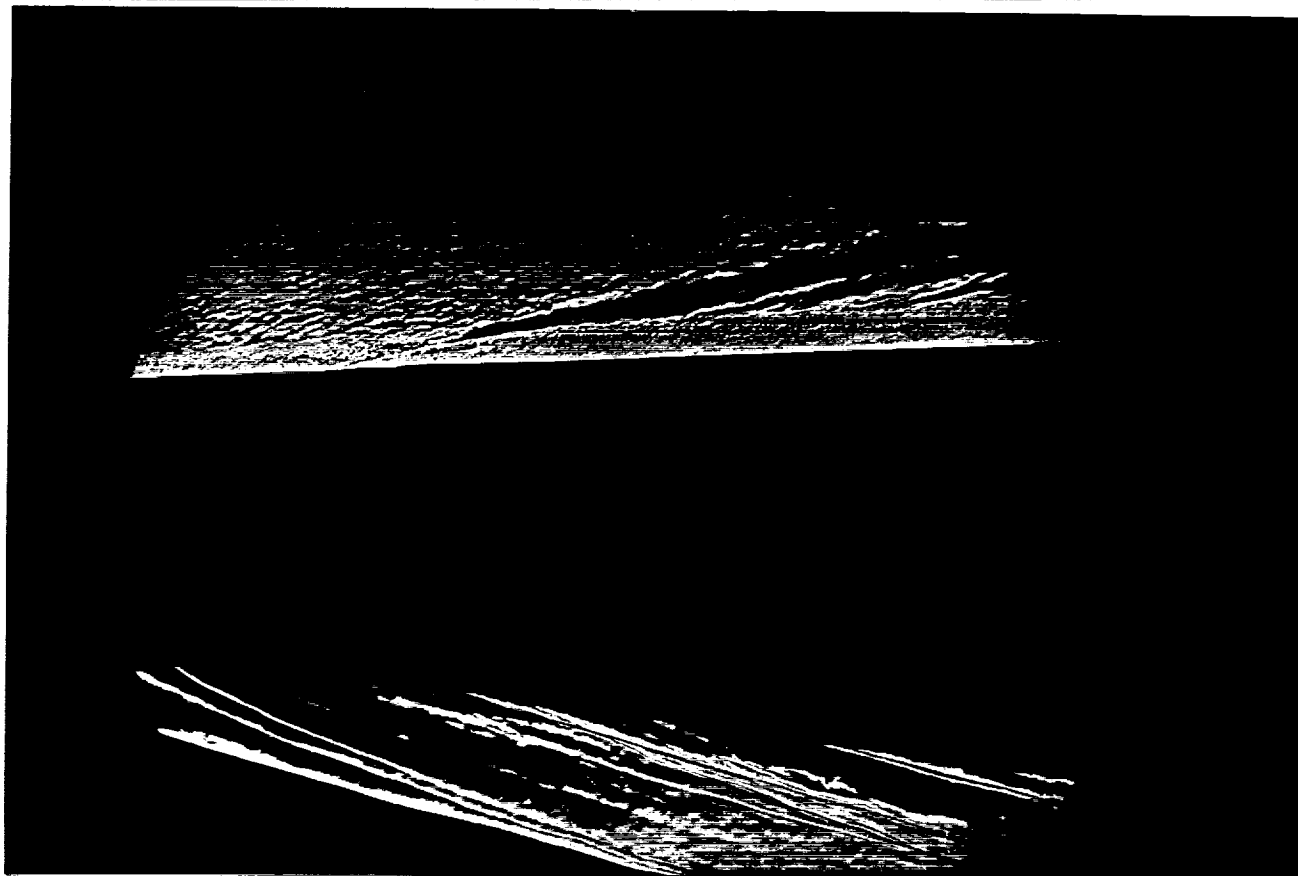
Po	= 3.666E+03 PSIA	Reservoir Total Pressure
Ho	= 1.433E+07 (Ft/sec) ²	Reservoir Total Enthalpy
To	= 2.227E+03 degR	Reservoir Total Temperature
M	= 7.867E+00	Freestream Mach Number
U	= 5.153E+03 Ft/sec	Freestream Velocity
T	= 1.784E+02 degR	Freestream Temperature
P	= 4.199E-01 PSIA	Freestream Static Pressure
Rho	= 1.976E-04 Slugs/Ft ³	Freestream Density
Mu	= 1.489E-07 Slugs/Ft-sec	Freestream Viscosity
Re	= 6.837E+06 1/Ft	Freestream Reynolds Number
Po'	= 3.363E+01 PSIA	Pitot Pressure
Q	= 1.821E+01 PSIA	Dynamic Pressure (Rho U ² /288)
Mi	= 2.884E+00	Shock Tube Incident Shock Mach Number
Tw	= 5.300E+02 degR	Wall Temperature (Test Gas = Air)
Hw	= 3.183E+06 (Ft/sec) ²	Wall Enthalpy (Cp Tw)
CPf	= 5.491E-02 1/PSIA	Pressure to CP factor (1/Q)
CHf	= 6.855E-05 Ft ² -s/BTU	Heat Rate to CH factor (778/(Rho U (Ho-Hw)))
QoFR	= 5.198E+01 BTU/Ft ² -s	Fay-Riddell Heat Transfer (.25' Diam Cylin.)



HEAT TRANSFER vs Gauge Position
Run 35

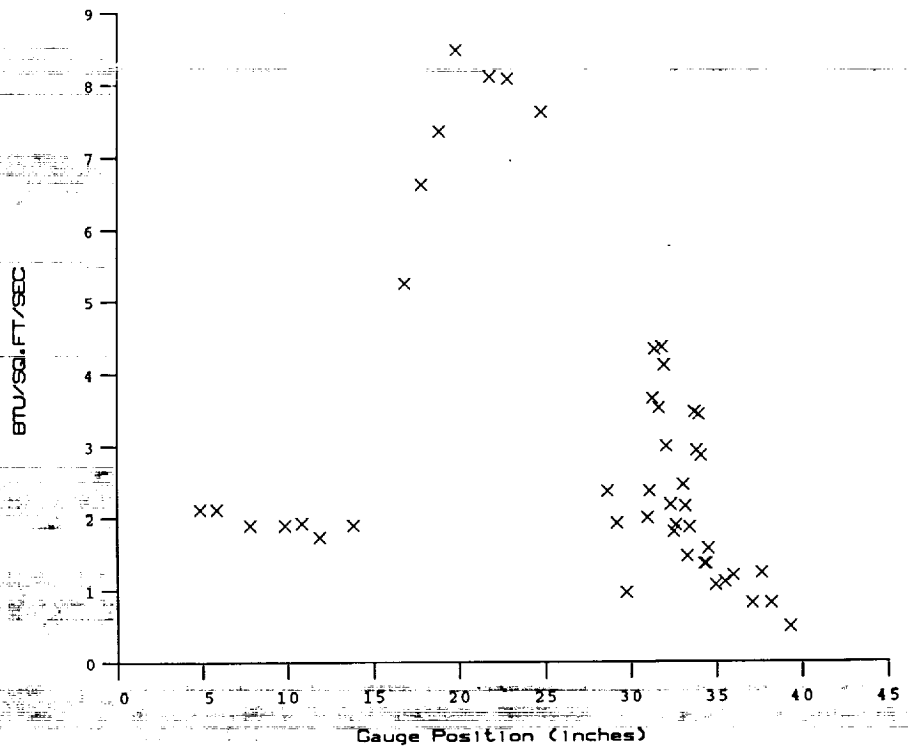


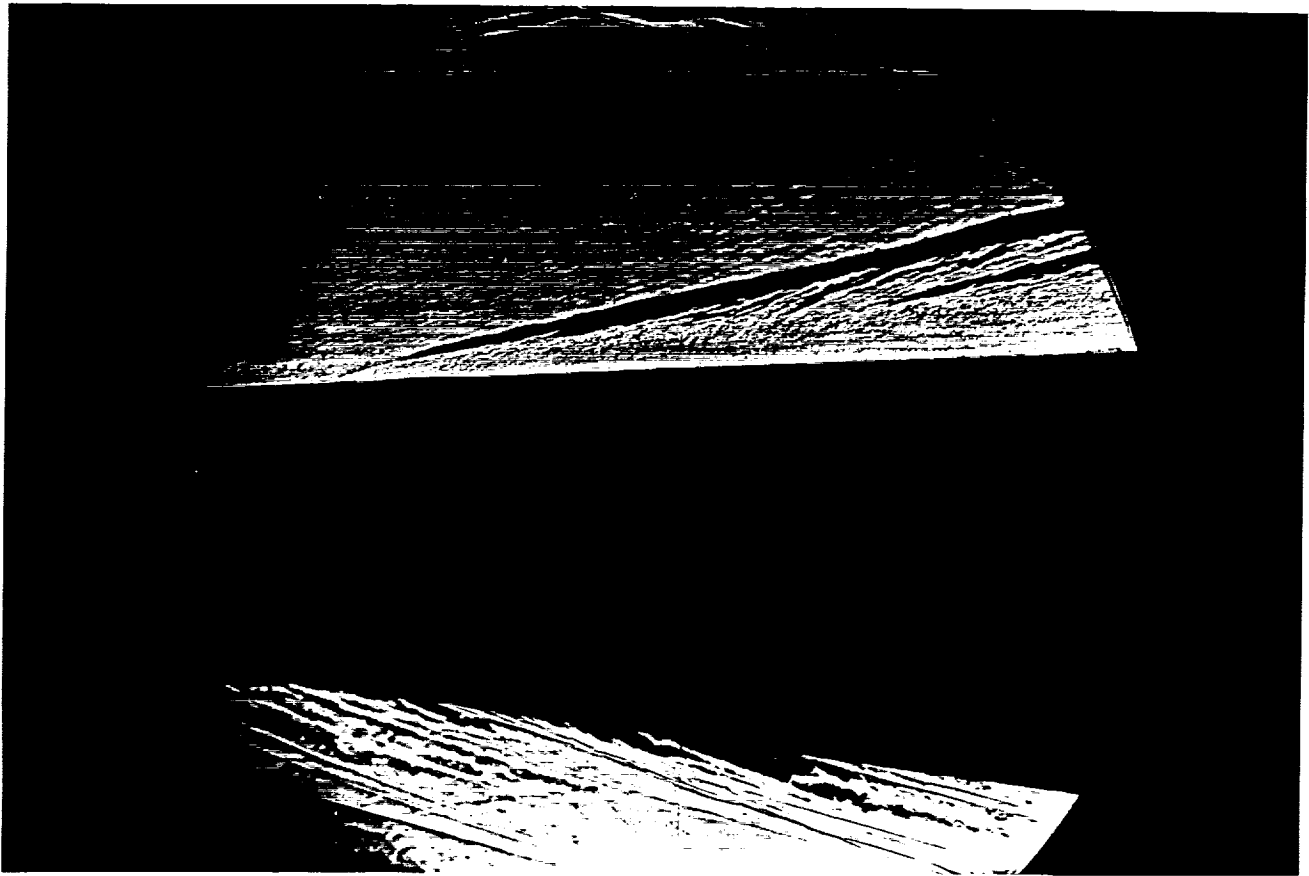
PRESSURE vs Gauge Position
Run 35



Test Conditions for Run 36 :

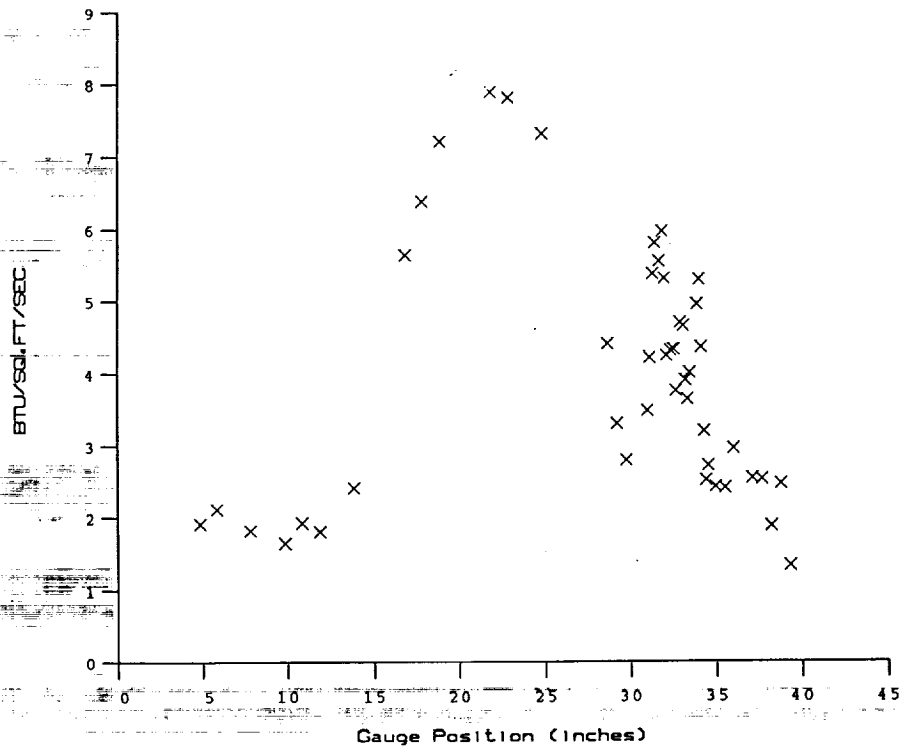
Po	= 3.675E+03 PSIA	Reservoir Total Pressure
Ho	= 1.402E+07 (Ft/sec) ²	Reservoir Total Enthalpy
To	= 2.183E+03 degR	Reservoir Total Temperature
M	= 7.872E+00	Freestream Mach Number
U	= 5.097E+03 Ft/sec	Freestream Velocity
T	= 1.743E+02 degR	Freestream Temperature
P	= 4.221E-01 PSIA	Freestream Static Pressure
Rho	= 2.032E-04 Slugs/Ft ³	Freestream Density
Mu	= 1.456E-07 Slugs/Ft-sec	Freestream Viscosity
Re	= 7.113E+06 1/Ft	Freestream Reynolds Number
Po'	= 3.384E+01 PSIA	Pitot Pressure
Q	= 1.833E+01 PSIA	Dynamic Pressure (Rho U ² /288)
Mi	= 2.867E+00	Shock Tube Incident Shock Mach Number
Tw	= 5.300E+02 degR	Wall Temperature (Test Gas = Air)
Hw	= 3.183E+06 (Ft/sec) ²	Wall Enthalpy (Cp Tw)
CPf	= 5.456E-02 1/PSIA	Pressure to CP factor (1/Q)
CHf	= 6.931E-05 Ft ² -s/BTU	Heat Rate to CH factor (778/(Rho U (Ho-Hw)))
QoFR	= 5.059E+01 BTU/Ft ² -s	Fay-Riddell Heat Transfer (.25' Diam Cylin.)



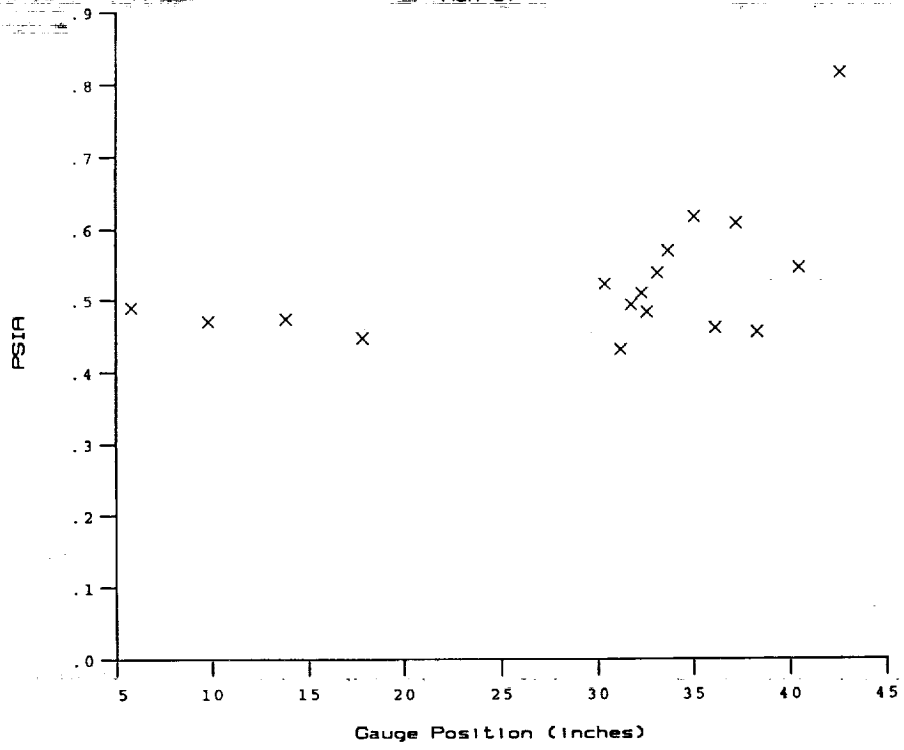


Test Conditions for Run 37 :

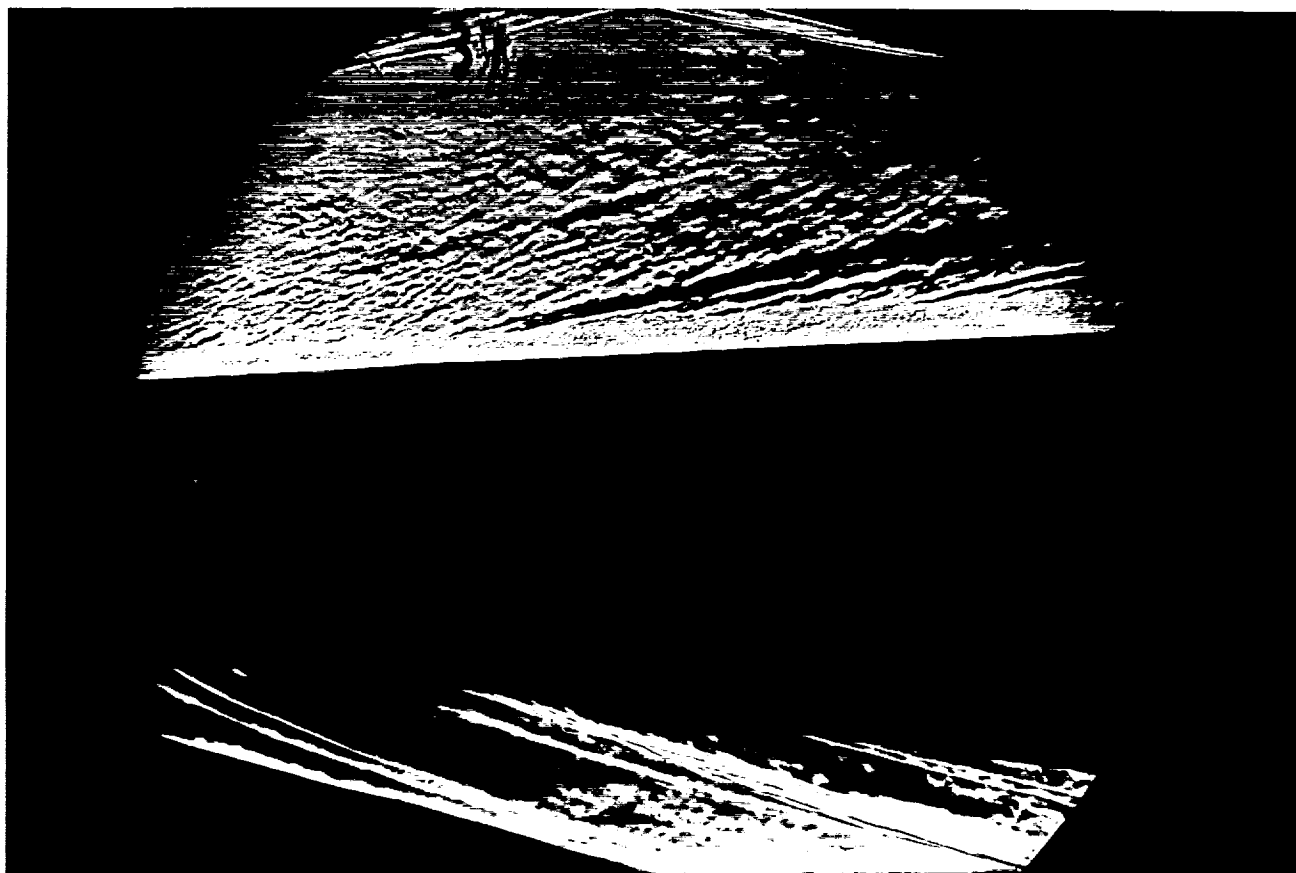
Po	= 3.646E+03 PSIA	Reservoir Total Pressure
Ho	= 1.444E+07 (Ft/sec) ²	Reservoir Total Enthalpy
To	= 2.242E+03 degR	Reservoir Total Temperature
M	= 7.862E+00	Freestream Mach Number
U	= 5.172E+03 Ft/sec	Freestream Velocity
T	= 1.800E+02 degR	Freestream Temperature
P	= 4.183E-01 PSIA	Freestream Static Pressure
Rho	= 1.951E-04 Slugs/Ft ³	Freestream Density
Mu	= 1.502E-07 Slugs/Ft-sec	Freestream Viscosity
Re	= 6.718E+06 1/Ft	Freestream Reynolds Number
Po'	= 3.347E+01 PSIA	Pitot Pressure
Q	= 1.812E+01 PSIA	Dynamic Pressure (Rho U ² /288)
Mi	= 2.901E+00	Shock Tube Incident Shock Mach Number
Tw	= 5.300E+02 degR	Wall Temperature (Test Gas = Air)
Hw	= 3.183E+06 (Ft/sec) ²	Wall Enthalpy (Cp Tw)
CPf	= 5.519E-02 1/PSIA	Pressure to CP factor (1/Q)
CHF	= 6.848E-05 Ft ² -s/BTU	Heat Rate to CH factor (778/(Rho U (Ho-Hw)))
QoFR	= 5.239E+01 BTU/Ft ² -s	Fay-Riddell Heat Transfer (.25' Diam Cylin.)



HEAT TRANSFER vs Gauge Position
Run 37

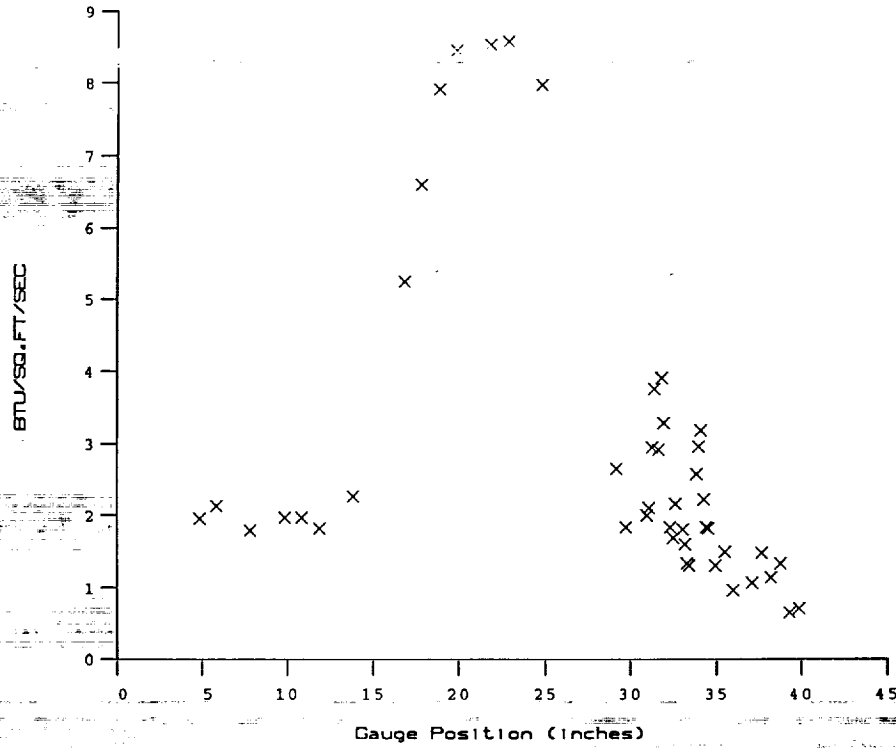


PRESSURE vs Gauge Position
Run 37

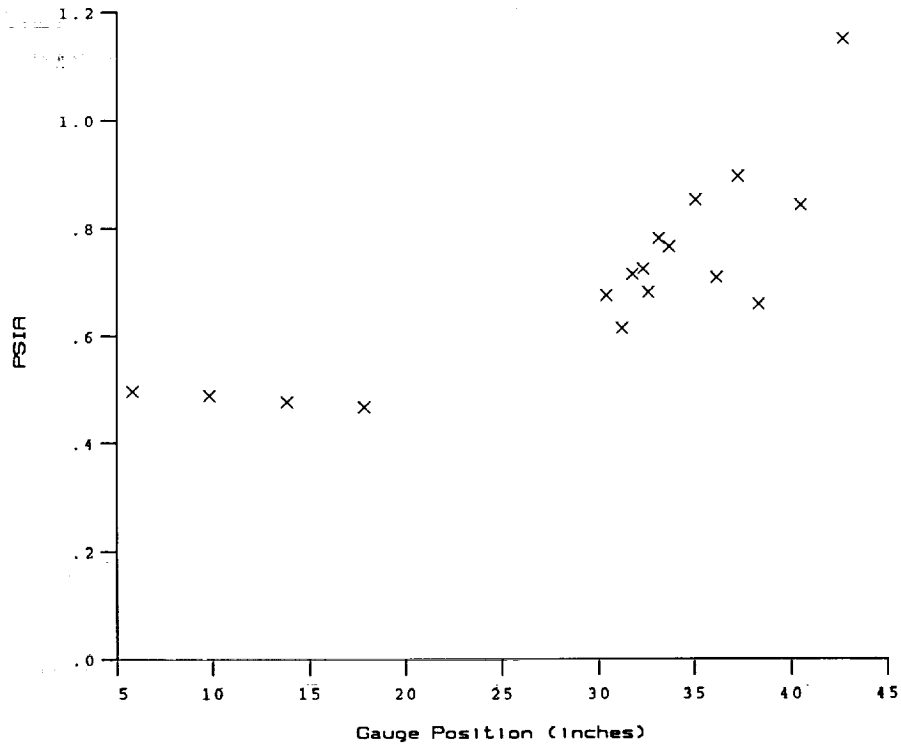


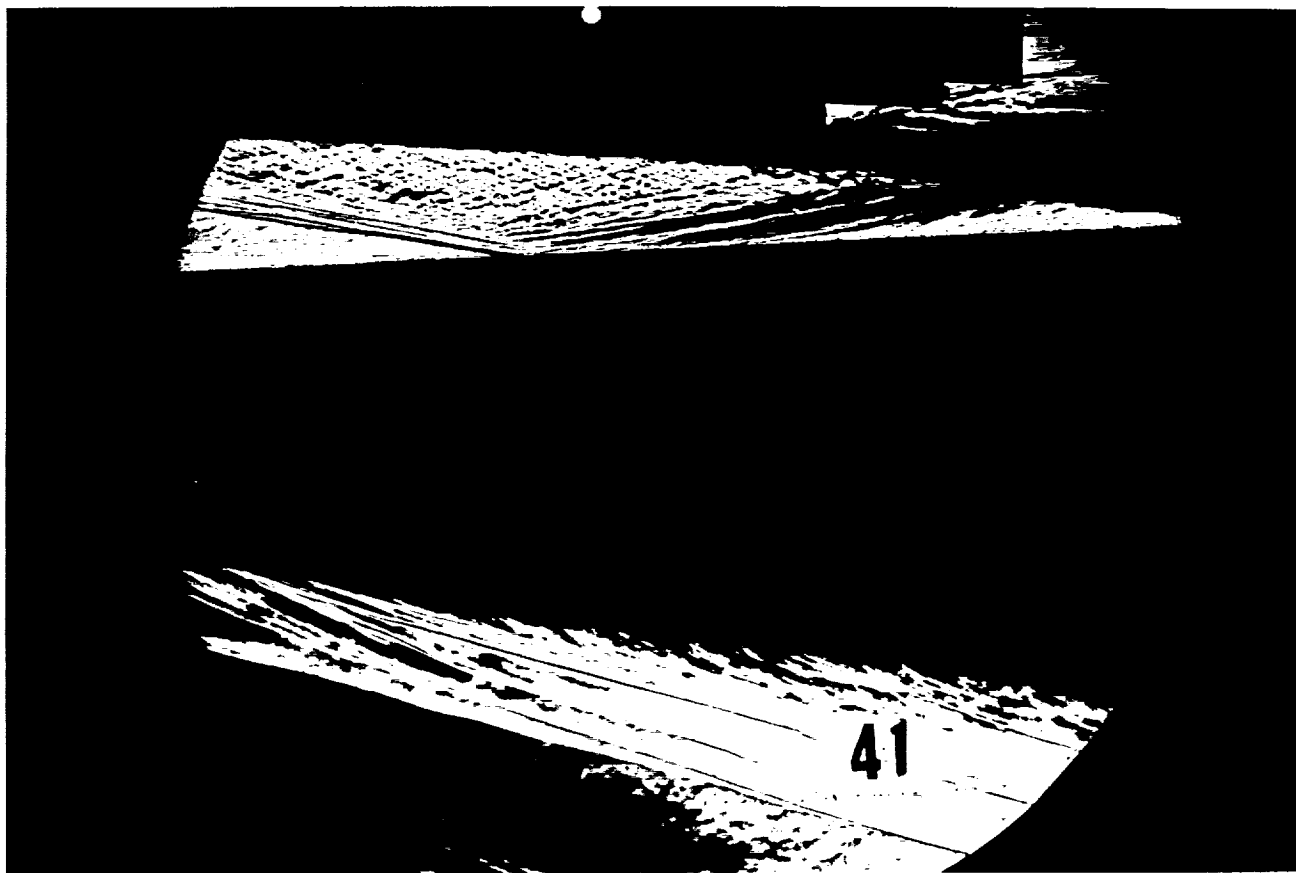
Test Conditions for Run 38 :

Po	= 3.633E+03 PSIA	Reservoir Total Pressure
Ho	= 1.447E+07 (Ft/sec) ²	Reservoir Total Enthalpy
To	= 2.246E+03 degR	Reservoir Total Temperature
M	= 7.861E+00	Freestream Mach Number
U	= 5.178E+03 Ft/sec	Freestream Velocity
T	= 1.804E+02 degR	Freestream Temperature
P	= 4.167E-01 PSIA	Freestream Static Pressure
Rho	= 1.939E-04 Slugs/Ft ³	Freestream Density
Mu	= 1.505E-07 Slugs/Ft-sec	Freestream Viscosity
Re	= 6.670E+06 1/Ft	Freestream Reynolds Number
Po'	= 3.333E+01 PSIA	Pitot Pressure
Q	= 1.805E+01 PSIA	Dynamic Pressure ($\rho U^2/288$)
Mi	= 2.901E+00	Shock Tube Incident Shock Mach Number
Tw	= 5.300E+02 degR	Wall Temperature (Test Gas = Air)
Hw	= 3.183E+06 (Ft/sec) ²	Wall Enthalpy ($C_p Tw$)
CPf	= 5.541E-02 1/PSIA	Pressure to CP factor (1/Q)
CHf	= 6.865E-05 Ft ² -s/BTU	Heat Rate to CH factor ($778/(\rho U (Ho-Hw))$)
QoFR	= 5.244E+01 BTU/Ft ² -s	Fay-Riddell Heat Transfer (.25' Diam Cylin.)



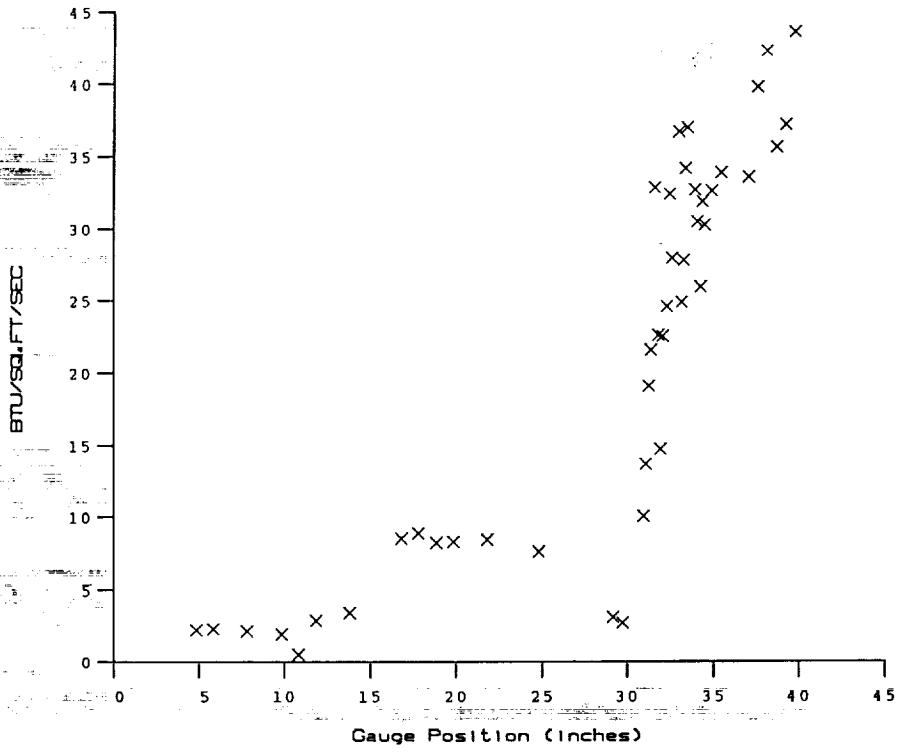
HEAT TRANSFER vs Gauge Position
Run 38



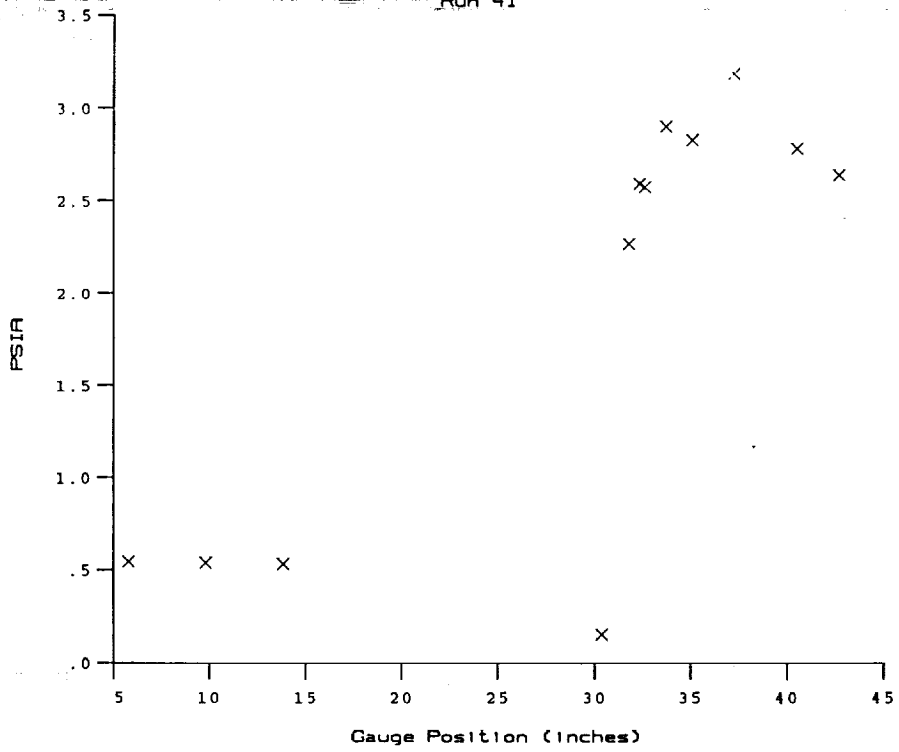


Test Conditions for Run 41 :

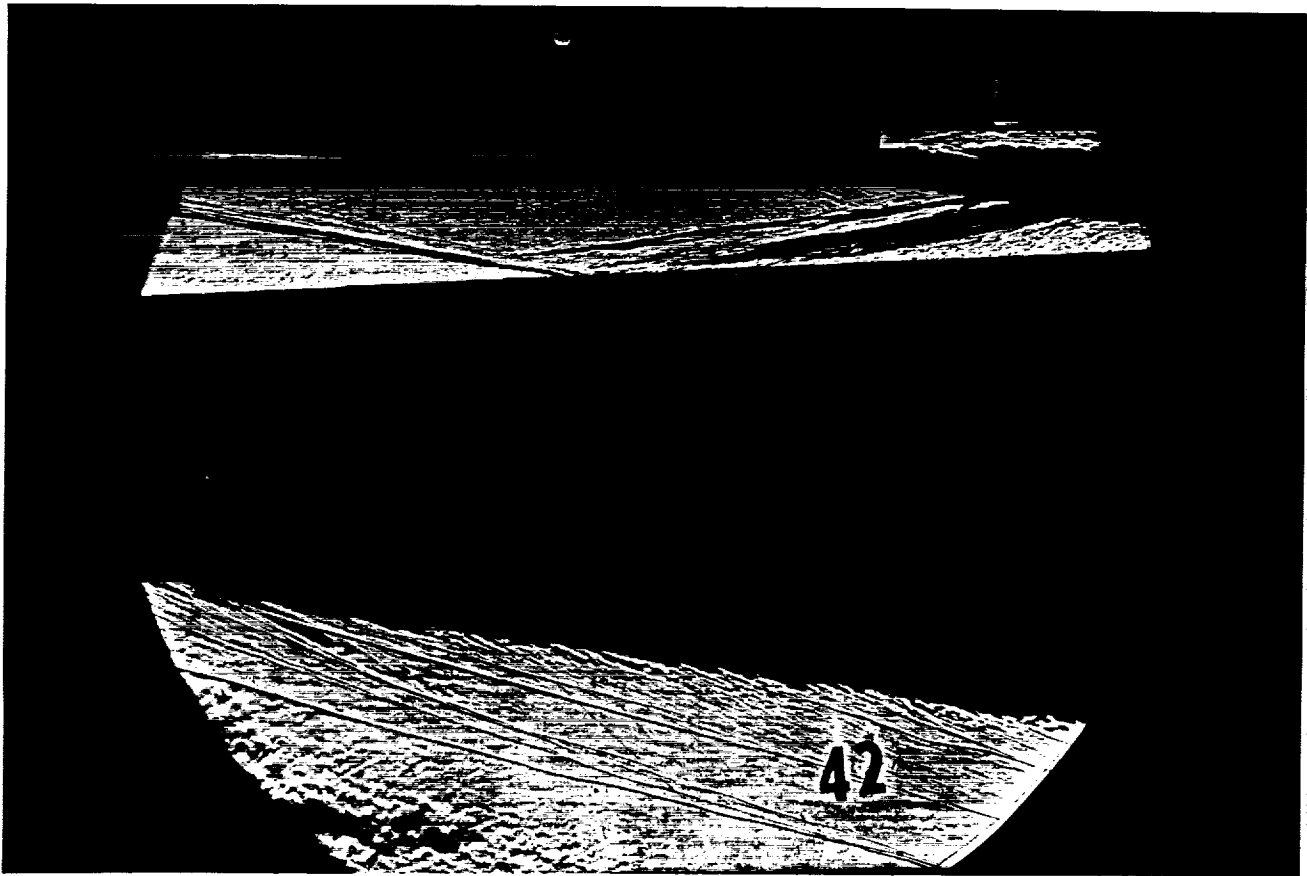
Po	= 4.086E+03 PSIA	Reservoir Total Pressure
Ho	= 1.389E+07 (Ft/sec) ²	Reservoir Total Enthalpy
To	= 2.165E+03 degR	Reservoir Total Temperature
M	= 7.893E+00	Freestream Mach Number
U	= 5.074E+03 Ft/sec	Freestream Velocity
T	= 1.718E+02 degR	Freestream Temperature
P	= 4.649E-01 PSIA	Freestream Static Pressure
Rho	= 2.271E-04 Slugs/Ft ³	Freestream Density
Mu	= 1.435E-07 Slugs/Ft-sec	Freestream Viscosity
Re	= 8.026E+06 1/Ft	Freestream Reynolds Number
Po'	= 3.747E+01 PSIA	Pitot Pressure
Q	= 2.030E+01 PSIA	Dynamic Pressure ($\rho U^2/288$)
Mi	= 2.846E+00	Shock Tube Incident Shock Mach Number
Tw	= 5.300E+02 degR	Wall Temperature (Test Gas = Air)
Hw	= 3.183E+06 (Ft/sec) ²	Wall Enthalpy ($C_p T_w$)
CPf	= 4.927E-02 1/PSIA	Pressure to CP factor (1/Q)
CHf	= 6.307E-05 Ft ² -s/BTU	Heat Rate to CH factor ($778/(\rho U (H_o - H_w))$)
QoFR	= 5.256E+01 BTU/Ft ² -s	Fay-Riddell Heat Transfer (.25' Diam Cylin.)



HEAT TRANSFER vs Gauge Position
Run 41

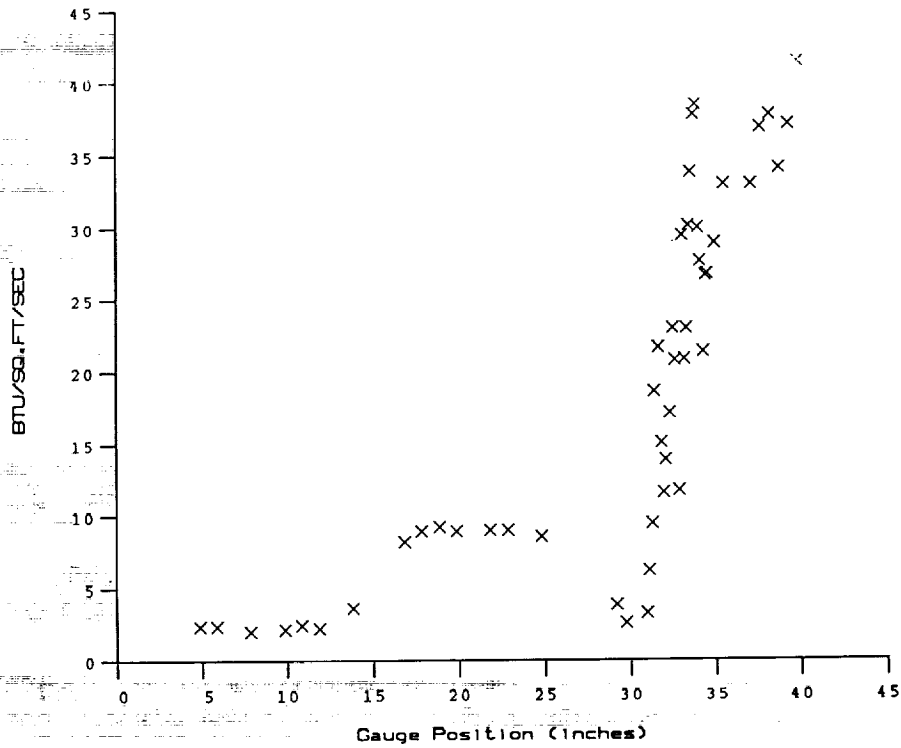


PRESSURE vs Gauge Position
Run 41

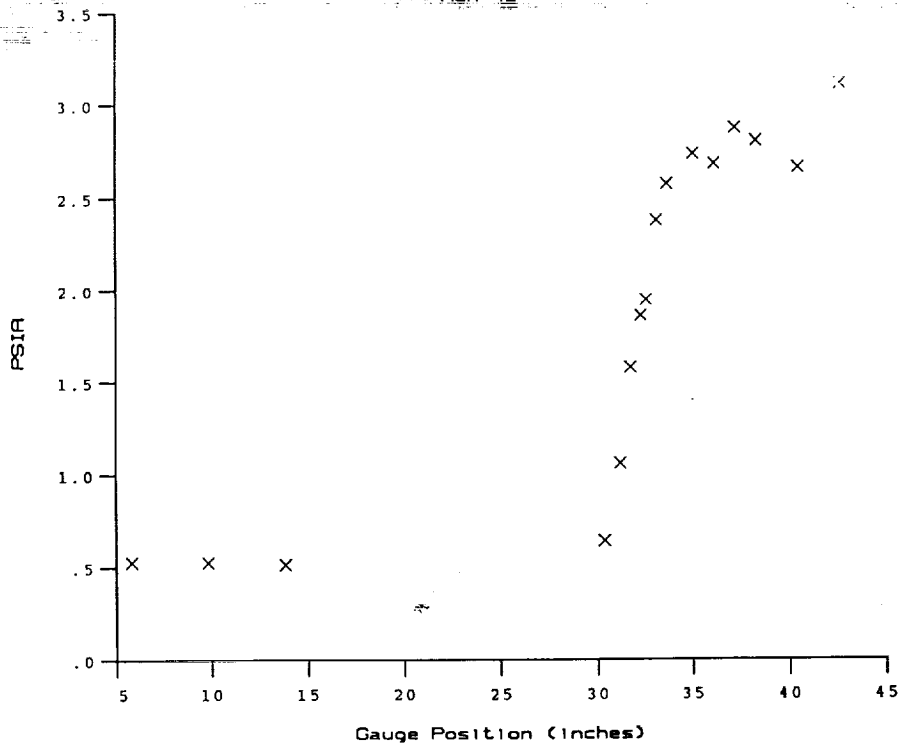


Test Conditions for Run 42 :

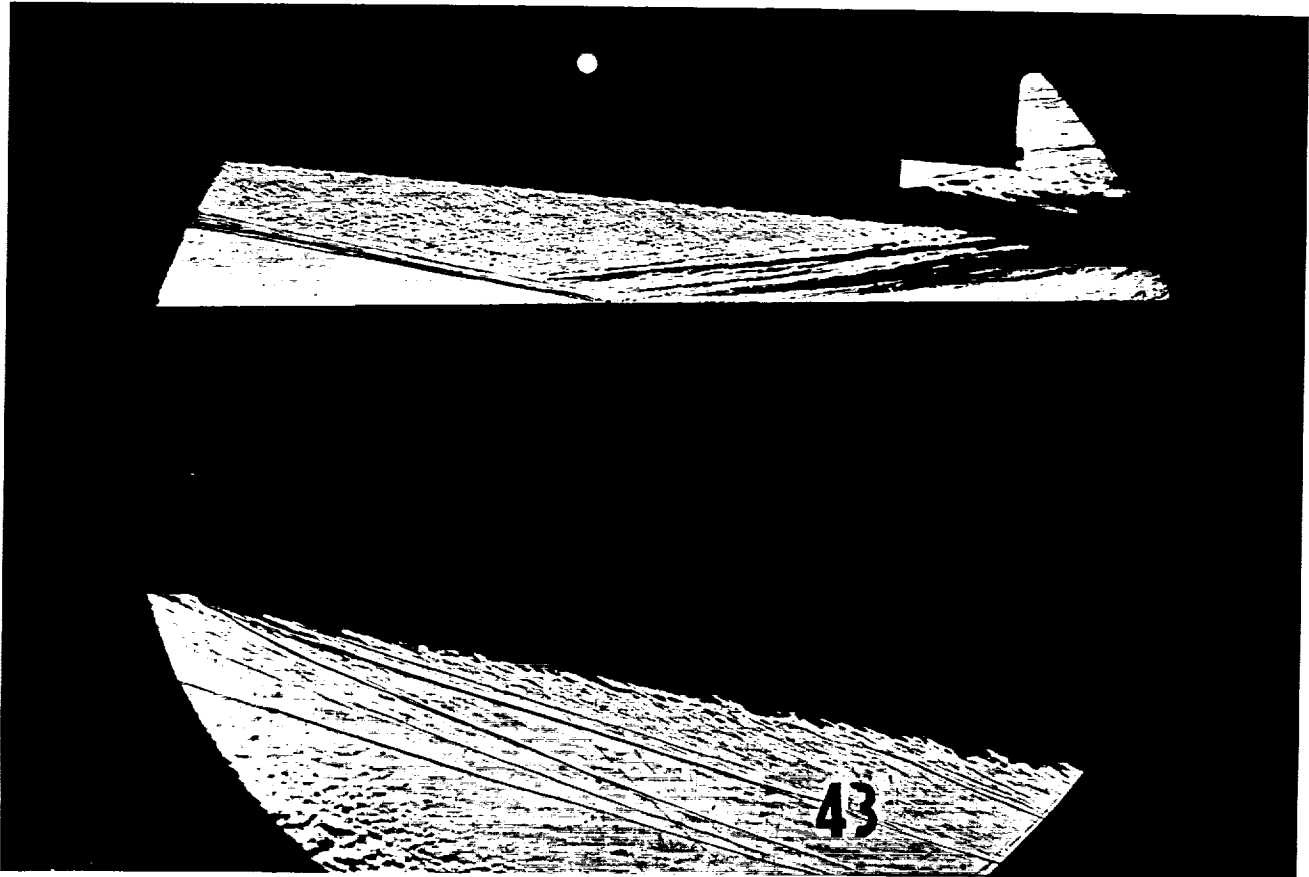
Po	= 3.936E+03 PSIA	Reservoir Total Pressure
Ho	= 1.487E+07 (Ft/sec) ²	Reservoir Total Enthalpy
To	= 2.300E+03 degR	Reservoir Total Temperature
M	= 7.859E+00	Freestream Mach Number
U	= 5.249E+03 Ft/sec	Freestream Velocity
T	= 1.854E+02 degR	Freestream Temperature
P	= 4.503E-01 PSIA	Freestream Static Pressure
Rho	= 2.038E-04 Slugs/Ft ³	Freestream Density
Mu	= 1.546E-07 Slugs/Ft-sec	Freestream Viscosity
Re	= 6.919E+06 1/Ft	Freestream Reynolds Number
Po'	= 3.601E+01 PSIA	Pitot Pressure
Q	= 1.949E+01 PSIA	Dynamic Pressure (Rho U ² /288)
Mi	= 2.955E+00	Shock Tube Incident Shock Mach Number
Tw	= 5.300E+02 degR	Wall Temperature (Test Gas = Air)
Hw	= 3.183E+06 (Ft/sec) ²	Wall Enthalpy (Cp Tw)
CPf	= 5.131E-02 1/PSIA	Pressure to CP factor (1/Q)
Chf	= 6.222E-05 Ft ² -s/BTU	Heat Rate to CH factor (778/(Rho U (Ho-Hw)))
QoFR	= 5.655E+01 BTU/Ft ² -s	Fay-Riddell Heat Transfer (.25' Diam Cylin.)



HEAT TRANSFER vs Gauge Position
Run 42

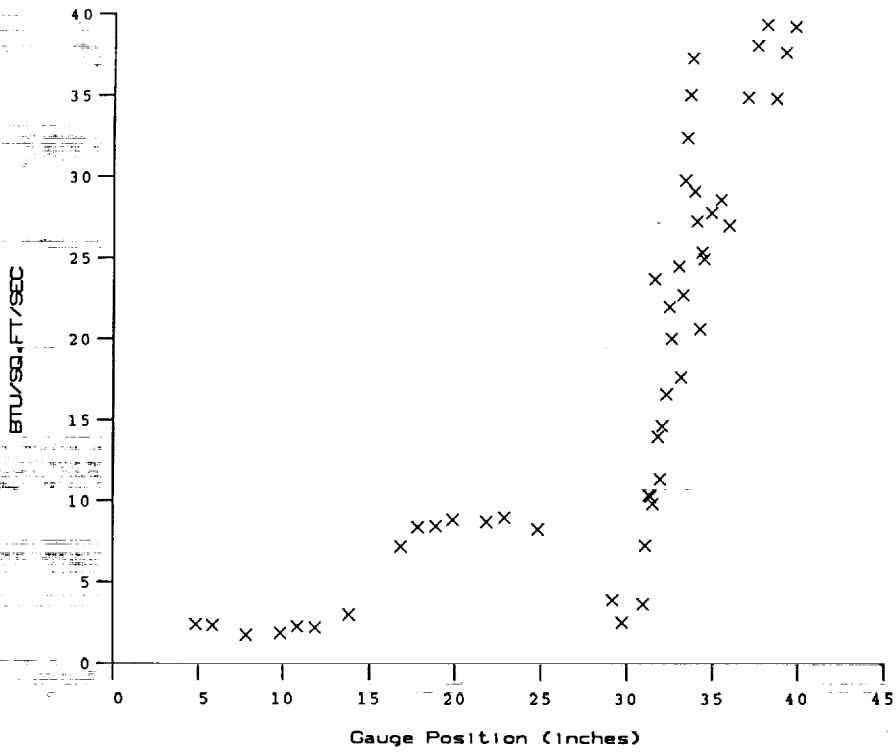


PRESSURE vs Gauge Position
Run 42

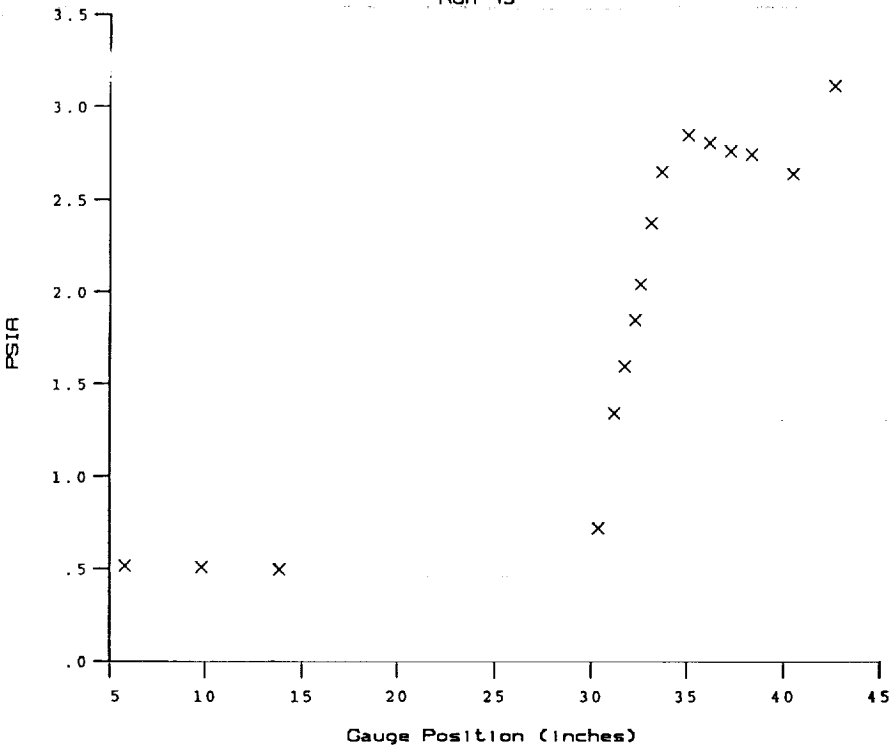


Test Conditions for Run 43 :

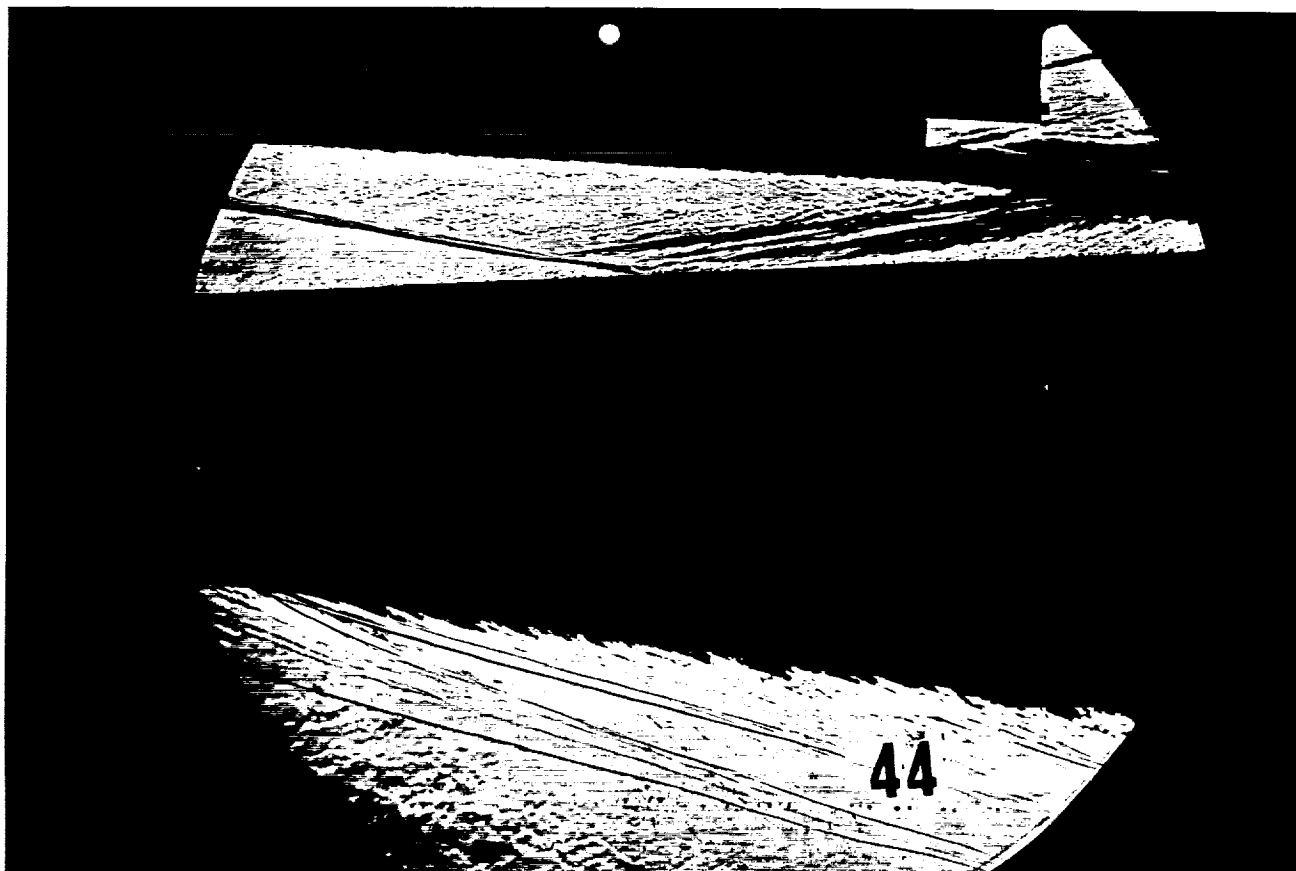
Po	= 4.000E+03 PSIA	Reservoir Total Pressure
Ho	= 1.473E+07 (Ft/sec) ²	Reservoir Total Enthalpy
To	= 2.280E+03 degR	Reservoir Total Temperature
M	= 7.866E+00	Freestream Mach Number
U	= 5.223E+03 Ft/sec	Freestream Velocity
T	= 1.834E+02 degR	Freestream Temperature
P	= 4.569E-01 PSIA	Freestream Static Pressure
Rho	= 2.091E-04 Slugs/Ft ³	Freestream Density
Mu	= 1.529E-07 Slugs/Ft-sec	Freestream Viscosity
Re	= 7.144E+06 1/Ft	Freestream Reynolds Number
Po'	= 3.660E+01 PSIA	Pitot Pressure
Q	= 1.981E+01 PSIA	Dynamic Pressure (Rho U ² /288)
Mi	= 2.940E+00	Shock Tube Incident Shock Mach Number
Tw	= 5.300E+02 degR	Wall Temperature (Test Gas = Air)
Hw	= 3.183E+06 (Ft/sec) ²	Wall Enthalpy (Cp Tw)
CPf	= 5.048E-02 1/PSIA	Pressure to CP factor (1/Q)
CHF	= 6.169E-05 Ft ² -s/BTU	Heat Rate to CH factor (778/(Rho U (Ho-Hw)))
QoFR	= 5.626E+01 BTU/Ft ² -s	Fay-Riddell Heat Transfer (.25' Diam Cylin.)



HEAT TRANSFER vs Gauge Position
Run 43

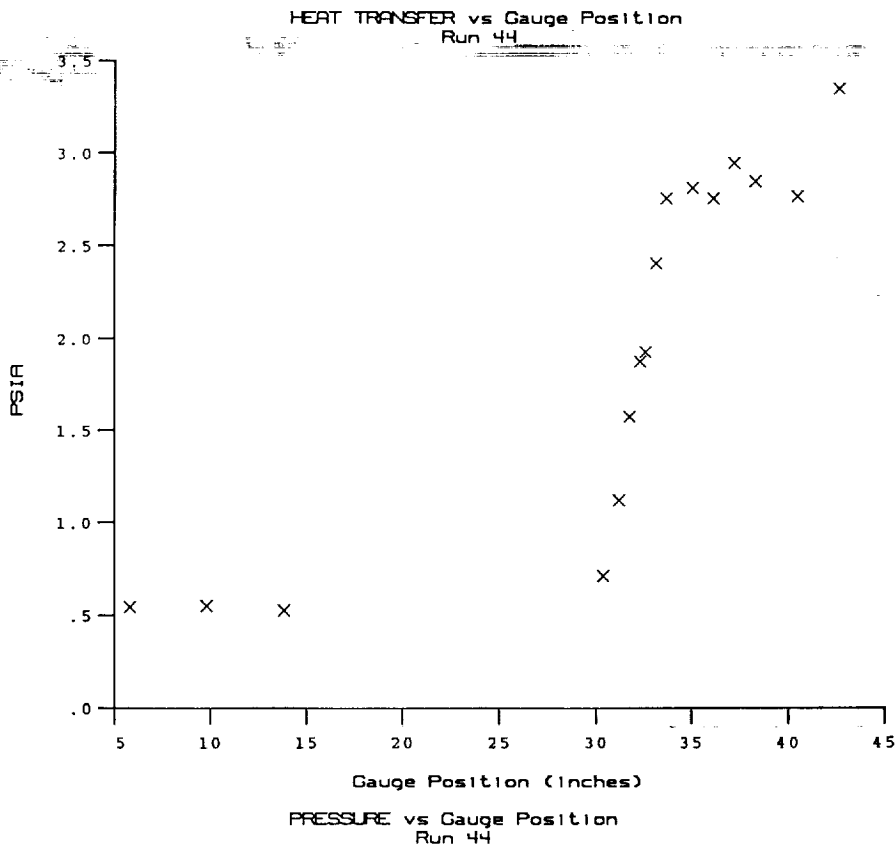
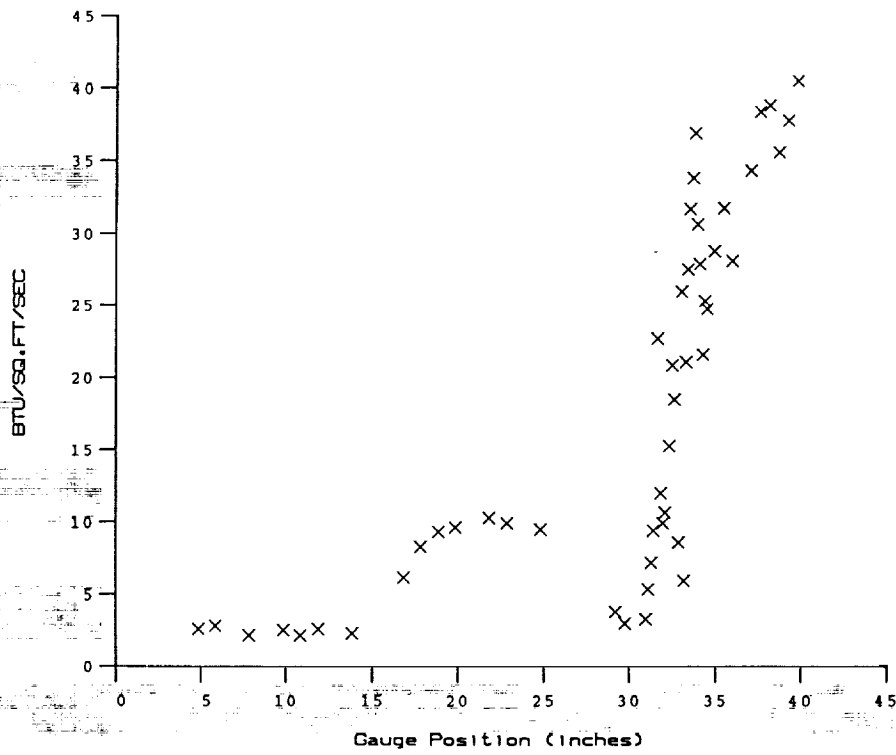


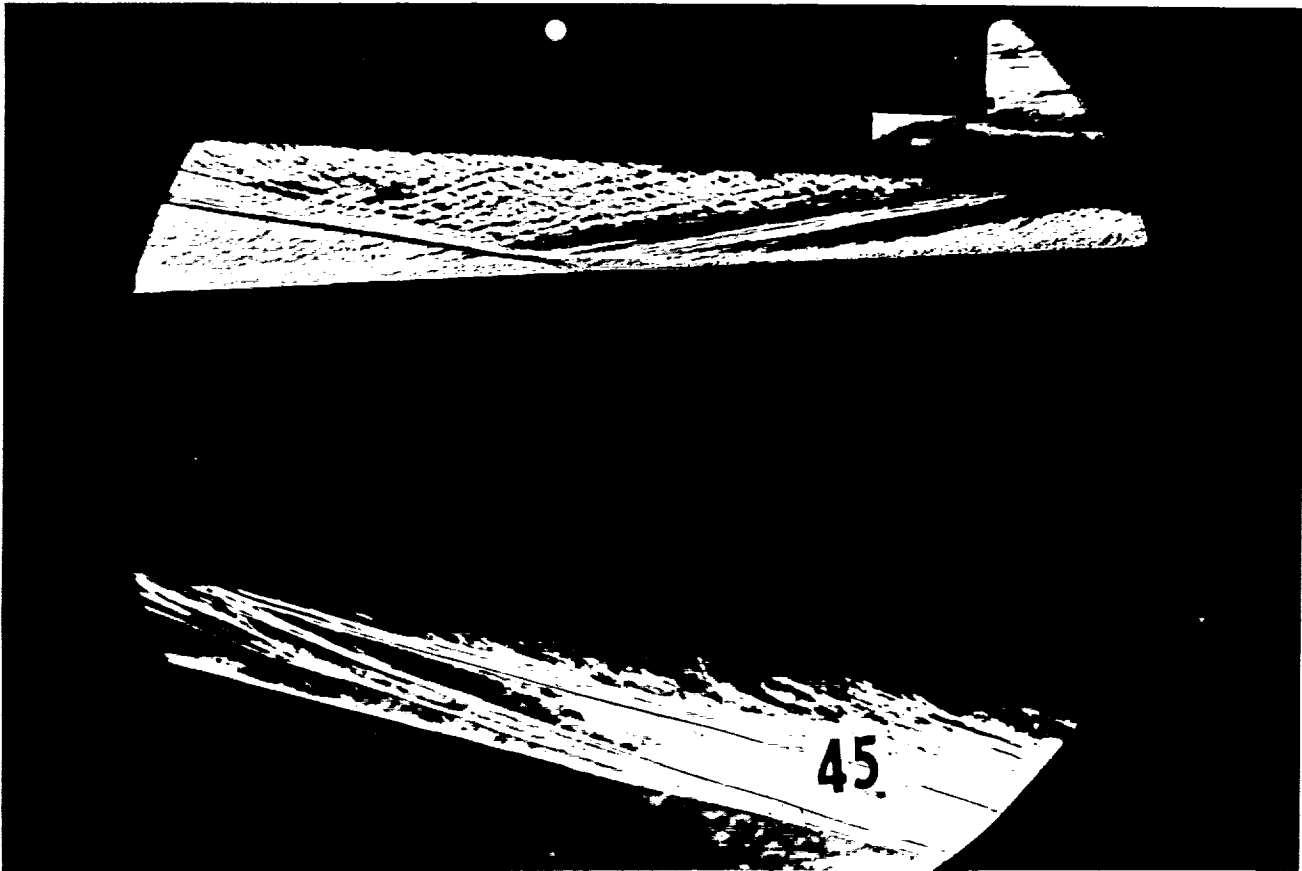
PRESSURE vs Gauge Position
Run 43



Test Conditions for Run 44 :

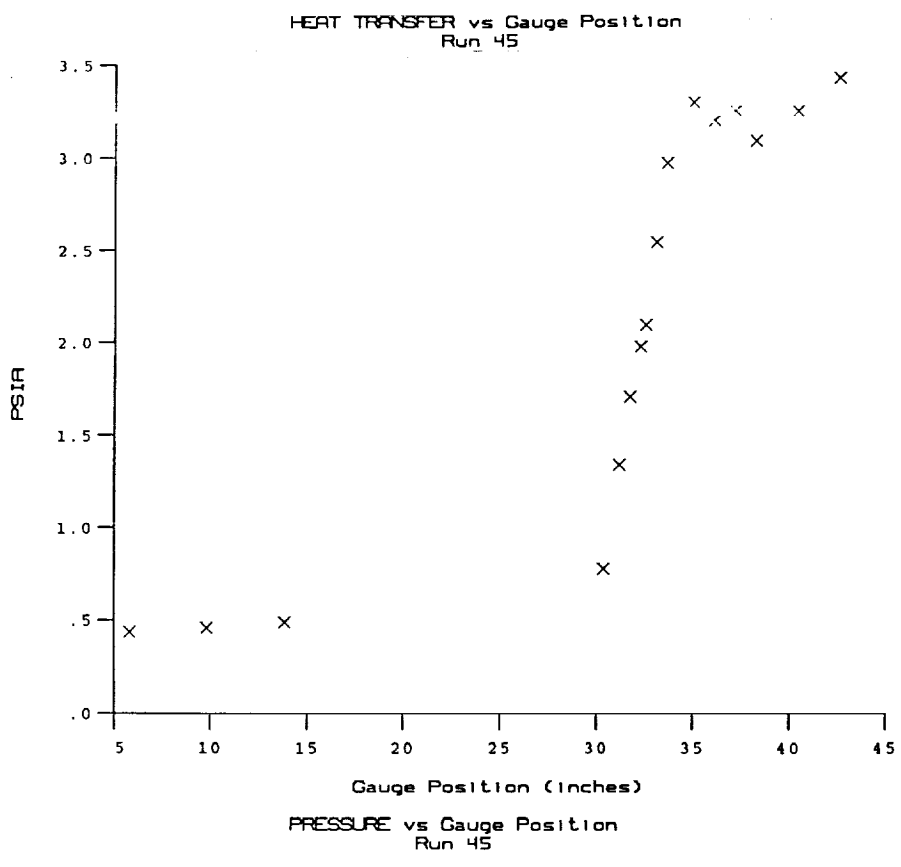
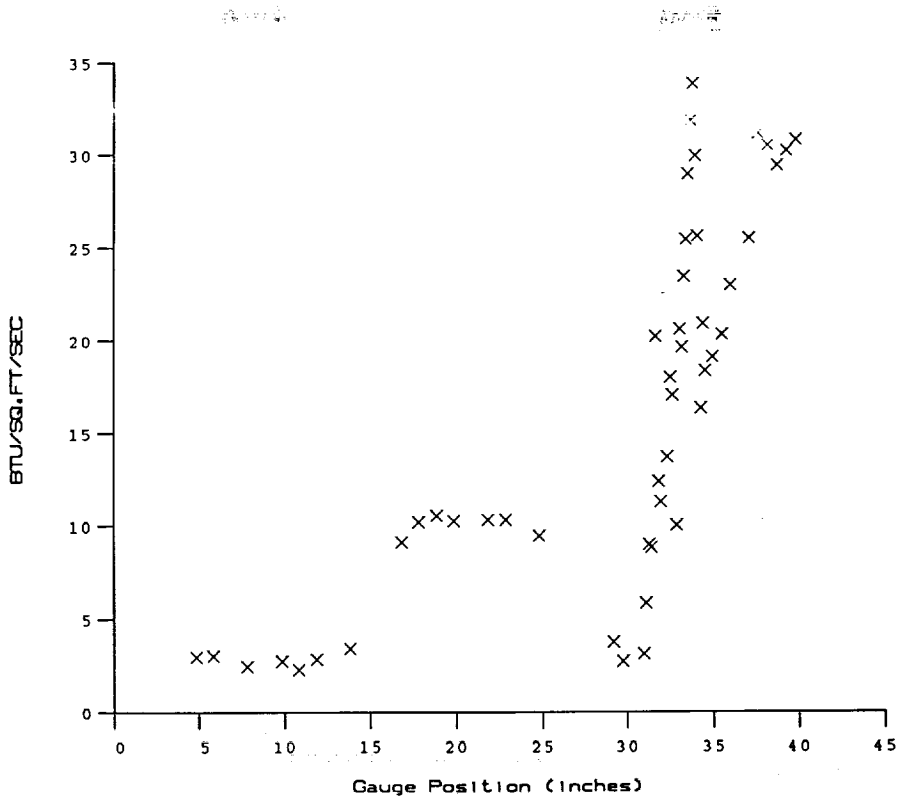
Po	= 4.087E+03 PSIA	Reservoir Total Pressure
Ho	= 1.522E+07 (Ft/sec) ²	Reservoir Total Enthalpy
To	= 2.347E+03 degR	Reservoir Total Temperature
M	= 7.855E+00	Freestream Mach Number
U	= 5.310E+03 Ft/sec	Freestream Velocity
T	= 1.900E+02 degR	Freestream Temperature
P	= 4.668E-01 PSIA	Freestream Static Pressure
Rho	= 2.062E-04 Slugs/Ft ³	Freestream Density
Mu	= 1.582E-07 Slugs/Ft-sec	Freestream Viscosity
Re	= 6.918E+06 1/Ft	Freestream Reynolds Number
Po'	= 3.731E+01 PSIA	Pitot Pressure
Q	= 2.018E+01 PSIA	Dynamic Pressure (Rho U ² /288)
Mi	= 2.995E+00	Shock Tube Incident Shock Mach Number
TW	= 5.300E+02 degR	Wall Temperature (Test Gas = Air)
Hw	= 3.183E+06 (Ft/sec) ²	Wall Enthalpy (Cp Tw)
CPf	= 4.955E-02 1/PSIA	Pressure to CP factor (1/Q)
CHf	= 5.903E-05 Ft ² -s/BTU	Heat Rate to CH factor (778/(Rho U (Ho-Hw)))
QoFR	= 5.937E+01 BTU/Ft ² -s	Fay-Riddell Heat Transfer (.25' Diam Cylin.)





Test Conditions for Run 45 :

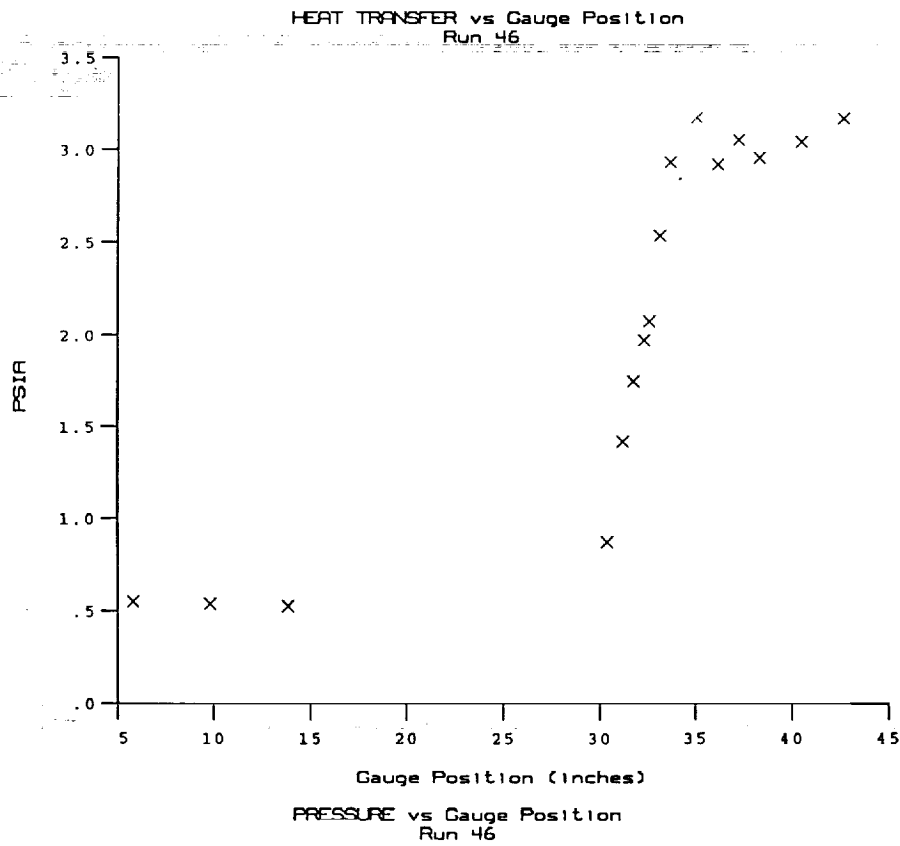
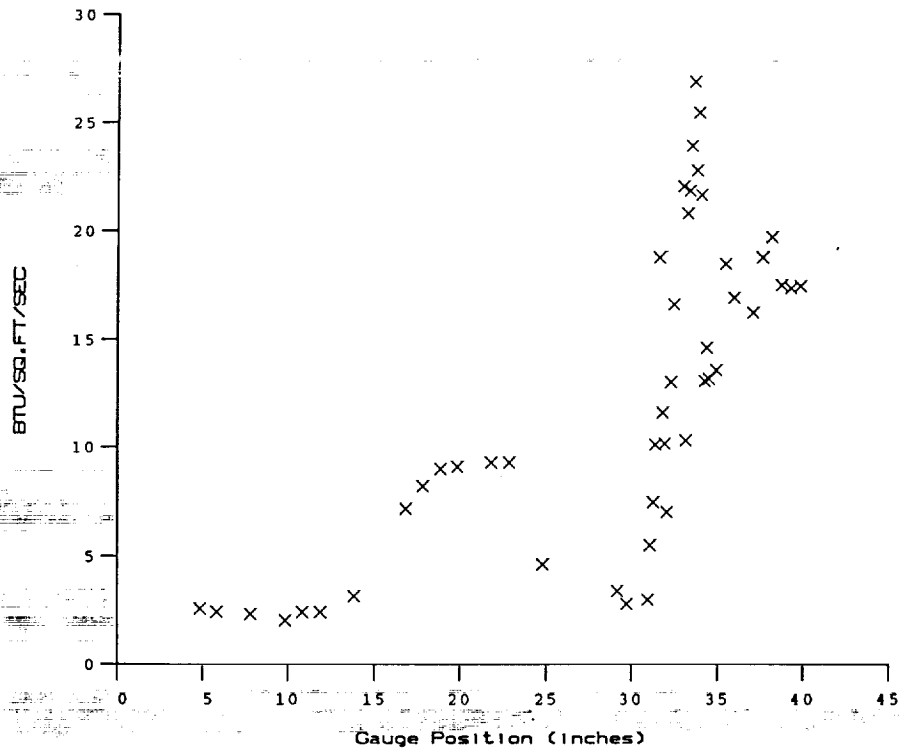
Po	- 4.179E+03 PSIA	Reservoir Total Pressure
Ho	- 1.535E+07 (Ft/sec) ²	Reservoir Total Enthalpy
To	- 2.364E+03 degR	Reservoir Total Temperature
M	- 7.856E+00	Freestream Mach Number
U	- 5.331E+03 Ft/sec	Freestream Velocity
T	- 1.915E+02 degR	Freestream Temperature
P	- 4.763E-01 PSIA	Freestream Static Pressure
Rho	- 2.087E-04 Slugs/Ft ³	Freestream Density
Mu	- 1.594E-07 Slugs/Ft-sec	Freestream Viscosity
Re	- 6.979E+06 1/Ft	Freestream Reynolds Number
Po'	- 3.808E+01 PSIA	Pitot Pressure
Q	- 2.060E+01 PSIA	Dynamic Pressure (Rho U ² /288)
Mi	- 3.005E+00	Shock Tube Incident Shock Mach Number
Tw	- 5.300E+02 degR	Wall Temperature (Test Gas = Air)
Hw	- 3.183E+06 (Ft/sec) ²	Wall Enthalpy (Cp Tw)
CPf	- 4.855E-02 1/PSIA	Pressure to CP factor (1/Q)
CHf	- 5.748E-05 Ft ² -s/BTU	Heat Rate to CH factor (778/(Rho U (Ho-Hw)))
QoFR	- 6.063E+01 BTU/Ft ² -s	Fay-Riddell Heat Transfer (.25' Diam Cylin.)

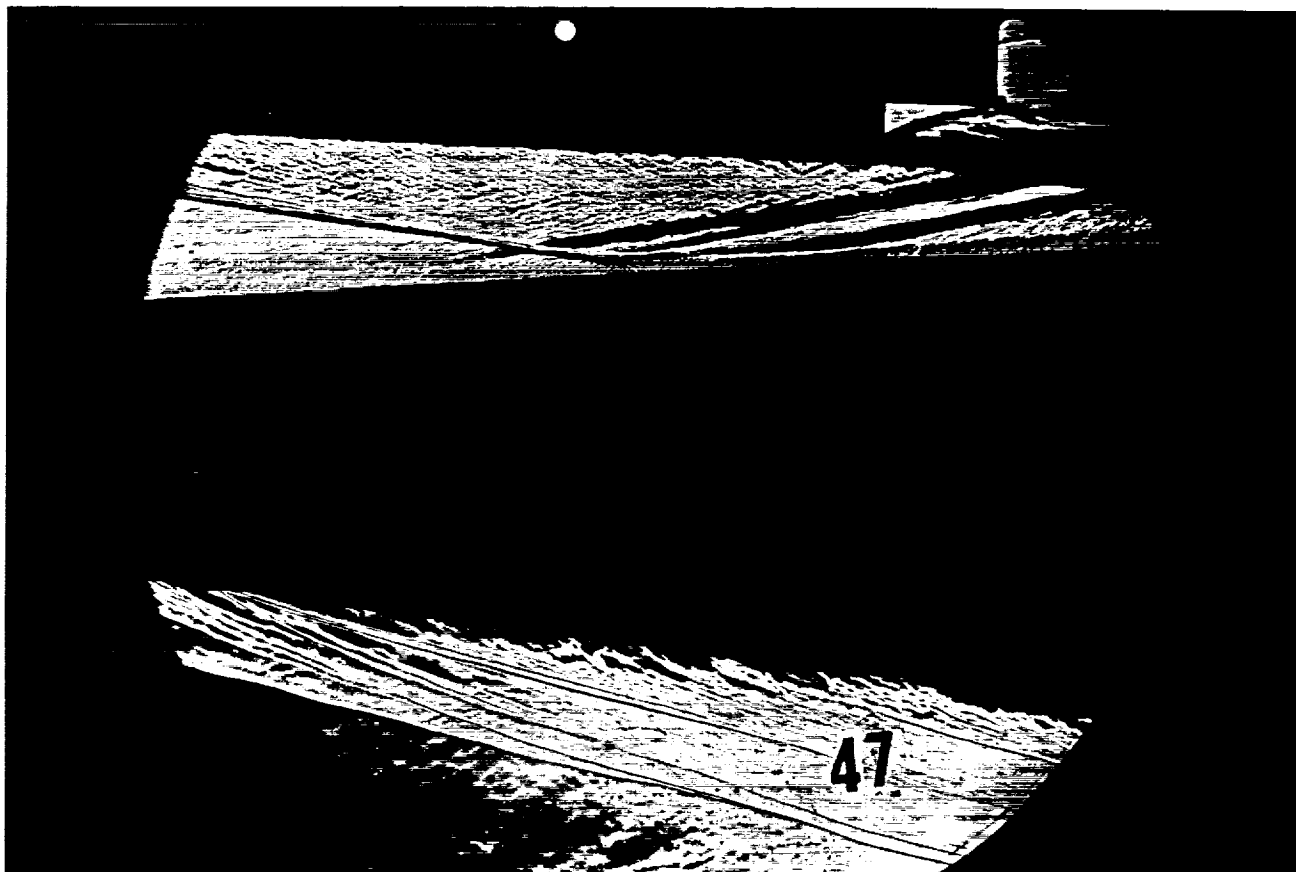


Test Conditions for Run 46 :

Po = 4.228E+03 PSIA
Ho = 1.479E+07 (Ft/sec)²
To = 2.288E+03 degR
M = 7.873E+00
U = 5.234E+03 Ft/sec
T = 1.838E+02 degR
P = 4.811E-01 PSIA
Rho = 2.196E-04 Slugs/Ft³
Mu = 1.532E-07 Slugs/Ft-sec
Re = 7.502E+06 1/Ft
Po' = 3.860E+01 PSIA
Q = 2.089E+01 PSIA
Mi = 2.949E+00
Tw = 5.300E+02 degR
Hw = 3.183E+06 (Ft/sec)²
CPf = 4.786E-02 1/PSIA
CHf = 5.832E-05 Ft²-s/BTU
QoFR = 5.808E+01 BTU/Ft²-s

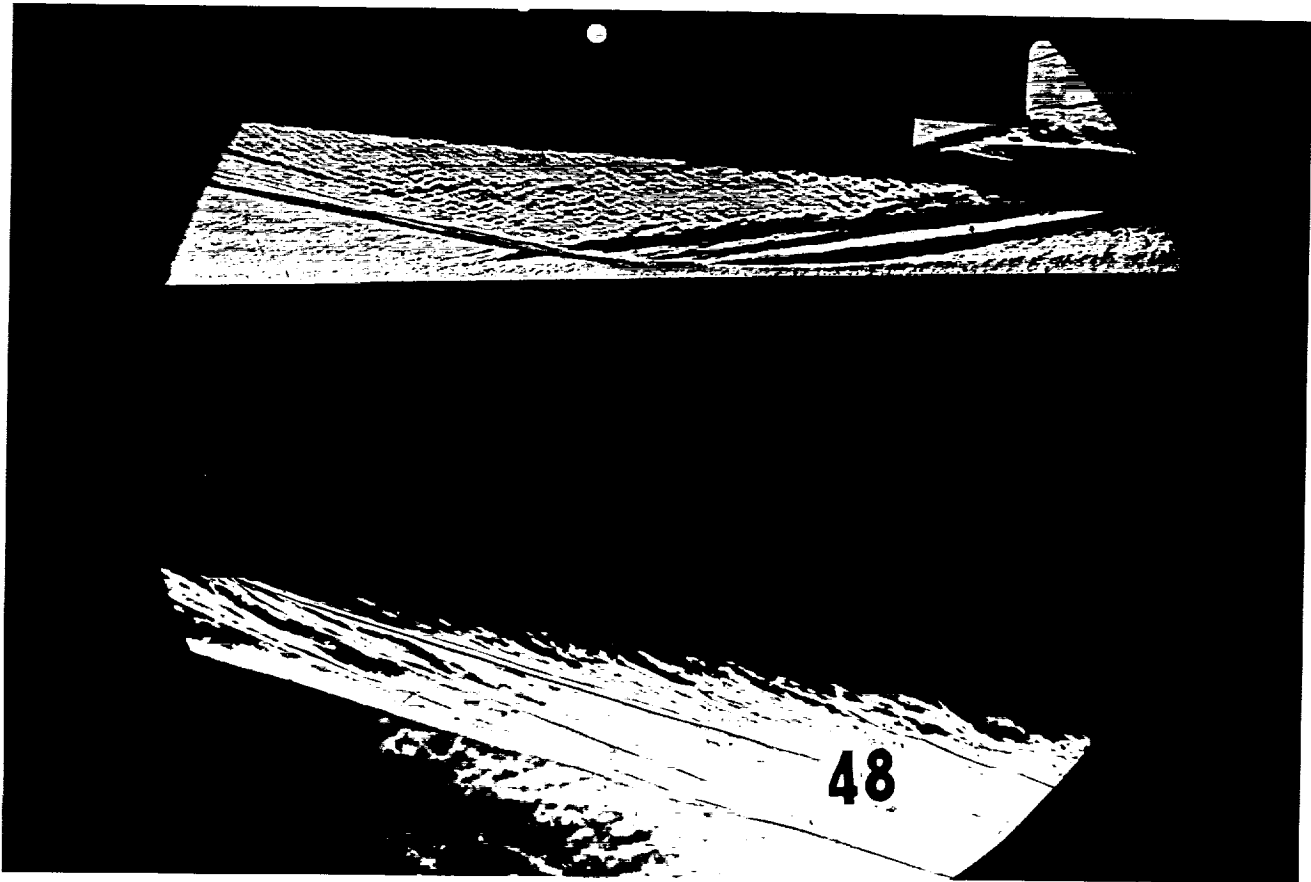
Reservoir Total Pressure
Reservoir Total Enthalpy
Reservoir Total Temperature
Freestream Mach Number
Freestream Velocity
Freestream Temperature
Freestream Static Pressure
Freestream Density
Freestream Viscosity
Freestream Reynolds Number
Pitot Pressure
Dynamic Pressure ($\rho U^2/288$)
Shock Tube Incident Shock Mach Number
Wall Temperature (Test Gas = Air)
Wall Enthalpy ($C_p T_w$)
Pressure to CP factor (1/Q)
Heat Rate to CH factor ($778/(\rho U (H_o - H_w))$)
Fay-Riddell Heat Transfer (.25' Diam Cylin.)





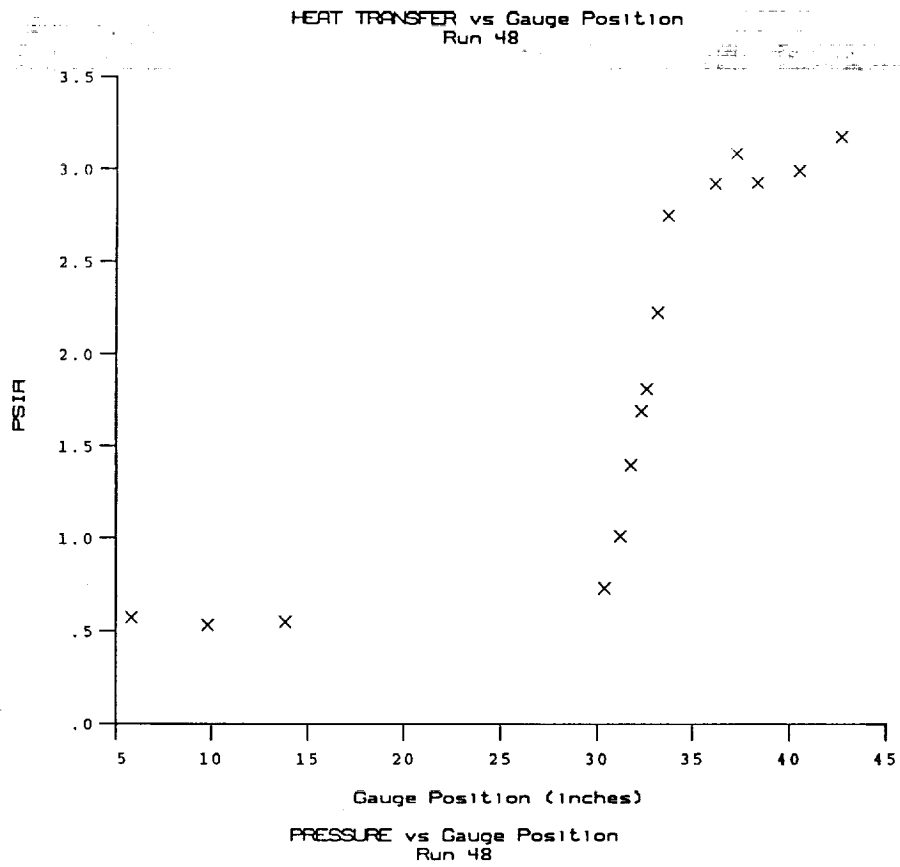
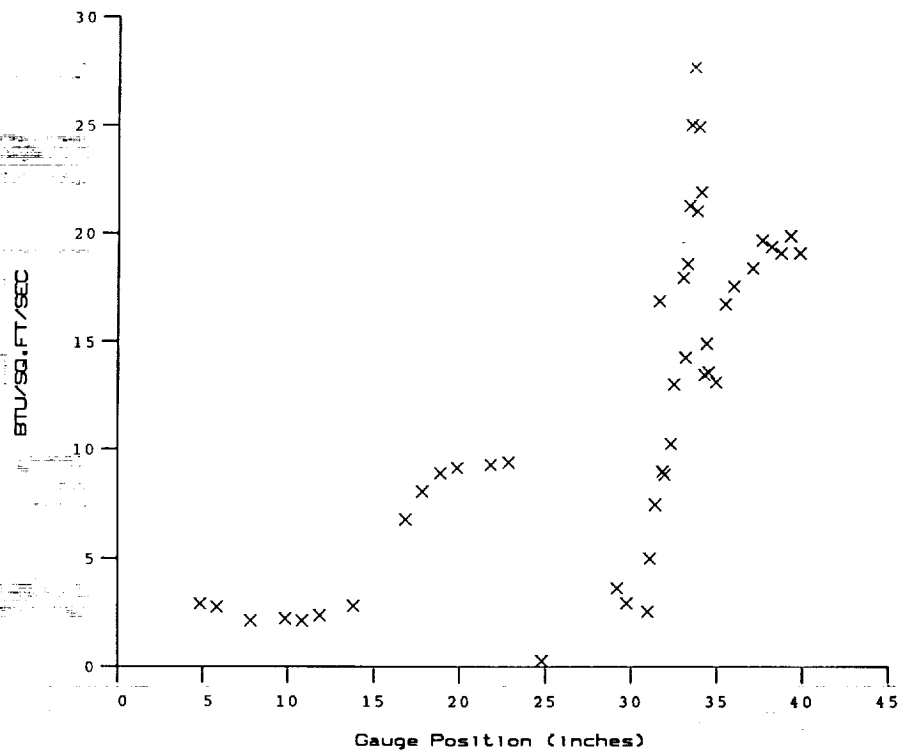
Test Conditions for Run 47 :

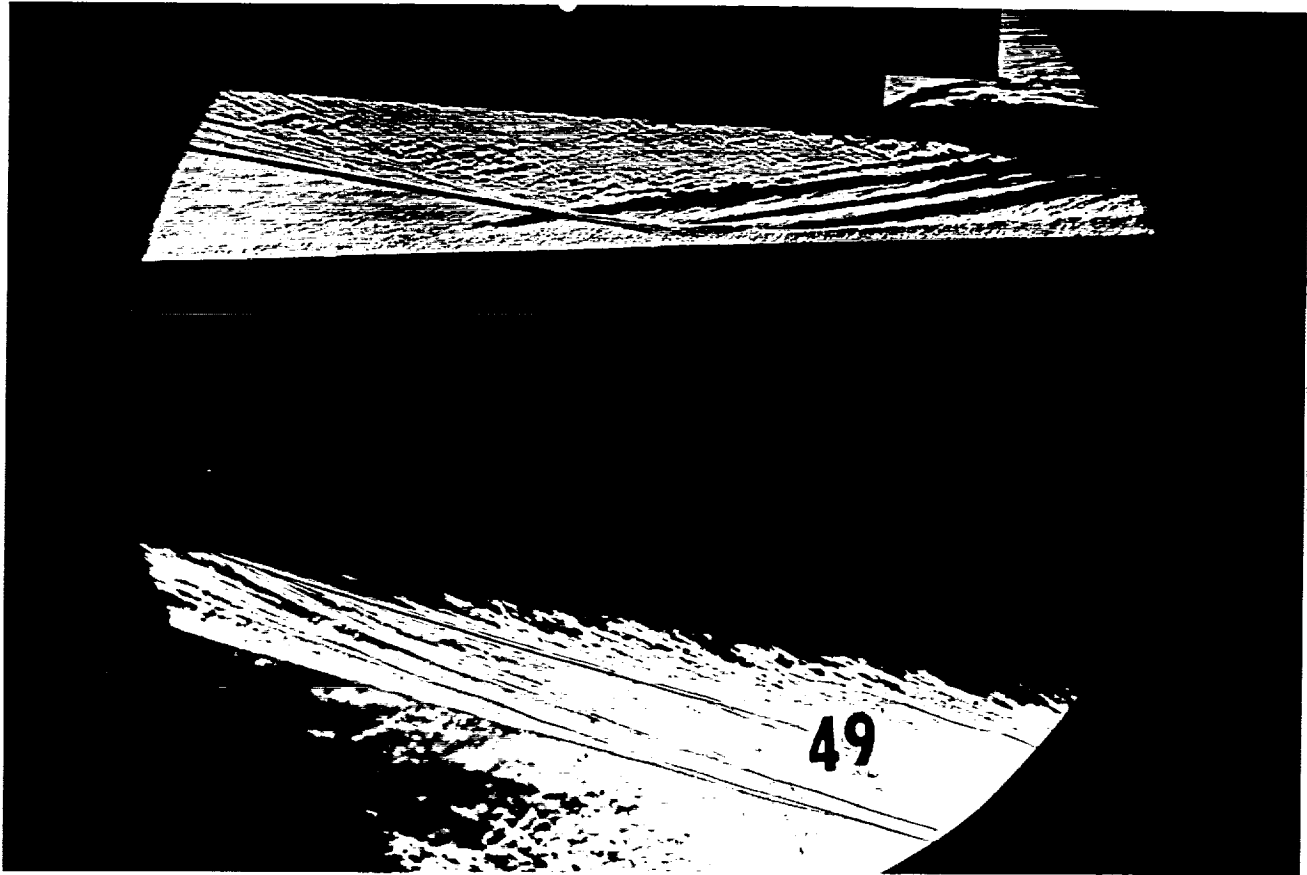
Po	- 4.109E+03 PSIA	Reservoir Total Pressure
Ho	- 1.488E+07 (Ft/sec) ²	Reservoir Total Enthalpy
To	- 2.300E+03 degR	Reservoir Total Temperature
M	- 7.866E+00	Freestream Mach Number
U	- 5.250E+03 Ft/sec	Freestream Velocity
T	- 1.852E+02 degR	Freestream Temperature
P	- 4.684E-01 PSIA	Freestream Static Pressure
Rho	- 2.123E-04 Slugs/Ft ³	Freestream Density
Mu	- 1.544E-07 Slugs/Ft-sec	Freestream Viscosity
Re	- 7.219E+06 1/Ft	Freestream Reynolds Number
Po'	- 3.753E+01 PSIA	Pitot Pressure
Q	- 2.031E+01 PSIA	Dynamic Pressure (Rho U ² /288)
Mi	- 2.955E+00	Shock Tube Incident Shock Mach Number
Tw	- 5.300E+02 degR	Wall Temperature (Test Gas = Air)
Hw	- 3.183E+06 (Ft/sec) ²	Wall Enthalpy (Cp Tw)
CPf	- 4.924E-02 1/PSIA	Pressure to CP factor (1/Q)
CHf	- 5.971E-05 Ft ² -s/BTU	Heat Rate to CH factor (778/(Rho U (Ho-Hw)))
QoFR	- 5.774E+01 BTU/Ft ² -s	Fay-Riddell Heat Transfer (.25' Diam Cylin.)



Test Conditions for Run 48 :

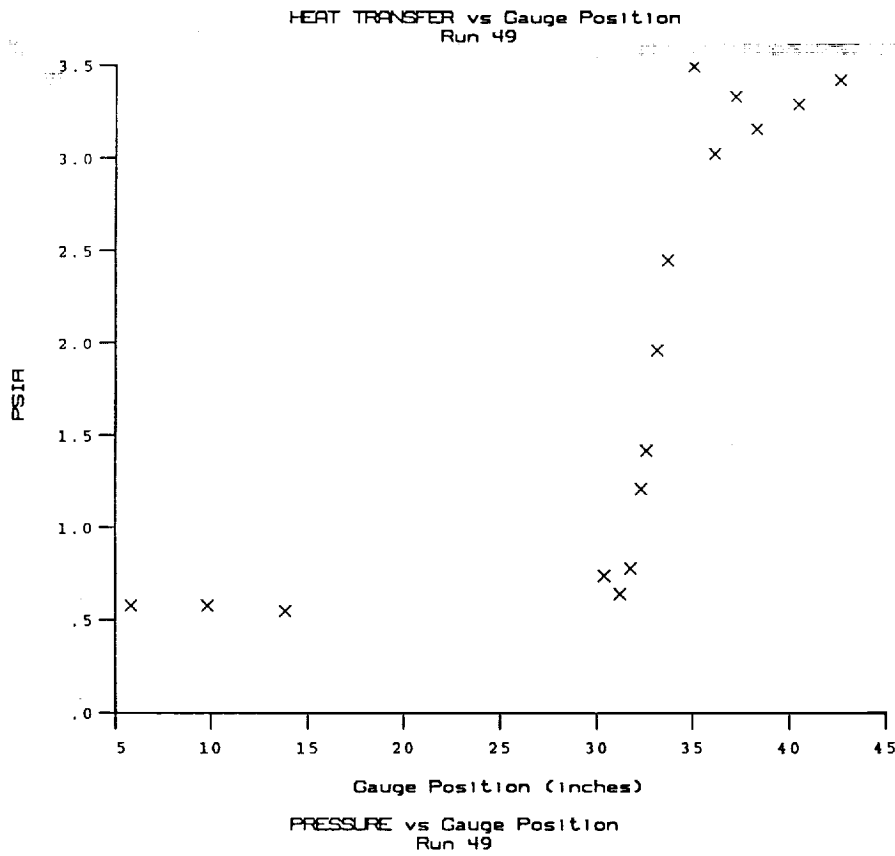
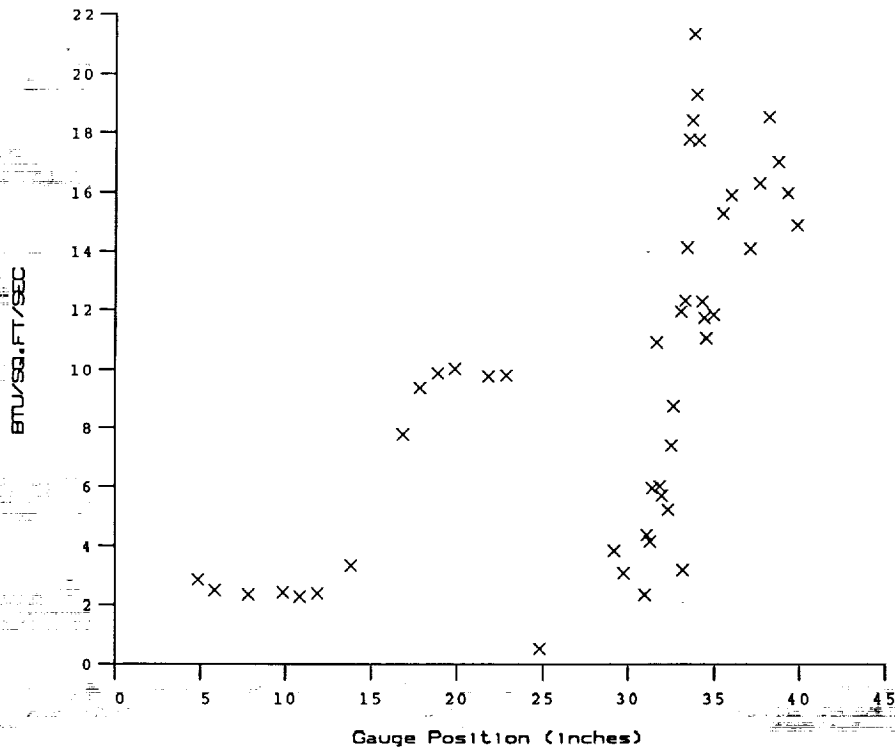
Po	= 4.213E+03 PSIA	Reservoir Total Pressure
Ho	= 1.528E+07 (Ft/sec) ²	Reservoir Total Enthalpy
To	= 2.356E+03 degR	Reservoir Total Temperature
M	= 7.860E+00	Freestream Mach Number
U	= 5.320E+03 Ft/sec	Freestream Velocity
T	= 1.905E+02 degR	Freestream Temperature
P	= 4.791E-01 PSIA	Freestream Static Pressure
Rho	= 2.111E-04 Slugs/Ft ³	Freestream Density
Mu	= 1.586E-07 Slugs/Ft-sec	Freestream Viscosity
Re	= 7.080E+06 1/Ft	Freestream Reynolds Number
Po'	= 3.835E+01 PSIA	Pitot Pressure
Q	= 2.075E+01 PSIA	Dynamic Pressure ($\rho U^2/288$)
Mi	= 2.993E+00	Shock Tube Incident Shock Mach Number
Tw	= 5.300E+02 degR	Wall Temperature (Test Gas = Air)
Hw	= 3.183E+06 (Ft/sec) ²	Wall Enthalpy (Cp Tw)
CPf	= 4.820E-02 1/PSIA	Pressure to CP factor (1/Q)
CHf	= 5.726E-05 Ft ² -s/BTU	Heat Rate to CH factor ($778/(\rho U (Ho-Hw))$)
QoFR	= 6.050E+01 BTU/Ft ² -s	Fay-Riddell Heat Transfer (.25' Diam Cylin.)

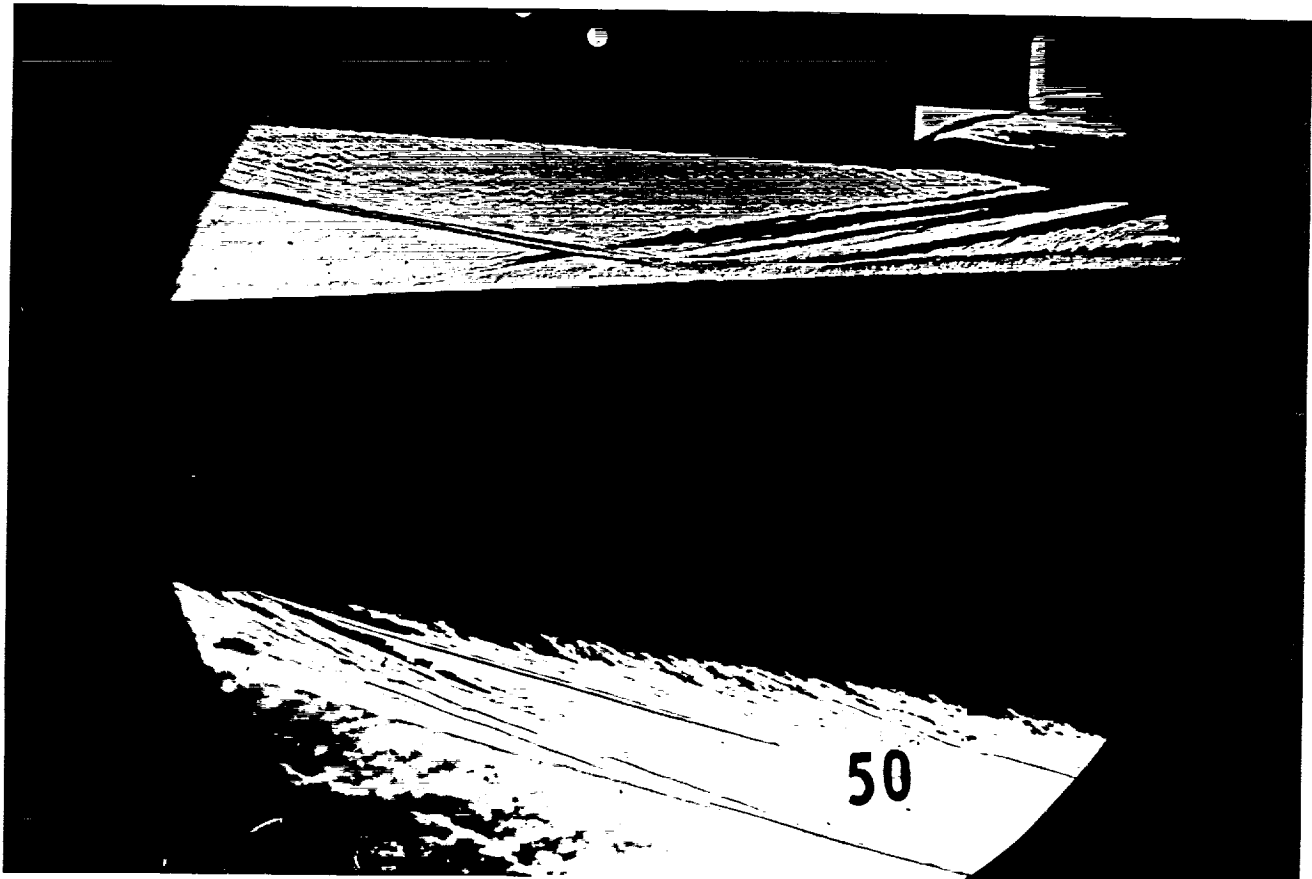




Test Conditions for Run 49 :

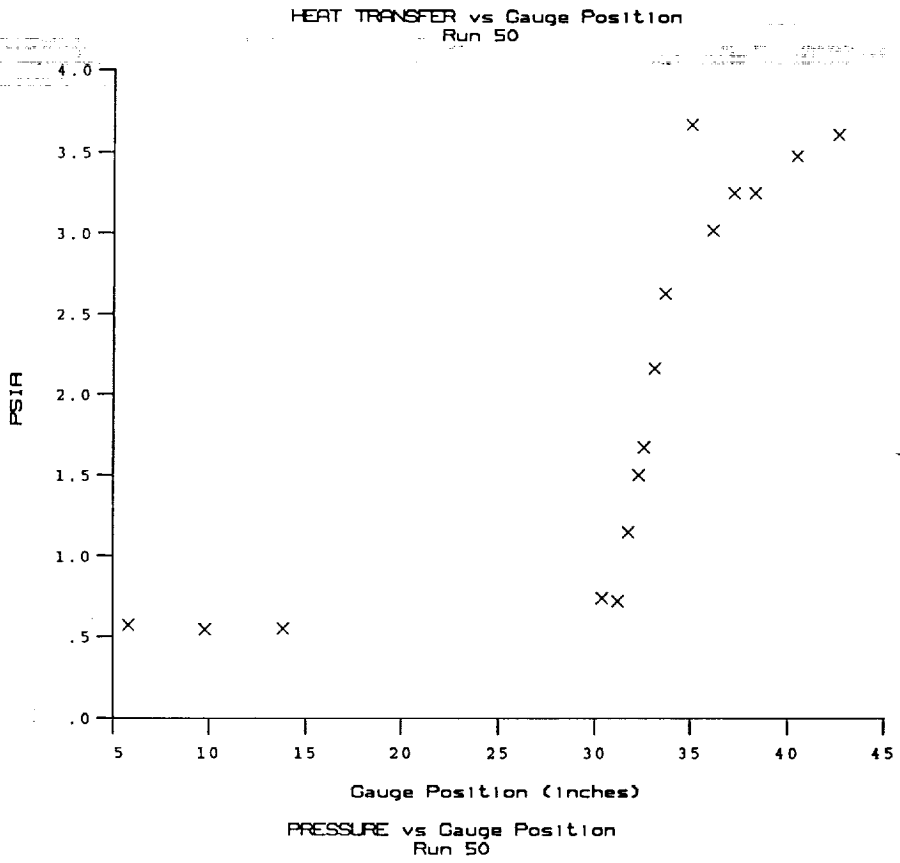
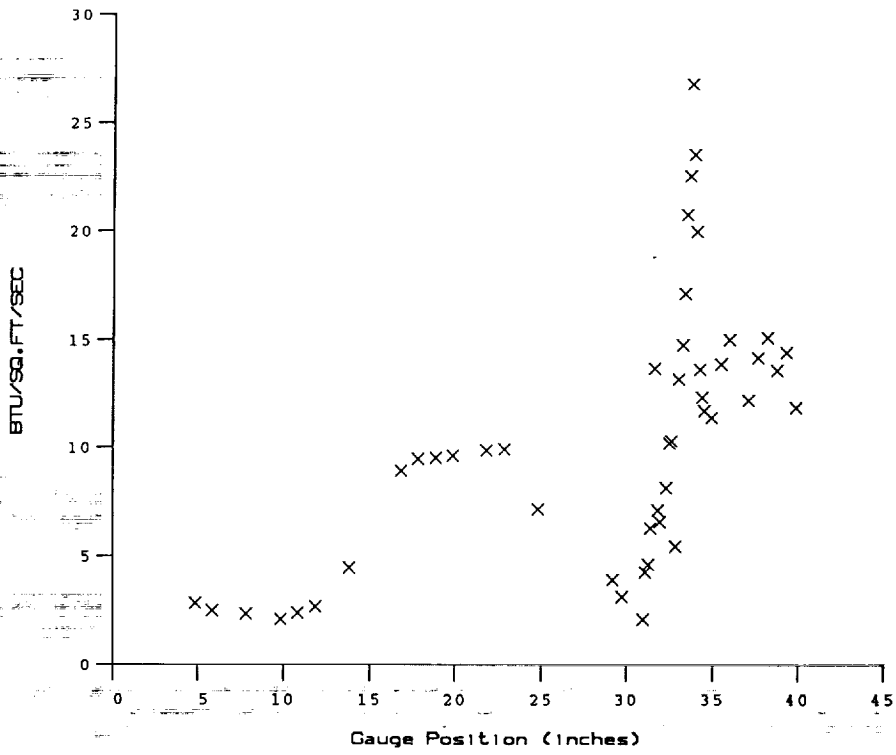
Po	= 4.442E+03 PSIA	Reservoir Total Pressure
Ho	= 1.496E+07 (Ft/sec) ²	Reservoir Total Enthalpy
To	= 2.310E+03 degR	Reservoir Total Temperature
M	= 7.873E+00	Freestream Mach Number
U	= 5.264E+03 Ft/sec	Freestream Velocity
T	= 1.859E+02 degR	Freestream Temperature
P	= 5.047E-01 PSIA	Freestream Static Pressure
Rho	= 2.278E-04 Slugs/Ft ³	Freestream Density
Mu	= 1.549E-07 Slugs/Ft-sec	Freestream Viscosity
Re	= 7.740E+06 1/Ft	Freestream Reynolds Number
Po'	= 4.051E+01 PSIA	Pitot Pressure
Q	= 2.192E+01 PSIA	Dynamic Pressure (Rho U ² /288)
Mi	= 2.980E+00	Shock Tube Incident Shock Mach Number
Tw	= 5.300E+02 degR	Wall Temperature (Test Gas = Air)
Hw	= 3.183E+06 (Ft/sec) ²	Wall Enthalpy (Cp Tw)
CPf	= 4.562E-02 1/PSIA	Pressure to CP factor (1/Q)
CHf	= 5.509E-05 Ft ² -s/BTU	Heat Rate to CH factor (778/(Rho U (Ho-Hw)))
QoFR	= 6.043E+01 BTU/Ft ² -s	Fay-Riddell Heat Transfer (.25' Diam Cylin.)

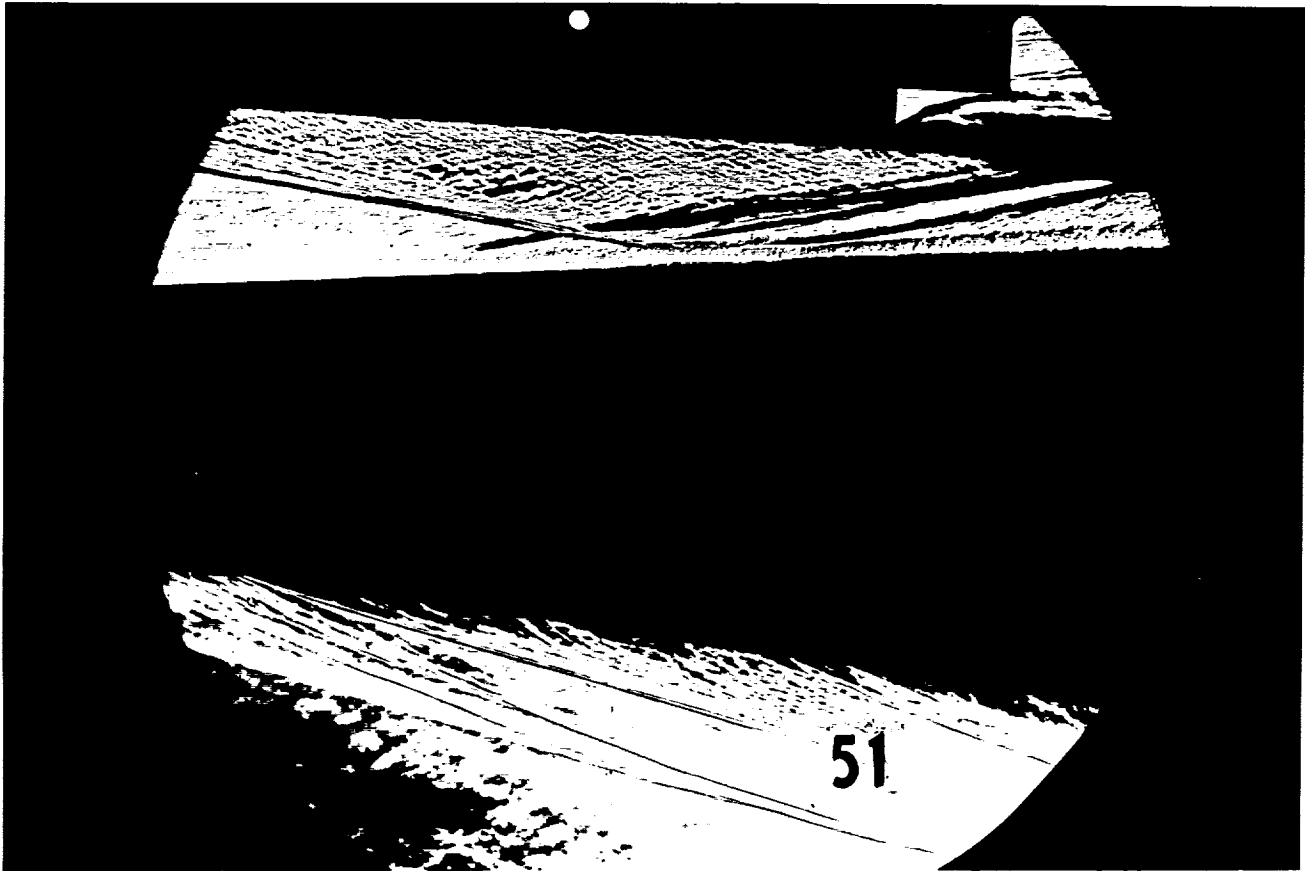




Test Conditions for Run 50 :

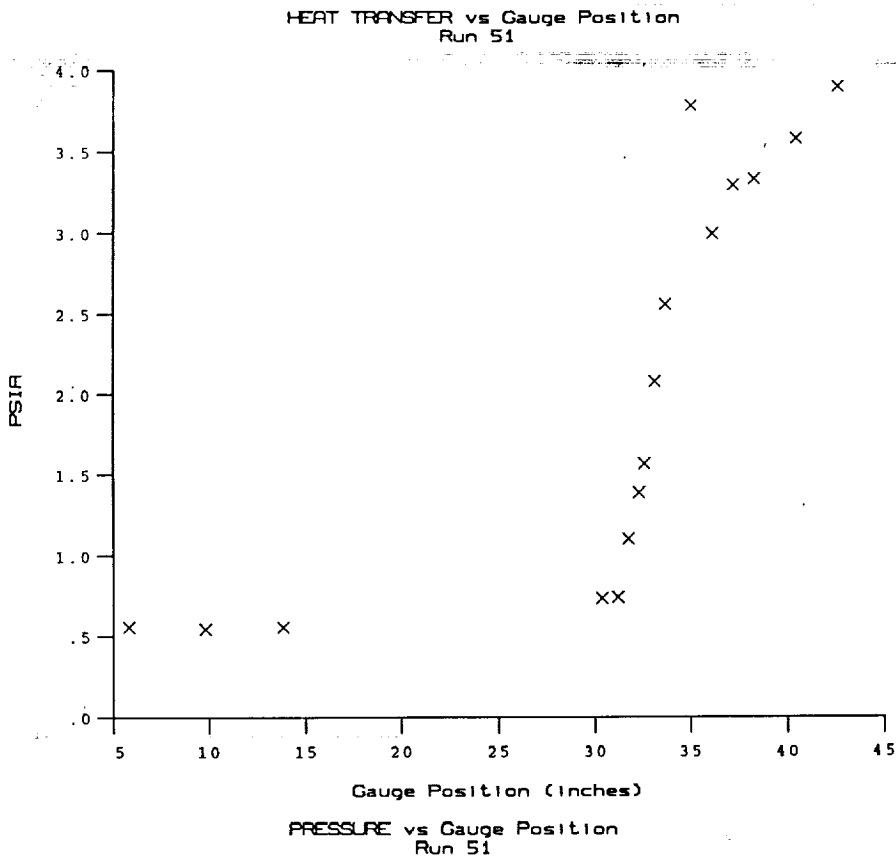
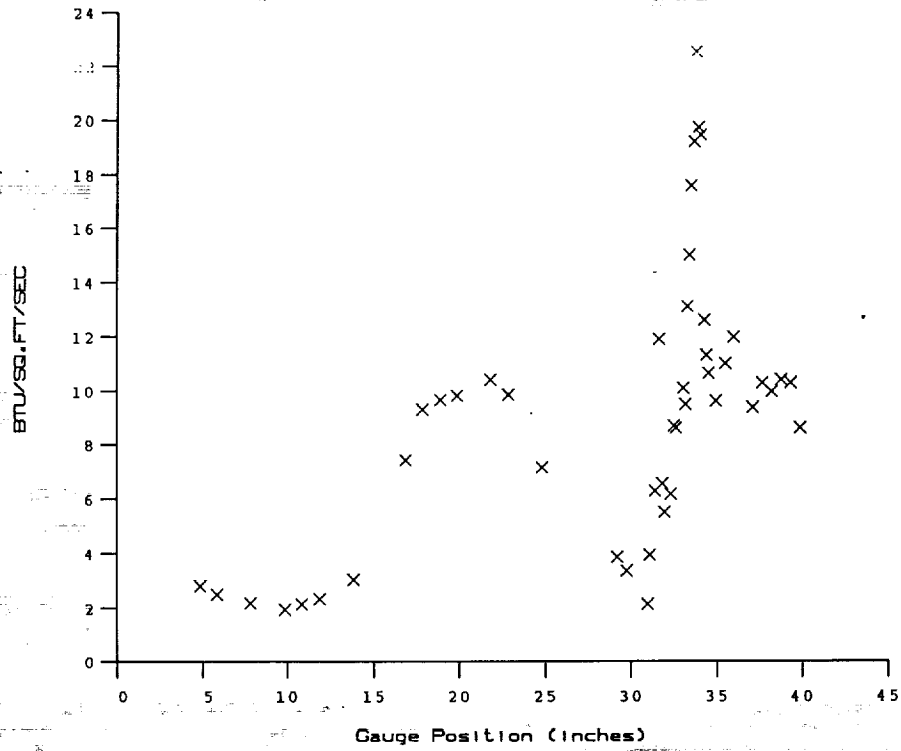
Po	= 4.528E+03 PSIA	Reservoir Total Pressure
Ho	= 1.562E+07 (Ft/sec) ²	Reservoir Total Enthalpy
To	= 2.400E+03 degR	Reservoir Total Temperature
M	= 7.861E+00	Freestream Mach Number
U	= 5.378E+03 Ft/sec	Freestream Velocity
T	= 1.946E+02 degR	Freestream Temperature
P	= 5.131E-01 PSIA	Freestream Static Pressure
Rho	= 2.212E-04 Slugs/Ft ³	Freestream Density
Mu	= 1.619E-07 Slugs/Ft-sec	Freestream Viscosity
Re	= 7.348E+06 1/Ft	Freestream Reynolds Number
Po'	= 4.108E+01 PSIA	Pitot Pressure
Q	= 2.222E+01 PSIA	Dynamic Pressure ($\rho U^2/288$)
Mi	= 3.041E+00	Shock Tube Incident Shock Mach Number
Tw	= 5.300E+02 degR	Wall Temperature (Test Gas = Air)
Hw	= 3.183E+06 (Ft/sec) ²	Wall Enthalpy ($C_p T_w$)
CPf	= 4.501E-02 1/PSIA	Pressure to CP factor (1/Q)
CHf	= 5.259E-05 Ft ² -s/BTU	Heat Rate to CH factor ($778/(\rho U (H_o - H_w))$)
QoFR	= 6.445E+01 BTU/Ft ² -s	Fay-Riddell Heat Transfer (.25' Diam Cylin.)

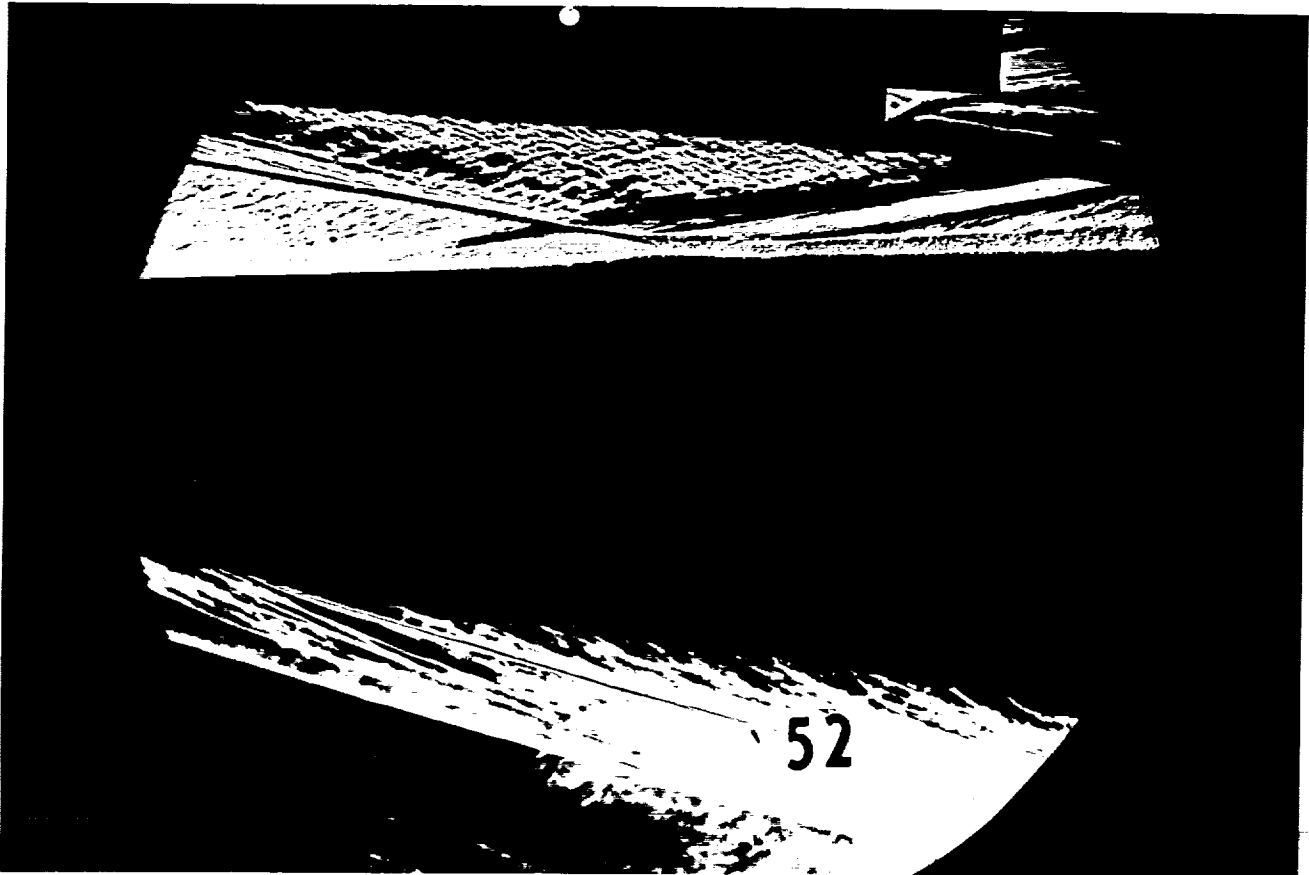




Test Conditions for Run 51 :

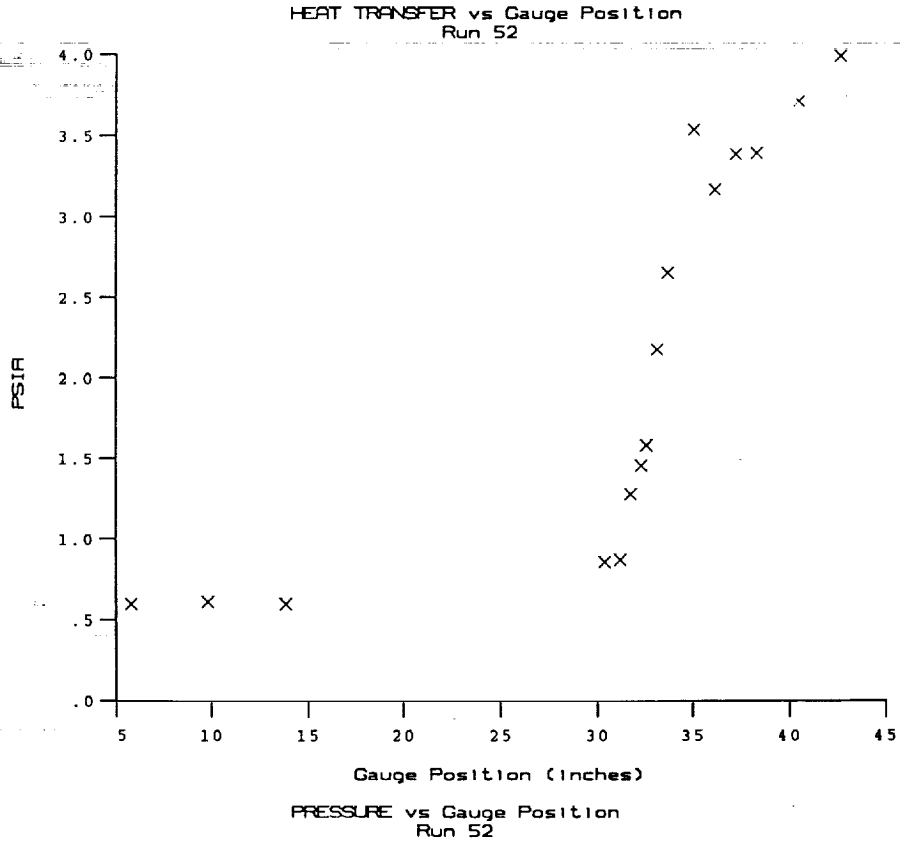
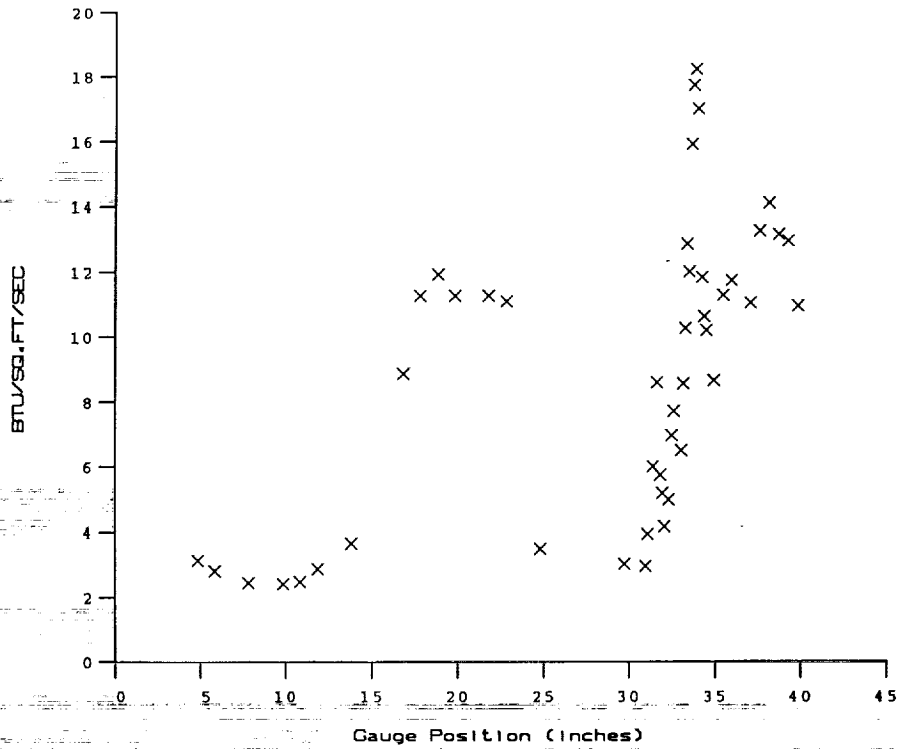
Po	- 4.399E+03 PSIA	Reservoir Total Pressure
Ho	- 1.591E+07 (Ft/sec) ²	Reservoir Total Enthalpy
To	- 2.441E+03 degR	Reservoir Total Temperature
M	- 7.851E+00	Freestream Mach Number
U	- 5.429E+03 Ft/sec	Freestream Velocity
T	- 1.988E+02 degR	Freestream Temperature
P	- 4.985E-01 PSIA	Freestream Static Pressure
Rho	- 2.105E-04 Slugs/Ft ³	Freestream Density
Mu	- 1.652E-07 Slugs/Ft-sec	Freestream Viscosity
Re	- 6.915E+06 1/Ft	Freestream Reynolds Number
Po'	- 3.983E+01 PSIA	Pitot Pressure
Q	- 2.153E+01 PSIA	Dynamic Pressure ($\rho U^2/288$)
Mi	- 3.055E+00	Shock Tube Incident Shock Mach Number
Tw	- 5.300E+02 degR	Wall Temperature (Test Gas = Air)
Hw	- 3.183E+06 (Ft/sec) ²	Wall Enthalpy ($C_p T_w$)
CPf	- 4.644E-02 1/PSIA	Pressure to CP factor (1/Q)
CHf	- 5.349E-05 Ft ² -s/BTU	Heat Rate to CH factor ($778/(\rho U (H_o - H_w))$)
QoFR	- 6.507E+01 BTU/Ft ² -s	Fay-Riddell Heat Transfer (.25' Diam Cylin.)

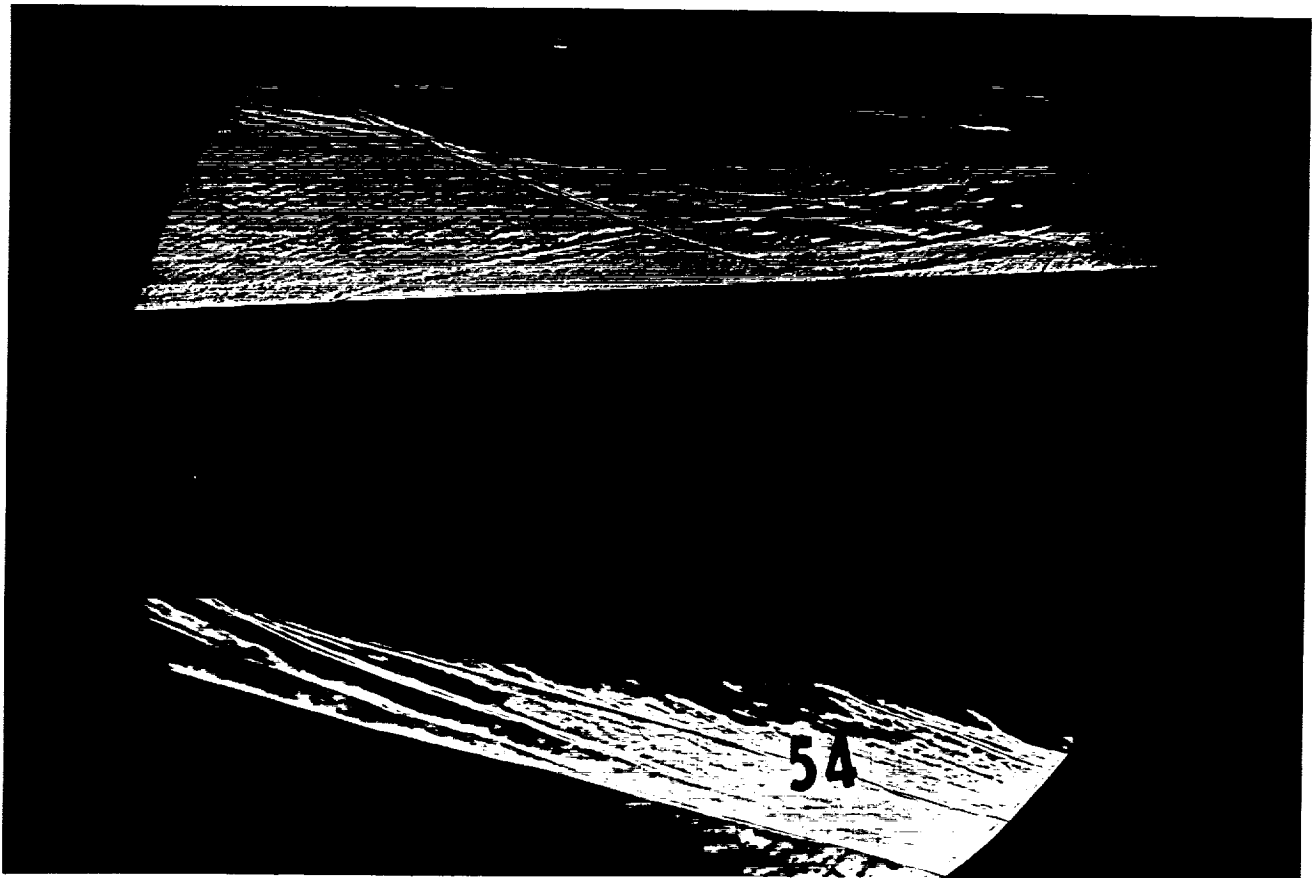




Test Conditions for Run 52 :

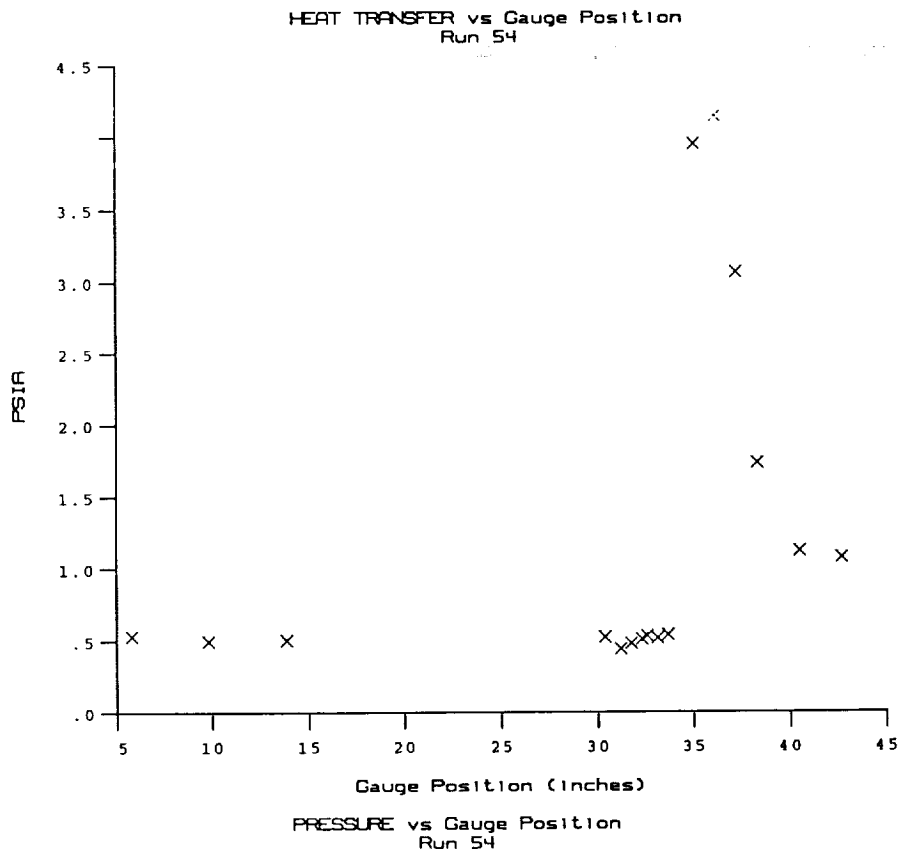
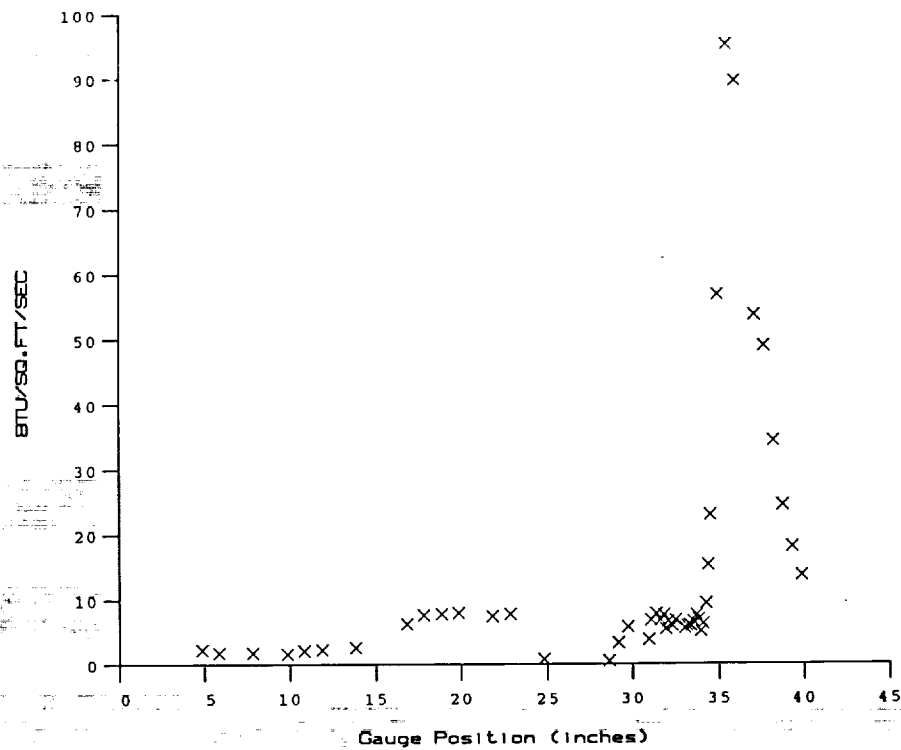
Po	= 4.652E+03 PSIA	Reservoir Total Pressure
Ho	= 1.550E+07 (Ft/sec) ²	Reservoir Total Enthalpy
To	= 2.384E+03 degR	Reservoir Total Temperature
M	= 7.868E+00	Freestream Mach Number
U	= 5.359E+03 Ft/sec	Freestream Velocity
T	= 1.929E+02 degR	Freestream Temperature
P	= 5.262E-01 PSIA	Freestream Static Pressure
Rho	= 2.289E-04 Slugs/Ft ³	Freestream Density
Mu	= 1.605E-07 Slugs/Ft-sec	Freestream Viscosity
Re	= 7.641E+06 1/Ft	Freestream Reynolds Number
Po'	= 4.220E+01 PSIA	Pitot Pressure
Q	= 2.282E+01 PSIA	Dynamic Pressure ($\rho U^2/288$)
Mi	= 3.036E+00	Shock Tube Incident Shock Mach Number
Tw	= 5.300E+02 degR	Wall Temperature (Test Gas = Air)
Hw	= 3.183E+06 (Ft/sec) ²	Wall Enthalpy ($C_p T_w$)
CPf	= 4.381E-02 1/PSIA	Pressure to CP factor ($1/Q$)
CHf	= 5.149E-05 Ft ² -s/BTU	Heat Rate to CH factor ($778/(\rho U (H_o - H_w))$)
QoFR	= 6.468E+01 BTU/Ft ² -s	Fay-Riddell Heat Transfer (.25' Diam Cylin.)

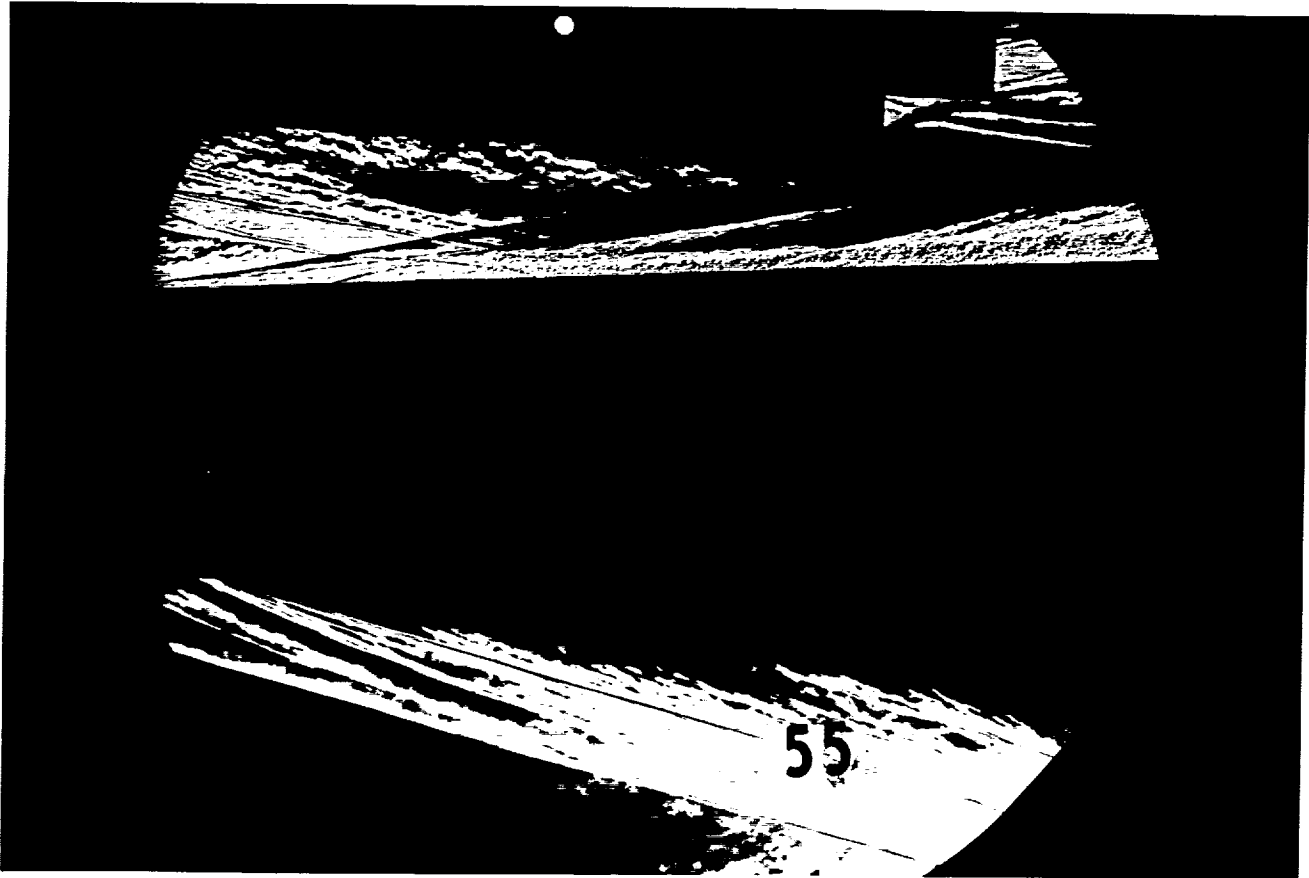




Test Conditions for Run 54 :

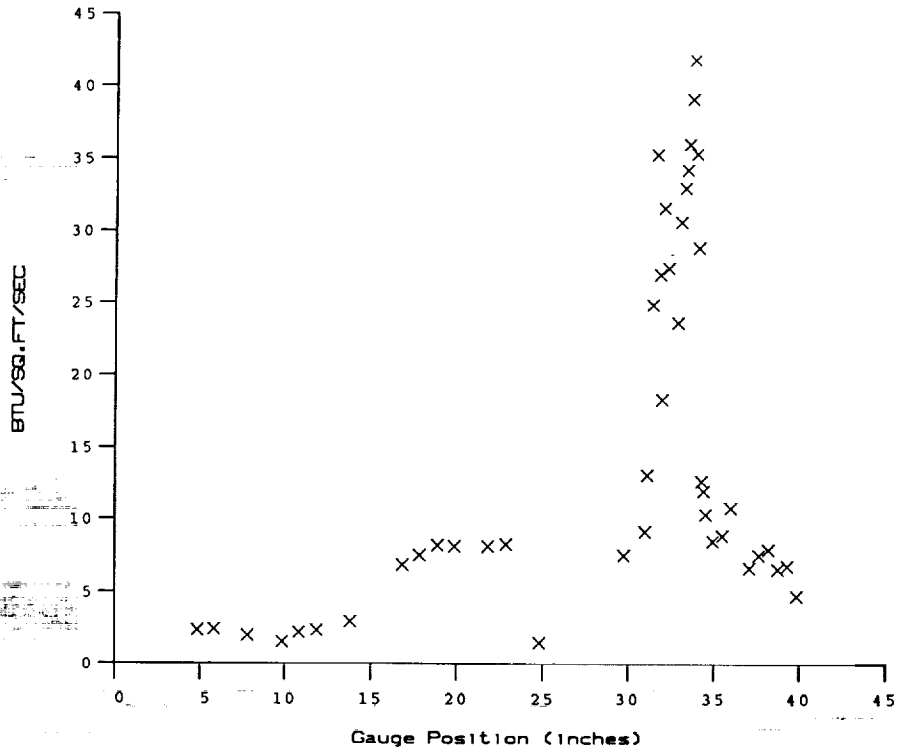
Po	= 3.934E+03 PSIA	Reservoir Total Pressure
Ho	= 1.418E+07 (Ft/sec) ²	Reservoir Total Enthalpy
To	= 2.205E+03 degR	Reservoir Total Temperature
M	= 7.879E+00	Freestream Mach Number
U	= 5.126E+03 Ft/sec	Freestream Velocity
T	= 1.760E+02 degR	Freestream Temperature
P	= 4.492E-01 PSIA	Freestream Static Pressure
Rho	= 2.142E-04 Slugs/Ft ³	Freestream Density
Mu	= 1.469E-07 Slugs/Ft-sec	Freestream Viscosity
Re	= 7.473E+06 1/Ft	Freestream Reynolds Number
Po'	= 3.609E+01 PSIA	Pitot Pressure
Q	= 1.954E+01 PSIA	Dynamic Pressure (Rho U ² /288)
Mi	= 2.878E+00	Shock Tube Incident Shock Mach Number
Tw	= 5.300E+02 degR	Wall Temperature (Test Gas - Air)
Hw	= 3.183E+06 (Ft/sec) ²	Wall Enthalpy (Cp Tw)
CPf	= 5.117E-02 1/PSIA	Pressure to CP factor (1/Q)
CHf	= 6.443E-05 Ft ² -s/BTU	Heat Rate to CH factor (778/(Rho U (Ho-Hw))
QoFR	= 5.306E+01 BTU/Ft ² -s	Fay-Riddell Heat Transfer (.25' Diam Cylin.)



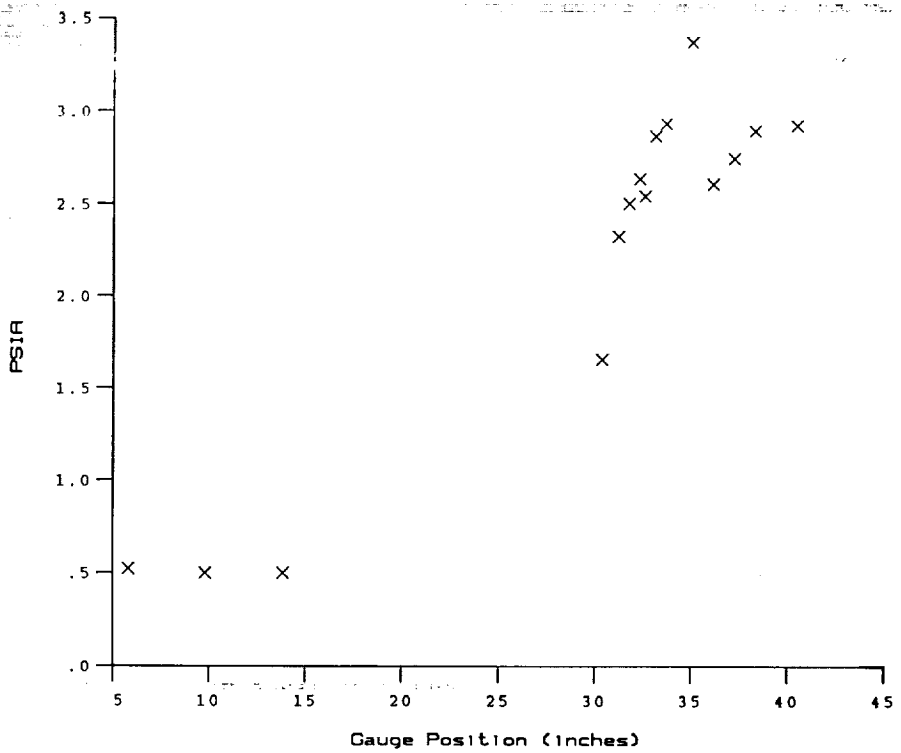


Test Conditions for Run 55 :

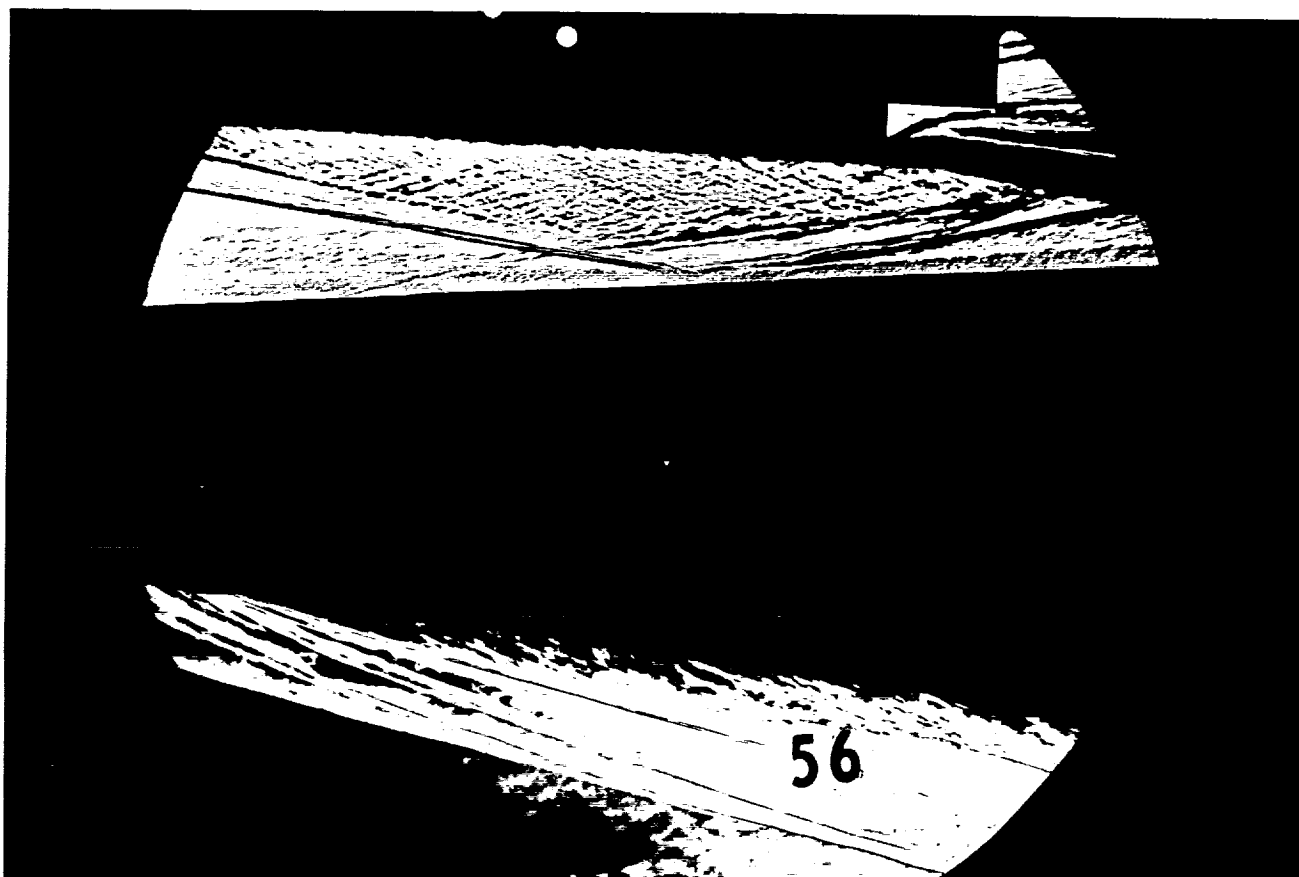
Po	= 3.891E+03 PSIA	Reservoir Total Pressure
Ho	= 1.452E+07 (Ft/sec) ²	Reservoir Total Enthalpy
To	= 2.252E+03 degR	Reservoir Total Temperature
M	= 7.868E+00	Freestream Mach Number
U	= 5.186E+03 Ft/sec	Freestream Velocity
T	= 1.806E+02 degR	Freestream Temperature
P	= 4.449E-01 PSIA	Freestream Static Pressure
Rho	= 2.067E-04 Slugs/Ft ³	Freestream Density
Mu	= 1.507E-07 Slugs/Ft-sec	Freestream Viscosity
Re	= 7.113E+06 1/Ft	Freestream Reynolds Number
Po'	= 3.565E+01 PSIA	Pitot Pressure
Q	= 1.930E+01 PSIA	Dynamic Pressure (Rho U ² /288)
Mi	= 2.914E+00	Shock Tube Incident Shock Mach Number
Tw	= 5.300E+02 degR	Wall Temperature (Test Gas = Air)
Hw	= 3.183E+06 (Ft/sec) ²	Wall Enthalpy (Cp Tw)
CPf	= 5.181E-02 1/PSIA	Pressure to CP factor (1/Q)
CHf	= 6.403E-05 Ft ² -s/BTU	Heat Rate to CH factor (778/(Rho U (Ho-Hw)))
QoFR	= 5.446E+01 BTU/Ft ² -s	Fay-Riddell Heat Transfer (.25' Diam Cylin.)



HEAT TRANSFER vs Gauge Position
Run 55

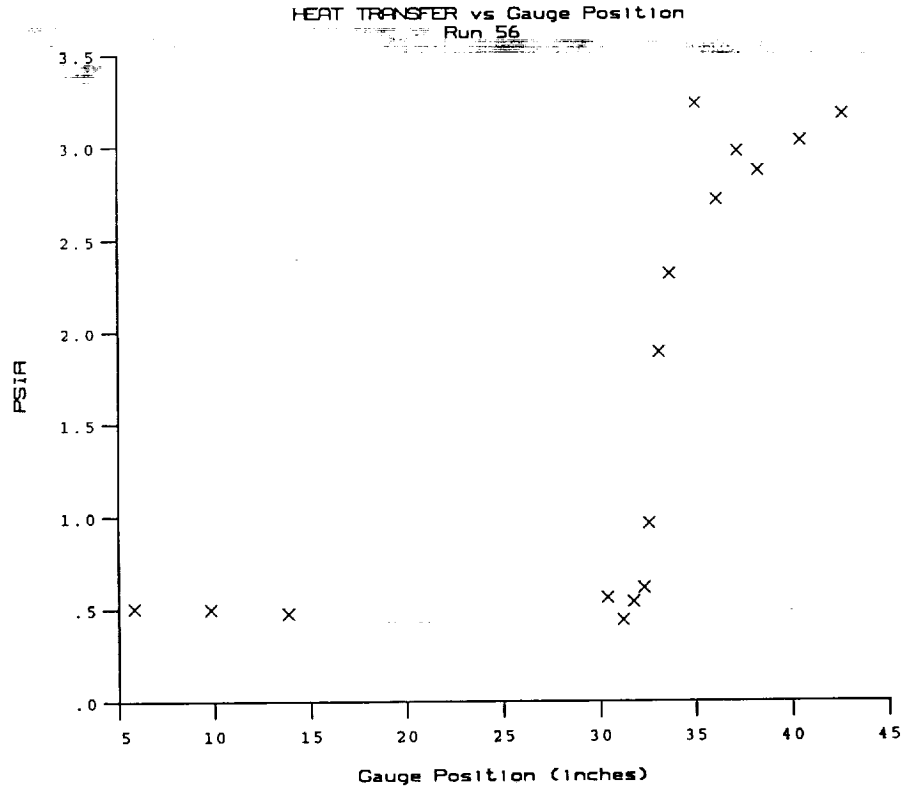
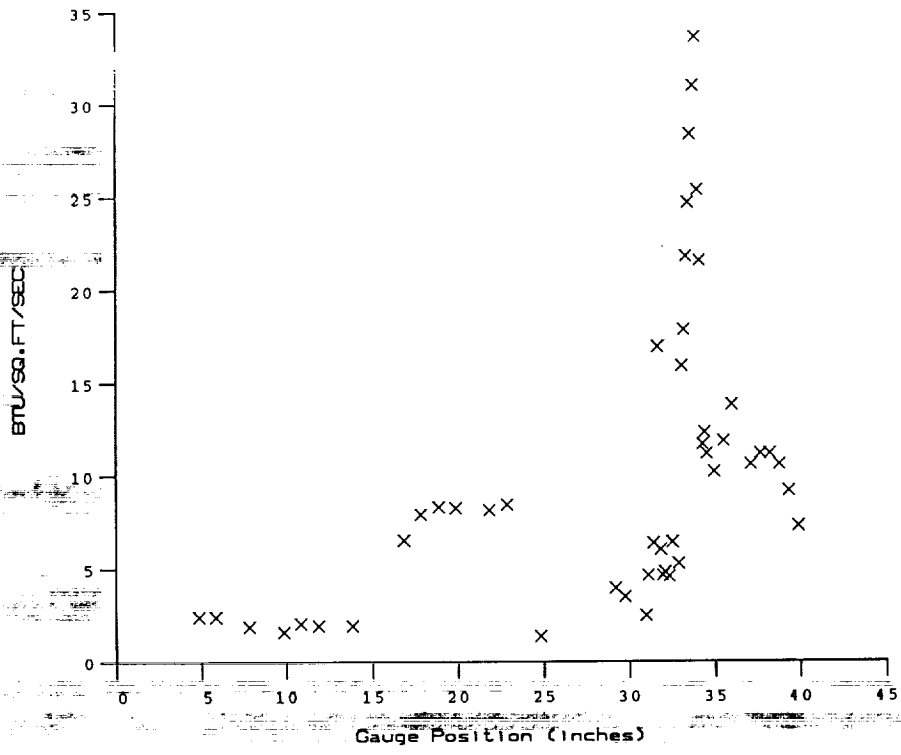


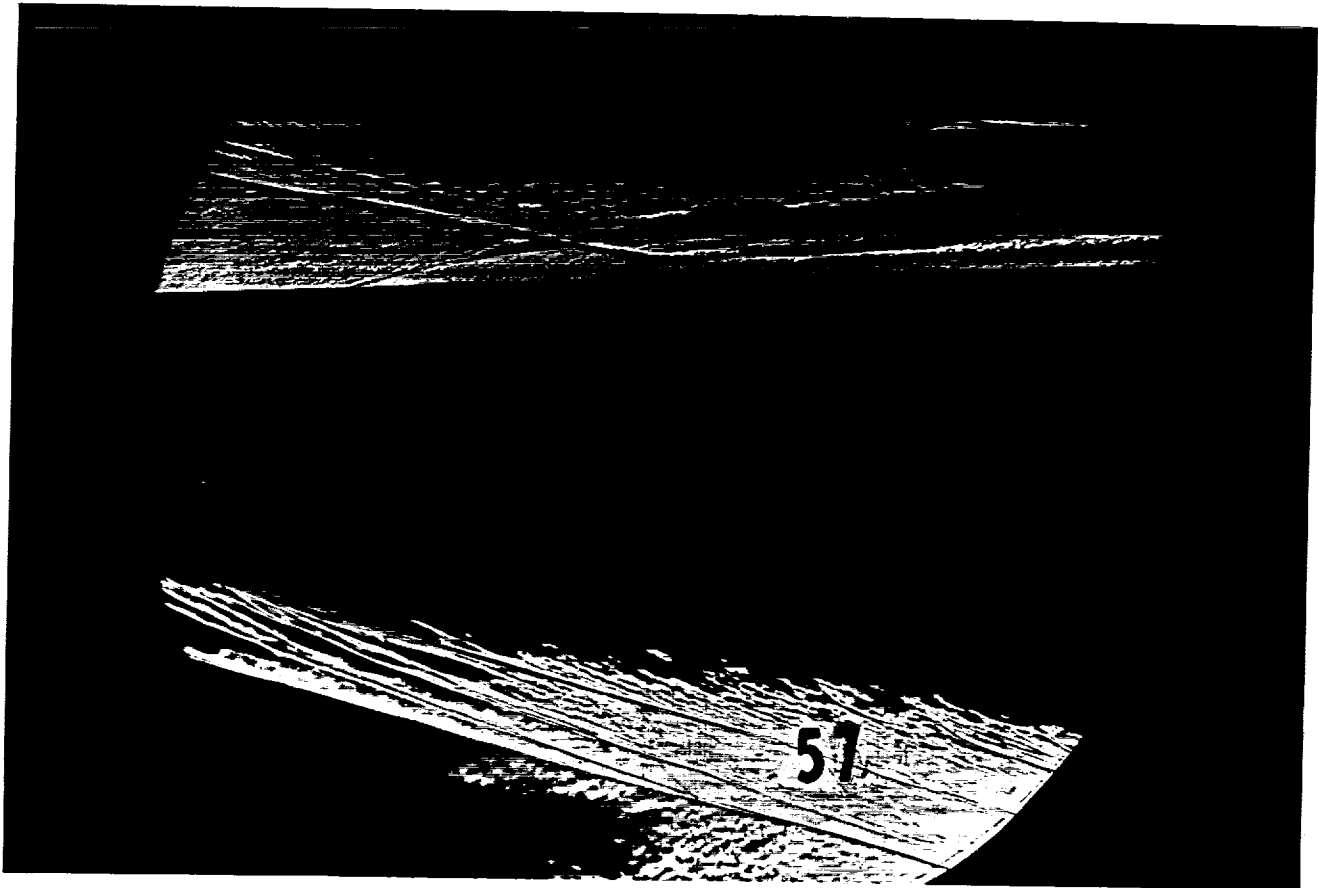
PRESSURE vs Gauge Position
Run 55



Test Conditions for Run 56 :

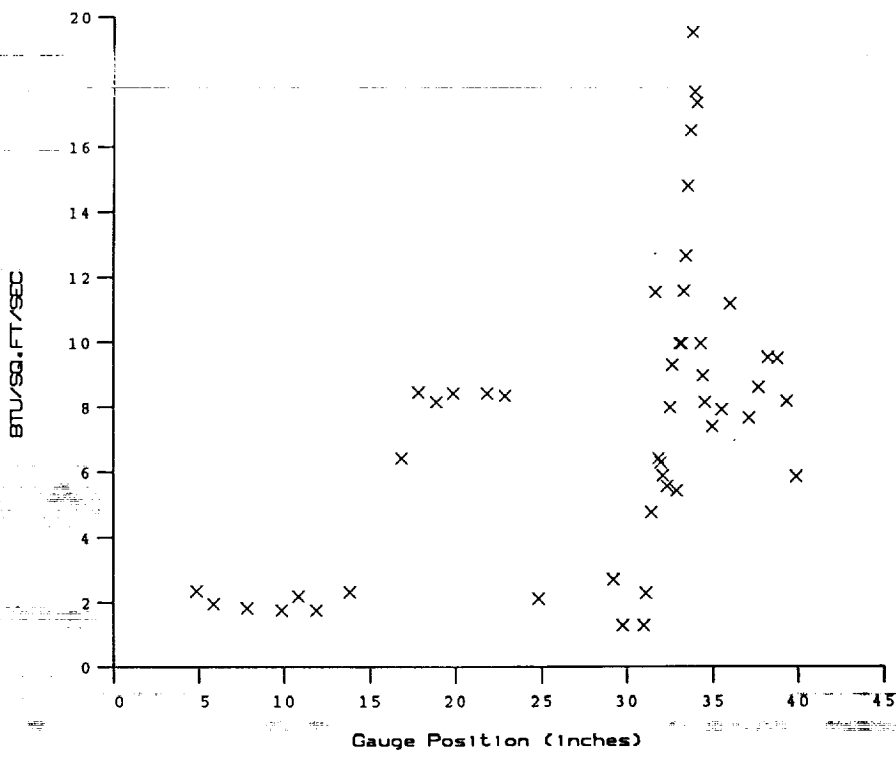
Po	= 3.882E+03 PSIA	Reservoir Total Pressure
Ho	= 1.446E+07 (Ft/sec) ²	Reservoir Total Enthalpy
To	= 2.244E+03 degR	Reservoir Total Temperature
M	= 7.868E+00	Freestream Mach Number
U	= 5.176E+03 Ft/sec	Freestream Velocity
T	= 1.800E+02 degR	Freestream Temperature
P	= 4.443E-01 PSIA	Freestream Static Pressure
Rho	= 2.072E-04 Slugs/Ft ³	Freestream Density
Mu	= 1.502E-07 Slugs/Ft-sec	Freestream Viscosity
Re	= 7.142E+06 1/Ft	Freestream Reynolds Number
Po'	= 3.560E+01 PSIA	Pitot Pressure
Q	= 1.928E+01 PSIA	Dynamic Pressure (Rho U ² /288)
Mi	= 2.913E+00	Shock Tube Incident Shock Mach Number
Tw	= 5.300E+02 degR	Wall Temperature (Test Gas = Air)
Hw	= 3.183E+06 (Ft/sec) ²	Wall Enthalpy (Cp Tw)
CPf	= 5.188E-02 1/PSIA	Pressure to CP factor (1/Q)
CHF	= 6.430E-05 Ft ² -s/BTU	Heat Rate to CH factor (778/(Rho U (Ho-Hw)))
QoFR	= 5.414E+01 BTU/Ft ² -s	Fay-Riddell Heat Transfer (.25' Diam Cylin.)



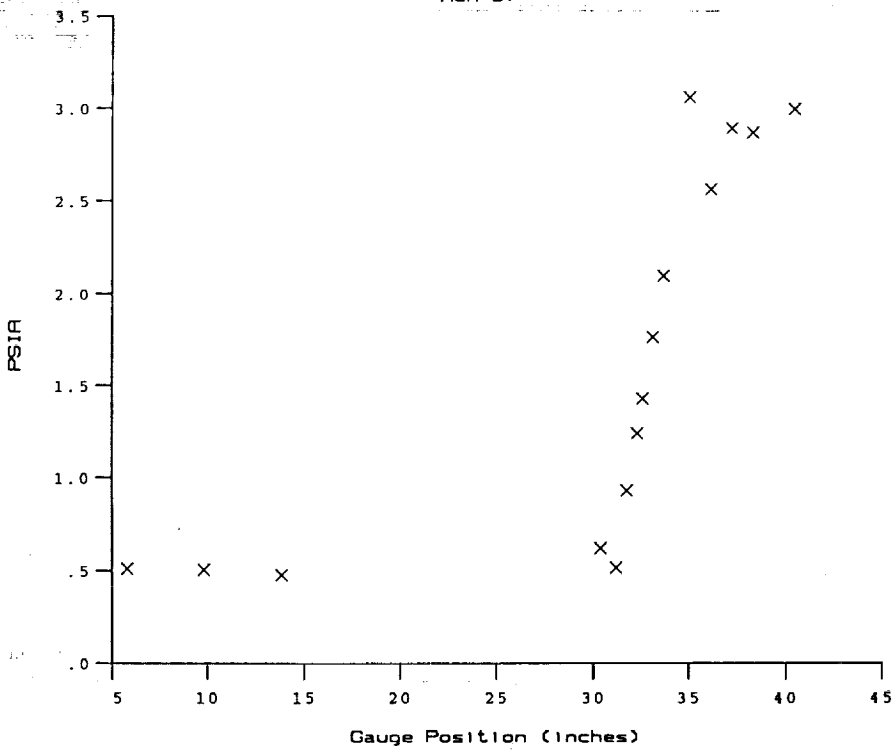


Test Conditions for Run 57 :

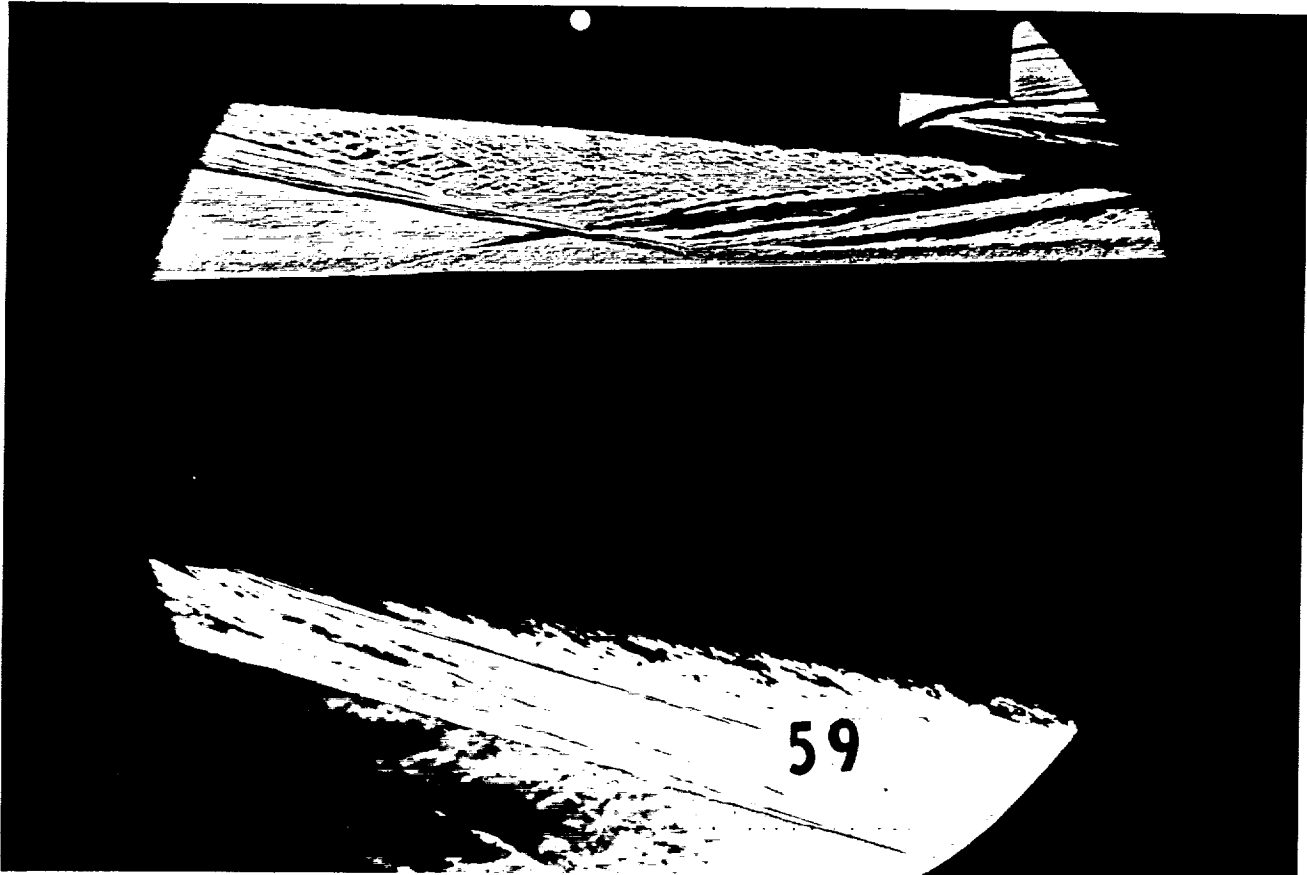
Po	= 3.883E+03 PSIA	Reservoir Total Pressure
Ho	= 1.462E+07 (Ft/sec) ²	Reservoir Total Enthalpy
To	= 2.265E+03 degR	Reservoir Total Temperature
M	= 7.866E+00	Freestream Mach Number
U	= 5.203E+03 Ft/sec	Freestream Velocity
T	= 1.820E+02 degR	Freestream Temperature
P	= 4.439E-01 PSIA	Freestream Static Pressure
Rho	= 2.048E-04 Slugs/Ft ³	Freestream Density
Mu	= 1.518E-07 Slugs/Ft-sec	Freestream Viscosity
Re	= 7.019E+06 1/Ft	Freestream Reynolds Number
Po'	= 3.556E+01 PSIA	Pitot Pressure
Q	= 1.925E+01 PSIA	Dynamic Pressure (Rho U ² /288)
Mi	= 2.922E+00	Shock Tube Incident Shock Mach Number
Tw	= 5.300E+02 degR	Wall Temperature (Test Gas = Air)
Hw	= 3.183E+06 (Ft/sec) ²	Wall Enthalpy (Cp Tw)
CPf	= 5.195E-02 1/PSIA	Pressure to CP factor (1/Q)
CHf	= 6.387E-05 Ft ² -s/BTU	Heat Rate to CH factor (778/(Rho U (Ho-Hw)))
QoFR	= 5.488E+01 BTU/Ft ² -s	Fay-Riddell Heat Transfer (.25' Diam Cylin.)



HEAT TRANSFER vs Gauge Position
Run 57

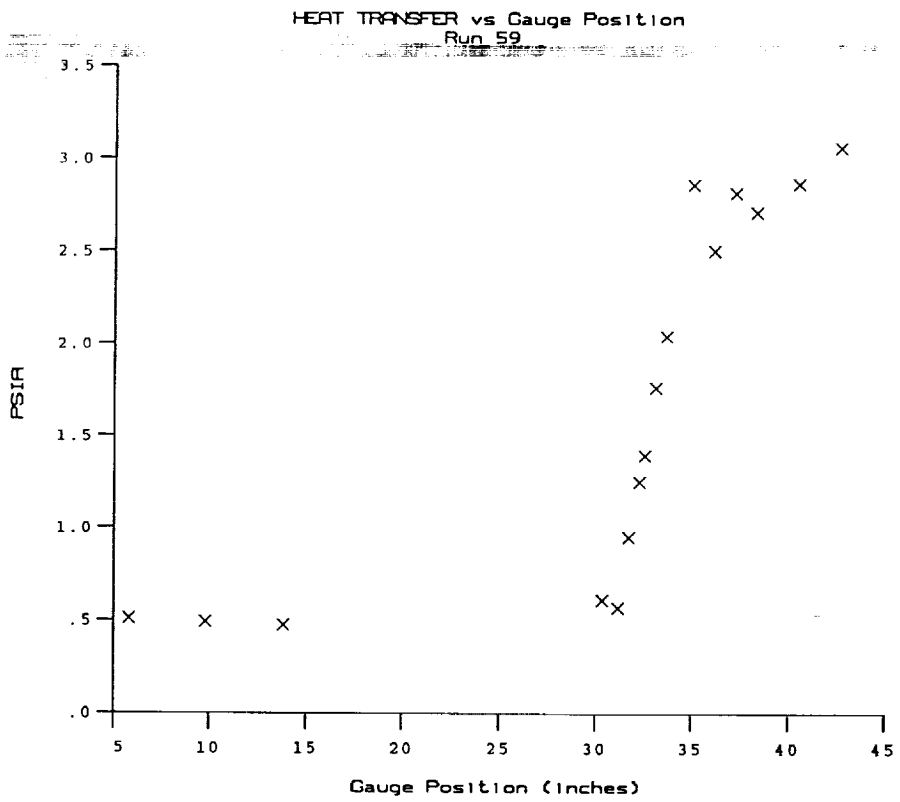
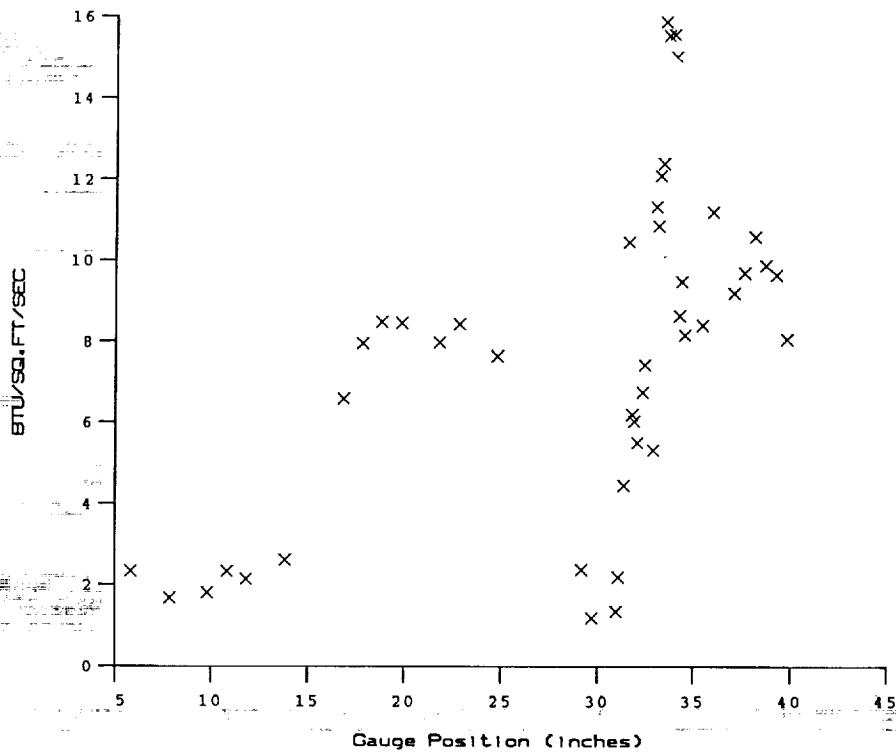


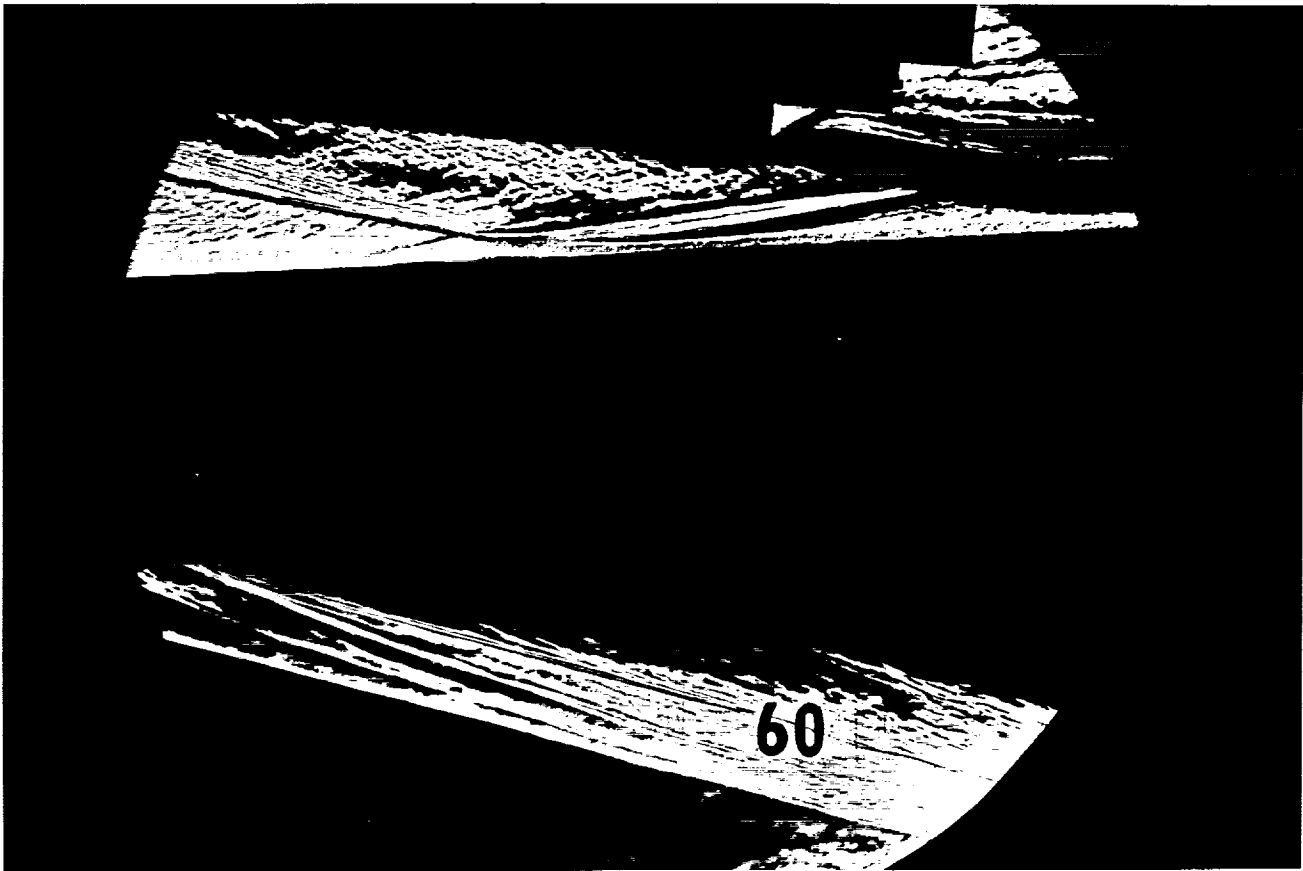
PRESSURE vs Gauge Position
Run 57



Test Conditions for Run 59 :

Po	= 3.879E+03 PSIA	Reservoir Total Pressure
Ho	= 1.430E+07 (Ft/sec) ²	Reservoir Total Enthalpy
To	= 2.221E+03 degR	Reservoir Total Temperature
M	= 7.869E+00	Freestream Mach Number
U	= 5.147E+03 Ft/sec	Freestream Velocity
T	= 1.779E+02 degR	Freestream Temperature
P	= 4.454E-01 PSIA	Freestream Static Pressure
Rho	= 2.100E-04 Slugs/Ft ³	Freestream Density
Mu	= 1.485E-07 Slugs/Ft-sec	Freestream Viscosity
Re	= 7.279E+06 1/Ft	Freestream Reynolds Number
Po'	= 3.569E+01 PSIA	Pitot Pressure
Q	= 1.932E+01 PSIA	Dynamic Pressure (Rho U ² /288)
Mi	= 2.911E+00	Shock Tube Incident Shock Mach Number
Tw	= 5.300E+02 degR	Wall Temperature (Test Gas = Air)
Hw	= 3.183E+06 (Ft/sec) ²	Wall Enthalpy (Cp Tw)
CPf	= 5.175E-02 1/PSIA	Pressure to CP factor (1/Q)
CHf	= 6.472E-05 Ft ² -s/BTU	Heat Rate to CH factor (778/(Rho U (Ho-Hw)))
QoFR	= 5.338E+01 BTU/Ft ² -s	Fay-Riddell Heat Transfer (.25' Diam Cylin.)

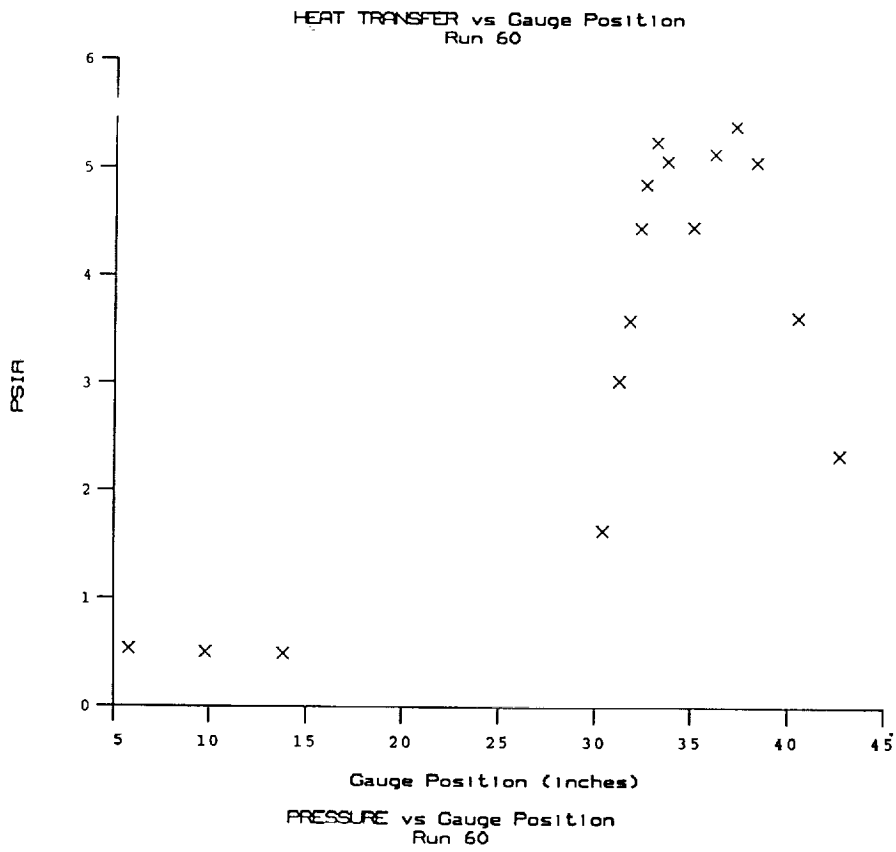
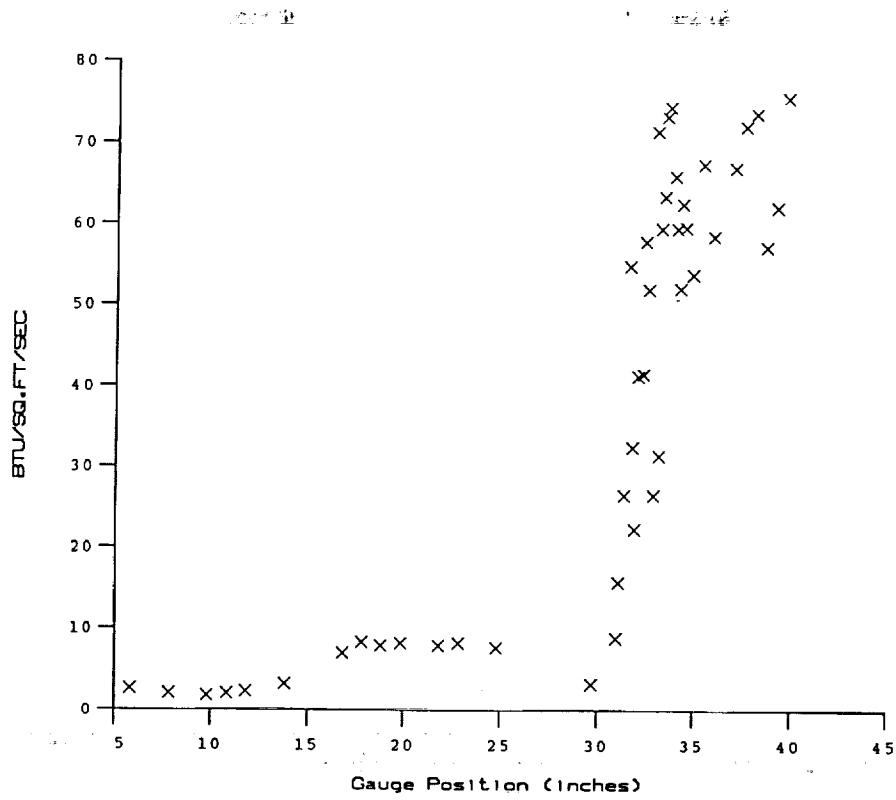




Test Conditions for Run 60 :

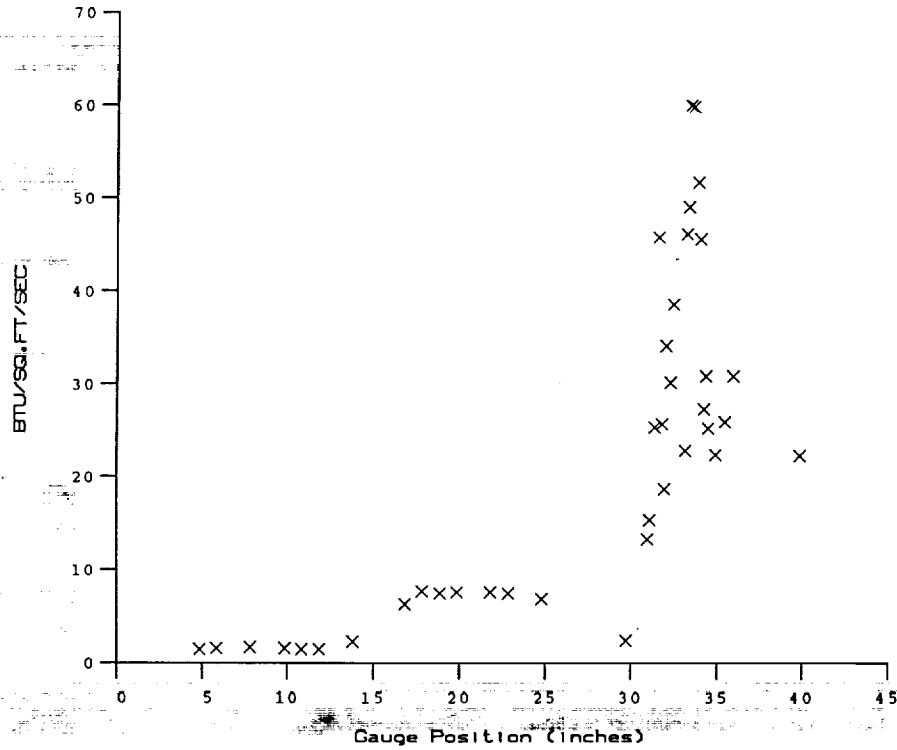
Po = 3.892E+03 PSIA
 Ho = 1.431E+07 (Ft/sec)²
 To = 2.222E+03 degR
 M = 7.872E+00
 U = 5.148E+03 Ft/sec
 T = 1.779E+02 degR
 P = 4.457E-01 PSIA
 Rho = 2.103E-04 Slugs/Ft³
 Mu = 1.485E-07 Slugs/Ft-sec
 Re = 7.292E+06 1/Ft
 Po' = 3.574E+01 PSIA
 Q = 1.935E+01 PSIA
 Mi = 2.900E+00
 Tw = 5.300E+02 degR
 Hw = 3.183E+06 (Ft/sec)²
 CPf = 5.167E-02 1/PSIA
 CHf = 6.460E-05 Ft²-s/BTU
 QoFR = 5.344E+01 BTU/Ft²-s

Reservoir Total Pressure
 Reservoir Total Enthalpy
 Reservoir Total Temperature
 Freestream Mach Number
 Freestream Velocity
 Freestream Temperature
 Freestream Static Pressure
 Freestream Density
 Freestream Viscosity
 Freestream Reynolds Number
 Pitot Pressure
 Dynamic Pressure ($\rho U^2/288$)
 Shock Tube Incident Shock Mach Number
 Wall Temperature (Test Gas = Air)
 Wall Enthalpy ($C_p T_w$)
 Pressure to CP factor ($1/Q$)
 Heat Rate to CH factor ($778/(\rho U (H_o - H_w))$)
 Fay-Riddell Heat Transfer (.25' Diam Cylin.)

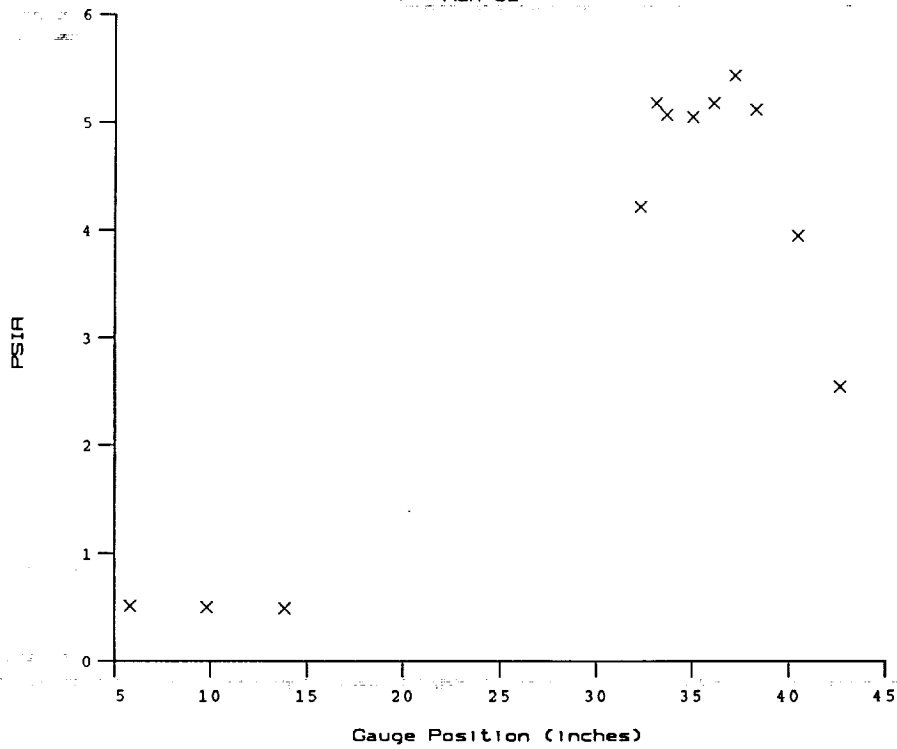


Test Conditions for Run 62 :

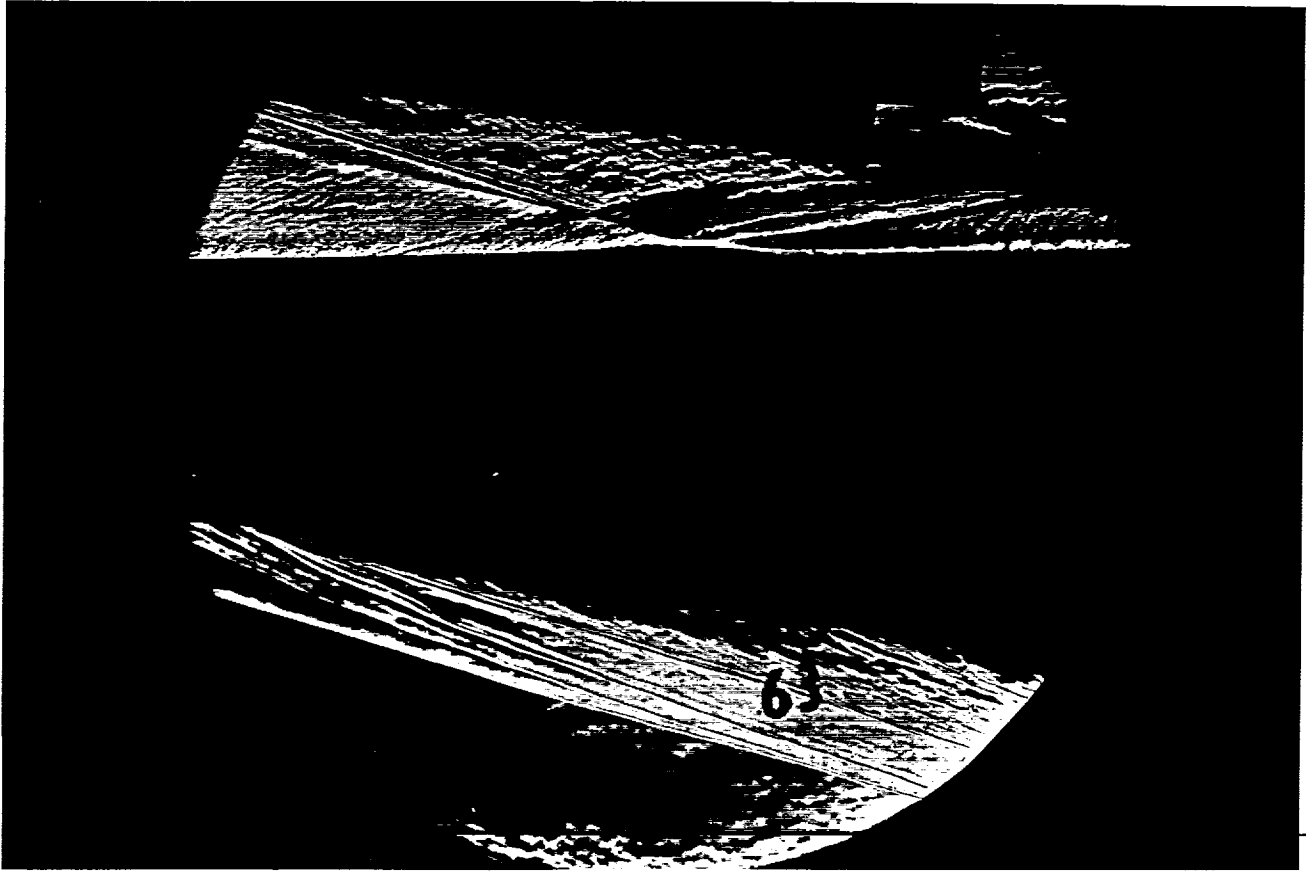
Po	= 3.959E+03 PSIA	Reservoir Total Pressure
Ho	= 1.432E+07 (Ft/sec) ²	Reservoir Total Enthalpy
To	= 2.225E+03 degR	Reservoir Total Temperature
M	= 7.876E+00	Freestream Mach Number
U	= 5.151E+03 Ft/sec	Freestream Velocity
T	= 1.779E+02 degR	Freestream Temperature
P	= 4.521E-01 PSIA	Freestream Static Pressure
Rho	= 2.133E-04 Slugs/Ft ³	Freestream Density
Mu	= 1.485E-07 Slugs/Ft-sec	Freestream Viscosity
Re	= 7.399E+06 1/Ft	Freestream Reynolds Number
Po'	= 3.629E+01 PSIA	Pitot Pressure
Q	= 1.965E+01 PSIA	Dynamic Pressure ($\text{Rho } U^2/288$)
Mi	= 2.895E+00	Shock Tube Incident Shock Mach Number
Tw	= 5.300E+02 degR	Wall Temperature (Test Gas = Air)
Hw	= 3.183E+06 (Ft/sec) ²	Wall Enthalpy ($C_p Tw$)
CPf	= 5.089E-02 1/PSIA	Pressure to CP factor (1/Q)
CHf	= 6.357E-05 Ft ² -s/BTU	Heat Rate to CH factor ($778/(\text{Rho } U (Ho-Hw))$)
QoFR	= 5.394E+01 BTU/Ft ² -s	Fay-Riddell Heat Transfer (.25' Diam Cylin.)



HEAT TRANSFER vs Gauge Position
Run 62



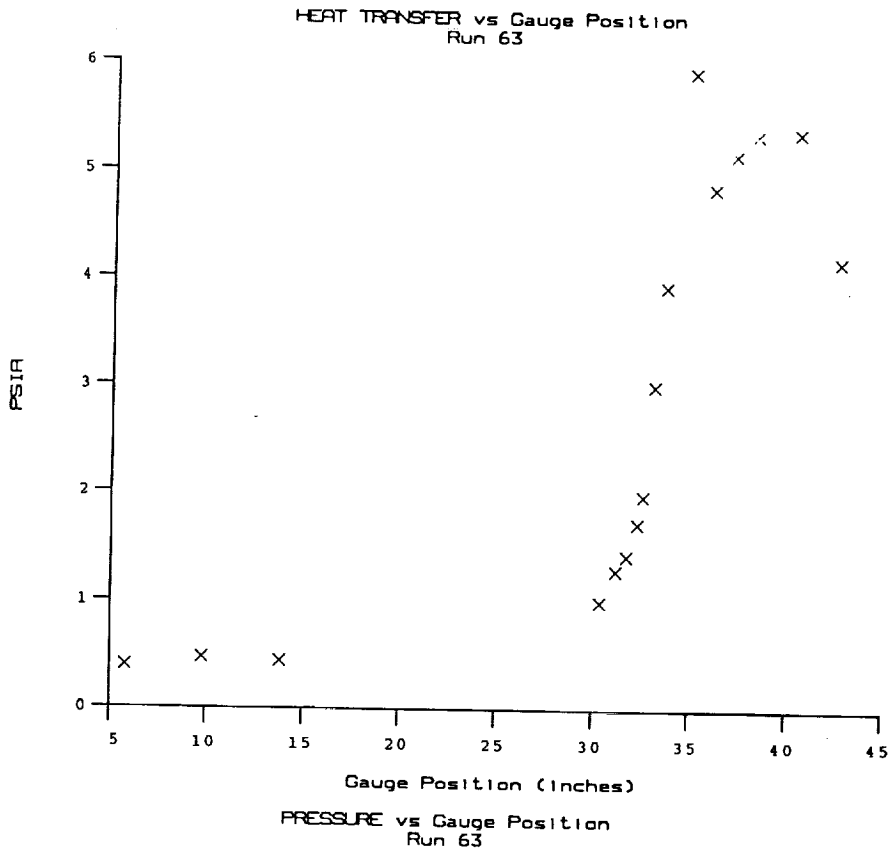
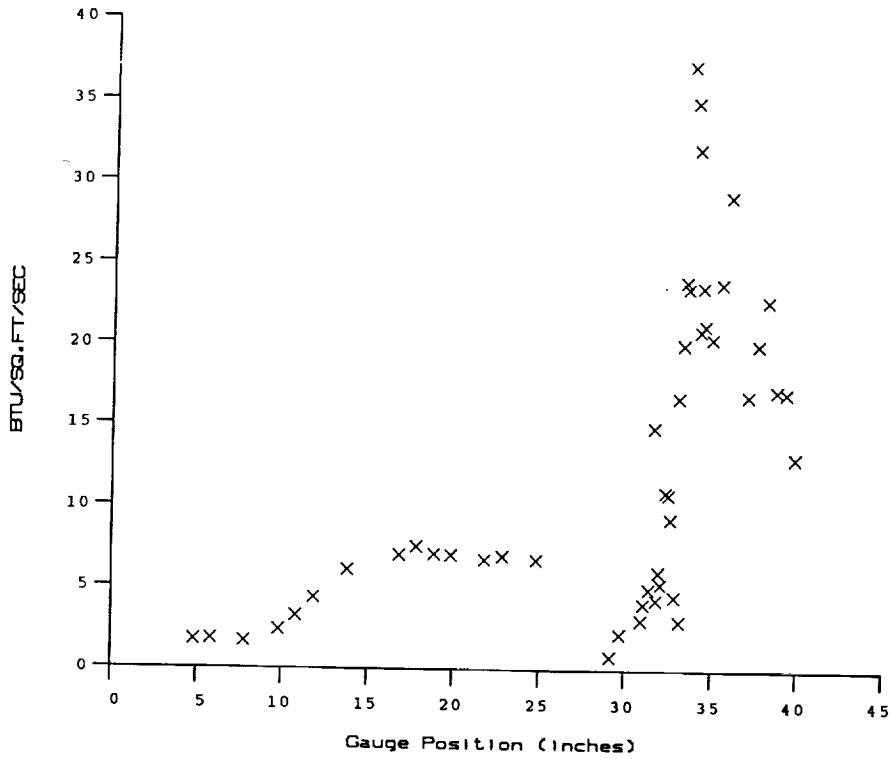
PRESSURE vs Gauge Position
Run 62

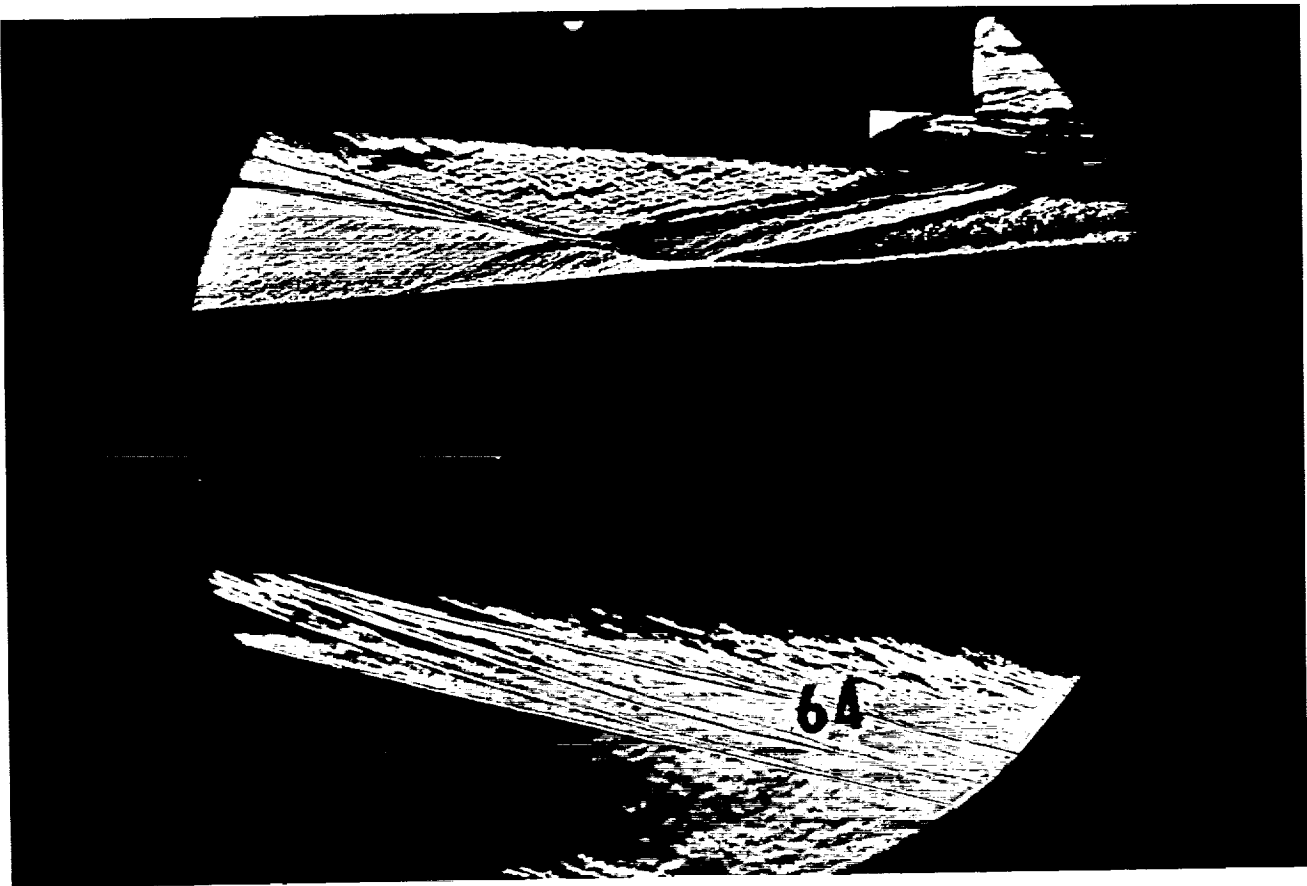


Test Conditions for Run 63 :

Po - 3.867E+03 PSIA
 Ho - 1.439E+07 (Ft/sec)²
 To - 2.233E+03 degR
 M - 7.869E+00
 U - 5.162E+03 Ft/sec
 T - 1.789E+02 degR
 P - 4.428E-01 PSIA
 Rho - 2.077E-04 Slugs/Ft³
 Mu - 1.494E-07 Slugs/Ft-sec
 Re - 7.179E+06 1/Ft
 Po' - 3.549E+01 PSIA
 Q - 1.922E+01 PSIA
 Mi - 2.906E+00
 Tw - 5.300E+02 degR
 Hw - 3.183E+06 (Ft/sec)²
 CPf - 5.203E-02 1/PSIA
 CHf - 6.477E-05 Ft²-s/BTU
 QoFR - 5.367E+01 BTU/Ft²-s

Reservoir Total Pressure
 Reservoir Total Enthalpy
 Reservoir Total Temperature
 Freestream Mach Number
 Freestream Velocity
 Freestream Temperature
 Freestream Static Pressure
 Freestream Density
 Freestream Viscosity
 Freestream Reynolds Number
 Pitot Pressure
 Dynamic Pressure ($\rho U^2/288$)
 Shock Tube Incident Shock Mach Number
 Wall Temperature (Test Gas = Air)
 Wall Enthalpy ($C_p T_w$)
 Pressure to CP factor ($1/Q$)
 Heat Rate to CH factor ($778/(\rho U (H_o - H_w))$)
 Fay-Riddell Heat Transfer (.25' Diam Cylin.)

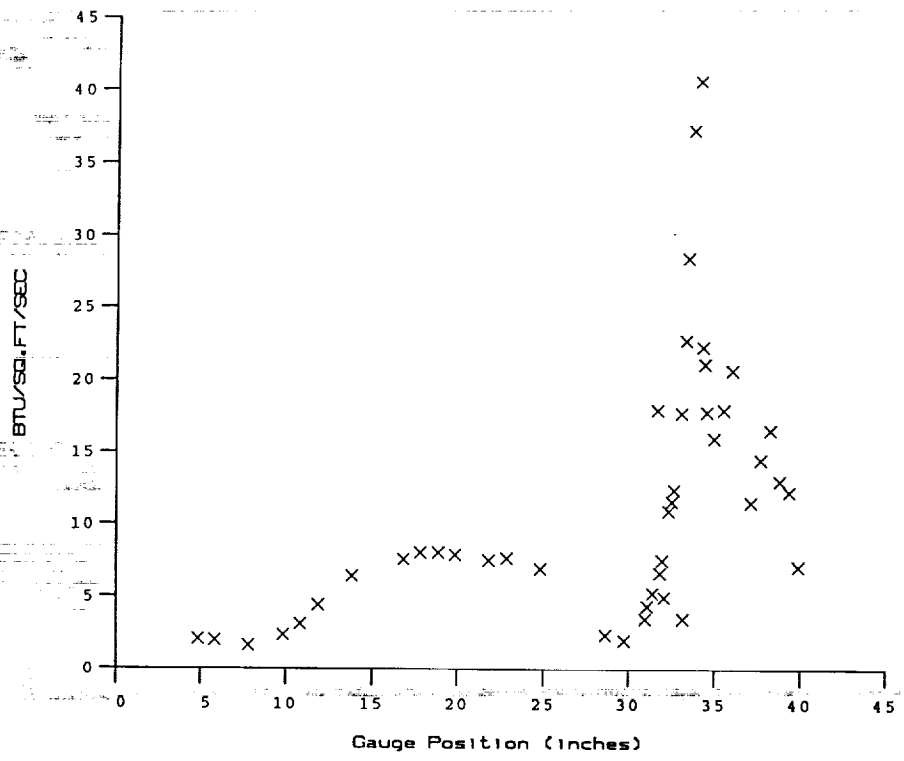




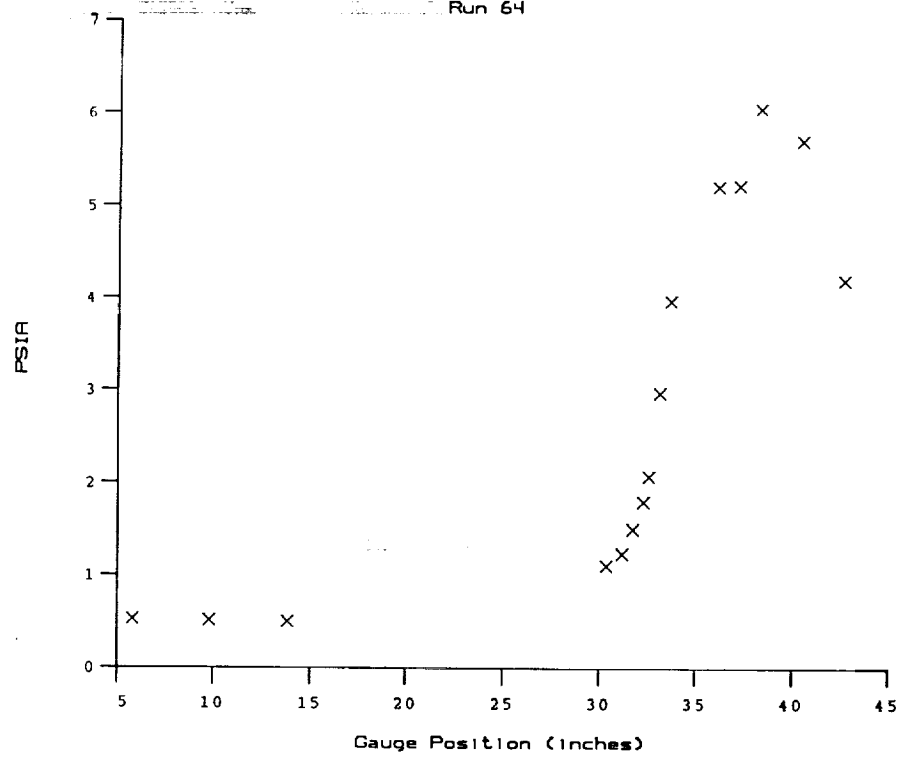
Test Conditions for Run 64 :

Po = 3.911E+03 PSIA
 Ho = 1.460E+07 (Ft/sec)²
 To = 2.264E+03 degR
 M = 7.868E+00
 U = 5.201E+03 Ft/sec
 T = 1.817E+02 degR
 P = 4.468E-01 PSIA
 Rho = 2.063E-04 Slugs/Ft³
 Mu = 1.516E-07 Slugs/Ft-sec
 Re = 7.080E+06 1/Ft
 Po' = 3.580E+01 PSIA
 Q = 1.938E+01 PSIA
 Mi = 2.920E+00
 Tw = 5.300E+02 degR
 Hw = 3.183E+06 (Ft/sec)²
 CPf = 5.160E-02 1/PSIA
 CHF = 6.348E-05 Ft²-s/BTU
 QoFR = 5.500E+01 BTU/Ft²-s

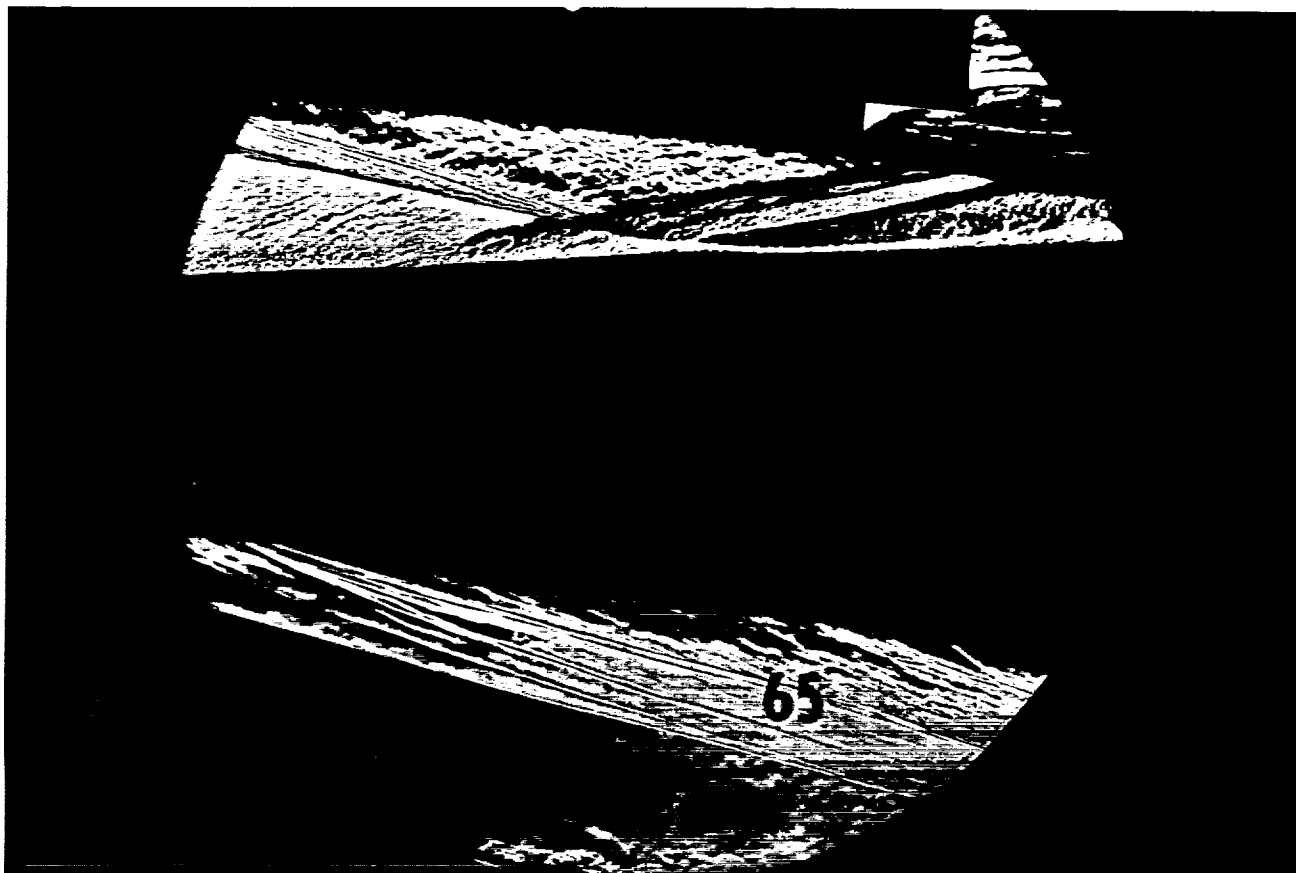
Reservoir Total Pressure
 Reservoir Total Enthalpy
 Reservoir Total Temperature
 Freestream Mach Number
 Freestream Velocity
 Freestream Temperature
 Freestream Static Pressure
 Freestream Density
 Freestream Viscosity
 Freestream Reynolds Number
 Pitot Pressure
 Dynamic Pressure ($\rho U^2/288$)
 Shock Tube Incident Shock Mach Number
 Wall Temperature (Test Gas = Air)
 Wall Enthalpy ($C_p T_w$)
 Pressure to CP factor ($1/Q$)
 Heat Rate to CH factor ($778/(\rho U (H_o - H_w))$)
 Fay-Riddell Heat Transfer (.25' Diam Cylin.)



HEAT TRANSFER vs Gauge Position
Run 64

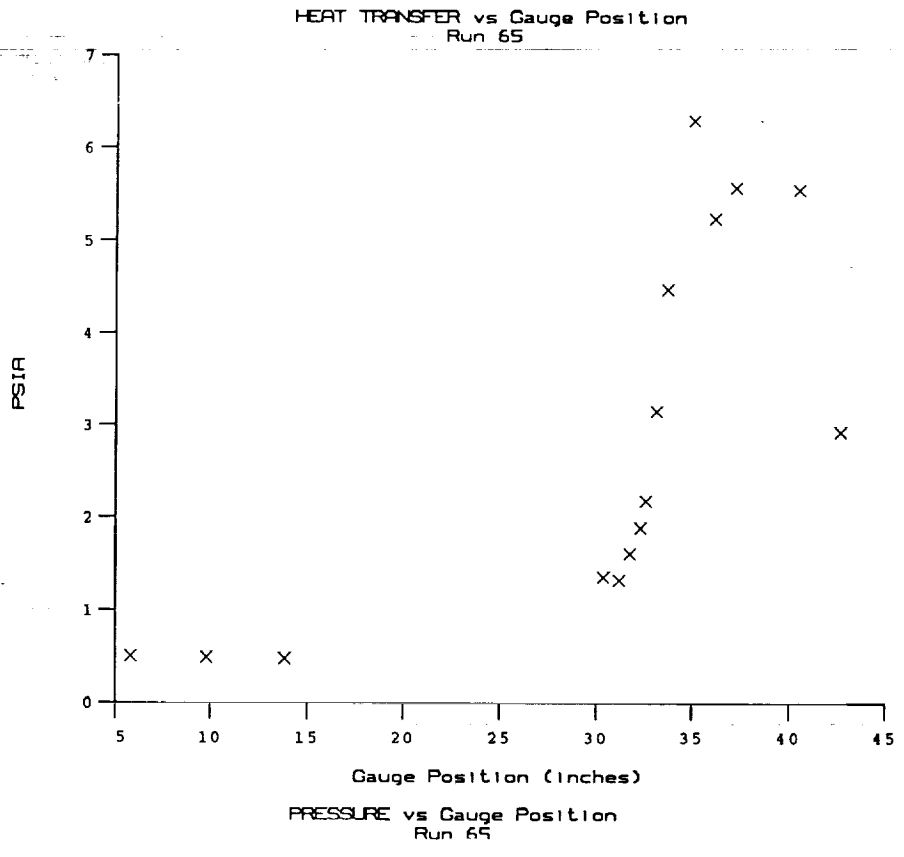
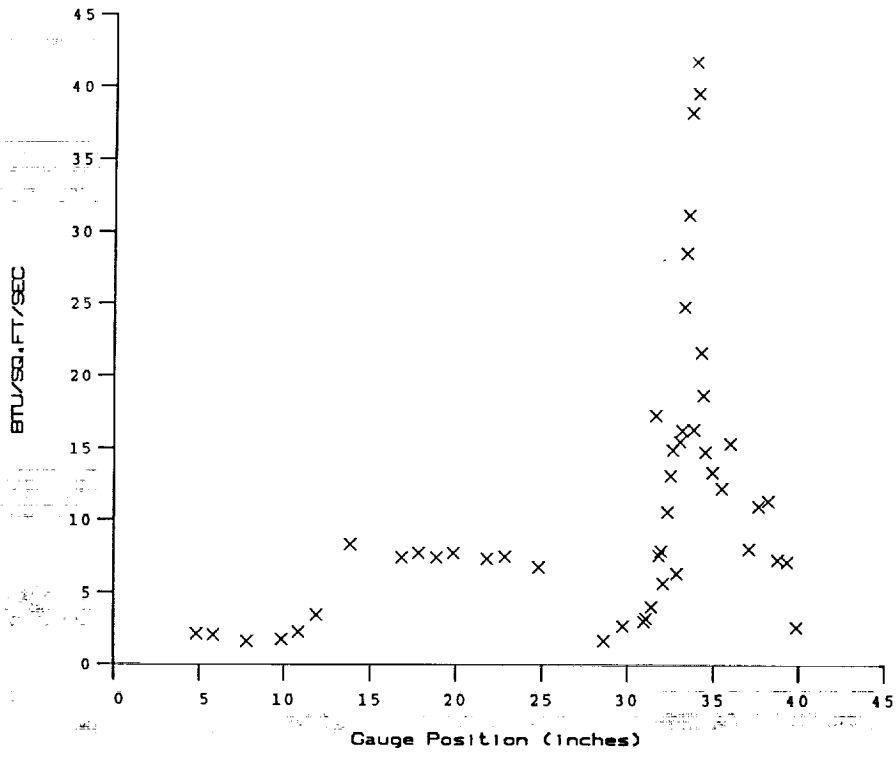


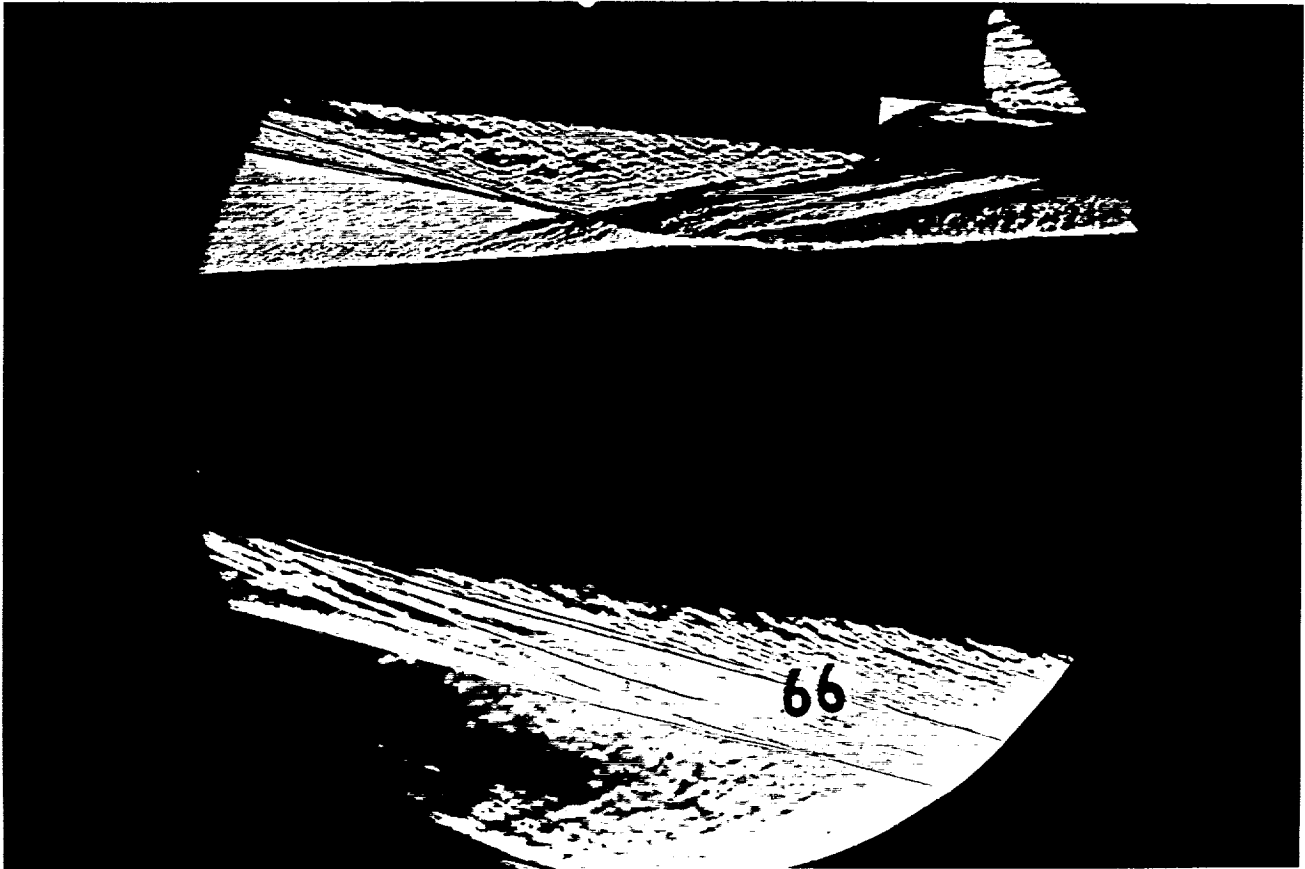
PRESSURE vs Gauge Position
Run 64



Test Conditions for Run 65 :

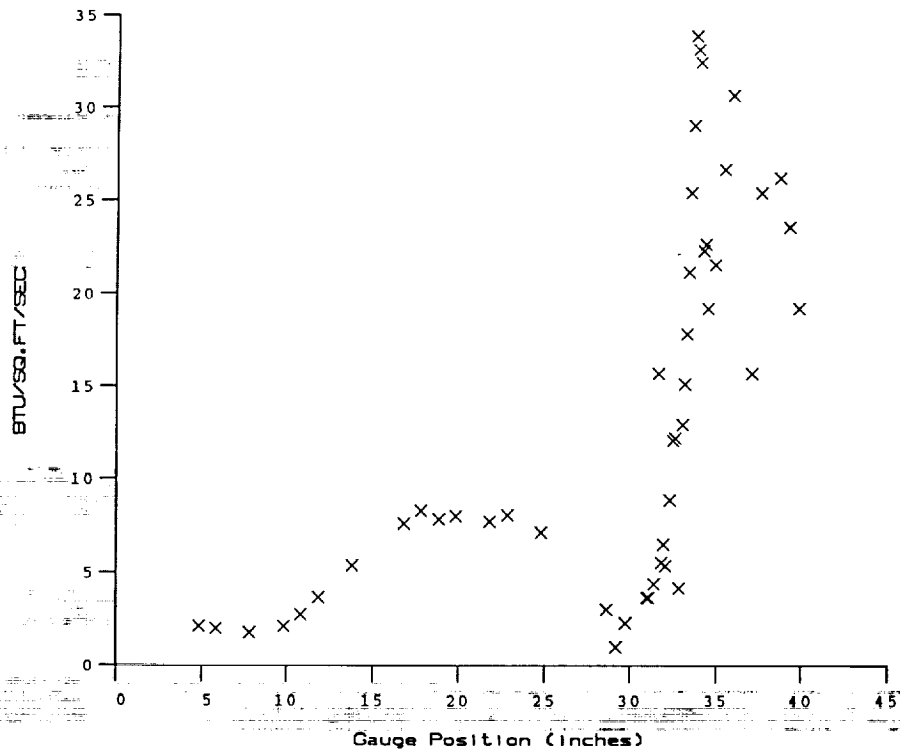
Po	= 3.770E+03 PSIA	Reservoir Total Pressure
Ho	= 1.455E+07 (Ft/sec) ²	Reservoir Total Enthalpy
To	= 2.257E+03 degR	Reservoir Total Temperature
M	= 7.865E+00	Freestream Mach Number
U	= 5.191E+03 Ft/sec	Freestream Velocity
T	= 1.812E+02 degR	Freestream Temperature
P	= 4.312E-01 PSIA	Freestream Static Pressure
Rho	= 1.998E-04 Slugs/Ft ³	Freestream Density
Mu	= 1.511E-07 Slugs/Ft-sec	Freestream Viscosity
Re	= 6.862E+06 1/Ft	Freestream Reynolds Number
Po'	= 3.453E+01 PSIA	Pitot Pressure
Q	= 1.869E+01 PSIA	Dynamic Pressure (Rho U ² /288)
Mi	= 2.908E+00	Shock Tube Incident Shock Mach Number
Tw	= 5.300E+02 degR	Wall Temperature (Test Gas = Air)
Hw	= 3.183E+06 (Ft/sec) ²	Wall Enthalpy (Cp Tw)
CPf	= 5.349E-02 1/PSIA	Pressure to CP factor (1/Q)
CHf	= 6.600E-05 Ft ² -s/BTU	Heat Rate to CH factor (778/(Rho U (Ho-Hw)))
QoFR	= 5.374E+01 BTU/Ft ² -s	Fay-Riddell Heat Transfer (.25' Diam Cylin.)



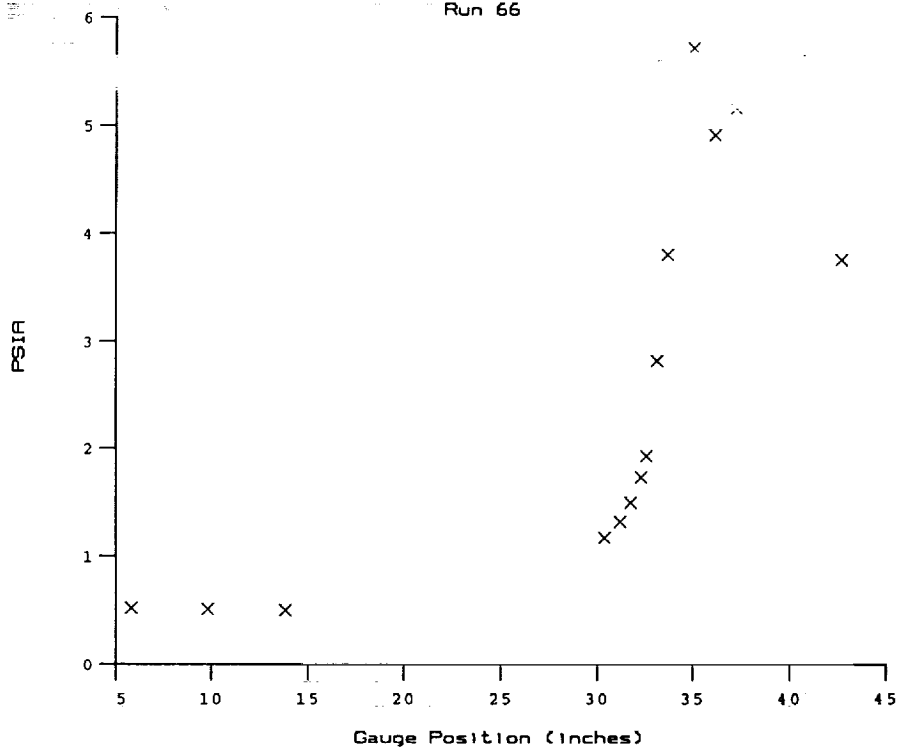


Test Conditions for Run 66 :

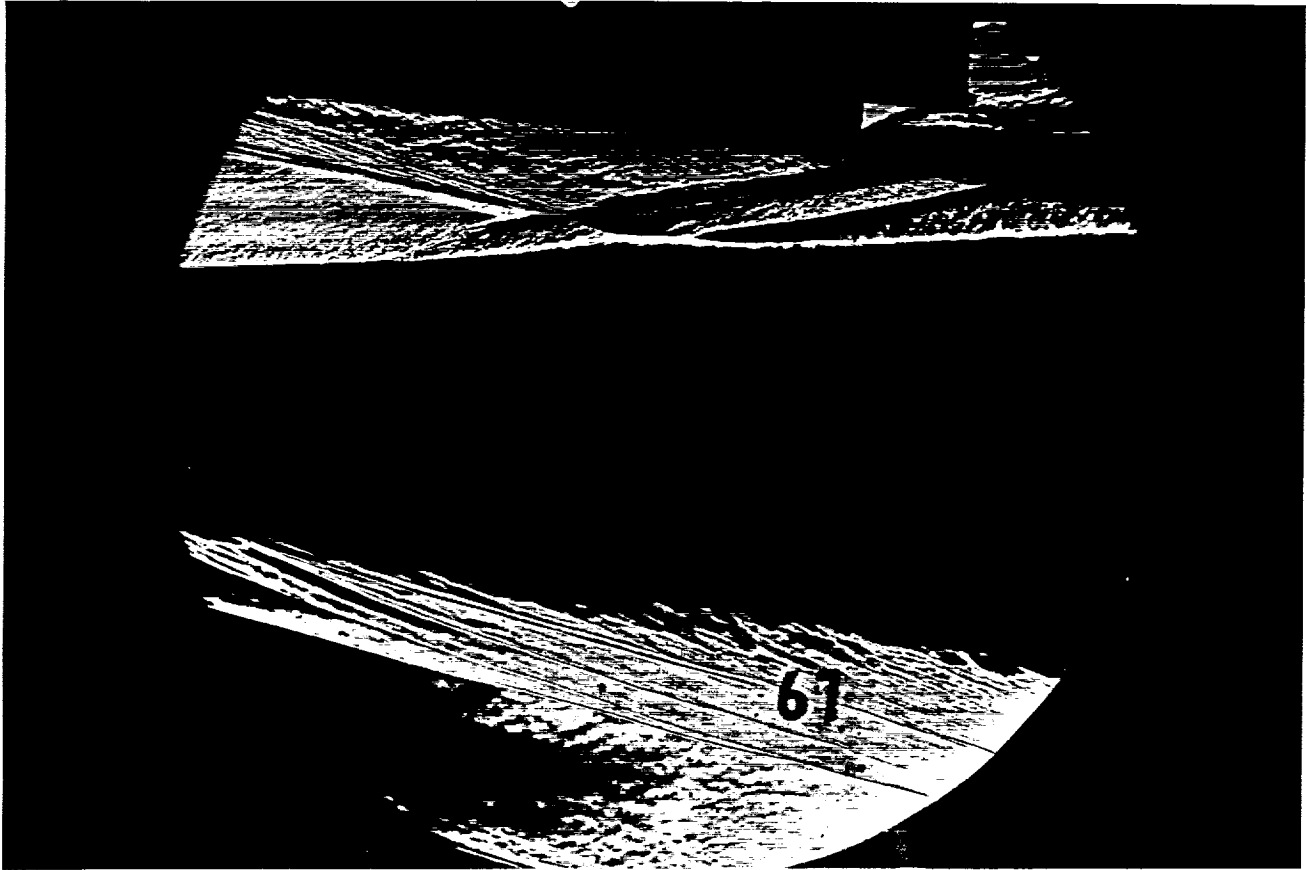
Po	= 3.907E+03 PSIA	Reservoir Total Pressure
Ho	= 1.464E+07 (Ft/sec) ²	Reservoir Total Enthalpy
To	= 2.268E+03 degR	Reservoir Total Temperature
M	= 7.866E+00	Freestream Mach Number
U	= 5.207E+03 Ft/sec	Freestream Velocity
T	= 1.822E+02 degR	Freestream Temperature
P	= 4.464E-01 PSIA	Freestream Static Pressure
Rho	= 2.056E-04 Slugs/Ft ³	Freestream Density
Mu	= 1.520E-07 Slugs/Ft-sec	Freestream Viscosity
Re	= 7.045E+06 1/Ft	Freestream Reynolds Number
Po'	= 3.576E+01 PSIA	Pitot Pressure
Q	= 1.936E+01 PSIA	Dynamic Pressure (Rho U ² /288)
Mi	= 2.924E+00	Shock Tube Incident Shock Mach Number
Tw	= 5.300E+02 degR	Wall Temperature (Test Gas = Air)
Hw	= 3.183E+06 (Ft/sec) ²	Wall Enthalpy (Cp Tw)
CPf	= 5.166E-02 1/PSIA	Pressure to CP factor (1/Q)
CHf	= 6.344E-05 Ft ² -s/BTU	Heat Rate to CH factor (778/(Rho U (Ho-Hw)))
QoFR	= 5.515E+01 BTU/Ft ² -s	Fay-Riddell Heat Transfer (.25' Diam Cylin.)



HEAT TRANSFER vs Gauge Position
Run 66

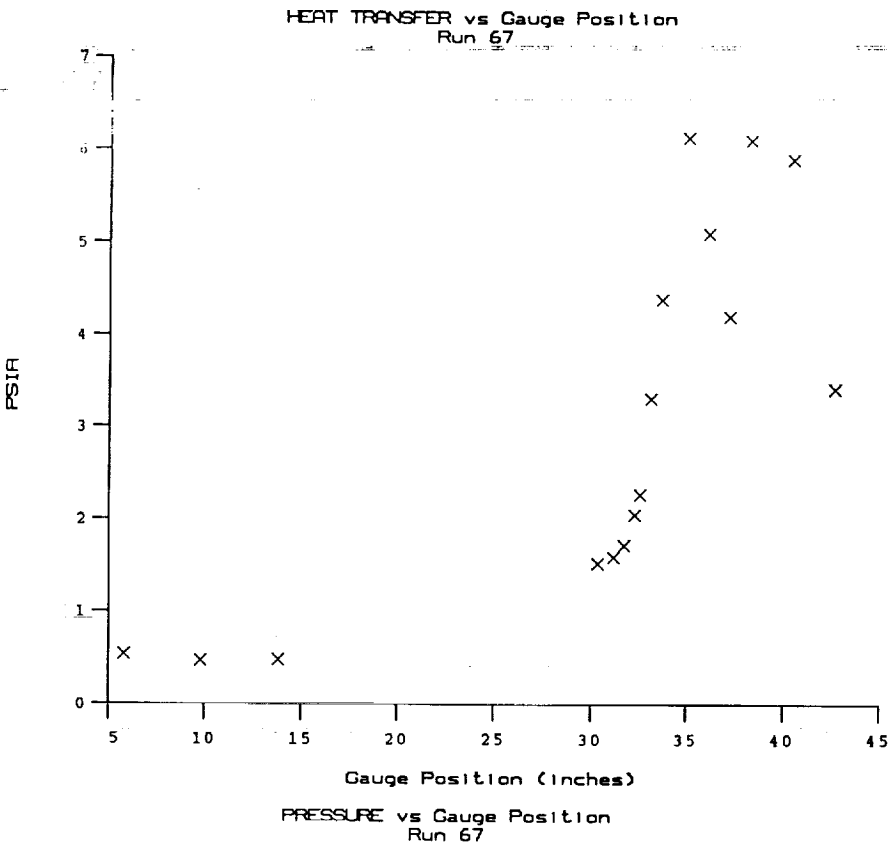
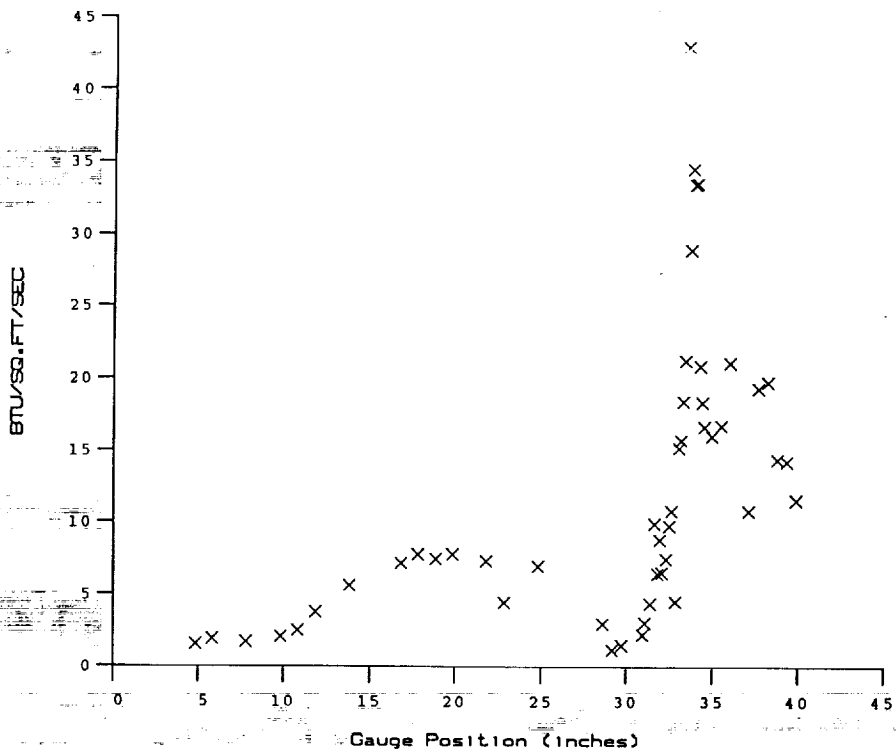


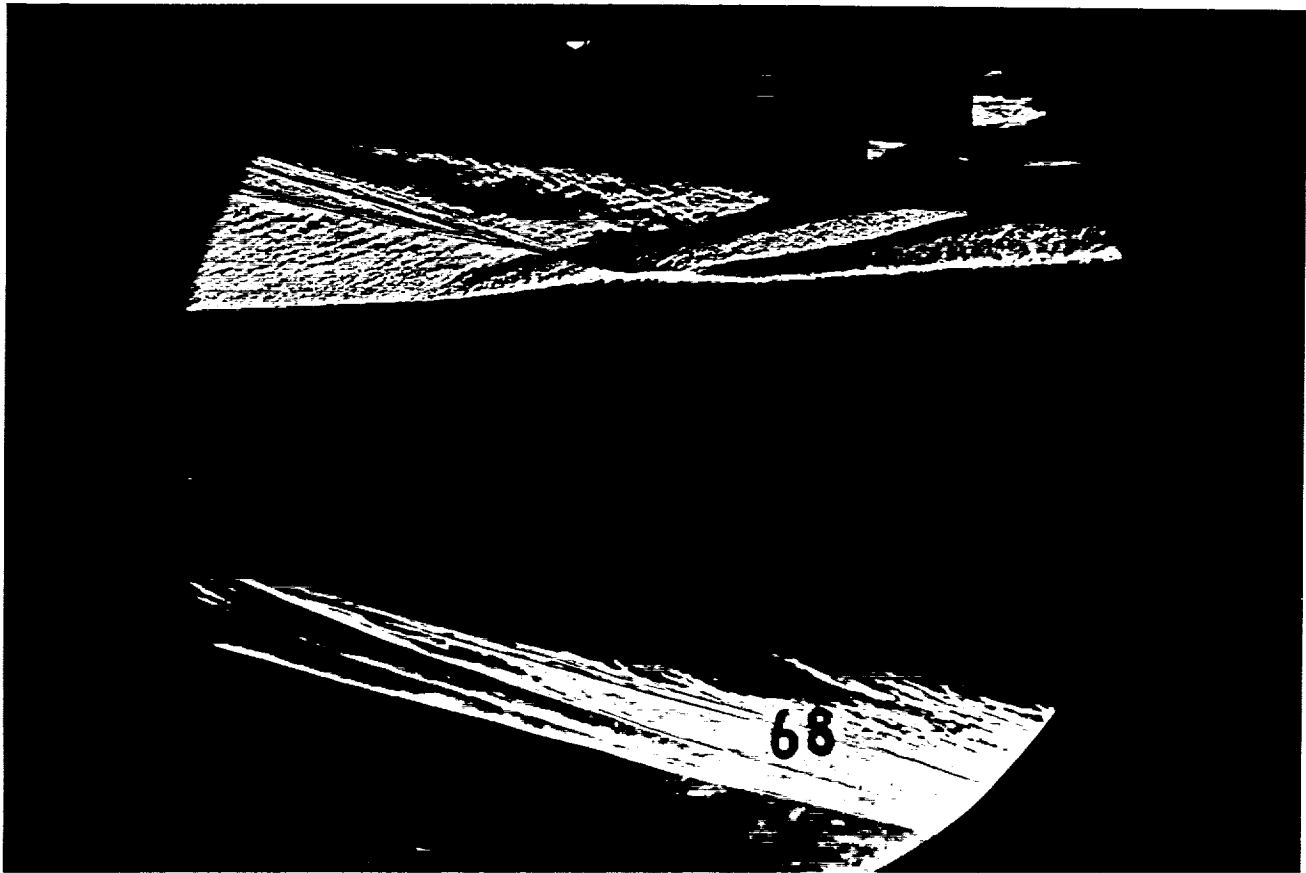
PRESSURE vs Gauge Position
Run 66



Test Conditions for Run 67 :

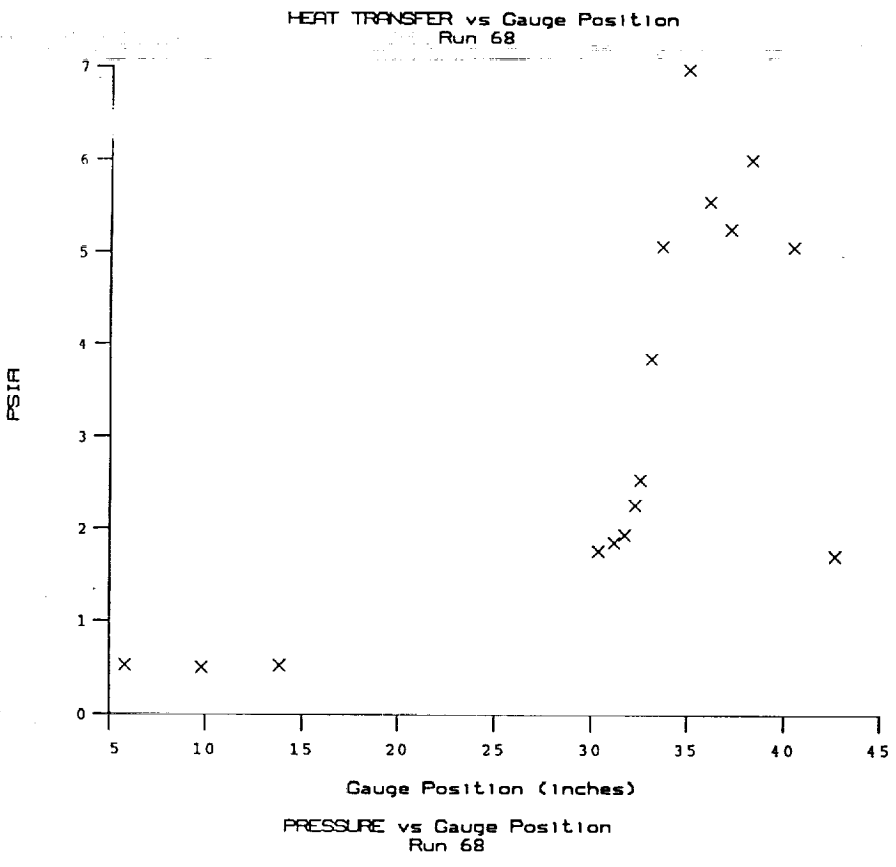
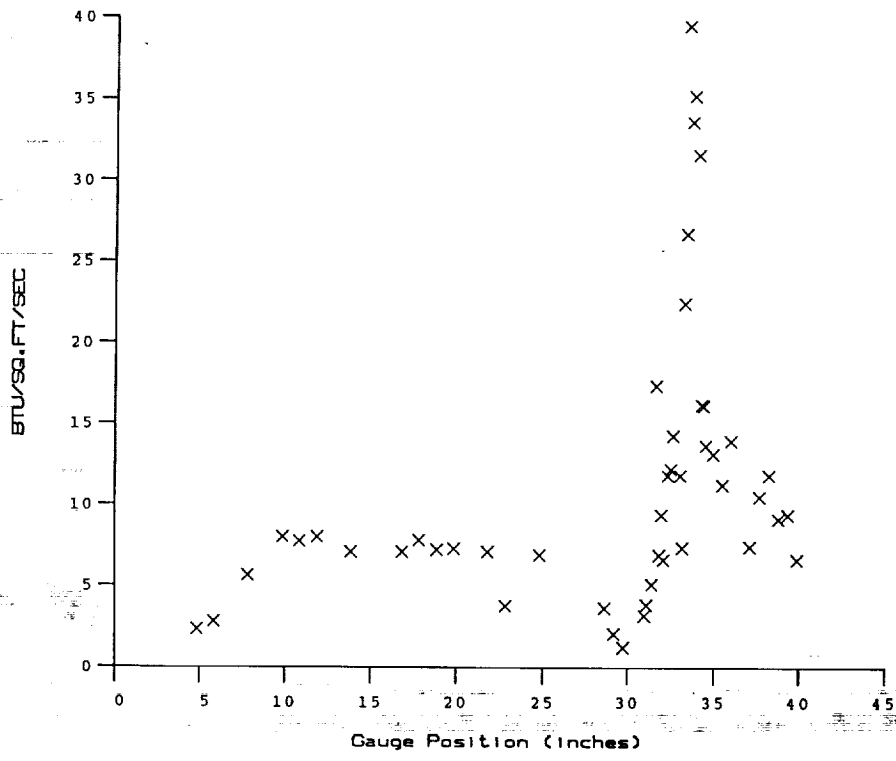
Po	= 3.930E+03 PSIA	Reservoir Total Pressure
Ho	= 1.469E+07 (Ft/sec) ²	Reservoir Total Enthalpy
To	= 2.276E+03 degR	Reservoir Total Temperature
M	= 7.867E+00	Freestream Mach Number
U	= 5.217E+03 Ft/sec	Freestream Velocity
T	= 1.829E+02 degR	Freestream Temperature
P	= 4.485E-01 PSIA	Freestream Static Pressure
Rho	= 2.058E-04 Slugs/Ft ³	Freestream Density
Mu	= 1.525E-07 Slugs/Ft-sec	Freestream Viscosity
Re	= 7.040E+06 1/Ft	Freestream Reynolds Number
Po'	= 3.593E+01 PSIA	Pitot Pressure
Q	= 1.945E+01 PSIA	Dynamic Pressure (Rho U ² /288)
Mi	= 2.926E+00	Shock Tube Incident Shock Mach Number
Tw	= 5.300E+02 degR	Wall Temperature (Test Gas = Air)
Hw	= 3.183E+06 (Ft/sec) ²	Wall Enthalpy (Cp Tw)
CPf	= 5.141E-02 1/PSIA	Pressure to CP factor (1/Q)
CHf	= 6.295E-05 Ft ² -s/BTU	Heat Rate to CH factor (778/(Rho U (Ho-Hw))
QoFR	= 5.556E+01 BTU/Ft ² -s	Fay-Riddell Heat Transfer (.25' Diam Cy'lin.)

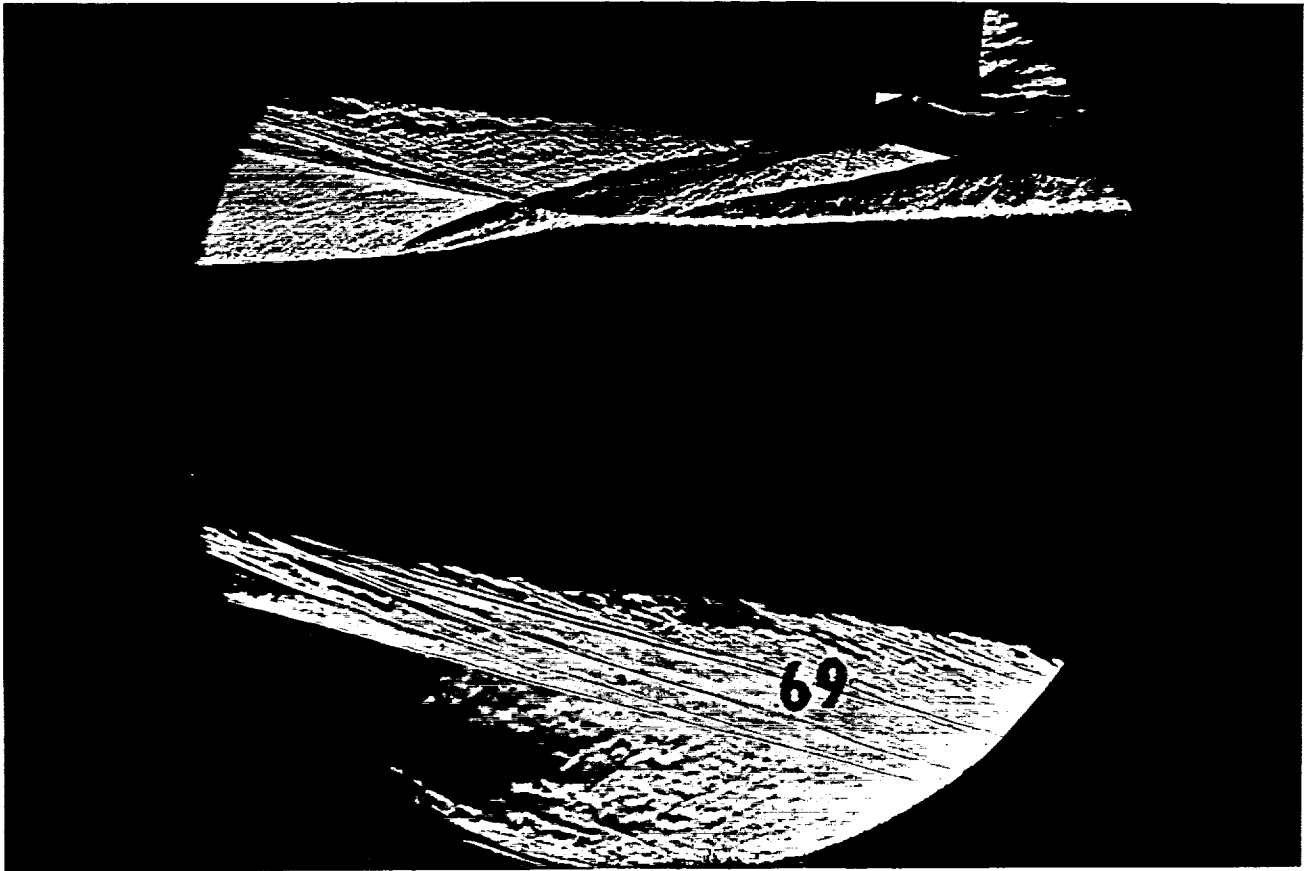




Test Conditions for Run 68 :

Po	= 3.841E+03 PSIA	Reservoir Total Pressure
Ho	= 1.441E+07 (Ft/sec) ²	Reservoir Total Enthalpy
To	= 2.236E+03 degR	Reservoir Total Temperature
M	= 7.868E+00	Freestream Mach Number
U	= 5.166E+03 Ft/sec	Freestream Velocity
T	= 1.793E+02 degR	Freestream Temperature
P	= 4.400E-01 PSIA	Freestream Static Pressure
Rho	= 2.060E-04 Slugs/Ft ³	Freestream Density
Mu	= 1.496E-07 Slugs/Ft-sec	Freestream Viscosity
Re	= 7.113E+06 1/Ft	Freestream Reynolds Number
Po'	= 3.526E+01 PSIA	Pitot Pressure
Q	= 1.909E+01 PSIA	Dynamic Pressure (Rho U ² /288)
Mi	= 2.908E+00	Shock Tube Incident Shock Mach Number
Tw	= 5.300E+02 degR	Wall Temperature (Test Gas = Air)
Hw	= 3.183E+06 (Ft/sec) ²	Wall Enthalpy (Cp Tw)
CPf	= 5.239E-02 1/PSIA	Pressure to CP factor (1/Q)
CHf	= 6.513E-05 Ft ² -s/BTU	Heat Rate to CH factor (778/(Rho U (Ho-Hw)))
QoFR	= 5.359E+01 BTU/Ft ² -s	Fay-Riddell Heat Transfer (.25' Diam Cylin.)

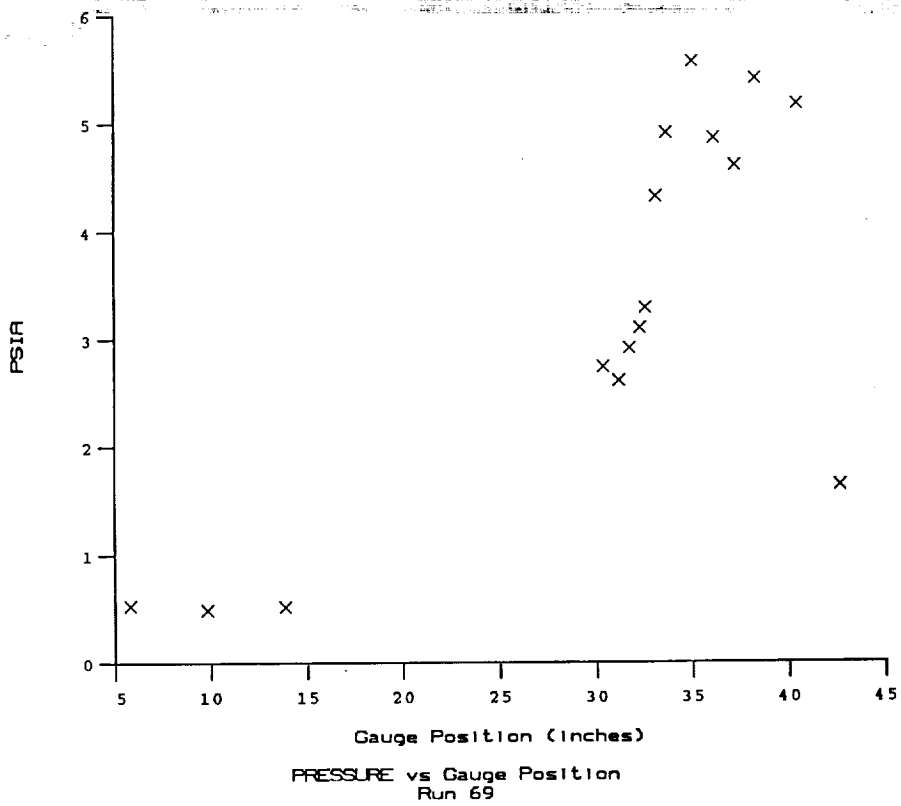
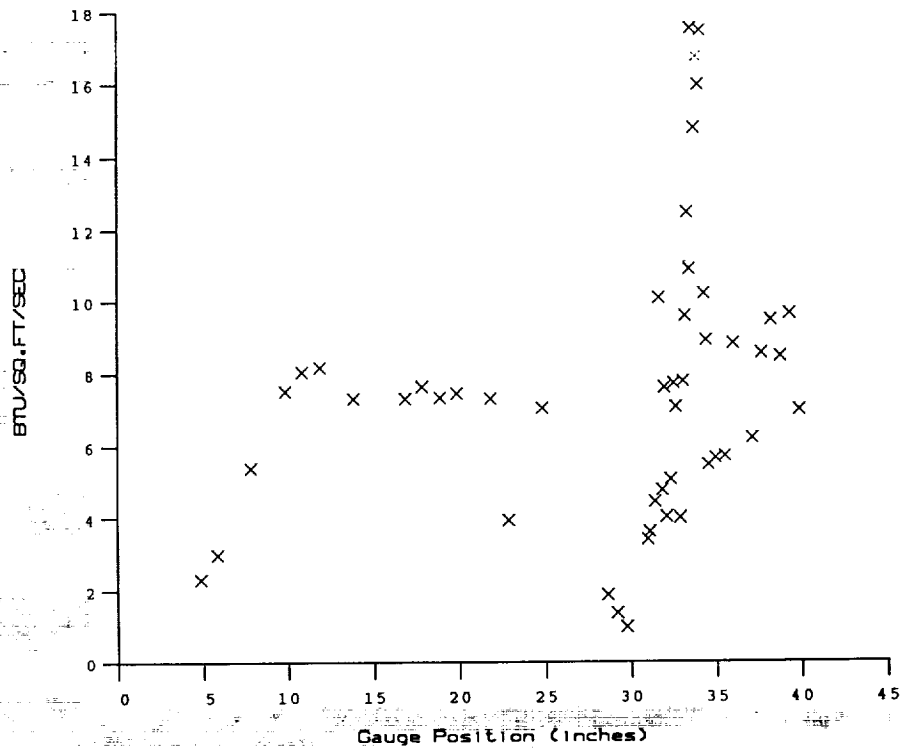


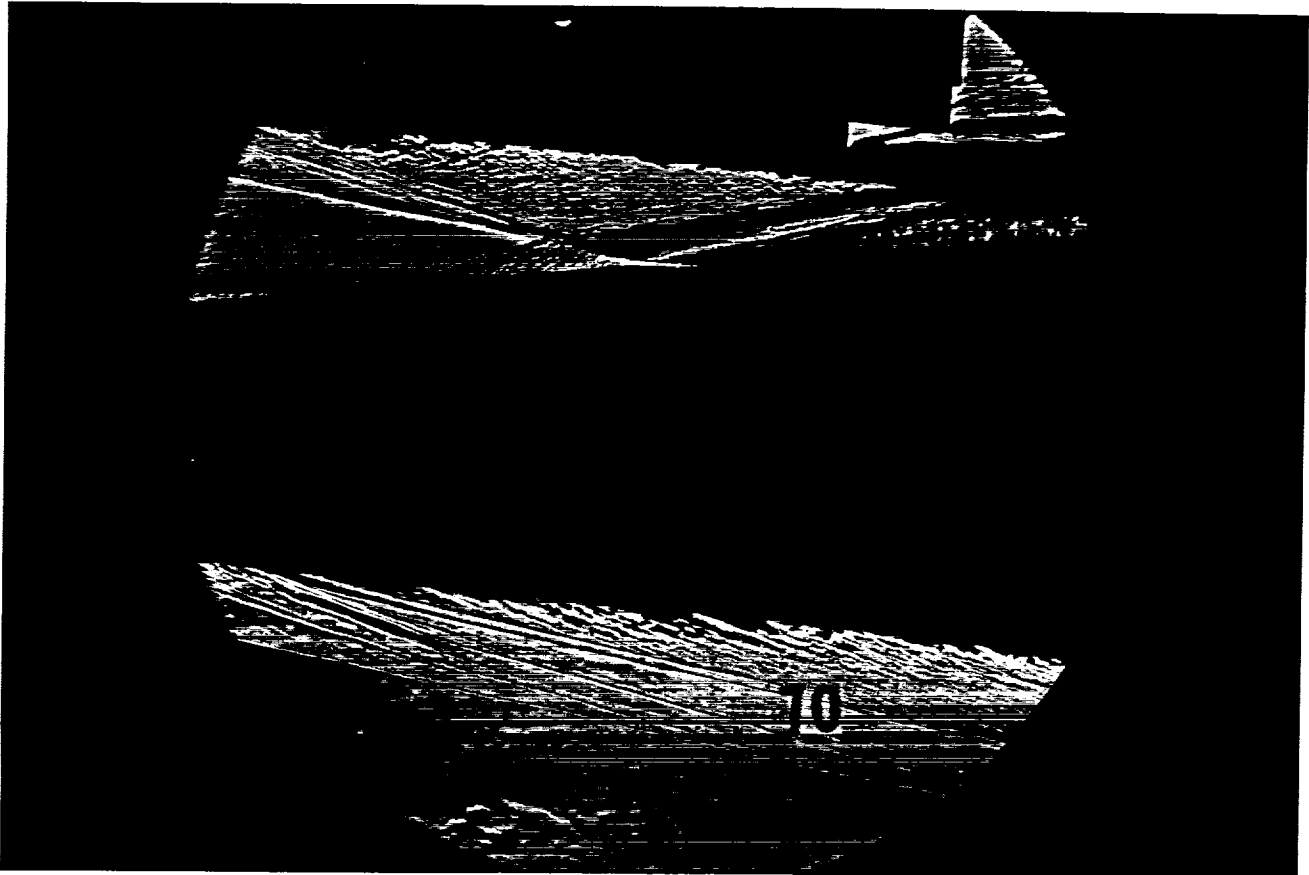


Test Conditions for Run 69 :

Po - 3.903E+03 PSIA
 Ho - 1.463E+07 (Ft/sec)²
 To - 2.268E+03 degR
 M - 7.867E+00
 U - 5.206E+03 Ft/sec
 T - 1.821E+02 degR
 P - 4.457E-01 PSIA
 Rho - 2.054E-04 Slugs/Ft³
 Mu - 1.519E-07 Slugs/Ft-sec
 Re - 7.040E+06 1/Ft
 Po' - 3.571E+01 PSIA
 Q - 1.933E+01 PSIA
 Mi - 2.921E+00
 Tw - 5.300E+02 degR
 Hw - 3.183E+06 (Ft/sec)²
 CPF - 5.173E-02 1/PSIA
 CHF - 6.354E-05 Ft²-s/BTU
 QoFR - 5.508E+01 BTU/Ft²-s

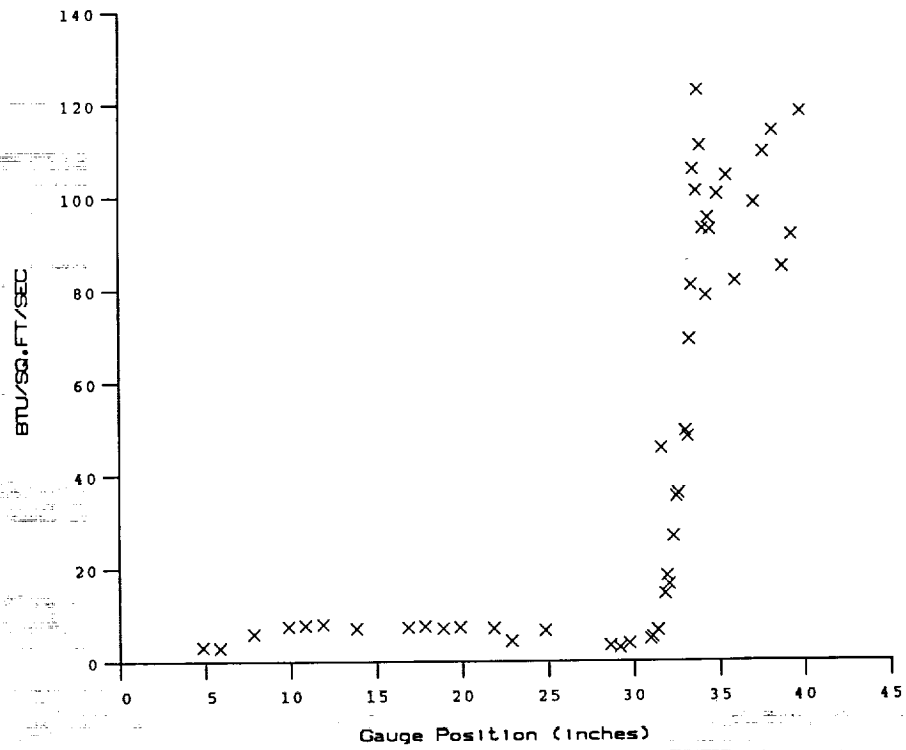
Reservoir Total Pressure
 Reservoir Total Enthalpy
 Reservoir Total Temperature
 Freestream Mach Number
 Freestream Velocity
 Freestream Temperature
 Freestream Static Pressure
 Freestream Density
 Freestream Viscosity
 Freestream Reynolds Number
 Pitot Pressure
 Dynamic Pressure ($\rho U^2/288$)
 Shock Tube Incident Shock Mach Number
 Wall Temperature (Test Gas = Air)
 Wall Enthalpy ($C_p T_w$)
 Pressure to CP factor ($1/Q$)
 Heat Rate to CH factor ($778/(\rho U (H_o - H_w))$)
 Fay-Riddell Heat Transfer (.25' Diam Cylin.)



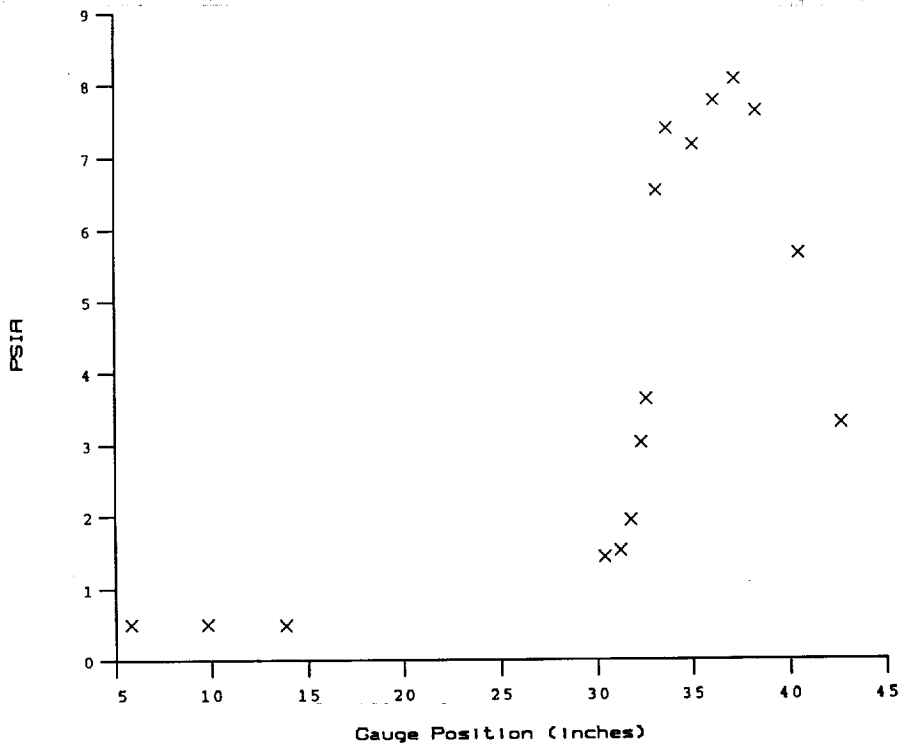


Test Conditions for Run 70 :

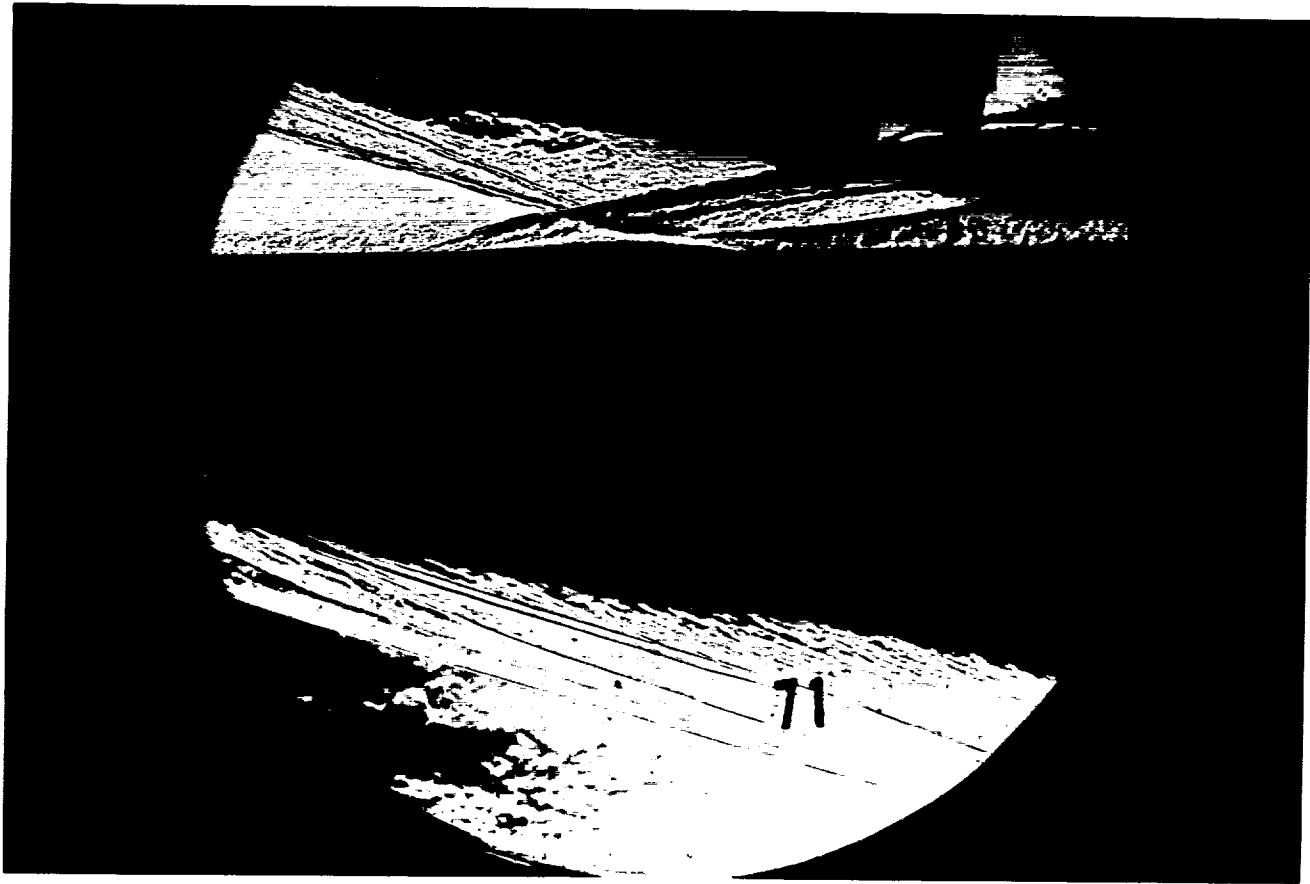
Po	= 3.882E+03 PSIA	Reservoir Total Pressure
Ho	= 1.462E+07 (Ft/sec) ²	Reservoir Total Enthalpy
To	= 2.266E+03 degR	Reservoir Total Temperature
M	= 7.868E+00	Freestream Mach Number
U	= 5.204E+03 Ft/sec	Freestream Velocity
T	= 1.819E+02 degR	Freestream Temperature
P	= 4.431E-01 PSIA	Freestream Static Pressure
Rho	= 2.044E-04 Slugs/Ft ³	Freestream Density
Mu	= 1.517E-07 Slugs/Ft-sec	Freestream Viscosity
Re	= 7.010E+06 1/Ft	Freestream Reynolds Number
Po'	= 3.551E+01 PSIA	Pitot Pressure
Q	= 1.922E+01 PSIA	Dynamic Pressure (Rho U ² /288)
Mi	= 2.915E+00	Shock Tube Incident Shock Mach Number
Tw	= 5.300E+02 degR	Wall Temperature (Test Gas - Air)
Hw	= 3.183E+06 (Ft/sec) ²	Wall Enthalpy (Cp Tw)
CPf	= 5.203E-02 1/PSIA	Pressure to CP factor (1/Q)
CHf	= 6.395E-05 Ft ² -s/BTU	Heat Rate to CH factor (778/(Rho U (Ho-Hw)))
QoFR	= 5.486E+01 BTU/Ft ² -s	Fay-Riddell Heat Transfer (.25' Diam Cylin.)



HEAT TRANSFER vs Gauge Position
Run 70

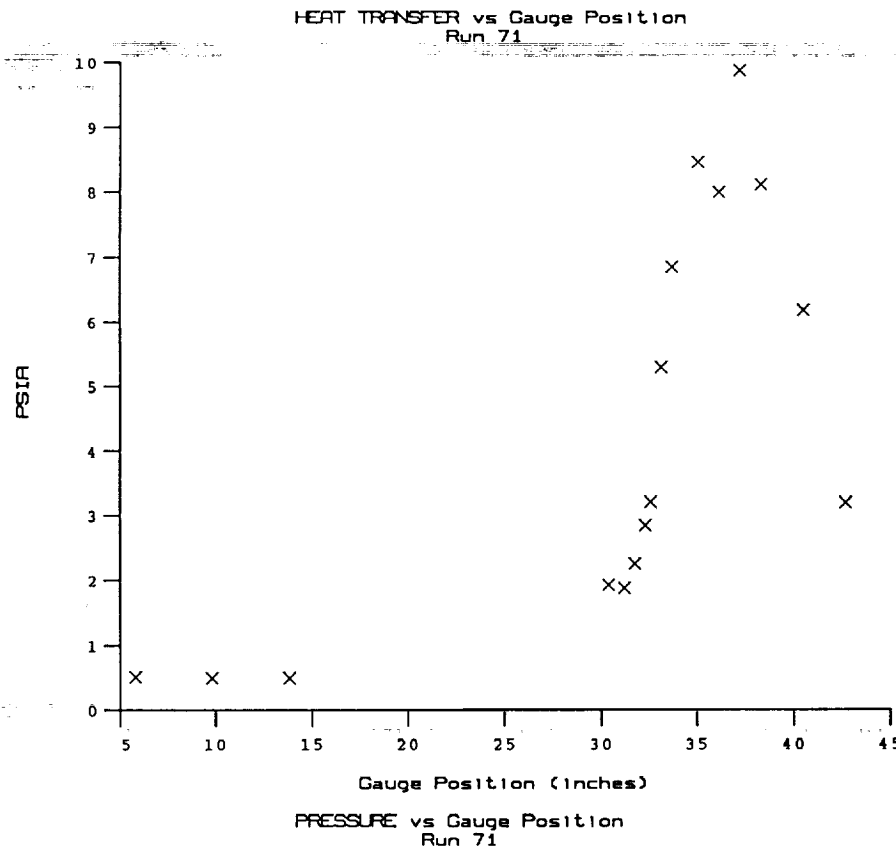
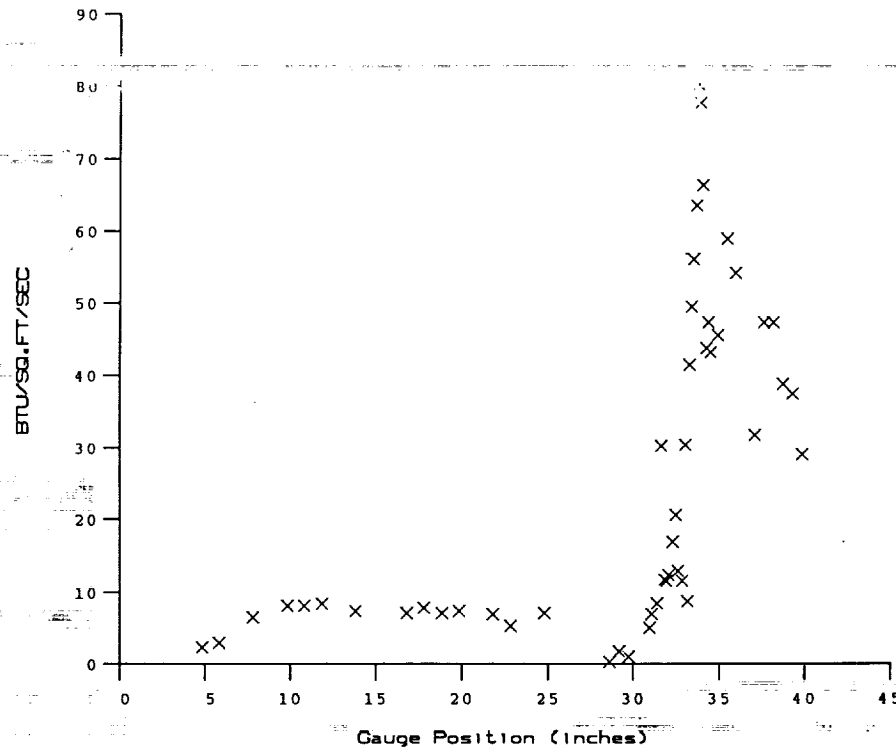


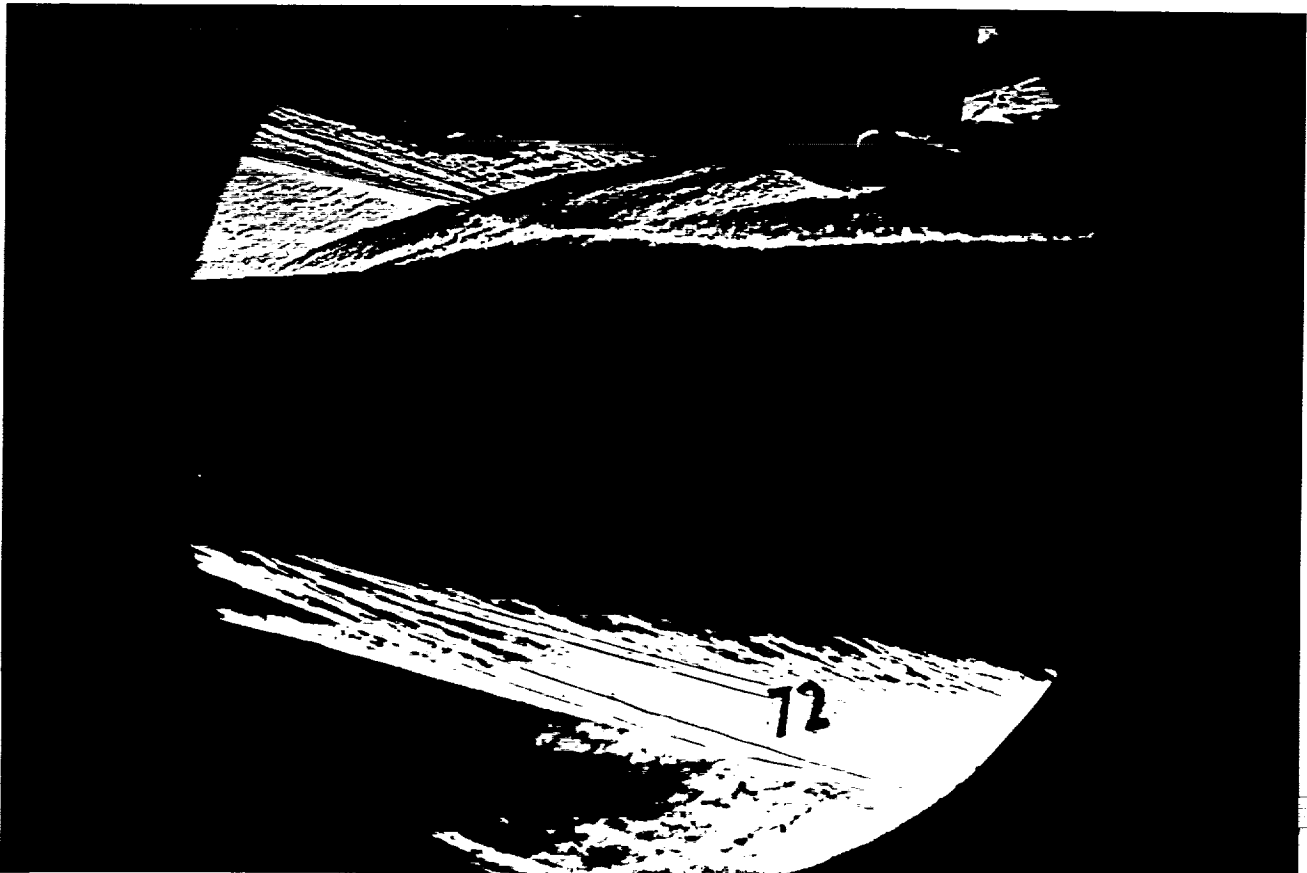
PRESSURE vs Gauge Position
Run 70



Test Conditions for Run 71 :

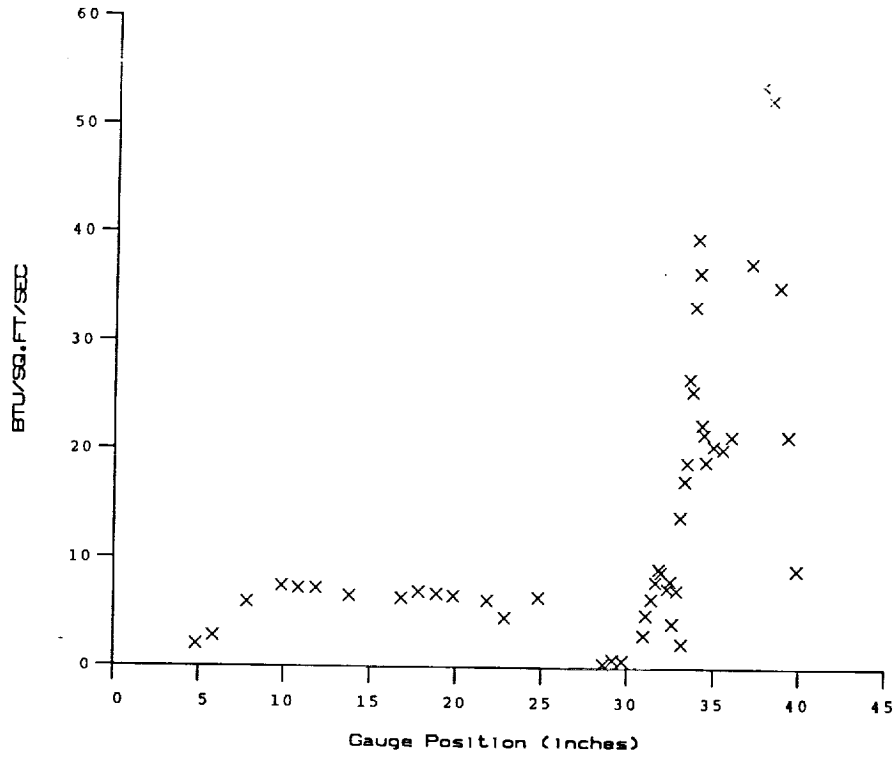
Po	- 3.858E+03 PSIA	Reservoir Total Pressure
Ho	- 1.448E+07 (Ft/sec) ²	Reservoir Total Enthalpy
To	- 2.246E+03 degR	Reservoir Total Temperature
M	- 7.865E+00	Freestream Mach Number
U	- 5.179E+03 Ft/sec	Freestream Velocity
T	- 1.803E+02 degR	Freestream Temperature
P	- 4.424E-01 PSIA	Freestream Static Pressure
Rho	- 2.059E-04 Slugs/Ft ³	Freestream Density
Mu	- 1.505E-07 Slugs/Ft-sec	Freestream Viscosity
Re	- 7.088E+06 1/Ft	Freestream Reynolds Number
Po'	- 3.543E+01 PSIA	Pitot Pressure
Q	- 1.918E+01 PSIA	Dynamic Pressure ($\rho U^2/288$)
Mi	- 2.922E+00	Shock Tube Incident Shock Mach Number
Tw	- 5.300E+02 degR	Wall Temperature (Test Gas - Air)
Hw	- 3.183E+06 (Ft/sec) ²	Wall Enthalpy (Cp Tw)
CPf	- 5.214E-02 1/PSIA	Pressure to CP factor (1/Q)
Chf	- 6.456E-05 Ft ² -s/BTU	Heat Rate to CH factor ($778/(\rho U (Ho-Hw))$)
QoFR	- 5.409E+01 BTU/Ft ² -s	Fay-Riddell Heat Transfer (.25' Diam Cylin.)



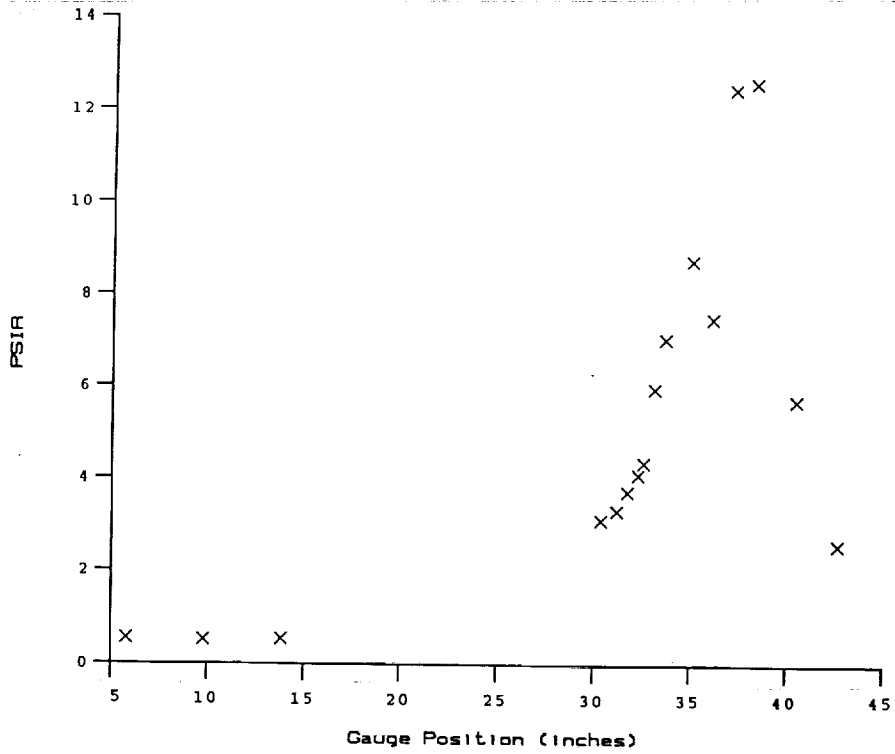


Test Conditions for Run 72 :

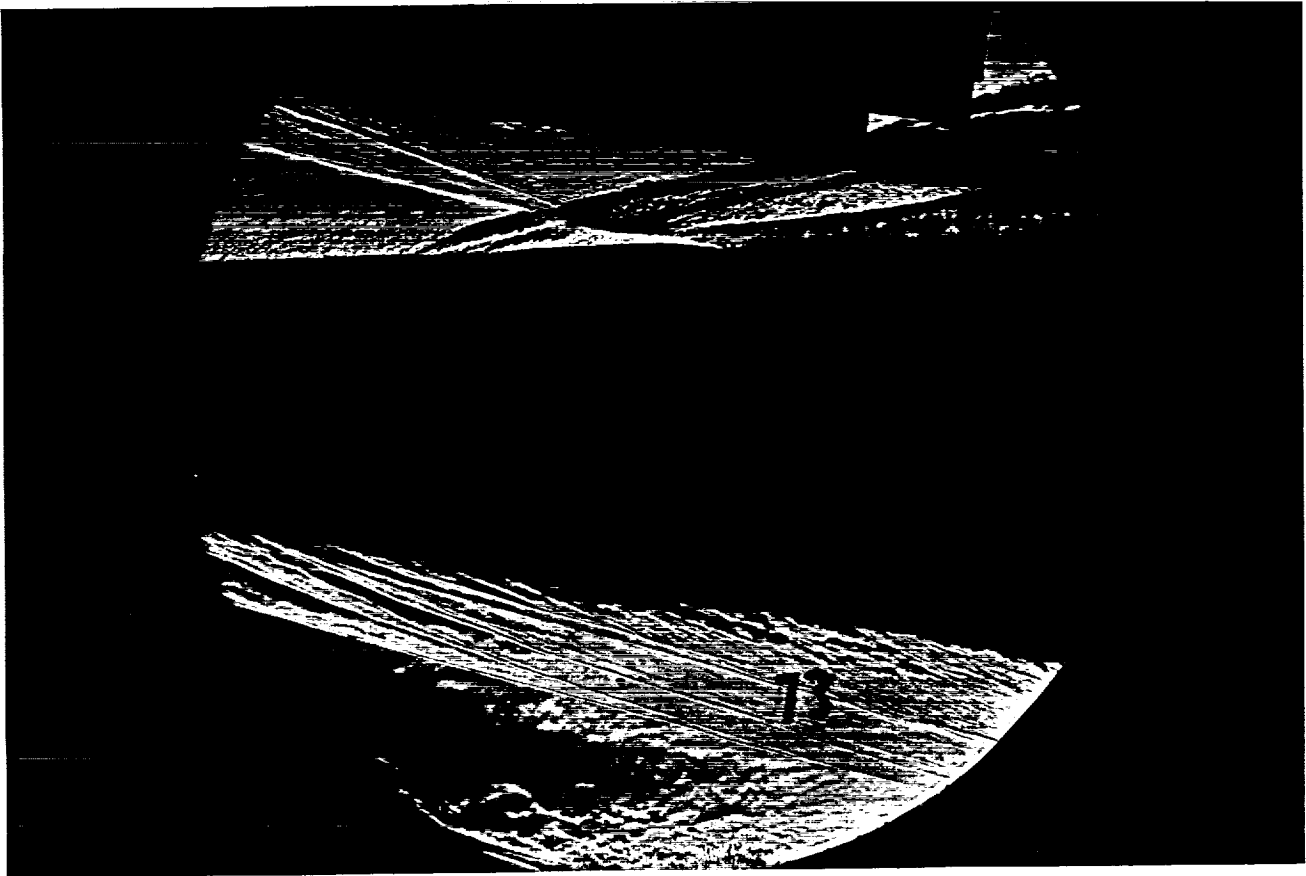
Po	= 3.935E+03 PSIA	Reservoir Total Pressure
Ho	= 1.457E+07 (Ft/sec) ²	Reservoir Total Enthalpy
To	= 2.258E+03 degR	Reservoir Total Temperature
M	= 7.869E+00	Freestream Mach Number
U	= 5.194E+03 Ft/sec	Freestream Velocity
T	= 1.812E+02 degR	Freestream Temperature
P	= 4.497E-01 PSIA	Freestream Static Pressure
Rho	= 2.083E-04 Slugs/Ft ³	Freestream Density
Mu	= 1.512E-07 Slugs/Ft-sec	Freestream Viscosity
Re	= 7.157E+06 1/Ft	Freestream Reynolds Number
Po'	= 3.604E+01 PSIA	Pitot Pressure
Q	= 1.951E+01 PSIA	Dynamic Pressure (Rho U ² /288)
Mi	= 2.921E+00	Shock Tube Incident Shock Mach Number
Tw	= 5.300E+02 degR	Wall Temperature (Test Gas = Air)
Hw	= 3.183E+06 (Ft/sec) ²	Wall Enthalpy (Cp Tw)
CPf	= 5.125E-02 1/PSIA	Pressure to CP factor (1/Q)
CHF	= 6.318E-05 Ft ² -s/BTU	Heat Rate to CH factor (778/(Rho U (Ho-Hw)))
QoFR	= 5.499E+01 BTU/Ft ² -s	Fay-Riddell Heat Transfer (.25' Diam Cylin.)



HEAT TRANSFER vs Gauge Position
Run 72

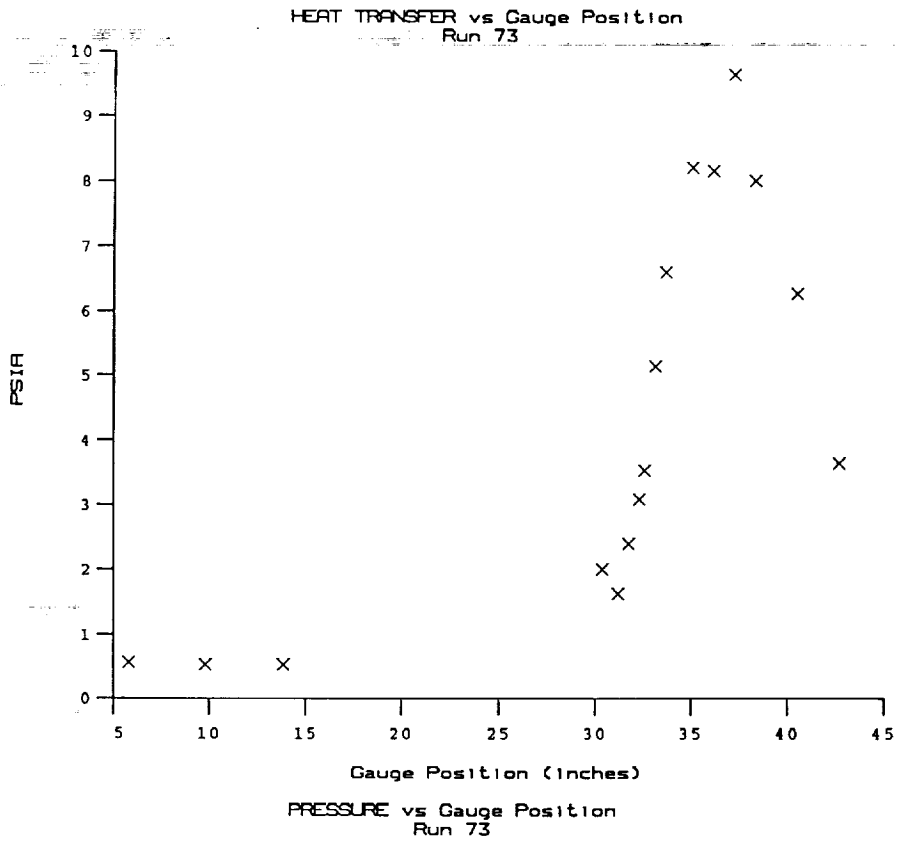
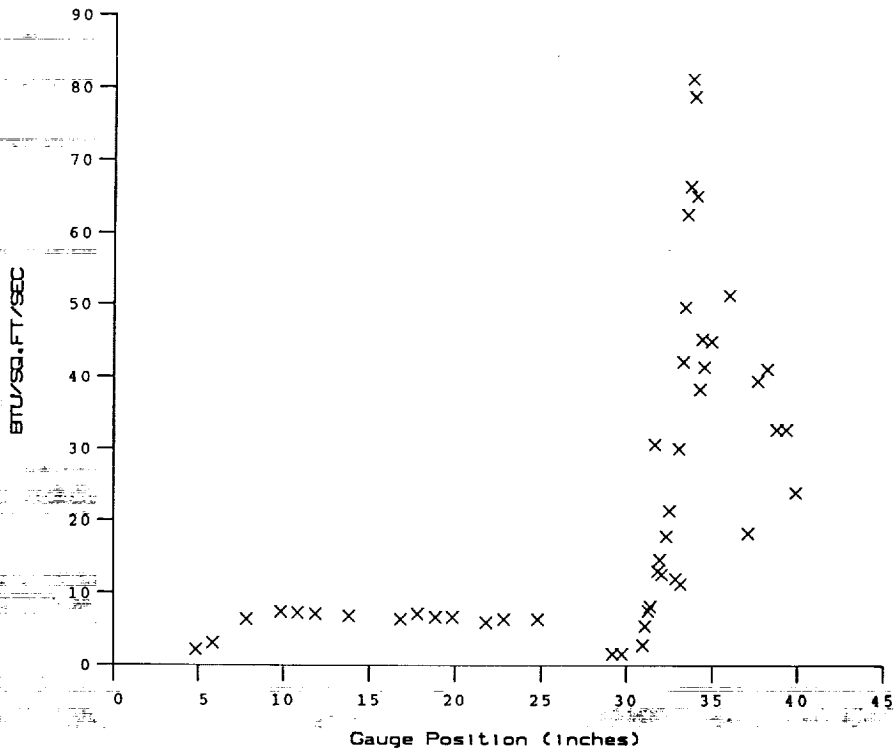


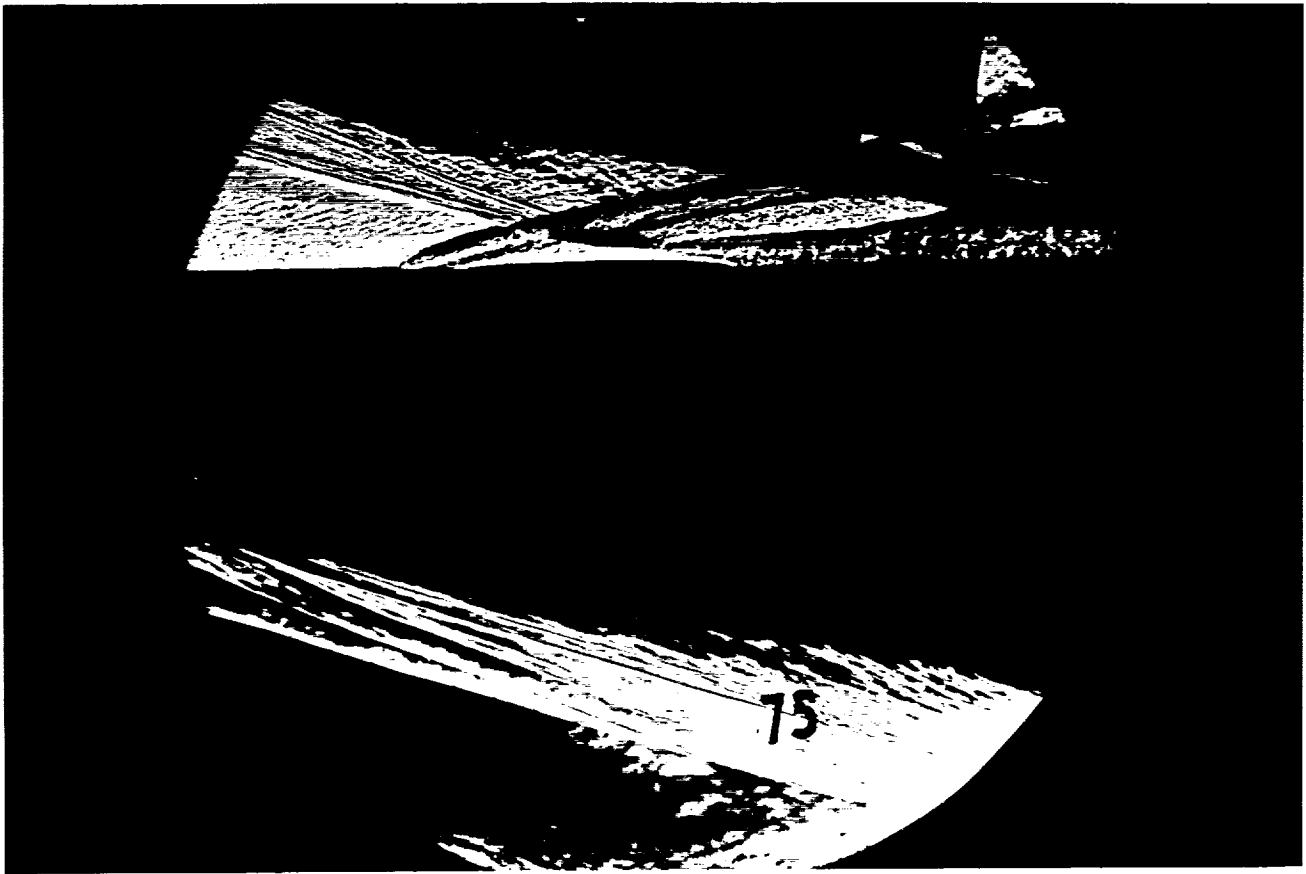
PRESSURE vs Gauge Position
Run 72



Test Conditions for Run 73 :

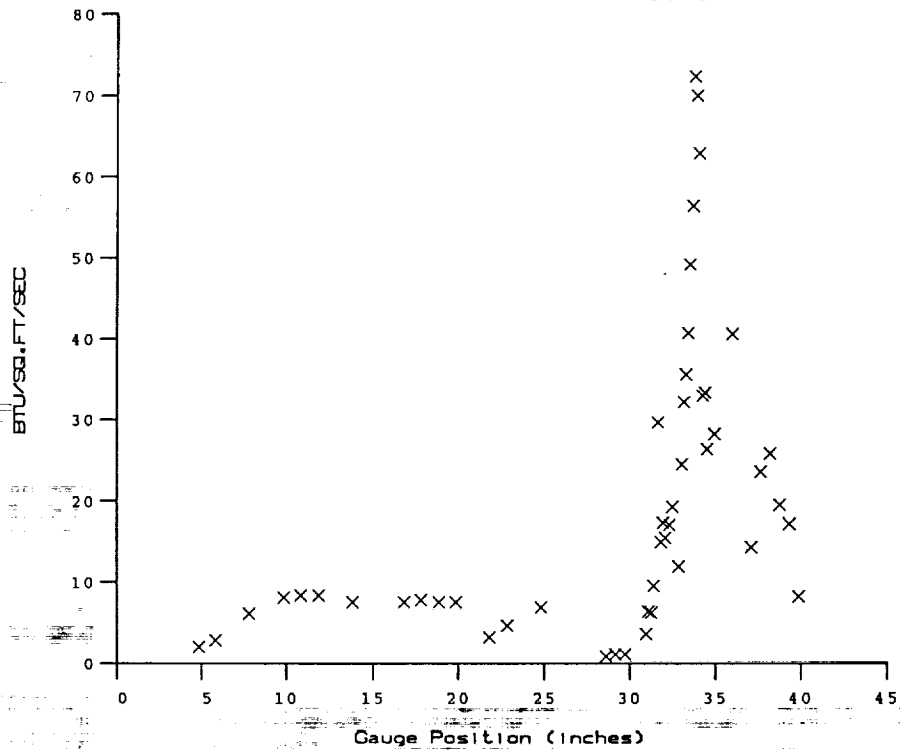
Po	= 3.906E+03 PSIA	Reservoir Total Pressure
Ho	= 1.464E+07 (Ft/sec) ²	Reservoir Total Enthalpy
To	= 2.269E+03 degR	Reservoir Total Temperature
M	= 7.867E+00	Freestream Mach Number
U	= 5.208E+03 Ft/sec	Freestream Velocity
T	= 1.822E+02 degR	Freestream Temperature
P	= 4.459E-01 PSIA	Freestream Static Pressure
Rho	= 2.054E-04 Slugs/Ft ³	Freestream Density
Mu	= 1.520E-07 Slugs/Ft-sec	Freestream Viscosity
Re	= 7.038E+06 1/Ft	Freestream Reynolds Number
Po'	= 3.573E+01 PSIA	Pitot Pressure
Q	= 1.934E+01 PSIA	Dynamic Pressure (Rho U ² /288)
Mi	= 2.920E+00	Shock Tube Incident Shock Mach Number
Tw	= 5.300E+02 degR	Wall Temperature (Test Gas = Air)
Hw	= 3.183E+06 (Ft/sec) ²	Wall Enthalpy (Cp Tw)
CPf	= 5.170E-02 1/PSIA	Pressure to CP factor (1/Q)
CHF	= 6.348E-05 Ft ² -s/BTU	Heat Rate to CH factor (778/(Rho U (Ho-Hw)))
QOFR	= 5.514E+01 BTU/Ft ² -s	Fay-Riddell Heat Transfer (.25' Diam Cylin.)



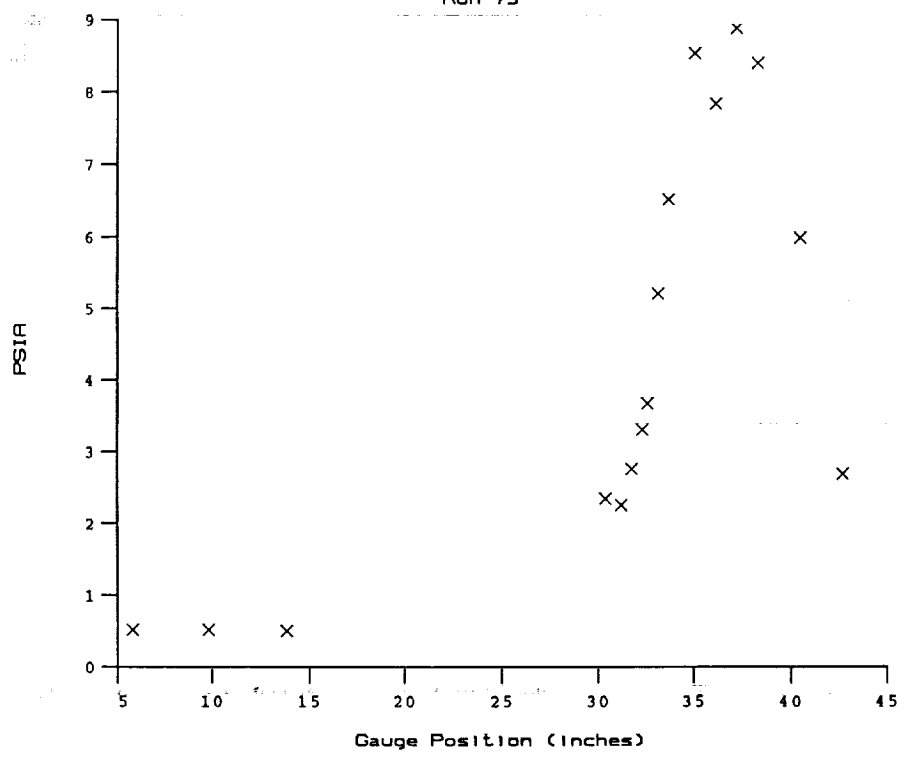


Test Conditions for Run 75 :

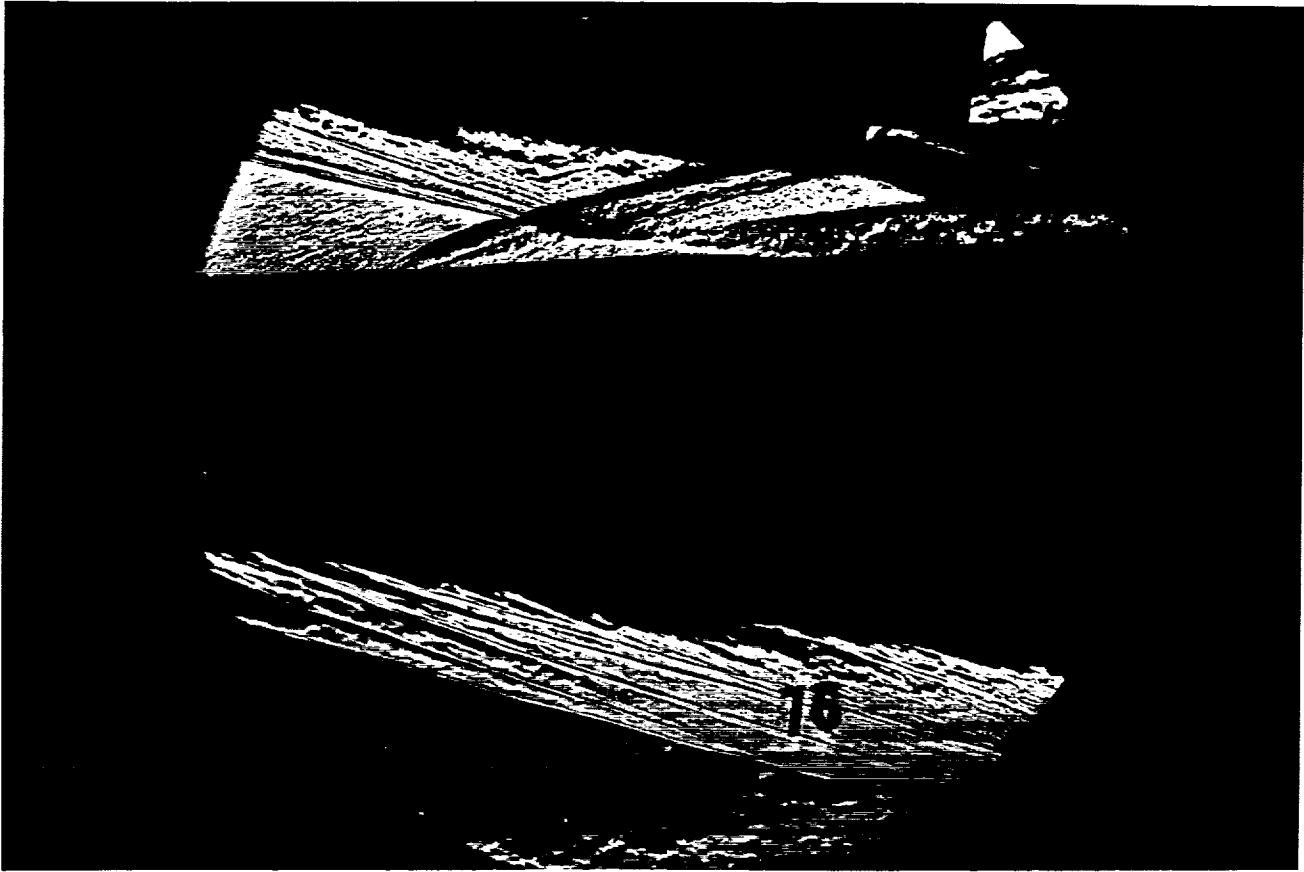
Po	= 3.946E+03 PSIA	Reservoir Total Pressure
Ho	= 1.456E+07 (Ft/sec) ²	Reservoir Total Enthalpy
To	= 2.258E+03 degR	Reservoir Total Temperature
M	= 7.868E+00	Freestream Mach Number
U	= 5.194E+03 Ft/sec	Freestream Velocity
T	= 1.812E+02 degR	Freestream Temperature
P	= 4.512E-01 PSIA	Freestream Static Pressure
Rho	= 2.090E-04 Slugs/Ft ³	Freestream Density
Mu	= 1.512E-07 Slugs/Ft-sec	Freestream Viscosity
Re	= 7.179E+06 1/Ft	Freestream Reynolds Number
Po'	= 3.616E+01 PSIA	Pitot Pressure
Q	= 1.958E+01 PSIA	Dynamic Pressure (Rho U ² /288)
Mi	= 2.924E+00	Shock Tube Incident Shock Mach Number
Tw	= 5.300E+02 degR	Wall Temperature (Test Gas = Air)
Hw	= 3.183E+06 (Ft/sec) ²	Wall Enthalpy (Cp Tw)
CPf	= 5.109E-02 1/PSIA	Pressure to CP factor (1/Q)
CHF	= 6.298E-05 Ft ² -s/BTU	Heat Rate to CH factor (778/(Rho U (Ho-Hw)))
QoFR	= 5.507E+01 BTU/Ft ² -s	Fay-Riddell Heat Transfer (.25' Diam Cylin.)



HEAT TRANSFER vs Gauge Position
Run 75

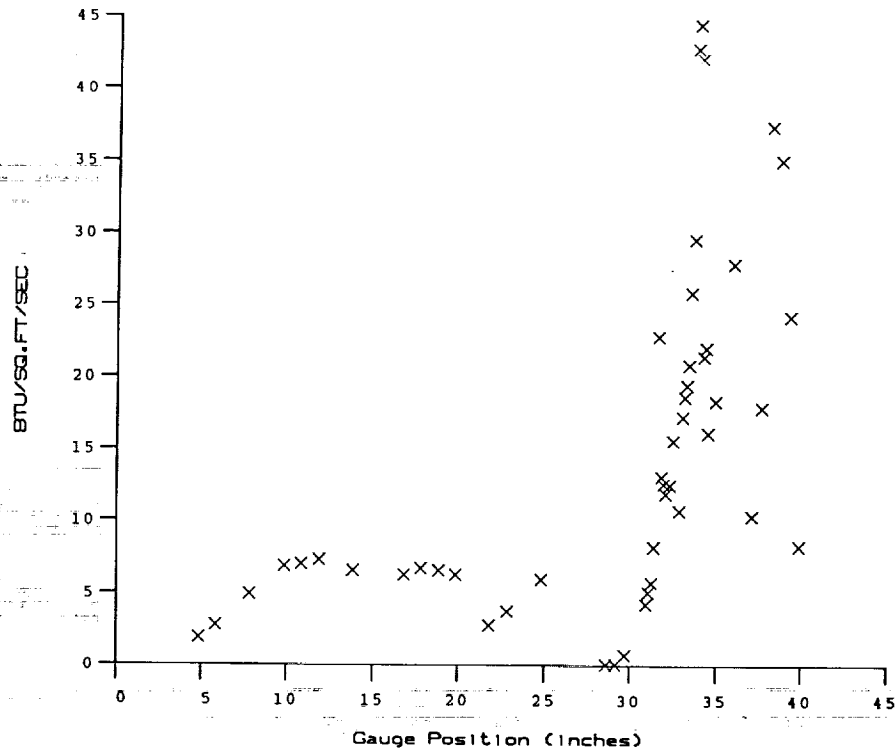


PRESSURE vs Gauge Position
Run 75

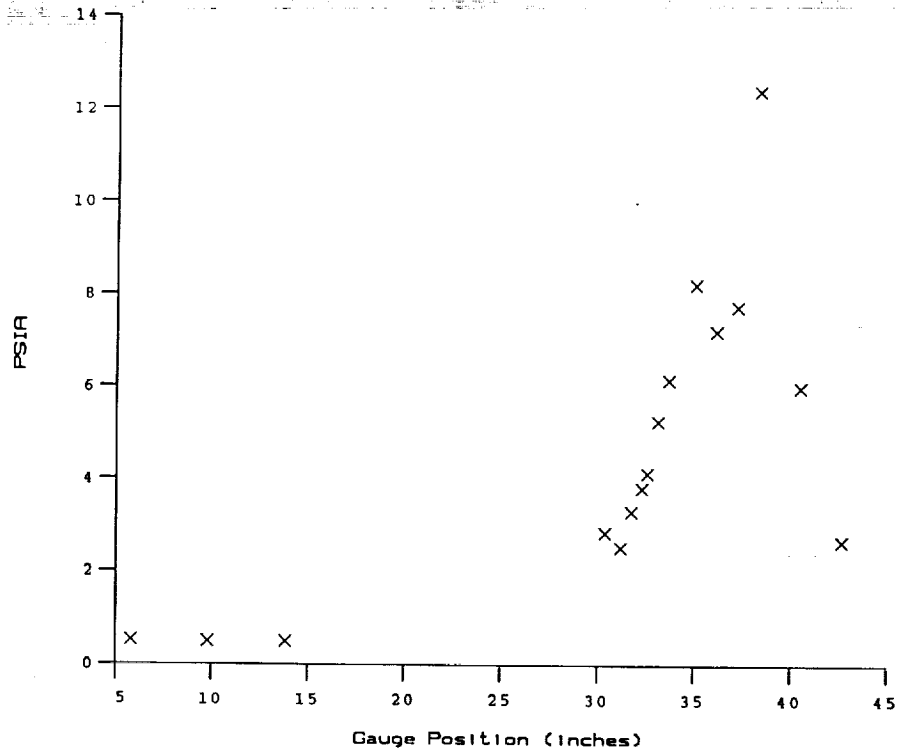


Test Conditions for Run 76 :

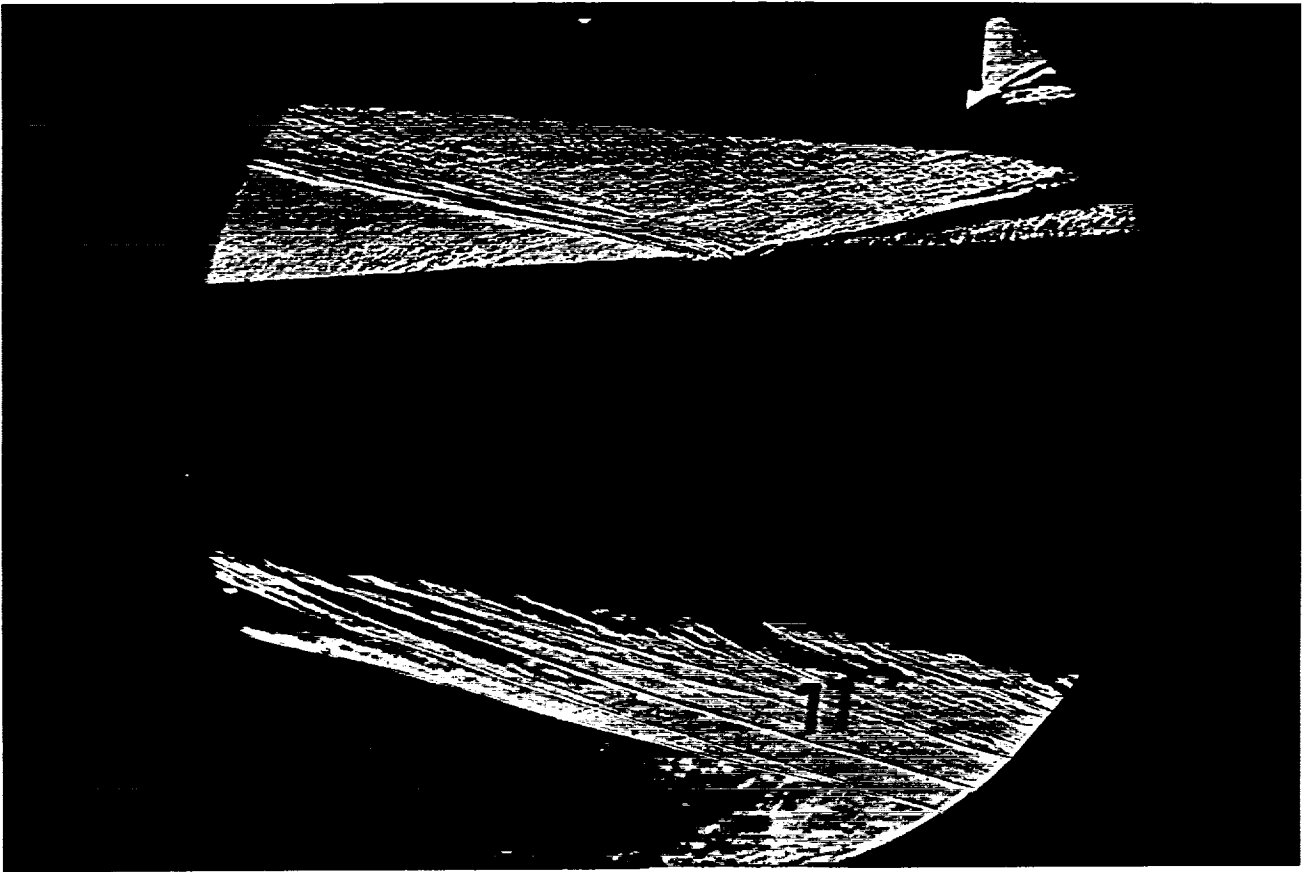
Po	= 3.898E+03 PSIA	Reservoir Total Pressure
Ho	= 1.439E+07 (Ft/sec) ²	Reservoir Total Enthalpy
To	= 2.234E+03 degR	Reservoir Total Temperature
M	= 7.873E+00	Freestream Mach Number
U	= 5.163E+03 Ft/sec	Freestream Velocity
T	= 1.789E+02 degR	Freestream Temperature
P	= 4.454E-01 PSIA	Freestream Static Pressure
Rho	= 2.090E-04 Slugs/Ft ³	Freestream Density
Mu	= 1.493E-07 Slugs/Ft-sec	Freestream Viscosity
Re	= 7.228E+06 1/Ft	Freestream Reynolds Number
Po'	= 3.573E+01 PSIA	Pitot Pressure
Q	= 1.934E+01 PSIA	Dynamic Pressure (Rho U ² /288)
Mi	= 2.899E+00	Shock Tube Incident Shock Mach Number
Tw	= 5.300E+02 degR	Wall Temperature (Test Gas = Air)
Hw	= 3.183E+06 (Ft/sec) ²	Wall Enthalpy (Cp Tw)
CPf	= 5.170E-02 1/PSIA	Pressure to CP factor (1/Q)
CHf	= 6.434E-05 Ft ² -s/BTU	Heat Rate to CH factor (778/(Rho U (Ho-Hw)))
QoFR	= 5.386E+01 BTU/Ft ² -s	Fay-Riddell Heat Transfer (.25' Diam Cylin.)



HEAT TRANSFER vs Gauge Position
Run 76

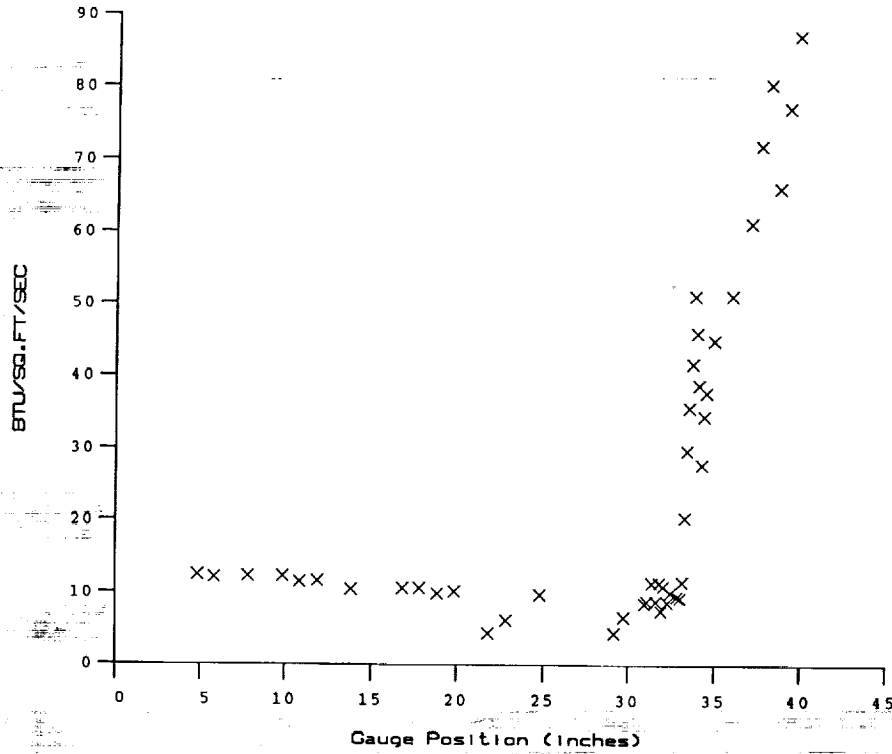


PRESSURE vs Gauge Position
Run 76

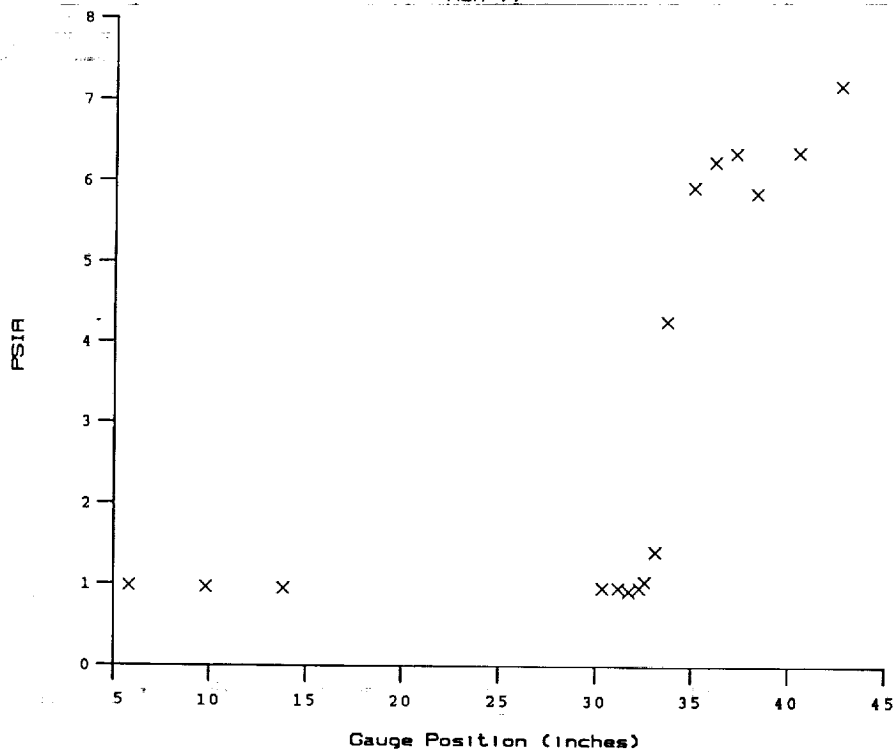


Test Conditions for Run 77 :

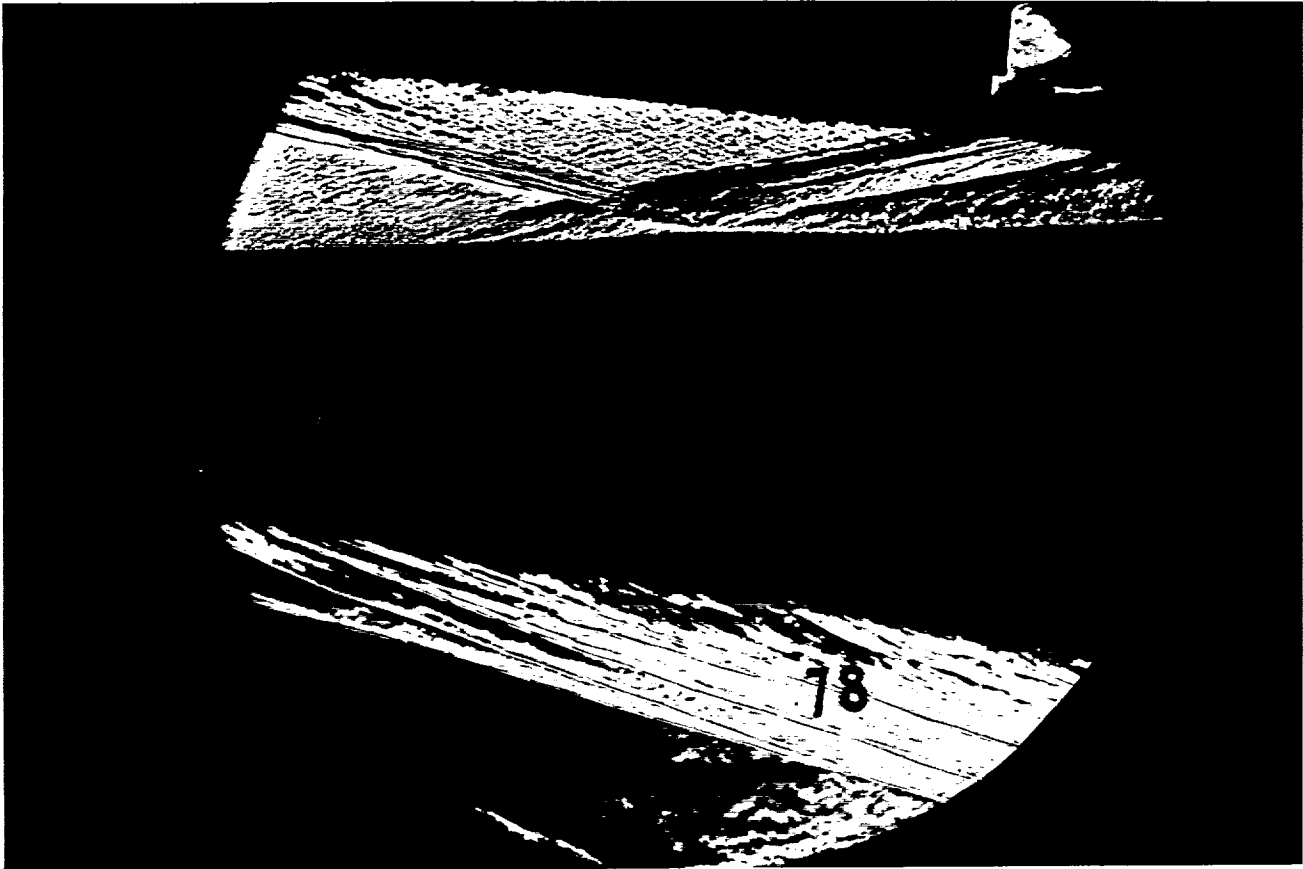
Po	= 2.248E+03 PSIA	Reservoir Total Pressure
Ho	= 1.371E+07 (Ft/sec) ²	Reservoir Total Enthalpy
To	= 2.148E+03 degR	Reservoir Total Temperature
M	= 6.424E+00	Freestream Mach Number
U	= 4.948E+03 Ft/sec	Freestream Velocity
T	= 2.467E+02 degR	Freestream Temperature
P	= 9.195E-01 PSIA	Freestream Static Pressure
Rho	= 3.128E-04 Slugs/Ft ³	Freestream Density
Mu	= 2.023E-07 Slugs/Ft-sec	Freestream Viscosity
Re	= 7.649E+06 1/Ft	Freestream Reynolds Number
Po'	= 4.958E+01 PSIA	Pitot Pressure
Q	= 2.659E+01 PSIA	Dynamic Pressure (Rho U ² /288)
Mi	= 2.831E+00	Shock Tube Incident Shock Mach Number
Tw	= 5.300E+02 degR	Wall Temperature (Test Gas = Air)
Hw	= 3.183E+06 (Ft/sec) ²	Wall Enthalpy (Cp Tw)
CPf	= 3.760E-02 1/PSIA	Pressure to CP factor (1/Q)
CHf	= 4.774E-05 Ft ² -s/BTU	Heat Rate to CH factor (778/(Rho U (Ho-Hw)))
QoFR	= 5.932E+01 BTU/Ft ² -s	Fay-Riddell Heat Transfer (.25' Diam Cylin.)



HEAT TRANSFER vs Gauge Position
Run 77

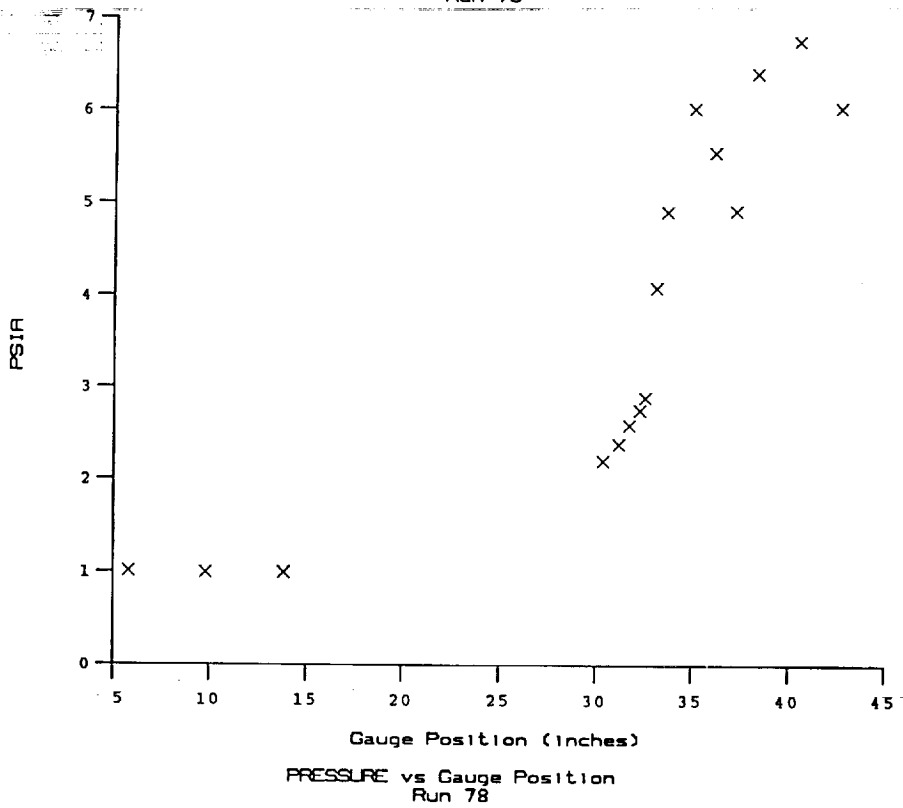
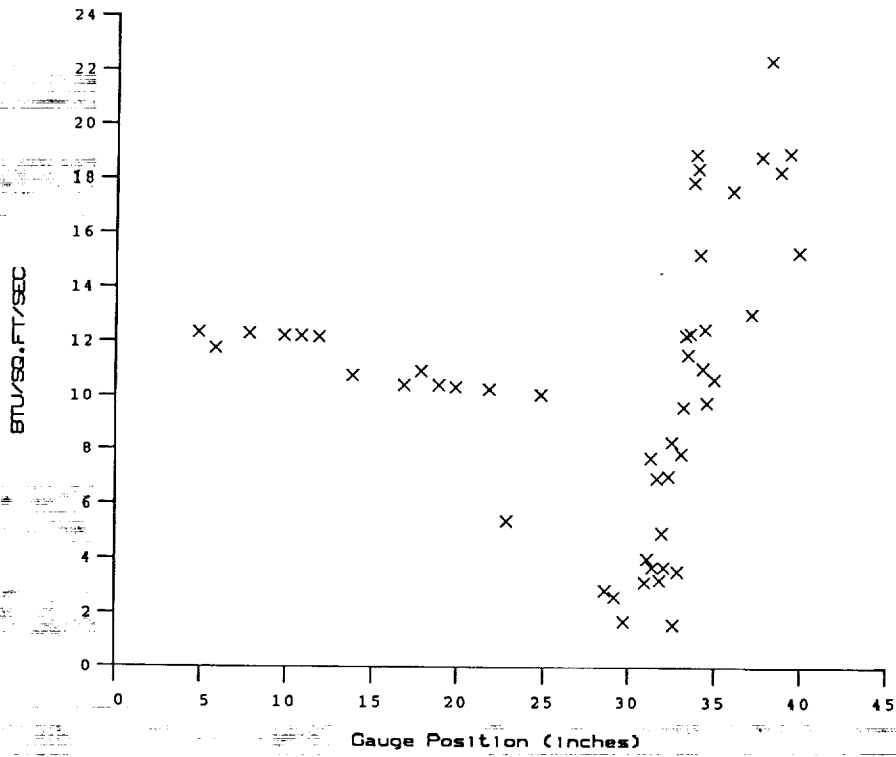


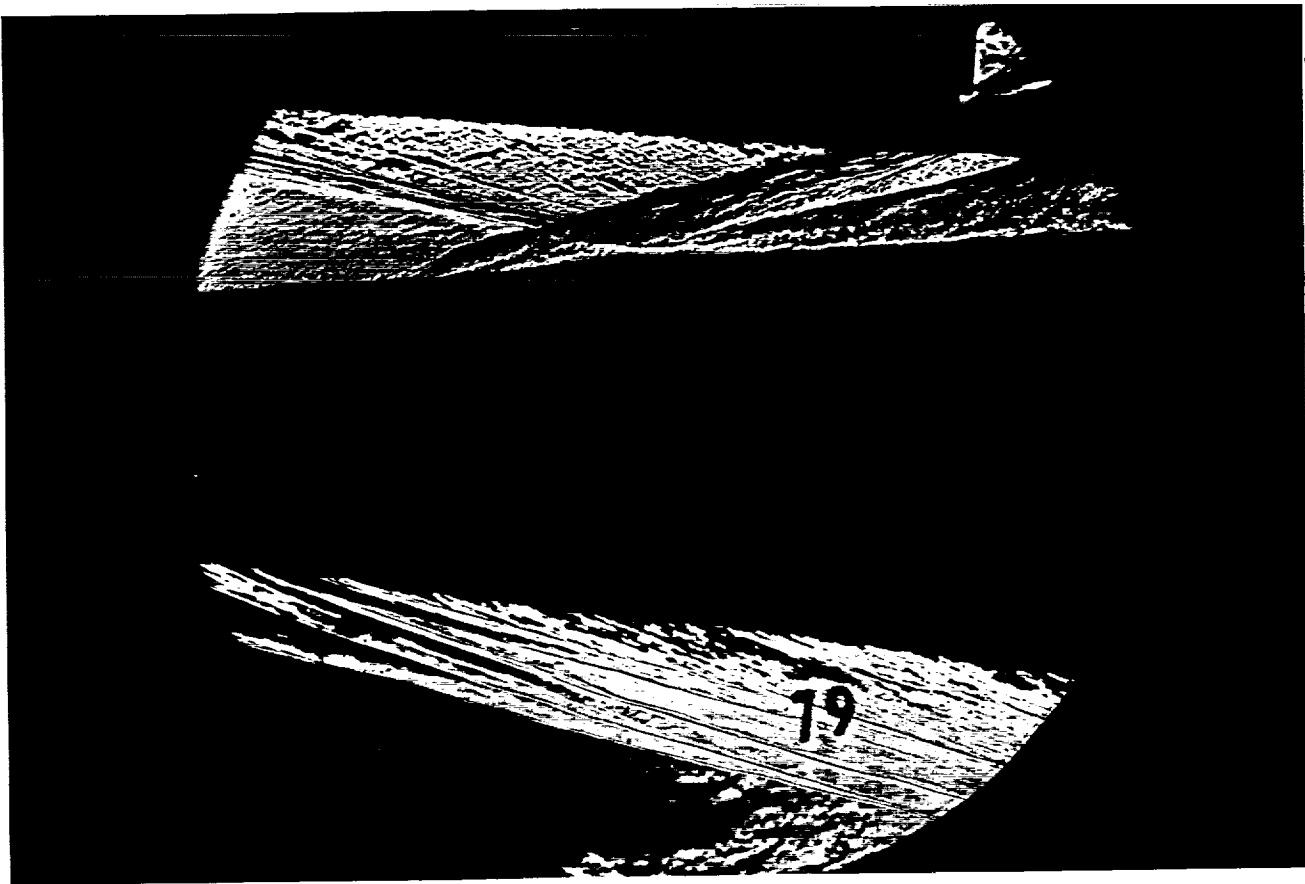
PRESSURE vs Gauge Position
Run 77



Test Conditions for Run 78 :

Po	- 2.252E+03 PSIA	Reservoir Total Pressure
Ho	- 1.370E+07 (Ft/sec) ²	Reservoir Total Enthalpy
To	- 2.146E+03 degR	Reservoir Total Temperature
M	- 6.425E+00	Freestream Mach Number
U	- 4.946E+03 Ft/sec	Freestream Velocity
T	- 2.464E+02 degR	Freestream Temperature
P	- 9.208E-01 PSIA	Freestream Static Pressure
Rho	- 3.136E-04 Slugs/Ft ³	Freestream Density
Mu	- 2.021E-07 Slugs/Ft-sec	Freestream Viscosity
Re	- 7.673E+06 1/Ft	Freestream Reynolds Number
Po'	- 4.966E+01 PSIA	Pitot Pressure
Q	- 2.664E+01 PSIA	Dynamic Pressure ($\rho U^2/288$)
Mi	- 2.829E+00	Shock Tube Incident Shock Mach Number
Tw	- 5.300E+02 degR	Wall Temperature (Test Gas - Air)
Hw	- 3.183E+06 (Ft/sec) ²	Wall Enthalpy ($C_p T_w$)
CPf	- 3.754E-02 1/PSIA	Pressure to CP factor (1/Q)
CHf	- 4.769E-05 Ft ² -s/BTU	Heat Rate to CH factor ($778/(\rho U (H_o - H_w))$)
QoFR	- 5.930E+01 BTU/Ft ² -s	Fay-Riddell Heat Transfer (.25' Diam Cylin.)

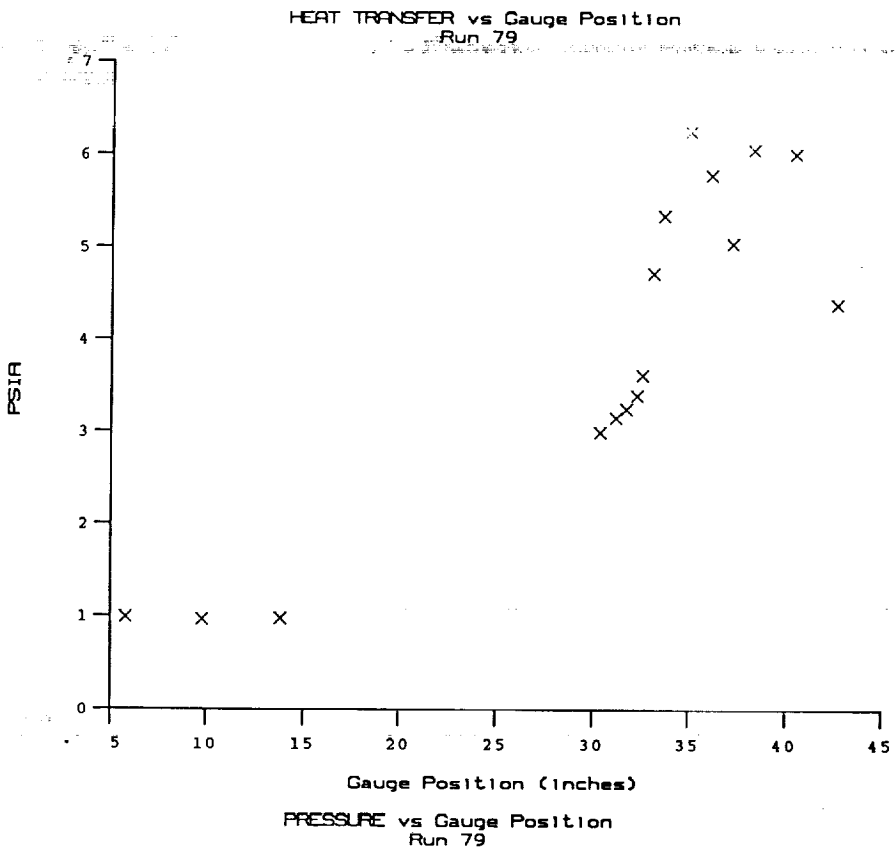
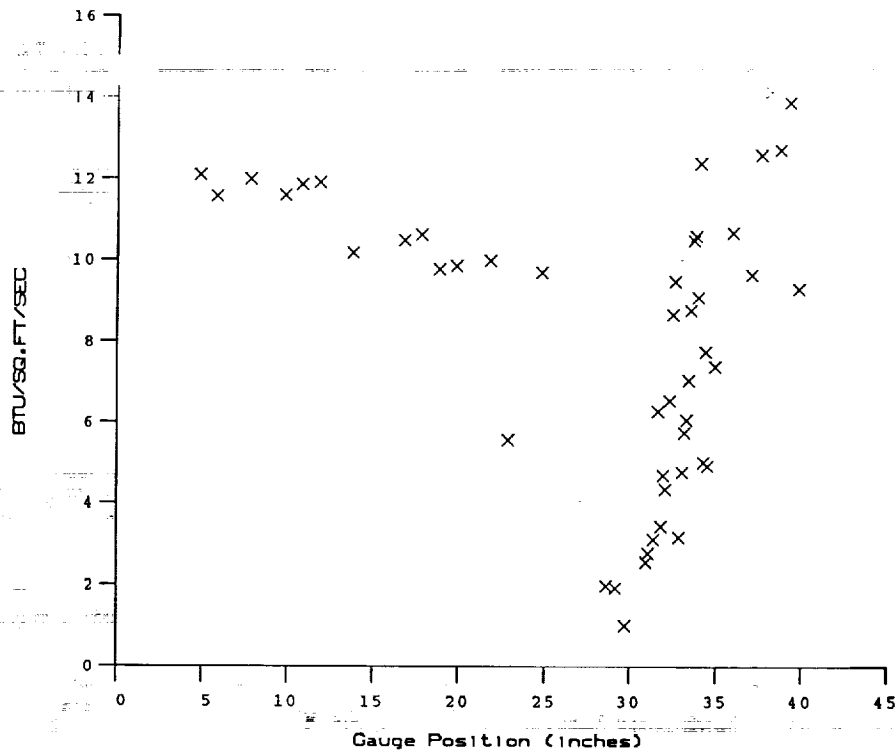


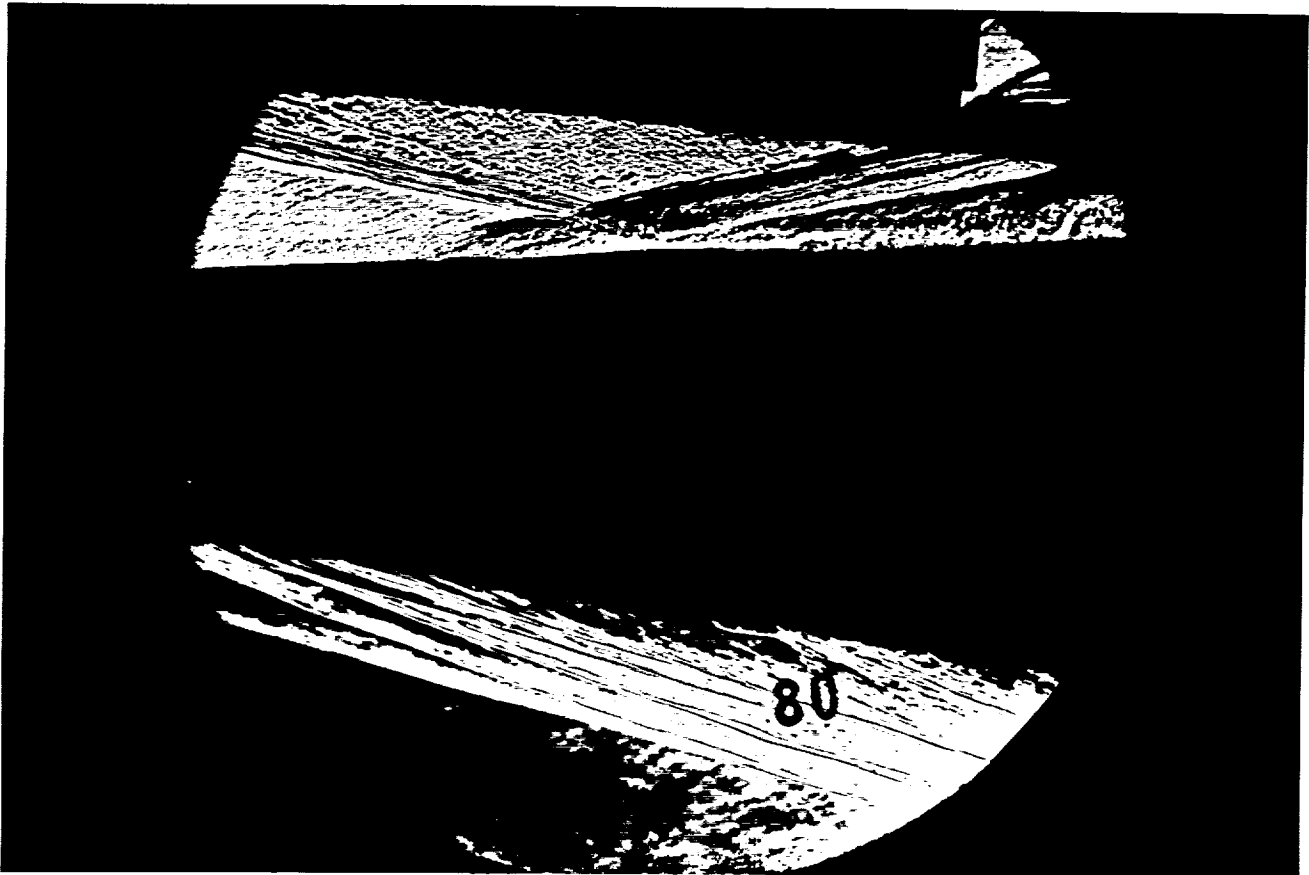


Test Conditions for Run 79 :

Po = 2.207E+03 PSIA
 Ho = 1.358E+07 (Ft/sec)²
 To = 2.129E+03 degR
 M = 6.426E+00
 U = 4.924E+03 Ft/sec
 T = 2.441E+02 degR
 P = 9.027E-01 PSIA
 Rho = 3.103E-04 Slugs/Ft³
 Mu = 2.004E-07 Slugs/Ft-sec
 Re = 7.623E+06 1/Ft
 Po' = 4.869E+01 PSIA
 Q = 2.612E+01 PSIA
 Mi = 2.811E+00
 Tw = 5.300E+02 degR
 Hw = 3.183E+06 (Ft/sec)²
 CPf = 3.828E-02 1/PSIA
 CHF = 4.899E-05 Ft²-s/BTU
 QoFR = 5.800E+01 BTU/Ft²-s

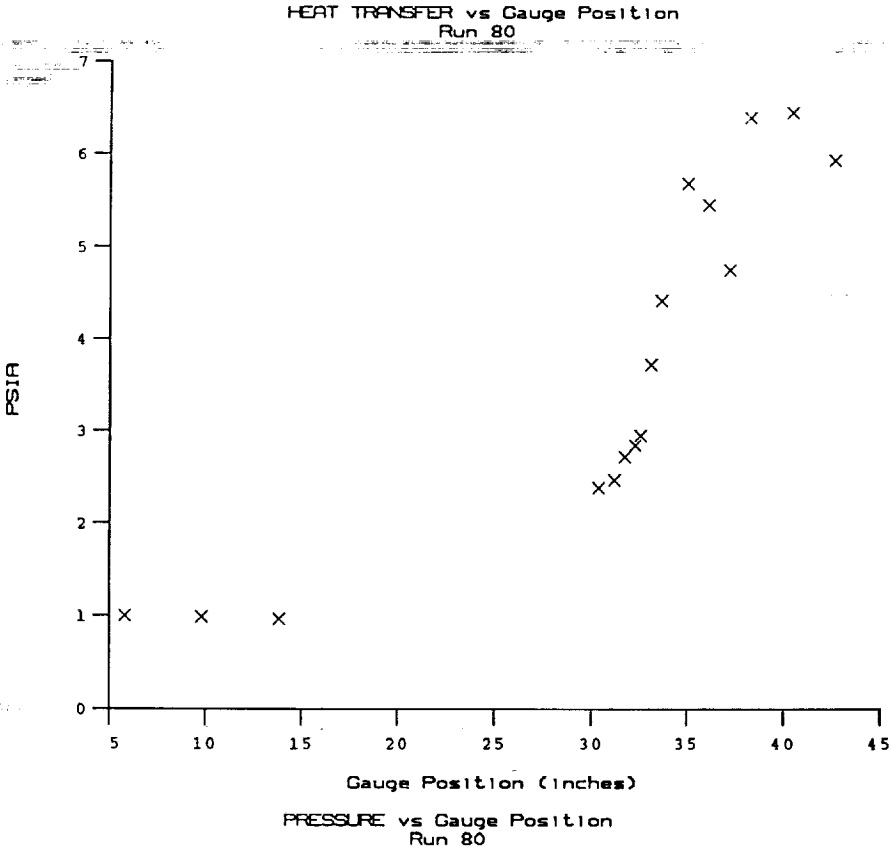
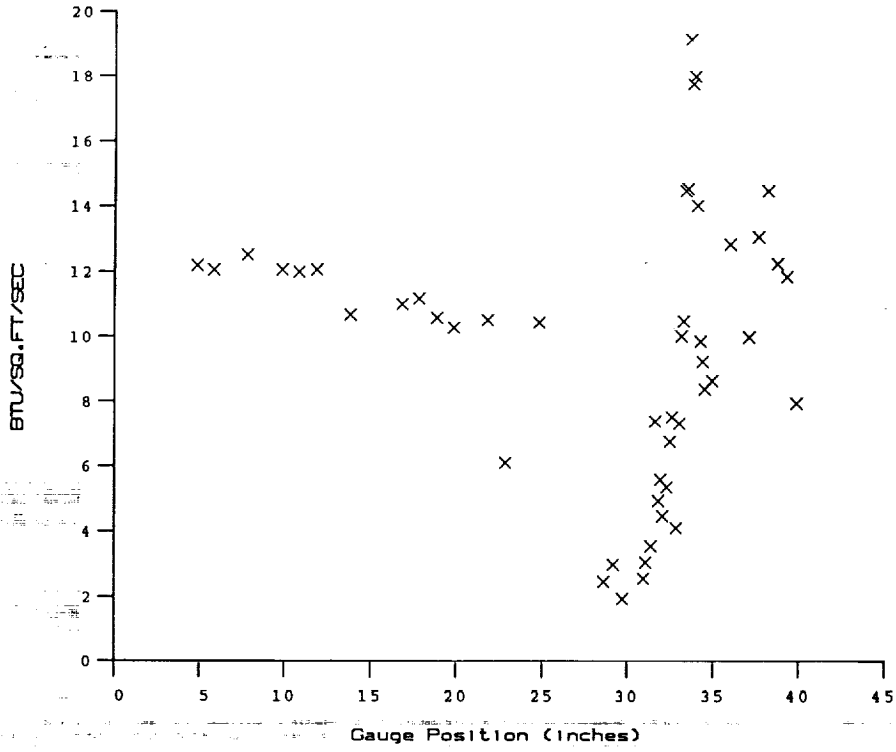
Reservoir Total Pressure
 Reservoir Total Enthalpy
 Reservoir Total Temperature
 Freestream Mach Number
 Freestream Velocity
 Freestream Temperature
 Freestream Static Pressure
 Freestream Density
 Freestream Viscosity
 Freestream Reynolds Number
 Pitot Pressure
 Dynamic Pressure ($\rho U^2/288$)
 Shock Tube Incident Shock Mach Number
 Wall Temperature (Test Gas = Air)
 Wall Enthalpy ($C_p T_w$)
 Pressure to CP factor ($1/Q$)
 Heat Rate to CH factor ($778/(\rho U (H_o - H_w))$)
 Fay-Riddell Heat Transfer (.25' Diam Cylin.)

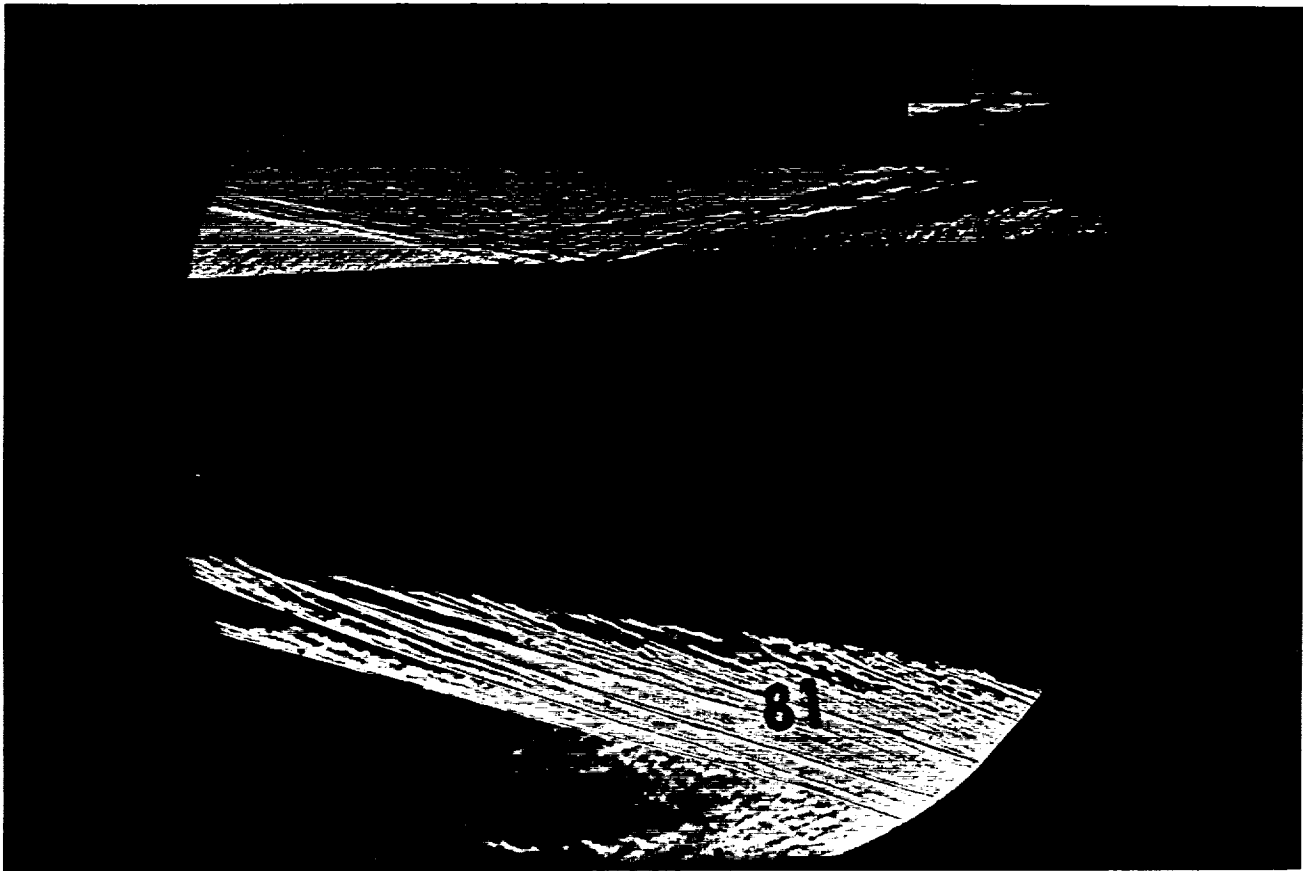




Test Conditions for Run 80 :

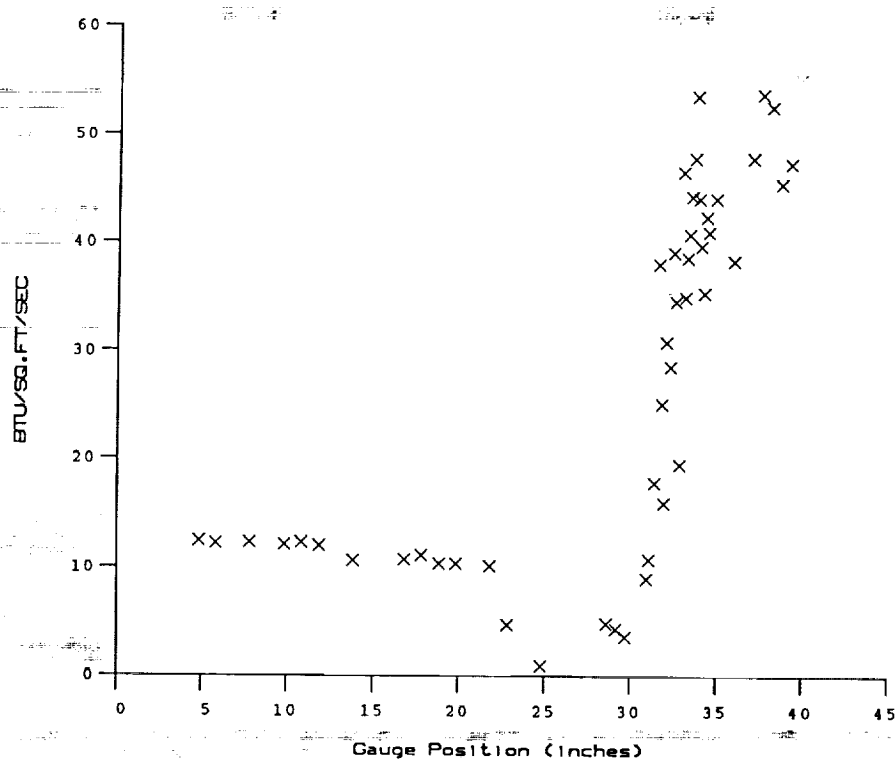
Po	= 2.232E+03 PSIA	Reservoir Total Pressure
Ho	= 1.375E+07 (Ft/sec) ²	Reservoir Total Enthalpy
To	= 2.153E+03 degR	Reservoir Total Temperature
M	= 6.425E+00	Freestream Mach Number
U	= 4.955E+03 Ft/sec	Freestream Velocity
T	= 2.473E+02 degR	Freestream Temperature
P	= 9.115E-01 PSIA	Freestream Static Pressure
Rho	= 3.093E-04 Slugs/Ft ³	Freestream Density
Mu	= 2.028E-07 Slugs/Ft-sec	Freestream Viscosity
Re	= 7.558E+06 1/Ft	Freestream Reynolds Number
Po'	= 4.916E+01 PSIA	Pitot Pressure
Q	= 2.637E+01 PSIA	Dynamic Pressure ($\rho U^2/288$)
Mi	= 2.824E+00	Shock Tube Incident Shock Mach Number
Tw	= 5.300E+02 degR	Wall Temperature (Test Gas = Air)
Hw	= 3.183E+06 (Ft/sec) ²	Wall Enthalpy ($C_p T_w$)
CPf	= 3.793E-02 1/PSIA	Pressure to CP factor (1/Q)
CHF	= 4.805E-05 Ft ² -s/BTU	Heat Rate to CH factor ($778/(\rho U (H_o - H_w))$)
QoFR	= 5.928E+01 BTU/Ft ² -s	Fay-Riddell Heat Transfer (.25' Diam Cylin.)



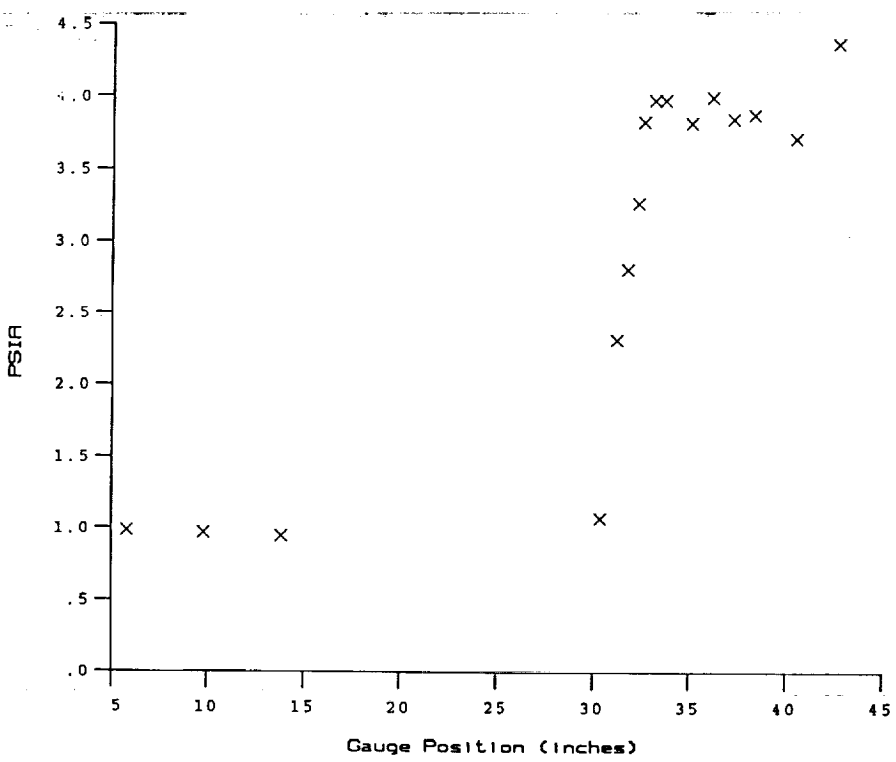


Test Conditions for Run 81 :

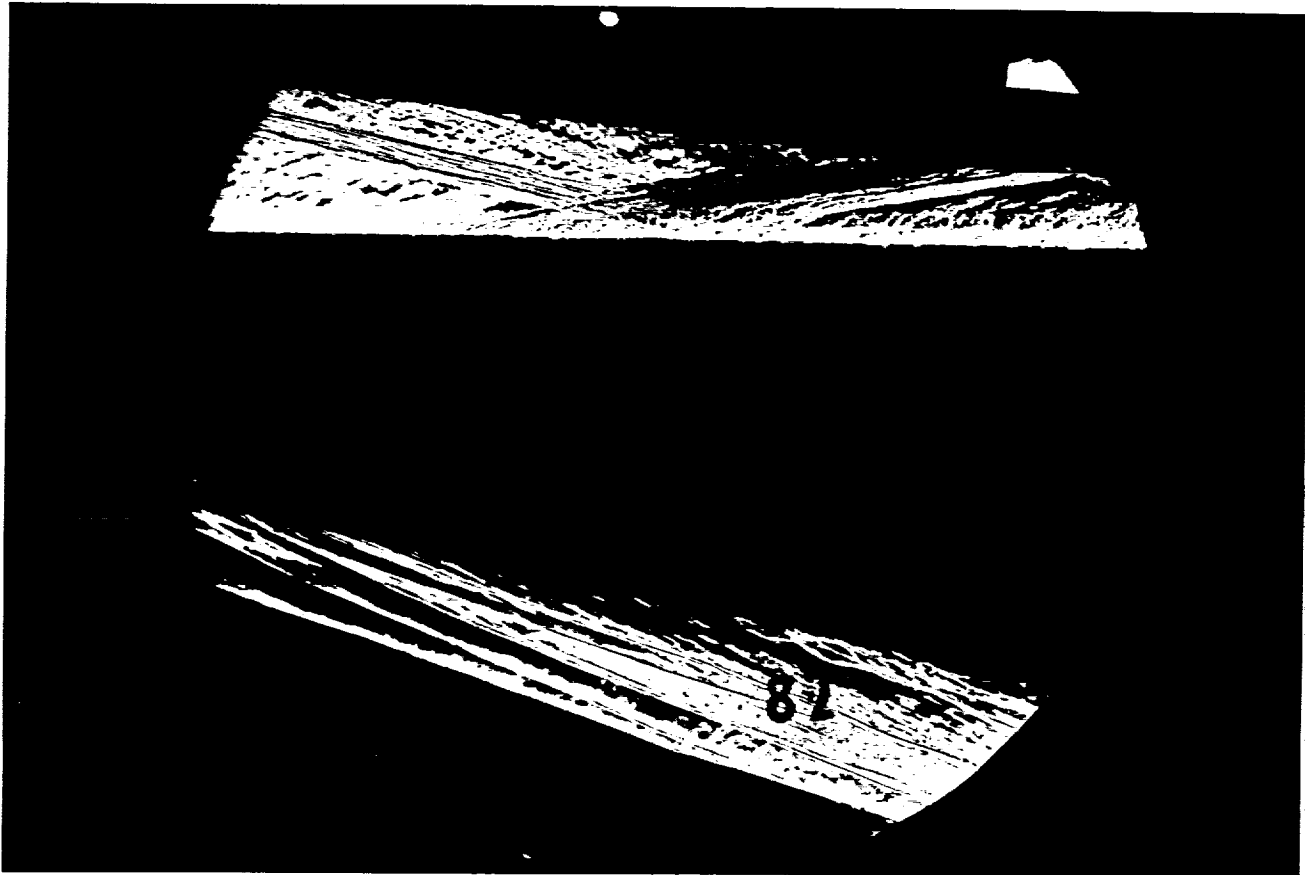
Po	= 2.233E+03 PSIA	Reservoir Total Pressure
Ho	= 1.375E+07 (Ft/sec) ²	Reservoir Total Enthalpy
To	= 2.154E+03 degR	Reservoir Total Temperature
M	= 6.425E+00	Freestream Mach Number
U	= 4.956E+03 Ft/sec	Freestream Velocity
T	= 2.474E+02 degR	Freestream Temperature
P	= 9.122E-01 PSIA	Freestream Static Pressure
Rho	= 3.094E-04 Slugs/Ft ³	Freestream Density
Mu	= 2.029E-07 Slugs/Ft-sec	Freestream Viscosity
Re	= 7.557E+06 1/Ft	Freestream Reynolds Number
Po'	= 4.919E+01 PSIA	Pitot Pressure
Q	= 2.639E+01 PSIA	Dynamic Pressure (Rho U ² /288)
Mi	= 2.826E+00	Shock Tube Incident Shock Mach Number
Tw	= 5.300E+02 degR	Wall Temperature (Test Gas = Air)
Hw	= 3.183E+06 (Ft/sec) ²	Wall Enthalpy (Cp Tw)
CPf	= 3.790E-02 1/PSIA	Pressure to CP factor (1/Q)
CHf	= 4.800E-05 Ft ² -s/BTU	Heat Rate to CH factor (778/(Rho U (Ho-Hw)))
QoFR	= 5.934E+01 BTU/Ft ² -s	Fay-Riddell Heat Transfer (.25' Diam Cylin.)



HEAT TRANSFER vs Gauge Position
Run 81

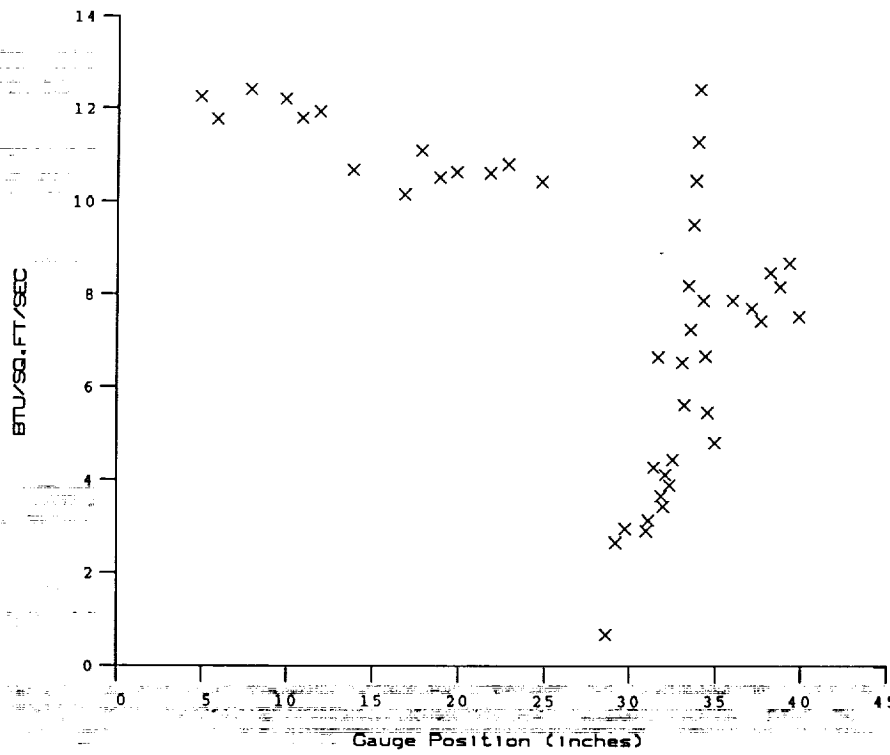


PRESSURE vs Gauge Position
Run 81

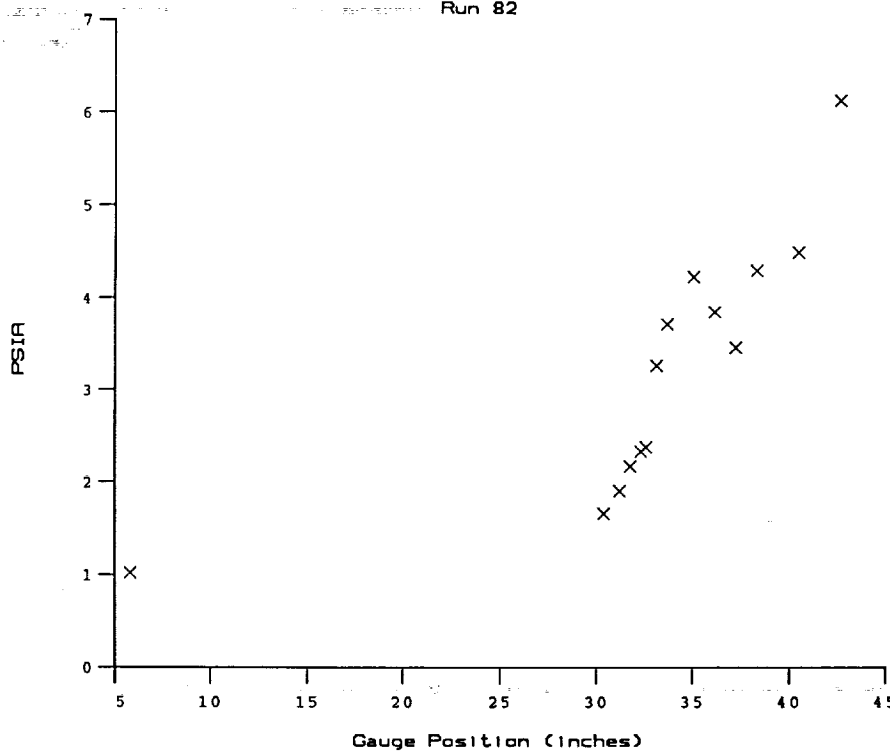


Test Conditions for Run 82 :

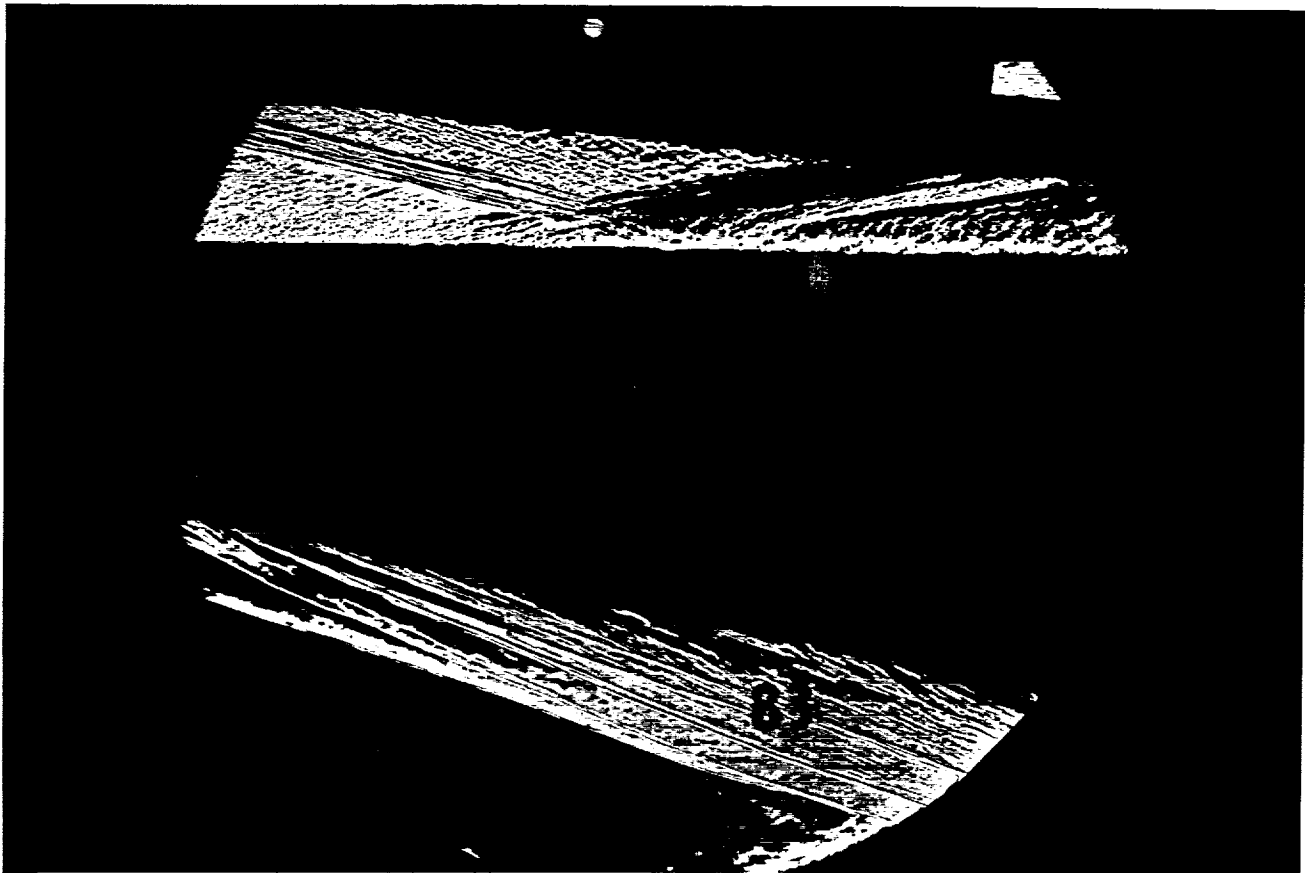
Po	= 2.393E+03 PSIA	Reservoir Total Pressure
Ho	= 1.417E+07 (Ft/sec) ²	Reservoir Total Enthalpy
To	= 2.211E+03 degR	Reservoir Total Temperature
M	= 6.421E+00	Freestream Mach Number
U	= 5.029E+03 Ft/sec	Freestream Velocity
T	= 2.551E+02 degR	Freestream Temperature
P	= 9.766E-01 PSIA	Freestream Static Pressure
Rho	= 3.213E-04 Slugs/Ft ³	Freestream Density
Mu	= 2.086E-07 Slugs/Ft-sec	Freestream Viscosity
Re	= 7.744E+06 1/Ft	Freestream Reynolds Number
Po'	= 5.263E+01 PSIA	Pitot Pressure
Q	= 2.822E+01 PSIA	Dynamic Pressure (Rho U ² /288)
Mi	= 2.883E+00	Shock Tube Incident Shock Mach Number
Tw	= 5.300E+02 degR	Wall Temperature (Test Gas = Air)
Hw	= 3.183E+06 (Ft/sec) ²	Wall Enthalpy (Cp Tw)
CPf	= 3.544E-02 1/PSIA	Pressure to CP factor (1/Q)
CHf	= 4.384E-05 Ft ² -s/BTU	Heat Rate to CH factor (778/(Rho U (Ho-Hw)))
QoFR	= 6.390E+01 BTU/Ft ² -s	Fay-Riddell Heat Transfer (.25' Diam Cylin.)



HEAT TRANSFER vs Gauge Position
Run 82

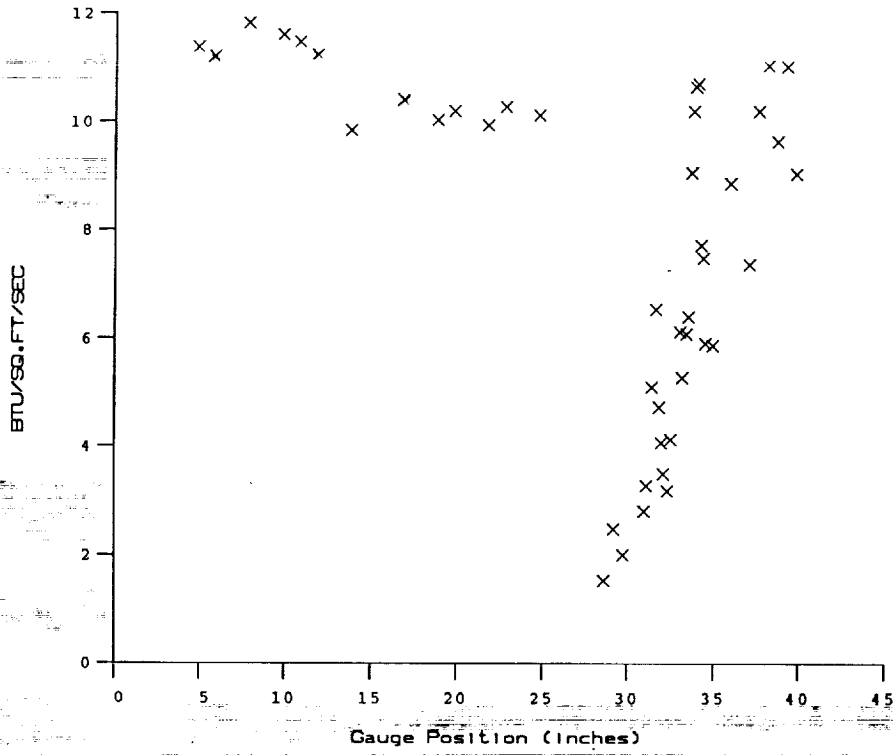


PRESSURE vs Gauge Position
Run 82

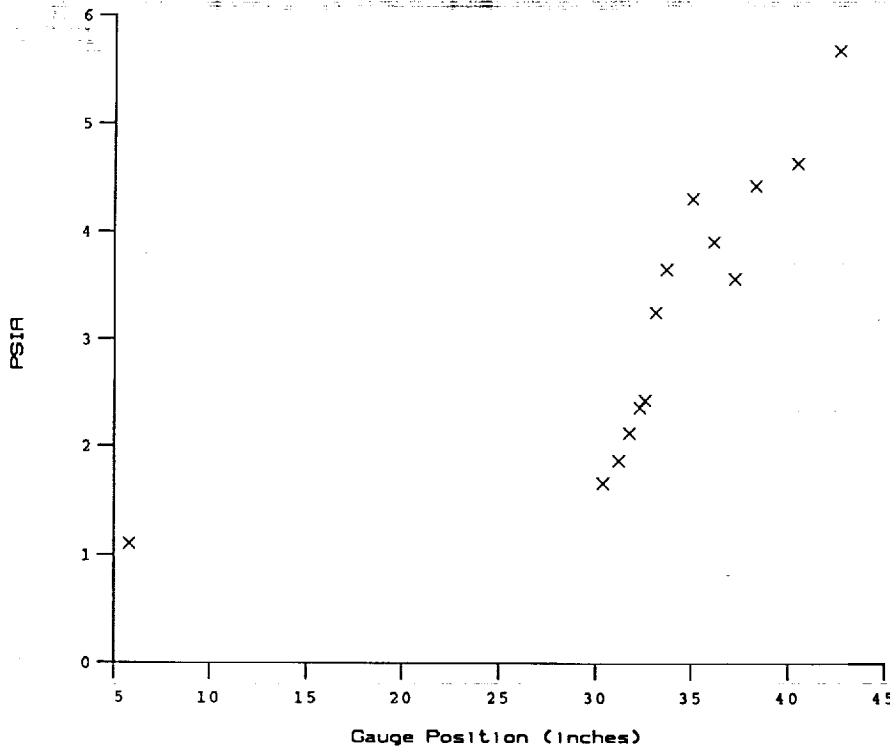


Test Conditions for Run 83 :

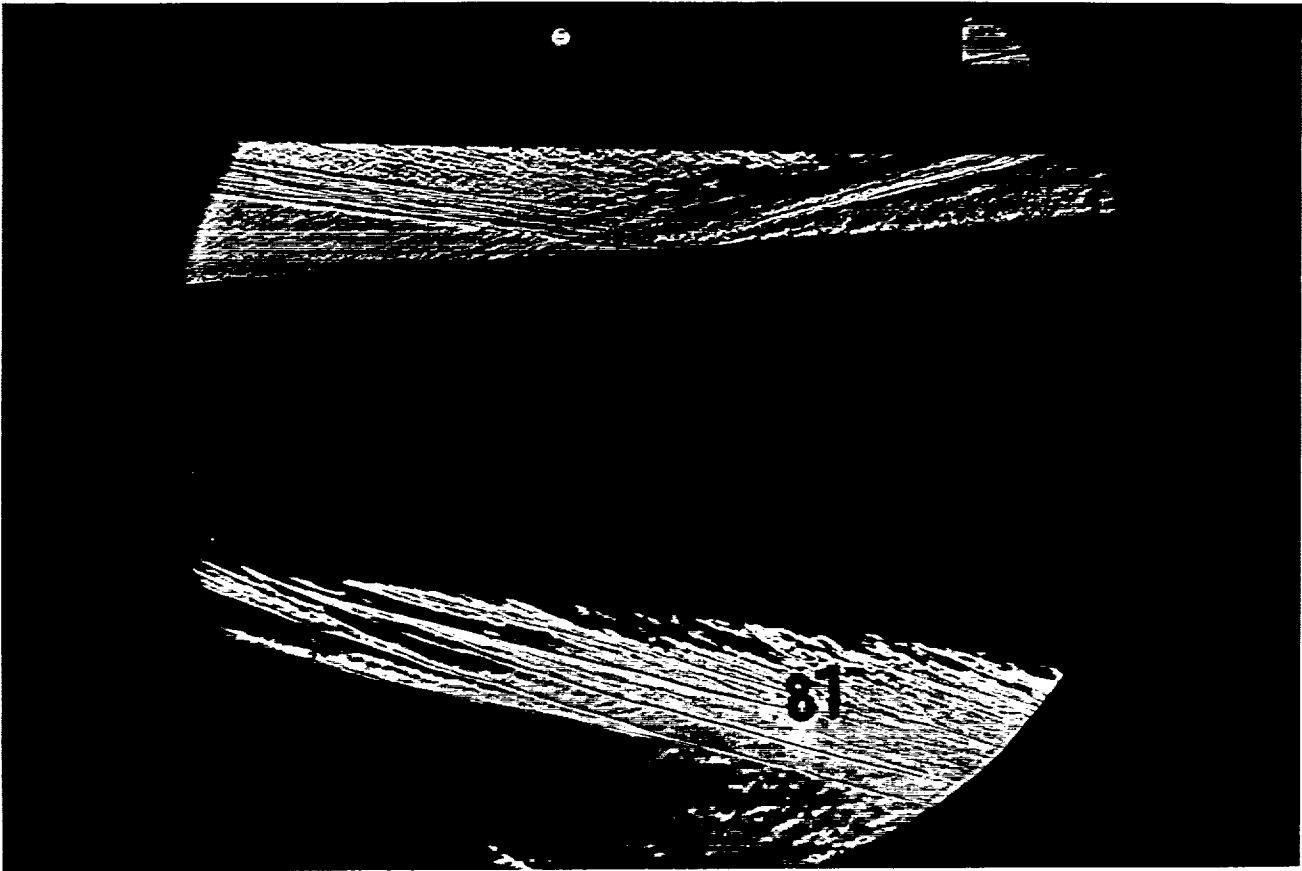
Po	= 2.340E+03 PSIA	Reservoir Total Pressure
Ho	= 1.427E+07 (Ft/sec) ²	Reservoir Total Enthalpy
To	= 2.228E+03 degR	Reservoir Total Temperature
M	= 6.422E+00	Freestream Mach Number
U	= 5.048E+03 Ft/sec	Freestream Velocity
T	= 2.570E+02 degR	Freestream Temperature
P	= 9.508E-01 PSIA	Freestream Static Pressure
Rho	= 3.105E-04 Slugs/Ft ³	Freestream Density
Mu	= 2.101E-07 Slugs/Ft-sec	Freestream Viscosity
Re	= 7.463E+06 1/Ft	Freestream Reynolds Number
Po'	= 5.126E+01 PSIA	Pitot Pressure
Q	= 2.748E+01 PSIA	Dynamic Pressure (Rho U ² /288)
Mi	= 2.865E+00	Shock Tube Incident Shock Mach Number
Tw	= 5.300E+02 degR	Wall Temperature (Test Gas - Air)
Hw	= 3.183E+06 (Ft/sec) ²	Wall Enthalpy (Cp Tw)
CPf	= 3.639E-02 1/PSIA	Pressure to CP factor (1/Q)
CHf	= 4.475E-05 Ft ² -s/BTU	Heat Rate to CH factor (778/(Rho U (Ho-Hw)))
QoFR	= 6.372E+01 BTU/Ft ² -s	Fay-Riddell Heat Transfer (.25' Diam Cylin.)



HEAT TRANSFER vs Gauge Position
Run 83

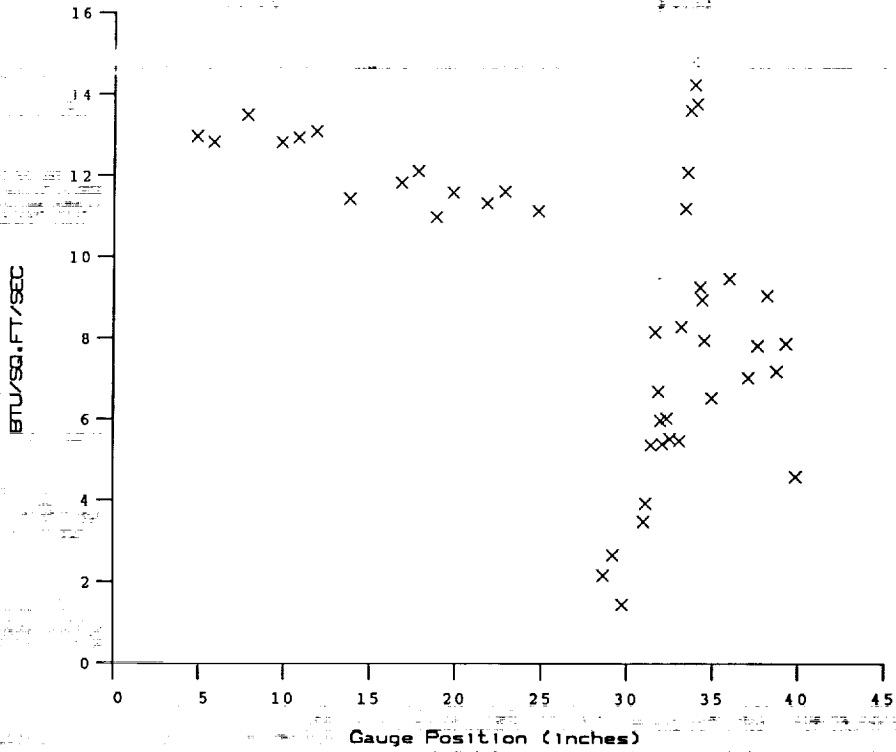


PRESSURE vs Gauge Position
Run 83

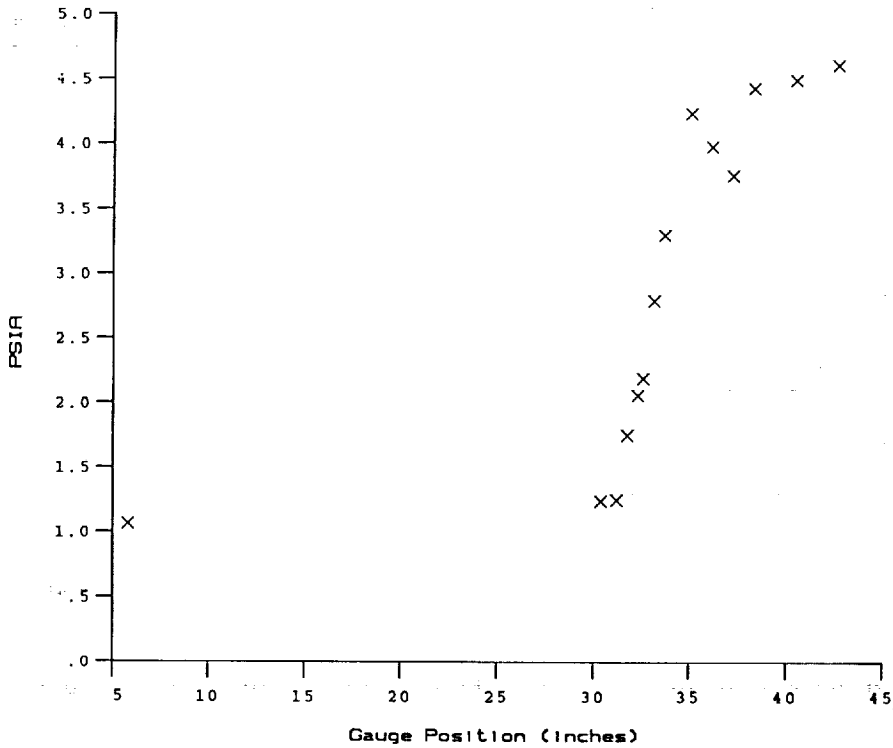


Test Conditions for Run 87 :

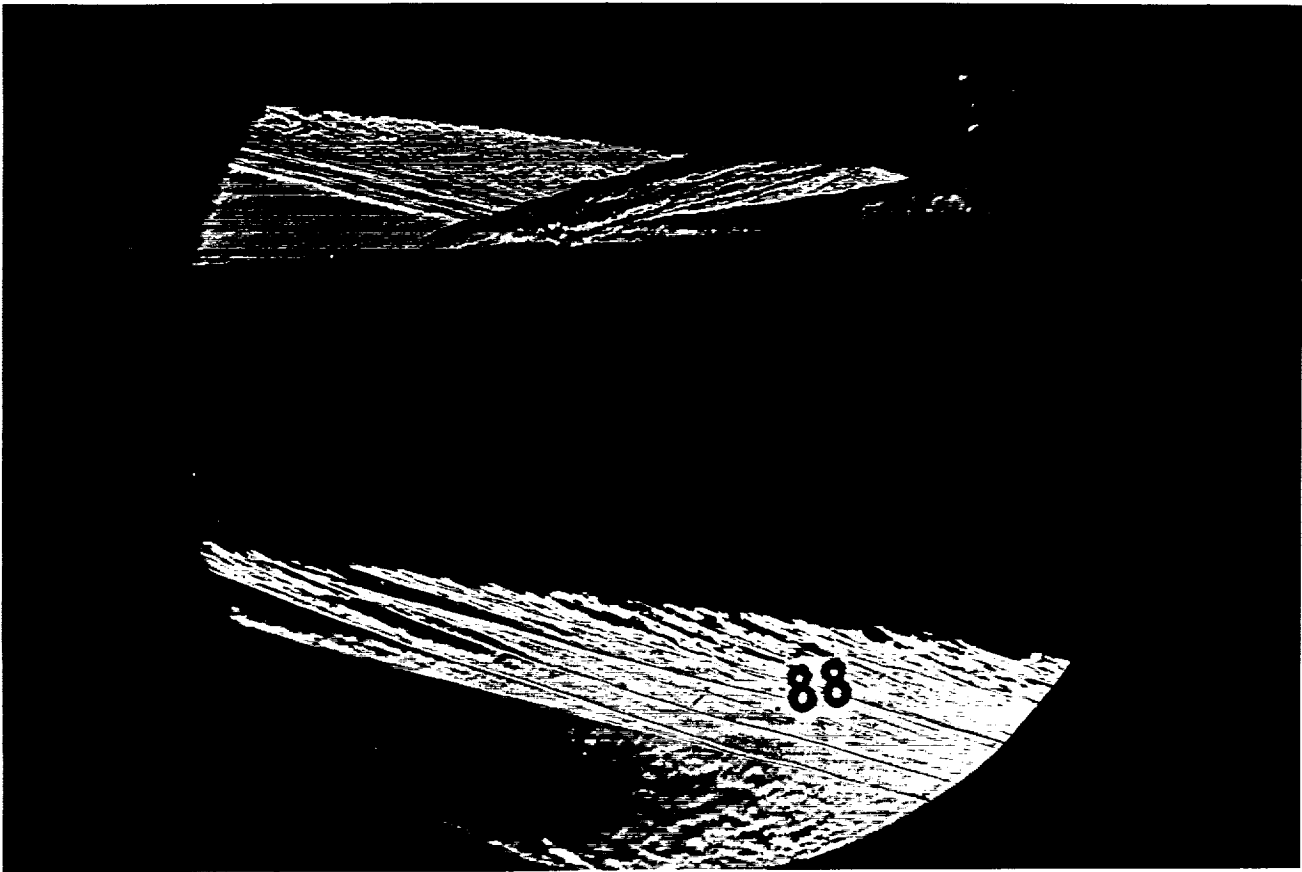
Po	= 2.363E+03 PSIA	Reservoir Total Pressure
Ho	= 1.421E+07 (Ft/sec) ²	Reservoir Total Enthalpy
To	= 2.218E+03 degR	Reservoir Total Temperature
M	= 6.420E+00	Freestream Mach Number
U	= 5.038E+03 Ft/sec	Freestream Velocity
T	= 2.560E+02 degR	Freestream Temperature
P	= 9.633E-01 PSIA	Freestream Static Pressure
Rho	= 3.158E-04 Slugs/Ft ³	Freestream Density
Mu	= 2.093E-07 Slugs/Ft-sec	Freestream Viscosity
Re	= 7.600E+06 1/Ft	Freestream Reynolds Number
Po'	= 5.190E+01 PSIA	Pitot Pressure
Q	= 2.783E+01 PSIA	Dynamic Pressure ($\rho U^2/288$)
Mi	= 2.878E+00	Shock Tube Incident Shock Mach Number
Tw	= 5.300E+02 degR	Wall Temperature (Test Gas = Air)
Hw	= 3.183E+06 (Ft/sec) ²	Wall Enthalpy ($C_p T_w$)
CPf	= 3.594E-02 1/PSIA	Pressure to CP factor (1/Q)
CHF	= 4.434E-05 Ft ² -s/BTU	Heat Rate to CH factor ($778/(\rho U (H_o - H_w))$)
QoFR	= 6.375E+01 BTU/Ft ² -s	Fay-Riddell Heat Transfer (.25' Diam Cylin.)



HEAT TRANSFER vs Gauge Position
Run 87

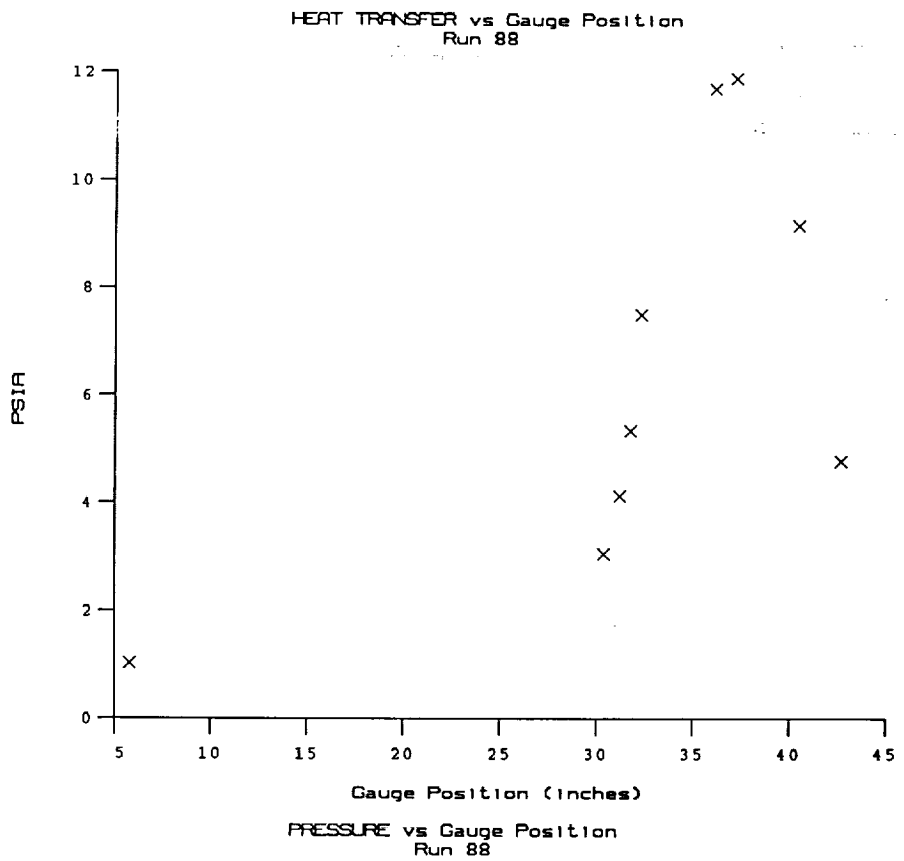
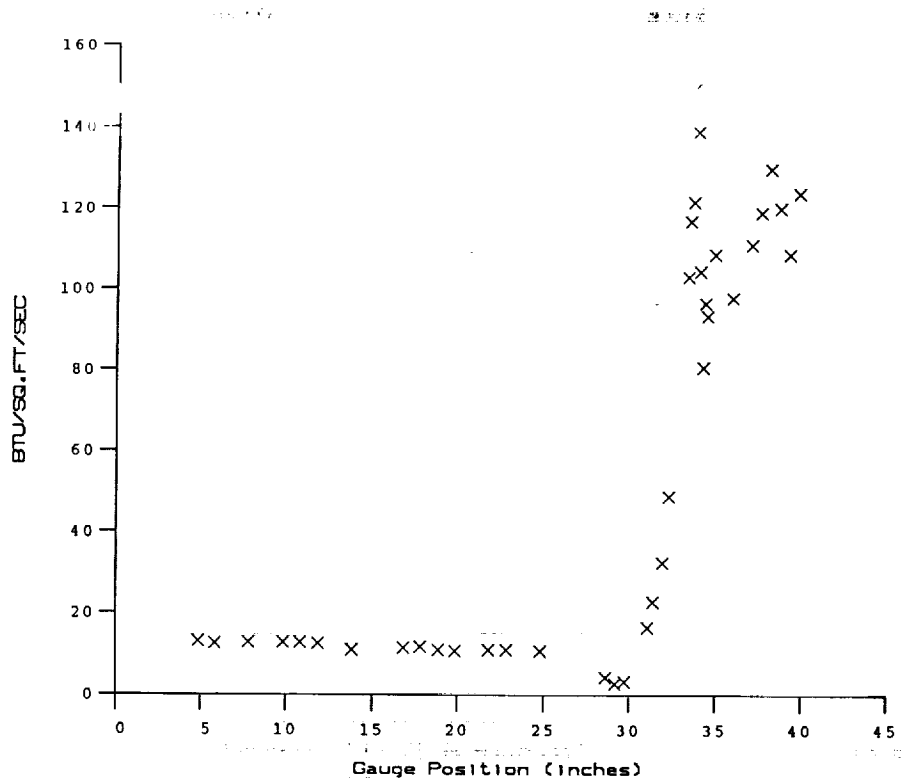


PRESSURE vs Gauge Position
Run 87



Test Conditions for Run 88 :

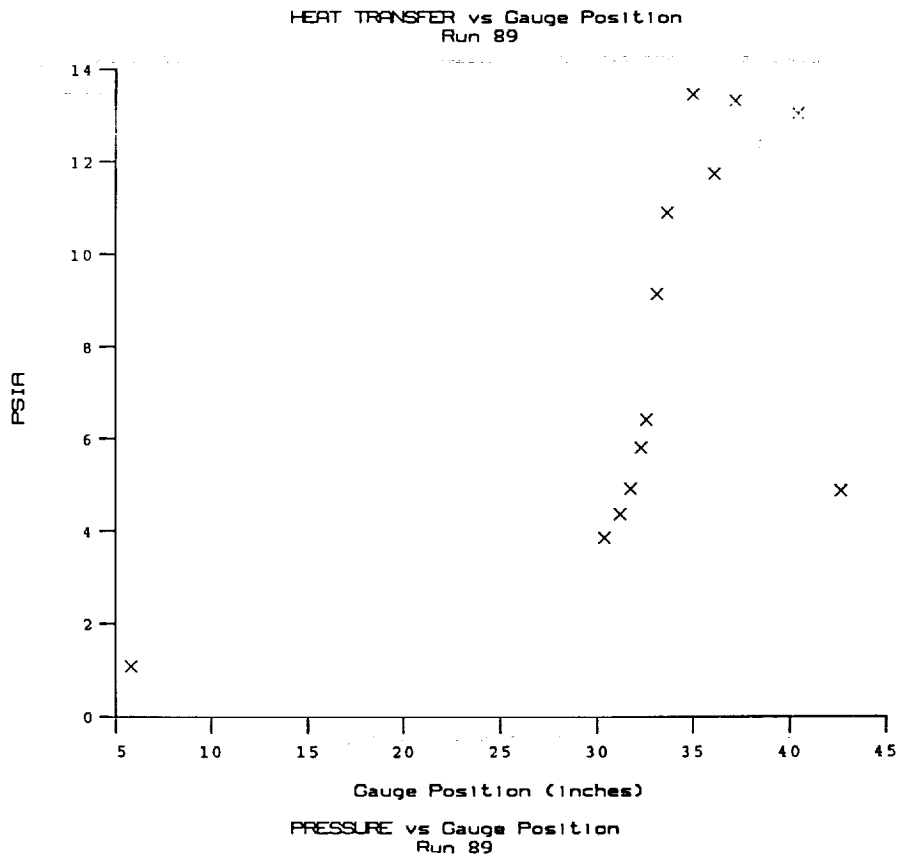
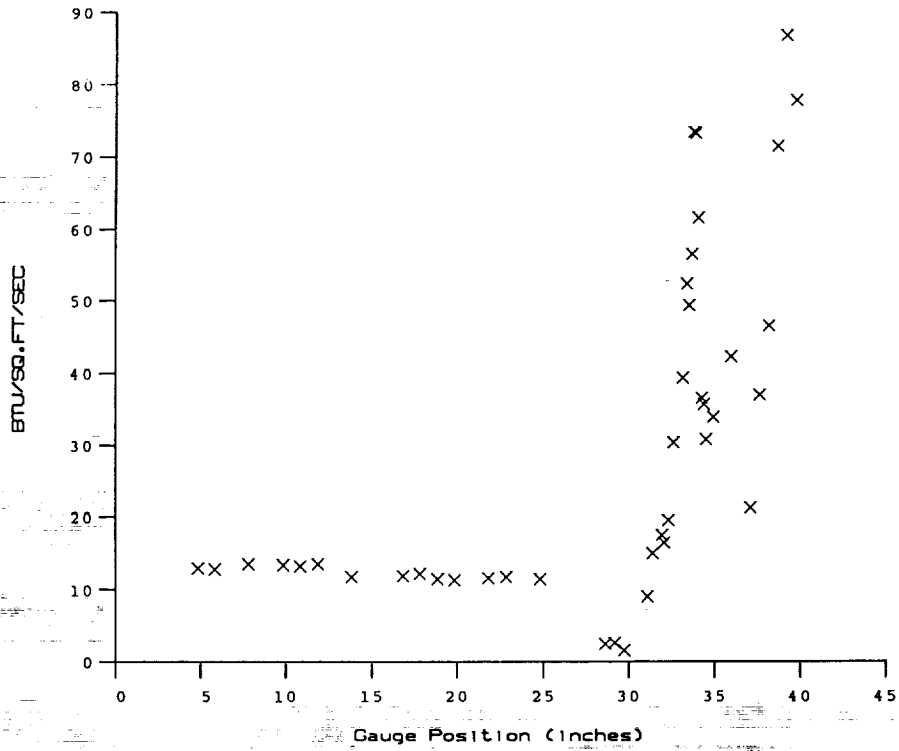
Po	= 2.366E+03 PSIA	Reservoir Total Pressure
Ho	= 1.411E+07 (Ft/sec) ²	Reservoir Total Enthalpy
To	= 2.204E+03 degR	Reservoir Total Temperature
M	= 6.422E+00	Freestream Mach Number
U	= 5.020E+03 Ft/sec	Freestream Velocity
T	= 2.541E+02 degR	Freestream Temperature
P	= 9.648E-01 PSIA	Freestream Static Pressure
Rho	= 3.187E-04 Slugs/Ft ³	Freestream Density
Mu	= 2.079E-07 Slugs/Ft-sec	Freestream Viscosity
Re	= 7.695E+06 1/Ft	Freestream Reynolds Number
Po'	= 5.201E+01 PSIA	Pitot Pressure
Q	= 2.789E+01 PSIA	Dynamic Pressure (Rho U ² /288)
Mi	= 2.871E+00	Shock Tube Incident Shock Mach Number
Tw	= 5.300E+02 degR	Wall Temperature (Test Gas = Air)
Hw	= 3.183E+06 (Ft/sec) ²	Wall Enthalpy (Cp Tw)
CPf	= 3.586E-02 1/PSIA	Pressure to CP factor (1/Q)
CHF	= 4.449E-05 Ft ² -s/BTU	Heat Rate to CH factor (778/(Rho U (Ho-Hw)))
QoFR	= 6.321E+01 BTU/Ft ² -s	Fay-Riddell Heat Transfer (.25' Diam Cylin.)

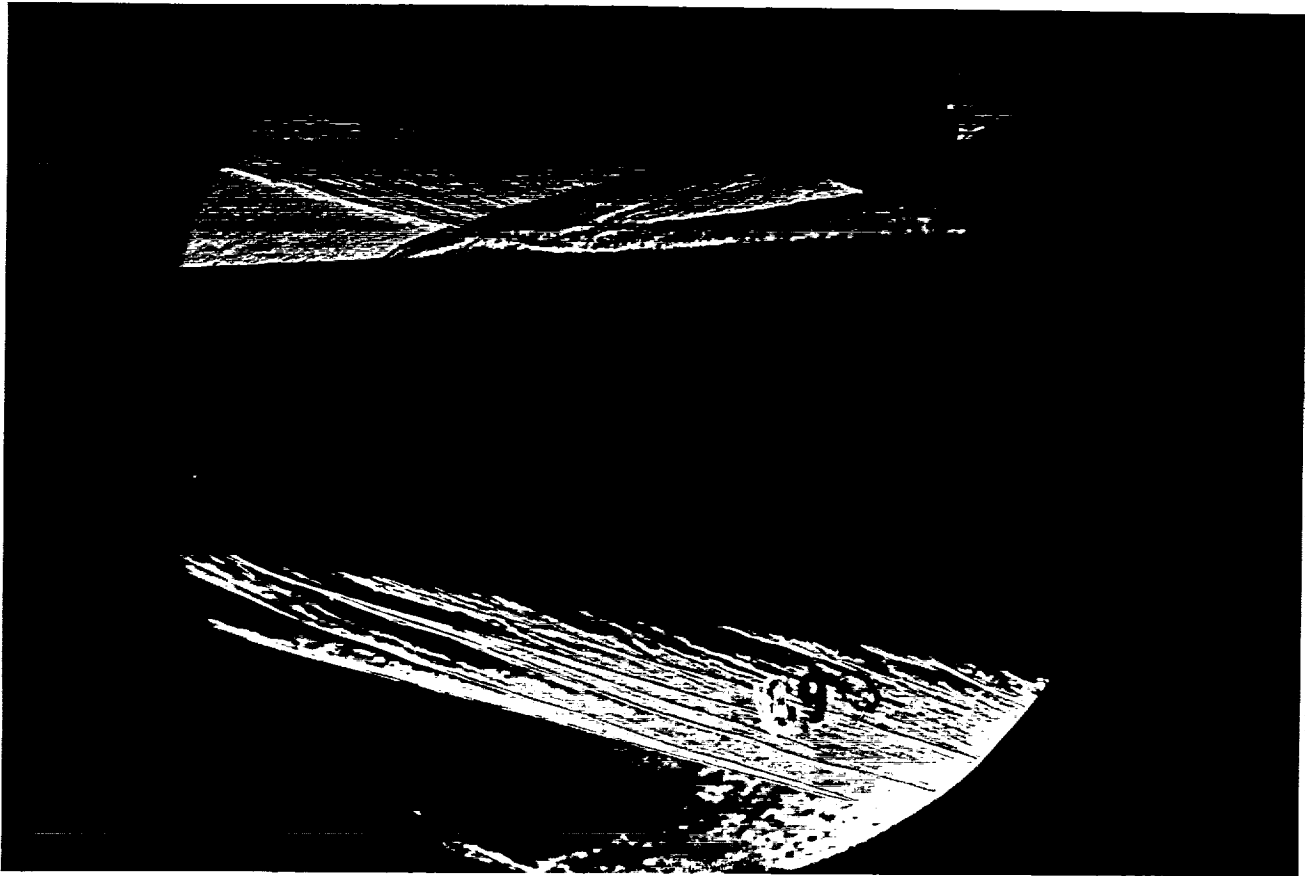


Test Conditions for Run 89 :

Po = 2.395E+03 PSIA
Ho = 1.429E+07 (Ft/sec)²
To = 2.229E+03 degR
M = 6.419E+00
U = 5.051E+03 Ft/sec
T = 2.575E+02 degR
P = 9.766E-01 PSIA
Rho = 3.183E-04 Slugs/Ft³
Mu = 2.104E-07 Slugs/Ft-sec
Re = 7.641E+06 1/Ft
Po' = 5.261E+01 PSIA
Q = 2.820E+01 PSIA
Mi = 2.891E+00
Tw = 5.300E+02 degR
Hw = 3.183E+06 (Ft/sec)²
Cpf = 3.546E-02 1/PSIA
Chf = 4.356E-05 Ft²-s/BTU
QoFR = 6.466E+01 BTU/Ft²-s

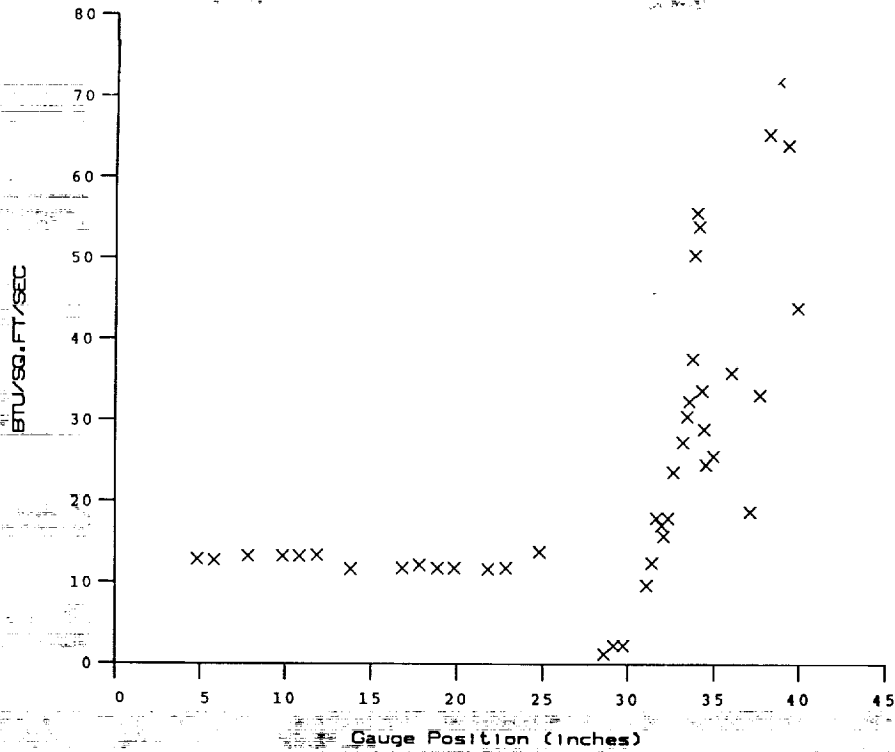
Reservoir Total Pressure
Reservoir Total Enthalpy
Reservoir Total Temperature
Freestream Mach Number
Freestream Velocity
Freestream Temperature
Freestream Static Pressure
Freestream Density
Freestream Viscosity
Freestream Reynolds Number
Pitot Pressure
Dynamic Pressure ($\text{Rho } U^2/288$)
Shock Tube Incident Shock Mach Number
Wall Temperature (Test Gas = Air)
Wall Enthalpy ($C_p Tw$)
Pressure to CP factor ($1/Q$)
Heat Rate to CH factor ($778/(\text{Rho } U (Ho-Hw))$)
Fay-Riddell Heat Transfer (.25' Diam Cylin.)



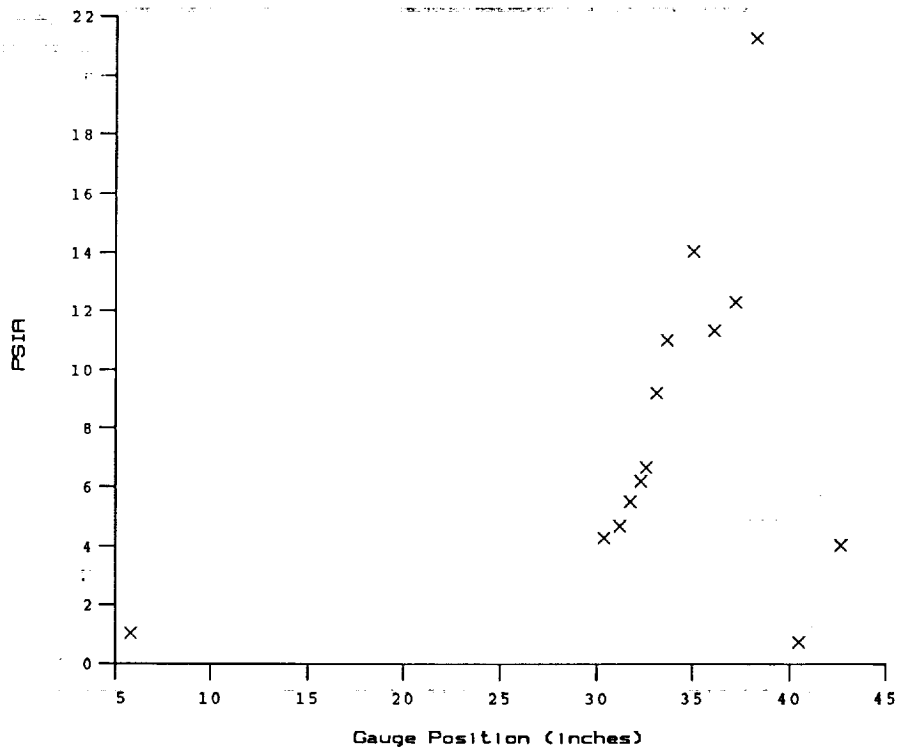


Test Conditions for Run 90 :

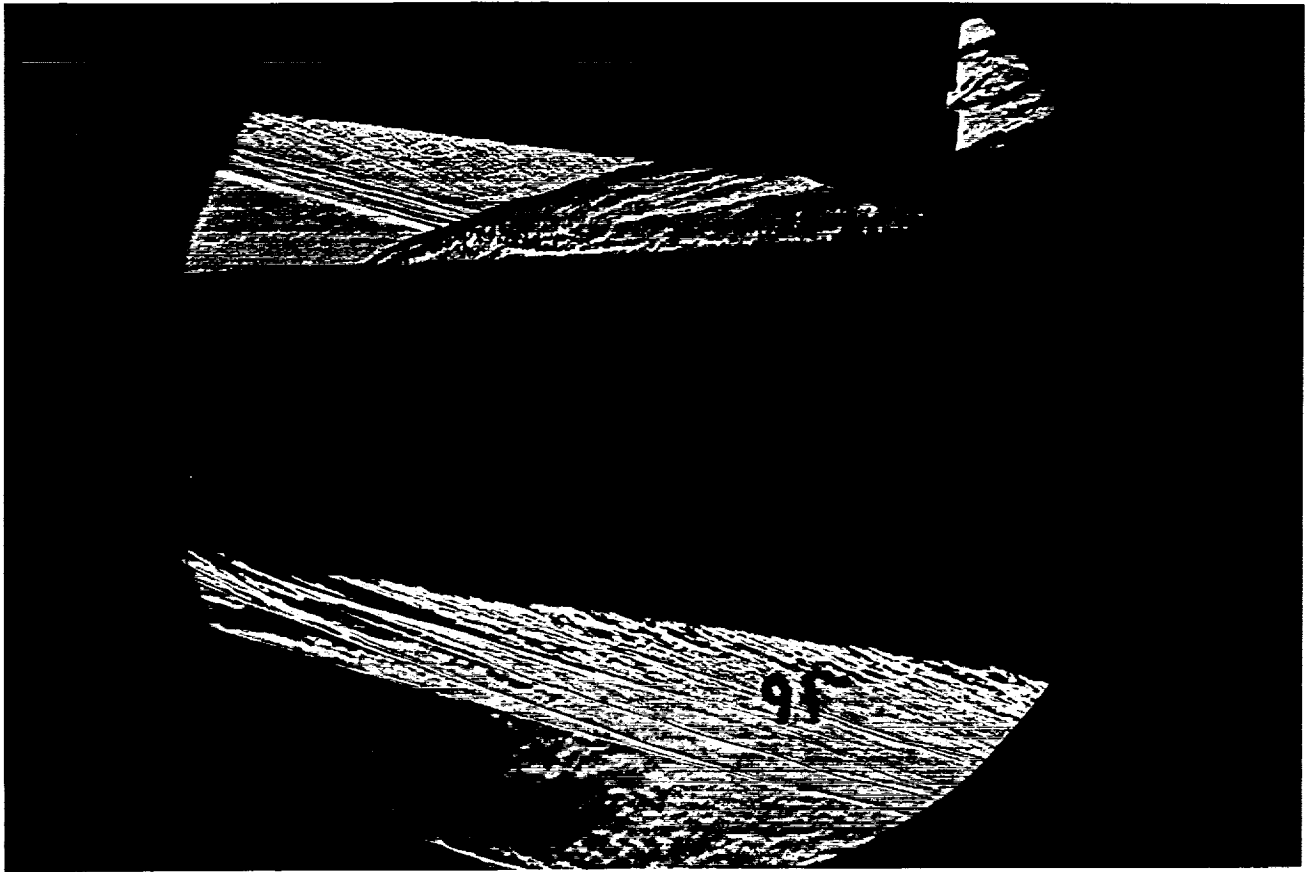
Po	= 2.385E+03 PSIA	Reservoir Total Pressure
Ho	= 1.435E+07 (Ft/sec) ²	Reservoir Total Enthalpy
To	= 2.238E+03 degR	Reservoir Total Temperature
M	= 6.420E+00	Freestream Mach Number
U	= 5.062E+03 Ft/sec	Freestream Velocity
T	= 2.585E+02 degR	Freestream Temperature
P	= 9.707E-01 PSIA	Freestream Static Pressure
Rho	= 3.151E-04 Slugs/Ft ³	Freestream Density
Mu	= 2.112E-07 Slugs/Ft-sec	Freestream Viscosity
Re	= 7.552E+06 1/Ft	Freestream Reynolds Number
Po'	= 5.230E+01 PSIA	Pitot Pressure
Q	= 2.803E+01 PSIA	Dynamic Pressure (Rho U ² /288)
Mi	= 2.886E+00	Shock Tube Incident Shock Mach Number
Tw	= 5.300E+02 degR	Wall Temperature (Test Gas = Air)
Hw	= 3.183E+06 (Ft/sec) ²	Wall Enthalpy (Cp Tw)
CPf	= 3.567E-02 1/PSIA	Pressure to CP factor (1/Q)
Chf	= 4.367E-05 Ft ² -s/BTU	Heat Rate to CH factor (778/(Rho U (Ho-Hw)))
CoFR	= 6.484E+01 BTU/Ft ² -s	Fay-Riddell Heat Transfer (.25' Diam Cylin.)



HEAT TRANSFER vs Gauge Position
Run 90

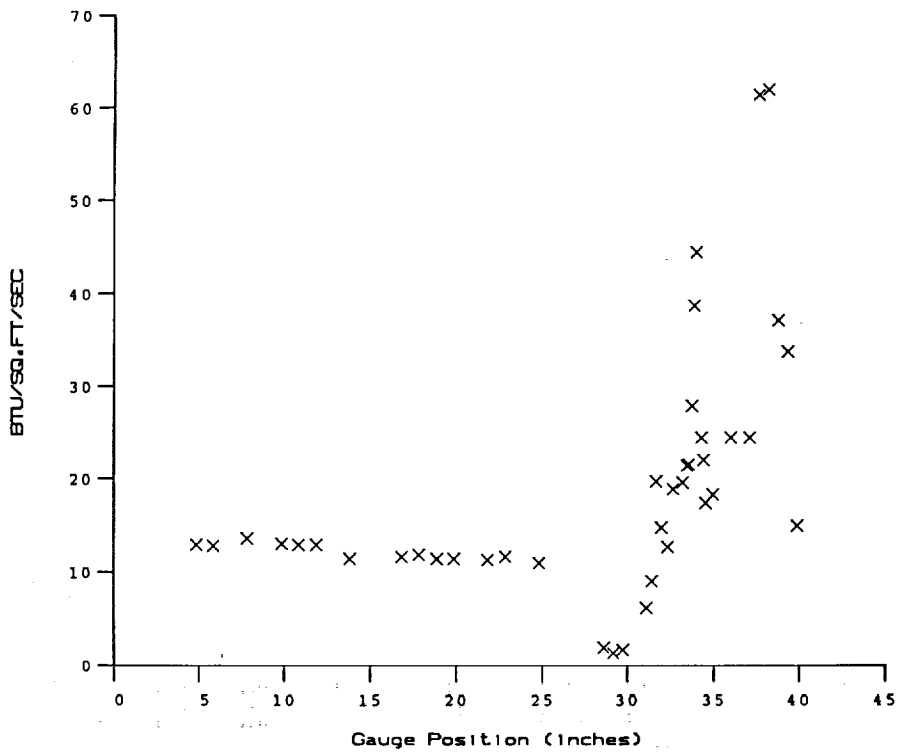


PRESSURE vs Gauge Position
Run 90

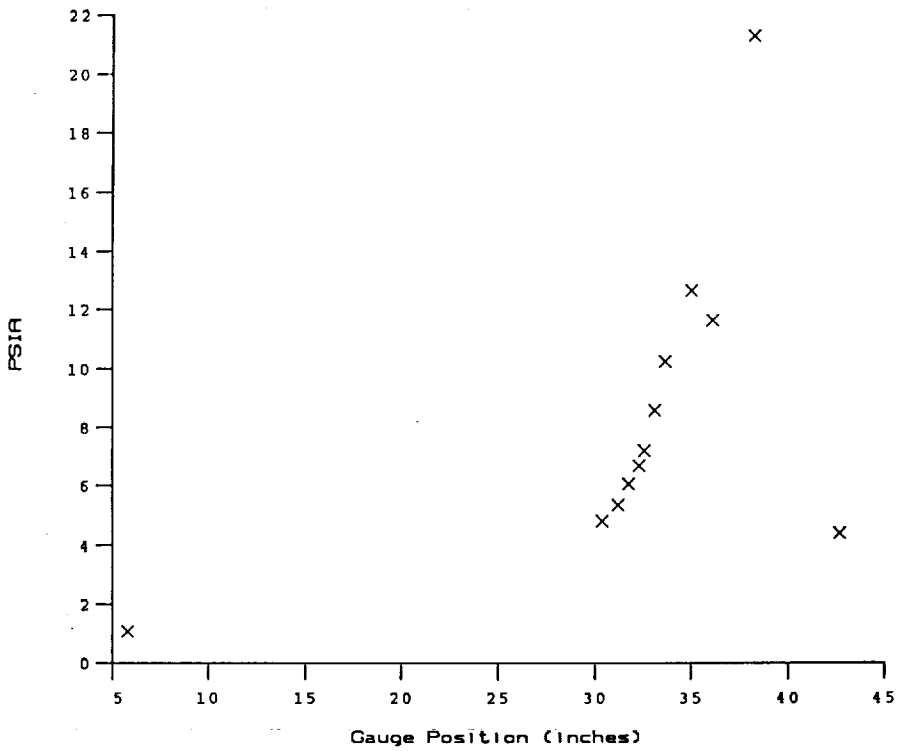


Test Conditions for Run 91 :

Po	= 2.383E+03 PSIA	Reservoir Total Pressure
Ho	= 1.434E+07 (Ft/sec) ²	Reservoir Total Enthalpy
To	= 2.237E+03 degR	Reservoir Total Temperature
M	= 6.420E+00	Freestream Mach Number
U	= 5.061E+03 Ft/sec	Freestream Velocity
T	= 2.583E+02 degR	Freestream Temperature
P	= 9.694E-01 PSIA	Freestream Static Pressure
Rho	= 3.149E-04 Slugs/Ft ³	Freestream Density
Mu	= 2.111E-07 Slugs/Ft-sec	Freestream Viscosity
Re	= 7.550E+06 1/Ft	Freestream Reynolds Number
Po'	= 5.224E+01 PSIA	Pitot Pressure
Q	= 2.800E+01 PSIA	Dynamic Pressure (Rho U ² /288)
Mi	= 2.883E+00	Shock Tube Incident Shock Mach Number
Tw	= 5.300E+02 degR	Wall Temperature (Test Gas = Air)
Hw	= 3.183E+06 (Ft/sec) ²	Wall Enthalpy (Cp Tw)
CPf	= 3.571E-02 1/PSIA	Pressure to CP factor (1/Q)
CHf	= 4.374E-05 Ft ² -s/BTU	Heat Rate to CH factor (778/(Rho U (Ho-Hw))
QoFR	= 6.476E+01 BTU/Ft ² -s	Fay-Riddell Heat Transfer (.25' Diam Cylin.)



HEAT TRANSFER vs Gauge Position
Run 91



PRESSURE vs Gauge Position
Run 91

Gauge Label	Loc. (in)	Value (PSIA) or (BTU/Ft2-Sec)	T Surf (DegR)	Gauge Label	Loc. (in)	Value (PSIA) or (BTU/Ft2-Sec)	T Surf (DegR)	Gauge Label	Loc. (in)	Value (PSIA) or (BTU/Ft2-Sec)	T Surf (DegR)
L28P1	5.85	4.773(-1)		L28H4	5.85	2.182(0)	535.61	TH16	32.35	3.687(0)	536.76
L28P2	9.85	4.482(-1)		L28H5	6.85	Null	Null	TH17	32.48	Null	Null
L28P3	13.85	4.578(-1)		L28H6	7.85	2.095(0)	535.43	TH18	32.62	3.473(0)	536.55
L28P4	17.85	4.438(-1)		L28H7	9.85	2.022(0)	535.36	TH20	32.89	4.391(0)	538.50
L28P5	21.85	Null		L28H8	10.85	2.107(0)	535.49	TH21	33.03	Null	Null
L28P6	25.85	Null		L28H9	11.85	2.069(0)	535.57	TH50	33.08	3.823(0)	536.73
TP1	28.75	Null		L28H10	12.85	Null	Null	TH22	33.16	3.409(0)	536.87
TP2	29.30	Null		L28H11	13.85	2.241(0)	535.78	TH23	33.31	3.463(0)	536.82
TP3	30.39	5.527(-1)		L28H13	16.85	5.474(0)	538.60	TH24	33.44	3.594(0)	536.87
TP4	30.94	Null		L28H14	17.85	7.250(0)	539.93	TH25	33.58	Null	Null
TP5	31.21	4.727(-1)		L28H15	18.85	7.619(0)	540.38	TH26	33.71	5.388(0)	537.57
TP6	31.48	Null		L28H16	19.85	8.338(0)	540.90	TH27	33.85	Null	Null
TP7	31.75	5.153(-1)		L28H17	21.85	7.794(0)	540.55	TH28	33.99	5.294(0)	537.92
TP8	32.03	Null		L28H18	22.85	7.647(0)	540.47	TH29	34.12	4.690(0)	537.64
TP9	32.30	5.346(-1)		L28H19	24.85	7.450(0)	540.20	TH30	34.26	2.819(0)	535.78
TP10	32.57	5.225(-1)		TH1	28.66	3.411(0)	536.17	TH31	34.39	2.651(0)	535.60
TP11	32.85	Null		TH2	29.21	3.422(0)	536.44	TH32	34.53	2.898(0)	535.74
TP12	33.11	5.869(-1)		TH3	29.75	3.498(0)	536.78	TH34	34.80	Null	Null
TP13	33.39	Null		TH4	30.30	Null	Null	TH35	34.94	2.828(0)	535.90
TP14	33.67	6.078(-1)		TH6	30.99	3.482(0)	536.30	TH36	35.49	2.917(0)	535.85
TP15	34.21	Null		TH7	31.12	3.988(0)	537.31	TH37	36.03	3.261(0)	536.30
TP16	34.49	Null		TH8	31.26	4.988(0)	537.97	TH38	36.58	Null	Null
TP17	34.99	Null		TH9	31.39	5.839(0)	538.88	TH39	37.12	2.992(0)	535.81
TP18	35.03	6.248(-1)		TH10	31.53	Null	Null	TH40	37.67	2.710(0)	535.82
TP19	35.03	6.248(-1)		TH11	31.67	6.120(0)	538.67	TH41	38.22	2.401(0)	535.20
TP20	36.12	5.170(-1)		TH12	31.80	5.807(0)	538.86	TH42	38.76	2.620(0)	535.58
TP21	37.21	6.323(-1)		TH13	31.94	5.071(0)	537.64	TH43	39.31	1.803(0)	534.90
TP22	38.31	5.202(-1)		TH14	32.07	4.197(0)	539.54	TH44	39.85	2.116(0)	535.36
TP24	40.48	5.623(-1)		TH15	32.21	Null	Null	TH45	40.41	Null	Null
TP26	42.66	8.316(-1)									
L28H3	4.85	1.979(0)	535.37								

Run 29 Reduced Data Tabulation

Gauge Label	Loc. (in)	Value (PSIA) or (BTU/Ft2-Sec)	T Surf (DegR)	Gauge Label	Loc. (in)	Value (PSIA) or (BTU/Ft2-Sec)	T Surf (DegR)	Gauge Label	Loc. (in)	Value (PSIA) or (BTU/Ft2-Sec)	T Surf (DegR)
L28P1	5.85	4.959(-1)		L28H5	6.85	Null	Null	TH17	32.48	Null	Null
L28P2	9.85	4.911(-1)		L28H6	7.85	Null	Null	TH18	32.62	Null	Null
L28P3	13.85	4.809(-1)		L28H7	9.85	Null	Null	TH20	32.89	5.589(0)	540.56
L28P4	17.85	4.802(-1)		L28H8	10.85	Null	Null	TH21	33.03	Null	Null
L28P5	21.85	Null		L28H9	11.85	Null	Null	TH50	33.08	4.616(0)	539.87
L28P6	25.85	Null		L28H10	12.85	Null	Null	TH22	33.16	Null	Null
TP1	28.75	Null		L28H11	13.85	Null	Null	TH23	33.31	Null	Null
TP2	29.30	Null		L28H13	16.85	Null	Null	TH24	33.44	Null	Null
TP3	30.39	5.081(-1)		L28H14	17.85	Null	Null	TH25	33.58	Null	Null
TP4	30.94	Null		L28H15	18.85	Null	Null	TH26	33.71	5.742(0)	540.02
TP5	31.21	4.520(-1)		L28H16	19.85	Null	Null	TH27	33.85	Null	Null
TP6	31.48	Null		L28H17	21.85	Null	Null	TH28	33.99	Null	Null
TP7	31.75	5.006(-1)		L28H18	22.85	Null	Null	TH29	34.12	Null	Null
TP8	32.03	Null		L28H19	24.85	Null	Null	TH30	34.26	Null	Null
TP9	32.30	5.186(-1)		TH1	28.66	Null	Null	TH31	34.39	Null	Null
TP10	32.57	4.731(-1)		TH2	29.21	Null	Null	TH32	34.53	Null	Null
TP11	32.85	Null		TH3	29.75	Null	Null	TH34	34.80	Null	Null
TP12	33.11	5.514(-1)		TH4	30.30	Null	Null	TH35	34.94	Null	Null
TP13	33.39	Null		TH6	30.99	Null	Null	TH36	35.49	Null	Null
TP14	33.67	5.669(-1)		TH7	31.12	Null	Null	TH37	36.03	3.668(0)	538.93
TP16	34.21	Null		TH8	31.26	Null	Null	TH38	36.58	Null	Null
TP17	34.49	Null		TH9	31.39	6.618(0)	541.75	TH39	37.12	3.116(0)	538.44
TP19	35.03	5.744(-1)		TH10	31.53	Null	Null	TH40	37.67	2.967(0)	538.43
TP20	36.12	4.688(-1)		TH11	31.67	Null	Null	TH41	38.22	2.496(0)	537.89
TP21	37.21	5.947(-1)		TH12	31.80	Null	Null	TH42	38.76	2.780(0)	537.97
TP22	38.31	5.099(-1)		TH13	31.94	Null	Null	TH43	39.31	1.698(0)	537.21
TP24	40.48	4.101(-1)		TH14	32.07	4.947(0)	540.48	TH44	39.85	2.634(0)	538.15
TP26	42.66	7.657(-1)		TH15	32.21	Null	Null	TH45	40.41	Null	Null
L28H4	5.85	2.163(0)	538.06	TH16	32.35	Null	Null				

Run 30 Reduced Data Tabulation

Gauge Label	Loc. (in)	Value (PSIA) or (BTU/Ft2-Sec)	T Surf (DegR)	Gauge Label	Loc. (in)	Value (PSIA) or (BTU/Ft2-Sec)	T Surf (DegR)	Gauge Label	Loc. (in)	Value (PSIA) or (BTU/Ft2-Sec)	T Surf (DegR)
L28P1	5.85	5.020(-1)		L28H4	5.85	1.827(0)	541.45	TH16	32.35	4.668(0)	543.49
L28P2	9.85	4.819(-1)		L28H5	6.85	Null	Null	TH17	32.48	4.700(0)	543.71
L28P3	13.85	4.789(-1)		L28H6	7.85	1.974(0)	541.22	TH18	32.62	Null	Null
L28P4	17.85	4.570(-1)		L28H7	9.85	1.723(0)	541.24	TH20	32.89	3.810(0)	542.71
L28P5	21.85	Null		L28H8	10.85	2.022(0)	541.41	TH21	33.03	Null	Null
L28P6	25.85	Null		L28H9	11.85	1.844(0)	541.45	TH50	33.08	5.048(0)	543.92
TP1	28.75	Null		L28H10	12.85	Null	Null	TH22	33.16	Null	Null
TP2	29.30	Null		L28H11	13.85	1.750(0)	541.59	TH23	33.31	5.042(0)	543.58
TP3	30.39	5.233(-1)		L28H13	16.85	4.847(0)	544.41	TH24	33.44	4.842(0)	543.61
TP4	30.94	Null		L28H14	17.85	6.725(0)	546.04	TH25	33.58	Null	Null
TP5	31.21	4.491(-1)		L28H15	18.85	7.160(0)	546.55	TH26	33.71	Null	Null
TP6	31.48	Null		L28H16	19.85	8.021(0)	547.26	TH27	33.85	4.741(0)	544.01
TP7	31.75	4.958(-1)		L28H17	21.85	8.217(0)	547.02	TH28	33.99	5.886(0)	544.38
TP8	32.03	Null		L28H18	22.85	7.713(0)	546.97	TH29	34.12	4.845(0)	543.98
TP9	32.30	5.100(-1)		L28H19	24.85	7.670(0)	546.61	TH30	34.26	3.507(0)	542.43
TP10	32.57	4.740(-1)		TH1	28.66	4.265(0)	543.25	TH31	34.39	3.188(0)	542.14
TP11	32.85	Null		TH2	29.21	3.721(0)	542.63	TH32	34.53	3.522(0)	542.49
TP12	33.11	5.367(-1)		TH3	29.75	3.787(0)	543.04	TH34	34.80	Null	Null
TP13	33.39	Null		TH4	30.30	Null	Null	TH35	34.94	2.991(0)	542.07
TP14	33.67	5.622(-1)		TH6	30.99	4.465(0)	543.36	TH36	35.49	3.341(0)	542.36
TP16	34.21	Null		TH7	31.12	4.722(0)	544.33	TH37	36.03	3.502(0)	543.36
TP17	34.49	Null		TH8	31.26	Null	Null	TH38	36.58	Null	Null
TP19	35.03	5.792(-1)		TH9	31.39	6.750(0)	545.88	TH39	37.12	3.469(0)	542.45
TP20	36.12	4.618(-1)		TH10	31.53	5.668(0)	550.87	TH40	37.67	2.924(0)	542.34
TP21	37.21	6.138(-1)		TH11	31.67	6.487(0)	545.26	TH41	38.22	2.171(0)	541.38
TP22	38.31	5.040(-1)		TH12	31.80	6.667(0)	545.43	TH42	38.76	3.110(0)	542.51
TP24	40.48	5.556(-1)		TH13	31.94	5.058(0)	544.21	TH43	39.31	1.687(0)	540.59
TP26	42.66	8.135(-1)		TH14	32.07	4.654(0)	545.33	TH44	39.85	2.651(0)	541.78
L28H3	4.85	1.926(0)	541.29	TH15	32.21	Null	Null	TH45	40.41	Null	Null

Run 31 Reduced Data Tabulation

Table with columns: Gauge Label, Loc. (in), Value (PSIA) or (BTU/Ft2-Sec), T Surf (DegR). Multiple columns for different gauge locations.

Run 52 Reduced Data Tabulation

Table with columns: Gauge Label, Loc. (in), Value (PSIA) or (BTU/Ft2-Sec), T Surf (DegR). Multiple columns for different gauge locations.

Run 54 Reduced Data Tabulation

Table with columns: Gauge Label, Loc. (in), Value (PSIA) or (BTU/Ft2-Sec), T Surf (DegR). Multiple columns for different gauge locations.

Run 55 Reduced Data Tabulation

Gauge Label	Loc. (in)	Value (PSIA) or (BTU/Ft ² -Sec)	T Surf (DegR)	Gauge Label	Loc. (in)	Value (PSIA) or (BTU/Ft ² -Sec)	T Surf (DegR)	Gauge Label	Loc. (in)	Value (PSIA) or (BTU/Ft ² -Sec)	T Surf (DegR)
L28P1	5.85	5.323(-1)		L28H5	6.85	Null		TH17	32.48	5.784(1)	592.14
L28P2	9.85	5.116(-1)		L28H6	7.85	2.193(0)	539.22	TH18	32.62	5.202(1)	586.83
L28P3	13.85	4.956(-1)		L28H7	9.85	1.963(0)	539.04	TH20	32.89	2.659(1)	562.39
L28P4	17.85	Null		L28H8	10.85	2.162(0)	538.97	TH21	33.03	Null	Null
L28P5	21.85	Null		L28H9	11.85	2.398(0)	539.27	TH50	33.08	7.137(1)	602.60
L28P6	25.85	Null		L28H10	12.85	Null		TH22	33.16	1.151(1)	563.25
TP1	28.75	Null		L28H11	13.85	3.299(0)	540.09	TH23	33.31	5.949(1)	594.25
TP2	29.30	Null		L28H13	16.85	7.196(0)	543.94	TH24	33.44	6.341(1)	597.51
TP3	30.39	1.640(0)		L28H14	17.85	8.441(0)	545.04	TH25	33.58	7.329(1)	595.15
TP4	30.94	Null		L28H15	18.85	8.048(0)	545.07	TH26	33.71	7.436(1)	607.05
TP5	31.21	3.034(0)		L28H16	19.85	8.312(0)	545.08	TH27	33.85	Null	Null
TP6	31.48	Null		L28H17	21.85	8.042(0)	544.90	TH28	33.99	6.584(1)	598.66
TP7	31.75	3.593(0)		L28H18	22.85	8.352(0)	544.88	TH29	34.12	5.940(1)	593.81
TP8	32.03	Null		L28H19	24.85	7.841(0)	544.49	TH30	34.26	5.203(1)	588.52
TP9	32.30	4.449(0)		TH1	28.66	Null		TH31	34.39	6.246(1)	598.35
TP10	32.57	4.852(0)		TH2	29.21	Null		TH32	34.53	5.952(1)	595.76
TP11	32.85	Null		TH3	29.75	3.340(0)	540.62	TH34	34.80	Null	Null
TP12	33.11	5.247(0)		TH4	30.30	Null		TH35	34.94	5.384(1)	588.21
TP13	33.39	Null		TH6	30.99	8.962(0)	544.18	TH36	35.49	6.728(1)	604.38
TP14	33.67	5.071(0)		TH7	31.12	1.580(1)	550.18	TH37	36.03	5.851(1)	592.28
TP16	34.21	Null		TH8	31.26	Null		TH38	36.58	Null	Null
TP17	34.49	Null		TH9	31.39	2.666(1)	556.87	TH39	37.12	6.691(1)	604.12
TP19	35.03	4.455(0)		TH10	31.53	Null		TH40	37.67	7.201(1)	608.77
TP20	36.12	5.138(0)		TH11	31.67	5.489(1)	590.56	TH41	38.22	7.363(1)	614.88
TP21	37.21	5.390(0)		TH12	31.80	3.257(1)	567.87	TH42	38.76	5.726(1)	591.73
TP22	38.31	5.060(0)		TH13	31.94	2.246(1)	559.02	TH43	39.31	6.208(1)	600.06
TP24	40.48	3.617(0)		TH14	32.07	4.131(1)	580.54	TH44	39.85	7.554(1)	611.65
TP26	42.66	2.343(0)		TH15	32.21	Null		TH45	40.41	Null	Null
L28H4	5.85	2.755(0)	539.41	TH16	32.35	4.158(1)	577.14				

Run 60 Reduced Data Tabulation

Gauge Label	Loc. (in)	Value (PSIA) or (BTU/Ft ² -Sec)	T Surf (DegR)	Gauge Label	Loc. (in)	Value (PSIA) or (BTU/Ft ² -Sec)	T Surf (DegR)	Gauge Label	Loc. (in)	Value (PSIA) or (BTU/Ft ² -Sec)	T Surf (DegR)
L28P1	5.85	5.189(-1)		L28H4	5.85	1.719(0)	540.64	TH16	32.35	3.030(1)	568.45
L28P2	9.85	5.050(-1)		L28H5	6.85	Null		TH17	32.48	3.869(1)	576.89
L28P3	13.85	5.009(-1)		L28H6	7.85	1.747(0)	540.15	TH18	32.62	Null	Null
L28P4	17.85	Null		L28H7	9.85	1.641(0)	540.17	TH20	32.89	Null	Null
L28P5	21.85	Null		L28H8	10.85	1.560(0)	540.29	TH21	33.03	Null	Null
L28P6	25.85	Null		L28H9	11.85	1.553(0)	540.46	TH50	33.08	Null	Null
TP1	28.75	Null		L28H10	12.85	Null		TH22	33.16	2.288(1)	558.49
TP2	29.30	Null		L28H11	13.85	2.402(0)	541.09	TH23	33.31	4.622(1)	586.10
TP3	30.39	Null		L28H13	16.85	6.326(0)	544.93	TH24	33.44	4.914(1)	589.17
TP4	30.94	Null		L28H14	17.85	7.703(0)	546.18	TH25	33.58	6.009(1)	596.82
TP5	31.21	Null		L28H15	18.85	7.522(0)	546.59	TH26	33.71	5.994(1)	601.46
TP6	31.48	Null		L28H16	19.85	7.682(0)	546.58	TH27	33.85	Null	Null
TP7	31.75	Null		L28H17	21.85	7.606(0)	546.63	TH28	33.99	5.175(1)	592.26
TP8	32.03	Null		L28H18	22.85	7.562(0)	546.54	TH29	34.12	4.563(1)	586.69
TP9	32.30	4.226(0)		L28H19	24.85	6.939(0)	545.85	TH30	34.26	2.743(1)	568.01
TP10	32.57	Null		TH1	28.66	Null		TH31	34.39	3.093(1)	571.91
TP11	32.85	Null		TH2	29.21	Null		TH32	34.53	2.535(1)	567.02
TP12	33.11	5.176(0)		TH3	29.75	2.500(0)	539.75	TH34	34.80	Null	Null
TP13	33.39	Null		TH4	30.30	Null		TH35	34.94	2.247(1)	564.88
TP14	33.67	5.070(0)		TH6	30.99	1.344(1)	551.14	TH36	35.49	2.600(1)	569.41
TP16	34.21	Null		TH7	31.12	1.547(1)	551.80	TH37	36.03	3.097(1)	574.07
TP17	34.49	Null		TH8	31.26	Null		TH38	36.58	Null	Null
TP19	35.03	5.052(0)		TH9	31.39	2.549(1)	562.93	TH39	37.12	Null	Null
TP20	36.12	5.176(0)		TH10	31.53	Null		TH40	37.67	Null	Null
TP21	37.21	5.433(0)		TH11	31.67	4.588(1)	583.59	TH41	38.22	Null	Null
TP22	38.31	5.122(0)		TH12	31.80	2.586(1)	563.22	TH42	38.76	Null	Null
TP24	40.48	3.954(0)		TH13	31.94	1.880(1)	558.44	TH43	39.31	Null	Null
TP26	42.66	2.552(0)		TH14	32.07	3.420(1)	571.80	TH44	39.85	2.238(1)	564.92
L28H3	4.85	1.573(0)	540.61	TH15	32.21	Null		TH45	40.41	Null	Null

Run 62 Reduced Data Tabulation

Gauge Label	Loc. (in)	Value (PSIA) or (BTU/Ft ² -Sec)	T Surf (DegR)	Gauge Label	Loc. (in)	Value (PSIA) or (BTU/Ft ² -Sec)	T Surf (DegR)	Gauge Label	Loc. (in)	Value (PSIA) or (BTU/Ft ² -Sec)	T Surf (DegR)
L28P1	5.85	3.965(-1)		L28H4	5.85	1.862(0)	539.84	TH16	32.35	1.101(1)	547.76
L28P2	9.85	4.816(-1)		L28H5	6.85	Null		TH17	32.48	1.086(1)	549.05
L28P3	13.85	4.446(-1)		L28H6	7.85	1.721(0)	539.63	TH18	32.62	9.347(0)	547.29
L28P4	17.85	Null		L28H7	9.85	2.446(0)	540.52	TH20	32.89	4.560(0)	543.79
L28P5	21.85	Null		L28H8	10.85	3.334(0)	541.42	TH21	33.03	Null	Null
L28P6	25.85	Null		L28H9	11.85	4.452(0)	542.62	TH50	33.08	1.676(1)	554.11
TP1	28.75	Null		L28H10	12.85	Null		TH22	33.16	3.080(0)	539.79
TP2	29.30	Null		L28H11	13.85	6.144(0)	544.03	TH23	33.31	2.008(1)	557.25
TP3	30.39	1.013(0)		L28H13	16.85	7.076(0)	545.78	TH24	33.44	2.395(1)	560.21
TP4	30.94	Null		L28H14	17.85	7.610(0)	545.76	TH25	33.58	2.352(1)	558.14
TP5	31.21	1.298(0)		L28H15	18.85	7.146(0)	545.36	TH26	33.71	3.721(1)	572.56
TP6	31.48	Null		L28H16	19.85	7.052(0)	545.24	TH27	33.85	Null	Null
TP7	31.75	1.432(0)		L28H17	21.85	6.807(0)	545.26	TH28	33.99	3.497(1)	570.76
TP8	32.03	Null		L28H18	22.85	7.010(0)	545.32	TH29	34.12	3.211(1)	569.53
TP9	32.30	1.733(0)		L28H19	24.85	6.813(0)	544.25	TH30	34.26	2.090(1)	558.31
TP10	32.57	1.983(0)		TH1	28.66	Null		TH31	34.39	2.362(1)	559.93
TP11	32.85	Null		TH2	29.21	8.806(-1)	538.60	TH32	34.53	2.127(1)	557.73
TP12	33.11	3.007(0)		TH3	29.75	2.240(0)	540.42	TH34	34.80	Null	Null
TP13	33.39	Null		TH4	30.30	Null		TH35	34.94	2.048(1)	557.05
TP14	33.67	3.935(0)		TH6	30.99	3.112(0)	542.20	TH36	35.49	2.381(1)	559.93
TP16	34.21	Null		TH7	31.12	4.097(0)	542.33	TH37	36.03	2.919(1)	566.65
TP17	34.49	Null		TH8	31.26	Null		TH38	36.58	Null	Null
TP19	35.03	5.916(0)		TH9	31.39	5.056(0)	544.64	TH39	37.12	1.690(1)	554.90
TP20	36.12	4.839(0)		TH10	31.53	Null		TH40	37.67	2.006(1)	558.89
TP21	37.21	5.160(0)		TH11	31.67	1.494(1)	552.88	TH41	38.22	2.278(1)	561.69
TP22	38.31	5.346(0)		TH12	31.80	4.349(0)	543.42	TH42	38.76	1.726(1)	556.69
TP24	40.48	5.363(0)		TH13	31.94	6.063(0)	544.37	TH43	39.31	1.714(1)	556.63
TP26	42.66	4.168(0)		TH14	32.07	5.354(0)	546.46	TH44	39.85	1.310(1)	552.30
L28H3	4.85	1.821(0)	539.87	TH15	32.21	Null		TH45	40.41	Null	Null

Run 63 Reduced Data Tabulation

Gauge Label	Loc. (in)	Value (PSIA) or (BTU/Fl ² -Sec)	T Surf (DegR)	Gauge Label	Loc. (in)	Value (PSIA) or (BTU/Fl ² -Sec)	T Surf (DegR)	Gauge Label	Loc. (in)	Value (PSIA) or (BTU/Fl ² -Sec)	T Surf (DegR)
L28P1	5.85	5.308(-1)		L28H4	5.85	2.022(0)	541.64	TH16	32.35	1.099(1)	551.22
L28P2	9.85	5.178(-1)		L28H5	6.85	Null	Null	TH17	32.48	1.166(1)	550.96
L28P3	13.85	5.103(-1)		L28H6	7.85	1.691(0)	541.64	TH18	32.62	1.247(1)	552.10
L28P4	17.85	Null		L28H7	9.85	2.405(0)	542.45	TH20	32.89	Null	Null
L28P5	21.85	Null		L28H8	10.85	3.132(0)	543.30	TH21	33.03	Null	Null
L28P6	25.85	Null		L28H9	11.85	4.497(0)	544.56	TH50	33.08	1.775(1)	557.93
TP1	28.75	Null		L28H10	12.85	Null	Null	TH22	33.16	3.528(0)	542.19
TP2	29.30	Null		L28H11	13.85	6.431(0)	546.30	TH23	33.31	2.279(0)	562.68
TP3	30.39	1.118(0)		L28H13	16.85	7.626(0)	547.46	TH24	33.44	2.849(1)	567.81
TP4	30.94	Null		L28H14	17.85	8.103(0)	548.52	TH25	33.58	Null	Null
TP5	31.21	1.248(0)		L28H15	18.85	8.078(0)	548.58	TH26	33.71	3.734(1)	576.96
TP6	31.48	Null		L28H16	19.85	7.974(0)	547.61	TH27	33.85	Null	Null
TP7	31.75	1.514(0)		L28H17	21.85	7.570(0)	547.65	TH28	33.99	Null	Null
TP8	32.03	Null		L28H18	22.85	7.726(0)	547.60	TH29	34.12	4.076(1)	579.13
TP9	32.30	1.815(0)		L28H19	24.85	6.969(0)	547.04	TH30	34.26	2.233(1)	562.40
TP10	32.57	2.082(0)		TH1	28.66	2.368(0)	541.77	TH31	34.39	2.114(1)	560.41
TP11	32.85	Null		TH2	29.21	Null	Null	TH32	34.53	1.783(1)	557.31
TP12	33.11	2.988(0)		TH3	29.75	2.024(0)	541.78	TH34	34.80	Null	Null
TP13	33.39	Null		TH4	30.30	Null	Null	TH35	34.94	1.603(1)	555.73
TP14	33.67	3.981(0)		TH6	30.99	3.493(0)	543.37	TH36	35.49	1.798(1)	554.46
TP16	34.21	Null		TH7	31.12	4.373(0)	544.23	TH37	36.03	2.071(1)	564.83
TP17	34.49	Null		TH8	31.26	Null	Null	TH38	36.58	Null	Null
TP19	35.03	6.428(0)		TH9	31.39	5.258(0)	545.88	TH39	37.12	1.154(1)	550.76
TP20	36.12	5.221(0)		TH10	31.53	Null	Null	TH40	37.67	1.449(1)	554.15
TP21	37.21	5.232(0)		TH11	31.67	1.799(1)	558.02	TH41	38.22	1.658(1)	558.14
TP22	38.31	6.065(0)		TH12	31.80	6.707(0)	546.75	TH42	38.76	1.306(1)	552.43
TP24	40.48	5.715(0)		TH13	31.94	7.582(0)	547.84	TH43	39.31	1.229(1)	551.79
TP26	42.66	4.215(0)		TH14	32.07	4.973(0)	547.12	TH44	39.85	7.102(0)	546.98
L28H3	4.85	2.073(0)	541.88	TH15	32.21	Null	Null	TH45	40.41	Null	Null

Run 64 Reduced Data Tabulation

Gauge Label	Loc. (in)	Value (PSIA) or (BTU/Fl ² -Sec)	T Surf (DegR)	Gauge Label	Loc. (in)	Value (PSIA) or (BTU/Fl ² -Sec)	T Surf (DegR)	Gauge Label	Loc. (in)	Value (PSIA) or (BTU/Fl ² -Sec)	T Surf (DegR)
L28P1	5.85	5.077(-1)		L28H4	5.85	2.072(0)	542.76	TH16	32.35	1.065(1)	552.85
L28P2	9.85	5.009(-1)		L28H5	6.85	Null	Null	TH17	32.48	1.321(1)	554.70
L28P3	13.85	4.910(-1)		L28H6	7.85	1.682(0)	542.48	TH18	32.62	1.497(1)	556.52
L28P4	17.85	Null		L28H7	9.85	1.824(0)	542.77	TH20	32.89	6.416(0)	547.58
L28P5	21.85	Null		L28H8	10.85	2.304(0)	543.48	TH21	33.03	Null	Null
L28P6	25.85	Null		L28H9	11.85	3.524(0)	544.54	TH50	33.08	1.559(1)	556.90
TP1	28.75	Null		L28H10	12.85	Null	Null	TH22	33.16	1.632(1)	548.71
TP2	29.30	Null		L28H11	13.85	8.395(0)	548.98	TH23	33.31	2.486(1)	562.89
TP3	30.39	1.375(0)		L28H13	16.85	7.506(0)	548.29	TH24	33.44	2.855(1)	564.76
TP4	30.94	Null		L28H14	17.85	7.798(0)	548.01	TH25	33.58	3.120(1)	561.31
TP5	31.21	1.339(0)		L28H15	18.85	7.531(0)	548.00	TH26	33.71	3.826(1)	573.49
TP6	31.48	Null		L28H16	19.85	7.763(0)	548.18	TH27	33.85	1.636(1)	554.59
TP7	31.75	1.629(0)		L28H17	21.85	7.397(0)	548.18	TH28	33.99	4.177(1)	575.70
TP8	32.03	Null		L28H18	22.85	7.562(0)	548.58	TH29	34.12	3.958(1)	574.12
TP9	32.30	1.908(0)		L28H19	24.85	6.805(0)	548.13	TH30	34.26	2.170(1)	560.01
TP10	32.57	2.184(0)		TH1	28.66	1.755(0)	542.92	TH31	34.39	1.870(1)	556.86
TP11	32.85	Null		TH2	29.21	Null	Null	TH32	34.53	1.479(1)	553.33
TP12	33.11	3.168(0)		TH3	29.75	2.764(0)	543.50	TH34	34.80	Null	Null
TP13	33.39	Null		TH4	30.30	Null	Null	TH35	34.94	1.342(1)	552.07
TP14	33.67	4.488(0)		TH6	30.99	3.035(0)	544.42	TH36	35.49	1.227(1)	551.81
TP16	34.21	Null		TH7	31.12	3.255(0)	544.95	TH37	36.03	1.537(1)	556.49
TP17	34.49	Null		TH8	31.26	Null	Null	TH38	36.58	Null	Null
TP19	35.03	6.300(0)		TH9	31.39	4.095(0)	547.06	TH39	37.12	8.087(0)	548.10
TP20	36.12	5.251(0)		TH10	31.53	Null	Null	TH40	37.67	1.106(1)	552.12
TP21	37.21	5.579(0)		TH11	31.67	1.736(1)	559.07	TH41	38.22	1.139(1)	552.67
TP22	38.31	6.347(0)		TH12	31.80	7.650(0)	548.62	TH42	38.76	7.334(0)	548.86
TP24	40.48	5.562(0)		TH13	31.94	7.941(0)	549.06	TH43	39.31	7.195(0)	548.83
TP26	42.66	2.941(0)		TH14	32.07	5.742(0)	547.83	TH44	39.85	2.728(0)	543.71
L28H3	4.85	2.183(0)	542.83	TH15	32.21	Null	Null	TH45	40.41	Null	Null

Run 65 Reduced Data Tabulation

Gauge Label	Loc. (in)	Value (PSIA) or (BTU/Fl ² -Sec)	T Surf (DegR)	Gauge Label	Loc. (in)	Value (PSIA) or (BTU/Fl ² -Sec)	T Surf (DegR)	Gauge Label	Loc. (in)	Value (PSIA) or (BTU/Fl ² -Sec)	T Surf (DegR)
L28P1	5.85	5.241(-1)		L28H4	5.85	2.047(0)	542.04	TH16	32.35	8.943(0)	547.68
L28P2	9.85	5.131(-1)		L28H5	6.85	Null	Null	TH17	32.48	1.217(1)	550.84
L28P3	13.85	5.036(-1)		L28H6	7.85	1.811(0)	541.73	TH18	32.62	1.224(1)	551.41
L28P4	17.85	Null		L28H7	9.85	2.148(0)	542.04	TH20	32.89	4.252(0)	545.17
L28P5	21.85	Null		L28H8	10.85	2.780(0)	542.61	TH21	33.03	Null	Null
L28P6	25.85	Null		L28H9	11.85	3.694(0)	543.68	TH50	33.08	1.299(1)	552.81
TP1	28.75	Null		L28H10	12.85	Null	Null	TH22	33.16	1.519(1)	554.74
TP2	29.30	Null		L28H11	13.85	5.422(0)	545.20	TH23	33.31	1.791(1)	557.16
TP3	30.39	1.176(0)		L28H13	16.85	7.691(0)	547.40	TH24	33.44	2.124(1)	559.62
TP4	30.94	Null		L28H14	17.85	8.345(0)	547.93	TH25	33.58	2.548(1)	558.17
TP5	31.21	1.324(0)		L28H15	18.85	7.895(0)	547.80	TH26	33.71	2.912(1)	566.08
TP6	31.48	Null		L28H16	19.85	8.055(0)	547.80	TH27	33.85	3.394(1)	569.93
TP7	31.75	1.503(0)		L28H17	21.85	7.795(0)	547.42	TH28	33.99	3.318(1)	570.16
TP8	32.03	Null		L28H18	22.85	8.156(0)	547.68	TH29	34.12	3.248(1)	567.99
TP9	32.30	1.740(0)		L28H19	24.85	7.217(0)	547.52	TH30	34.26	2.241(1)	559.41
TP10	32.57	1.939(0)		TH1	28.66	3.090(0)	543.04	TH31	34.39	2.273(1)	557.09
TP11	32.85	Null		TH2	29.21	1.037(0)	540.84	TH32	34.53	1.925(1)	556.10
TP12	33.11	2.818(0)		TH3	29.75	2.314(0)	542.68	TH34	34.80	Null	Null
TP13	33.39	Null		TH4	30.30	Null	Null	TH35	34.94	2.163(1)	556.71
TP14	33.67	3.808(0)		TH6	30.99	3.700(0)	544.05	TH36	35.49	2.676(1)	561.65
TP16	34.21	Null		TH7	31.12	3.685(0)	544.15	TH37	36.03	3.072(1)	566.16
TP17	34.49	Null		TH8	31.26	Null	Null	TH38	36.58	Null	Null
TP19	35.03	5.715(0)		TH9	31.39	4.438(0)	546.29	TH39	37.12	1.577(1)	556.66
TP20	36.12	4.909(0)		TH10	31.53	Null	Null	TH40	37.67	2.547(1)	563.39
TP21	37.21	5.162(0)		TH11	31.67	1.577(1)	554.88	TH41	38.22	Null	Null
TP22	38.31	5.494(0)		TH12	31.80	5.579(0)	545.97	TH42	38.76	2.628(1)	565.74
TP24	40.48	5.609(0)		TH13	31.94	6.585(0)	546.40	TH43	39.31	2.363(1)	563.98
TP26	42.66	3.763(0)		TH14	32.07	5.457(0)	545.75	TH44	39.85	1.929(1)	559.41
L28H3	4.85	2.133(0)	542.12	TH15	32.21	Null	Null	TH45	40.41	Null	Null

Run 66 Reduced Data Tabulation

Value				Value				Value			
Gauge Label	Loc. (in)	(PSIA) or (BTU/Ft2-Sec)	T Surf (DegR)	Gauge Label	Loc. (in)	(PSIA) or (BTU/Ft2-Sec)	T Surf (DegR)	Gauge Label	Loc. (in)	(PSIA) or (BTU/Ft2-Sec)	T Surf (DegR)
L28P1	5.85	5.434(-1)		L28H4	5.85	1.972(0)	542.97	TH16	32.35	7.511(0)	550.25
L28P2	9.85	4.764(-1)		L28H5	6.85	Null	542.97	TH17	32.48	9.794(0)	552.90
L28P3	13.85	4.865(-1)		L28H6	7.85	1.759(0)	542.48	TH18	32.62	1.085(1)	553.13
L28P4	17.85	Null		L28H7	9.85	2.129(0)	542.92	TH20	32.89	4.577(0)	546.87
L28P5	21.85	Null		L28H8	10.85	2.542(0)	543.42	TH21	33.03	Null	Null
L28P6	25.85	Null		L28H9	11.85	3.818(0)	544.61	TH50	33.08	1.520(1)	556.74
TP1	28.75	Null		L28H10	12.85	Null	545.70	TH22	33.16	1.570(1)	557.79
TP2	29.30	Null		L28H11	13.85	5.676(0)	545.70	TH23	33.31	1.844(1)	560.37
TP3	30.39	1.540(0)		L28H13	16.85	7.238(0)	548.04	TH24	33.44	2.126(1)	562.62
TP4	30.94	Null		L28H14	17.85	7.769(0)	548.60	TH25	33.58	4.295(1)	569.76
TP5	31.21	1.600(0)		L28H15	18.85	7.486(0)	548.59	TH26	33.71	2.892(1)	570.22
TP6	31.48	Null		L28H16	19.85	7.773(0)	548.68	TH27	33.85	3.452(1)	574.05
TP7	31.75	1.734(0)		L28H17	21.85	7.383(0)	547.97	TH28	33.99	3.342(1)	572.14
TP8	32.03	Null		L28H18	22.85	4.441(0)	545.00	TH29	34.12	3.351(1)	569.36
TP9	32.30	2.060(0)		L28H19	24.85	7.007(0)	548.28	TH30	34.26	2.089(1)	559.20
TP10	32.57	2.283(0)		TH1	28.66	2.978(0)	544.29	TH31	34.39	1.838(1)	556.94
TP11	32.85	Null		TH2	29.21	1.255(0)	541.81	TH32	34.53	1.667(1)	554.89
TP12	33.11	3.313(0)		TH3	29.75	1.479(0)	543.57	TH34	34.80	Null	Null
TP13	33.39	Null		TH4	30.30	Null	544.47	TH35	34.94	1.598(1)	554.10
TP14	33.67	4.399(0)		TH6	30.99	2.232(0)	544.47	TH36	35.49	1.674(1)	556.18
TP16	34.21	Null		TH7	31.12	3.033(0)	544.73	TH37	36.03	2.112(1)	561.23
TP17	34.49	Null		TH8	31.26	Null	546.93	TH38	36.58	Null	Null
TP19	35.03	6.130(0)		TH9	31.39	4.360(0)	546.93	TH39	37.12	1.080(1)	551.63
TP20	36.12	5.104(0)		TH10	31.53	Null	550.66	TH40	37.67	1.931(1)	560.13
TP21	37.21	4.210(0)		TH11	31.67	9.973(0)	548.29	TH41	38.22	1.979(1)	561.44
TP22	38.31	6.112(0)		TH12	31.80	6.473(0)	549.75	TH42	38.76	1.440(1)	556.54
TP24	40.48	5.907(0)		TH13	31.94	8.844(0)	549.75	TH43	39.31	1.419(1)	556.14
TP26	42.66	3.417(0)		TH14	32.07	6.549(0)	550.14	TH44	39.85	1.153(1)	551.82
L28H3	4.85	1.570(0)	542.64	TH15	32.21	Null	Null	TH45	40.41	Null	Null

Run 67 Reduced Data Tabulation

Value				Value				Value			
Gauge Label	Loc. (in)	(PSIA) or (BTU/Ft2-Sec)	T Surf (DegR)	Gauge Label	Loc. (in)	(PSIA) or (BTU/Ft2-Sec)	T Surf (DegR)	Gauge Label	Loc. (in)	(PSIA) or (BTU/Ft2-Sec)	T Surf (DegR)
L28P1	5.85	5.400(-1)		L28H4	5.85	2.826(0)	541.08	TH16	32.35	1.185(1)	549.93
L28P2	9.85	5.127(-1)		L28H5	6.85	Null	Null	TH17	32.48	1.224(1)	551.36
L28P3	13.85	5.325(-1)		L28H6	7.85	5.675(0)	543.45	TH18	32.62	1.428(1)	552.76
L28P4	17.85	Null		L28H7	9.85	8.034(0)	545.58	TH20	32.89	Null	Null
L28P5	21.85	Null		L28H8	10.85	7.800(0)	544.27	TH21	33.03	Null	Null
L28P6	25.85	Null		L28H9	11.85	8.023(0)	545.54	TH50	33.08	1.187(1)	551.14
TP1	28.75	Null		L28H10	12.85	Null	545.09	TH22	33.16	7.395(0)	545.02
TP2	29.30	Null		L28H11	13.85	7.095(0)	545.09	TH23	33.31	2.242(1)	558.19
TP3	30.39	1.773(0)		L28H13	16.85	7.111(0)	545.11	TH24	33.44	2.668(1)	560.93
TP4	30.94	Null		L28H14	17.85	7.825(0)	545.49	TH25	33.58	3.948(1)	566.21
TP5	31.21	1.865(0)		L28H15	18.85	7.273(0)	545.27	TH26	33.71	3.360(1)	566.74
TP6	31.48	Null		L28H16	19.85	7.297(0)	545.21	TH27	33.85	3.518(1)	567.65
TP7	31.75	1.943(0)		L28H17	21.85	7.115(0)	545.04	TH28	33.99	Null	Null
TP8	32.03	Null		L28H18	22.85	3.842(0)	541.52	TH29	34.12	3.156(1)	561.12
TP9	32.30	2.269(0)		L28H19	24.85	6.911(0)	545.20	TH30	34.26	1.620(1)	550.95
TP10	32.57	2.551(0)		TH1	28.66	3.710(0)	542.14	TH31	34.39	1.611(1)	549.86
TP11	32.85	Null		TH2	29.21	2.142(0)	541.55	TH32	34.53	1.371(1)	547.52
TP12	33.11	3.857(0)		TH3	29.75	1.250(0)	541.24	TH34	34.80	Null	Null
TP13	33.39	Null		TH4	30.30	Null	543.67	TH35	34.94	1.316(1)	547.89
TP14	33.67	5.074(0)		TH6	30.99	3.234(0)	543.67	TH36	35.49	1.126(1)	547.37
TP16	34.21	Null		TH7	31.12	3.880(0)	544.31	TH37	36.03	1.398(1)	550.32
TP17	34.49	Null		TH8	31.26	Null	546.73	TH38	36.58	Null	Null
TP19	35.03	6.981(0)		TH9	31.39	5.152(0)	547.40	TH39	37.12	7.470(0)	545.83
TP20	36.12	5.563(0)		TH10	31.53	Null	553.40	TH40	37.67	1.056(1)	548.22
TP21	37.21	5.258(0)		TH11	31.67	1.738(1)	546.95	TH41	38.22	1.189(1)	550.27
TP22	38.31	6.004(0)		TH12	31.80	6.910(0)	547.95	TH42	38.76	9.183(0)	546.81
TP24	40.48	5.063(0)		TH13	31.94	9.445(0)	547.95	TH43	39.31	9.418(0)	547.15
TP26	42.66	1.720(0)		TH14	32.07	6.643(0)	548.32	TH44	39.85	6.635(0)	544.50
L28H3	4.85	2.383(0)	540.49	TH15	32.21	Null	Null	TH45	40.41	Null	Null

Run 68 Reduced Data Tabulation

Value				Value				Value			
Gauge Label	Loc. (in)	(PSIA) or (BTU/Ft2-Sec)	T Surf (DegR)	Gauge Label	Loc. (in)	(PSIA) or (BTU/Ft2-Sec)	T Surf (DegR)	Gauge Label	Loc. (in)	(PSIA) or (BTU/Ft2-Sec)	T Surf (DegR)
L28P1	5.85	5.410(-1)		L28H4	5.85	2.986(0)	543.57	TH16	32.35	5.083(0)	546.35
L28P2	9.85	5.006(-1)		L28H5	6.85	Null	Null	TH17	32.48	7.730(0)	548.72
L28P3	13.85	5.290(-1)		L28H6	7.85	5.397(0)	545.77	TH18	32.62	7.086(0)	548.76
L28P4	17.85	Null		L28H7	9.85	7.517(0)	547.56	TH20	32.89	4.010(0)	546.11
L28P5	21.85	Null		L28H8	10.85	8.048(0)	548.08	TH21	33.03	Null	Null
L28P6	25.85	Null		L28H9	11.85	8.158(0)	548.18	TH50	33.08	7.786(0)	548.66
TP1	28.75	Null		L28H10	12.85	Null	547.40	TH22	33.16	9.588(0)	550.10
TP2	29.30	Null		L28H11	13.85	7.320(0)	547.45	TH23	33.31	1.246(1)	561.72
TP3	30.39	2.743(0)		L28H13	16.85	7.315(0)	547.80	TH24	33.44	1.088(1)	551.13
TP4	30.94	Null		L28H14	17.85	7.650(0)	547.24	TH25	33.58	1.753(1)	553.99
TP5	31.21	2.612(0)		L28H15	18.85	7.340(0)	547.24	TH26	33.71	1.480(1)	556.20
TP6	31.48	Null		L28H16	19.85	7.454(0)	547.55	TH27	33.85	1.675(1)	556.81
TP7	31.75	2.919(0)		L28H17	21.85	7.301(0)	547.24	TH28	33.99	1.596(1)	557.02
TP8	32.03	Null		L28H18	22.85	3.937(0)	543.77	TH29	34.12	1.748(1)	555.53
TP9	32.30	3.109(0)		L28H19	24.85	7.042(0)	546.79	TH30	34.26	1.023(1)	549.63
TP10	32.57	3.293(0)		TH1	28.66	1.891(0)	542.07	TH31	34.39	8.921(0)	548.33
TP11	32.85	Null		TH2	29.21	1.388(0)	542.07	TH32	34.53	5.475(0)	546.47
TP12	33.11	4.335(0)		TH3	29.75	9.756(-1)	541.77	TH34	34.80	Null	Null
TP13	33.39	Null		TH4	30.30	Null	544.49	TH35	34.94	5.648(0)	545.55
TP14	33.67	4.913(0)		TH6	30.99	3.427(0)	544.93	TH36	35.49	5.722(0)	546.66
TP16	34.21	Null		TH7	31.12	3.622(0)	544.93	TH37	36.03	8.823(0)	550.31
TP17	34.49	Null		TH8	31.26	Null	547.25	TH38	36.58	Null	Null
TP19	35.03	5.570(0)		TH9	31.39	4.448(0)	547.25	TH39	37.12	6.221(0)	547.85
TP20	36.12	4.860(0)		TH10	31.53	Null	551.30	TH40	37.67	8.547(0)	550.39
TP21	37.21	4.617(0)		TH11	31.67	1.008(1)	546.66	TH41	38.22	9.477(0)	552.37
TP22	38.31	5.410(0)		TH12	31.80	4.782(0)	547.45	TH42	38.76	8.455(0)	550.54
TP24	40.48	5.177(0)		TH13	31.94	7.596(0)	547.45	TH43	39.31	9.658(0)	551.55
TP26	42.66	1.645(0)		TH14	32.07	4.027(0)	545.93	TH44	39.85	6.994(0)	549.14
L28H3	4.85	2.315(0)	543.14	TH15	32.21	Null	Null	TH45	40.41	Null	Null

Run 69 Reduced Data Tabulation

Gauge Label	Loc. (in)	Value (PSIA) or (BTU/Ft ² -Sec)	T Surf (DegR)	Gauge Label	Loc. (in)	Value (PSIA) or (BTU/Ft ² -Sec)	T Surf (DegR)	Gauge Label	Loc. (in)	Value (PSIA) or (BTU/Ft ² -Sec)	T Surf (DegR)
L28P1	5.85	5.107(-1)		L28H4	5.85	3.206(0)	543.50	TH16	32.35	2.698(1)	562.24
L28P2	9.85	5.037(-1)		L28H5	6.85	Null		TH17	32.48	3.552(1)	567.17
L28P3	13.85	4.936(-1)		L28H6	7.85	6.024(0)	546.40	TH18	32.62	3.616(1)	569.88
L28P4	17.85	Null		L28H7	9.85	7.646(0)	547.56	TH20	32.89	Null	Null
L28P5	21.85	Null		L28H8	10.85	7.843(0)	547.44	TH21	33.03	Null	Null
L28P6	25.85	Null		L28H9	11.85	8.225(0)	548.35	TH50	33.08	4.953(1)	581.27
TP1	28.75	Null		L28H10	12.85	Null		TH23	33.16	4.835(1)	572.27
TP2	29.30	Null		L28H11	13.85	7.323(0)	547.46	TH23	33.31	6.935(1)	595.79
TP3	30.39	1.435(0)		L28H13	16.85	7.373(0)	547.59	TH24	33.44	8.114(1)	603.74
TP4	30.94	Null		L28H14	17.85	7.661(0)	548.07	TH25	33.58	1.059(2)	617.17
TP5	31.21	1.529(0)		L28H15	18.85	7.209(0)	547.59	TH26	33.71	1.013(2)	621.27
TP6	31.48	Null		L28H16	19.85	7.378(0)	547.50	TH27	33.85	1.229(2)	637.49
TP7	31.75	1.944(0)		L28H17	21.85	7.206(0)	547.31	TH28	33.99	1.109(2)	628.44
TP8	32.03	Null		L28H18	22.85	4.426(0)	543.68	TH29	34.12	9.319(1)	615.81
TP9	32.30	3.016(0)		L28H19	24.85	6.692(0)	547.27	TH30	34.26	7.873(1)	607.03
TP10	32.57	3.622(0)		TH1	28.66	3.514(0)	544.72	TH31	34.39	9.543(1)	620.37
TP11	32.85	Null		TH2	29.21	3.170(0)	545.09	TH32	34.53	9.307(1)	620.28
TP12	33.11	6.521(0)		TH3	29.75	3.937(0)	545.41	TH34	34.80	Null	Null
TP13	33.39	Null		TH4	30.30	Null		TH35	34.94	1.005(2)	628.15
TP14	33.67	7.384(0)		TH6	30.99	4.890(0)	546.83	TH36	35.49	1.045(2)	634.88
TP16	34.21	Null		TH7	31.12	5.398(0)	547.32	TH37	36.03	8.189(1)	619.04
TP17	34.49	Null		TH8	31.26	Null		TH38	36.58	Null	Null
TP19	35.03	7.154(0)		TH9	31.39	6.668(0)	548.40	TH39	37.12	9.884(1)	632.02
TP20	36.12	7.766(0)		TH10	31.53	Null		TH40	37.67	1.096(2)	641.27
TP21	37.21	8.065(0)		TH11	31.67	4.588(1)	577.58	TH41	38.22	1.142(2)	647.41
TP22	38.31	7.611(0)		TH12	31.80	1.464(1)	552.87	TH42	38.76	8.495(1)	627.82
TP24	40.48	5.651(0)		TH13	31.94	1.850(1)	554.41	TH43	39.31	9.195(1)	637.59
TP26	42.66	3.283(0)		TH14	32.07	1.666(1)	557.99	TH44	39.85	1.183(2)	660.00
L28H3	4.85	3.234(0)	543.28	TH15	32.21	Null		TH45	40.41	Null	Null

Run 70 Reduced Data Tabulation

Gauge Label	Loc. (in)	Value (PSIA) or (BTU/Ft ² -Sec)	T Surf (DegR)	Gauge Label	Loc. (in)	Value (PSIA) or (BTU/Ft ² -Sec)	T Surf (DegR)	Gauge Label	Loc. (in)	Value (PSIA) or (BTU/Ft ² -Sec)	T Surf (DegR)
L28P1	5.85	5.155(-1)		L28H4	5.85	3.086(0)	540.16	TH16	32.35	1.689(1)	553.19
L28P2	9.85	5.052(-1)		L28H5	6.85	Null		TH17	32.48	2.066(1)	556.50
L28P3	13.85	5.067(-1)		L28H6	7.85	6.645(0)	543.53	TH18	32.62	1.298(1)	547.54
L28P4	17.85	Null		L28H7	9.85	8.252(0)	544.78	TH20	32.89	1.158(1)	547.33
L28P5	21.85	Null		L28H8	10.85	8.271(0)	544.91	TH21	33.03	Null	Null
L28P6	25.85	Null		L28H9	11.85	8.515(0)	544.90	TH50	33.08	3.038(1)	565.51
TP1	28.75	Null		L28H10	12.85	Null		TH23	33.16	8.743(0)	543.59
TP2	29.30	Null		L28H11	13.85	7.405(0)	544.32	TH23	33.31	4.147(1)	576.28
TP3	30.39	1.928(0)		L28H13	16.85	7.201(0)	544.22	TH24	33.44	4.956(1)	577.51
TP4	30.94	Null		L28H14	17.85	7.894(0)	544.67	TH25	33.58	5.608(1)	587.50
TP5	31.21	1.879(0)		L28H15	18.85	7.182(0)	544.46	TH26	33.71	6.345(1)	593.77
TP6	31.48	Null		L28H16	19.85	7.534(0)	544.40	TH27	33.85	8.023(1)	604.74
TP7	31.75	2.252(0)		L28H17	21.85	6.961(0)	544.00	TH28	33.99	7.760(1)	605.10
TP8	32.03	Null		L28H18	22.85	5.448(0)	540.94	TH29	34.12	6.631(1)	593.38
TP9	32.30	2.841(0)		L28H19	24.85	7.142(0)	544.21	TH30	34.26	4.382(1)	574.96
TP10	32.57	3.206(0)		TH1	28.66	3.936(-1)	537.29	TH31	34.39	4.737(1)	581.15
TP11	32.85	Null		TH2	29.21	1.914(0)	539.64	TH32	34.53	4.317(1)	577.86
TP12	33.11	5.300(0)		TH3	29.75	1.074(0)	539.17	TH34	34.80	Null	Null
TP13	33.39	Null		TH4	30.30	Null		TH35	34.94	4.554(1)	581.77
TP14	33.67	6.852(0)		TH6	30.99	5.048(0)	542.00	TH36	35.49	5.882(1)	591.51
TP16	34.21	Null		TH7	31.12	6.955(0)	543.74	TH37	36.03	5.423(1)	588.04
TP17	34.49	Null		TH8	31.26	Null		TH38	36.58	Null	Null
TP19	35.03	8.461(0)		TH9	31.39	8.514(0)	546.29	TH39	37.12	3.173(1)	560.51
TP20	36.12	8.001(0)		TH10	31.53	Null		TH40	37.67	4.735(1)	584.98
TP21	37.21	9.871(0)		TH11	31.67	3.015(1)	563.28	TH41	38.22	4.733(1)	591.03
TP22	38.31	8.116(0)		TH12	31.80	1.170(1)	548.24	TH42	38.76	3.882(1)	581.40
TP24	40.48	6.178(0)		TH13	31.94	1.158(1)	548.58	TH43	39.31	3.753(1)	579.52
TP26	42.66	3.202(0)		TH14	32.07	1.229(1)	549.55	TH44	39.85	2.897(1)	572.48
L28H3	4.85	2.496(0)	539.71	TH15	32.21	Null		TH45	40.41	Null	Null

Run 71 Reduced Data Tabulation

Gauge Label	Loc. (in)	Value (PSIA) or (BTU/Ft ² -Sec)	T Surf (DegR)	Gauge Label	Loc. (in)	Value (PSIA) or (BTU/Ft ² -Sec)	T Surf (DegR)	Gauge Label	Loc. (in)	Value (PSIA) or (BTU/Ft ² -Sec)	T Surf (DegR)
L28P1	5.85	5.620(-1)		L28H4	5.85	2.935(0)	542.88	TH16	32.35	7.471(0)	551.87
L28P2	9.85	5.299(-1)		L28H5	6.85	Null		TH17	32.48	8.102(0)	555.11
L28P3	13.85	5.652(-1)		L28H6	7.85	6.057(0)	545.97	TH18	32.62	4.207(0)	546.08
L28P4	17.85	Null		L28H7	9.85	7.498(0)	547.32	TH20	32.89	7.258(0)	550.28
L28P5	21.85	Null		L28H8	10.85	7.327(0)	547.21	TH21	33.03	Null	Null
L28P6	25.85	Null		L28H9	11.85	7.318(0)	547.35	TH50	33.08	1.394(1)	557.98
TP1	28.75	Null		L28H10	12.85	Null		TH23	33.16	2.321(0)	541.54
TP2	29.30	Null		L28H11	13.85	6.663(0)	546.39	TH23	33.31	1.726(1)	557.75
TP3	30.39	3.128(0)		L28H13	16.85	6.500(0)	546.37	TH24	33.44	1.894(1)	559.12
TP4	30.94	Null		L28H14	17.85	7.091(0)	546.94	TH25	33.58	2.678(1)	564.80
TP5	31.21	3.339(0)		L28H15	18.85	6.869(0)	546.97	TH26	33.71	2.559(1)	567.22
TP6	31.48	Null		L28H16	19.85	6.663(0)	547.09	TH27	33.85	3.343(1)	574.03
TP7	31.75	3.747(0)		L28H17	21.85	6.227(0)	547.25	TH28	33.99	3.968(1)	575.51
TP8	32.03	Null		L28H18	22.85	4.707(0)	544.17	TH29	34.12	3.651(1)	574.42
TP9	32.30	4.126(0)		L28H19	24.85	6.563(0)	547.38	TH30	34.26	2.249(1)	561.93
TP10	32.57	4.386(0)		TH1	28.66	4.036(-1)	540.13	TH31	34.39	2.164(1)	559.96
TP11	32.85	Null		TH2	29.21	8.181(-1)	542.10	TH32	34.53	1.905(1)	558.11
TP12	33.11	5.999(0)		TH3	29.75	7.450(-1)	541.37	TH34	34.80	Null	Null
TP13	33.39	Null		TH4	30.30	Null		TH35	34.94	2.054(1)	558.02
TP14	33.67	7.060(0)		TH6	30.99	3.118(0)	547.10	TH36	35.49	2.028(1)	561.03
TP16	34.21	Null		TH7	31.12	5.023(0)	548.36	TH37	36.03	2.146(1)	568.02
TP17	34.49	Null		TH8	31.26	Null		TH38	36.58	Null	Null
TP19	35.03	8.769(0)		TH9	31.39	6.481(0)	551.06	TH39	37.12	3.737(1)	567.46
TP20	36.12	7.495(0)		TH10	31.53	Null		TH40	37.67	5.372(1)	592.85
TP21	37.21	1.248(1)		TH11	31.67	8.049(0)	556.36	TH41	38.22	5.246(1)	585.74
TP22	38.31	1.260(1)		TH12	31.80	9.226(0)	553.35	TH42	38.76	3.526(1)	572.68
TP24	40.48	5.734(0)		TH13	31.94	8.927(0)	553.56	TH43	39.31	2.147(1)	559.92
TP26	42.66	2.604(0)		TH14	32.07	Null		TH44	39.85	9.069(0)	548.10
L28H3	4.85	2.109(0)	541.90	TH15	32.21	Null		TH45	40.41	Null	Null

Run 72 Reduced Data Tabulation

Gauge Label	Loc. (in)	Value (PSIA) or (BTU/Ft ² -Sec)	T Surf (DegR)	Gauge Label	Loc. (in)	Value (PSIA) or (BTU/Ft ² -Sec)	T Surf (DegR)	Gauge Label	Loc. (in)	Value (PSIA) or (BTU/Ft ² -Sec)	T Surf (DegR)
L28P1	5.85	5.591(-1)		L28H4	5.85	3.151(0)	543.93	L28P1	5.85	5.591(-1)	
L28P2	9.85	5.373(-1)		L28H5	6.85	Null	Null	L28P2	9.85	5.373(-1)	
L28P3	13.85	5.385(-1)		L28H6	7.85	6.398(0)	547.50	L28P3	13.85	5.385(-1)	
L28P4	17.85	Null		L28H7	9.85	7.491(0)	548.76	L28P4	17.85	Null	
L28P5	21.85	Null		L28H8	10.85	7.370(0)	548.27	L28P5	21.85	Null	
L28P6	25.85	Null		L28H9	11.85	7.108(0)	548.63	L28P6	25.85	Null	
TP1	28.75	Null		L28H10	12.85	Null	Null	TP1	28.75	Null	
TP2	29.30	Null		L28H11	13.85	6.906(0)	548.00	TP2	29.30	Null	
TP3	30.39	2.019(0)		L28H12	16.85	6.477(0)	547.95	TP3	30.39	2.019(0)	
TP4	30.94	Null		L28H13	17.85	7.210(0)	548.00	TP4	30.94	Null	
TP5	31.21	1.640(0)		L28H14	17.85	7.210(0)	548.00	TP5	31.21	1.640(0)	
TP6	31.48	Null		L28H15	18.85	6.703(0)	547.90	TP6	31.48	Null	
TP7	31.75	2.398(0)		L28H16	19.85	6.756(0)	547.97	TP7	31.75	2.398(0)	
TP8	32.03	Null		L28H17	21.85	5.929(0)	547.07	TP8	32.03	Null	
TP9	32.30	3.094(0)		L28H18	22.85	6.494(0)	547.76	TP9	32.30	3.094(0)	
TP10	32.57	3.534(0)		L28H19	24.85	6.407(0)	547.50	TP10	32.57	3.534(0)	
TP11	32.85	Null		TH1	28.66	Null	Null	TP11	32.85	Null	
TP12	33.11	5.148(0)		TH2	29.21	1.668(0)	541.63	TP12	33.11	5.148(0)	
TP13	33.39	Null		TH3	29.75	1.758(0)	541.19	TP13	33.39	Null	
TP14	33.67	6.604(0)		TH4	30.30	Null	Null	TP14	33.67	6.604(0)	
TP16	34.21	Null		TH6	30.99	2.918(0)	543.93	TP16	34.21	Null	
TP17	34.49	Null		TH7	31.12	5.595(0)	546.40	TP17	34.49	Null	
TP19	35.03	8.218(0)		TH8	31.26	7.659(0)	550.04	TP19	35.03	8.218(0)	
TP20	36.12	8.174(0)		TH9	31.39	8.160(0)	548.47	TP20	36.12	8.174(0)	
TP21	37.21	9.652(0)		TH10	31.53	Null	Null	TP21	37.21	9.652(0)	
TP22	38.31	8.026(0)		TH11	31.67	3.071(1)	570.78	TP22	38.31	8.026(0)	
TP24	40.48	6.284(0)		TH12	31.80	1.311(1)	552.96	TP24	40.48	6.284(0)	
TP26	42.66	3.652(0)		TH13	31.94	1.472(1)	553.48	TP26	42.66	3.652(0)	
L28H3	4.85	2.280(0)	543.03	TH14	32.07	1.259(1)	553.74	L28H3	4.85	2.280(0)	543.03
				TH15	32.21	Null	Null				

Run 73 Reduced Data Tabulation

Gauge Label	Loc. (in)	Value (PSIA) or (BTU/Ft ² -Sec)	T Surf (DegR)	Gauge Label	Loc. (in)	Value (PSIA) or (BTU/Ft ² -Sec)	T Surf (DegR)	Gauge Label	Loc. (in)	Value (PSIA) or (BTU/Ft ² -Sec)	T Surf (DegR)
L28P1	5.85	5.298(-1)		L28H4	5.85	2.980(0)	541.47	L28P1	5.85	5.298(-1)	
L28P2	9.85	5.280(-1)		L28H5	6.85	Null	Null	L28P2	9.85	5.280(-1)	
L28P3	13.85	5.148(-1)		L28H6	7.85	6.260(0)	544.82	L28P3	13.85	5.148(-1)	
L28P4	17.85	Null		L28H7	9.85	8.170(0)	546.65	L28P4	17.85	Null	
L28P5	21.85	Null		L28H8	10.85	8.458(0)	546.82	L28P5	21.85	Null	
L28P6	25.85	Null		L28H9	11.85	8.456(0)	547.09	L28P6	25.85	Null	
TP1	28.75	Null		L28H10	12.85	Null	Null	TP1	28.75	Null	
TP2	29.30	Null		L28H11	13.85	7.636(0)	546.04	TP2	29.30	Null	
TP3	30.39	2.342(0)		L28H12	16.85	7.670(0)	546.22	TP3	30.39	2.342(0)	
TP4	30.94	Null		L28H13	17.85	7.890(0)	546.30	TP4	30.94	Null	
TP5	31.21	2.251(0)		L28H14	17.85	7.890(0)	546.30	TP5	31.21	2.251(0)	
TP6	31.48	Null		L28H15	18.85	7.681(0)	546.33	TP6	31.48	Null	
TP7	31.75	2.757(0)		L28H16	19.85	7.620(0)	546.20	TP7	31.75	2.757(0)	
TP8	32.03	Null		L28H17	21.85	3.385(0)	541.57	TP8	32.03	Null	
TP9	32.30	3.298(0)		L28H18	22.85	4.822(0)	543.04	TP9	32.30	3.298(0)	
TP10	32.57	3.670(0)		L28H19	24.85	7.084(0)	546.38	TP10	32.57	3.670(0)	
TP11	32.85	Null		TH1	28.66	9.838(-1)	539.28	TP11	32.85	Null	
TP12	33.11	5.211(0)		TH2	29.21	1.232(0)	539.96	TP12	33.11	5.211(0)	
TP13	33.39	Null		TH3	29.75	1.190(0)	539.75	TP13	33.39	Null	
TP14	33.67	6.506(0)		TH4	30.30	Null	Null	TP14	33.67	6.506(0)	
TP16	34.21	Null		TH6	30.99	3.681(0)	541.91	TP16	34.21	Null	
TP17	34.49	Null		TH7	31.12	6.513(0)	544.42	TP17	34.49	Null	
TP19	35.03	8.529(0)		TH8	31.26	6.399(0)	546.24	TP19	35.03	8.529(0)	
TP20	36.12	7.833(0)		TH9	31.39	9.703(0)	547.64	TP20	36.12	7.833(0)	
TP21	37.21	8.883(0)		TH10	31.53	Null	Null	TP21	37.21	8.883(0)	
TP22	38.31	8.409(0)		TH11	31.67	2.979(1)	564.14	TP22	38.31	8.409(0)	
TP24	40.48	5.975(0)		TH12	31.80	1.508(1)	550.07	TP24	40.48	5.975(0)	
TP26	42.66	2.688(0)		TH13	31.94	1.735(1)	551.68	TP26	42.66	2.688(0)	
L28H3	4.85	2.136(0)	540.98	TH14	32.07	1.561(1)	551.29	L28H3	4.85	2.136(0)	540.98
				TH15	32.21	Null	Null				

Run 75 Reduced Data Tabulation

Gauge Label	Loc. (in)	Value (PSIA) or (BTU/Ft ² -Sec)	T Surf (DegR)	Gauge Label	Loc. (in)	Value (PSIA) or (BTU/Ft ² -Sec)	T Surf (DegR)	Gauge Label	Loc. (in)	Value (PSIA) or (BTU/Ft ² -Sec)	T Surf (DegR)
L28P1	5.85	5.400(-1)		L28H4	5.85	2.835(0)	542.22	L28P1	5.85	5.400(-1)	
L28P2	9.85	5.076(-1)		L28H5	6.85	Null	Null	L28P2	9.85	5.076(-1)	
L28P3	13.85	5.239(-1)		L28H6	7.85	4.976(0)	544.67	L28P3	13.85	5.239(-1)	
L28P4	17.85	Null		L28H7	9.85	6.930(0)	546.44	L28P4	17.85	Null	
L28P5	21.85	Null		L28H8	10.85	7.062(0)	546.53	L28P5	21.85	Null	
L28P6	25.85	Null		L28H9	11.85	7.334(0)	546.87	L28P6	25.85	Null	
TP1	28.75	Null		L28H10	12.85	Null	Null	TP1	28.75	Null	
TP2	29.30	Null		L28H11	13.85	6.629(0)	546.12	TP2	29.30	Null	
TP3	30.39	2.862(0)		L28H12	16.85	6.308(0)	545.99	TP3	30.39	2.862(0)	
TP4	30.94	Null		L28H13	17.85	6.783(0)	546.30	TP4	30.94	Null	
TP5	31.21	2.551(0)		L28H14	17.85	6.649(0)	546.12	TP5	31.21	2.551(0)	
TP6	31.48	Null		L28H15	18.85	6.354(0)	545.93	TP6	31.48	Null	
TP7	31.75	3.322(0)		L28H16	19.85	6.354(0)	545.93	TP7	31.75	3.322(0)	
TP8	32.03	Null		L28H17	21.85	2.878(0)	542.04	TP8	32.03	Null	
TP9	32.30	3.818(0)		L28H18	22.85	3.726(0)	543.11	TP9	32.30	3.818(0)	
TP10	32.57	4.149(0)		L28H19	24.85	6.047(0)	546.28	TP10	32.57	4.149(0)	
TP11	32.85	Null		TH1	28.66	9.840(-2)	538.74	TP11	32.85	Null	
TP12	33.11	5.285(0)		TH2	29.21	9.157(-2)	538.78	TP12	33.11	5.285(0)	
TP13	33.39	Null		TH3	29.75	7.732(-1)	539.27	TP13	33.39	Null	
TP14	33.67	6.178(0)		TH4	30.30	Null	Null	TP14	33.67	6.178(0)	
TP16	34.21	Null		TH6	30.99	4.297(0)	544.02	TP16	34.21	Null	
TP17	34.49	Null		TH7	31.12	5.112(0)	545.36	TP17	34.49	Null	
TP19	35.03	8.242(0)		TH8	31.26	5.835(0)	549.51	TP19	35.03	8.242(0)	
TP20	36.12	7.241(0)		TH9	31.39	8.267(0)	548.61	TP20	36.12	7.241(0)	
TP21	37.21	7.765(0)		TH10	31.53	Null	Null	TP21	37.21	7.765(0)	
TP22	38.31	1.243(1)		TH11	31.67	2.287(1)	561.33	TP22	38.31	1.243(1)	
TP24	40.48	6.019(0)		TH12	31.80	1.312(1)	552.08	TP24	40.48	6.019(0)	
TP26	42.66	2.674(0)		TH13	31.94	1.260(1)	553.17	TP26	42.66	2.674(0)	
L28H3	4.85	1.967(0)	541.18	TH14	32.07	1.191(1)	552.52	L28H3	4.85	1.967(0)	541.18
				TH15	32.21	Null	Null				

Run 76 Reduced Data Tabulation

Gauge Label	Loc. (in)	Value (PSIA) or (BTU/Ft ² -Sec)	T Surf (DegR)	Gauge Label	Loc. (in)	Value (PSIA) or (BTU/Ft ² -Sec)	T Surf (DegR)	Gauge Label	Loc. (in)	Value (PSIA) or (BTU/Ft ² -Sec)	T Surf (DegR)
L28P1	5.85	9.961(-1)		L28H4	5.85	1.222(1)	546.69	TH16	32.35	8.805(0)	545.40
L28P2	9.85	9.758(-1)		L28H5	6.85	Null	Null	TH17	32.48	1.016(0)	546.77
L28P3	13.85	9.634(-1)		L28H6	7.85	1.230(1)	546.78	TH18	32.62	Null	Null
L28P4	17.85	Null		L28H7	9.85	1.237(1)	547.06	TH20	32.89	9.557(0)	545.36
L28P5	21.85	Null		L28H8	10.85	1.154(1)	548.58	TH21	33.03	Null	Null
L28P6	25.85	Null		L28H9	11.85	1.178(1)	546.96	TH50	33.08	9.364(0)	546.02
TP1	28.75	Null		L28H10	12.85	Null	Null	TH22	33.16	1.159(1)	546.26
TP2	29.30	Null		L28H11	13.85	1.057(1)	546.00	TH23	33.31	2.042(1)	551.45
TP3	30.39	9.788(-1)		L28H13	16.85	1.072(1)	545.81	TH24	33.44	2.984(1)	558.18
TP4	30.94	Null		L28H14	17.85	1.069(1)	547.97	TH25	33.58	3.567(1)	562.64
TP5	31.21	9.745(-1)		L28H15	18.85	9.997(0)	546.05	TH26	33.71	4.174(1)	567.52
TP6	31.48	Null		L28H16	19.85	1.024(1)	546.01	TH27	33.85	5.127(1)	573.49
TP7	31.75	9.342(-1)		L28H17	21.85	4.453(0)	540.80	TH28	33.99	4.601(1)	569.88
TP8	32.03	Null		L28H18	22.85	6.262(0)	542.30	TH29	34.12	3.882(1)	565.19
TP9	32.30	9.729(-1)		L28H19	24.85	9.863(0)	545.28	TH30	34.26	2.793(1)	558.76
TP10	32.57	1.059(0)		TH1	28.66	Null	Null	TH31	34.39	3.445(1)	564.51
TP11	32.85	Null		TH2	29.21	4.467(0)	541.91	TH32	34.53	3.774(1)	567.15
TP12	33.11	1.427(0)		TH3	29.75	6.707(0)	544.84	TH34	34.80	Null	Null
TP13	33.39	Null		TH4	30.30	Null	Null	TH35	34.94	4.494(1)	581.00
TP14	33.67	4.278(0)		TH6	30.99	8.702(0)	545.46	TH36	35.49	Null	Null
TP16	34.21	Null		TH7	31.12	8.964(0)	545.48	TH37	36.03	5.124(1)	582.09
TP17	34.49	Null		TH8	31.26	Null	Null	TH38	36.58	Null	Null
TP19	35.03	5.936(0)		TH9	31.39	1.141(1)	547.22	TH39	37.12	6.118(1)	591.96
TP20	36.12	6.240(0)		TH10	31.53	Null	Null	TH40	37.67	7.210(1)	601.59
TP21	37.21	6.357(0)		TH11	31.67	8.929(0)	545.96	TH41	38.22	8.054(1)	606.55
TP22	38.31	5.864(0)		TH12	31.80	1.144(1)	547.07	TH42	38.76	6.610(1)	595.74
TP24	40.48	6.362(0)		TH13	31.94	7.677(0)	544.08	TH43	39.31	7.727(1)	602.85
TP26	42.66	7.186(0)		TH14	32.07	1.095(1)	547.13	TH44	39.85	8.729(1)	630.18
L28H3	4.85	1.252(1)	547.49	TH15	32.21	Null	Null	TH45	40.41	Null	Null

Run 77 Reduced Data Tabulation

Gauge Label	Loc. (in)	Value (PSIA) or (BTU/Ft ² -Sec)	T Surf (DegR)	Gauge Label	Loc. (in)	Value (PSIA) or (BTU/Ft ² -Sec)	T Surf (DegR)	Gauge Label	Loc. (in)	Value (PSIA) or (BTU/Ft ² -Sec)	T Surf (DegR)
L28P1	5.85	1.019(0)		L28H4	5.85	1.176(1)	547.68	TH16	32.35	7.074(0)	544.47
L28P2	9.85	1.008(0)		L28H5	6.85	Null	Null	TH17	32.48	8.321(0)	545.61
L28P3	13.85	1.006(0)		L28H6	7.85	1.230(1)	548.19	TH18	32.62	1.588(0)	538.24
L28P4	17.85	Null		L28H7	9.85	1.224(1)	547.73	TH20	32.89	3.562(0)	541.57
L28P5	21.85	Null		L28H8	10.85	1.223(1)	549.56	TH21	33.03	Null	Null
L28P6	25.85	Null		L28H9	11.85	1.220(1)	548.13	TH50	33.08	7.887(0)	546.09
TP1	28.75	Null		L28H10	12.85	Null	Null	TH22	33.16	9.623(0)	548.32
TP2	29.30	Null		L28H11	13.85	1.078(1)	546.83	TH23	33.31	1.229(1)	550.13
TP3	30.39	2.210(0)		L28H13	16.85	1.041(1)	546.81	TH24	33.44	1.156(1)	550.33
TP4	30.94	Null		L28H14	17.85	1.092(1)	547.39	TH25	33.58	1.236(1)	551.02
TP5	31.21	2.391(0)		L28H15	18.85	1.042(1)	547.00	TH26	33.71	1.792(1)	553.75
TP6	31.48	Null		L28H16	19.85	1.033(1)	547.44	TH27	33.85	1.895(1)	554.56
TP7	31.75	2.607(0)		L28H17	21.85	1.026(1)	546.48	TH28	33.99	1.842(1)	554.75
TP8	32.03	Null		L28H18	22.85	5.408(0)	542.09	TH29	34.12	1.527(1)	552.19
TP9	32.30	2.768(0)		L28H19	24.85	1.007(1)	546.28	TH30	34.26	1.107(1)	547.78
TP10	32.57	2.902(0)		TH1	28.66	2.843(0)	540.14	TH31	34.39	1.251(1)	548.69
TP11	32.85	Null		TH2	29.21	2.636(0)	540.24	TH32	34.53	9.778(0)	546.07
TP12	33.11	4.092(0)		TH3	29.75	1.712(0)	539.84	TH34	34.80	Null	Null
TP13	33.39	Null		TH4	30.30	Null	Null	TH35	34.94	1.066(1)	547.46
TP14	33.67	4.911(0)		TH6	30.99	3.170(0)	541.09	TH36	35.49	Null	Null
TP16	34.21	Null		TH7	31.12	4.034(0)	542.02	TH37	36.03	1.759(1)	552.81
TP17	34.49	Null		TH8	31.26	7.742(0)	546.28	TH38	36.58	Null	Null
TP19	35.03	6.028(0)		TH9	31.39	3.717(0)	542.42	TH39	37.12	1.306(1)	548.46
TP20	36.12	5.552(0)		TH10	31.53	Null	Null	TH40	37.67	1.885(1)	553.92
TP21	37.21	4.924(0)		TH11	31.67	6.987(0)	547.88	TH41	38.22	2.240(1)	557.51
TP22	38.31	6.408(0)		TH12	31.80	3.238(0)	542.09	TH42	38.76	1.830(1)	554.98
TP24	40.48	6.769(0)		TH13	31.94	4.993(0)	542.86	TH43	39.31	1.898(1)	555.81
TP26	42.66	6.037(0)		TH14	32.07	3.716(0)	542.93	TH44	39.85	1.535(1)	552.42
L28H3	4.85	1.237(1)	547.92	TH15	32.21	Null	Null	TH45	40.41	Null	Null

Run 78 Reduced Data Tabulation

Gauge Label	Loc. (in)	Value (PSIA) or (BTU/Ft ² -Sec)	T Surf (DegR)	Gauge Label	Loc. (in)	Value (PSIA) or (BTU/Ft ² -Sec)	T Surf (DegR)	Gauge Label	Loc. (in)	Value (PSIA) or (BTU/Ft ² -Sec)	T Surf (DegR)
L28P1	5.85	9.996(-1)		L28H4	5.85	1.158(1)	547.86	TH16	32.35	6.558(0)	545.21
L28P2	9.85	9.699(-1)		L28H5	6.85	Null	Null	TH17	32.48	8.688(0)	547.26
L28P3	13.85	9.850(-1)		L28H6	7.85	1.201(1)	548.84	TH18	32.62	9.499(0)	548.02
L28P4	17.85	Null		L28H7	9.85	1.160(1)	548.24	TH20	32.89	3.183(0)	542.65
L28P5	21.85	Null		L28H8	10.85	1.185(1)	549.18	TH21	33.03	Null	Null
L28P6	25.85	Null		L28H9	11.85	1.192(1)	548.90	TH50	33.08	4.806(0)	546.15
TP1	28.75	Null		L28H10	12.85	Null	Null	TH22	33.16	5.758(0)	546.75
TP2	29.30	Null		L28H11	13.85	1.017(1)	547.73	TH23	33.31	6.095(0)	548.28
TP3	30.39	3.005(0)		L28H13	16.85	1.048(1)	547.06	TH24	33.44	7.044(0)	549.06
TP4	30.94	Null		L28H14	17.85	1.064(1)	547.78	TH25	33.58	8.795(0)	550.24
TP5	31.21	3.166(0)		L28H15	18.85	9.797(0)	546.80	TH26	33.71	1.049(1)	552.13
TP6	31.48	Null		L28H16	19.85	9.866(0)	547.17	TH27	33.85	1.060(1)	553.10
TP7	31.75	3.257(0)		L28H17	21.85	1.001(1)	547.51	TH28	33.99	9.113(0)	553.25
TP8	32.03	Null		L28H18	22.85	5.579(0)	542.92	TH29	34.12	1.239(1)	550.14
TP9	32.30	3.403(0)		L28H19	24.85	9.718(0)	547.06	TH30	34.26	5.035(0)	545.20
TP10	32.57	3.624(0)		TH1	28.66	2.018(0)	540.28	TH31	34.39	7.756(0)	545.14
TP11	32.85	Null		TH2	29.21	1.965(0)	540.39	TH32	34.53	4.942(0)	543.51
TP12	33.11	4.724(0)		TH3	29.75	1.046(0)	539.61	TH34	34.80	Null	Null
TP13	33.39	Null		TH4	30.30	Null	Null	TH35	34.94	7.401(0)	543.48
TP14	33.67	5.351(0)		TH6	30.99	2.582(0)	541.71	TH36	35.49	Null	Null
TP16	34.21	Null		TH7	31.12	2.805(0)	542.28	TH37	36.03	1.067(1)	548.23
TP17	34.49	Null		TH8	31.26	Null	Null	TH38	36.58	Null	Null
TP19	35.03	6.259(0)		TH9	31.39	3.135(0)	543.18	TH39	37.12	9.661(0)	544.94
TP20	36.12	5.790(0)		TH10	31.53	Null	Null	TH40	37.67	1.259(1)	550.30
TP21	37.21	5.049(0)		TH11	31.67	6.291(0)	548.02	TH41	38.22	1.414(1)	552.39
TP22	38.31	6.058(0)		TH12	31.80	3.454(0)	544.00	TH42	38.76	1.273(1)	550.41
TP24	40.48	6.018(0)		TH13	31.94	4.708(0)	543.60	TH43	39.31	1.388(1)	550.78
TP26	42.66	4.401(0)		TH14	32.07	4.372(0)	544.94	TH44	39.85	9.326(0)	547.81
L28H3	4.85	1.211(1)	548.06	TH15	32.21	Null	Null	TH45	40.41	Null	Null

Run 79 Reduced Data Tabulation

Value				Value				Value			
Gauge Label	Loc. (in)	(PSIA) or (BTU/Ft ² -Sec)	T Surf (DegR)	Gauge Label	Loc. (in)	(PSIA) or (BTU/Ft ² -Sec)	T Surf (DegR)	Gauge Label	Loc. (in)	(PSIA) or (BTU/Ft ² -Sec)	T Surf (DegR)
L28P1	5.85	1.003(0)		L28H4	5.85	1.206(1)	549.82	TH16	32.35	5.372(0)	544.06
L28P2	9.85	9.901(-1)		L28H5	6.85	Null	Null	TH17	32.48	6.767(0)	545.26
L28P3	13.85	9.479(-1)		L28H6	7.85	1.254(1)	549.20	TH18	32.62	7.535(0)	545.78
L28P4	17.85	Null		L28H7	9.85	1.205(1)	549.08	TH20	32.89	4.114(0)	543.54
L28P5	21.85	Null		L28H8	10.85	1.202(1)	549.70	TH21	33.03	Null	Null
L28P6	25.85	Null		L28H9	11.85	1.208(1)	550.22	TH50	33.08	7.338(0)	545.71
TP1	28.75	Null		L28H10	12.85	Null	Null	TH22	33.16	1.003(1)	547.20
TP2	29.30	Null		L28H11	13.85	1.068(1)	548.50	TH23	33.31	1.048(1)	548.14
TP3	30.39	2.400(0)		L28H13	16.85	1.102(1)	548.57	TH24	33.44	1.451(1)	549.95
TP4	30.94	Null		L28H14	17.85	1.117(1)	548.90	TH25	33.58	1.456(1)	551.05
TP5	31.21	2.478(0)		L28H15	18.85	1.059(1)	548.47	TH26	33.71	1.916(1)	555.50
TP6	31.48	Null		L28H16	19.85	1.028(1)	548.21	TH27	33.85	1.779(1)	554.27
TP7	31.75	2.734(0)		L28H17	21.85	1.052(1)	548.54	TH28	33.99	1.801(1)	555.51
TP8	32.03	Null		L28H18	22.85	6.119(0)	544.93	TH29	34.12	1.403(1)	552.05
TP9	32.30	2.858(0)		L28H19	24.85	1.046(1)	548.81	TH30	34.26	9.867(0)	546.60
TP10	32.57	2.960(0)		TH1	28.66	2.481(0)	541.08	TH31	34.39	9.242(0)	545.82
TP11	32.85	Null		TH2	29.21	3.003(0)	541.67	TH32	34.53	8.389(0)	545.04
TP12	33.11	3.735(0)		TH3	29.75	1.959(0)	540.79	TH34	34.80	Null	Null
TP13	33.39	Null		TH4	30.30	Null	Null	TH35	34.94	8.667(0)	545.34
TP14	33.67	4.420(0)		TH6	30.99	2.583(0)	541.61	TH36	35.49	Null	Null
TP16	34.21	Null		TH7	31.12	3.078(0)	542.71	TH37	36.03	1.285(1)	550.07
TP17	34.49	Null		TH8	31.26	Null	Null	TH38	36.58	Null	Null
TP19	35.03	5.682(0)		TH9	31.39	3.553(0)	542.96	TH39	37.12	9.986(0)	547.30
TP20	36.12	5.455(0)		TH10	31.53	Null	Null	TH40	37.67	1.309(1)	550.51
TP21	37.21	4.756(0)		TH11	31.67	7.415(0)	548.29	TH41	38.22	1.450(1)	552.10
TP22	38.31	6.392(0)		TH12	31.80	4.931(0)	544.09	TH42	38.76	1.227(1)	549.35
TP24	40.48	6.452(0)		TH13	31.94	5.594(0)	543.45	TH43	39.31	1.186(1)	550.97
TP26	42.66	5.932(0)		TH14	32.07	4.486(0)	543.58	TH44	39.85	7.973(0)	546.76
L28H3	4.85	1.221(1)	549.50	TH15	32.21	Null	Null	TH45	40.41	Null	Null

Run 80 Reduced Data Tabulation

Value				Value				Value			
Gauge Label	Loc. (in)	(PSIA) or (BTU/Ft ² -Sec)	T Surf (DegR)	Gauge Label	Loc. (in)	(PSIA) or (BTU/Ft ² -Sec)	T Surf (DegR)	Gauge Label	Loc. (in)	(PSIA) or (BTU/Ft ² -Sec)	T Surf (DegR)
L28P1	5.85	9.901(-1)		L28H4	5.85	1.228(1)	549.34	TH16	32.35	2.866(1)	562.03
L28P2	9.85	9.724(-1)		L28H5	6.85	Null	Null	TH17	32.48	3.914(1)	569.96
L28P3	13.85	9.518(-1)		L28H6	7.85	1.240(1)	549.26	TH18	32.62	3.465(1)	567.12
L28P4	17.85	Null		L28H7	9.85	1.217(1)	549.19	TH20	32.89	1.955(1)	554.14
L28P5	21.85	Null		L28H8	10.85	1.238(1)	549.42	TH21	33.03	Null	Null
L28P6	25.85	Null		L28H9	11.85	1.206(1)	549.40	TH50	33.08	4.654(1)	577.15
TP1	28.75	Null		L28H10	12.85	Null	Null	TH22	33.16	3.501(1)	567.73
TP2	29.30	Null		L28H11	13.85	1.067(1)	548.08	TH23	33.31	3.867(1)	570.70
TP3	30.39	1.078(0)		L28H13	16.85	1.077(1)	548.21	TH24	33.44	4.087(1)	572.64
TP4	30.94	Null		L28H14	17.85	1.116(1)	548.39	TH25	33.58	4.427(1)	575.54
TP5	31.21	2.319(0)		L28H15	18.85	1.044(1)	548.02	TH26	33.71	4.784(1)	578.03
TP6	31.48	Null		L28H16	19.85	1.035(1)	547.78	TH27	33.85	5.352(1)	582.89
TP7	31.75	2.809(0)		L28H17	21.85	1.018(1)	547.71	TH28	33.99	4.409(1)	574.29
TP8	32.03	Null		L28H18	22.85	4.808(0)	543.12	TH29	34.12	3.980(1)	571.27
TP9	32.30	3.267(0)		L28H19	24.85	1.004(0)	539.58	TH30	34.26	3.539(1)	569.76
TP10	32.57	3.831(0)		TH1	28.66	4.871(0)	544.58	TH31	34.39	4.245(1)	575.51
TP11	32.85	Null		TH2	29.21	4.372(0)	544.88	TH32	34.53	4.103(1)	574.78
TP12	33.11	3.977(0)		TH3	29.75	3.683(0)	544.03	TH34	34.80	Null	Null
TP13	33.39	Null		TH4	30.30	Null	Null	TH35	34.94	4.411(1)	578.14
TP14	33.67	3.982(0)		TH6	30.99	8.983(0)	546.55	TH36	35.49	Null	Null
TP16	34.21	Null		TH7	31.12	1.075(1)	547.95	TH37	36.03	3.840(1)	575.59
TP17	34.49	Null		TH8	31.26	Null	Null	TH38	36.58	Null	Null
TP19	35.03	3.826(0)		TH9	31.39	1.788(1)	552.99	TH39	37.12	4.783(1)	583.44
TP20	36.12	4.000(0)		TH10	31.53	Null	Null	TH40	37.67	5.374(1)	586.23
TP21	37.21	3.856(0)		TH11	31.67	3.807(1)	569.66	TH41	38.22	5.254(1)	589.99
TP22	38.31	3.886(0)		TH12	31.80	2.513(1)	558.60	TH42	38.76	4.546(1)	581.23
TP24	40.48	3.721(0)		TH13	31.94	1.603(1)	552.01	TH43	39.31	4.735(1)	584.10
TP26	42.66	4.377(0)		TH14	32.07	3.093(1)	563.82	TH44	39.85	5.513(1)	598.38
L28H3	4.85	1.242(1)	549.59	TH15	32.21	Null	Null	TH45	40.41	Null	Null

Run 81 Reduced Data Tabulation

Value				Value				Value			
Gauge Label	Loc. (in)	(PSIA) or (BTU/Ft ² -Sec)	T Surf (DegR)	Gauge Label	Loc. (in)	(PSIA) or (BTU/Ft ² -Sec)	T Surf (DegR)	Gauge Label	Loc. (in)	(PSIA) or (BTU/Ft ² -Sec)	T Surf (DegR)
L28P1	5.85	1.028(0)		L28H4	5.85	1.178(1)	551.51	TH16	32.35	3.921(0)	542.44
L28P2	9.85	Null		L28H5	6.85	Null	Null	TH17	32.48	4.477(0)	543.35
L28P3	13.85	Null		L28H6	7.85	1.242(1)	551.33	TH18	32.62	Null	Null
L28P4	17.85	Null		L28H7	9.85	1.222(1)	550.68	TH20	32.89	Null	Null
L28P5	21.85	Null		L28H8	10.85	1.181(1)	551.40	TH21	33.03	Null	Null
L28P6	25.85	Null		L28H9	11.85	1.195(1)	550.69	TH50	33.08	6.556(0)	544.82
TP1	28.75	Null		L28H10	12.85	Null	Null	TH22	33.16	5.637(0)	544.56
TP2	29.30	Null		L28H11	13.85	1.070(1)	549.59	TH23	33.31	Null	Null
TP3	30.39	1.667(0)		L28H13	16.85	1.016(1)	549.16	TH24	33.44	8.228(0)	547.34
TP4	30.94	Null		L28H14	17.85	1.111(1)	549.16	TH25	33.58	7.282(0)	546.59
TP5	31.21	1.913(0)		L28H15	18.85	1.055(1)	549.60	TH26	33.71	9.539(0)	549.32
TP6	31.48	Null		L28H16	19.85	1.065(1)	549.31	TH27	33.85	1.047(1)	550.07
TP7	31.75	2.181(0)		L28H17	21.85	1.064(1)	549.40	TH28	33.99	1.129(1)	550.71
TP8	32.03	Null		L28H18	22.85	1.082(1)	549.77	TH29	34.12	1.242(1)	550.34
TP9	32.30	2.334(0)		L28H19	24.85	1.044(1)	549.56	TH30	34.26	7.906(0)	545.71
TP10	32.57	2.382(0)		TH1	28.66	6.935(-1)	538.62	TH31	34.39	6.694(0)	544.84
TP11	32.85	Null		TH2	29.21	2.681(0)	541.70	TH32	34.53	5.492(0)	543.34
TP12	33.11	3.274(0)		TH3	29.75	2.977(0)	541.45	TH34	34.80	Null	Null
TP13	33.39	Null		TH4	30.30	Null	Null	TH35	34.94	4.850(0)	542.31
TP14	33.67	3.715(0)		TH6	30.99	2.941(0)	541.55	TH36	35.49	Null	Null
TP16	34.21	Null		TH7	31.12	3.153(0)	541.62	TH37	36.03	7.902(0)	546.76
TP17	34.49	Null		TH8	31.26	Null	Null	TH38	36.58	Null	Null
TP19	35.03	4.232(0)		TH9	31.39	4.315(0)	543.16	TH39	37.12	7.732(0)	544.97
TP20	36.12	3.862(0)		TH10	31.53	Null	Null	TH40	37.67	7.466(0)	547.46
TP21	37.21	3.461(0)		TH11	31.67	6.688(0)	545.23	TH41	38.22	8.490(0)	548.42
TP22	38.31	4.301(0)		TH12	31.80	3.679(0)	542.84	TH42	38.76	8.204(0)	547.35
TP24	40.48	4.501(0)		TH13	31.94	3.461(0)	542.64	TH43	39.31	8.691(0)	548.20
TP26	42.66	6.127(0)		TH14	32.07	4.143(0)	542.57	TH44	39.85	7.553(0)	545.71
L28H3	4.85	1.225(1)	551.41	TH15	32.21	Null	Null	TH45	40.41	Null	Null

Run 82 Reduced Data Tabulation

Gauge Label	Loc. (in)	Value (PSIA) or (BTU/Ft ² -Sec)	T Surf (DegR)	Gauge Label	Loc. (in)	Value (PSIA) or (BTU/Ft ² -Sec)	T Surf (DegR)	Gauge Label	Loc. (in)	Value (PSIA) or (BTU/Ft ² -Sec)	T Surf (DegR)
L28P1	5.85	1.109(0)		L28H4	5.85	1.122(1)	554.45	TH16	32.35	3.195(0)	546.86
L28P2	9.85	Null		L28H5	6.85	Null		TH17	32.48	4.157(0)	547.69
L28P3	13.85	Null		L28H6	7.85	1.184(1)	554.69	TH18	32.62	Null	Null
L28P4	17.85	Null		L28H7	9.85	1.161(1)	554.54	TH20	32.89	Null	Null
L28P5	21.85	Null		L28H8	10.85	1.148(1)	554.50	TH21	33.03	Null	Null
L28P6	25.85	Null		L28H9	11.85	1.125(1)	554.66	TH50	33.08	6.148(0)	549.55
TP1	28.75	Null		L28H10	12.85	Null		TH22	33.16	5.299(0)	548.80
TP2	29.30	Null		L28H11	13.85	9.833(0)	553.23	TH23	33.31	Null	Null
TP3	30.39	1.671(0)		L28H13	16.85	1.041(1)	553.69	TH24	33.44	6.090(0)	550.19
TP4	30.94	Null		L28H14	17.85	1.069(1)	553.93	TH25	33.58	6.412(0)	550.46
TP5	31.21	1.873(0)		L28H15	18.85	1.003(1)	553.48	TH26	33.71	9.065(0)	552.40
TP6	31.48	Null		L28H16	19.85	1.019(1)	553.37	TH27	33.85	1.020(1)	553.51
TP7	31.75	2.133(0)		L28H17	21.85	9.944(0)	553.36	TH28	33.99	1.066(1)	553.51
TP8	32.03	Null		L28H18	22.85	1.027(1)	553.68	TH29	34.12	1.072(1)	553.30
TP9	32.30	2.369(0)		L28H19	24.85	1.011(1)	553.30	TH30	34.26	7.738(0)	550.11
TP10	32.57	2.441(0)		TH1	28.66	1.547(0)	544.81	TH31	34.39	7.492(0)	549.79
TP11	32.85	Null		TH2	29.21	2.500(0)	546.15	TH32	34.53	5.931(0)	548.42
TP12	33.11	3.255(0)		TH3	29.75	2.028(0)	545.28	TH34	34.80	Null	Null
TP13	33.39	Null		TH4	30.30	Null		TH35	34.94	5.885(0)	548.38
TP14	33.67	3.663(0)		TH6	30.99	2.819(0)	546.53	TH36	35.49	Null	Null
TP16	34.21	Null		TH7	31.12	3.308(0)	546.68	TH37	36.03	8.886(0)	552.73
TP17	34.49	Null		TH8	31.26	Null		TH38	36.58	Null	Null
TP19	35.03	4.311(0)		TH9	31.39	5.119(0)	548.31	TH39	37.12	7.386(0)	549.38
TP20	36.12	3.912(0)		TH10	31.53	Null		TH40	37.67	1.020(1)	553.53
TP21	37.21	3.570(0)		TH11	31.67	6.560(0)	550.22	TH41	38.22	1.104(1)	555.20
TP22	38.31	4.432(0)		TH12	31.80	4.747(0)	548.48	TH42	38.76	9.636(0)	553.27
TP24	40.48	4.639(0)		TH13	31.94	4.091(0)	547.50	TH43	39.31	1.103(1)	553.91
TP26	42.66	5.679(0)		TH14	32.07	3.521(0)	547.48	TH44	39.85	9.051(0)	551.84
L28H3	4.85	1.138(1)	554.37	TH15	32.21	Null		TH45	40.41	Null	Null

Run 83 Reduced Data Tabulation

Gauge Label	Loc. (in)	Value (PSIA) or (BTU/Ft ² -Sec)	T Surf (DegR)	Gauge Label	Loc. (in)	Value (PSIA) or (BTU/Ft ² -Sec)	T Surf (DegR)	Gauge Label	Loc. (in)	Value (PSIA) or (BTU/Ft ² -Sec)	T Surf (DegR)
L28P1	5.85	1.063(0)		L28H4	5.85	1.284(1)	551.60	TH16	32.35	6.044(0)	544.49
L28P2	9.85	Null		L28H5	6.85	Null		TH17	32.48	5.552(0)	544.96
L28P3	13.85	Null		L28H6	7.85	1.349(1)	551.73	TH18	32.62	Null	Null
L28P4	17.85	Null		L28H7	9.85	1.285(1)	551.58	TH20	32.89	Null	Null
L28P5	21.85	Null		L28H8	10.85	1.294(1)	551.58	TH21	33.03	Null	Null
L28P6	25.85	Null		L28H9	11.85	1.310(1)	552.21	TH50	33.08	5.515(0)	546.19
TP1	28.75	Null		L28H10	12.85	Null		TH22	33.16	8.319(0)	547.98
TP2	29.30	Null		L28H11	13.85	1.144(1)	550.33	TH23	33.31	Null	Null
TP3	30.39	1.247(0)		L28H13	16.85	1.184(1)	550.99	TH24	33.44	1.121(1)	550.52
TP4	30.94	Null		L28H14	17.85	1.213(1)	551.45	TH25	33.58	1.210(1)	551.13
TP5	31.21	1.256(0)		L28H15	18.85	1.100(1)	550.32	TH26	33.71	1.361(1)	552.33
TP6	31.48	Null		L28H16	19.85	1.160(1)	551.04	TH27	33.85	1.483(1)	552.05
TP7	31.75	1.755(0)		L28H17	21.85	1.135(1)	550.76	TH28	33.99	1.425(1)	553.80
TP8	32.03	Null		L28H18	22.85	1.162(1)	550.97	TH29	34.12	1.377(1)	553.66
TP9	32.30	2.062(0)		L28H19	24.85	1.115(1)	550.51	TH30	34.26	9.275(0)	548.09
TP10	32.57	2.196(0)		TH1	28.66	2.207(0)	541.71	TH31	34.39	8.972(0)	547.42
TP11	32.85	Null		TH2	29.21	2.704(0)	541.83	TH32	34.53	7.964(0)	546.13
TP12	33.11	2.792(0)		TH3	29.75	1.497(0)	540.95	TH34	34.80	Null	Null
TP13	33.39	Null		TH4	30.30	Null		TH35	34.94	6.551(0)	545.08
TP14	33.67	3.303(0)		TH6	30.99	3.504(0)	542.36	TH36	35.49	Null	Null
TP16	34.21	Null		TH7	31.12	3.943(0)	542.90	TH37	36.03	9.500(0)	548.46
TP17	34.49	Null		TH8	31.26	Null		TH38	36.58	Null	Null
TP19	35.03	4.240(0)		TH9	31.39	5.392(0)	545.50	TH39	37.12	7.056(0)	544.72
TP20	36.12	3.983(0)		TH10	31.53	Null		TH40	37.67	7.838(0)	547.69
TP21	37.21	3.765(0)		TH11	31.67	8.183(0)	547.10	TH41	38.22	9.080(0)	549.84
TP22	38.31	4.438(0)		TH12	31.80	6.700(0)	546.17	TH42	38.76	7.199(0)	547.48
TP24	40.48	4.501(0)		TH13	31.94	6.007(0)	545.43	TH43	39.31	7.902(0)	548.62
TP26	42.66	4.618(0)		TH14	32.07	5.425(0)	545.00	TH44	39.85	4.622(0)	545.33
L28H3	4.85	1.296(1)	553.40	TH15	32.21	Null		TH45	40.41	Null	Null

Run 87 Reduced Data Tabulation

Gauge Label	Loc. (in)	Value (PSIA) or (BTU/Ft ² -Sec)	T Surf (DegR)	Gauge Label	Loc. (in)	Value (PSIA) or (BTU/Ft ² -Sec)	T Surf (DegR)	Gauge Label	Loc. (in)	Value (PSIA) or (BTU/Ft ² -Sec)	T Surf (DegR)
L28P1	5.85	1.043(0)		L28H4	5.85	1.266(1)	549.52	TH16	32.35	4.908(1)	577.77
L28P2	9.85	Null		L28H5	6.85	Null		TH17	32.48	Null	Null
L28P3	13.85	Null		L28H6	7.85	1.302(1)	550.33	TH18	32.62	Null	Null
L28P4	17.85	Null		L28H7	9.85	1.311(1)	549.56	TH20	32.89	Null	Null
L28P5	21.85	Null		L28H8	10.85	1.292(1)	550.13	TH21	33.03	Null	Null
L28P6	25.85	Null		L28H9	11.85	1.281(1)	550.04	TH50	33.08	Null	Null
TP1	28.75	Null		L28H10	12.85	Null		TH22	33.16	Null	Null
TP2	29.30	Null		L28H11	13.85	1.126(1)	548.88	TH23	33.31	Null	Null
TP3	30.39	3.065(0)		L28H13	16.85	1.169(1)	548.97	TH24	33.44	1.031(2)	624.04
TP4	30.94	Null		L28H14	17.85	1.185(1)	549.18	TH25	33.58	1.168(2)	634.62
TP5	31.21	4.157(0)		L28H15	18.85	1.109(1)	548.72	TH26	33.71	1.216(2)	637.98
TP6	31.48	Null		L28H16	19.85	1.086(1)	548.58	TH27	33.85	1.499(2)	659.16
TP7	31.75	5.345(0)		L28H17	21.85	1.108(1)	548.50	TH28	33.99	1.388(2)	650.97
TP8	32.03	Null		L28H18	22.85	1.129(1)	548.76	TH29	34.12	1.044(2)	626.20
TP9	32.30	7.512(0)		L28H19	24.85	1.090(1)	548.28	TH30	34.26	8.067(1)	611.60
TP10	32.57	Null		TH1	28.66	4.491(0)	544.49	TH31	34.39	9.655(1)	625.39
TP11	32.85	Null		TH2	29.21	3.004(0)	543.73	TH32	34.53	9.351(1)	623.69
TP12	33.11	Null		TH3	29.75	3.427(0)	543.91	TH34	34.80	Null	Null
TP13	33.39	Null		TH4	30.30	Null		TH35	34.94	1.087(2)	635.27
TP14	33.67	Null		TH6	30.99	Null		TH36	35.49	Null	Null
TP16	34.21	Null		TH7	31.12	1.664(1)	552.85	TH37	36.03	9.774(1)	629.13
TP17	34.49	Null		TH8	31.26	Null		TH38	36.58	Null	Null
TP19	35.03	1.102(1)		TH9	31.39	2.309(1)	558.57	TH39	37.12	1.109(2)	642.80
TP20	36.12	1.169(1)		TH10	31.53	Null		TH40	37.67	1.190(2)	650.99
TP21	37.21	1.190(1)		TH11	31.67	Null		TH41	38.22	1.296(2)	657.15
TP22	38.31	1.099(1)		TH12	31.80	Null		TH42	38.76	1.198(2)	647.89
TP24	40.48	9.170(0)		TH13	31.94	3.271(1)	565.67	TH43	39.31	1.085(2)	642.33
TP26	42.66	4.790(0)		TH14	32.07	Null		TH44	39.85	1.237(2)	673.00
L28H3	4.85	1.317(1)	548.30	TH15	32.21	Null		TH45	40.41	Null	Null

Run 88 Reduced Data Tabulation

Gauge Label	Loc. (in)	Value (PSIA) or (BTU/Ft ² -Sec)	T Surf (DegR)	Gauge Label	Loc. (in)	Value (PSIA) or (BTU/Ft ² -Sec)	T Surf (DegR)	Gauge Label	Loc. (in)	Value (PSIA) or (BTU/Ft ² -Sec)	T Surf (DegR)
L28P1	5.85	1.083(0)		L28H4	5.85	1.285(1)	551.48	TH16	32.35	1.961(1)	559.15
L28P2	9.85	Null		L28H5	6.85	Null	Null	TH17	32.48	Null	Null
L28P3	13.85	Null		L28H6	7.85	1.347(1)	551.60	TH18	32.62	3.043(1)	566.44
L28P4	17.85	Null		L28H7	9.85	1.343(1)	551.60	TH20	32.89	Null	Null
L28P5	21.85	Null		L28H8	10.85	1.326(1)	551.47	TH21	33.03	Null	Null
L28P6	25.85	Null		L28H9	11.85	1.346(1)	551.95	TH50	33.08	Null	Null
TP1	28.75	Null		L28H10	12.85	Null	Null	TH22	33.16	3.931(1)	571.62
TP2	29.30	Null		L28H11	13.85	1.176(1)	550.68	TH23	33.31	Null	Null
TP3	30.39	3.880(0)		L28H13	16.85	1.188(1)	550.71	TH24	33.44	5.243(1)	578.97
TP4	30.94	Null		L28H14	17.85	1.223(1)	550.97	TH25	33.58	4.937(1)	586.72
TP5	31.21	4.374(0)		L28H15	18.85	1.152(1)	550.74	TH26	33.71	5.651(1)	593.50
TP6	31.48	Null		L28H16	19.85	1.133(1)	550.78	TH27	33.85	7.341(1)	605.91
TP7	31.75	4.925(0)		L28H17	21.85	1.156(1)	550.28	TH28	33.99	7.324(1)	608.13
TP8	32.03	Null		L28H18	22.85	1.177(1)	551.30	TH29	34.12	6.154(1)	596.73
TP9	32.30	5.818(0)		L28H19	24.85	1.144(1)	550.05	TH30	34.26	3.651(1)	575.80
TP10	32.57	6.422(0)		TH1	28.66	2.586(0)	542.03	TH31	34.39	3.571(1)	574.52
TP11	32.85	Null		TH2	29.21	2.691(0)	542.15	TH32	34.53	3.086(1)	568.95
TP12	33.11	9.163(0)		TH3	29.75	1.741(0)	542.95	TH34	34.80	Null	Null
TP13	33.39	Null		TH4	30.30	Null	Null	TH35	34.94	3.392(1)	571.79
TP14	33.67	1.091(1)		TH6	30.99	Null	Null	TH36	35.49	Null	Null
TP16	34.21	Null		TH7	31.12	9.085(0)	549.95	TH37	36.03	4.228(1)	589.99
TP17	34.49	Null		TH8	31.26	Null	Null	TH38	36.58	Null	Null
TP19	35.03	1.346(1)		TH9	31.39	1.502(1)	554.15	TH39	37.12	2.136(1)	565.65
TP20	36.12	1.177(1)		TH10	31.53	Null	Null	TH40	37.67	3.703(1)	586.04
TP21	37.21	1.331(1)		TH11	31.67	Null	Null	TH41	38.22	4.670(1)	591.44
TP22	38.31	1.237(1)		TH12	31.80	Null	Null	TH42	38.76	7.144(1)	618.12
TP24	40.48	1.305(1)		TH13	31.94	1.749(1)	557.12	TH43	39.31	6.681(1)	626.35
TP26	42.66	4.888(0)		TH14	32.07	1.654(1)	559.59	TH44	39.85	7.780(1)	612.25
L28H3	4.85	1.300(1)	551.70	TH15	32.21	Null	Null	TH45	40.41	Null	Null

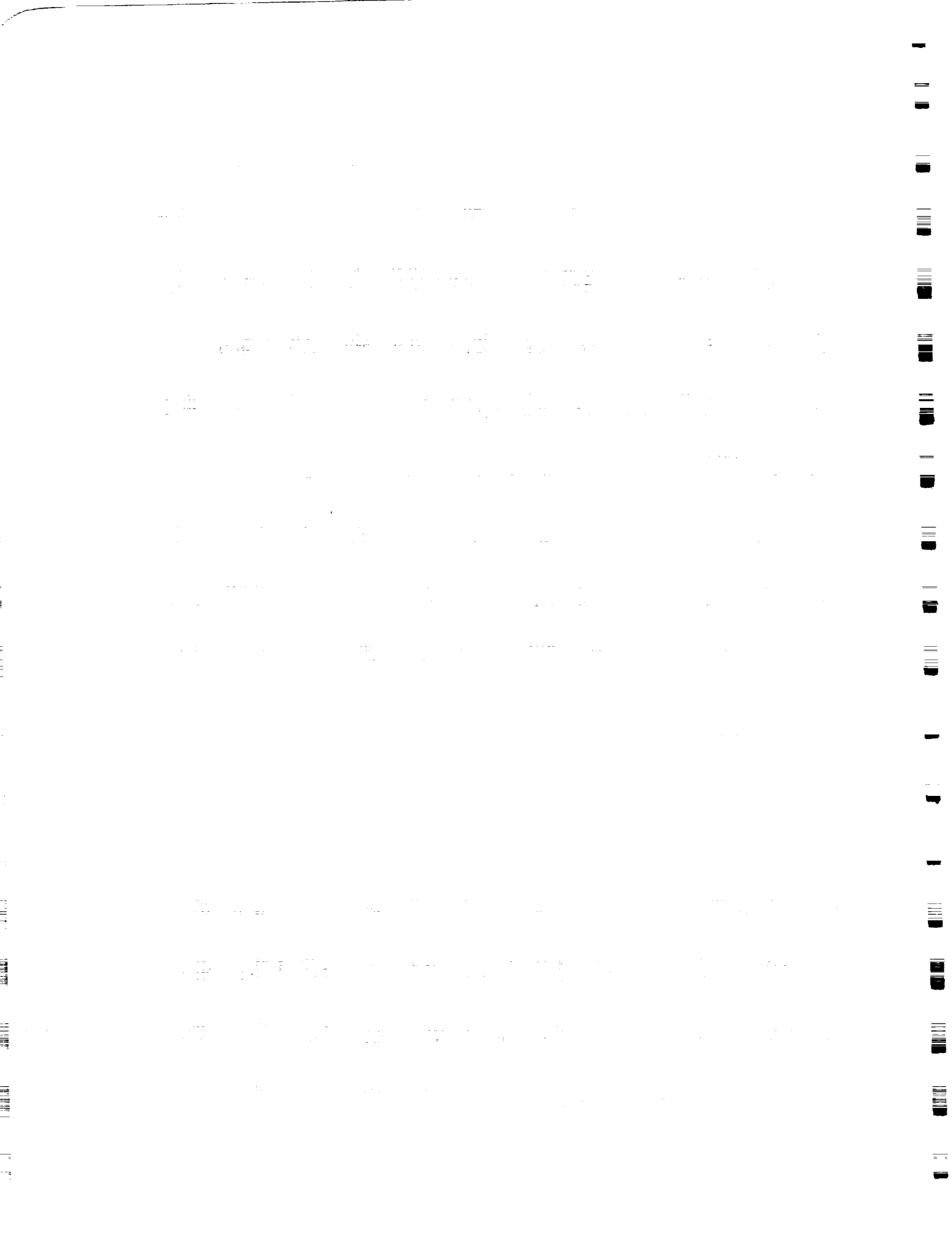
Run 89 Reduced Data Tabulation

Gauge Label	Loc. (in)	Value (PSIA) or (BTU/Ft ² -Sec)	T Surf (DegR)	Gauge Label	Loc. (in)	Value (PSIA) or (BTU/Ft ² -Sec)	T Surf (DegR)	Gauge Label	Loc. (in)	Value (PSIA) or (BTU/Ft ² -Sec)	T Surf (DegR)
L28P1	5.85	1.051(0)		L28H4	5.85	1.287(1)	553.80	TH16	32.35	1.810(1)	561.35
L28P2	9.85	Null		L28H5	6.85	Null	Null	TH17	32.48	Null	Null
L28P3	13.85	Null		L28H6	7.85	1.337(1)	553.73	TH18	32.62	2.366(1)	568.24
L28P4	17.85	Null		L28H7	9.85	1.334(1)	553.99	TH20	32.89	Null	Null
L28P5	21.85	Null		L28H8	10.85	1.334(1)	554.55	TH21	33.03	Null	Null
L28P6	25.85	Null		L28H9	11.85	1.349(1)	555.06	TH50	33.08	Null	Null
TP1	28.75	Null		L28H10	12.85	Null	Null	TH22	33.16	2.739(1)	570.96
TP2	29.30	Null		L28H11	13.85	1.171(1)	552.44	TH23	33.31	Null	Null
TP3	30.39	4.304(0)		L28H13	16.85	1.191(1)	553.12	TH24	33.44	3.059(1)	574.80
TP4	30.94	Null		L28H14	17.85	1.234(1)	553.66	TH25	33.58	3.240(1)	576.71
TP5	31.21	4.712(0)		L28H15	18.85	1.187(1)	553.00	TH26	33.71	3.770(1)	581.69
TP6	31.48	Null		L28H16	19.85	1.183(1)	553.26	TH27	33.85	5.036(1)	594.24
TP7	31.75	5.541(0)		L28H17	21.85	1.178(1)	552.90	TH28	33.99	5.569(1)	598.57
TP8	32.03	Null		L28H18	22.85	1.191(1)	553.08	TH29	34.12	5.397(1)	594.30
TP9	32.30	6.241(0)		L28H19	24.85	1.388(1)	554.35	TH30	34.26	3.375(1)	575.28
TP10	32.57	6.708(0)		TH1	28.66	1.407(0)	543.20	TH31	34.39	2.894(1)	571.71
TP11	32.85	Null		TH2	29.21	2.368(0)	544.29	TH32	34.53	2.463(1)	567.12
TP12	33.11	9.228(0)		TH3	29.75	2.448(0)	545.54	TH34	34.80	Null	Null
TP13	33.39	Null		TH4	30.30	Null	Null	TH35	34.94	2.568(1)	568.25
TP14	33.67	1.105(1)		TH6	30.99	Null	Null	TH36	35.49	Null	Null
TP16	34.21	Null		TH7	31.12	9.728(0)	553.46	TH37	36.03	3.593(1)	583.73
TP17	34.49	Null		TH8	31.26	Null	Null	TH38	36.58	Null	Null
TP19	35.03	1.405(1)		TH9	31.39	1.253(1)	557.26	TH39	37.12	1.891(1)	565.82
TP20	36.12	1.137(1)		TH10	31.53	Null	Null	TH40	37.67	3.317(1)	583.37
TP21	37.21	1.233(1)		TH11	31.67	1.809(1)	568.64	TH41	38.22	6.519(1)	612.23
TP22	38.31	2.130(1)		TH12	31.80	Null	Null	TH42	38.76	7.180(1)	611.92
TP24	40.48	7.854(-1)		TH13	31.94	1.712(1)	559.12	TH43	39.31	6.396(1)	603.50
TP26	42.66	4.081(0)		TH14	32.07	1.579(1)	561.34	TH44	39.85	4.389(1)	583.12
L28H3	4.85	1.297(1)	553.97	TH15	32.21	Null	Null	TH45	40.41	Null	Null

Run 90 Reduced Data Tabulation

Gauge Label	Loc. (in)	Value (PSIA) or (BTU/Ft ² -Sec)	T Surf (DegR)	Gauge Label	Loc. (in)	Value (PSIA) or (BTU/Ft ² -Sec)	T Surf (DegR)	Gauge Label	Loc. (in)	Value (PSIA) or (BTU/Ft ² -Sec)	T Surf (DegR)
L28P1	5.85	1.092(0)		L28H4	5.85	1.298(1)	554.16	TH16	32.35	1.283(1)	553.67
L28P2	9.85	Null		L28H5	6.85	Null	Null	TH17	32.48	Null	Null
L28P3	13.85	Null		L28H6	7.85	1.377(1)	554.47	TH18	32.62	1.906(1)	559.49
L28P4	17.85	Null		L28H7	9.85	1.319(1)	554.28	TH20	32.89	Null	Null
L28P5	21.85	Null		L28H8	10.85	1.307(1)	553.92	TH21	33.03	Null	Null
L28P6	25.85	Null		L28H9	11.85	1.306(1)	554.19	TH50	33.08	Null	Null
TP1	28.75	Null		L28H10	12.85	Null	Null	TH22	33.16	1.969(1)	560.91
TP2	29.30	Null		L28H11	13.85	1.154(1)	552.78	TH23	33.31	Null	Null
TP3	30.39	4.837(0)		L28H13	16.85	1.177(1)	553.00	TH24	33.44	2.161(1)	561.20
TP4	30.94	Null		L28H14	17.85	1.205(1)	553.46	TH25	33.58	2.166(1)	563.22
TP5	31.21	5.373(0)		L28H15	18.85	1.153(1)	553.16	TH26	33.71	2.799(1)	568.06
TP6	31.48	Null		L28H16	19.85	1.156(1)	553.97	TH27	33.85	3.083(1)	577.02
TP7	31.75	6.100(0)		L28H17	21.85	1.142(1)	553.95	TH28	33.99	4.449(1)	580.99
TP8	32.03	Null		L28H18	22.85	1.176(1)	553.87	TH29	34.12	Null	Null
TP9	32.30	6.683(0)		L28H19	24.85	1.111(1)	554.46	TH30	34.26	2.456(1)	564.36
TP10	32.57	7.191(0)		TH1	28.66	1.961(0)	543.80	TH31	34.39	2.217(1)	561.10
TP11	32.85	Null		TH2	29.21	1.489(0)	544.50	TH32	34.53	1.749(1)	557.66
TP12	33.11	8.597(0)		TH3	29.75	1.816(0)	544.32	TH34	34.80	Null	Null
TP13	33.39	Null		TH4	30.30	Null	Null	TH35	34.94	1.849(1)	558.71
TP14	33.67	1.023(1)		TH6	30.99	Null	Null	TH36	35.49	Null	Null
TP16	34.21	Null		TH7	31.12	6.264(0)	550.19	TH37	36.03	2.459(1)	573.80
TP17	34.49	Null		TH8	31.26	Null	Null	TH38	36.58	Null	Null
TP19	35.03	1.266(1)		TH9	31.39	9.147(0)	553.27	TH39	37.12	2.459(1)	570.87
TP20	36.12	1.165(1)		TH10	31.53	Null	Null	TH40	37.67	6.138(1)	597.03
TP21	37.21	1.331(1)		TH11	31.67	1.983(1)	562.09	TH41	38.22	6.207(1)	600.49
TP22	38.31	2.130(1)		TH12	31.80	Null	Null	TH42	38.76	3.717(1)	582.64
TP24	40.48	Null		TH13	31.94	1.492(1)	555.14	TH43	39.31	3.380(1)	577.59
TP26	42.66	4.426(0)		TH14	32.07	Null	Null	TH44	39.85	1.509(1)	557.16
L28H3	4.85	1.302(1)	554.26	TH15	32.21	Null	Null	TH45	40.41	Null	Null

Run 91 Reduced Data Tabulation



Appendix B

VELOCITY-PROFILE MEASUREMENTS

Test Conditions

Po = 2.7447X10+3 PSIA	Reservoir Total Pressure
Ho = 1.2530X10+7 (Ft/sec) ²	Reservoir Total Enthalpy
To = 1.9825X10+3 degR	Reservoir Total Temperature
M = 6.4843	Freestream Mach Number
U = 4.7350X10+3 Ft/sec	Freestream Velocity
T = 2.2173X10+2 degR	Freestream Temperature
P = 1.0970 PSIA	Freestream Static Pressure
Rho = 4.1520X10-4 Slugs/Ft ³	Freestream Density
Mu = 1.8322X10-7 Slugs/Ft-sec	Freestream Viscosity
Re = 1.0730X10+7 1/Ft	Freestream Reynolds Number
Po' = 6.0187X10+1 PSIA	Pitot Pressure
Q = 3.2323X10+1 PSIA	Dynamic Pressure (Rho U ² /288)
Mi = 2.6723	Shock Tube Incident Shock Mach Number
Tw = 5.3840X10+2 degR	Wall Temperature
QoFR = 5.6783X10+1 BTU/Ft ² -s	Fay-Riddell Heat Transfer (.25' Diam Cylin.)

Model Parameter Value

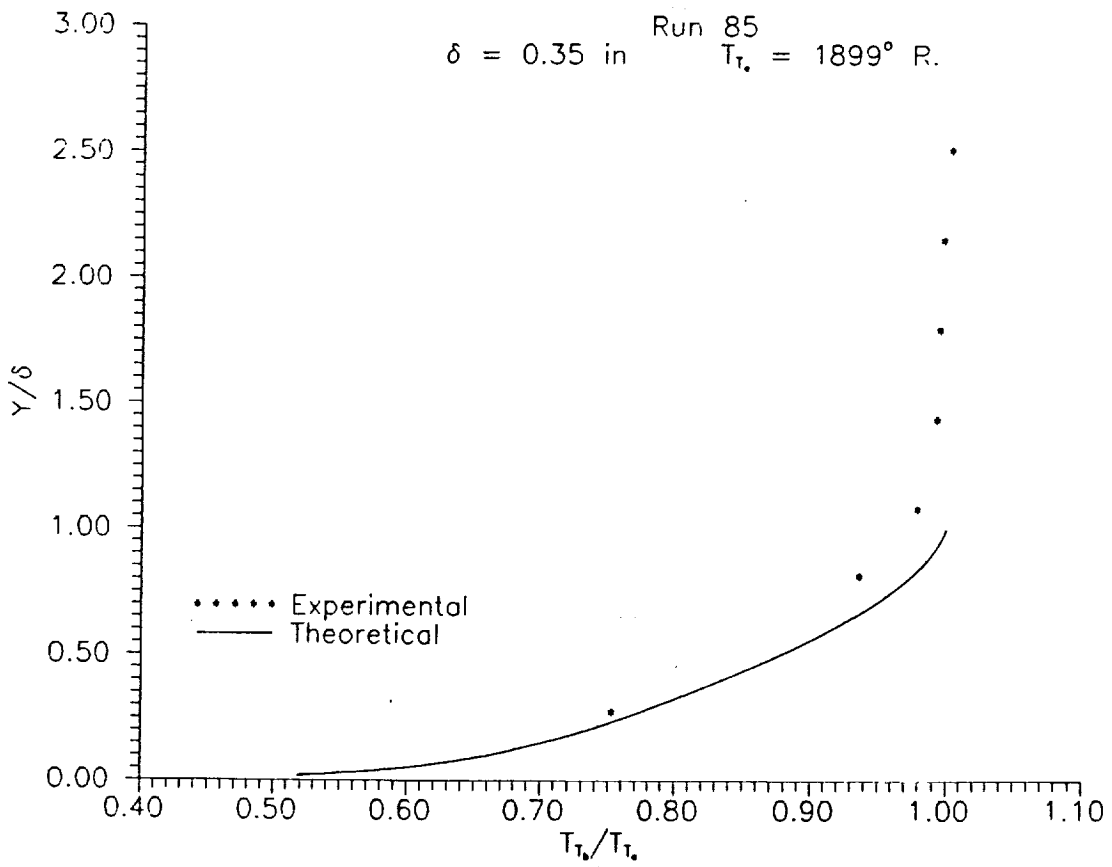
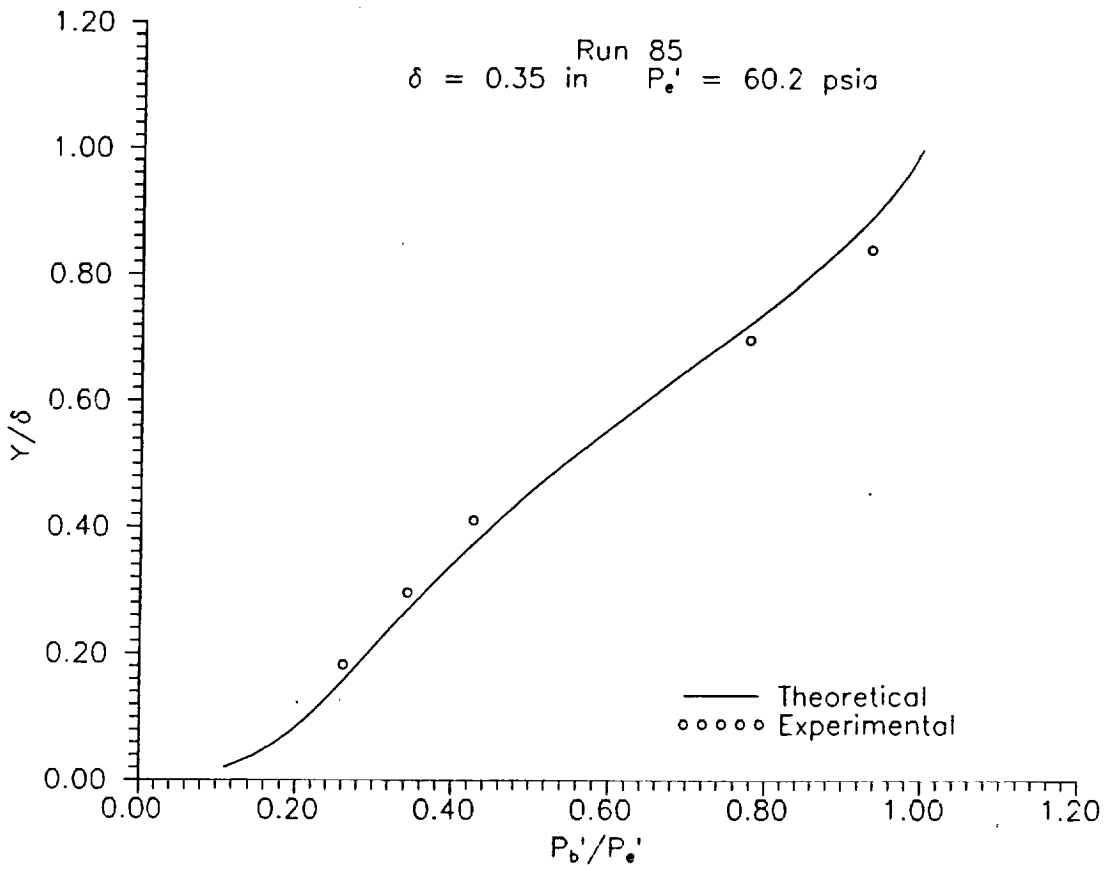
Plate length (in) 27.0

Run 85

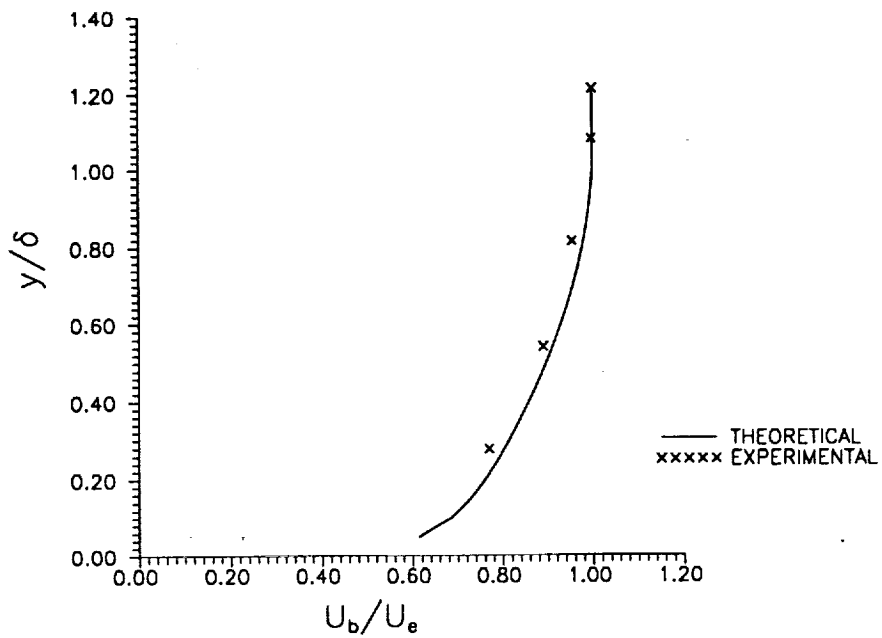
Gauge#	Location (inches)	Pressure (psia)	Gauge#	Location (inches)	Temperature deg R
BL1	0.024	Null	TT1	0.097	1430.0
BL2	0.064	15.780	TT2	0.191	Null
BL3	0.104	20.700	TT3	0.285	1779.0
BL4	0.144	25.700	TT4	0.378	1860.0
BL5	0.194	Null	TT5	0.503	1886.0
BL6	0.244	46.870	TT6	0.628	1890.0
BL7	0.294	56.340	TT7	0.753	1895.0
BL8	0.354	Null	TT8	0.878	1905.0
BL9	0.414	Null	TT9	1.003	1898.0

Pressure Data for Run 85

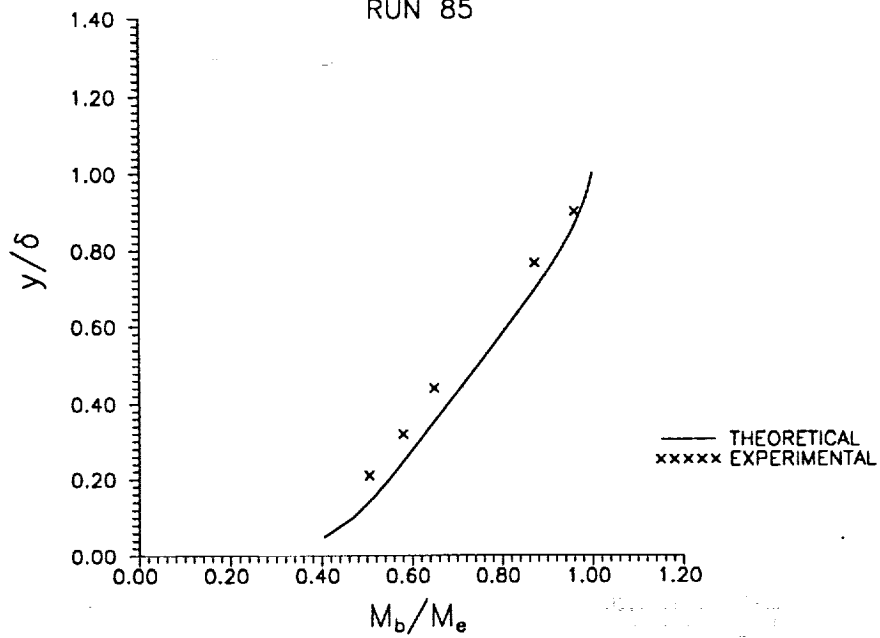
Total Temperature for Run 85



VELOCITY PROFILE
RUN 85



MACH NUMBER PROFILE
RUN 85



Test Conditions

Po = 2.7688X10+3 PSIA	Reservoir Total Pressure
Ho = 1.2078X10+7 (Ft/sec) ²	Reservoir Total Enthalpy
To = 1.9164X10+3 degR	Reservoir Total Temperature
M = 6.4911	Freestream Mach Number
U = 4.6493X10+3 Ft/sec	Freestream Velocity
T = 2.1333X10+2 degR	Freestream Temperature
P = 1.1101 PSIA	Freestream Static Pressure
Rho = 4.3669X10-4 Slugs/Ft ³	Freestream Density
Mu = 1.7667X10-7 Slugs/Ft-sec	Freestream Viscosity
Re = 1.1492X10+7 1/Ft	Freestream Reynolds Number
Po' = 6.1001X10+1 PSIA	Pitot Pressure
Q = 3.2776X10+1 PSIA	Dynamic Pressure (Rho U ² /288)
Mi = 2.6453	Shock Tube Incident Shock Mach Number
Tw = 5.3250X10+2 degR	Wall Temperature
QoFR= 5.4456X10+1 BTU/Ft ² -s	Fay-Riddell Heat Transfer (.25' Diam Cylin.)

Model Parameter Value

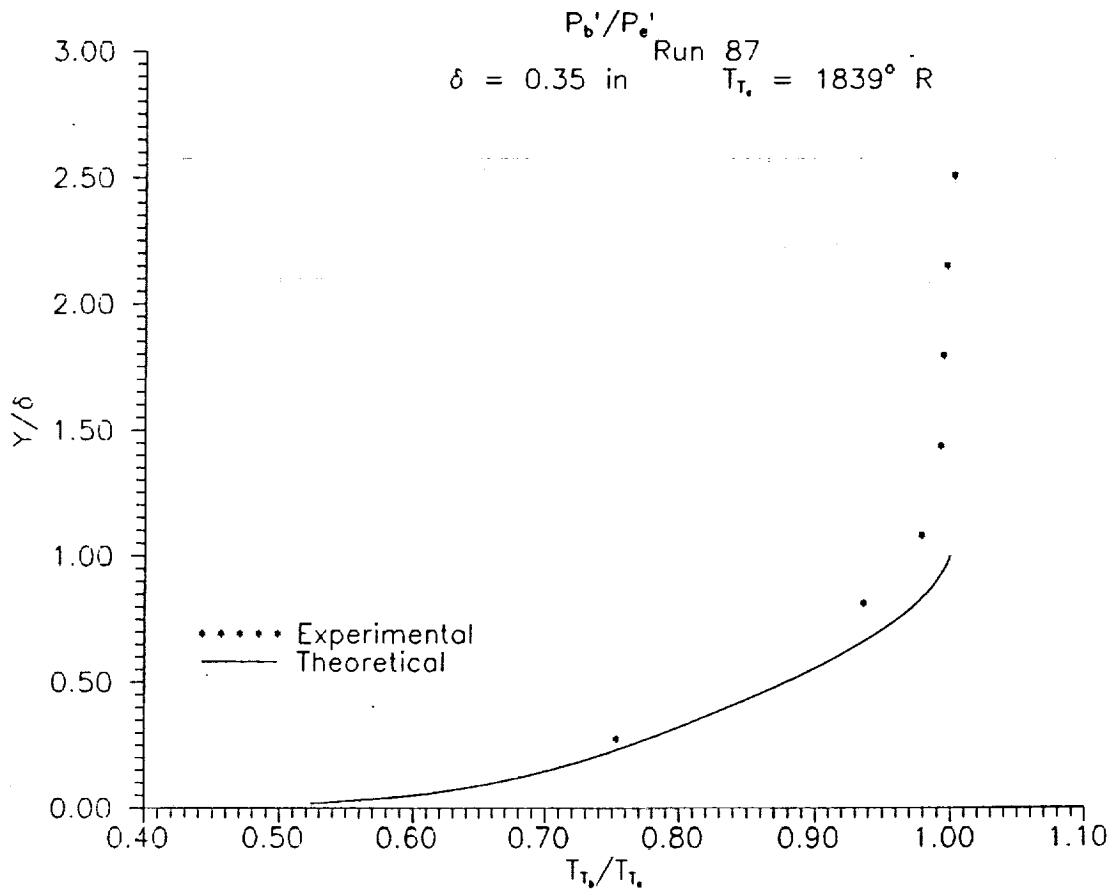
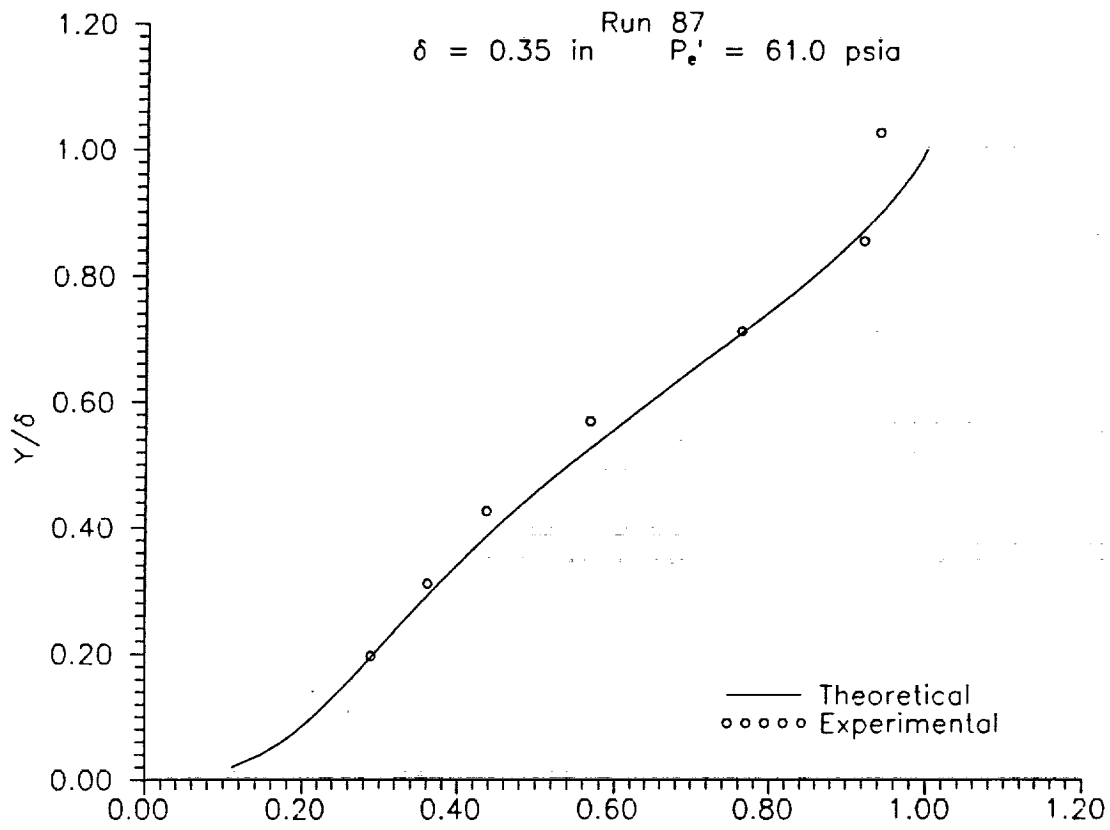
Plate length (in) 27.0

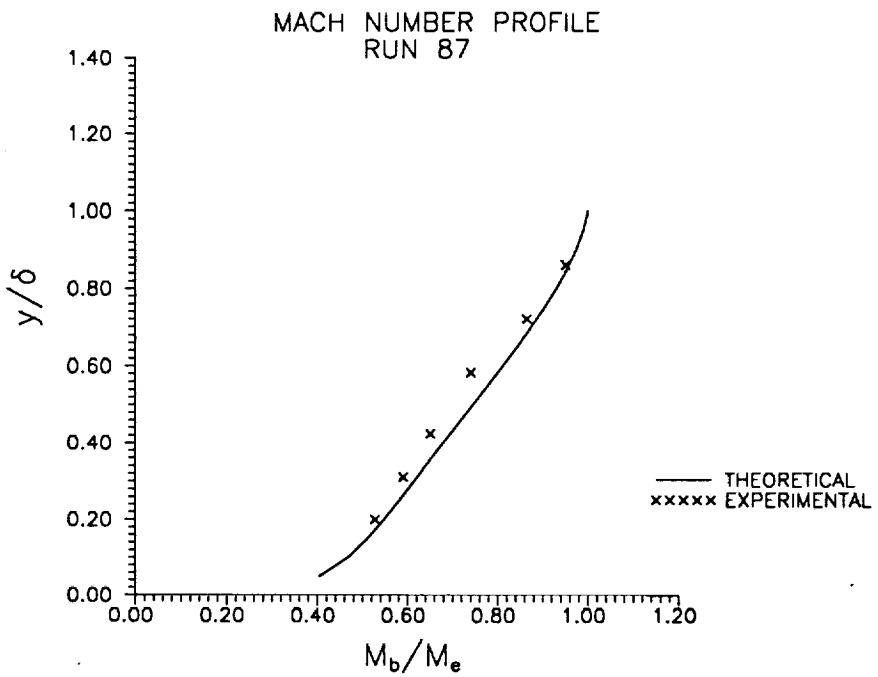
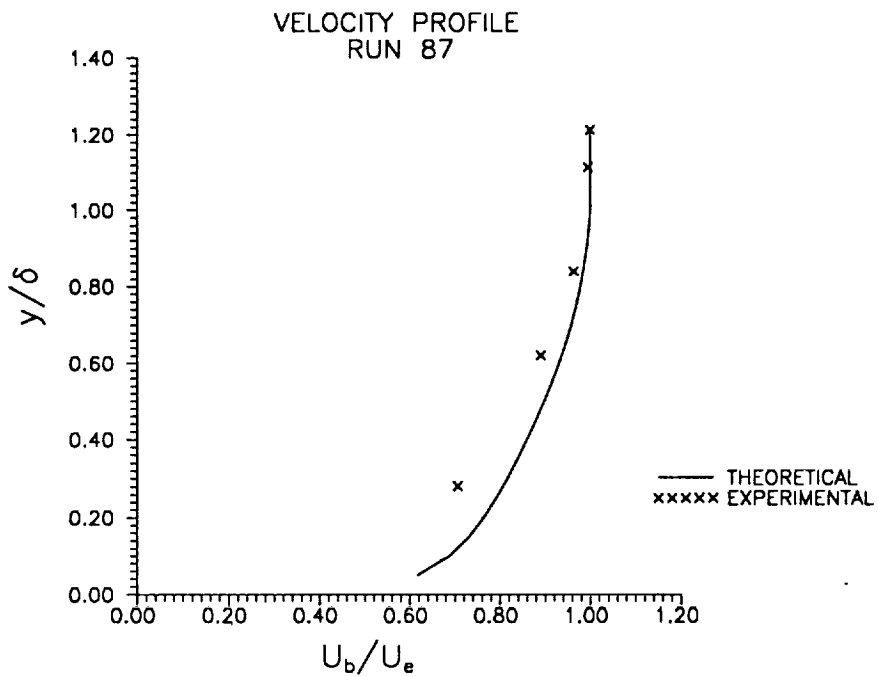
Run 87

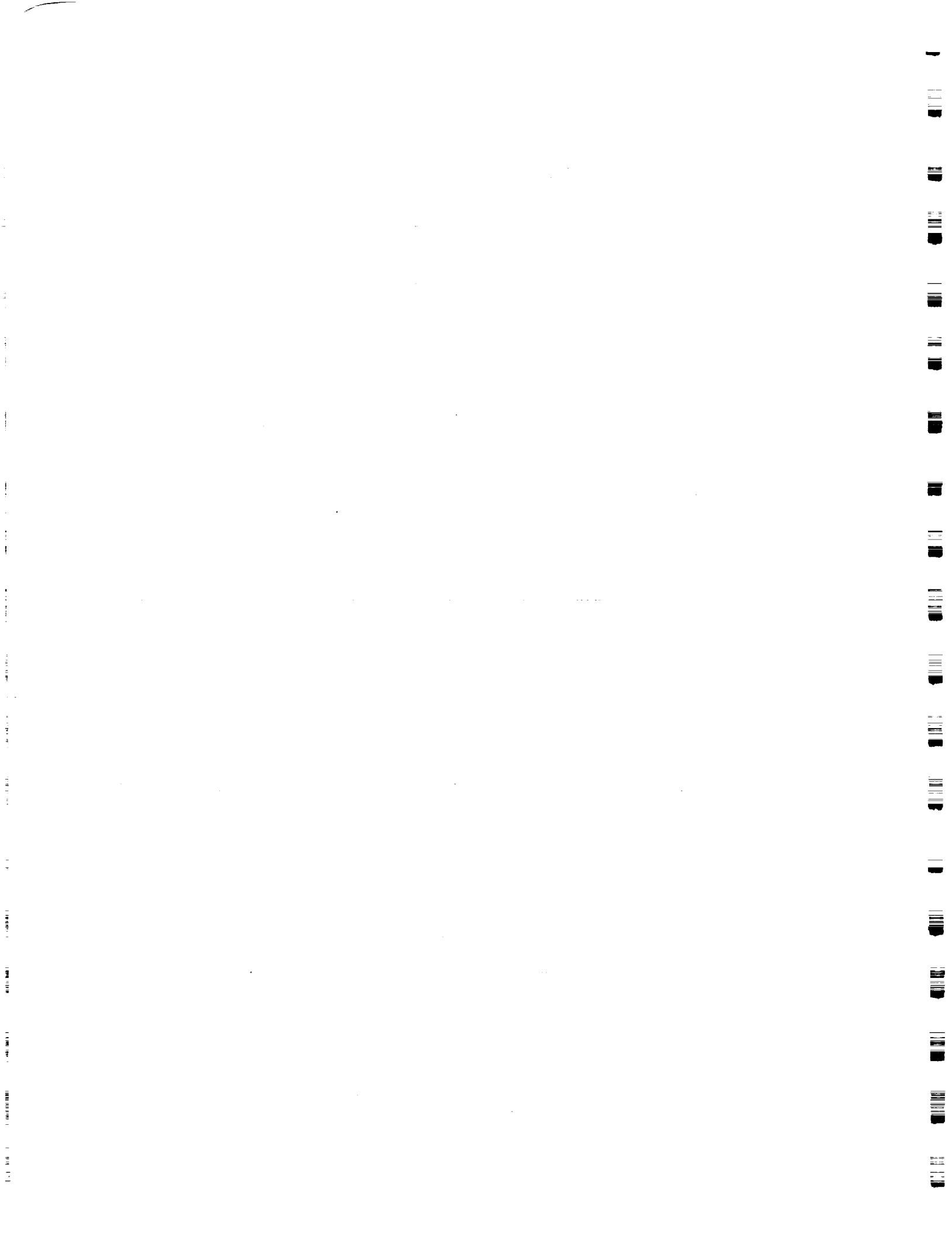
Gauge#	Location (inches)	Pressure (psia)	Gauge#	Location (inches)	Temperature deg R
BL1	0.024	Null	TT1	0.097	1299.0
BL2	0.064	17.630	TT2	0.191	Null
BL3	0.104	22.040	TT3	0.285	1771.0
BL4	0.144	26.680	TT4	0.378	1830.0
BL5	0.194	34.640	TT5	0.503	1837.0
BL6	0.244	46.530	TT6	0.628	1827.0
BL7	0.294	56.160	TT7	0.753	1840.0
BL8	0.354	57.390	TT8	0.878	1849.0
BL9	0.414	Null	TT9	1.003	Null

Pressure Data for Run 87

Total Temperature for Run 87







Appendix C

CUBDAT COMPUTER PROGRAM

Distribution of Program CUBDAT on 5-1/4" Floppy Diskettes

CUBDAT is a program which runs on an IBM PC AT or compatible computer having 640kB of RAM, hard disk, math coprocessor, graphics card and a 5-1/4" high density floppy drive. Under limited conditions, the program may be run from "MAIN_DISK", a bootable diskette which uses COMPAQ PC DOS Version 3.31. However, it is advisable to install the necessary software on the system hard disk and run the program there.

Until recently, program CUBDAT has been distributed to interested parties on a fixed number of 5-1/4", High Density (1.2MB), DOS formatted floppy diskettes. The experience gained as a result of that methodology has led to a more practical approach to handling the continually expanding database and the ability to correct errors detected after distribution. This document will discuss the rationale behind the structure of each diskette and serve as a guide for potential users.

CUBDAT, in its entirety, is delivered on four diskettes whose contents are described at the bottom of this page. However, in general practice, the data files from a single experimental study are delivered on a single diskette with the executable and configuration files needed to access them. In this instance CUBDAT may be run from diskette.

The current complete set of CUBDAT diskettes follows:

1. MAIN_DISK (All executable and configuration files);
2. DISK_1 (Subdirectories noted below);
 - A. BDYFIXTR
 - B. BICONIC3
 - C. BICONIC4
 - D. BLOWRUFF
 - E. BLUNTBOD
 - F. BLUNTLE
 - G. CURVSURF
 - H. INCIPSEP
 - I. LAMINAR
3. DISK_2 (Subdirectories noted below);
 - A. MRVPAT
 - B. MRVSAND
 - C. NASAFP
 - D. SEP-K90
 - E. SHK-SHK
 - F. SWEPTSKU
 - G. TURBFLO
4. DISK_3 (Subdirectories noted below);
 - A. SLOT_080
 - B. SLOT_120
 - C. SCANT
 - D. SMTHBLW1
 - E. SMTHBLW2
 - F. CONEFLAR
 - G. SHK-COMP

Whenever CUBDAT is invoked the default drive and directory are checked for the existence of files "summary.fil" and "summary.mtx". An error message is delivered if either file is missing. The user is then asked to specify in which drive and directory the program is to confine its searches. Unless all files are copied to the hard disk, it is necessary to place the appropriate diskette in the floppy drive. Subsequently, a menu of options is presented which gives the user the ability to select a specific experimental run's data for plotting or tabulation. Reduced data may be stored for pressure, skin friction, force/moment, heat transfer and calorimeter measurements. Test conditions and model configuration parameters may also be displayed for individual runs. The data from a particular run is stored in an ASCII file named "run*.lts" (* = run sequence # w/o leading zeroes). These files are also capable of being "imported" to LOTUS 1-2-3.

A new feature has been incorporated to enable users to plot data from other sources for comparison with reduced data in the database. An external ASCII file named "plot.add" must be included in the directory of the study of interest to provide this capability. The form of "plot.add" is as follows:

1. The initial line contains literal data, not to exceed 75 characters, which is not processed.
2. Two integer entries: Run# and Number of sets of data, N, to follow.
[N.B. Run# < 0 --> all runs. Run#s must be given in numerical order.]
3. For each set of data a single line containing, in order:
 - a. The number of points M to be plotted.
 - b. A type# defining the measurement of interest from the following list:
1=Pressure; 2=CP; 3=Skin Friction; 4=CF; 5=Force & Moment; 6=Heat Transfer;
7=CH; 8=Q/Qo(Fay-Riddell); 9=Calorimeter; 10=CC; 11=Temperature.
 - c. A symbol# defining the symbol to be drawn from the following list:
0=None; 1=Arrow Up; 2=X; 3=Arrow Down; 4=Square; 5=Arrow Right; 6=Diamond;
7=Arrow Left; 8=Circle; 9=Pentagon; 10=5 Pt Star; 11=Hexagon; 12=6 Pt Star;
13=Asterisk(*); 14=Plus(+); 15=Y; 16=Y Inverted; 17=Up&Down Arrows; 18=Dot.
[N.B. Use a negative value for a symbol only plot.]
 - d. A line# selecting the line type to be used to connect data points from:
1=Solid; 2=Dotted; 3=Dot-Dash; 4=Short Dash; 5=Long Dash.
[N.B. A negative line# causes a double width line to be drawn.]
 - e. Up to eight characters, in single quotes, for the plot legend.
4. M lines containing the x,y coordinates of each point to be plotted.
5. Repeat 3 & 4 until N sets of data have been input.
6. Loop back to 2 until data to be input have been exhausted.

Plotting to the screen employs a Tektronix 4014 emulator for the PC from MicroPlot Systems Inc. The mapping of the 1024 pixels wide by 780 pixels high Tektronix plot window to the size supported by individual PCs is accomplished through a device assignment in the "config.sys" file when the system is booted. The files named "plotdev.xxx", where the extension "xxx" relates to a specific graphics adaptor, are provided for this purpose. To date, only the AT&T 6300 (works with COMPAQ plasma displays), CGA, EGA and Hercules graphics adaptors have been accounted for in the distribution.

In the course of running CUBDAT, files containing graphic information may be produced. These files will be Tektronix compatible and may be directed to the screen for review using the "draw" utility provided. It is invoked by entering the command "draw xxx", where xxx is the name of the file created using CUBDAT. If more than one

plot is present in file xxx, the image on the screen will remain until the "Enter" key is pressed for another page or the "Esc" key is struck to terminate execution. An attempt to print the information in xxx will produce nonsense unless the Tektronix language is supported. Since most current generation laser printers do not "speak" Tektronix, the "tek2ps" utility will convert plot files to PostScript, a more common language. The same file may be converted to PostScript format by entering the command "tek2ps xxx > yyy", where yyy is the name of the translated file to be printed.

MAIN_DISK contains all the programs needed to successfully access and display the reduced data stored in the other diskettes. In addition to CUBDAT, DRAW and TEK2PS, several other programs (filenames with "EXE" extensions) are included. CLR should be used instead of the DOS command CLS to clear the screen and place the prompt at the top of the display. The remaining executable files extract information from the "run*.lts" files and place it on program prescribed or user designated filenames. Each is used by first entering its name and then responding to the prompts.

Optimum use of CUBDAT can be obtained by copying all files from MAIN_DISK into a single subdirectory on the system's hard disk. CALSPAN will be assumed for the purpose of illustration but the user is free to choose any name which is unique to DOS. The "config.sys" file in the system's root directory should be edited to include the lines "files=20", "buffers=40" and "device=\calspan\plotdev.?" (see below) to provide the environment required to successfully execute CUBDAT. Always transfer to the CALSPAN subdirectory by entering "cd \calspan" before invoking CUBDAT.

A slight improvement in performance can be obtained by also copying the files from the remaining diskettes into appropriately named subdirectories. If space on the hard disk is limited, CUBDAT can be directed to search for data on the floppy drive.

A list of all filenames delivered on "MAIN_DISK", with remarks enclosed in parentheses, follows:

- ASCIIDAT.EXE (appends selected run info to file ASCIIDAT.OUT)
- AUTOEXEC.BAT (consult your DOS reference manual for file's content)
- BOOTDISK.DOC (enter "TYPE BOOTDISK.DOC" to display useful info)
- CLR.EXE (use instead of "CLS" to clear screen display)
- COMMAND.COM (needed for booting from MAIN_DISK)
- CONFIG.SYS (must contain "DEVICE=PLOTDEV.?" for ?=ATT,CGA,EGA or HGC)
- CUBDAT.EXE (invoke CUBDAT where SUMMARY.FIL and SUMMARY.MTX reside)
- DRAW.EXE (draws plot files created by CUBDAT)
- GETTALL.EXE (appends selected test conditions to ALLPARMS.LTS)
- GETMODEL.EXE (appends run information to MODELSIN.LTS)
- GETTCS.EXE (appends all test conditions to TESTCONS.LIS)
- IBMBIO.COM (system hidden file)
- IBMDOS.COM (system hidden file)
- PLOTDEV.ATT (CONFIG.SYS device name for COMPAQ plasma display)
- PLOTDEV.CGA (CONFIG.SYS device name for Color Graphics Adaptor (CGA))
- PLOTDEV.EGA (CONFIG.SYS device name for Enhanced Graphics Adaptor (EGA))
- PLOTDEV.HGC (CONFIG.SYS device name for Hercules Graphics Card (HGC))
- PSTEK.PRO (required to successfully run TEK2PS.EXE)
- SUMMARY.FIL (used by CUBDAT for valid study (directory) names)
- SUMMARY.MTX (used by CUBDAT for test matrix specifications)
- TABULATE.EXE (tabulates selected calibration type(s) to named file)
- TEK2PS.EXE (translates Tektronix plot files to PostScript)

CUBDAT was created with the intention of providing a useful PC tool for accessing experimental data from Calspan's shock tunnels. In the course of time, the program has evolved based on in-house analysis and reporting needs. It is hoped that use of CUBDAT by others will lead to a greater understanding of the information contained in the data files and foster a dialogue to improve its usefulness. Toward that end, please address your comments to

John R. Moselle (716) 631-6850
Calspan Corporation
P.O. Box 400
Buffalo, NY 14225

**CUBDAT: A CUBRC Program to Access Hypersonic Experimental Database
Compiled from Studies in Calspan Shock Tunnels**

CUBDAT is a program which provides access to reduced data from a number of experimental studies conducted in Calspan's shock tunnels from 1964 to present. Data from each study are stored in ASCII files which are compatible for use with LOTUS 1-2-3. The sequence number, n, of each run performed is part of its associated filename which is of the form "RUNn.LTS". The use of appropriately named subdirectories provides the ability to discriminate data from different experimental series. A file named "CONFIGUR" must also be present in each subdirectory. It defines the single character abbreviations used in place of lengthy descriptions for model parameters related to the experiments. For instance, the phrase "Distance from the Leading Edge" might be represented by the letter "A" in the data files.

Although CUBDAT provides the user with a number of options for the plotting and tabulation of the information within the ASCII files, the ability to use the data in other contexts is essential. Toward this end, added information is provided in the form of:

1. Brief description of file organization;
2. Sample RUNn.LTS file;
3. Sample CONFIGUR file;
4. Plots derived from data in item 2.

When the CUBDAT user requests a display of run test conditions, some parameters which are not contained in the RUNn.LTS files are also reported. Their definitions follow:

Hw = Wall Enthalpy = Cp•Tw	[(Ft/sec) ²]
CPf = Converts Pressure to CP = 1/Q	[PSIA ⁻¹]
CHf = Converts Heat Rate to CH = 778/(Rho•U•(Ho-Hw))	[(BTU/Ft ² /sec) ⁻¹]
QoFR= Fay-Riddell* Heat Transfer to 3" Diam. Cylinder	[BTU/Ft ² /sec]

* Fay, J.A. and Riddell, F.R., "Theory of Stagnation Point Heat Transfer in Dissociated Air," Journal of Aeronautical Sciences, Vol. 25, No. 2

Organization of Information in RUNn.LTS Files

Line(s)	Description of Entry	Units
1	The run sequence number is the initial entry in the file. Lines 2 thru 7 contain the number of entries for the type of measurement [units] indicated:	
2	Pressure	[PSIA]
3	Skin Friction	[PSIA]
4	Force/Moment	[LBF/IN-LBF]
5	Heat Transfer	[BTU/Ft ² /SEC]
6	Calorimeter	[BTU/Ft ² /SEC]
7	Pressure (for separation from data levels in line 2)	[PSIA]

Let N be the total number of entries for all the types of measurement. Then, there follow three groups of N entries whose contents are:

Line(s)	Description of Entry
8,N+7	Group 1 -- Gauge labels within double quotes which may be preceded by a single non-blank character
N+8,2•N+7	Group 2 -- Gauge positions (inches) relative to a reference point provided in report documentation
2•N+8,3•N+7	Group 3 -- Data level in units appropriate to the type of measurement a) Heat transfer measurements may contain a second entry for the temperature at the surface in ⁰ R b) "N" indicates no measurement or nulled data

Thirteen values, one per line, corresponding to some of the conditions during the test follow:

Line(s)	Description of Entry	Units
3•N+8	Mi = Shock Tube Incident Shock Mach#	
3•N+9	Po = Reservoir Total Pressure	[PSIA]
3•N+10	Ho = Reservoir Total Enthalpy	[(Ft/sec) ²]
3•N+11	To = Reservoir Total Temperature	[⁰ R]
3•N+12	M = Freestream Mach#	
3•N+13	U = Freestream Velocity	[Ft/sec]
3•N+14	T = Freestream Temperature	[⁰ R]
3•N+15	P = Freestream Static Pressure	[PSIA]
3•N+16	Q = Dynamic Pressure = ½ • Rho • U ² /144	[PSIA]
3•N+17	Rho = Freestream Density	[Slugs/Ft ³]
3•N+18	Mu = Freestream Viscosity	[Slugs/Ft-sec]
3•N+19	Re = Freestream Reynolds Number	[Ft ⁻¹]
3•N+20	Po' = Pitot Pressure	[PSIA]

The remaining lines in the file contain a single character abbreviation from file CONFIGUR in column one followed by the datum for the associated model parameter.

Organization of Information in RUNn.LTS Files

Sample RUNn.LTS File

Entry	Line#	Comment
59	1	Run# is 59
24	2	24 Pressure gauges
0	3	No Skin Friction data
0	4	No Force/Moment data
32	5	32 H.T. gauges
0	6	No Calorimeter data
0	7	No extra Pressure data

$N = 24 + 32 = 56$ Gauge labels follow:

Entry	Line#	Comment
"P 30 "	8	Pressure label
"P 28 "	9	Pressure label
"P 26 "	10	Pressure label
"P 25 "	11	Pressure label
"P 24 "	12	Pressure label
"P 23 "	13	Pressure label
"P 22 "	14	Pressure label
"P 21 "	15	Pressure label
"P 20 "	16	Pressure label
"P 15 "	17	Pressure label
"P 19 "	18	Pressure label
"P 14 "	19	Pressure label
"P 18 "	20	Pressure label
"P 13 "	21	Pressure label
"P 17 "	22	Pressure label
"P 12 "	23	Pressure label
"P 16 "	24	Pressure label
"P 11 "	25	Pressure label
"P 10 "	26	Pressure label
"P 9 "	27	Pressure label
"P 7 "	28	Pressure label
"P 5 "	29	Pressure label
"P 3 "	30	Pressure label
"P 1 "	31	Pressure label
"HT 32 "	32	Heat Transfer label
"HT 31 "	33	Heat Transfer label
"HT 29 "	34	Heat Transfer label
"HT 28 "	35	Heat Transfer label
"HT 25 "	36	Heat Transfer label

Organization of Information in RUNn.LTS Files

"HT 24 "	37	Heat Transfer label
"HT 64 "	38	Heat Transfer label
"HT 65 "	39	Heat Transfer label
"HT 66 "	40	Heat Transfer label
"HT 67 "	41	Heat Transfer label
"HT 68 "	42	Heat Transfer label
"HT 69 "	43	Heat Transfer label
"HT 70 "	44	Heat Transfer label
"HT 10 "	45	Heat Transfer label
"HT 71 "	46	Heat Transfer label
"HT 9 "	47	Heat Transfer label
"HT 7 "	48	Heat Transfer label
"HT 6 "	49	Heat Transfer label
"HT 5 "	50	Heat Transfer label
"HT 4 "	51	Heat Transfer label
"HT 3 "	52	Heat Transfer label
"HT 2 "	53	Heat Transfer label
"HT 1 "	54	Heat Transfer label
"HT 62 "	55	Heat Transfer label
"HT 61 "	56	Heat Transfer label
"HT 59 "	57	Heat Transfer label
"HT 58 "	58	Heat Transfer label
"HT 57 "	59	Heat Transfer label
"HT 56 "	60	Heat Transfer label
"HT 55 "	61	Heat Transfer label
"HT 54 "	62	Heat Transfer label
"HT 53 "	63	Heat Transfer label

56 Gauge positions follow:

Entry	Line#	Comment
0.0000	64	Press. gauge location
0.3750	65	Press. gauge location
0.7500	66	Press. gauge location
0.9375	67	Press. gauge location
1.1250	68	Press. gauge location
1.3125	69	Press. gauge location
1.5000	70	Press. gauge location
1.6875	71	Press. gauge location
1.8125	72	Press. gauge location
1.8750	73	Press. gauge location
1.9375	74	Press. gauge location
2.0000	75	Press. gauge location
2.0625	76	Press. gauge location

Organization of Information in RUNn.LTS Files

2.1250	77	Press. gauge location
2.1875	78	Press. gauge location
2.2500	79	Press. gauge location
2.3125	80	Press. gauge location
2.3750	81	Press. gauge location
2.5000	82	Press. gauge location
2.6875	83	Press. gauge location
3.0625	84	Press. gauge location
3.4375	85	Press. gauge location
3.8125	86	Press. gauge location
4.1875	87	Press. gauge location
1.2600	88	H.T. gauge location
1.3400	89	H.T. gauge location
1.5000	90	H.T. gauge location
1.5800	91	H.T. gauge location
1.8200	92	H.T. gauge location
1.9000	93	H.T. gauge location
2.0250	94	H.T. gauge location
2.0500	95	H.T. gauge location
2.0750	96	H.T. gauge location
2.1000	97	H.T. gauge location
2.1250	98	H.T. gauge location
2.1500	99	H.T. gauge location
2.1750	100	H.T. gauge location
2.1870	101	H.T. gauge location
2.2000	102	H.T. gauge location
2.2080	103	H.T. gauge location
2.2500	104	H.T. gauge location
2.2707	105	H.T. gauge location
2.2916	106	H.T. gauge location
2.3125	107	H.T. gauge location
2.3334	108	H.T. gauge location
2.3543	109	H.T. gauge location
2.3753	110	H.T. gauge location
2.3753	111	H.T. gauge location
2.4553	112	H.T. gauge location
2.6153	113	H.T. gauge location
2.6953	114	H.T. gauge location
2.7753	115	H.T. gauge location
2.8553	116	H.T. gauge location
2.9353	117	H.T. gauge location
3.0153	118	H.T. gauge location
3.0953	119	H.T. gauge location

Organization of Information in RUNn.LTS Files

56 Data levels follow:

Entry	Line#	Comment
"N"	120	Pressure data
2.9817E+00	121	Pressure data
4.8875E+00	122	Pressure data
4.4496E+00	123	Pressure data
2.4228E+00	124	Pressure data
1.2506E+00	125	Pressure data
9.3307E-01	126	Pressure data
2.3393E+00	127	Pressure data
5.2630E+00	128	Pressure data
7.0792E+00	129	Pressure data
1.3301E+01	130	Pressure data
1.7795E+01	131	Pressure data
3.1199E+01	132	Pressure data
4.9766E+01	133	Pressure data
1.0579E+02	134	Pressure data
8.7510E+01	135	Pressure data
6.0132E+01	136	Pressure data
3.1908E+01	137	Pressure data
2.5303E+01	138	Pressure data
2.5834E+01	139	Pressure data
2.1739E+01	140	Pressure data
1.6147E+01	141	Pressure data
9.5870E+00	142	Pressure data
4.3132E+00	143	Pressure data
1.6407E+01 5.5659E+02	144	H.T. & SurfaceT data
8.2543E+00 5.5309E+02	145	H.T. & SurfaceT data
8.0836E+00 5.5710E+02	146	H.T. & SurfaceT data
1.2132E+01 5.6029E+02	147	H.T. & SurfaceT data
4.9894E+01 6.4553E+02	148	H.T. & SurfaceT data
7.9512E+01 7.1050E+02	149	H.T. & SurfaceT data
2.0241E+02 8.3680E+02	150	H.T. & SurfaceT data
"N"	151	H.T. & SurfaceT data
3.0849E+02 8.7951E+02	152	H.T. & SurfaceT data
3.9993E+02 9.1072E+02	153	H.T. & SurfaceT data
4.6382E+02 9.2251E+02	154	H.T. & SurfaceT data
5.5120E+02 9.3979E+02	155	H.T. & SurfaceT data
6.3309E+02 9.5299E+02	156	H.T. & SurfaceT data
7.6012E+02 9.8267E+02	157	H.T. & SurfaceT data
7.3708E+02 9.7058E+02	158	H.T. & SurfaceT data
7.3548E+02 9.5051E+02	159	H.T. & SurfaceT data
5.1358E+02 8.9748E+02	160	H.T. & SurfaceT data

Organization of Information in RUNn.LTS Files

6.0265E+02	9.2167E+02	161	H.T. & SurfaceT data
6.2253E+02	9.2078E+02	162	H.T. & SurfaceT data
4.8431E+02	8.6673E+02	163	H.T. & SurfaceT data
4.3188E+02	8.4131E+02	164	H.T. & SurfaceT data
3.4912E+02	8.0254E+02	165	H.T. & SurfaceT data
3.2089E+02	7.8725E+02	166	H.T. & SurfaceT data
3.4024E+02	7.9381E+02	167	H.T. & SurfaceT data
2.1714E+02	7.2924E+02	168	H.T. & SurfaceT data
2.0662E+02	7.1388E+02	169	H.T. & SurfaceT data
1.7707E+02	6.9167E+02	170	H.T. & SurfaceT data
1.6153E+02	6.8830E+02	171	H.T. & SurfaceT data
1.4524E+02	6.7237E+02	172	H.T. & SurfaceT data
1.4748E+02	6.7381E+02	173	H.T. & SurfaceT data
1.2867E+02	6.5669E+02	174	H.T. & SurfaceT data
1.1740E+02	6.4460E+02	175	H.T. & SurfaceT data

13 Test conditions follow:

Entry	Line#	Comment
3.4120E+00	176	Mi
1.3520E+03	177	Po
1.8554E+07	178	Ho
2.8191E+03	179	To
8.0357E+00	180	M
5.8716E+03	181	U
2.2201E+02	182	T
1.1847E-01	183	P
5.3608E+00	184	Q
4.4783E-05	185	Rho
1.8344E-07	186	Mu
1.4334E+06	187	Re
9.9386E+00	188	Po'

Organization of Information in RUNn.LTS Files

Model parameters follow:

Entry	Line#	Comment
A 15.0	189	Parameter abbreviation, Value
B Blunt	190	Parameter abbreviation, Value
C 22.5	191	Parameter abbreviation, Value
D Yes	192	Parameter abbreviation, Value
E 20	193	Parameter abbreviation, Value
F 50	194	Parameter abbreviation, Value

A possible CONFIGUR file for the above model parameters is shown below.

A	Angle of Attack (Degrees)
B	Nose Type --
C	Model Width (Inches)
D	Angular Trip (Yes/No)
E	Bluntness Ratio (Rn/Rb) (Percent)
F	Heat Transfer Reference Run Number =

